ZooKeys

Research Article

Identification of two new species of *Mecistocephalus* (Chilopoda, Geophilomorpha, Mecistocephalidae) from southern China and the re-description of *Mecistocephalus smithii* Pocock, 1895

Yang-Yang Pan[1,2*], Jia-Bo Fan[1,2*], Chun-Xue You[1], Chao Jiang[2]

1 Tianjin Key Laboratory of Agricultural Animal Breeding and Healthy Husbandry, College of Animal Science and Veterinary Medicine, Tianjin Agricultural University, Tianjin 300392, China

2 State Key Laboratory for Quality Ensurance and Sustainable Use of Dao-di Herbs, National Resource Center for Chinese Materia Medica, China Academy of Chinese Medical Sciences, Beijing 100700, China

Corresponding authors: Chao Jiang (jiangchao0411@126.com); Chun-Xue You (youchunxue@mail.bnu.edu.cn)

Citation: Pan Y-Y, Fan J-B, You C-X, Jiang C (2024) Identification of two new species of *Mecistocephalus* (Chilopoda, Geophilomorpha, Mecistocephalidae) from southern China and the re-description of *Mecistocephalus smithii* Pocock, 1895. ZooKeys 1218: 1–23. https://doi.org/10.3897/zookeys.1218.130709

Abstract

Mecistocephalus Newport, 1843 is the most diverse genus in the family Mecistocephalidae; however, only two species have been recorded in mainland China to date. Therefore, taxonomic research on Chinese *Mecistocephalus* needs further research. In this study, the species diversity of *Mecistocephalus* in southern China was investigated using the mitochondrial marker COI integrated with morphological evidence. Species delimitation using Automatic Barcode Gap Discovery, Poisson Tree Processes, and phylogenetic and morphological analyses revealed ten species, including two newly described species, *M. chuensis* Jiang & You, **sp. nov.** and *M. huangi* Jiang & You, **sp. nov.** Furthermore, based on newly collected specimens, the presence of the little-known species *M. smithii* Pocock, 1895 was confirmed in China and thoroughly re-described.

Key words: COI, phylogeny, taxonomic key, taxonomy

Introduction

Mecistocephalus Newport, 1843 is the most diverse genus in the family Mecistocephalidae Bollman, 1893, comprising nearly 70% of mecistocephalid species. Approximately 135 species in the genus have been reported to date, most of which are distributed in tropical and subtropical Asia, particularly in South Asia (India, Sri Lanka, and Nepal), Southeast Asia (Cambodia, Laos, Indonesia, Malaysia, Myanmar, Philippines, Singapore, Thailand, and Vietnam), and East Asia (southern China and Japan), with fewer records from Africa, America, and temperate areas, such as Northeast China (Bonato et al. 2011, 2016).

The earliest species discovered in China is *Mecistocephalus smithii* Pocock, 1895, reported in Ningbo, Zhejiang Province (Pocock 1895). Subsequently, taxonomic and faunistic contributions were made by F. Silvestri (1919), K.W. Verhoeff (1937), Y. Takakuwa (1940), and C.G. Attems (1947). A dozen *Mecistocephalus* species have been recorded in Taiwan and its adjacent regions. Wang and

---

* These authors contributed equally to this work.

Mauries (1996) compiled a comprehensive record of 16 *Mecistocephalus* species from China. However, subsequent assessments by Uliana et al. (2007) identified four of these as synonyms (*M. fenestratus* Verhoeff, 1934 = *M. japonicus* Meinert, 1886; *M. insulomontanus* Gressitt, 1941 = *M. marmoratus* Verhoeff, 1934; *M. mirandus* Pocock, 1895 = *M. japonicus* Meinert, 1886; *M. takakuwai* Verhoeff, 1934 = *M. diversisternus* (Silvestri 1919)), and records of another two species in Taiwan were doubtful (*M. punctifrons* Newport, 1843 and *M. insularis* (Lucas, 1863)). Two species were misclassified: *Formosocephalus longichilatus* (Takakuwa, 1936) = *M. longichilatus* Takakuwa, 1936 and *Taiwanella yanagiharai* Takakuwa, 1936 = *M. yanagiharai* (Takakuwa, 1936) (Bonato et al. 2002, 2003); accordingly, 14 *Mecistocephalus* species have been reported in China to date. Chao et al. (2020) have reported only the occurrence of *M. rubriceps* Wood, 1862 in Yunnan province; however, earlier research has primarily concentrated on Taiwan, and taxonomic knowledge of Chinese *Mecistocephalus* is incomplete.

In this study, we describe two new species of *Mecistocephalus* from southern China and re-describe *M. smithii*. Through a molecular analysis of the COI sequence, we verified the boundaries between the new species and their congeners.

Materials and methods

Specimen collection and identification

In China, 92 *Mecistocephalus* specimens were collected from seven provinces (Sichuan, Yunnan, Guangxi, Guangdong, Hunan, Hubei, and Jiangsu) (Fig. 1). All specimens were preserved in 75% ethanol. The forcipular segment was dissected and mounted for examination with lactic acid. Temporary mounts were clarified using lactic acid. The specimens are deposited in the National Resource Center for Chinese Materia Medica, China Academy of Chinese Medical Sciences, China (**CMMI**).

The terminology used in descriptions follows Bonato et al. (2010). Specimens were examined and photographed by using a Leica M205 FCA stereomicroscope and an Olympus BX51 Microscope. Line drawings were prepared from photographs taken with the microscope. The ArcMap 10.7.1 software tool was used to produce distribution maps.

DNA extraction and fragment amplification

According to the DNeasy Blood & Tissue Kit (Qiagen, Hilden, Germany) requirements, ~ 6 walking legs from each specimen were used to extract genomic DNA; the isolated DNA being resuspended in 100 µL of buffer and stored at −20 °C for subsequent analysis. Polymerase chain reaction (PCR) was used to amplify the cytochrome c oxidase subunit I (COI). The PCR primers and programs used are listed in Table 1 (TFP682 and TRP682 are newly developed primers for more efficient amplification of *Mecistocephalus* CO1 sequences). PCR reaction mixtures (total volume 25 µL) contained 12.5 µL of 2 × M5 Mix (Transgen, Beijing, China), 0.4 µL each of the forward and reverse primers (10 µmol·L^{-1}, Sangon, Shanghai, China), and 1 µL (~ 20 ng) of genomic DNA. Amplification was performed in a Veriti™ thermal cycler (Applied Biosystems, Foster City, CA, USA) using cycling conditions in Table 1.

Figure 1. The known distribution of *Mecistocephalus* specimens in mainland China.

Table 1. Primers and PCR conditions employed.

Loci	Primer name	Sequence 5'– 3'	Program	Reference
CO1	LCO1490	GGTCAACAAATCATAAAGATATTGG	95 °C 5 min; 38 cycles of 20 s at 95 °C, 20 s at 45 °C and 1 min at 72 °C; 3 min at 72 °C	Folmer et al. 1994
	HCOUTOUT	GTAAATATATGRTGDGCTC		
CO1	LCO1490	GGTCAACAAATCATAAAGATATTGG	2 min at 94 °C; 35 cycles of 15 s at 95 °C, 40 s at 45– 47 °C and 15 s at 72 °C; 10 min at 72 °C	Folmer et al. 1994; Joshi and Karanth 2011
	HCO2198	TAAACTTCAGGGTGACCAAAAAATCA		
CO1	TFP682	TTGGAGATGACCAAACATATAA	5 min at 94 °C, 30 s at 94 °C; 35 cycles of 30 s at 52 °C and 1 min at 72 °C; 5 min at 72 °C	This study
	TRP682	CAAAAAATCAGAATAGGTGTTG		

Species delimitation, phylogenetic analysis, and genetic distance calculation

Species delimitation analyses were conducted using the Automatic Barcode Gap Discovery (ABGD) method (Puillandre et al. 2012) and the Poisson Tree Processes (PTP) model (Zhang et al. 2013) based on *COI* sequences. We ran ABGD under the following parameters: Pmin = 0.001, Pmax = 0.1, Steps = 20, X (relative gap width) = 1.0, Kimura (K80) TS/TV distances = 2.0, Nb bins (for distance distribution) = 20. We ran PTP under the following parameters: No. MCMC generations = 100000, Thinning = 100, Burn-in = 0.1, Seed = 123. The genetic distance between *Mecistocephalus* species was calculated using the Kimura 2-parameter model in MEGA 11 (Tamura et al. 2021). Using *Tygarrup javanicus* (Attems, 1907) as an outgroup, the ClustalW tool (Thompson et al.

1994) in BIOEDIT 7.1.3.0 (Hall 1999) was used to align a total of 28 COI sequences obtained from 15 newly sequenced *Mecistocephalus* sequences and 13 sequences obtained from GenBank (12 sequences were *Mecistocephalus* and 1 sequence was *Tygarrup*) (Table 2). Phylogenetic trees based on Bayesian Inference (BI) and Maximum Likelihood (ML) were respectively constructed with the PHYLOSUITE 1.2.2 platform (Zhang et al. 2020). In addition, MODELFINDER (Kalyaanamoorthy et al. 2017) was used to select suitable models, in which the best ML model was TIM2+F+I+G4, and the best BI model was SYM+I+G4. IQ-TREE 1.6.8 (Nguyen et al. 2015) was used to perform ML analysis with 500,000 ultrafast bootstraps (Hoang et al. 2018). MRBAYES 3.2.6 (Ronquist et al. 2012) was used to run Bayesian analyses. In the process, four Markov Chain Monte Carlo (MCMC) chains were used to run 10,000,000 generations at the same time with a sampling frequency of 1000 generations and dividing 25% of the trees as burn-in. Branch support was evaluated through standard statistical testing (bootstrap support and posterior probability).

Table 2. Vouchers of *Mecistocephalus* species and outgroup and their GenBank accession numbers.

No.	Species	Voucher	Locality	COI	Reference
1	*M. chuensis* sp. nov.	CMMI 20200121008	Hengyang, Hunan, China	OR864658	This study
2	*M. chuensis* sp. nov.	CMMI 20210408124	Wuhan, Hubei, China	OR864659	This study
3	*M. chuensis* sp. nov.	CMMI 20210409130	Jinmen, Hubei, China	OR864660	This study
4	*M. diversisternus*	–	–	AB610776.1	Chao and Chang (unpublished)
5	*M. guildingii*	–	–	AF370837.1	Giribet et al. 2001
6	*M. guildingii*	CMMI 20201214103	Nantong, Jiangsu, China	OR864662	This study
7	*M. guildingii*	CMMI 20200608031	Yuanjiang, Hunan, China	OR864663	This study
8	*M. huangi* sp. nov.	CMMI 20230705004D	Gejiu, Yunnan, China	OR864653	This study
9	*M. huangi* sp. nov.	CMMI 20230830001D	Gejiu, Yunnan, China	OR864654	This study
10	*M. huangi* sp. nov.	CMMI 20201022122	Honghe Hani and Yi Autonomous Prefecture, Yunnan, China	OR864655	This study
11	*M. japonicus*	–	–	AB610480.1	Chao and Chang (unpublished)
12	*M. marmoratus*	–	–	AB672644.1	Chao and Chang (unpublished)
13	*M. marmoratus*	–	–	AB672611.1	Chao and Chang (unpublished)
14	*M. marmoratus*	–	–	AB610773.1	Chao and Chang (unpublished)
15	*M. marmoratus*	–	–	AB610772.1	Chao and Chang (unpublished)
16	*M. marmoratus*	–	–	AB610501.1	Chao and Chang (unpublished)
17	*M. marmoratus*	–	–	AB610500.1	Chao and Chang (unpublished)
18	*M. multidentatus*	–	–	AB610774.1	Chao and Chang (unpublished)
19	*M. multidentatus*	–	–	AB672610.1	Chao and Chang (unpublished)
20	*M. multidentatus*	–	–	AB610775.1	Chao and Chang (unpublished)
21	*M. multidentatus*	CMMI 20201205104	Shenzhen, Guangdong, China	OR864661	This study
22	*M. multidentatus*	CMMI 20230307001D	Shenzhen, Guangdong, China	OR864664	This study
23	*M. mikado*	CMMI 20200515001	Laibin, Guangxi Zhuang Autonomous Region, China	OR864668	This study
24	*M. mikado*	CMMI 20190418026	Laibin, Guangxi Zhuang Autonomous Region, China	OR864669	This study
25	*M. rubriceps*	CMMI 20210419105	Chengdu, Sichuan, China	OR864666	This study
26	*M. smithii*	CMMI 20201108126	Nanjing, Jiangsu, China	OR864667	This study
27	*M. smithii*	CMMI 20191031042	Zhoushan, Zhejiang, China	PP101253	This study
28	*Tygarrup javanicus*	–	–	KM491598.1	Thormann and von der Mark (unpublished)

Results

Molecular phylogenetic analyses and species delimitation

Both the PTP and ABGD methods classified *M. huangi* sp. nov. and *M. chuensis* sp. nov. as distinct species. Eleven candidate species were identified using the ABGD method (0.001 < P < 0.037927). Using the PTP (ML) and PTP (BI) methods, 17 and 18 units were identified, respectively. Furthermore, Kimura two-parameter (K2P) distances between *Mecistocephalus* species ranged from 15.6% (*M. smithii* against *M. diversisternus*) to 23.9% (*M. chuensis* sp. nov. against *M. guildingii* Newport, 1843), and the average K2P genetic distance was 19.8% (Table 3). The intraspecific divergence within *Mecistocephalus* taxa was low, ranging from 0.5% (*M. multidentatus* Takakuwa, 1936) to 5.7% (*M. mikado* Attems, 1928). The mean distance within *M. chuensis* sp. nov. was second highest at 5.0% (Table 4). The K2P genetic distance between the two new species was 18.4%, well above the upper limit for intraspecific genetic distance. Considering the morphological characteristics of the samples and intraspecific genetic distances, both PTP methods (ML and PI) likely overestimated the number of species within *Mecistocephalus*.

A phylogenetic analysis and the ABGD method revealed 11 species. For *M. marmoratus*, the observed internal branch length was consistent with multiple taxonomic units identified though ABGD and PTP delimitation but disagreed with results based on morphological characters (Fig. 2). The two new species described here were recovered as sister taxa, with moderate support in phylogenetic analyses (Posterior Probability, PP = 0.897; Bootstrap Support, BS = 73%). In the phylogeny, a basal dichotomy was observed between *M. mikado* and the remaining

Table 3. Mean K2P genetic distance between the *Mecistocephalus* species based on COI sequences.

		(1)	(2)	(3)	(4)	(5)	(6)	(7)	(8)	(9)
(1)	*M. multidentatus*									
(2)	*M. guildingii*	21.0%								
(3)	*M. marmoratus*	18.8%	21.5%							
(4)	*M. diversisternus*	18.8%	20.9%	19.1%						
(5)	*M. japonicus*	18.2%	20.8%	17.6%	16.9%					
(6)	*M. huangi* sp. nov.	17.5%	20.9%	18.6%	20.3%	20.1%				
(7)	*M. smithii*	18.0%	18.3%	17.3%	15.6%	16.4%	18.1%			
(8)	*M. chuensis* sp. nov.	18.1%	23.9%	20.6%	19.2%	19.7%	18.4%	21.3%		
(9)	*M. rubriceps*	21.0%	22.7%	19.0%	23.0%	19.1%	21.1%	18.6%	23.6%	
(10)	*M. mikado*	21.0%	23.5%	21.3%	22.2%	17.2%	19.3%	19.2%	23.4%	21.3%

Table 4. Mean K2P genetic distance within the *Mecistocephalus* species based on COI sequences.

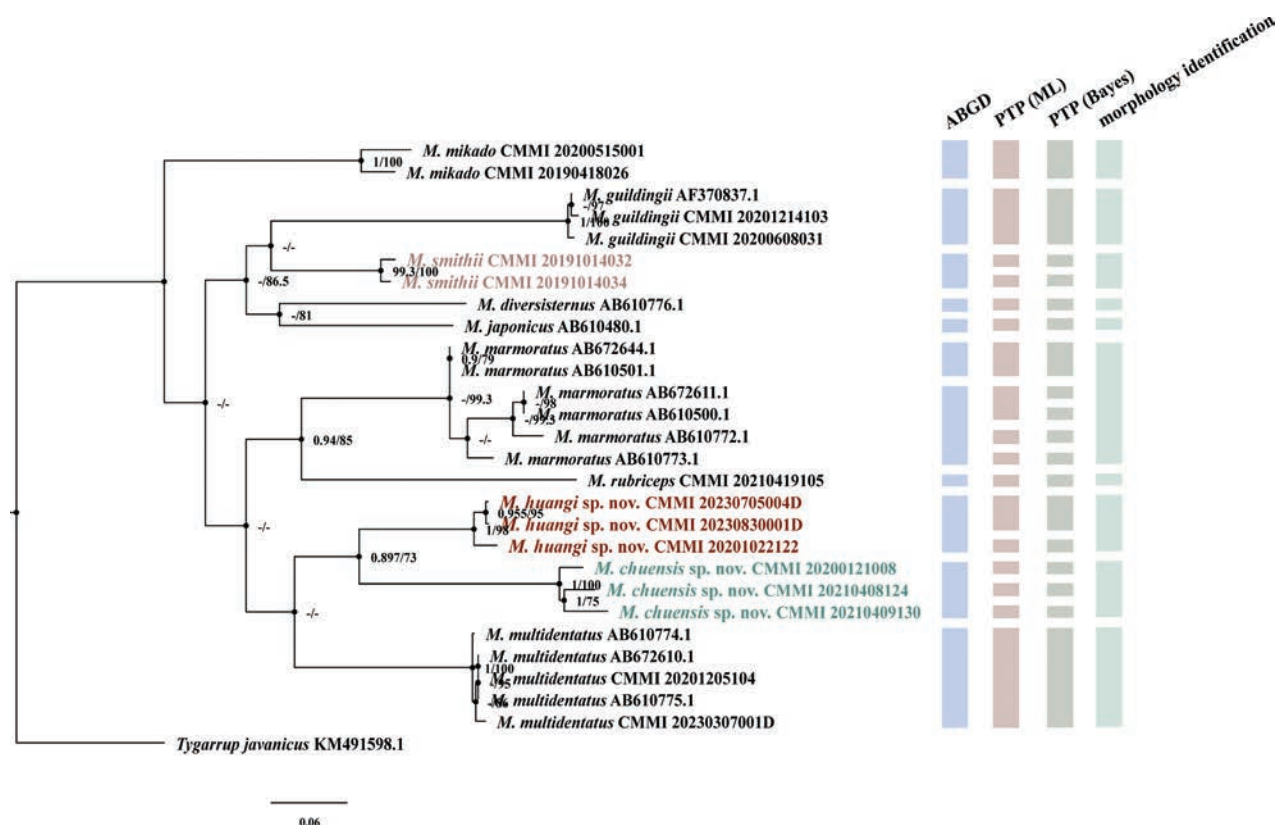| Examined species	Mean distance	Standard error
M. multidentatus	0.5%	0.2%
M. guildingii	0.8%	0.3%
M. marmoratus	3.6%	0.7%
M. diversisternus	-	-
M. japonicus	-	-
M. huangi sp. nov.	2.0%	0.5%
M. smithii	1.6%	0.6%
M. chuensis sp. nov.	5.0%	0.8%
M. rubriceps	-	-
M. mikado	5.7%	1.0%

Figure 2. Phylogenetic tree based on COI for *Mecistocephalus* with Bayesian posterior probability (PP > 0.9 / BS > 70%, PP marked in the left and BS in the right) values and bootstrap support following ML analysis for each node and the result of species delimitation of single locus COI are based on using three species delimitation methods ABGD, PTP(ML), and PTP(BI).

species. All other *Mecistocephalus* taxa were resolved into three clades. *Mecistocephalus huangi* sp. nov. and *M. chuensis* sp. nov. were recovered as a clade with *M. multidentatus*, sister to a clade containing *M. marmoratus* and *M. rubriceps*. The remaining species, *M. guildingii*, *M. smithii*, *M. diversisternus*, and *M. japonicus*, all formed one clade sister to the other two. Internal structure was observed. Notably, samples from Hubei Province (CMMI 20210408124, 20210409130) within *M. chuensis* sp. nov. were separated from those from Hunan Province (PP = 1, BS = 100%). Similarly, samples from Gejiu City (CMMI 20201022122) and Jianshui County (CMMI 20230705004D, 20230830001D) in Yunnan Province, identified as *M. huangi* sp. nov., exhibited clear differentiation into two branches, with high nodal support (PP = 1, BS = 98%). Conversely, samples collected from the same geographic site exhibited relatively small intraspecific distances, as exemplified by *M. smithii* and *M. chuensis* sp. nov. in PTP analyses.

Taxonomic accounts

Family Mecistocephalidae Bollmann, 1893

Genus *Mecistocephalus* Newport, 1843

Diagnosis. Mecistocephalids with at least 45 leg-bearing segments. Two clypeal plagulae, separated by a mid-longitudinal stripe. Spiculum usually present. Buccae with setae at least in the posterior half. Posterior alae of the

labrum smooth. Coxosternum of the first maxillae divided, with a mid-longitudinal suture. Coxosternum of the second maxillae undivided; groove from the metameric pore reaching the lateral margin of the coxosternum. Telopodites of the second maxillae well developed, overreaching those of the first maxillae; pretarsus present. Forcipular trochanteroprefemur with a distal tooth and often with another tooth at approximately mid-length. Sternal sulcus of trunk segments furcate or not. Last leg-bearing segment: Coxopleura usually without a macropore distinct from other pores; legs usually as slender in males as in females, with or without one or two short apical spines (Uliana et al. 2007).

Mecistocephalus chuensis Jiang & You, sp. nov.

https://zoobank.org/CBECBDD2-1928-49AB-ADAA-859E4D7D74AA
Figs 3, 4
Chinese name: 楚地蜈蚣

Material examined. *Holotype*. • ♂; (CMMI 20210409134); Сʜɪɴᴀ, **Hubei Province,** Jingshan County, Kongshandong Scenic Area; 30.9735°N, 113.0377°E; 110 m a.s.l.; 9 Apr. 2021; coll. Tianyun Chen & Zhidong Wang. *Paratypes*. • 2 ♂♂, 2 ♀♀; (CMMI 20210409130−133); same data as holotype. • 1 ♂, 7 ♀♀; (CMMI 20210408121−20210408124, -129, -131, -132, -134); **Hubei Province, Wuhan,** Ma'anshan Forest Park; 30.5146°N, 114.4394°E; 110 m a.s.l.; 8 Apr. 2021; coll. Tianyun Chen & Zhidong Wang. • 1 ♀ (CMMI 202100121008); **Hunan Province, Hengyang,** Chuanshan Ave; 30.5146°N, 114.4394°E; 120 m a.s.l.; 12 Jan. 2021; coll. Chao Jiang.

Diagnosis. A *Mecistocephalus* species with 49 leg pairs. Head length-to-width ratio 1.77, each side of clypeus with five or six smooth insulae, clypeal ratio (areolate part/ non-areolate part) of 1.22, sensilla on plagulae absent, posterior 1/2 of cephalic pleurite bearing a group of setae, forcipular cerrus composed of two paramedian rows of setae, mandible with ~ 8 well-developed lamellae, and first lamella with seven teeth. Sternal sulcus furcated at an obtuse angle.

Description. *Holotype* (CMMI 20210409134).

Body length: 58 mm; posterior part slightly slender. Head and forcipular segment dark red in color; remainder yellow.

Cephalic plate (Fig. 3A−C): sub-rectangular, length-to-width ratio of 1.77; lateral margins slightly convergent backward, strongly convergent backward at proximal three-fourths, maximum width 2.88 mm; transverse suture protrudes to the back edge of the cephalic plate in an arc; two or three setae in the anterior of back side, punctate depressions interspersed throughout. Antennae 5.3 × as long as the head width. Apical sensilla ~ 8 μm long.

Clypeus (Fig. 3D): clypeal ratio (areolate part/ non-areolate part) ~ 1.22; five or six insulae on each side of clypeus, only four bearing setae on each side; the transverse suture of clypeal plagulae almost straight, sensilla inside plagulae absent.

Labrum (Fig. 3D): anterior ala with medial margin not reduced to a vertex, medial margin ~ 1/3 of the length of posterior ala; mid piece protruding forward over side pieces; posterior margin of side pieces sinuous, concave or convex with respect to straight anterior margin; the hair-like fringes and projections on the labral side pieces absent, the comma-shaped sclerite lateral to the labral side pieces present.
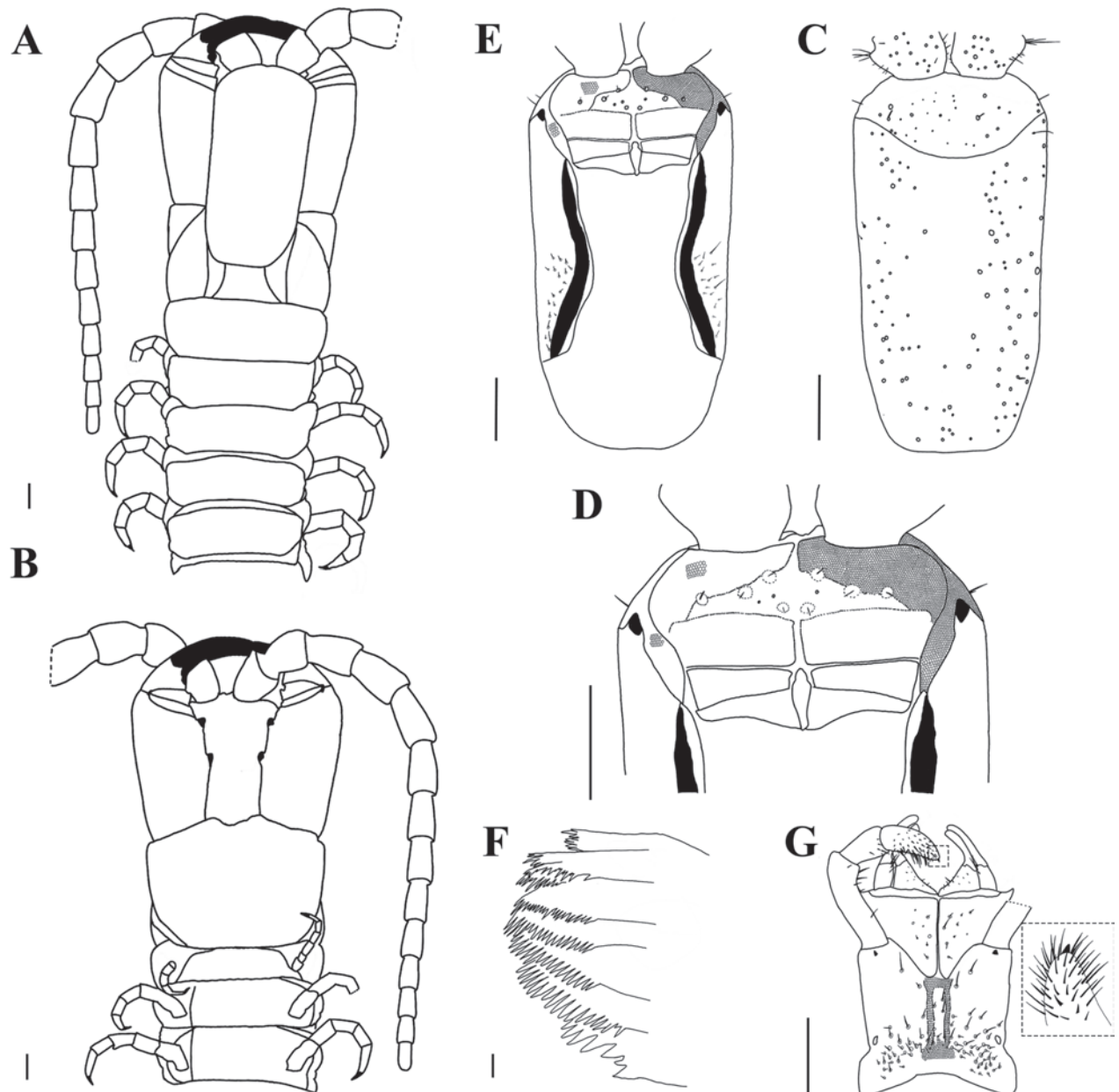
Figure 3. *Mecistocephalus chuensis* Jiang & You, sp. nov., holotype (CMMI 20210409134) **A** anterior part of body, dorsal view (right antenna not drawn) **B** anterior part of body, ventral view (right antenna not drawn) **C** cephalic plate, dorsal view **D** anterior part of head, ventral view (maxillae removed) **E** cephalic plate, ventral view (maxillae removed) **F** mandible **G** maxillae and inner illustration shows the telopodite article III of the second maxillae, ventral view (right telopodite of the second maxillae removed) Part of areolation not drawn. Scale bars: 20 μm (**F**); 1 mm (**A–E, G**).

Cephalic pleurite (Fig. 3E): spiculum present, group of setae only on the posterior 1/2.

Mandible (Fig. 3F): approximately eight well-developed lamellae; first lamella with seven teeth; average intermediate lamella with ~ 22 teeth; basal teeth as same size as distal teeth; basal tooth large, shorter than the teeth of the first lamella.

First maxillae (Fig. 3G): antero-external corners of coxosternite protruding and short; coxosternite divided by mid-longitudinal sulcus, with eight or nine setigerous insulae on each side; coxal projection 1.2 × wider than long, eleven setae on medial marginal and clavate lappet present; telopodites 2.86 × longer than wide, clavate lappet present.
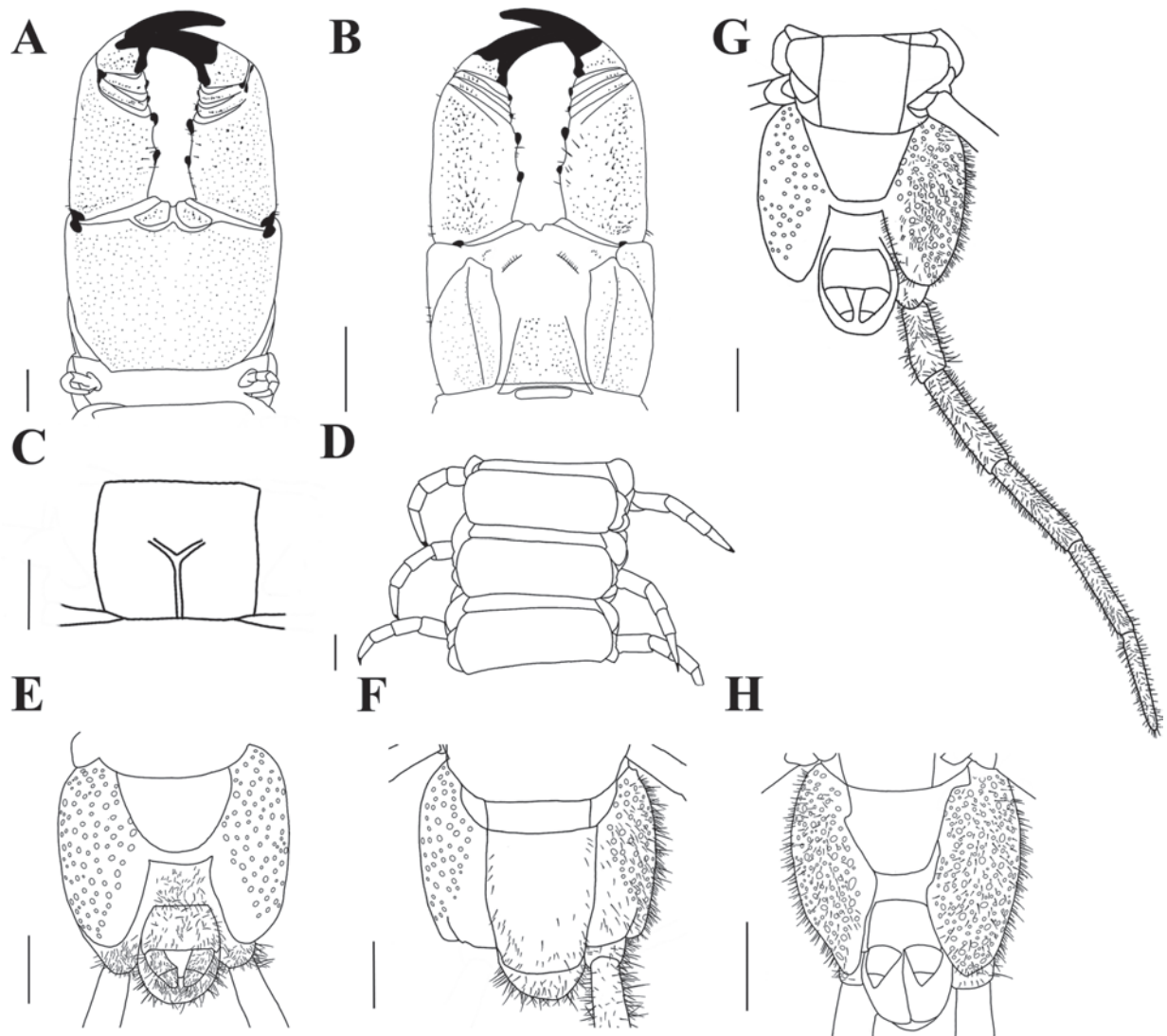
Figure 4. *Mecistocephalus chuensis* Jiang & You, sp. nov., holotype (CMMI 20210409134) **A** forcipular segment, ventral view **B** forcipular segment, dorsal view **C** sternite of leg-bearing segment VI, ventral view **D** tergites of leg-bearing segments VI–VIII, dorsal view **E** ultimate leg-bearing segment, ventral view **F** ultimate leg-bearing segment, dorsal view **G** ultimate leg-bearing segment and left leg, ventral view **H** ultimate leg-bearing segment, ventral view (paratype CMMI 20210408122). Scale bars: 500 μm (**H**); 1 mm (**A–G**).

Second maxillae (Fig. 3G): sclerotic ridge on the middle of coxosternite circumscribing three or four setigerous insulae; each side of coxosternite with setae on the lateral to each metameric pore; telopodite article I 1.4 × longer than wide; anterior end of article II with six surrounding setae; article III 2.78 × longer than wide, with distal end densely setose, pretarsus present, conical in shape.

Forcipular segment (Fig. 4A, B): exposed part of the coxosternite with a width-to-length ratio of 0.68; cerrus composed of two convergent rows of setae and a pair of setae on each side. Forcipular trochanteroprefemur length-to-width ratio of 1.7, proximal tooth slightly smaller than the distal tooth; femur and tibia each with one tooth, equal in size; tarsungulum with two dark brown, small. basal teeth, one dorsal to the other.

Leg-bearing segments (Fig. 4C, D): 49 leg-bearing segments; a few sternites with sternal sulcus and dispersed setae; sternal sulcus of anterior segments furcate, branches at an obtuse angle.

Ultimate leg-bearing segment (Fig. 4E–H): metasternite trapezoidal, length-to-width ratio of 1; each coxopleuron covered with dense pore-field into the distal end ultimate leg telopodite with short setae, apical claw absent.

Postpedal segments (Fig. 4E, G, H): male gonopods tapered and biarticulated.

Variation in paratypes. Body length up to 64 mm, cephalic plate length-to-width ratio of 1.77–1.97, antennae length-to-head width ratio of 4.8–5.5, medial projection of first maxillae width-to-length ratio of 1.2–2.14 and telopodites length-to-width ratio of 1.43–2.86, telopodites article I of second maxillae length-to-width ratio of 4–6.88, article III ratio of 2.78–3.18, forcipular trochanteroprefemur length-to-width ratio of 1.27–1.7, exposed part of coxosternite length-to-width ratio of 0.68–0.79. Female gonopods also biarticulated.

Remarks. As shown in Table 5, *M. megittii* Verhoeff, 1937, *M. stenoceps* Chamberlin, 1944, *M. enigmus* Chamberlin, 1944 and *M. chuensis* sp. nov. are similar in the numbers of leg-bearing segments, furcate sternal sulcus and clypeal ratio, but other features distinguish them. *Mecistocephalus megittii* notably differs from *M. chuensis* sp. nov. in the presence of a large tooth on the tarsungulum (only a small tooth at the base of the tarsungulum in the latter) and the presence of one or two setae on each side of clypeus (3 setae on each side of clypeus in the latter) (Attems 1947).

Similarly, the other two species and *M. chuensis* sp. nov. can be distinguished by the location of the setae and presence or absence of a tooth on the forcipular femur. The clypeus of *M. stenoceps* Chamberlin has a series of three setae in a transverse row on each side farther anteriorly than in *M. chuensis* sp. nov., and *M. enigmus* lacks a femoral tooth (Chamberlin 1944), which is present in *M. chuensis* sp. nov.

Distribution. China (Hubei, Hunan).

Table 5. Distinguishing characteristics of new species from similar species, incorporating data from Attems (1947), Chamberlin (1944), Matic and Dărăbanțu (1969), original descriptions, and re-descriptions.

	M. chuensis sp. nov.	*M. huangi* sp. nov.	*M. megittii* Verhoeff, 1937	*M. stenoceps* Chamberlin, 1944	*M. enigmus* Chamberlin, 1944	*M. lanzai* Matic & Dărăbanțu, 1969
Locality	Hunan, China	Yunnan, China	Rangoon, Myanmar	Purmerend, Batavia Bay	Poentjak, Java	Giohar
Number of leg-bearing segments	49	49	49	49	49	49
Head length-to-width ratio	1.77	2	2.5	2.03	1.73	1.58
Clypeal ratio	1.22	1	1.1	1.47		1.63
Setae on each side of clypeus	4	2–3	1–2	4		3
Cephalic pleurite	only on the posterior 1/2	only on the posterior 1/2				only on the posterior 1/2
Mandible with well-developed lamellae	8	6			~ 9 or 10	9 or 10
Forciples	trochanteroprefemur with both basal and distal teeth	trochanteroprefemur with both basal and distal teeth	tooth on tarsungulum very prominent	trochanteroprefemur with both basal and distal teeth	femur without tooth	trochanteroprefemur with both basal and distal teeth
Sternal sulcus	furcate	furcate	furcate		furcate	furcate
Metasternite of ultimate leg-bearing segment	trapezoid	with a pillow-like protrusion		significantly narrow, the posterior end rather narrowly rounded		

Etymology. The specific name is derived from its distribution in Hunan Province and Hubei Province, where "Chu" in ancient China usually referred to these regions.

Mecistocephalus huangi Jiang & You, sp. nov.

https://zoobank.org/5654176E-38FF-4C11-9F9C-9B20CEE6DDA7

Figs 5, 6

Chinese name: 黄氏地蜈蚣

Material examined. *Holotype.* • ♂; (CMMI 20201022122); Cʜɪɴᴀ, **Yunnan Province,** Honghe Hani and Yi Autonomous Prefecture, Jianshui County, Yanzidong Scenic Area; 23.6359°N, 103.0537°E; 1260 m a.s.l.; 22 Oct. 2021; coll. Chao Jiang & Zhidong Wang. *Paratypes.* • 2 ♂♂, 4 ♀♀; (CMMI 20201022119, -121, -123, -125, -126, -137); same data as holotype; 22 Oct, 2021. • 3 ♂♂, 4 ♀♀; (CMMI 20190122001D–007D); **Yunnan Province**, **Gejiu,** Baohua Park; 23.3545°N, 103.1621°E; 1770 m a.s.l.; 22 Jan. 2019; coll. Huiqin Ma; • 2 ♂♂; (CMMI 20230705004D, 20230705005D); same location but collected at 5 Jul. 2023; coll. Yangyang Pan & Jiabo Fan. • 1 ♂, 8 ♀♀; (CMMI 20230830001D–20230830009D); same location but collected at 30 Aug. 2023; coll. Tianyun Chen & Jiabo Fan.

Diagnosis. A *Mecistocephalus* species with 49 leg pairs. Head length-to-width ratio 2, each side of clypeus with two or three smooth insulae, clypeal ratio (areolate part/ non-areolate part) ~ 1, plagulae without sensilla, posterior 1/2 of cephalic pleurite bearing a group of setae, mandible with ~ 6 well-developed lamellae and first lamella with ~ 6 teeth. Sternal sulcus furcated at an obtuse angle. Metasternite trapezoid and with a pillow-like protrusion.

Holotype description. Body length 69 mm; the posterior part slightly slender; head and forcipular segment dark brown in color; remainder yellow.

Cephalic plate (Fig. 5A–C): sub-rectangular, length-to-width ratio 2; lateral margins slightly convergent backward, strongly convergent backward at proximal four-fifths, the maximum width 2.58 mm; transverse suture protruding to the back edge of the cephalic plate in an arc; six or seven setae on each side of back, punctate depressions interspersed throughout; dorsal side of cephalic plate with scattered puncta. Antennae 5.35 × as long as the head width. Apical sensilla at the actual distal apex of article XIV ~ 8 μm long.

Clypeus (Fig. 5D): clypeal ratio (areolate part/ non-areolate part) ~ 1; each side bearing two or three insulae, each circumscribing one seta; transverse suture of the clypeal plagulae slightly protruding from the front cephalic plate, concave inward near cephalic pleurite, sensilla absent.

Labrum (Fig. 5D): anterior ala medial margin ~ 5/12 of length of posterior ala; the middle piece protrudes forward into a vertex over side pieces; posterior margin of side pieces curved, concave with respect to straight anterior margin; the hair-like fringes and projections on the labral side pieces absent, the comma-shaped sclerite lateral to the labral side pieces present.

Cephalic pleurite (Fig. 5E): spiculum present; a group of setae only on the posterior 1/2.

Mandible (Fig. 5F): approximately six well developed lamellae; first lamella with six teeth; average intermediate lamella with ~ 22 teeth, all teeth of similar size, the region before the first lamella without teeth.
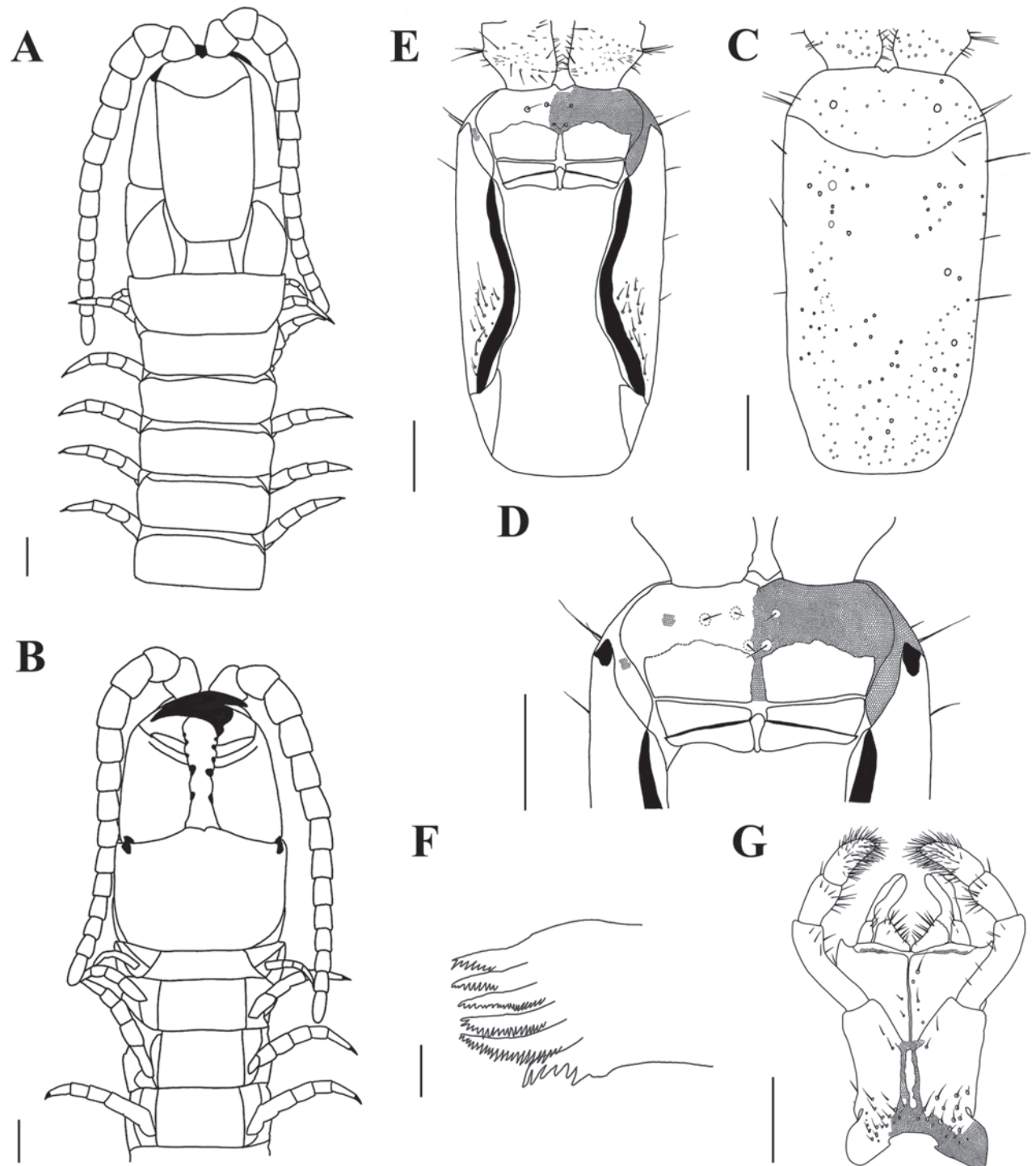
Figure 5. *Mecistocephalus huangi* Jiang & You, sp. nov., holotype (CMMI 20201022122) **A** anterior part of body, dorsal view **B** anterior part of body, ventral view **C** cephalic plate, dorsal view **D** anterior part of head, ventral view (maxillae removed) **E** cephalic plate, ventral view (maxillae removed) **F** mandible **G** maxillae, ventral view. Scale bars: 50 µm (**F**); 1 mm (**A–E, G**). Part of areolation not drawn.

First maxillae (Fig. 5G): antero-external corners of coxosternite protruding and short; coxosternite divided by mid-longitudinal sulcus, three to four setigerous insulae on each side; coxal projections 1.1 × as wide as long, nine setae on medial margin; clavate lappets present on coxal projections; telopodites 2.14 × as long as wide, clavate lappet present.
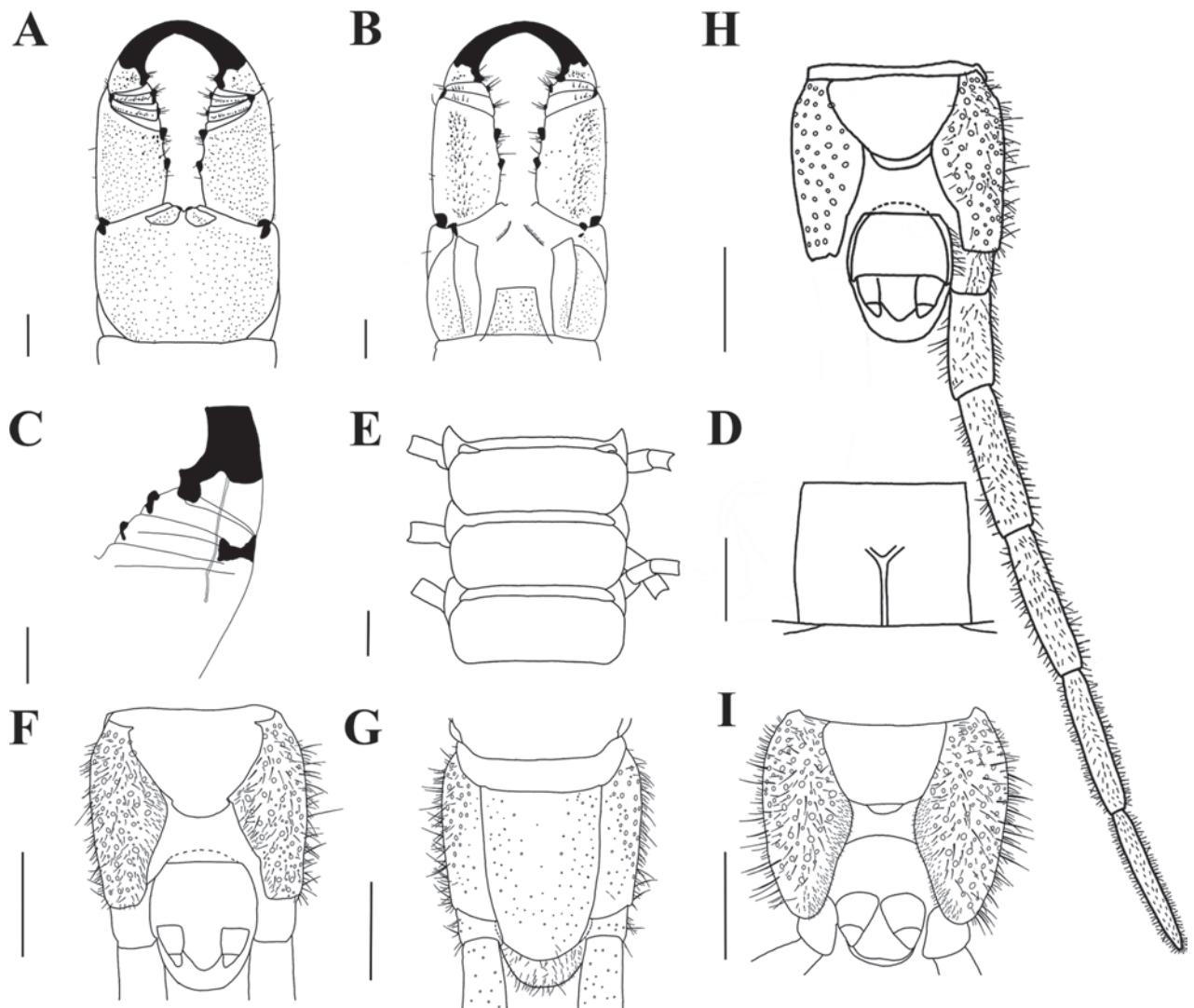
Figure 6. *Mecistocephalus huangi* Jiang & You, sp. nov., holotype (CMMI 20201022122) **A** forcipular segment, ventral view **B** forcipular segment, dorsal view **C** part of right forcipule, ventral view **D** sternite of leg-bearing segment VI, ventral view **E** tergites of leg-bearing segments VI–VIII, dorsal view **F** ultimate leg-bearing segment, ventral view **G** ultimate leg-bearing segment, dorsal view **H** ultimate leg-bearing segment and left leg, ventral view **I** ultimate leg-bearing segment, ventral view (paratype CMMI 20230803003D). Scale bars:100 μm (**C**); 500 μm (**I**); 1 mm (**A, B, D–H**).

Second maxillae (Fig. 5G): sclerotic ridge on the middle of coxosternite with two setigerous insulae on the posterior ridge; each side of coxosternite with at least 17 setigerous insulae on the posterior side; telopodite article I 3.85 × as long as wide, the ventral and dorsal part of anterior telopodites both with five vertical setae; anterior article II with ten surrounding setae; article III 2.75 × as long as wide, apex densely setose, pretarsus present.

Forcipular segment (Fig. 6A–C): exposed part of coxosternite width-to-length radio 1.4; cerrus only composed of two convergent rows of setae. Trochantero-prefemur length-to-width radio 1.43, proximal tooth slightly smaller than the distal tooth; both femur and tibia with one tooth and the former smaller than the latter; tarsungulum with two dark brown and small basal teeth, one dorsal to the other; poison calyx reaching the distal part of trochanteroprefemur.

Leg-bearing segments (Fig. 6D, E): 49 leg-bearing segments; a few sternites in the anterior part of leg-bearing segment with sternal sulcus and dispersed

setae; sternal sulcus of anterior segments furcate, branches at an obtuse angle; the first pair of legs much smaller than the rest, apical claw simple.

Ultimate leg-bearing segment (Fig. 6F−I): metasternite trapezoid in shape and with a small pillow-like protrusion in the end, length-to-width radio of 1.45; each coxopleura covered by a dense pore-field except for the distal end; ultimate leg telopodite with short setae, apical claw absent; the last leg-bearing segment covered with setae.

Postpedal segments (Fig. 6F, H, I): male gonopods tapered and biarticulated.

Variation in paratypes. Body length up to 69 mm, cephalic plate length-to-width ratio 1.84−1.97, antennae length to head width ratio 3.57−5.17, medial projection of first maxillae width to length ratio 1.07−1.29 and telopodites length to width ratio 2.5−4.8, telopodites article I of second maxillae length-to-width radio 3.43−4.29, article III ratio 4−4.29, forcipular trochanteroprefemur length-to-width ratio 1.16−1.19, exposed part of coxosternite length to width ratio 0.69−0.75. The end of female metasternite also with a small pillow-like protrusion. Females gonopods also biarticulated.

Remarks. This new species resembles *M. lanzai* Matic & Dărăbanțu (1969) in the furcate sternal sulci, three pairs of setae on the clypeus, and a cluster of setae located exclusively on the posterior 1/2 of the cephalic pleurite (Table 5). However, a distinguishing feature of *M. lanzai* is the absence of a basal tooth on the tarsungulum.

Mecistocephalus huangi sp. nov. exhibits a clear morphological resemblance with *M. chuensis* sp. nov. However, it can be differentiated from the latter by the presence of five to six smooth insulae on the clypeus of the former and a pillow-like protrusion on the metasternite which is common in both paratypes and non-type material of *M. huangi* sp. nov. (Figs 5E, 6F−I). Furthermore, this species and *M. chuensis* sp. nov. were found to form two distinct but closely related clades in the phylogenetic analysis (Fig. 2).

Distribution. China (Yunnan).

Etymology. The specific name is dedicated to Dr. Luqi Huang for his generous help in the intensive fieldwork for collecting specimens of geophilomorphs.

Mecistocephalus smithii Pocock, 1895
Figs 7, 8

Mecistocephalus smithii Pocock, 1895: 351.

Material examined. • 2 ♂♂, 5 ♀♀; (CMMI 20191014012, −032, 20191014034−20191014036); **Cʜɪɴᴀ, Guangdong Province,** Guangzhou, Maofengshan Forest Park; 23.2983°N, 113.4644°E; 330 m a.s.l.; 14 Oct. 2019; coll. Chao Jiang. • 2 ♀♀; (CMMI 20201217111, 20201217112); **Guangdong Province, Heyuan,** Xinfengjiang Reservoir; 23.7703°N, 114.6300°E; 180 m a.s.l.; 17 Dec. 2020; coll. Zhidong Wang. • 1 ♀; (CMMI 20191031042); **Zhejiang Province, Zhoushan,** Changgangshan Forest Park; 30.0355°N, 122.1201°E; 130 m a.s.l.; 31 Oct. 2019; coll. Chao Jiang. • 2 ♂♂, 1 ♀; (CMMI 20201108123, -124, -126); **Jiangsu Province, Nanjing,** Fuguishan Forest Park; 32.1006°N, 118.586°E; 130 m a.s.l.; 8 Nov. 2020; coll. Zhidong Wang.
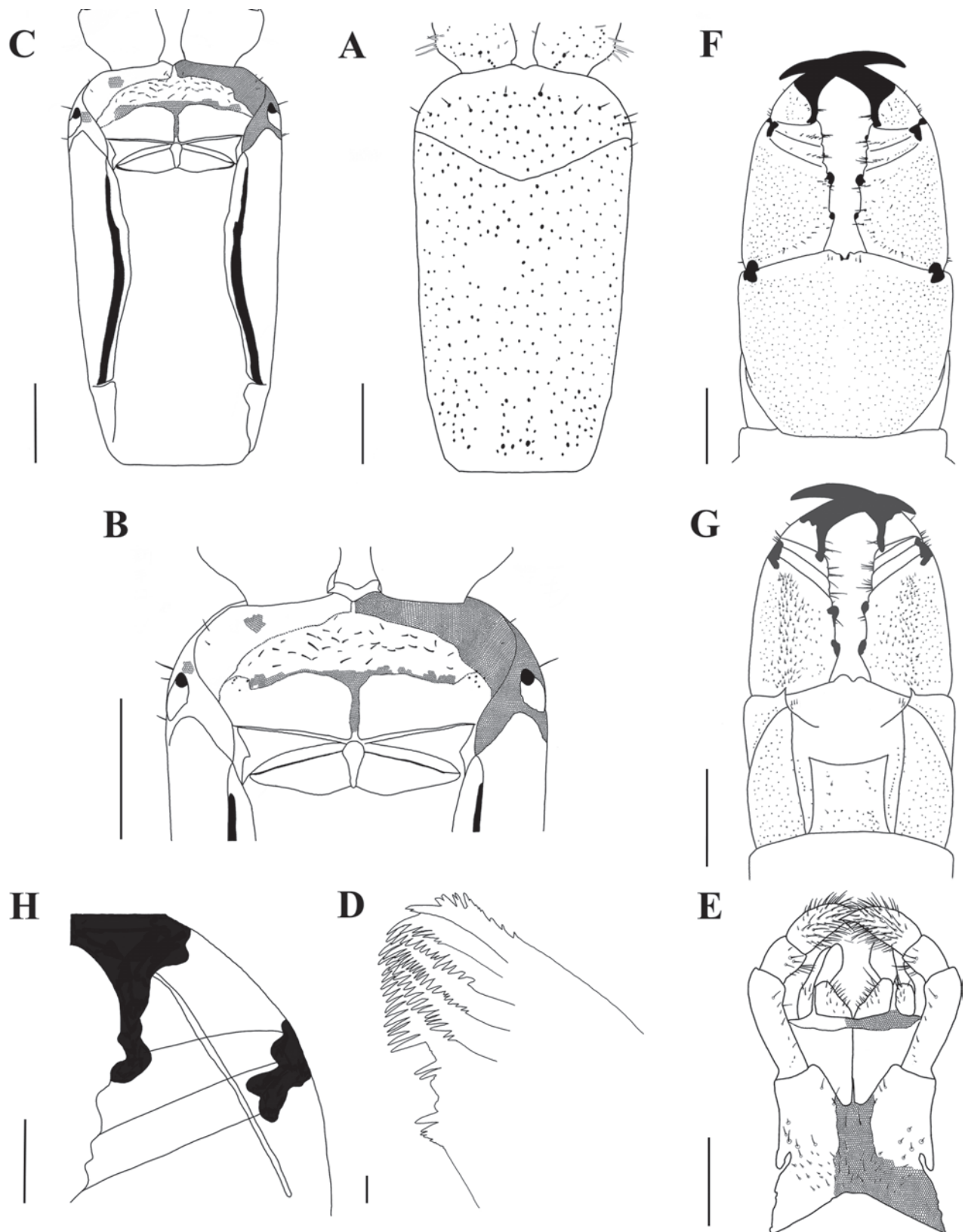
Figure 7. *Mecistocephalus smithii* Pocock, 1895 (spm. CMMI 20191014031) **A** clypeus and cephalic pleurite, ventral view **B** anterior part of head, ventral view (maxillae removed) **C** cephalic plate, ventral view (maxillae removed) **D** mandible **E** maxillae, ventral view **F** forcipular segment, ventral view **G** forcipular segment, dorsal view **H** a part of right forcipule, ventral view. Part of areolation not drawn. Scale bars: 20 μm (**D**), 100 μm (**H**); 1 mm (**A–C, E–G**).
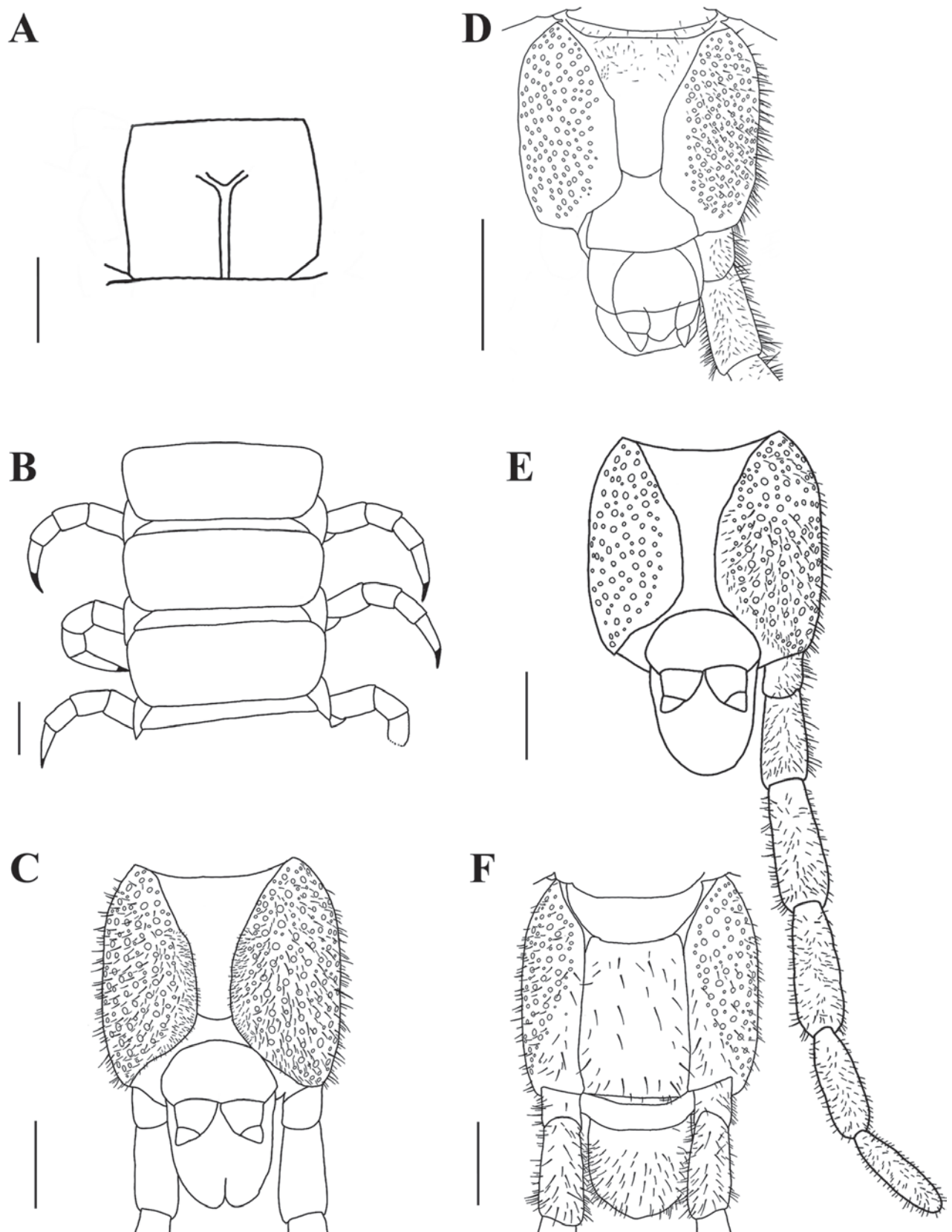
Figure 8. *Mecistocephalus smithii* Pocock, 1895 (spm. CMMI 20191014031) **A** sternite of leg-bearing segment VI, ventral view **B** tergite of leg-bearing segments VI–VIII, dorsal view **C** ultimate leg-bearing segment, ventral view **D** ultimate leg-bearing segment, ventral view (spm. CMMI 20191014012) **E** ultimate leg-bearing segment and left leg, ventral view **F** ultimate leg-bearing segment, dorsal view. Scale bars: 1 mm.

Diagnosis. A *Mecistocephalus* species with 59 leg pairs. Head length-to-width ratio ~ 1.7, each side of clypeus with ~ 20–22 setae, clypeal ratio (areolate part/ non-areolate part) of ~ 1, plagulae with sensilla, cephalic pleurite without setae, forcipular coxosternite only with a part of short cerrus. Sternal sulcus with short branches.

Re-description. Body length 74–88 mm (limited to the above samples); posterior part slightly slender. Head and forcipular segment dark red in color; remainder yellow.

Cephalic plate (Fig. 7A): sub-rectangular, length-to-width ratio 1.7–2.1; lateral margins slightly convergent backward, the maximum width 2.65 mm; transverse suture protruded to the back edge of the cephalic plate, vertex pointed; suture line on the back side of the cephalic plate with four to six setae; dorsal cephalic plate with scattered puncta. Antennae 5.3 × as long as the head width. Apical sensilla ~ 10 μm long.

Clypeus (Fig. 7B): clypeal ratio (areolate part/ non-areolate part) ~ 1; each side with 20–22 setae; the transverse suture of clypeal plagulae slightly protrude from the front cephalic plate; plagulae with groups of small sensilla localized to anterolateral corners.

Labrum (Fig. 7B): anterior ala medial marginal ~ 1/3 of posterior ala; middle piece protrudes forward into a vertex over side pieces; posterior line of side pieces curve, convex with respect to straight anterior margin; the hair-like fringes and projections on the labral side pieces absent, the comma-shaped sclerite lateral to the labral side pieces present.

Cephalic pleurite (Fig. 7C): spiculum present; cephalic pleurite without setae.

Mandible (Fig. 7D): approximately seven to eleven well developed lamellae; first lamella with ~ 5 teeth; average intermediate lamella with ~ 22 teeth; basal teeth small and protruding.

First maxillae (Fig. 7E): antero–external corners of coxosternite protruding and short; coxosternite divided by mid–longitudinal sulcus; coxal projection 1–1.2 × as wide as long, 17 setae on medial margin and clavate lappet present; telopodites 2.5–3.4 × as long as wide, clavate lappet present.

Second maxillae (Fig. 7E): one sclerotic ridge on the middle of coxosternite with ~ 8 setigerous insulae; telopodite article I 3.33–4.5 × as long as wide, the ventral and dorsal part of interior telopodites both with four vertical setae; anterior article II with nine surrounding setae; article III 2.5–3 × as long as wide, distal end densely setose, pretarsus present.

Forcipular segment (Fig. 7F–H): exposed part of coxosternite width-to-length radio 0.8–0.85; cerrus composed of a pair of setae on each side. Forcipular Trochanteroprefemur length-to-width radio of 1.13–1.35, two teeth present; both femur and tibia with one tooth and the former smaller than the latter; tarsungulum with one dark brown and small basal tooth; poison calyx reaching the distal part of trochanteroprefemur.

Leg-bearing segments (Fig. 8A, B): 59 leg-bearing segments, a few sternite with sternal sulcus, almost all posterior sternite with setae; sternal sulcus of anterior segments furcate, and with short branches; the first pair of legs much smaller than the others, only one claw at the front.

Ultimate leg-bearing segment (Fig. 8C, F): posterior line of metasternite protruding no more than intermediate sternite, sandwiched between two coxopleura; each of coxopleura covered with dense pore-fields except for the ends;

ultimate leg-bearing with short setae, claw absent; setae distributed in various parts of the last leg-bearing segment.

Postpedal segments (Fig. 8C, E, F): gonopods of both males and females tapered and biarticulated.

Remarks. To date, within Asia, only two species of the genus *Mecistocephalus* possess 59 leg-bearing segments: *M. diversisternus* Silvestri, 1919 and *M. smithii* Pocock, 1895. It is noteworthy that some researchers have previously raised concerns regarding the accuracy of *M. smithii* records in Japan and Taiwan, suggesting that they may represent misidentification of *M. diversisternus* (Uliana et al. 2007). *Mecistocephalus smithii* was originally described from "Da-laen-Saen 30 miles S.W. of Ningpo" and "Wo Lee Lake, 25 miles S. of Ningpo" in the Chinese mainland. The locality "Da-laen-Saen 30 miles S.W. of Ningpo" is very likely "Dalei Shan" near (45 km SW) Ningbo, Zhejiang (Schawaller and Aston 2017), while the locality of "Wo Lee Lake, 25 miles S. of Ningpo" does not match any present geographical name in Ningbo after a survey among local residents. The original account was too brief, and the true identity of *M. smithii* remained unclear (Uliana et al. 2007).

To address this problem, we collected and examined new specimens near the type locality, as well as in other provinces. Therefore, we can confidently state that *M. smithii* is a distinct species to *M. diversisternus* and that it is present in China. The distinguishing features of *M. diversisternus* include a limited number of clypeal setae, typically less than ten, and a sternal sulcus that lacks bifurcation. In contrast, *M. smithii* has abundant setae on each side of the clypeus ranging from 20 to 22 and a bifurcate sternal sulcus with short branches.

Distribution. China (Zhejiang, Guangdong).

Key to the species of the *Mecistocephalus* in China

1 Number of leg-bearing segments invariably 49 ....**2**
– Number of leg-bearing segments not 49...**13**
2 Medial projection and telopodites of first maxillae longer than the telopodite of the second maxillae.....................***M. longichilatus* Takakuwa, 1936**
– Medial projection and telopodites of first maxillae shorter than the telopodite of the second maxillae..**3**
3 Areolate part of the clypeus with smooth insulae **4**
– Areolate part of the clypeus without smooth insulae...............................**9**
4 Sternal sulcus furcate **5**
– Sternal sulcus not furcate...................................***M. rubriceps* Wood, 1862**
5 Posterior 1/2 of the cephalic pleurite bearing a group of setae **6**
– Both the anterior and posterior halves of the cephalic pleurite bearing a group of setae .... ***M. mikado* Attems, 1928**
6 Fewer than 6 smooth insulae on each side of clypeus..............................**7**
– More than 6 smooth insulae on each side of clypeus ....
....***M. multidentatus* Takakuwa, 1936**
7 More than 4 smooth insulae on each side of clypeus....***M. chuensis* sp. nov.**
– Fewer than 4 smooth insulae on each side of clypeus..............................**8**
8 Each plagula covered with pore-like sensilla...
....***M. marmoratus* Verhoeff, 1934**
– Plagulae without pore-like sensilla................................. ***M. huangi* sp. nov.**

9   Clypeal ratio (areolate part/ non-areolate part) > 2.................................**10**
−   Clypeal ratio (areolate part/ non-areolate part) < 2.................................**12**
10   Sternal sulcus furcate **11**
−   Sternal sulcus not furcate.............***M. changi* Uliana, Bonato, Minelli, 2007**
11   Metasternite of ultimate leg-bearing segment approx. as wide as long .....
        ....***M. ongi* Takakuwa, 1934**
−   Metasternite of ultimate leg-bearing segment width-to-length ratio ~ 2.....
        ....***M. brevisternalis* Takakuwa, 1934**
12   Trochanteroprefemur with a distal tooth, spiculum absent ....
        ....***M. yanagiharai* Takakuwa, 1936**
−   Trochanteroprefemur with both basal and distal teeth, spiculum present..
        ....***M. monticolens* Chamberlin, 1920**
13   Number of leg-bearing segments invariantly 45 ....
        ....***M. nannocornis* Chamberlin, 1920**
−   Number of leg-bearing segments not 45..**14**
14   Number of leg-bearing segments < 60 ....**15**
−   Number of leg-bearing segments > 60 ....***M. japonicus* Meinert, 1886**
15   20 setae on each side of clypeus, sternal sulcus furcate............................
        ....***M. smithii* Pocock, 1895**
−   Approx. 3 or 4 setae on each side of clypeus, sternal sulcus not furcate...
        ....***M. diversisternus* Silvestri,1919**

Discussion

Attems (1929) proposed *Mecistocephalus punctifrons* Newport, 1843 as the type species of the genus *Mecistocephalus*, encompassing 27 species at the time. We report two new species as belonging to the genus, *M. chuensis* sp. nov. and *M. huangi* sp. nov. Identifying new species within the genus *Mecistocephalus* is highly challenging owing to the lack of adequate illustrations and complete records; for example, images of *M. angustior* Chamberlin, 1920 are lacking and the original description is brief (only a few sentences) (Chamberlin 1920). Furthermore, descriptions of certain species (such as *M. apator* Chamberlin, 1920) often lack diagnostic information, such as the number of clypeal insulae with setae and placement of the buccal setae. In the case of the new species *M. chuensis* sp. nov. and *M. huangi* sp. nov., similarities in external morphology pose difficulties in their differentiation. The most noticeable distinction between these two species lies in the metasternite of the ultimate leg-bearing segment, with or without a pillow-like protrusion, and in the arrangement of setae on each side of the clypeus. However, these characteristics have not been consistently documented across all species and require further scrutiny to adequately characterize intraspecific variation. Therefore, redescribing poorly known species is a priority, and molecular methods might help in identifying species with insufficient descriptions.

In this study, we analyzed the phylogenetic relationships of *Mecistocephalus* in China. However, only a few *Mecistocephalus* COI sequences have been documented in the literature, in addition to several unpublished COI sequences deposited in the NCBI GenBank database (https://www.ncbi.nlm.nih.gov/genbank/). We selected twelve COI sequences from five species collected in Taiwan, including *M. guildingii*, *M. marmoratus*, *M. multidentatus*, *M. diversisternus*,

and *M. japonicus*. To eliminate incorrect identifications, we also remotely examined photographs of specimens obtained from the authors who submitted the sequences (Jui-Lung Chao, pers. comm., 4th Oct 2023). Phylogenetic analyses based on COI sequences from ten species with *M. rubriceps* and *M. mikado* demonstrate that *Mecistocephalus* species in China can be divided into four distinct clades. The number of leg-bearing segments in species of *Mecistocephalus* found in China can be divided into three groups: 45, 49, and > 50. Moreover, studies have shown the number of leg-bearing segments can vary within the same species (Bonato et al. 2001). In this study, neither the phylogenetic trees nor the genetic distances among *Mecistocephalus* species indicated that the evolutionary relationships are linked to the number of leg-bearing segments. This could be explained the utilization of COI sequences alone for phylogenetic reconstruction owing to inadequate 16S and 28S rRNA sequences in public databases for most *Mecistocephalus* species or could indicate that the number of leg-bearing segments does not vary within a species in China; further data are needed to evaluate this.

According to the results of the phylogenetic analysis, *M. chuensis* sp. nov. and *M. huangi* sp. nov. exhibit a close evolutionary relationship, forming a well-supported clade distinct from other species. The genetic distances between different samples of the same species were related to physical distances between localities. However, this pattern was not observed for *M. guildingii*. To improve the data set for constructing the phylogenetic tree, two additional COI sequences of *M. guildingii* (CMMI 20201214103 and CMMI 20200608031) from Yunnan Province, China were included in this study. Interestingly, the type locality of *M. guildingii* is St. Vincent and the Grenadines, a considerable distance away. Despite this, the phylogenetic analysis did not reveal a similar pattern in *M. guildingii* to those observed in *M. chuensis* sp. nov. and *M. huangi* sp. nov. The mean genetic distance of *M. guildingii* was 0.8%, compared with 5.0% for *M. chuensis* sp. nov., suggesting the possibility of cryptic species or a connection to geographic variation in *M. chuensis* sp. nov. Similarly, *M. mikado* showed an intraspecific genetic distance of 5.7%, which raises the possibility of individual variation or geographic divergence. Additionally, it should be noted that we have not examined the holotype of *M. mikado* and have classified the species based solely on the original description and illustrations, which could account for the observed genetic distance, to some extent. Moreover, a phylogenetic analysis using 78 COI sequences of *Nannarrup* did not reveal a significant correlation between the phylogenetic relationships of *Nannarrup innuptus* samples and their geographic locations (Tsukamoto et al. 2022). Thus, the unique characteristics observed in *M. chuensis* sp. nov. and *M. huangi* sp. nov. require further confirmation with broader data. Nevertheless, genetic distance, species delimitation, and morphological identification results confirmed the taxonomic status of *M. chuensis* sp. nov. and *M. huangi* sp. nov. as new species.

The limitations of single-locus molecular data for species delimitation, the broad geographic distribution of samples, intraspecific variation, and morphological changes in individuals during development likely contributed to identification of 17 and 18 distinct units using the PTP method in this study. These constraints in species classification underscore the importance of gathering extensive genetic data across a wider range of taxa for more comprehensive analysis of the relationships within *Mecistocephalus*.

Acknowledgements

Additional information

Conflict of interest

The authors have declared that no competing interests exist.

Ethical statement

No ethical statement was reported.

Funding

Author contributions

Yang−Yang Pan: Methodology, Software, Data Curation, Writing – Original Draft, Writing – review & editing. Jia-Bo Fan: Software, Data Curation, Hand drawing picture, Writing – review & editing. Chun−Xue You: Conceptualization, Methodology, Supervision, Writing – Review & Editing, Project administration, Funding acquisition. Chao Jiang: Conceptualization, Methodology, Supervision, Writing – Review & Editing, Project administration, Funding acquisition.

Author ORCIDs

Yang-Yang Pan ⓘ https://orcid.org/0000-0002-8096-8550
Jia-Bo Fan ⓘ https://orcid.org/0009-0006-0390-4285
Chun-Xue You ⓘ https://orcid.org/0000-0002-3315-6090
Chao Jiang ⓘ https://orcid.org/0000-0003-1841-1169

Data availability

All of the data that support the findings of this study are available in the main text.

References

Attems CG (1929) Das Tierreich. 52 Myriapoda. I. Geophilomorpha. De Gruyter & Co., Berlin−Leipzig, 388 pp. https://doi.org/10.1515/9783111430638

Attems CG (1947) Neue Geophilomorpha des Wiener Museums. Annalen des Naturhistorischen Museums, Wien 55(1944−1947): 50−149.

Bonato L, Foddai D, Minelli A (2001) Increase by duplication and loss of invariance of segment number in the centipede *Mecistocephalus microporus* Haase, 1887 (Chilopoda, Geophilomorpha, Mecistocephalidae). Italian Journal of Zoology 68: 345−352. https://doi.org/10.1080/11250000109356429

Bonato L, Foddai D, Minelli A (2002) A new mecistocephalid centipede from Ryukyu Islands and a revisitation of "Taiwanella" (Chilopoda: Geophilomorpha: Mecistocephalidae). Zootaxa 86: 1–12. https://doi.org/10.11646/zootaxa.86.1.1

Bonato L, Foddai D, Minelli A (2003) Evolutionary trends and patterns in centipede segment number based on a cladistic analysis of Mecistocephalidae (Chilopoda: Geophilomorpha). Systematic Entomology 28: 539–579. https://doi.org/10.1046/j.1365-3113.2003.00217.x

Bonato L, Edgecombe GD, Lewis JGE, Minelli A, Pereira L, Shelley RM, Zapparoli M (2010) A common terminology for the external anatomy of centipedes (Chilopoda). ZooKeys 69: 17–51. https://doi.org/10.3897/zookeys.69.737

Bonato L, Edgecombe GD, M. Zapparoli, Minelli A (2011) Chilopoda – Taxonomic overview: Geophilomorpha. Treatise on Zoology – Anatomy, Taxonomy, Biology. The Myriapoda, volume 1. Minelli A, Brill-Leiden, 407–443.

Bonato L, Chagas Junior A, Edgecombe GD, Lewis JGE, Minelli A, Pereira LA., Shelley RM., Stoev P, Zapparoli M (2016) ChiloBase 2.0 – A World Catalogue of Centipedes (Chilopoda). https://chilobase.biologia.unipd.it [accessed 28 Sept 2023]

Chamberlin RV (1920) The Myriopoda of the Australian region. Bulletin of the Museum of Comparative Zoology 64: 1–269.

Chamberlin RV (1944) Some chilopods from the Indo–Australian Archipelago – Notulae Naturae, Academy of Natural Sciences in Philadelphia 147: 1–14.

Chao JL, Lee KS, Yang ZZ, Chang HW (2020) Two new species of centipedes, *Tygarrup daliensis* sp. nov. (Mecistocephalidae) and *Australobius cangshanensis* sp. nov. (Lithobiidae), from Southwestern China. Opuscula Zoologica Budapest 51: 57–67. https://doi.org/10.18348/opzool.2020.S2.57

Folmer O, Black M, Hoeh W, Lutz R, Vrijenhoek R (1994) DNA primers for amplification of mitochondrial cytochrome C oxidase subunit I from diverse metazoan invertebrates. Molecular Marine Biology and Biotechnology 3(5): 294–299.

Giribet G, Edgecombe GD, Wheeler WC (2001) Arthropod phylogeny based on eight molecular loci and morphology. Nature 13 413(6852): 157–161. https://doi.org/10.1038/35093097

Hall T (1999) BioEdit: A user–friendly biological sequence alignment editor and analysis program for Windows 95/98/NT. Nucleic Acids Symposium Series 41: 95–98.

Hoang DT, Chernomor O, Von Haeseler A, Minh BQ, Vinh LS (2018) UFBoot2: Improving the ultrafast bootstrap approximation. Molecular Biology and Evolution 35(2): 518–522. https://doi.org/10.1093/molbev/msx281

Joshi J, Karanth KP (2011) Cretaceous–Tertiary diversification among select scolopendrid centipedes of South India. Molecular Phylogenetics and Evolution 60(3): 287–294. https://doi.org/10.1016/j.ympev.2011.04.024

Kalyaanamoorthy S, Minh BQ, Wong TK, Von Haeseler A, Jermiin LS (2017) ModelFinder: Fast model selection for accurate phylogenetic estimates. Nature Methods 14(6): 587–589. https://doi.org/10.1038/nmeth.4285

Matic Z, Darabantu C (1969) Su alcuni chilopodi della Somalia. Monitore Zoologico Italiano N.S 3: 1–8. https://doi.org/10.1080/03749444.1970.10736758

Newport G (1843) On some new genera of the class Myriapoda. Zoological Society of London 10 (1842): 177–181. https://doi.org/10.1080/03745484309442474

Nguyen LT, Schmidt HA, Von HA, Minh BQ (2015) IQ–TREE: a fast and effective stochastic algorithm for estimating maximum–likelihood phylogenies. Molecular Biology and Evolution 32(1): 268–274. https://doi.org/10.1093/molbev/msu300

Pocock RI (1895) Report upon the Chilopoda and Diplopoda obtained by P. W. Bassett-Smith Esq. Surgeon R. N. and J. J. Walker Esq. R. N. during the cruise in the Chinese

seas of H.M.S. "Penguin" Commander W. U. Moore commanding. Annals and Magazine of Natural History 15: 346–372. https://doi.org/10.1080/00222939508677895

Puillandre N, Lambert A, Brouillet S, Achaz G (2012) ABGD, Automatic Barcode Gap Discovery for primary species delimitation. Molecular Ecology 21(8): 1864–1877. https://doi.org/10.1111/j.1365-294X.2011.05239.x

Ronquist F, Teslenko M, Mark P, Ayres DL, Darling A, Höhna S, Larget L, Suchard MA, Huelsenbeck JP (2012) MrBayes 3.2: Efficient Bayesian phylogenetic inference and model choice across a large model space. Systematic Biology 61(3): 539–542. https://doi.org/10.1093/sysbio/sys029

Schawaller W, Aston P (2017) Two new species of the genus *Laena* Dejean (Coleoptera: Tenebrionidae: Lagriinae) from Hong Kong. Zootaxa 4344(1): 169–173. https://doi.org/10.11646/zootaxa.4344.1.10

Silvestri F (1919) Contributions to a knowledge of the Chilopoda Geophilomorpha of India-Record of the Indian Museum, Calcutta 16: 45–107.

Takakuwa Y (1940) Geophilomorpha. Fauna Nipponica, Vol. 9. Okada et al., Sansei-do-Tokyo 8(1): 1–156.

Tamura K, Stecher G, Kumar S (2021) MEGA11: Molecular Evolutionary Genetics Analysis Version 11. Molecular Biology and Evolution 38(7): 3022–3027. https://doi.org/10.1093/molbev/msab120

Thompson JD, Higgins DG, Gibson TJ (1994) CLUSTAL W: Improving the sensitivity of progressive multiple sequence alignment through sequence weighting, position specific gap penalties and weight matrix choice. Nucleic Acids Research 22(22): 4673–4680. https://doi.org/10.1093/nar/22.22.4673

Tsukamoto S, Shimano S, Eguchi K (2022) Two new species of the dwarf centipede genus *Nannarrup* Foddai, Bonato, Pereira & Minelli, 2003 (Chilopoda, Geophilomorpha, Mecistocephalidae) from Japan. Zookeys 1115: 117–150. https://doi.org/10.3897/zookeys.1115.83946

Uliana M, Bonato L, Minelli A (2007) The Mecistocephalidae of the Japanese and Taiwanese islands (Chilopoda: Geophilomorpha). Zootaxa 1396: 56–59. https://doi.org/10.11646/zootaxa.1396.1.1

Verhoeff KW (1937) Über einige Chilopoden aus Australien und Brasilien. Zoologische Jahrbücher 70: 1–16.

Wang D, Mauries JP (1996) Review and perspective of study on myriapodology of China. Acta Myriapodologica, Mémoires du Museum national d'Histoire Naturelle, Paris, 169: 81–99.

Zhang Jiajie, Kapli P, Pavlidis P, Stamatakis A (2013) A General Species Delimitation Method with Applications to Phylogenetic Placements. Bioinformatics 29(22): 2869–2876. https://doi.org/10.1093/bioinformatics/btt499

Zhang D, Gao F, Jakovlić I, Zou H, Zhang J, Li WX, Wang GT (2020) PhyloSuite: An integrated and scalable desktop platform for streamlined molecular sequence data management and evolutionary phylogenetics studies. Molecular Ecology Resources 20(1): 348–355. https://doi.org/10.1111/1755-0998.13096

Two new species and additional records of *Sinlathrobium* Assing (Coleoptera, Staphylinidae, Paederinae) from southern China

Xi Chen[1], Jian-Ping Ye[2], Zhong Peng[1]

1   *1 College of Life Sciences, Shanghai Normal University, 100 Guilin Road, 1st Educational Building 323 Room, Shanghai, 200234, China*

2   *Guangxi Maoershan National Nature Reserve, Guilin, Guangxi, 541001, China*

Corresponding author: Zhong Peng (lathrobium@163.com)

Abstract

New taxonomic and faunistic data for three species of the genus *Sinlathrobium* Assing, 2013 from China are provided. *Sinlathrobium assingi* Chen & Peng, **sp. nov.** (Chongqing: West Daba Shan) and *Sinlathrobium chenzhilini* Chen & Peng, **sp. nov.** (Guangxi: Maoer Shan) are described and illustrated. Additional records from Chongqing, detailed bionomic data and female sexual characters of *S. lobrathioides* (Assing, 2012) are provided. A key to the species of *Sinlathrobium* is given.

Key words: New species, rove beetles, taxonomic key

Introduction

The small genus *Sinlathrobium* Assing, 2013 currently contains four species scattered in the south of China: *S. densepunctatum* Assing, 2013 (Sichuan), *S. iniquum* Assing, 2013 (Yunnan), *S. lobrathiforme* (Assing, 2012) (Yunnan) and *S. lobrathioides* (Assing, 2012) (Chonqing) (Assing, 2013). *Sinlathrobium* is allied to the widely distributed genus *Lathrobium* Gravenhorst, 1802 by sharing a similar general habitus (the morphology of the mouthparts, the broad neck, the absence of a supramarginal line of the elytra, punctation of the pronotum, elytra and abdomen, the ventral aspect of the head, thorax and abdomen), and the presence of sexual dimorphism of tergites IX and X. However, *Sinlathrobium* is distinguished from *Lathrobium* by the different morphology of the head (more transverse, an uneven dorsal surface, with dense and somewhat areolate punctation), the large and strongly bulging eyes, the slightly more oblong mesoventrite, the stouter pronotum, the coloration of the elytra, the truncate anterior margin of the male sternite VII (usually with a convex median projection in *Lathrobium*), the simple internal sac of the aedeagus (usually with distinct internal structures in *Lathrobium*), and by the different chaetotaxy of the female sternite VIII (posterior portion without micropubescence) (Assing 2013).

This paper presents taxonomic and faunistic data for three Chinese species, including two new species (*Sinlathrobium assingi* Chen & Peng, sp. nov. and *Sinlathrobium chenzhilini* Chen & Peng, sp. nov.), and detailed bionomic data for the previously unknown females of *S. lobrathioides* (Assing, 2012).

Material and methods

The following abbreviations are used in the text, with all measurements in millimeters.

Body length (**BL**)	length of body from the anterior margin of the mandibles (in resting position) to the abdominal apex;
Forebody length (**FL**)	length of forebody from the anterior margin of the mandibles (in resting position) to the posterior margin of the elytra;
Head length (**HL**)	length of head from the anterior margin of the frons to the posterior margin of the head;
Head width (**HW**)	maximum width of head;
Antennal length (**AL**)	length of antennae from the base of antennomere 1 to the apex of antennomere 11;
Pronotum length (**PL**)	length of pronotum along midline;
Pronotum width (**PW**)	maximum width of pronotum;
Elytral length (**EL**)	length at suture from apex of scutellum to elytral hind margin;
Aedeagus length (**AeL**)	length of aedeagus from apex of ventral process to base of aedeagal capsule.

All material treated in this paper is deposited in the Insect Collection of Shanghai Normal University, Shanghai, China (SNUC). The type labels are cited using the original spelling; different labels are separated by slashes.

Results

Staphylinidae Latrielle, 1802
Paederinae Fleming, 1821

***Sinlathrobium assingi* X. Chen & Z. Peng, sp. nov.**
https://zoobank.org/ECEA11E1-F830-4446-8152-1DDB63001CFD
Figs 1A, 1D, 2

Type material. *Holotype.* Cʜɪɴᴀ − Chongqing • ♂; glued on a card with two labels as follows: "China: Chongqing City, Chengkou County, Gaoxing Xiang, West Daba Shan, Gou-Di-Tang; 32°08'N, 108°37'E; alt. 1830 m; 24.IV.2008; Huang & Xu leg." "HOLOTYPE: *Sinlathrobium assingi* sp. nov., Chen & Peng des. 2024" [red handwritten label]; SNUC. **Paratypes.** Cʜɪɴᴀ − Chongqing • 1♀; Chengkou County, Gaoxing Xiang, West Daba Shan, Gou-Di-Tang, 32°08'N, 108°37'E, alt. 1830 m, 24.IV.2008, Huang & Xu leg; SNUC.

Description. Measurements (in mm) and ratios: BL 7.67−7.73, FL 3.61−3.67, HL 0.85−0.92, HW 1.02−1.04, PL 1.05−1.11, PW 0.96−0.98, EL 1.04−1.05, AL 1.94−2.04, AeL 1.02, HL/HW 0.83−0.88, HW/PW 1.06, HL/PL 0.81−0.83, PL/PW 1.09−1.13, EL/PL 0.95−0.99.

Habitus as in Fig. 1A. Coloration: body black, elytra with moderately large, transverse yellowish spot posteriorly reaching lateral and posterior margins; legs yellowish with darker femora; antennae dark brown to brown.
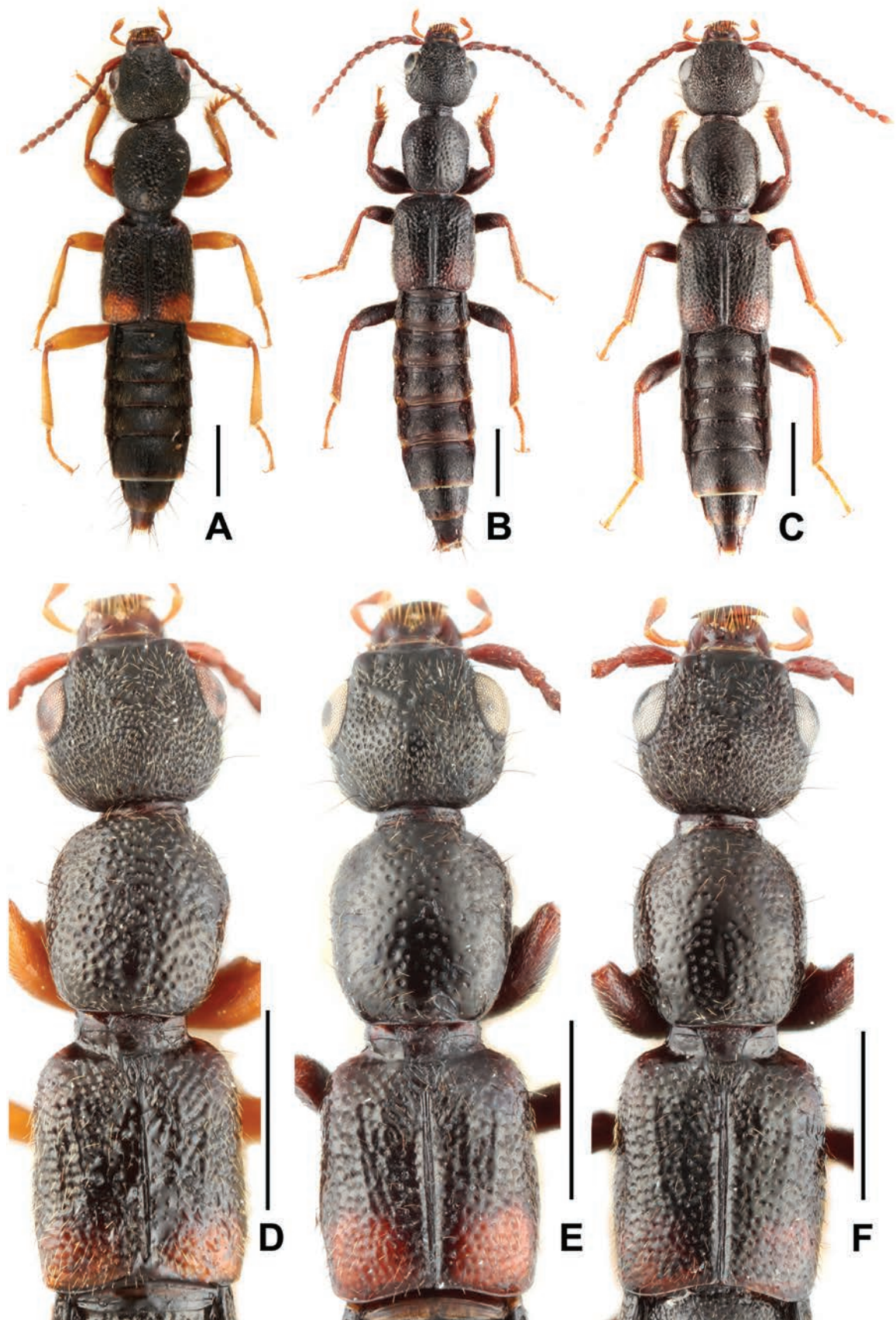
Figure 1. Habitus (**A–C**): **A** *Sinlathrobium assingi* sp. nov. **B** *Sinlathrobium chenzhilini* sp. nov. **C** *Sinlathrobium lobrathioides*. Forebody (**D–F**): **D** *Sinlathrobium assingi* sp. nov. **E** *Sinlathrobium chenzhilini* sp. nov. **F** *Sinlathrobium lobrathioides*. Scale bars: 1.0 mm.
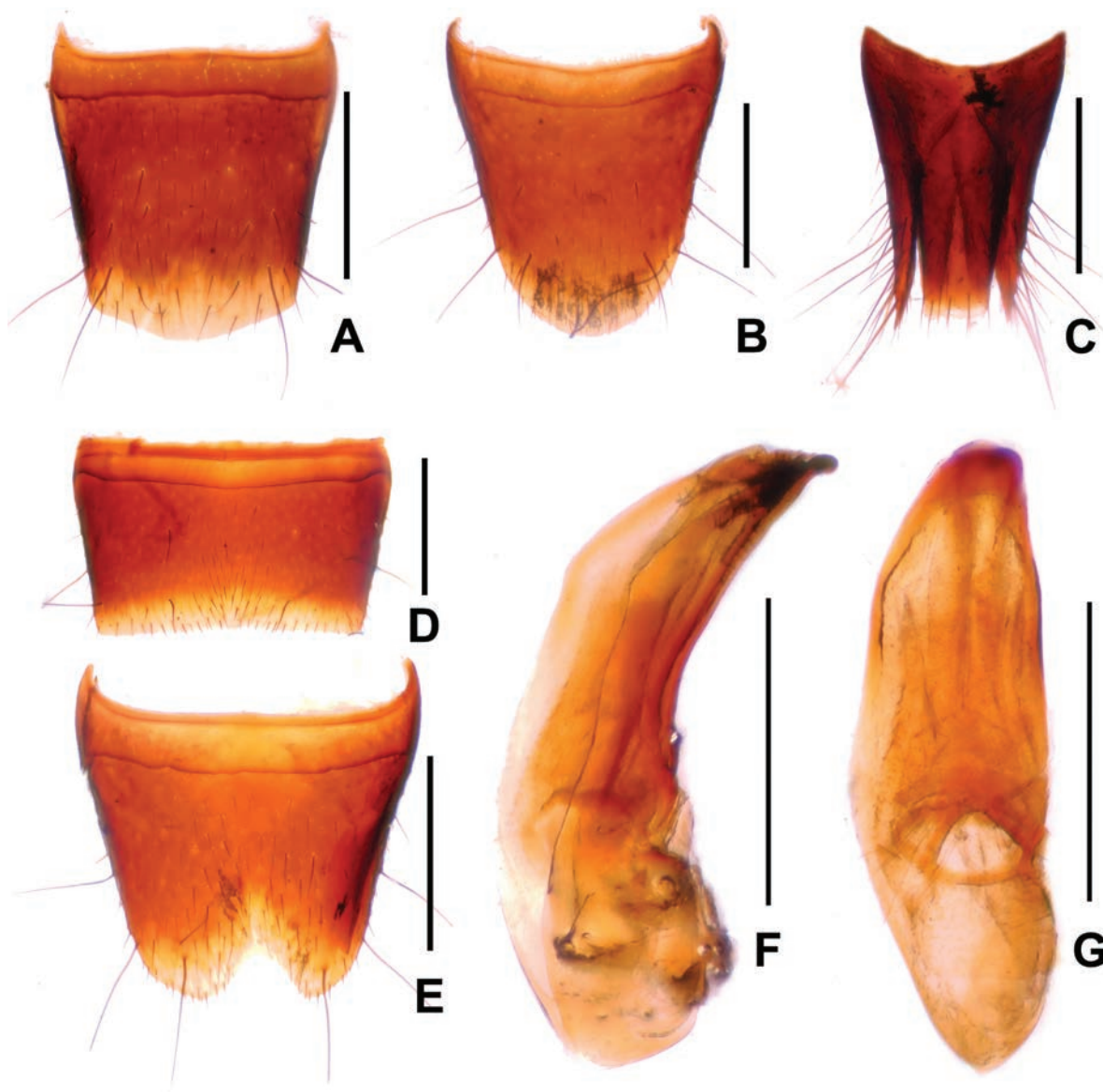
Figure 2. *Sinlathrobium assingi* sp. nov. **A** female tergite VIII **B** female sternite VIII **C** female tergites IX−X **D** male sternite VII **E** male sternite VIII **F** aedeagus in lateral view **G** aedeagus in ventral view. Scale bars: 0.2 mm.

Head (Fig. 1D) transverse, widest across eyes; punctation coarse and very dense, in median dorsal portion and on frons somewhat sparser; interstices with shallow microsculpture. Eyes large and bulging, 0.80−0.83 times as long as postocular region in dorsal view. Antennae not particularly slender.

Pronotum (Fig. 1D) nearly parallel-sided; punctation sparser and distinctly coarser than that of head; interstices without microsculpture and glossy.

Elytra (Fig. 1D) broader than pronotum; humeral angles weakly pronounced; punctation coarse and rather dense; interstices without microsculpture and glossy. Hind wings presumably fully developed.

Abdomen somewhat narrower than elytra; punctation conspicuously dense and fine on all tergites; interstices with distinct microsculpture and subdued gloss; posterior margin of tergite VII with palisade fringe.

Male. Sternites III−VI unmodified; sternite VII (Fig. 2D) strongly transverse, with shallow median impression without modified pubescence, posterior margin

broadly and shallowly concave; sternite VIII (Fig. 2E) weakly transverse, with shallow median impression posteriorly, this impression without modified setae, posterior excision V-shaped and moderately deep; aedeagus as in Fig. 2F, G, ventral process somewhat asymmetric, dorsal plate lamellate and weakly sclerotized.

Female. Tergite VIII (Fig. 2A) with strongly convex posterior margin; sternite VIII (Fig. 2B) weakly oblong, and with strongly convex posterior margin; tergite IX (Fig. 2C) with slender posterior processes; tergite X flat, nearly reaching anterior margin of tergite IX.

Distribution and biological notes. The type locality is situated to the west of Chengkou, northern Chongqing. The specimens were sifted from leaf litter, moss, and grass roots in shrub habitats at an altitude of 1830 m.

Etymology. This species is dedicated to our friend, Volker Assing, who prematurely passed away. He was a renowned specialist on mainly Palaearctic Staphylinidae.

Comparative notes. The highly similar male sexual characters, particularly the shape of the male sternites VII–VIII and the similarly derived morphology of the aedeagus, suggest that *S. assingi* is very closely related to *S. chenzhilini* sp. nov. and *S. lobrathioides* (Assing, 2012). It differs from *S. chenzhilini* and *S. lobrathioides* by the yellowish legs, particularly by the distinctly denser and coarser punctation of the pronotum, by the somewhat asymmetric ventral process of the aedeagus, and by the differently shaped female tergites IX–X. For illustrations of *S. chenzhilini* see Figs 1B, 1E, 3 and for *S. lobrathioides* see Figs 1C, 1F, 4A–C and Assing (2012: figs 315–320).

Sinlathrobium chenzhilini X. Chen & Z. Peng, sp. nov.
https://zoobank.org/3577BC92-4D2E-4E06-B0B9-A25B8F974FD0
Figs 1B, 1E, 3

Material examined. *Holotype.* China – Guangxi Prov. • ♂; glued on a card with two labels as follows: "China: Guangxi Prov., Xing'an County, Maoer Shan, 25°52'27"N, 110°24'44"E, alt. 1940 m, 29.VII.2014, Peng, Song, Yu & Yan leg." "HOLOTYPE: *Sinlathrobium chenzhilini* sp. nov., Chen & Peng des. 2024" [red handwritten label]; SNUC. *Paratypes.* China – Guangxi Prov. • 7♂♂, 5♀♀; Xing'an County, Maoer Shan, 25°52'27"N, 110°24'44"E, alt. 1940 m, 29.VII.2014, Peng, Song, Yu & Yan leg; SNUC • 2♂♂; Xing'an County, Maoer Shan, 25°53'15"N, 110°25'47"E, alt. 2030 m, 30.VII.2014, Peng, Song, Yu & Yan leg; SNUC.

Description. Measurements (in mm) and ratios: BL 6.12–7.78, FL 3.67–3.89, HL 0.89–0.94, HW 1.04–1.09, PL 1.11–1.20, PW 0.96–1.05, EL 1.07–1.15, AL 1.81–1.91, AeL 1.04–1.14, HL/HW 0.85–0.87, HW/PW 1.03–1.08, HL/PL 0.78–0.80, PL/PW 1.14–1.16, EL/PL 0.95–0.96.

Habitus as in Fig. 1B. Coloration: body black, elytra with extensive orange spot in postero-lateral angles, this spot reaching posterior and lateral margins, near suture; legs with the femora blackish, tibiae dark brown and tarsi brown; antennae dark brown to brown.

Head (Fig. 1E) transverse, widest across eyes; punctation coarse and very dense, in median dorsal portion and on frons distinctly sparser; interstices with shallow microsculpture. Eyes large and bulging, 0.90–0.92 times as long as postocular region in dorsal view. Antennae not particularly slender.
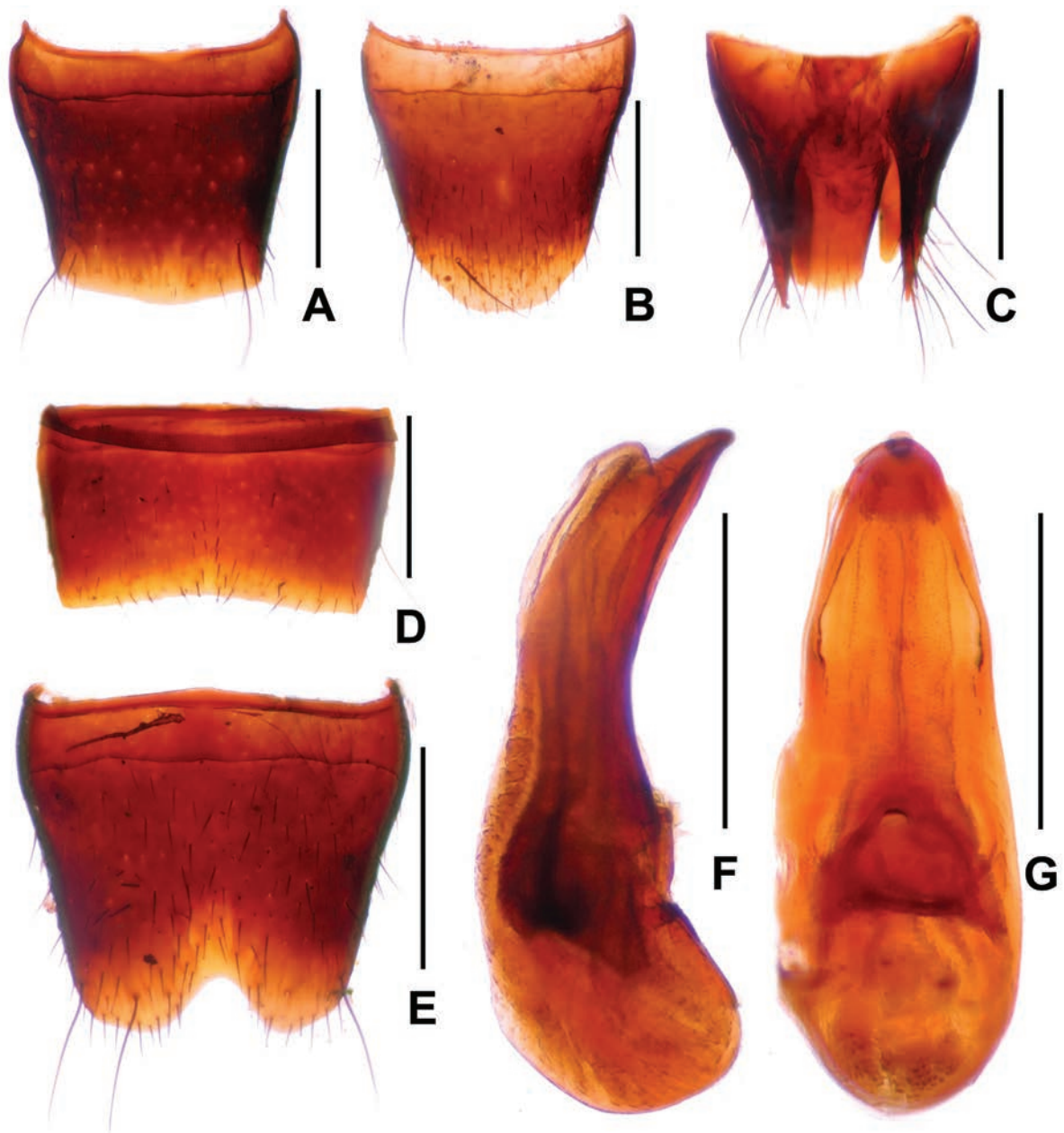
Figure 3. *Sinlathrobium chenzhilini* sp. nov. **A** female tergite VIII **B** female sternite VIII **C** female tergites IX–X **D** male sternite VII **E** male sternite VIII **F** aedeagus in lateral view **G** aedeagus in ventral view. Scale bars: 0.2 mm.

Pronotum (Fig. 1E) nearly parallel-sided; punctation distinctly sparser and distinctly coarser than that of head; interstices without microsculpture and glossy.

Elytra (Fig. 1E) broader than pronotum; humeral angles pronounced; punctation coarse and rather dense; interstices without microsculpture and glossy. Hind wings fully developed.

Abdomen somewhat narrower than elytra; tergites III–VI with very fine and dense punctation, tergites VII–VIII with distinctly sparser punctation; posterior margin of tergite VII with palisade fringe.

Male. Sternites III–VI unmodified; sternite VII (Fig. 3D) strongly transverse, with shallow median impression without modified pubescence, posterior margin broadly concave; sternite VIII (Fig. 3E) transverse, with shallow median im-

pression posteriorly, this impression without modified setae, posterior excision V-shaped and moderately deep; aedeagus as in Fig. 3F, G, ventral process symmetric, dorsal plate long and strongly sclerotized.

Female. Tergite VIII (Fig. 3A) with broadly convex posterior margin; sternite VIII (Fig. 3B) weakly oblong, and with strongly convex posterior margin; anterior portion of tergite IX (Fig. 3C) divided in middle, tergite X (Fig. 3C) approximately twice as long as tergite IX in the middle.

Distribution and biological notes. The type locality is situated in the Maoer Shan to the north of Guilin, northern Guangxi. The specimens were sifted from leaf litter and dead wood in mixed deciduous forests at altitudes from approximately 1940 up to 2030 m.

Etymology. This species is dedicated to Zhi-Lin Chen, who supported us on our field trips.

Comparative notes. The highly similar male sexual characters, particularly the shape of the male sternites VII–VIII and the similarly derived morphology of the aedeagus, suggest that *S. chenzhilini* is very closely related to *S. assingi* sp. nov. and *S. lobrathioides* (Assing, 2012). It differs from *S. assingi* by the coloration of legs, particularly by the distinctly sparser and finer punctation of the pronotum, and by the differently shaped ventral process of the aedeagus. It differs from *S. lobrathioides* by the somewhat longer elytra, particularly by the sparser punctation of the head and pronotum, and by the longer dorsal plate of the aedeagus. For illustrations of *S. assingi* see Figs 1A, 1D, 2.

Sinlathrobium lobrathioides (Assing, 2012)
Figs 1C, 1F, 4

Lathrobium lobrathioides Assing, 2012: 125.

Material examined. China – Chongqing • 3♂♂, 3♀♀; Jinfo Shan, 29°01'25"N, 107°11'01"E, alt. 2160 m, 09.VII.2015, Jiang, Peng, Tu & Zhou leg; SNUC.

Comment. The original description is based on a single male. The previously unknown female sexual characters are as follows: tergite VIII (Fig. 4A) with strongly convex posterior margin; sternite VIII (Fig. 4B) oblong, and with strongly convex posterior margin; anterior portion of tergite IX (Fig. 4C) divided in middle, tergite X (Fig. 4C) nearly reaching anterior margin of tergite IX. For illustrations of the male sexual characters see Assing (2012: figs 315–320). The specimens were sifted from dead wood in mixed deciduous forests at an altitude of about 2160 m (Fig. 4D, E).

Key to the species of *Sinlathrobium*

1   Femora blackish; tibiae blackish-brown to brown.......................................**2**
–   Femora yellowish-brown to brown; tibiae reddish......................................**4**
2   Pronotum weakly oblong (PL/PW 1.08). Elytra with shallow longitudinal impressions. China: northwestern Yunnan...........***S. iniquum* Assing, 2013**
–   Pronotum slenderer (PL/PW ≥ 1.13). Elytra with smooth surface and without longitudinal impressions **3**

3   Median dorsal portion of head with small impression. Posterior margin of male sternite VII with numerous stout black setae. China: western Sichuan.. ***S. densepunctatum* Assing, 2013**
–   Median dorsal portion of head with moderately dense punctation and glossy. Posterior margin of male sternite VII with unmodified pubescence. China: Guangxi: Maoer Shan .... ***S. chenzhilini* sp. nov.**
4   Male sternite VII with weakly defined pair of clusters of black setae posteriorly. Ventral process of aedeagus apically acute in ventral view. China: Yunnan: Gaoligong Shan..........................***S. lobrathiforme* (Assing, 2012)**
–   Male sternite VII without modified setae posteriorly. Ventral process of aedeagus apically convex in ventral view..**5**
5   Coloration of legs darker. Pronotum with less coarse and sparser punctation. Ventral process of aedeagus symmetric in ventral view. China: Chonqing: Jinfo Shan...***S. lobrathioides* (Assing, 2012)**
–   Coloration of legs lighter. Pronotum with more coarse and denser punctation. Ventral process of aedeagus somewhat asymmetric in ventral view. China: Chonqing: West Daba Shan...................................***S. assingi* sp. nov.**
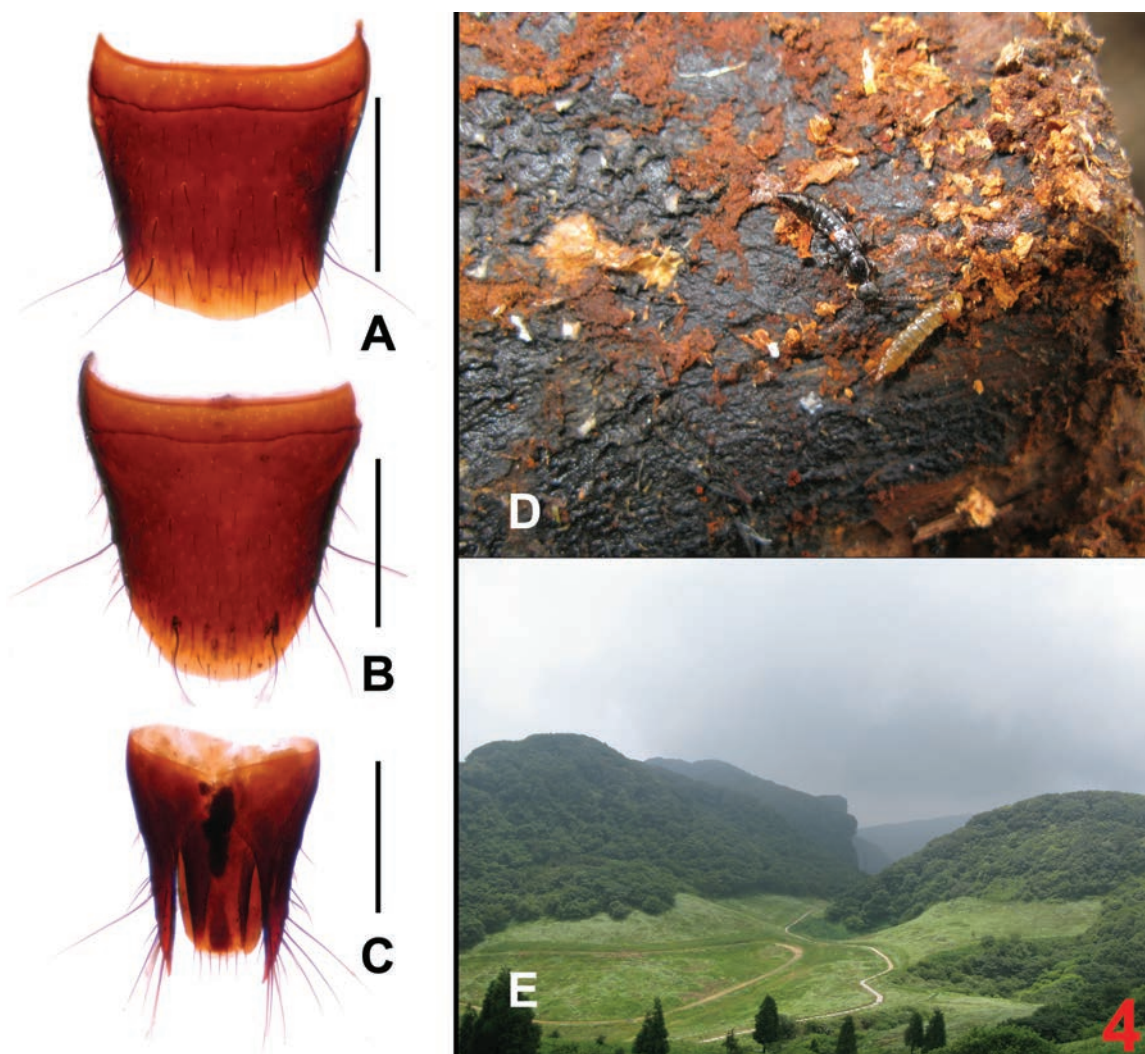
Figure 4. *Sinlathrobium lobrathioides*. **A** female tergite VIII **B** female sternite VIII **C** female tergites IX–X **D** *S. lobrathioides* walking on the dead wood **E** habitat (Jinfo Shan). Scale bars: 0.2 mm.

Acknowledgements

Additional information

Conflict of interest

The authors have declared that no competing interests exist.

Ethical statement

No ethical statement was reported.

Funding

Author contributions

Data curation: XC. Resources: JPY. Writing – original draft: ZP.

Author ORCIDs

Xi Chen ⓘ https://orcid.org/0000-0001-9903-8700
Jian-Ping Ye ⓘ https://orcid.org/0000-0002-2498-0010
Zhong Peng ⓘ https://orcid.org/0000-0001-5959-1536

Data availability

All of the data that support the findings of this study are available in the main text.

References

Assing V (2012) A revision of East Palaearctic *Lobrathium* (Coleoptera: Staphylinidae: Paederinae). Bonn Zoological Bulletin 61(1): 49–128. https://doi.org/10.21248/contrib.entomol.61.1.89-148

Assing V (2013) Two new genera of Lathrobiina from the East Palaearctic region (Coleoptera: Staphylinidae: Paederinae). Contributions to Entomology, Beiträge zur Entomologie 63(2): 219–239. https://doi.org/10.21248/contrib.entomol.63.2.219-239

ZooKeys

Research Article

Taxonomic notes on the genus *Chaitoregma* (Hemiptera, Aphididae, Hormaphidinae), with description of a new species from China

Yizhe Wang[1], Xiaolei Huang[1]

1 *State Key Laboratory of Ecological Pest Control for Fujian and Taiwan Crops, College of Plant Protection, Fujian Agriculture and Forestry University, Fuzhou 350002, China*
Corresponding author: Xiaolei Huang (*huangxl@fafu.edu.cn*)

Abstract

A new aphid species, *Chaitoregma kirlia* **sp. nov.**, from Fujian and Guangdong, China, is described, which feeds on bamboo. The diagnostic morphological characteristics of the new species are described and illustrated. A key to apterous viviparous females of *Chaitoregma* species is provided. The COI barcode sequence of this new species is also provided. Due to its unique morphological characteristics, the diagnosis of the genus has been revised. Other species within the genus are also reviewed and discussed.

Key words: *Chaitoregma*, China, Hormaphidinae, new species, taxonomy

Introduction

The aphid genus *Chaitoregma* was established by Hille Ris Lambers and Basu in 1966, with *Oregma tattakana* Takahashi, 1925 as the type species. This small genus belongs to the tribe Cerataphidini (Aphididae, Hormaphidinae). Currently, *Chaitoregma* comprises only two species and one (non-nominotypical) subspecies: *C. tattakana tattakana* (Takahashi, 1925), *C. tattakana suishana* (Takahashi, 1929), and *C. aderuensis* (Takahashi, 1935) (Eastop and Hille Ris Lambers 1976; Remaudière and Remaudière 1997; Fang et al. 2006; Favret 2024). These species were originally discovered on Taiwan Island, China, where they feed on various bamboo species, such as *Phyllostachys pubescens*, *Yushania niitakayamensis*, and *Bambusa* spp. (Takahashi 1925, 1929, 1931, 1935; Qiao et al. 2018).

The genus *Chaitoregma* is characterized by cylindrical frontal horns with rounded tips and nymphs that exhibit blunt frontal horns from birth. The pronotum is fused to the head; the mesonotum, metanotum, and abdominal tergites I and VIII remain free, whereas the other segments are completely fused without distinct sutures. Roundish to irregular stippled wax facets can be found everywhere on the dorsal surface of the body, but wax glands are not present in localized groups (Hille Ris Lambers and Basu 1966; Basant and Ghosh 1985; Tao 1991).

In this study, a new species, *Chaitoregma kirlia* sp. nov., is described, found on bamboo in Fujian and Guangdong, China. A key to apterous viviparous females of *Chaitoregma* species is provided. Other species within the genus are reviewed and discussed.

Materials and methods

Field sampling

The specimens of the new species were collected from Wuyishan Mountain, Fujian Province, China on August 2, 2016, and Mount Lianhuashan, Guangdong Province, China on July 16, 2024. During the fieldwork, photographs of live individuals were taken using a digital camera (Canon EOS 7D plus Canon EF 100 mm f/2.8L Macro IS USM Lens).

Specimens of *C. tattakana tattakana* were collected from Kunming, Yunnan Province, China on November 9, 2017.

All samples were preserved in 95% ethanol and kept at −80 °C for further morphological measurement and molecular experiments.

Morphological description

Aphid terminology and the morphological measurements used in this paper follow Cheng and Huang (2023) (Table 1). Specimens were examined and measurements and images were taken by using Nikon SMZ18 stereomicroscope. The measurements and the micrographs of mounted specimens were performed

Table 1. Biometric data (mean, range) of *Chaitoregma kirlia* sp. nov. and *Chaitoregma tattakana tattakana*.

Part		*Chaitoregma kirlia* sp. nov. Apterous vivipara (*n* = 8)		*Chaitoregma tattakana* Apterous vivipara (*n* = 7)	
		Mean	**Range**	**Mean**	**Range**
Length (mm)	BL	1.164	1.012−1.372	1.322	1.209−1.395
	BW	0.690	0.624−0.789	0.734	0.645−0.852
	WA	0.198	0.187−0.210	0.236	0.230−0.241
	Ant. I	0.031	0.025−0.037	0.033	0.030−0.040
	Ant. II	0.028	0.025−0.030	0.035	0.029−0.038
	Ant. III	0.070	0.064−0.073	0.089	0.087−0.094
	Ant. III_WD	0.029	0.027−0.033	0.029	0.027−0.030
	Ant. IV	0.047	0.040−0.052	0.056	0.052−0.063
	PT	0.022	0.018−0.027	0.020	0.016−0.025
	HF	0.225	0.201−0.254	0.273	0.245−0.286
	HF_WD	0.059	0.053−0.069	0.056	0.054−0.058
	HT	0.288	0.262−0.307	0.362	0.340−0.384
	HT_WD	0.036	0.031−0.040	0.032	0.030−0.035
	2HT	0.071	0.065−0.079	0.092	0.088−0.101
	SIPH_DW	0.029	0.024−0.033	0.032	0.028−0.038
	Cauda	0.034	0.030−0.046	0.039	0.030−0.051
	Cauda_ BW	0.065	0.058−0.070	0.078	0.072−0.086
	URS	0.047	0.040−0.051	0.053	0.051−0.056
	URS_BW	0.048	0.042−0.055	0.041	0.039−0.044
	MF	0.038	0.029−0.047	0.041	0.030−0.050
	FH	0.045	0.039−0.054	0.059	0.053−0.062
	FH_BW	0.033	0.028−0.048	0.035	0.032−0.041
	Setae on dorsum head	0.059	0.050−0.066	0.090	0.079−0.112
	Setae on abd. tergites I	0.048	0.035−0.059	0.087	0.056−0.113
	Setae on abd. tergites VIII	0.060	0.042−0.072	0.081	0.062−0.096
	Setae on Ant. III	0.026	0.020−0.045	0.032	0.026−0.036
	Distance between the apex of horns	0.121	0.109−0.135	0.103	0.098−0.110
	Setae on hind tibia	0.037	0.033−0.044	0.058	0.050−0.065

Part		*Chaitoregma kirlia* sp. nov. Apterous vivipara (*n* = 8)		*Chaitoregma tattakana* Apterous vivipara (*n* = 7)	
		Mean	**Range**	**Mean**	**Range**
No. of setae	URS	6	6−7	6	6
	Ant. I	1	1−2	2	1−2
	Ant. II	2	2−3	2	2
	Ant. III	4	3−6	4	4−5
	Ant. IV	2	1−2	1	1
	PT	4	2−5	4	3−5
	HF	15	10−19	17	24−21
	HT	22	18−28	24	21−28
	CAUDA	5	3−7	10	8−12
	AP	11	10−13	13	11−15
	GP	11	9−19	14	11−18
	GONA	10	9−13	12	10−15
	Around SIPH	5	4−6	4	3−4
	FH	8	6−12	7	6−7
	Dorsum head	18	15−20	26	25−28
	Dorsum mesonotum	11	7−12	13	11−14
	Dorsum metanotum	11	8−13	14	12−17
	Dorsum tergites I	9	7−12	15	13−16
	Dorsum tergites VIII	11	8−16	17	15−19
Ratio (times)	BL/BW	1.69	1.60−1.80	1.81	1.59−2.01
	WA/BL	0.17	0.14−0.20	0.18	0.17−0.19
	HT/BL	0.25	0.22−0.26	0.27	0.25−0.3
	HF/BL	0.19	0.18−0.21	0.21	0.18−0.23
	PT/WA	0.11	0.09−0.13	0.09	0.07−0.10
	Ant. III/WA	0.36	0.32−0.39	0.38	0.36−0.40
	PT/Ant.IV	0.48	0.39−0.68	0.37	0.27−0.48
	URS/URS_BW	0.96	0.78−1.04	1.28	1.16−1.44
	URS/2HT	0.66	0.60−0.75	0.56	0.54−0.58
	Cauda_BW/Cauda	1.88	1.52−2.16	2.10	1.53−2.87
	HF/Ant. III	3.20	2.79−3.86	3.06	2.75−3.29
	2HT/Ant. III	1.02	0.92−1.13	1.06	0.98−1.16
	URS/Ant. III	0.66	0.56−0.74	0.59	0.57−0.63

using a computer-connected Nikon set: Nikon Eclipse Ci-L upright microscope, 16 MP digital camera with 0.55 × adapter and imaging software NIS-Elements D v. 4.60.00. The unit of measurement in this paper is millimeter (mm).

The following abbreviations have been used: BL, body length; BW, body width; WA, whole length of antenna; Ant. I, Ant. II, Ant.III, Ant. IV, for antennal segment I, II, III, IV, respectively; Ant. III_WD, the widest diameter of Ant. III; PT, processus terminalis; HF, hind femur; HF_WD, the widest diameter of HF; HT, hind tibia; HT_WD, the widest diameter of HT; 2HT, second hind tarsal segment; SIPH, siphunculus; SIPH_DW, distal width of siphunculus; Cauda_BW, basal width of cauda; URS, ultimate rostral segment; URS_BW, basal width of URS; MF, mesosternal furca; FH, frontal horns; FH_BW, basal width of frontal horns; AP, anal plate; GP, genital plate; GONA, gonapophyses.

DNA sequencing

Whole genomic DNA was extracted from a single individual preserved in 95% ethanol using the DNeasy Blood & Tissue Kit (Qiagen, Hilden, Germany). The standard DNA barcode gene of animals, cytochrome c oxidase subunit I (5'

region of COI) was amplified with primer LepF (5'-ATTCAACCAATCATAAAGA-TATTGG-3') and LepR (5'-TAAACTTCTGGATGTCCAAAAAATCA-3') (Foottit et al. 2008). PCR amplifications were performed in a final volume of 25 µL reaction mixture containing 2 µL of template DNA, 0.5 µL of both forward and reverse primer (10 µM), 0.25 µL of Taq DNA polymerase (5 U/µL), 17.25 µL of double distilled H2O, 2.5 µL of 10 × buffer and 2 µL of dNTP. PCR thermal regime was as follows: 5 min of initial denaturation at 95 °C, 35 cycles of 20 s at 94 °C, 30 s at 50 °C (the annealing temperature) and 2 min at 72 °C, and 10 min of final extension at 72 °C. The products of PCR were visualized by electrophoresis on a 1% agarose gel and then bidirectionally sequenced at Beijing Tsingke Biotech Co., Ltd (Beijing, China). All sequences were assembled by ContigExpress (Vector NTI Suite 6.0, InforMax Inc.), and the reliability was checked by BLAST. The COI sequence was submitted to GenBank under the accession number PP910380.

The phylogenetic analysis was performed based on the sequence of the new species and 15 COI sequences downloaded from NCBI: four sequences of *C. tattakana tattakana*, two unidentified *Chaitoregma* species sequences, and seven sequences representing seven species within the tribe Cerataphidini; two sequences representing two species within the tribe Nipponaphidini were used as outgroups (Table 2).

Multiple alignment was conducted using MUSCLE (Edgar 2004). Maximum-likelihood phylogenies were inferred using MEGA X (Tamura et al. 2021) under the GTR+G+I model for 500 bootstraps. The mean genetic distances among the *Chaitoregma* species were calculated using MEGA X (Tamura et al. 2021) under Kimura's two-parameter (K2P) model (Kimura 1980).

Specimen deposition

The holotype and paratypes of the new species examined here are deposited in the Insect Systematics & Diversity Lab, Fujian Agriculture and Forestry University, Fuzhou, China.

Table 2. Voucher information and GenBank accession numbers of aphid samples used in molecular data analysis.

Species	Host	Locality	GenBank accession number	References
Astegopteryx bambusae	Bambusoideae spp.	Fujian, China	MH821551	Li et al. (2023)
Astegopteryx styracophila	Zingiberaceae spp.	Hainan, China	JX489626	Chen et al. (2014)
Ceratovacuna graminum	Bambusoideae spp.	Fujian, China	MH821618	Li et al. (2023)
Ceratovacuna lanigera	Bambusoideae spp.	Fujian, China	MH821646	Li et al. (2023)
Ceratovacuna keduensis	*Bambusa ventricosa*	Fujian, China	MH821625	Li et al. (2023)
Chaitoregma sp.	Bambusoideae spp.	Fujian, China	MH821702	Li et al. (2023)
Chaitoregma sp.	Bambusoideae spp.	Fujian, China	MH821703	Li et al. (2023)
Chaitoregma kirlia	Bambusoideae spp.	Fujian, China	PP910380	This study
Chaitoregma tattakana tattakana	Bambusoideae spp.	Yunnan, China	MH821704	Li et al. (2023)
Chaitoregma tattakana tattakana	Bambusoideae spp.	Yunnan, China	MH821705	Li et al. (2023)
Chaitoregma tattakana tattakana	Bambusoideae spp.	Yunnan, China	JX489629	Chen et al. (2014)
Chaitoregma tattakana tattakana	Bambusoideae spp.	Guizhou, China	JN032707	Huang et al. (2012)
Metanipponaphis lithocarpicola	*Castanopsis* spp.	Fujian, China	JX489637	Chen et al. (2014)
Neohormaphis wuyiensis	*Quercus* spp.	Fujian, China	JX489762	Chen et al. (2014)
Pseudoregma panicola	*Cyrtococcum patens*	Fujian, China	MH820756	Li et al. (2023)
Pseudoregma bambucicola	Bambusoideae spp.	Fujian, China	MH820693	Li et al. (2023)

Taxonomy

Genus *Chaitoregma* Hille Ris Lambers & Basu, 1966

Chaitoregma Hille Ris Lambers & Basu, 1966: 15; Eastop and Hille Ris Lambers 1976: 143; Ghosh et al. 1977: 102; Blackman and Eastop 1984: 258; Remaudière and Remaudière 1997: 182; Qiao and Zhang 2003: 146; Aoki and Kurosu 2010: 2; Nieto Nafría et al. 2011: 171.
Chaetoregma Tao, 1991: 41. (incorrect subsequent spelling).

Generic diagnosis. In apterae, body round, flat, and strongly sclerotized. Head with 1 pair of frontal horns, cylindrical with broadly rounded tips, nymph with blunt frontal horns from birth. Head plus pronotum, meso- and metanotum, and abd. tergites I and VIII mutually free, the other abdominal tergites completely fused without sutures. Body dorsum with irregularly shaped wax facets, sometimes wax plates appear in groups along the abdominal margin. Eyes with 3 facets. Antennae 4- or 5-segmented, with primary rhinaria on the terminal segment. Rostrum short and thick. Ultimate rostral segment blunt, wedge-shaped, with 3 pairs of long primary setae. Legs normal, claws normal, first tarsal chaetotaxy: 4, 3, 2. Siphunculi pore-like, not situated on hairy cones. Cauda knobbed and constricted at base. Anal plate bilobed.

Distribution. China (Fujian, Guangdong, Taiwan, Yunan), India (Darjeeling).
Host plants. Various species of Bambusoideae.
Type species. *Oregma tattakana* Takahashi, 1925 by original designation.

Chaitoregma tattakana tattakana (Takahashi, 1925)

Oregma tattakana Takahashi, 1925: 47; Takahashi 1931: 96; Tao and Tseng 1938: 218; Shinji 1941: 1115; Chu 1957: 144; Tao 1969: 57.
Chaitoregma tattakana Hille Ris Lambers & Basu, 1966: 16; Eastop and Hille Ris Lambers 1976: 143, 327; Ghosh et al. 1977: 102; Blackman and Eastop 1984: 258; Fukatsu et al. 1994: 617; Remaudière and Remaudière 1997: 182; Stern et al. 1997: 84; Fang et al. 2006: 993; Aoki and Kurosu 2010: 22; Fang et al. 2011: 160.
Chaetoregma tattakana Tao, 1991: 42.

Specimens examined. • 7 apterous viviparous females, CHINA: Yunnan (24.886°N, 102.839°E), 9 Nov. 2017, No. HL_zld20171109_2_A to G, coll. L. D. Zeng (FAFU).

Chaitoregma kirlia sp. nov.

https://zoobank.org/3EAB9F31-3213-4EEE-8DCF-1E0732092F78
Figs 1–3, Table 1

Etymology. The specific epithet "kirlia" is a noun in apposition, named after Kirlia, a character from the popular Pokémon series. They both have a pair of front horns. The name was chosen to honor the graceful and elegant nature of this new species, reminiscent of the character.
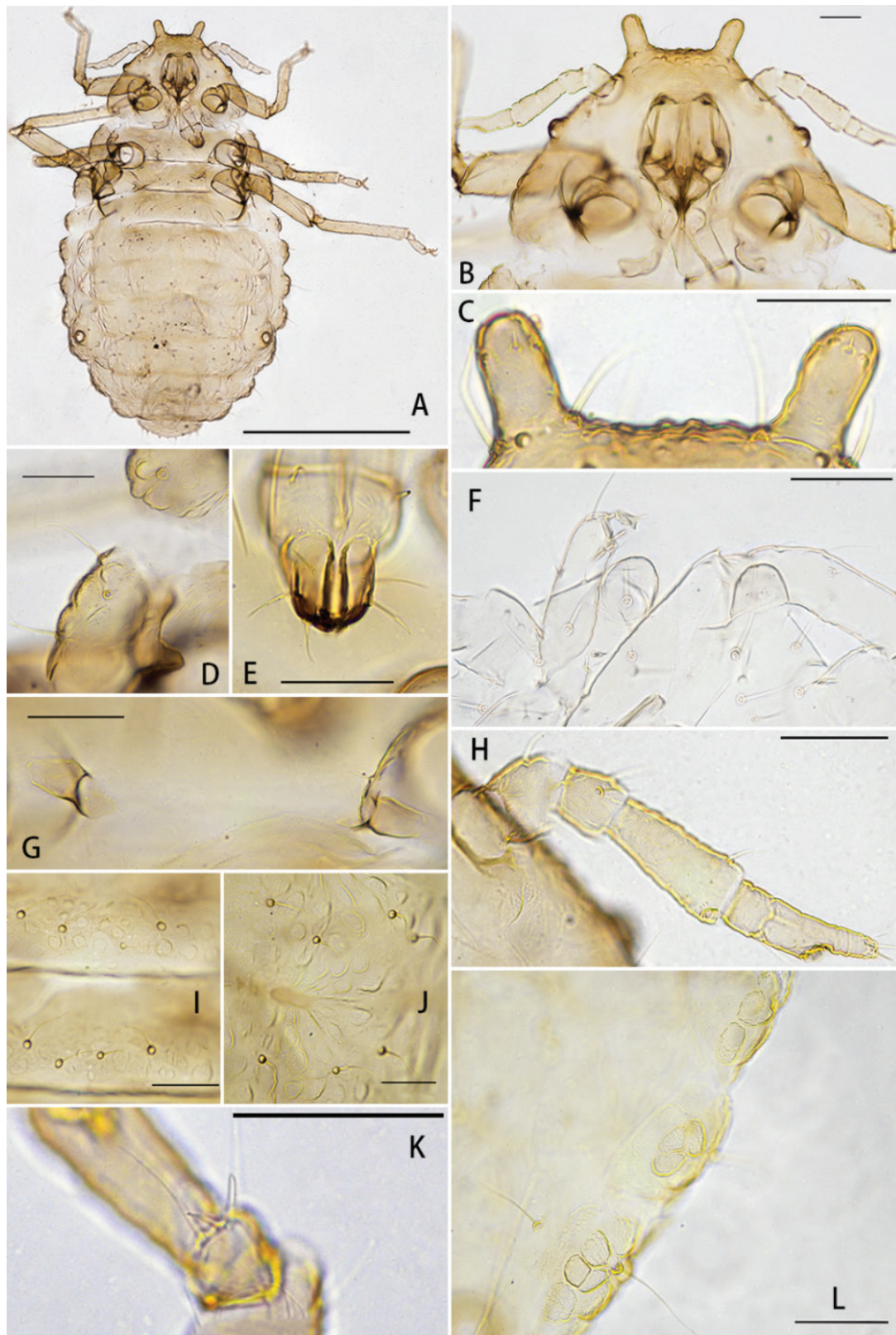
Figure 1. *Chaitoregma kirlia*, apterous viviparous female **A** dorsal view of body **B** head and pronotum **C** frontal horns **D** marginal wax gland plates on mesonotum **E** ultimate rostral segment **F** blunt frontal horns in embryo **G** mesosternal furca **H** antenna **I** spinal setae and wax facets on mesonotum and metanotum **J** wax facets on dorsal abdomen **K** setae on first fore tarsal joint **L** wax gland plates on marginal abdomen (**A–E, G–K** from HL_20160812_19_A; **F** from HL_20160812_19_C; **L** from HL_20160812_19_D). Scale bars: 0.5 mm (**A**); 0.05 mm (**B–L**).
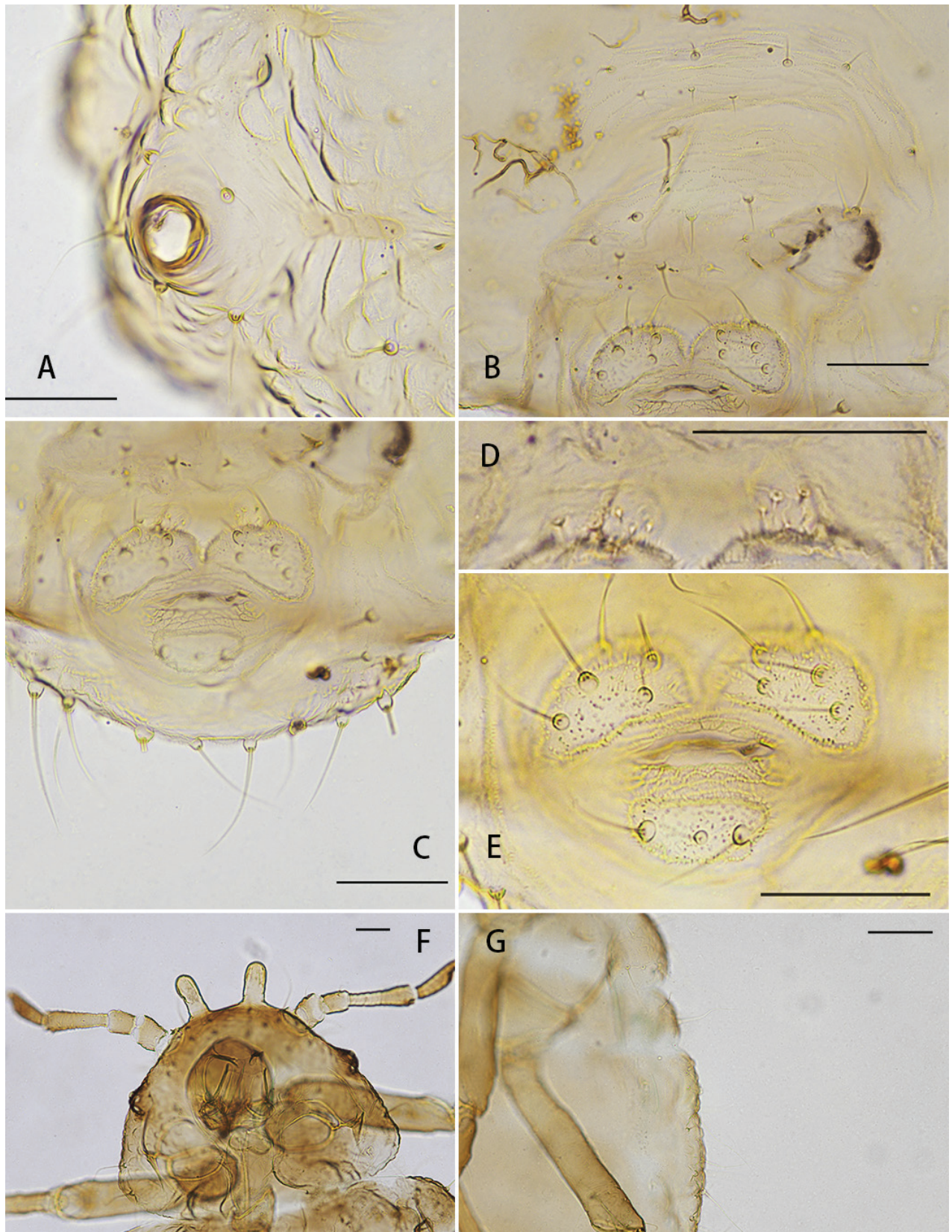
Figure 2. A–E *Chaitoregma kirlia*, apterous viviparous female **A** siphunculi with 5 setae around **B** genital plate **C** abdominal tergites VIII **D** gonapophysis **E** cauda and anal plate **F, G** *Chaitoregma tattakana* apterous viviparous female **F** head and pronotum **G** dorsal view of body (**A–E** from HL_20160812_19_A, **F–G** from HL_zld20171109_2_C). Scale bars: 0.05 mm (**A–G**).

Figure 3. *Chaitoregma. kirlia* sp. nov., colony on the underside of leaf of one undefined bamboo species, attended by an ant species, *Crematogaster* sp.

Description. Apterous viviparous female: body oval, dark purple in life. Body dorsum slightly covered with white wax powders, marginal areas on body with undeveloped flaky wax powders in life. For morphometric data see Table 1.

Mounted specimens. Body oval and dark sclerotic (Fig. 1A), 1.62−1.82 × as long as its width, sclerotic areas evenly covered with numerous irregularly shaped wax facets, wax facets arranged radially at the intersegmental area (Fig. 1J). Head and pronotum fused (Fig. 1B), mesonotum, metanotum, abdominal segment I and VIII mutually free; abdominal segment II to VII completely fused, sutures not clearly distinct.

Head. Frons with a pair of frontal horns, frontal horns cylindrical with broadly rounded tips, about 1.2−1.7 × as long as their basal width, smooth, with 6−12 short setae (Fig. 1C). Distance between the apex of the horns about 0.109−0.125 mm. Embryo with blunt frontal horns (Fig. 1F). Antennae 4-segmented, sometimes 5-segmented, about 0.15−0.19 × body length (Fig. 1H); length in proportion of segments I−IV: 25−37, 25−30, 64−73, 40−52, and 18−27. Antennal setae all fine, long with acute apices; segments I−V with 1−2, 2−3, 3−6, 1−2 setae, respectively; apical part of processus terminalis with 2−5 setae (Fig. 1F). Length of setae on segment III 0.02−0.045 mm. Segment III narrowed toward base, sensorium very small. Eyes with 3 facets in apterae. Rostrum short, reaching or nearly reaching mid-coxae; URS wedge-shaped (Fig. 1E), about 0.60−0.75 × of second joint of hind tarsi, with 3 pairs of long primary setae. Dorsal head and pronotum with 15−20 setae, 0.050−0.066 mm, fine wavy, with acute apices.

Thorax. Margin of the pronotum to metanotum each with some wax facets (Fig. 1D). Dorsal setae on thorax similar to head setae. Pronotum with 2 pairs

of spinal setae and 2 pairs of marginal setae; mesonotum, and metanotum each with 2 pairs of spinal, 1–2 pair of pleural and 2 pairs of marginal setae, respectively. Mesosternal furca with 2 separated arms (Fig. 1G), each arm 1.53–2.47 × as long as basal diameter of antenna segment III. Legs short, trochanters nearly fused with femora; hind tibia 0.22–0.26 × as long as body. Setae on legs fine and slightly long; setae on hind tibia 0.90–1.27 × as long as its diameter. First tarsal chaetotaxy: 4, 3, 2. The first fore tarsal joint of the legs with 2 long setae and 2 short setae (Fig. 1K), while the first hind tarsal joint with 2 long setae.

Abdomen. Abdominal tergites I–VII each with 1 pair of wax gland plates on marginal sclerites, composed with irregularly shaped to rounded wax gland facets (Fig. 1L), surrounding 1 marginal seta, wax gland facets composed with 2–5 facets. Abdominal tergites I–V each with 2 pair of spinal setae, 2–4 pair of pleural and 1 pair of marginal setae; tergites VI with 1 pair of spinal, 1 pair of pleural and 1 pair of marginal setae; tergites VI with 1 pair of spinal and 1 pair of marginal setae; tergite VIII with 8–16 setae (Fig. 2C), setae on abdominal tergite VIII 2.9–3.7 × as long as basal diameter of antennal segment III. Spiracles round, open. Siphunculae pore-like, about 0.03 mm, slightly elevated, not situated on setaceous cones (Fig. 2A). Cauda knobbed and constricted at base, with about 3–7 setae (Fig. 2E). Anal plate bilobed, with 5–7 setae on each lobe (Fig. 2E). Genital plate with 4 anterior setae and 7–9 posterior setae (Fig. 2B). Gonapophyses two, each with 5–7 setae (Fig. 2D).

Specimens examined. *Holotype* • 1 apterous viviparous female, China: Fujian (Mount Wuyishan, 27.630°N, 117.394°E, alt. 234 m), 12 Aug. 2016, HL_20160812_19_A, coll. X. L. Huang and X. L. Lin (FAFU). *Paratypes* • 7 apterous viviparous females (HL_20160812_19_B to D on the same slide as holotype; HL_20160812_19_E to G on another slide), with the same collection data as holotype.

Other examined material. • 3 apterous viviparous females on the same slide, China: Guangdong (Mount Lianhuashan, 23.067°N, 115.241°E, Alt. 905 m), 16 July 2024, WYZ_20240716_6_A to D, coll. Y. Z. Wang (FAFU).

Distribution. China: Fujian (Mount Wuyishan), Guangdong (Mount Lianhuashan).

Host plants. One unknown species of Bambusoideae.

Biology. According to our records, *Chaitoregma kirlia* forms large colonies on the undersides of leaves of the host plant, and can be attended by ants, *Crematogaster* sp. (Fig. 3). In the wild, it has been observed that in addition to the purple individuals of this new species within the colony, there are occasionally a few yellow individuals; these are suspected to be mixed colonies with another *Chaitoregma* species, possibly *C. tattakana suishana* (Fig. 3). The entire life cycle is unknown.

Taxonomic notes. The new species resembles the type species *C. tattakana* (Takahashi, 1925), they but differ as follows: *C. kirlia* sp. nov. has distinct wax gland plates on the margin of abd. I–VI (Fig. 1L), while other species in this genus do not have distinct wax gland plates (Qiao and Zhang 2003, Fig. 2G); The new species has a greater distance between the apex of the frontal horns (0.109–0.135 mm) compared to *C. tattakana tattakana* (0.098–0.110 mm); length of the setae on the dorsum of head (0.050–0.066 mm), abd. tergites I (0.035–0.059 mm) and VIII (0.042–0.072 mm) are significantly shorter than *C. tattakana tattakana* (0.079–0.112 mm; 0.056–0.113 mm; 0.062–0.096 mm); HT 0.22–0.26 × body length (*C. tattakana tattakana*: 0.25–0.30×), PT 0.4–0.68 × Ant.IV (*C. tattakana tattakana*: 0.27–0.48×), URS 0.78–1.04 × URS_BW (*C. tattakana tattakana*: 1.16–1.43×), URS 0.60–0.75 × 2HT (*C. tattakana tattakana*: 0.54–0.58×). Number of setae on various body parts are also different (Table 1).
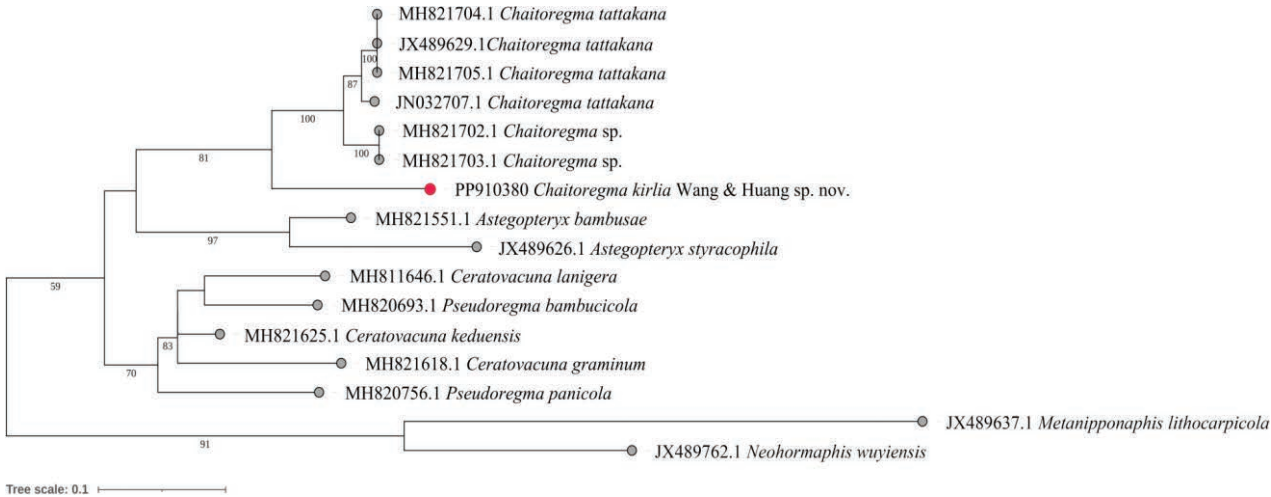
Figure 4. The maximum-likelihood phylogenetic tree of the samples based on COI sequences. Numbers beside main nodes are bootstrap support values (>50). Solid red circle marks the new species.

Table 3. Mean genetic distances (K2P) among new species and some other species in *Chaitoregma* based on COI sequences. The percentage of genetic distances are shown in the lower left half of the matrix, and the percentage of standard errors are shown in the upper right half of the matrix.

	PP910380 *C. kirlia*	MH821705.1 *C. tattakana tattakana*	JX489629.1 *C. tattakana tattakana*	JN032707.1 *C. tattakana tattakana*	MH821702.1 *C.* sp.
PP910380 *C. kirlia*		1.20	1.20	1.18	1.2
MH821705.1 *C. tattakana tattakana*	7.40		0	0.56	0.73
JX489629.1 *C. tattakana tattakana*	7.40	0		0.56	0.73
JN032707.1 *C. tattakana tattakana*	7.19	1.82	1.82		0.76
MH821702.1 *C.* sp.	7.61	3.32	3.32	3.32	

According to the original description, *C. kirlia* sp. nov. differs from *C. aderuensis* at least by following: HT 0.26–0.30 mm (*C. aderuensis*: 0.37 mm); WA 0.18–0.21 mm (*C. aderuensis*: 0.23 mm).

Molecular analyses

The phylogenetic results illustrate the evolutionary relationships among some species within the tribe Cerataphidini, highlighting the new species marked in red. The sequences of *C. kirlia* and *C. tattakana tattakana* cluster into two distinct clades, indicating clear genetic divergence between them (Fig. 4).

Genetic distance threshold has been used as the basis for species classification, and in aphid groups, a generally applicable threshold range is from 2% to 2.5% (Liu ei al. 2013; Lee et al. 2017; Zhu et al. 2017; Li et al. 2019, 2023). The K2P distances between *C. kirlia* and other species was around 7.19–7.61% (Table 3). This significant genetic distance, exceeding the typical threshold range, supports *C. kirlia* as a distinct species.

Discussion

When the genus *Chaitoregma* was established by Hille Ris Lambers and Basu (1966), they redescribed *C. tattakana tattakana* only using the samples collected

from southern Himalayas. There could be some subspecific differences between these samples, which could have led to inaccuracies in their redescription.

On Blackman and Eastop's website "Aphid on world's plants" (Blackman and Eastop 2024), they mentioned that *C. aderuensis* was not clearly distinct from *C. tattakana tattakana* based solely on the original description. After examining the original description, we determined that the shape of the frontal horns is key in distinguishing them: the frontal horns of *C. aderuensis* are narrowed on the apical part, while the frontal horns of *C. tattakana tattakana* are broadly rounded at the apical part. This distinction is based solely on the original description, and we need more sampling in the future to confirm the relationship between these two species.

According to the original description, the subspecies *C. tattakana suishana* can be distinguished from *C. tattakana tattakana* by its yellowish-brown body color in life, frontal horns not constricted at the base and slightly narrowed towards the apex, SIPH_DW longer, about 0.037 mm, and a slightly less sclerotic body (Takahashi 1929). These limited features indicate that *C. tattakana suishana* should likely be considered a distinct species rather than a subspecies. In the future, we need more sampling or the opportunity to examine type specimens to clarify the relationships between these species (subspecies).

Key to species of *Chaitoregma* (Apterous viviparous females)

1 Body yellow in life..*C. tattakana suishana*
– Body hazy bule purple in life **2**
2 Abdominal tergites I–VII each with 1 pair of wax gland plates on marginal sclerites, composed of irregularly-shaped to rounded wax gland facets....
....*C. kirlia* **sp. nov.**
– Abdominal tergites I–VII only with roundish stippled wax facets, which are not in groups...**3**
3 Head narrowed between antenna, and horns narrowed on apical part.......
....*C. aderuensis*
– Horns not expanded at base, not narrowed toward apex, but sometimes very slightly narrowed toward base, broadly rounded at apical part ....
....*C. tattakana tattakana*

Additional information

Conflict of interest

The authors have declared that no competing interests exist.

Ethical statement

No ethical statement was reported.

Funding

Author contributions

Writing - original draft: YW. Writing - review and editing: XH.

Author ORCIDs

Yizhe Wang ⬤ https://orcid.org/0009-0004-4703-2226
Xiaolei Huang ⬤ https://orcid.org/0000-0002-6839-9922

Data availability

All of the data that support the findings of this study are available in the main text.

References

Aoki S, Kurosu U (2010) A review of the biology of Cerataphidini (Hemiptera, Aphididae, Hormaphidinae), focusing mainly on their life cycles, gall formation, and soldiers. Psyche, a Journal of Entomology 2010: 380351. https://doi.org/10.1155/2010/380351

Basant AK, Ghosh AK (1985) Monograph on oriental aphidoidea: key to the genera and synoptic list. Zoological Survey of India 16: 1–118.

Blackman RL, Eastop VF (1984) Aphids on the World's Crops: an Identification and Information Guide. John Wiley & Sons, Chichester. 466 pp.

Blackman RL, Eastop VF (2024) Aphids on the World's Plants: an Online Identification and Information Guide. https://aphidsonworldsplants.info/ [Accessed: June 6, 2024].

Chen J, Jiang LY, Qiao GX (2014) A total-evidence phylogenetic analysis of Hormaphidinae (Hemiptera: Aphididae), with comments on the evolution of galls. Cladistics 30: 26–66. https://doi.org/10.1111/cla.12024

Cheng ZT, Huang XL (2023) Two new species of *Aphis* (*Toxoptera*) Koch (Hemiptera, Aphididae) from China. ZooKeys 1172: 31–46. https://doi.org/10.3897/zookeys.1172.106518

Eastop VF, Hille Ris Lambers D (1976) Survey of the World's Aphids. Dr. W. Junk, The Hague, 573 pp.

Edgar RC (2004) MUSCLE: a multiple sequence alignment method with reduced time and space complexity. BMC Bioinformatics 5: 113. https://doi.org/10.1186/1471-2105-5-113

Fang Y, Qiao GX, Zhang GX (2006) Morphometric variation of eight aphid species feeding on the leaves of bamboos. Acta Entomologica Sinica 49(6): 991–1001. https://doi.org/10.16380/J.KCXB.2006.06.016

Favret C (2024) Aphid Species File. http://Aphid.SpeciesFile.org [Accessed: June 6, 2024]

Foottit RG, Maw HE, Von Dohlen CD, Hebert PD (2008) Species identification of aphids (Insecta: Hemiptera: Aphididae) through DNA barcodes. Molecular Ecology Resources 8: 1189–1201. https://doi.org/10.1111/j.1755-0998.2008.02297.x

Fukatsu T, Aoki S, Kurosu U, Ishikawa H (1994) Phylogeny of Cerataphidini aphids revealed by their symbiotic microorganisms and basic structure of their galls: implications for host-symbiont coevolution and evolution of sterile soldier castes. Zoological Science 11(4): 613–623.

Ghosh MR, Pal PK, Raychaudhuri DN (1977) Studies on the aphids (Homoptera: Aphididae) from eastern India 21. The genus *Astegopteryx* Karsch and other related genera (Hormaphidinae), with descriptions of three new genera and two new species. Proceedings of the Zoological Society, Calcutta 27: 81–116.

Hille Ris Lambers D, Basu AN (1966) Some new or little known genera, subgenera, species and subspecies of Aphididae from India (Homoptera, Aphididae). Entomologische Berichten 26(1): 12–20. https://natuurtijdschriften.nl/pub/1014032/EB1966026001004.pdf

Huang XL, Xiang Yu JG, Ren SS, Zhang RL, Zhang YP, Qiao GX (2012), Molecular phylogeny and divergence times of Hormaphidinae (Hemiptera: Aphididae) indicate Late Cretaceous tribal diversification. Zoological Journal of the Linnean Society 165: 73–87. https://doi.org/10.1111/j.1096-3642.2011.00795.x

Kimura M (1980) A simple method for estimating evolutionary rates of base substitutions through comparative studies of nucleotide sequences. Journal of Molecular Evolution 16(2): 111–120. https://doi.org/10.1007/BF01731581

Lee Y, Lee W, Kanturski M, Foottit RG, Akimoto SI, Lee S (2017) Cryptic diversity of the subfamily Calaphidinae (Hemiptera: Aphididae) revealed by comprehensive DNA barcoding. PLoS ONE 12: e0176582. https://doi.org/10.1371/journal.pone.0176582

Li Q, Yao JM, Zeng LD, Lin XL, Huang XL (2019) Molecular and morphological evidence for the identity of two nominal species of *Astegopteryx* (Hemiptera, Aphididae, Hormaphidinae). ZooKeys 833: 59–74. https://doi.org/10.3897/zookeys.833.30592

Li Q, Liu Q, Yu YH, Lin XL, He XY, Huang XL (2023) Revealing cryptic diversity and population divergence in subtropical aphids through DNA barcoding. Zoologica Scripta 52(5): 517–530. https://doi.org/10.1111/zsc.12613

Liu QH, Jiang LY, Qiao GX (2013) DNA barcoding of Greenideinae (Hemiptera: Aphididae) with resolving taxonomy problems. Invertebrate Systematics 27: 428–438. https://doi.org/10.1071/IS13014

Nieto Nafría JM, Favret C, Akimoto S-ichi, Barbagallo S, Chakrabarti S, Mier Durante MP, Miller GL, Qiao GX., Sano M, Pérez Hidalgo N, Stekolshchikov AV, Węgierek P (2011) Register of genus-group taxa of Aphidoidea. In: Nieto Nafría JM, Favret C (Eds) Registers of Family-group and Genus-group Taxa of Aphidoidea (Hemiptera Sternorrhyncha). Universidad de León, León, 81–404.

Qiao GX, Zhang GX (2003) *Ctenopteryx* (Hemiptera: Hormaphidinae), a new genus from China, and a description of a new species. The Pan-Pacific Entomologist 79(2): 145–150.

Qiao GX, Jiang LY, Chen J, Zhang GX, Zhong TS (2018) Fauna of China (Hemiptera: Hormaphididae and Phloeomyzidae). China Science Press, Beijing, 398 pp.

Remaudière G, Remaudière M (1997) Catalogue of the World's Aphididae. INRA, Paris, 473 pp.

Shinji GO (1941) Monograph of Japanese Aphididae. Shinkyo Sha Shoin, Tokyo, 1215 pp.

Stern DL, Aoki S, Kurosu U (1997) Determining aphid taxonomic affinities and life cycles with molecular data: a case study of the tribe Cerataphidini (Hormaphididae: Aphidoidea: Hemiptera). Systematic Entomology 22(1): 81–96. https://doi.org/10.1046/j.1365-3113.1997.d01-20.x

Takahashi R (1925) Aphididae of Formosa Part 4. Report of the Department of Agriculture Government Research Institute Formosa 16: 65 pp.

Takahashi R (1929) Notes on some Formosan Aphididae (3). The Journal of Natural History Society of Taiwan. Natural History Society of Taiwan 19(105): 525–532.

Takahashi R (1931) Aphididae of Formosa Part 6. Report of the Department of Agriculture Government Research Institute Formosa 53: 127 pp.

Takahashi R (1935) Additions to the aphid fauna of Formosa (Hemiptera), III. Philippine Journal of Science 56(4): 499–507.

Tamura K, Stecher G, Kumar S (2021) MEGA11: Molecular Evolutionary Genetics Analysis version 11. Molecular Biology and Evolution 38: 3022–3027. https://doi.org/10.1093/molbev/msab120

Tao CC (1991) Aphid Fauna of Taiwan Province, China. Taiwan Provincial Museum, Taipei, 327 pp.

Zhu XC, Chen J, Chen R, Jiang LY, Qiao GX (2017) DNA barcoding and species delimitation of Chaitophorinae (Hemiptera, Aphididae). ZooKeys 656: 25–50. https://doi.org/10.3897/zookeys.656.11440

Four new species of *Leuctra* Stephens, 1836 from the Balkans (Plecoptera, Leuctridae)

Dávid Murányi[1], Tibor Kovács[2]

1   Department of Zoology, Eszterházy Károly Catholic University, Leányka út 6, Eger H-3300, Hungary
2   Mátra Museum of the Hungarian Natural History Museum, Kossuth Lajos u. 40, Gyöngyös H-3200, Hungary
Corresponding author: Dávid Murányi (d.muranyi@gmail.com)

Abstract

Four, presumably microendemic new *Leuctra* species are described on the basis of morphology of the adult males and females. Each species was collected only in a single mountain range of the western Balkans: *Leuctra enigma* Kovács & Murányi, **sp. nov.** (Albania, Çermenikë), *L. golija* **sp. nov.** (Serbia, Golija), *L. puskasi* **sp. nov.** (Bosnia & Herzegovina, Kozara), *L. visitor* **sp. nov.** (Montenegro, Visitor). Their morphological affinities and ecology are discussed, phylogenetic relations will be described in the framework of ongoing molecular studies of Balkan *Leuctra* species. The occurrences of the new species are depicted on a map. A list of Balkan endemic *Leuctra* species is given. *Leuctra dalmoni* Vinçon & Murányi, 2007 is new for Albania and Montenegro, *Nemoura uncinata* Despax, 1934, *N. marginata* Pictet, 1836 and *Isoperla buresi* Raušer, 1962 are new for Albania, *Nemoura sciurus* Aubert, 1949 is new for Bosnia & Herzegovina, while *Capnia* s. l. *vidua rilensis* Raušer, 1962 and *L. metsovonica* Aubert, 1956 are new for Montenegro.

Key words: Albania, Bosnia & Herzegovina, *Leuctra enigma*, *L. golija*, *L. puskasi*, *L. visitor*, Montenegro, Serbia

Introduction

The Balkan Peninsula is one of the hot spots of West Palaearctic Plecoptera diversity, with more than 200 species reported from the area to date (Graf et al. 2009; DeWalt et al. 2023). However, exploration of the region is far from complete (Sánchez-Campaña et al. 2023), and our knowledge on the fauna of different countries rather unbalanced (Kaćanski 1979; Popijač and Sivec 2009b; Murányi et al. 2014b; Petrović et al. 2014; Karaouzas et al. 2016; Pešić et al. 2018; Tyufekchieva et al. 2019; Bilalli et al. 2020; Murányi and Kovács 2024) According to the latest checklist (Murányi 2009a), the Balkans harbours 197 species, of which 84 have wider distribution, while 113 species are endemic or subendemic to the peninsula. Since then, twelve new species and a subspecies were described from the Balkans (Murányi 2009b, 2011; Graf and Bálint 2010; Graf et al. 2012, 2018; Kovács et al. 2012; Murányi et al. 2014a; Vinçon 2015; Hlebec et al. 2021; Reding et al. 2023), and eleven species were reported first from the peninsula (Popijač and Sivec 2009a; Petrović et al. 2014; Kazanci 2015).

During the last twenty years, we conducted several collecting trips to all Balkan countries. Some of the results, mostly new species descriptions, were published separately but the bulk of the faunistic data and several undescribed species still remained unpublished. We faced several complex taxonomic problems that requires an integrative approach (e.g., Murányi et al. 2016), and so most species descriptions were postponed. While molecular studies are underway, herein we give the morphological description of four distinctive new *Leuctra* Stephens, 1836, three of which were collected in the Dinaric, and one in the Western-Central Balkans (Fig. 1).

Materials and methods

Specimens were collected by hand or by beating sheet and stored in vials with 70% ethanol. Further specimens for molecular studies were transferred in 96% ethanol. Holotypes and most paratypes are deposited in the Collection of Smaller Insect Orders, Department of Zoology, Hungarian Natural History Museum, Budapest, Hungary (**HNHM**) and in the Mátra Museum of the Hungarian Natural History Museum, Gyöngyös, Hungary (**MM**), further paratypes are deposited in the Monte L. Bean Life Science Museum, Brigham Young University, Provo, Utah, US (**BYU**), Gilles Vinçon Collection, Grenoble, France (**CGV**), Department of Zoology, Eszterházy Károly Catholic University, Eger, Hungary (**EKCU**) and in the Stuttgart State Museum of Natural History, Stuttgart, Germany (**SMNS**).

Drawings were made with the aid of a drawing tube applied on a Nikon SMZ1500 and a Nikon SMZ10 microscopes. Terminology of the species description follows Murányi (2007) and Vinçon and Murányi (2007).
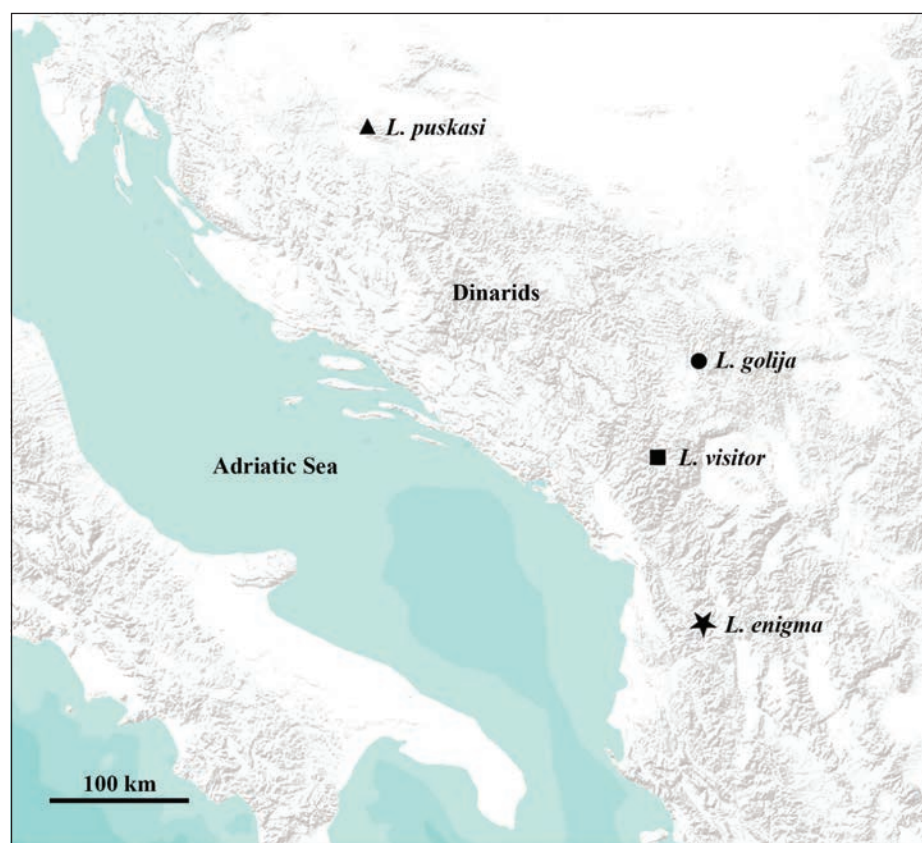
Figure 1. Collection sites of the four new *Leuctra* species.

Distribution and ecology of the Balkan endemic *Leuctra* were compiled from the following literature (in addition to the original descriptions): Braasch and Joost (1971), Darilmaz et al. (2016), Ikonomov (1986), Kaćanski (1975), Kovács and Murányi (2023), Murányi (2011), Murányi et al. (2014b, 2016), Pešić et al. (2018), Petrović et al. (2014), Ravizza (2002a), Sivec (1980), and Tierno de Figueroa and Fochetti (2001).

Taxonomic account

Leuctra enigma Kovács & Murányi, sp. nov.

https://zoobank.org/F0FF7DC4-7EA8-4BDE-9042-34D956A63609
Figs 1–4, 7A, E

Type material. *Holotype* male: ALBANIA: • Dibër county, Bulqizë municipality, Çermenikë Mts, brooks in open forest beneath Mt. Kaptinë, 1600 m, 41°23.199'N, 20°17.338'E, 10.x.2012 (field number: loc.25), leg. P. Juhász, T. Kovács, D. Murányi, G. Puskás (MM: 2012-178, PLETYP-30). *Paratypes*: • same locality and date: 1♂ 1♀ (BYU) • 1♂ 1♀ (CGV) • 5♂ 6♀ (HNHM: PLP4184) • 5♂ 10♀ (MM: 2012-178, PLETYP-31) • 1♂ 1♀ (SMNS).

Other materials. • Same locality, 21.vi.2012 (loc.58), leg. Z. Fehér, T. Kovács, D. Murányi: 3 putative larvae (HNHM: PLP4099) • 2 putative larvae (MM: 2012-1) • same locality, 27.v.2013 (loc.19), leg. P. Juhász, T. Kovács, G. Magos, G. Puskás: 2 putative larvae (MM: 2013-19).

Diagnosis. Macropterous in both sexes. Male tergite VII with huge membranous portion; tergite VIII with large, triangular posteromedial process, terminating in bi- or trilobed tip; tergite IX with large, lobed posteromedial sclerite supported by anterior sclerotised spots; tergite X posterior margin with deep and wide notch; sternite IX bears a vesicle shorter than 1/5 segment length; paraproct tip pointed, specillum slightly longer than paraproct, tip blunt. Female terga I–VIII with medial sclerite; subgenital plate with large lobes terminating in swollen and raised apex, central plate with anterolateral swellings and pale medial portion, posterior portion trapezoid in ventral view and nose-shaped in lateral view, well past by the lobes. Larva stout and with long setation, eyes small, clypeus lacks pointed corners.

Description. Medium sized, robust species, both sexes macropterous. Forewing length: holotype 6.0 mm, male paratypes 5.8–6.4 mm, female paratypes 6.5–7.8 mm; body length: holotype 6.5 mm, male paratypes 6.0–6.8 mm, female paratypes 8.0–8.8 mm. Setation generally short and dense. General colour dark brown. Head brown with distinct M-line and occipital rugosities, compound eyes relatively small; antennae dark brown, palpi brown. Pronotum brown to dark brown, wider than long and having rounded corners, rugosities distinct. Legs brown to dark brown, tarsi slightly darker. Wings brownish but hyaline, venation brown.

Male abdomen (Figs 2A–E, 7A): Tergite I membranous posteriorly and medially, with two medial spots; tergite II poorly sclerotised anteriorly. Transverse row of four pigmented spots distinct on terga II–VIII. Terga II–III with poorly developed antecosta, terga IV–VII with entire antecosta, terga III–VI full sclerotised. Tergite VII with huge medial membranous portion, a rounded or arrow-shaped sclerotised area extends between the medial pair of pigmented spots. Tergite
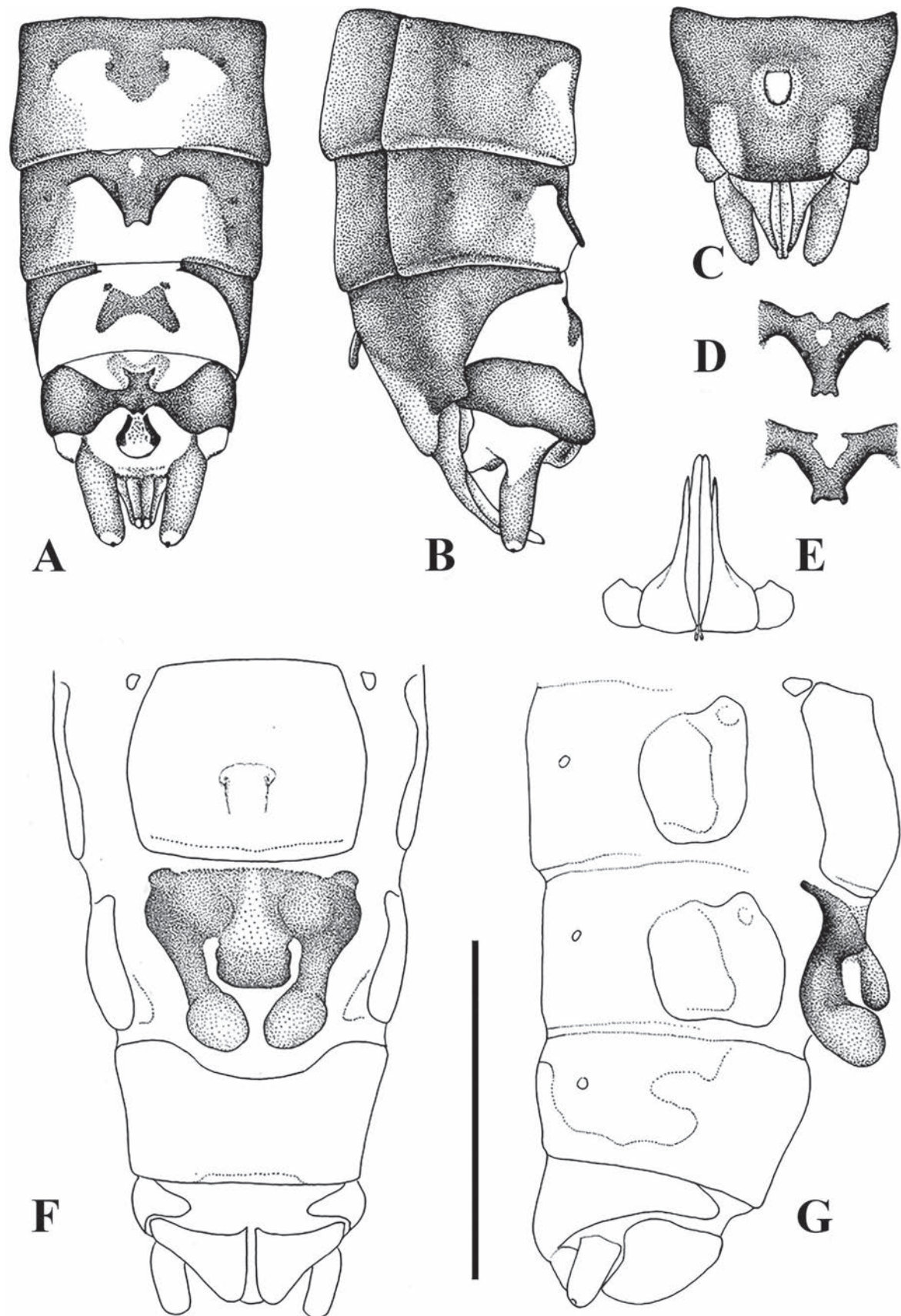
Figure 2. Terminalia of *Leuctra enigma* sp. nov. with setation omitted **A** male terminalia, dorsal view **B** same, lateral view **C** same, ventral view **D** variations of male tergite 8, dorsal view **E** male paraprocts and specillae, caudal view **F** female terminalia, ventral view **G** same, lateral view. Scale bar: 1 mm.
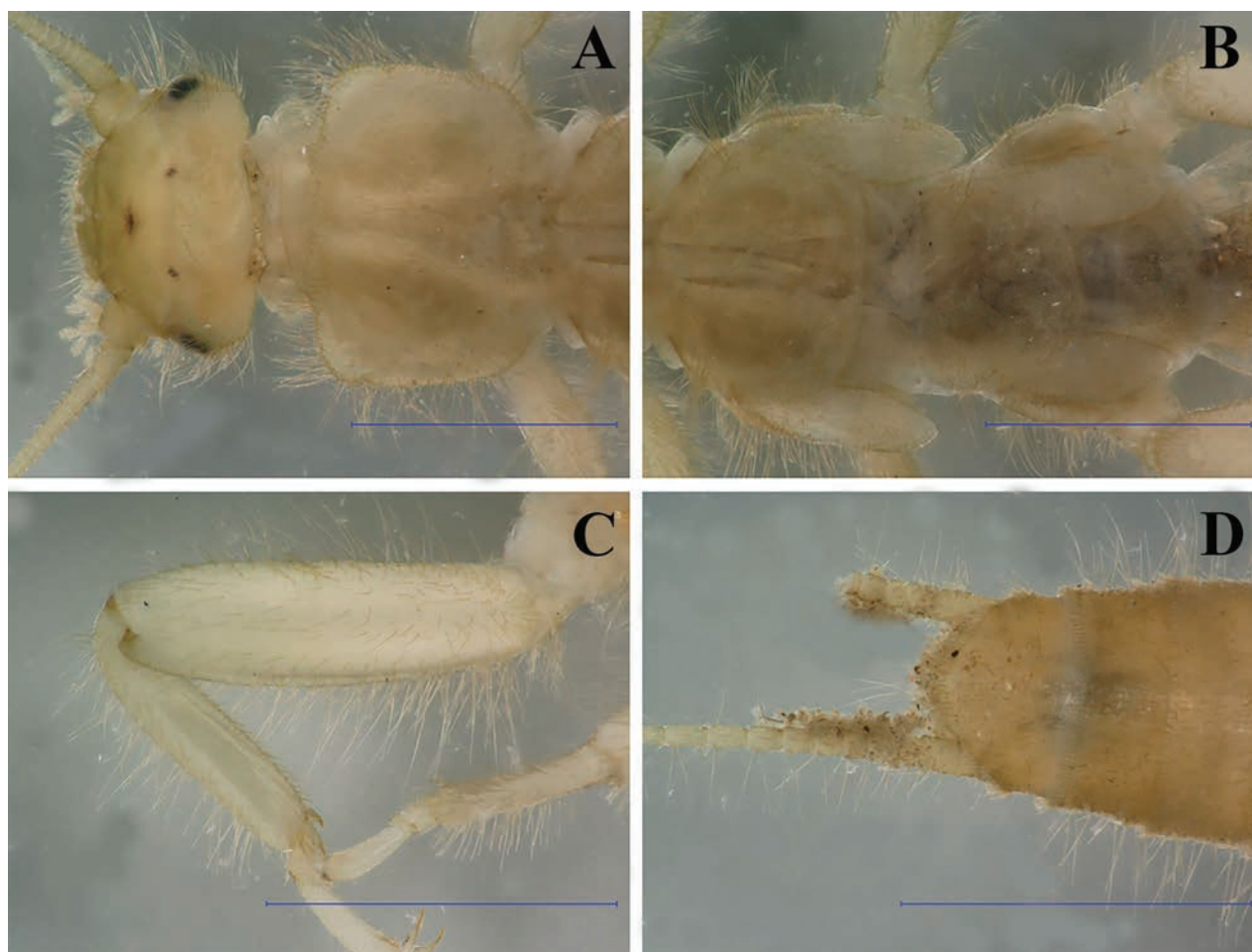
Figure 3. Putative larva of *Leuctra enigma* sp. nov. **A** head and pronotum, dorsal view **B** meso- and metathorax, dorsal view **C** hind leg, dorsal view **D** terminalia, dorsal view. Scale bars: 1 m.

VIII: antecosta nearly entire, gradually weakened in the medial 1/5, sometimes interrupted by a narrow medial notch; the posteromedial process is triangular, originated in the anterior 1/3 of the segment and reach the posterior 1/3 by its weakly bilobed or trilobed tip, medial portion with small membranous portion, medial pair of pigmented spots recognisable by the lateral sides of the process; the process is not darker than the lateral areas of the segment, wider than 1/3 segment width, slightly erect in side view; lateral edges of the medial membranous area obscure, while the anterior edge is sharply defined. Tergite IX mostly membranous, antecosta interrupted in the medial 1/3 of its length; posteromedial sclerite large, weakly bilobed anteriorly while posterior portion with long, diverging lobes, the sclerite is anteriorly supported by two sclerotised spots. Anterior margin of tergite X bilobed anteriorly but sclerotisation of lobes obscure; posterior margin with deep notch, as wide as 1/2 tergite width; medial portion of the notch with small protrusion at the origin of epiproct. Epiproct drop-shaped, sclerotised only at its sides, stalk gradually widening. Cercus simple, covered with long setae. Sterna II–VIII simple, sternite IX bears a very small, rounded vesicle shorter than 1/5 of segment length; posterolateral portions of the sternum pale coloured and weakly sclerotised. Paraproct with moderately wide base, narrowing after basal 1/3, apex gently curved in lateral view and tapering towards a pointed tip. Base of paraproct connected to a subrectangular
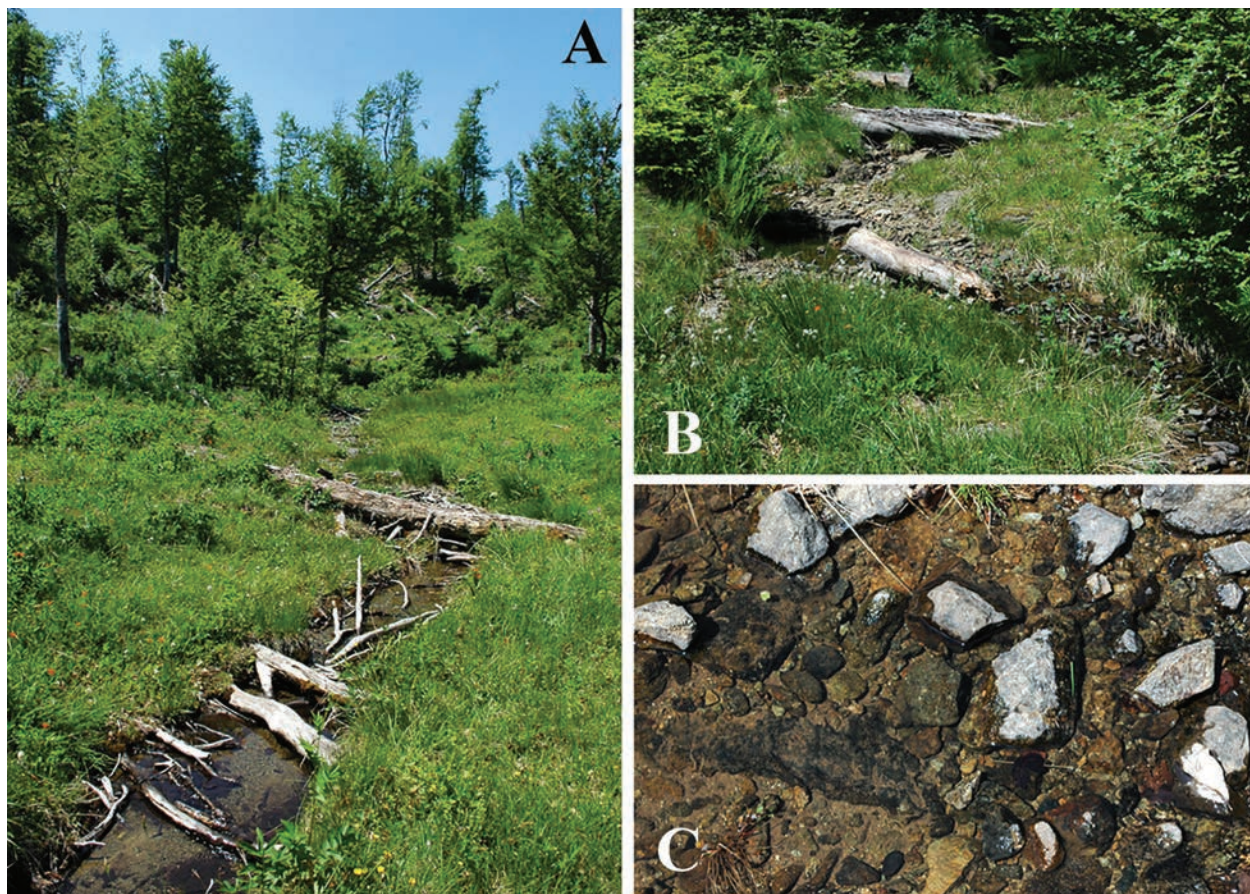
Figure 4. Habitat of *Leuctra enigma* sp. nov. **A** type locality: partly open brook in the Çermenikë Mts. **B** section at forest edge **C** substrate of the type locality.

lateral expansion. Specillum longer than the paraproct, gently curved in lateral view and ending in a blunt tip.

Female abdomen (Figs 2F–G, 7E): Terga I–VIII with transverse row of four pigmented spots clearly visible; terga I–VIII mostly membranous but with lateral sclerites and a medial sclerite as well; medial sclerite is a longitudinal stripe, more widened on terga II and III; tergite IX mostly, tergite X fully sclerotised. Sterna I–VII simple, sterna II–VII with one subrectangular median sclerite and two small anterior sclerites that are not fused. Subgenital plate of sternite VIII large and complex, not fused with other sclerites, lacks distinct setation. It has two large and well-defined lobes, darker brown than the remainder of the plate; the lobes terminate in a swollen, rounded apex that are paler than the base of the lobes, raised in lateral view and converging in ventral view. The central plate has two anterolateral swellings, medial portion pale and lightly sclerotised; the plate terminates in a trapezoidal bulge, raised and nose-shaped in lateral view, clearly separated from the lateral lobes that extend beyond it. Sternite IX with wide but shallow anterior indentation. Paraproct, cercus, and epiproct simple. Spermathecal sclerite thin, ring-shaped, with small anterior teeth and long posterior teeth.

Putative larva (Fig. 3): Body stout, length of the penultimate or younger larvae 7.0–7.5 mm. General colour pale brown, without distinctive markings, pilosity long and distinct. Head much wider than long, eye small, shorter than the widely rounded occipital region, ocelli distinct, clypeus not modified. Palpi simple,

antenna longer than 1/2 body length. Pronotum much wider than long. Wing pads under development, posterior edge of meso- and metathorax between wing pads rounded, not like the typical *prima-hippopus-inermis* group shape. Legs short, tibiae not longer than femora, stretched hind leg reaches back to the seventh abdominal segment. Abdomen stout, integument matt pale brown, paraproct triangular. Cercus nearly as long as abdomen, with 25 cylindrical segments, medial segments twice longer than wide. Setation of the larva: antenna and palpi with short setae but head and clypeus with dense and erect setation, longest setae as long as the distance between hind ocelli; marginal setae continuous on pronotum, as long as the setae of the head; wing pads with similar long, erect and dense setae; femora and tibiae with hairs as long as the width of each femora, distributed on the whole surface but not forming swimming fringe; tarsi with short and scarce setation; abdominal segments evenly setose, with erect setae approximately as long as the setae of the head; cercomeres bald besides the erect apical whorl, slightly shorter than abdominal setae.

Affinities. The new species is an isolated member of the *hippopus* group. The male is rather distinctive, the only *Leuctra* with comparable posteromedial process of tergite VIII is the Caucasian-Anatolian *L. martynovi* Zhiltzova, 1960. However, *L. martynovi* differs by larger posteromedial sclerite of tergite IX, shallow posterior notch of tergite X, and larger vesicle of sternite IX. The subgenital plate of the female shows similarity with the narrowly defined *hippopus* group (*hippopus* subgroup, sensu, e.g., Ravizza 2002b), having large lobes and a pale central plate. However, the combination of bulging lobes of the subgenital plate, central plate with anterolateral swellings and trapezoid, bulging posterior portion, already distinguish it from all other *Leuctra*. The putative larva is distinctive by its stout body and dense, long setation. Among the Balkanian *Leuctra*, only *L. nigra* (Olivier, 1811) and *L. hirsuta* Bogoesco & Tabacaru, 1960 are having similar long setation, however, their body is less stout, and their eyes are larger. The Alpine-Carpathian *L. braueri* Kempny, 1898 has similarly stout and hairy larva, but its clypeus is armed with prominent pointed corners.

Distribution and ecology. The species was collected at a single high elevation site of the Çermenikë Mts, central Albania (Fig. 1). It was not found at any further localities, despite of intensive collecting efforts during the last twenty years conducted in central Albania. The habitat is disturbed by partial deforestation, most sections of the two confluent brooks run open or in bush of young beech (Fig. 4A, B). The brooks run moderately fast, 0.5–1 meter wide and not deeper than 20 centimetres (both in June and October). The substrate is stony, mixed with small sandy patches, few patches of dead wood and partly submerged plants (Fig. 4B, C). The specimens were swarming together with *L. hirsuta* in October 2012. When we visited the locality in late spring and early summer, a more diverse fauna was found: 21.vi.2012 (leg. Z. Fehér, T. Kovács, D. Murányi): adults of *Brachyptera helenica* Aubert, 1956b, *Leuctra hippopoides* Kaćanski & Zwick, 1970, *L. metsovonica* Aubert, 1956, *Nemurella pictetii* (Klapálek, 1900), *Nemoura cinerea cinerea* (Retzius, 1783), *N. marginata* Pictet, 1836, *Perla* cf. *pallida* Guérin-Méneville, 1843, *Isoperla buresi* Raušer, 1962 and *Siphonoperla neglecta* (Rostock, 1881); 27.v.2013 (leg. P. Juhász, T. Kovács, G. Magos, G. Puskás): adults of *B. helenica*, *L. hippopoides*, *L.* cf. *dalmoni* Vinçon & Murányi, 2007, *Nemoura cinerea cinerea*, *N. uncinata* Despax, 1934, *N. marginata*, *Nemurella pictetii*, *Siphonoperla neglecta* and *S. graeca* (Aubert, 1956), and

putative larvae of the new species were found. *Leuctra* cf. *dalmoni*, *Nemoura uncinata*, *N. marginata* and *Isoperla buresi* are new findings for Albania. Records of other aquatic insects collected at the type locality were already published: Ephemeroptera (Kovács and Murányi 2013): *Baetis muticus*, *Habrophlebia lauta*; Odonata (Murányi and Kovács 2013): *Cordulegaster bidentata*; Trichoptera (Oláh and Kovács 2012b, 2013): *Agapetus iridipennis*, *Chaetopteryx bosniaca*, *Psychomyia pusilla*, *Cyrnus trimaculatus*, *Lepidostoma hirtum*, *Drusus plicatus*, *Mystacides azureus*.

Etymology. The name *enigma* (Latin; enigma or riddle) refers to the strange fact that such a distinctive new species was found only at a single locality. Used as a noun, gender neutral.

Leuctra golija sp. nov.

https://zoobank.org/776454AB-1086-4B10-A56B-636E13224914
Figs 1, 5, 6, 7B, F

Type material. *Holotype* male: Serbia: • Moravica district, Ivanjica municipality, Golija Mts, Dajići, Moravica Stream at Milošica, 1505 m, 43.3384°N, 20.2507°E, 6.v.2023 (field number: loc.16), leg. L.P. Kolcsár, T. Kovács, D. Murányi (MM: 2023-51, PLETYP-32). *Paratypes*: • same locality and date: 1♂ 1♀ (BYU) • 1♂ 1♀ (CGV) • 14♂ 6♀ (EKCU: PLP5721) • 10♂ 3♀ (MM: 2023-51, PLETYP-33) • 1♂ 1♀ (SMNS) • same locality, 26.vi.2018 (loc.1), leg. P. Juhász, T. Kovács, D. Murányi: 1♀ (HNHM: PLP5003) • 1♂ (MM: 2018-43, PLETYP-34) • Raška district, Novi Pazar municipality, Golija Mts, Radaljica, spring brooks in forest edge, 1575 m, 43.2743°N, 20.3467°E, 6.v.2023 (loc.17), leg. L.P. Kolcsár, T. Kovács, D. Murányi: 1♂ (EKCU: PLP5727) • 2♂ 1♀ (MM: 2023-52, PLETYP-35).

Diagnosis. Macropterous in both sexes. Male tergite VII mostly membranous, with bicoloured antecosta; tergite VIII with converging pair of slender, pale brown processes, medial membranous area rounded between the processes, triangular between the processes and the lateral sclerotised portions; tergite IX with small posteromedial sclerite, divided into leaf-like portions; tergite X posterior margin with wide and deep notch; epiproct sclerotised only at its sides, stalk nearly as long as the rounded apex; sternite IX bears a vesicle 1/2 as long as segment length; specillum slightly longer than paraproct, tip of paraproct acute, tip of specillum blunt. Female subgenital plate large and bicoloured, lobes large, triangular, and not converging, slightly raised in lateral view and the notch between them is triangular; spermathecal sclerite ring-shaped, with large and converging posterior teeth.

Description. Medium sized, slender species, both sexes macropterous. Forewing length: holotype 5.6 mm, male paratypes 5.4–6.0 mm, female paratypes 6.6–7.0 mm; body length: holotype 5.4 mm, male paratypes 5.2–6.4 mm, female paratypes 5.5–7.2 mm. Setation generally short and dense. General colour brown to dark brown. Head and antennae dark brown, palpi brown. Pronotum brown to dark brown, as wide as long or slightly wider, having rounded corners, rugosities distinct. Legs brown to dark brown. Wings brownish but hyaline, venation brown.

Male abdomen (Figs 5A–D, 7B): Tergite I membranous medially, with two medial spots; terga II and III poorly sclerotised anteriorly. Transverse row of
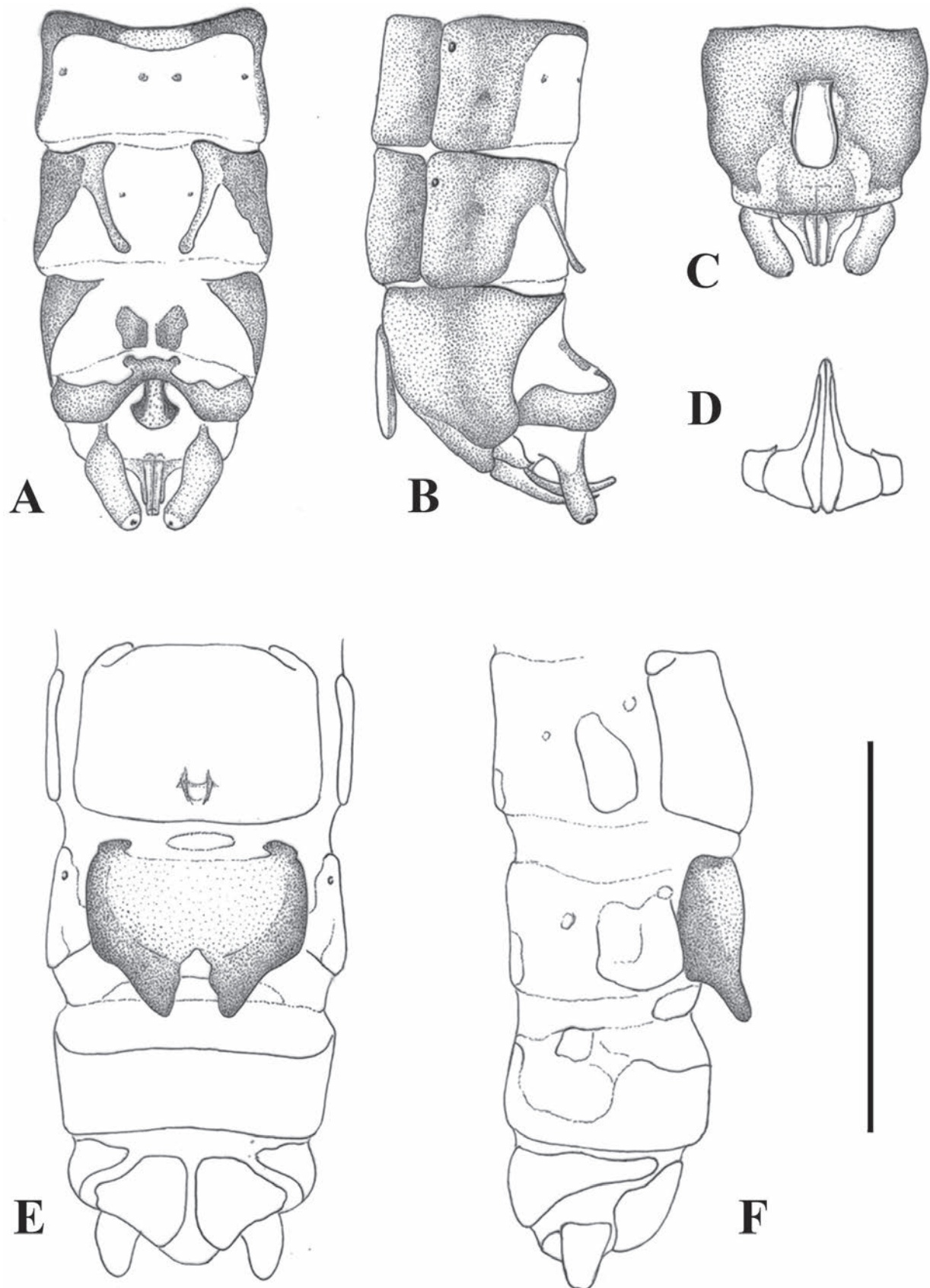
Figure 5. Terminalia of *Leuctra golija* sp. nov. with setation omitted **A** male terminalia, dorsal view **B** same, lateral view **C** same, ventral view **D** male paraprocts and specillae, caudal view **E** female terminalia, ventral view **F** same, lateral view. Scale bar: 1 mm.

Figure 6. Habitat of *Leuctra golija* sp. nov.: Moravica Stream in the Golija Mts (type locality, 23.x.2023).

four pigmented spots distinct on terga II–VII. Terga II–III with widely divided antecosta, terga IV–VII with entire antecosta, terga IV–VI full sclerotised. Tergite VII mostly membranous, sclerotised only laterally and in the widened antecosta that is distinctly bicoloured: dark brown laterally and pale brown medially. Tergite VIII: antecosta medially divided nearly in the 1/2 width of the segment; paired processes originated from the end of antecosta and reaches the posterior end of the segment, pale brown coloured, converging posteriorly, very slender, and only slightly widened apically, raised in lateral view; the medial membranous area well limited, rounded between the processes and with two sclerotised spots, triangular between the processes and the lateral sclerotised portion of the segment. Tergite IX mostly membranous, antecosta interrupted in the medial 1/2 of its length; posteromedial sclerite small, divided into leaf-like portions. Anterior margin of tergite X bilobed anteriorly; posterior margin with deep and wide notch, as wide as 1/2 tergite width. Epiproct large, sclerotised only at its sides, stalk nearly as long as the rounded apex. Cercus simple, covered with long setae. Sterna II–VIII simple. Sternite IX bears a long, tongue-shaped vesicle 1/2 as long as segment length; posterolateral portions of the sternum pale coloured and weakly sclerotised, connected to pale area around the base of vesicle. Paraproct with moderately wide base, narrowing after basal 1/3, apex gently curved in lateral view and tapering towards an acute tip. Base of paraproct connected to a subrectangular lateral expansion, having a small
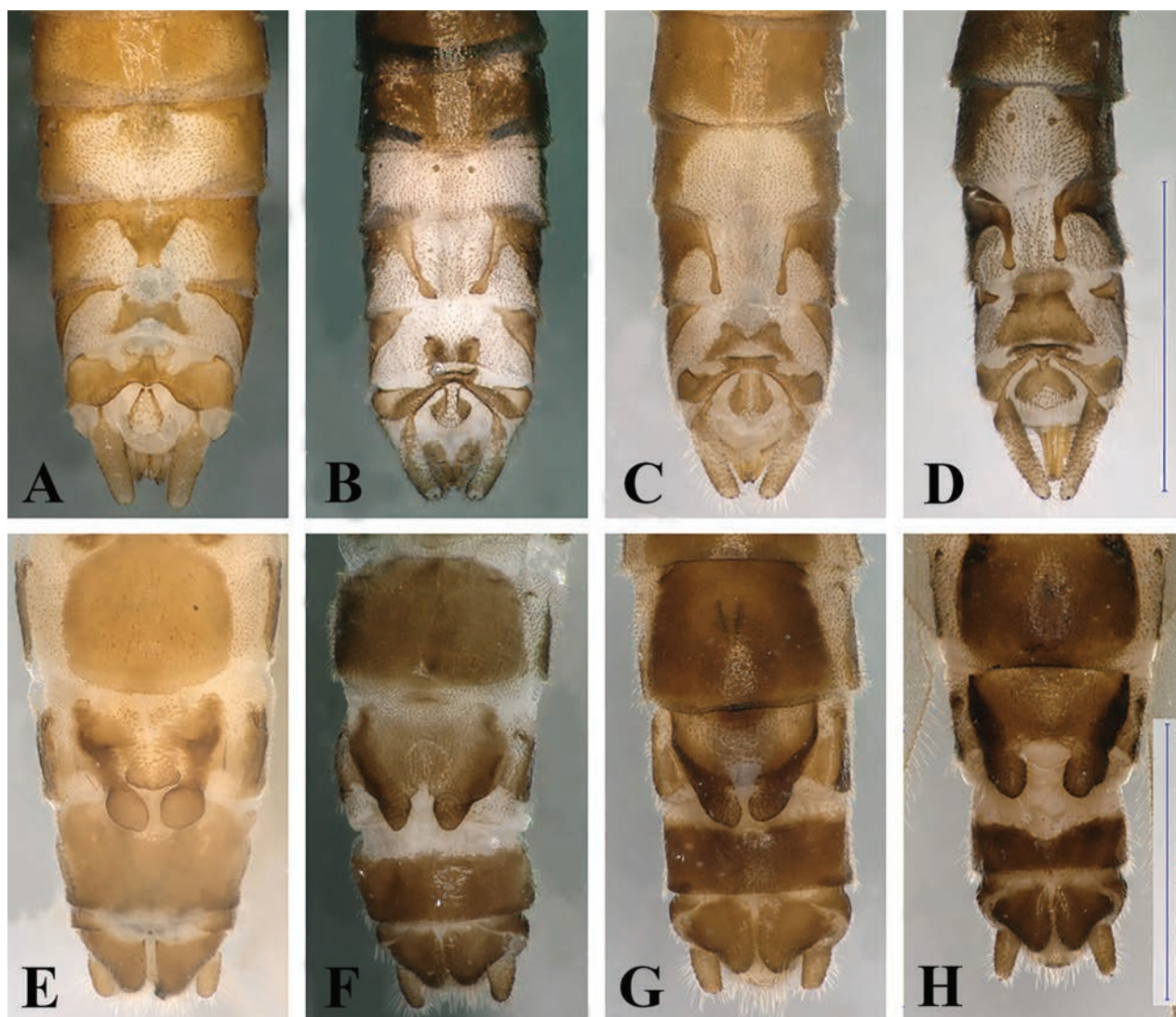
Figure 7. Terminalia of four Balkan members of the *Leuctra hippopus* group **A−D** male terminalia, dorsal view **E−H** female terminalia, ventral view. **A, E** *L. enigma* sp. nov., Çermenikë Mts, Albania **B, F** *L. golija* sp. nov., Golija Mts, Serbia **C, G** *L. pseudohippopus* Raušer, 1965, Stara Planina, Serbia **D, H** *L. hippopoides* Kaćanski & Zwick, 1970, Sutjeska, Bosnia & Herzegovina. Scale bars: 1 mm (**D** for **A−D**, **H** for **E−H**).

inner apical tip. Specillum longer than the paraproct, gently curved in lateral view and ending in a blunt tip.

Female abdomen (Figs 5E, F, 7F): Terga I−VIII with transverse row of four pigmented spots clearly visible; terga I−VIII mostly membranous but with lateral sclerites; small medial sclerite is present on terga VII−VIII, sometimes also on tergite II; tergite IX mostly, tergite X fully sclerotised. Sterna I−VII simple, sterna II−VII with one subrectangular median sclerite and two small anterior sclerites that are fused with median sclerite only on sternite VII. Subgenital plate of sternite VIII large, setation not distinctive; not fused with lateral sclerites but touching with, a small sclerotised portion is visible on the integument anterior to the plate, as well a wider, pale sclerite on the posterior edge of segment. The subgenital plate with two large and well-defined lobes, the plate is distinctly bicoloured: lateral sides and lobes dark brown, while the rest of the plate pale brown. The lobes are triangular, not swollen, slightly raised in lateral view, not

converging in ventral view and overhang the segment end, the notch between them has wavy sides but the proximal part is triangular. The central plate is smooth, only very slightly and evenly bulging in lateral view. Sternite IX without anterior indentation but the anterior 1/3 is membranous. Paraproct, cercus and epiproct simple. Spermathecal sclerite thin, ring-shaped, with small anterior teeth and converging, longer posterior teeth.

Affinities. The new species is a member of the narrowly defined *hippopus* group (*hippopus* subgroup, sensu, e.g., Ravizza 2002b), and morphologically closest to the West Balkan endemic *L. hippopoides* and the East Balkan endemic *L. pseudohippopus* Raušer, 1965. The male can be distinguished from both on the basis of a nearly fully membranous tergite VII, convergent pair of processes of tergite VIII that delimit the rounded median membranous area, the membranous area triangular lateral to the processes, the small posteromedial sclerite of tergite IX divided into leaf-like portions, and the epiproct sclerotised only at its sides, but with long stalk. Both *L. hippopoides* and *L. pseudohippopus* have a bell-shaped membranous area on tergite VII, the pair of processes not converging on tergite VIII and delimiting a square median membranous area, while the membranous area is rounded laterad to the processes, their epiproct more heavily sclerotised and with a short stalk; the posteromedial sclerite of tergite IX is divided into triangular portions in *L. pseudohippopus*, while the undivided sclerite is large and trapezoidal in *L. hippopoides*. The island endemic *L. pavesii* Vinçon, 2015 from Cephalonia, Greece, resembling *L. hippopoides* but differs by having a straight specillum in lateral view, contrary to the gentle curve for males of all other Balkan species of the species group. The widespread *L. hippopus* Kempny, 1899, co-occurring with the new species, is morphologically less related, and the male can easily be distinguished by its mostly sclerotised tergite VII, robust paired processes of tergite VIII, large and complex posteromedial sclerite of tergite IX, and heavily sclerotised epiproct with a short stalk. The female of the new species distinctly differs from all members of the narrowly defined *hippopus* group by having triangular lobes of the subgenital plate, contrary to the bulging, rounded, square, or finger-like lobes of the other species. The subgenital plate most resembles the not closely related *L. armata* Kempny, 1899, which has a small central lobule between the base of the lobes.

Distribution and ecology. The species was collected at two high elevation localities of the Golija Mts of southwestern Serbia (Fig. 1). The Golija is a south-eastern range of the Dinarids, a mostly volcanic area with a large plateau, its highest peak reaching more than 1800 meters. Most of the specimens were found at the Moravica Stream, 1−2 meters wide, < 0.5 meter deep, running in alder forest (Fig. 6). The other habitat, where only a few specimens were found, is a spring brook that belongs to the watershed of the Ibar River, being rather steep and only 0.5 meter wide with a few centimetres depth, running at the edge of a beech forest. Both streams have stony substrates mixed with gravel and small sandy patches. We visited the localities three times (Murányi and Kovács 2024): the new species was swarming in early May (6.v.2023, leg. L.P. Kolcsár, T. Kovács, D. Murányi), only a few individuals were found in late June (26.vi.2018, leg. P. Juhász, T. Kovács, D. Murányi), while no specimens were present in October (23.x.2023, leg. T. Kovács, D. Murányi, D. Pifkó). At the Moravica Stream, the following species were found to be cohabiting: *Brachyptera bulgarica* Raušer, 1962 (adults and larvae, May), *B. seticornis* (Klapálek, 1902)

(adults, larvae, and exuviae, May), *Capnia* s.l. *vidua rilensis* Raušer, 1962 (adults, May), *Leuctra nigra* (adults, May and June), *L. cingulata* Kempny, 1899 (adults, October), *L. dalmoni* (adults, May) (Fig. 12D, H), *L. prima* Kempny, 1899 (adults, May), *L.* cf. *balcanica* Raušer, 1965 (adults, June), *Nemoura cinerea cinerea* (adults, June), *N. uncinata* Despax, 1934 (adults, May), *N. marginata* (adults, June), an undescribed *Nemoura* species of the *marginata* group (adults, May), an undescribed *Nemoura* related to *N. bulgarica* Raušer, 1962 (adults, June), *Protonemura praecox praecox* (Morton, 1894) (adults, May), *P. intricata intricata* (Ris, 1902) (adults, June), *P. hrabei* Raušer, 1956 (adults, October), *P. nitida* (Pictet, 1836) (adults, October), *Perla* cf. *pallida* (larvae, May to October), *Isoperla* cf. *russevi* Sowa, 1970 (adults, June), *Chloroperla russevi* Braasch, 1969 (adults, June) and *Siphonoperla neglecta* (adults, June). At the spring brook, a different set of species were collected: *Brachyptera bulgarica* (adults, May), *Leuctra nigra* (adults, May and June), *L. fusca fusca* (Linnaeus, 1758) (adults, October), *L. cingulata* (adults, October), *L. hirsuta* (adults, October), *L. hippopus* (adults, May), *L. dalmoni* (adults, May), *L. prima* (adults, May), *L.* cf. *balcanica* (adults, June), *Amphinemura standfussi* (Ris, 1902) (adults, June), *Protonemura hrabei* (adults, October), an undescribed *Protonemura* species of the *auberti* group (adults in October, larvae in May and June), *Nemoura cinerea cinerea* (adults, June), *N. marginata* (adults, June), the undescribed *Nemoura* species of the *marginata* group (adults, May), the undescribed *Nemoura* related to *N. bulgarica* (adults, June), *Perla* cf. *pallida* (larvae, October), *Isoperla russevi* (adults, June) and an unidentified *Isoperla* (adult female, June).

Etymology. The name *golija* is derived from the Golija Mountains of Serbia, where the new species was found and is probably restricted to these mountains and the nearby ranges. Used as a noun, gender neutral.

Leuctra prima species complex

Within the West Palaearctic, *Leuctra* species are morphologically characterised by having tergal process only on male tergite VIII; closely related autumnal species of this lineage were recently defined as the *L. signifera* group (Reding et al. 2023). A similar, closely related lineage that are emerging during the late winter and spring months can be regarded as the *L. prima* species complex. This species complex consists of three widespread European species (*L. prima*, *L. pseudosignifera* Aubert, 1954, *L. dalmoni*), species restricted to the Alps and the northern Apennines (*L. niveola* Schmid, 1947, *L. helvetica* Aubert, 1956a, *L. ligurica* Aubert, 1962, *L. ravizzai* Ravizza Dematteis & Vinçon, 1994), the Pyrenees (*L. joani* Vinçon & Pardo, 1994), the Transylvanian Alps (*L. transsylvanica* Kis, 1964) and the eastern Balkans (*L. joosti* Braasch, 1970). While redefining the identity of the three widespread species (Vinçon and Murányi 2007), we faced several problems. First, in Western Europe, the Alps, and most of the Carpathians, the morphological distinction of the three species is not problematic; however, we observed notable variability and intermediate (hybrid?) specimens in the Eastern Carpathians and among the sparse Balkan materials. Second, the females of *L. pseudosignifera*, *L. transsylvanica*, and *L. joosti* seemed to be morphologically indistinguishable, and the distinction between the males of *L. transsylvanica* and *L. joosti* proved to be very problematic on the few available specimens. Third, a presumably new species was found among Bosnian

specimens, but we postponed its description because only a single male was available. During the last decade, we collected rich materials in the Balkans, and found several populations where the identity cannot be solved on the basis of morphology. Molecular studies are underway, but two distinctive new species can be described on the basis of their morphology and ecology.

Leuctra puskasi Murányi & Kovács, sp. nov.
https://zoobank.org/9C2CF7D9-F7F4-469C-AF6D-B78117E2078E
Figs 1, 8, 9, 12A, E

Type material. *Holotype* male: Bosnia & Herzegovina • Republika Srpska, Kozara Mts, forest brook along the Gornji Podgradci-Kozarac road, 595 m, 45.0414°N, 16.9040°E, 16.iii.2012 (field number: loc.6), leg. T. Kovács, D. Murányi, G. Puskás (HNHM: PLP4185). *Paratypes:* • same locality and date: 1♂ 1♀ (BYU) • 1♂ 1♀ (CGV) • 10♂ 4♀ (HNHM: PLP3853) • 12♂ 5♀ (MM: 2012-10, PLETYP-36) • 1♂ 1♀ (SMNS).

Diagnosis. Brachypterous in both sexes. Male tergite VII with small membranous portion; tergite VIII with strong posteromedial process that is not erect in side view and bear rounded lobes, membranous area usually shorter than 1/2 of segment length, the posterior margin is nearly straight between the posteromedial process and segment sides; tergite IX with short but wide posteromedial sclerite; tergite X posterior margin with deep but narrow notch; sternite IX bears a vesicle shorter than 1/2 segment length; specillum longer than paraproct, tip subterminally constricted. Female subgenital plate large and trapezoid, incision between the long lobes widening towards the median bulge but not forming a triangular field, median bulge is narrow in ventral view and distinctly raised in lateral view, lacking distinct setation; spermathecal sclerite ring-shaped, with large converging posterior teeth.

Description. Medium sized, slender species, females brachypterous (Fig. 9A), males strongly brachypterous (Fig. 9B, C). Forewing length: holotype 1.4 mm, male paratypes 1.0−1.4 mm, female paratypes 2.6−3.0 mm; body length: holotype 5.4 mm, male paratypes 4.5−5.8 mm, female paratypes 5.5−6.8 mm. Setation generally short and dense. General colour dark brown to blackish. Head and antennae dark brown, palpi brown. Pronotum brown to dark brown, slightly longer than wide and having rounded corners, rugosities distinct. Legs dark brown, tarsi slightly paler. Wings brownish but hyaline, venation brown.

Male abdomen (Figs 8A−E, 12A): Tergite I sclerotised only anteriorly and in lateral stripes, with two medial spots. Transverse row of four pigmented spots distinct on terga II−VII. Terga II and III with medially divided antecosta, tergite II with triangular membranous area anteriorly. Terga IV−VII with entire antecosta and full sclerotised, tergite VII with weakly sclerotised posterior edge and small membranous portion. Tergite VIII: antecosta interrupted by a wide membranous area, each part ends into a small triangular plate; the membranous area is ~ 1/3 segment width, and usually do not reach the 1/2 of the segment length but in some specimens it reach down to 2/3 above the posteromedial process, posterior margin of the membranous portion wavy; the surrounding sclerotisation of the membranous area lighter than the rest of the segment; posteromedial process not darker than the lateral areas of the segment, not erect in side
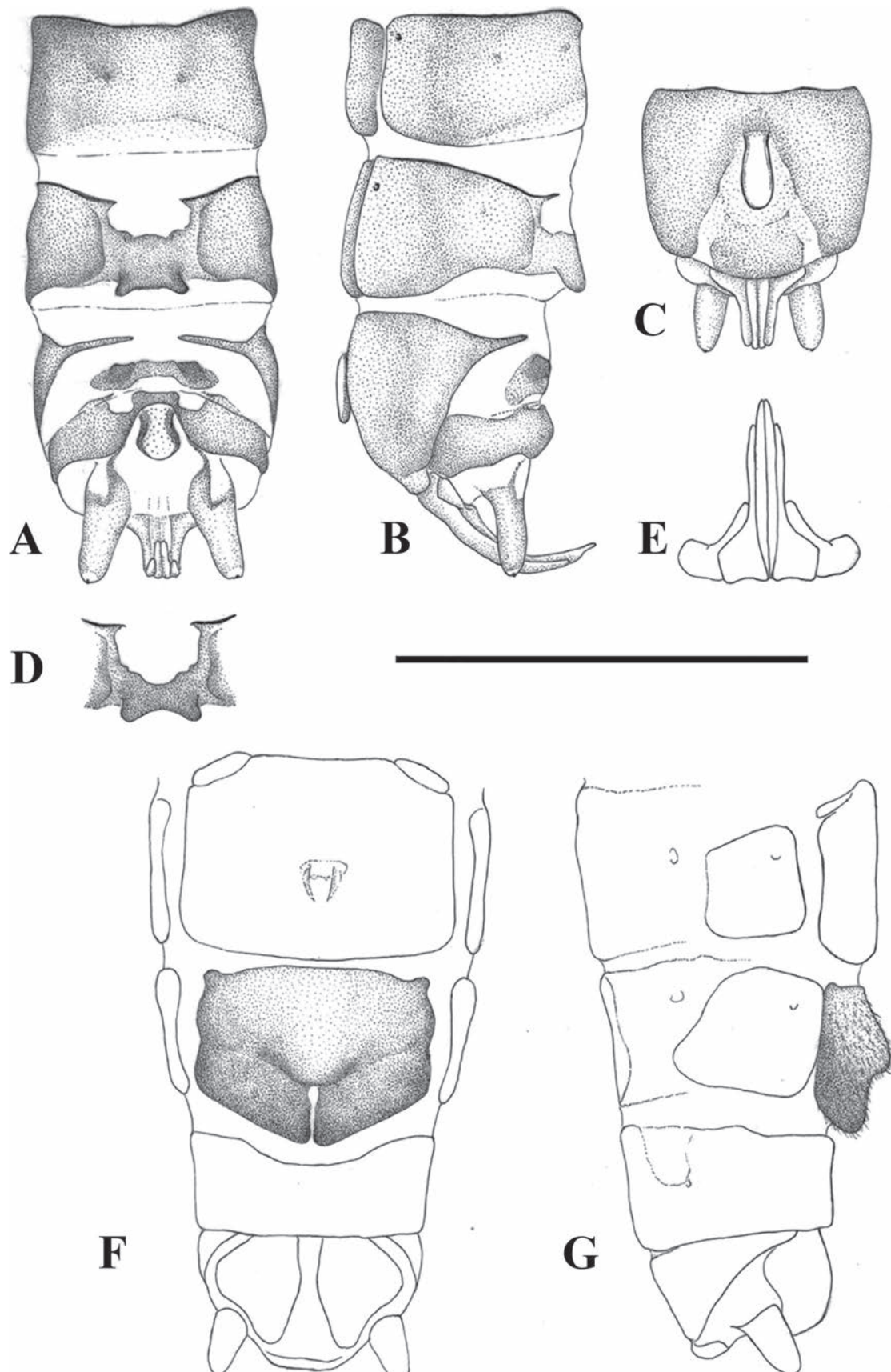
Figure 8. Terminalia of *Leuctra puskasi* sp. nov. **A** male terminalia, dorsal view **B** same, lateral view **C** same, ventral view **D** variation of male tergite 8, dorsal view **E** male paraprocts and specillae, caudal view **F** female terminalia, ventral view **G** same, lateral view. Setation omitted with the exception of subgenital plate on **G**. Scale bar: 1 mm.
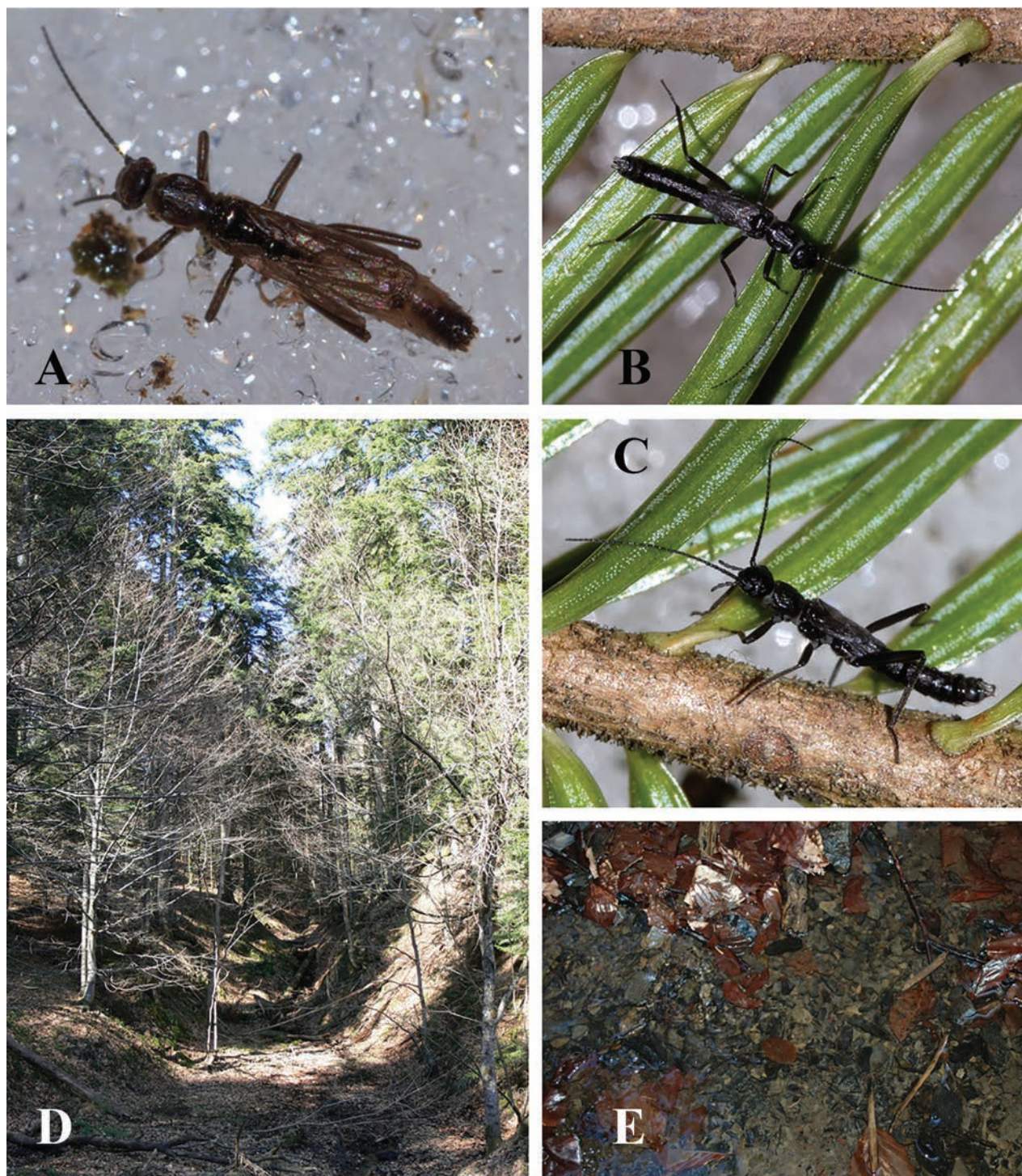
Figure 9. Habitus and habitat of *Leuctra puskasi* sp. nov. **A** female habitus **B, C** male habitus **D** type locality: forest brook in the Kozara Mts. **E** substrate of the type locality. Photographs **A–C** by Gellért Puskás.

view and not or only slightly overhangs the segment posterior edge, nearly as wide as the membranous area above, bilobed with rounded lobes slightly pointed laterad, the space between the lobes is concave to nearly straight; posterior margin between the posteromedial process and segment sides nearly straight, not indenting nor distinctly lobed. Tergite IX mostly membranous, antecosta interrupted in the medial 1/3 to 1/2 of its length; posteromedial sclerite short but wide, sublateral areas darker, the medial portion usually narrower than the

lateral portions. Anterior margin of tergite X bilobed anteriorly, posterior margin with deep notch, not wider than 1/3 tergite width. Epiproct large, posteriorly rounded, sclerotised only at its sides, stalk short. Cercus simple, covered with long setae. Sterna II–VIII simple, sternite IX bears a vesicle shorter than 1/2 segment length, its width more than 1/2 its length; posteromedial 1/2 of the sternum is delimited by a pale and weakly sclerotised area. Paraproct with moderately wide base, abruptly narrowing after basal 1/3, apex gently curved in lateral view and tapering towards a sharp tip. Base of paraproct connected to a subrectangular lateral expansion with an apical, blunt triangular process. Specillum longer than the paraproct, gently curved in lateral view and ending in a subterminally constricted, sharp tip.

Female abdomen (Figs 8F, G, 12E): Terga I–VIII with transverse row of four pigmented spots clearly visible; terga I–IV mostly membranous but with lateral sclerites, terga V–VIII with medial sclerite as well; medial sclerite is a longitudinal stripe on tergite V, gradually widens on the following segments and as wide as 1/2 segment width on tergite VIII; terga IX–X fully sclerotised. Sterna I–VII simple, sterna II–VII with one subrectangular median sclerite and two small anterior sclerites that are fused with the median sclerite on sternite VII. Subgenital plate of sternite VIII large and trapezoid, not fused with other sclerites. It has two large and wide lobes, slightly darker brown than the rest of the plate; posterior margin convex, incision between the lobes is a membranous strip, widening towards the median bulge near the centre of the plate but not forming a triangular field; median bulge is narrow in ventral view, distinctly raised, nose shaped to rounded in lateral view, lacking distinct setation. Sternite IX with wide but shallow anterior indentation. Paraproct, cercus and epiproct simple. Spermathecal sclerite ring-shaped, with small anterior teeth and large, converging the posterior teeth.

Affinities. Both sexes are morphologically the closest to *L. dalmoni* (compare with Fig. 12C, D). Males can be distinguished on the basis of the following characters: posteromedial process of tergite VIII stronger, its lobes are not teeth-like, and preceded by a more shallow membranous area than of those of *L. dalmoni*; the posterior margin of tergite VIII is nearly straight between the posteromedial process and segment sides, while it is clearly indented in a rounded membranous field in *L. dalmoni*; the posterior indentation of tergite X is a deep notch that is not wider than 1/3 tergite width, while that is usually wider than 1/2 tergite width in *L. dalmoni*; the ventral vesicle of sternite IX is shorter than 1/2 segment length, while that is clearly longer than 1/2 segment length in *L. dalmoni*. Females are nearly identical (compare with Fig. 12G, H), but variability might be high; however, in the available females, the incision between the lobes of the subgenital plate widens towards the median bulge, while it is only a narrow strip in *L. dalmoni*, and the median bulge is more robust in lateral view. The males of the new species can be easily distinguished from the other regional early spring species of the *prima* species complex: *L. pseudosignifera* is characterised by a pair of rounded sclerotised expansions, located between the posteromedial process and segment sides of tergite VIII (Fig. 12K); the posteromedial process of tergite VIII is erect in lateral view in case of *L. prima*. Furthermore, this species has a divided posteromedial sclerite on tergite IX (Fig. 12I); *L. visitor* has a crossband on the membranous area of tergite VIII, the membranous area is deeper, and the posteromedial process

has stronger, angular teeth; additionally, the posterior notch of tergite X is a wide V-shape (Fig. 12B). The females are also easily distinguishable: *L. pseudosignifera* is characterised by a triangular membranous field at the end of the incision between the lobes of the subgenital plate (Fig. 12L); the median bulge of the subgenital plate is much wider in *L. prima*, and the lobes of the subgenital plate are shorter (Fig. 12J); *L. visitor* has a wide median bulge of the subgenital plate, and the plate has distinctive, erect setation in lateral view (Fig. 10F). In addition, all the other species are macropterous.

Distribution and ecology. The species was collected at a single forest brook in the Kozara Mts of northwestern Bosnia & Herzegovina (Fig. 1). The Kozara is of low elevation, a northern foothill of the Dinarids, rather separated from the higher ranges and also stands far from the Slavonian mountains, separated by the plain of the Sava River. The habitat is a slowly running small brook in mixed forest dominated by fir and beech, which probably often runs dry in summer (Fig. 9D). It has a stony substrate mixed with mud and plenty of dead wood and fallen leaves (Fig. 9E). This habitat type is very different from those of the closely related *L. dalmoni*, and probably unsuitable even for the more eurytopic *L. prima*. No other member of the *Leuctra prima* species complex was found in the Kozara, despite the fact that some other habitats seemed suitable at least for *L. prima*. The type specimens were the only adult stoneflies found there (in partial snow cover), but last instar larvae of *Leuctra nigra*, *Nemoura sciurus* Aubert, 1949, and a *Nemoura marginata* group member were found in the brook. We visited the locality twice more, once in May (24.v.2012, leg. T. Kovács, G. Puskás) and once in November (7.xi.2012, leg. T. Kovács, G. Magos). In May, adults of *Leuctra nigra*, single females of a *N. marginata* group member and of *Siphonoperla torrentium* (Pictet, 1841) were collected. In November, no stoneflies but only autumnal Trichoptera were collected (Oláh and Kovács 2012a; Oláh et al. 2012): *Chaetopteryx gonospina*, *C. papukensis*.

Etymology. We dedicate this species to our friend and orthopterologist colleague, Gellért Puskás, with whom we made several collecting expeditions in the Balkans, and who regularly provides us stoneflies from his travels. Used as a noun, gender masculine.

Leuctra visitor sp. nov.

https://zoobank.org/6E2C2B5D-5228-4A6A-B501-C2FB65A162EC
Figs 1, 10, 11, 12B, F

Type material. *Holotype* male: MONTENEGRO: • Plav municipality, Visitor Mts, forest springs and their outlet along the Katun road, 1730 m, 42.6308°N, 19.8358°E, 5.v.2023 (field number: loc.13), leg. T. Kovács, D. Murányi (MM: 2023-49, PLETYP-37). *Paratypes*: • same locality and date: 1♂ 1♀ (BYU) • 1♂ 1♀ (CGV) • 11♂ 8♀ (3 pairs in copula) (EKCU: PLP5706) • 1♂ 2♀ (MM: 2023-49, PLETYP-38) • 1♂ 1♀ (SMNS) • Plav municipality, Visitor Mts, partly open brook and spring along the Katun road, 1845 m, 42.6185°N, 19.8378°E, 11.vi.2022 (loc.24), leg. A. Hunyadi, T. Kovács, D. Murányi, P. Olajos: 5♂ 3♀ (EKCU: PLP5584) • 8♂ 9♀ (1 pair in copula) (MM: 2022-90, PLETYP-39) • Plav municipality, Visitor Mts, forest streams and brooks along the Katun road, 1515 m, 42.6294°N, 19.8442°E, 11.vi.2022 (loc.22),
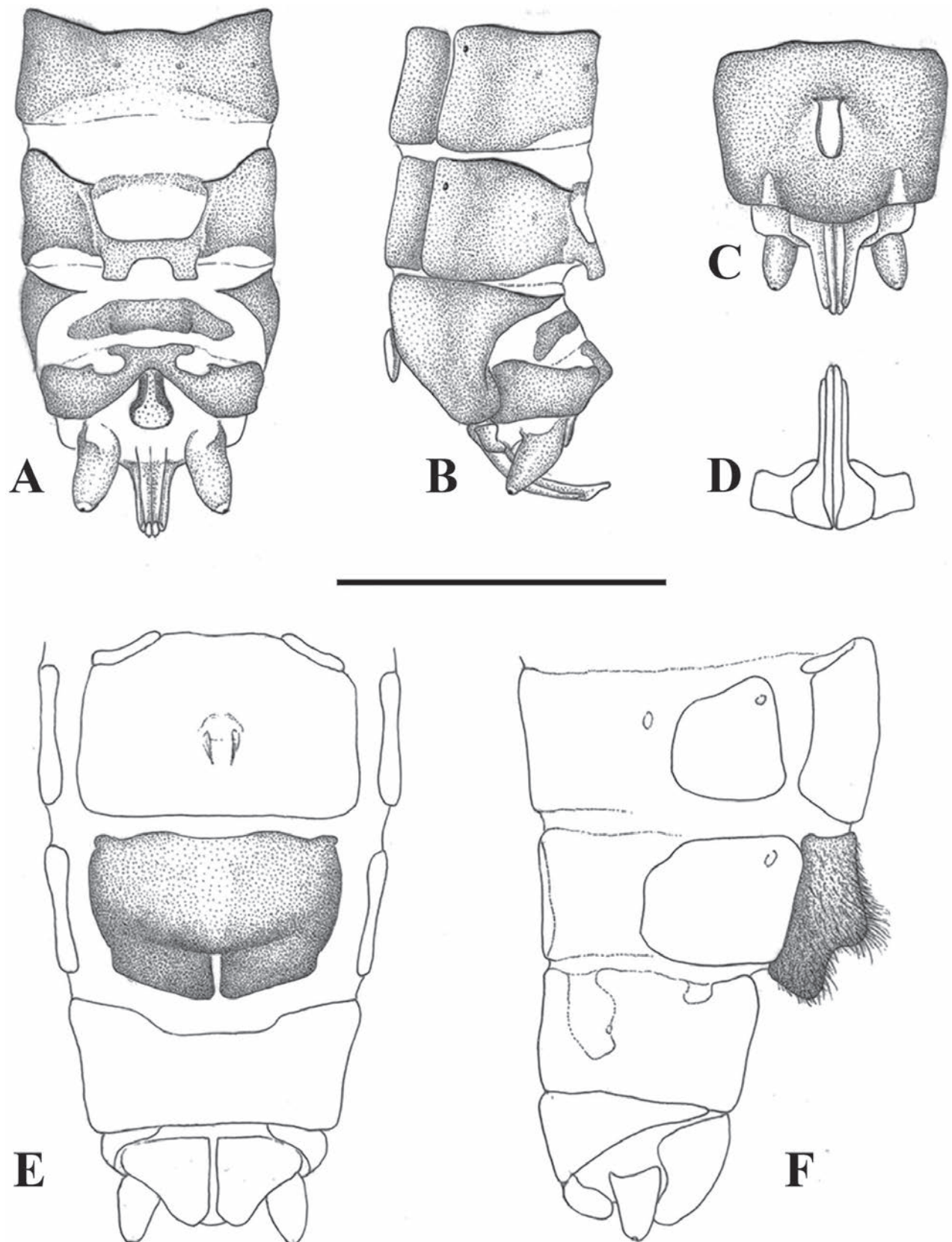
Figure 10. Terminalia of *Leuctra visitor* sp. nov. **A** male terminalia, dorsal view **B** same, lateral view **C** same, ventral view **D** male paraprocts and specillae, caudal view **E** female terminalia, ventral view **F** same, lateral view. Setation omitted with the exception of subgenital plate on **F**. Scale bar: 1 mm.

Figure 11. Habitus and habitat of *Leuctra visitor* sp. nov. **A** male habitus **B** female habitus **C** copula **D** partly open brook at 1845 m in the Visitor Mts. **E** type locality: forest springs and their outlet at 1730 m in the Visitor Mts.

leg. A. Hunyadi, T. Kovács, D. Murányi, P. Olajos: 1♀ (EKCU: PLP5572) • same locality, 5.v.2023 (loc.12), leg. L.P. Kolcsár, T. Kovács, D. Murányi: 8♂ 7♀ (2 pairs in copula) (EKCU: PLP5701) • 6♂ 8♀ (1 pair in copula) (MM: 2023-48, PLETYP-40).

Diagnosis. Brachypterous in both sexes. Male tergite VII with small membranous portion; tergite VIII with strong posteromedial process that is not erect in side view and bear angular teeth, membranous area longer than 1/2 segment length with a crossband, the posterior margin indented in a rounded membranous field between the posteromedial process and segment sides; tergite IX with short but wide posteromedial sclerite; tergite X posterior margin with a
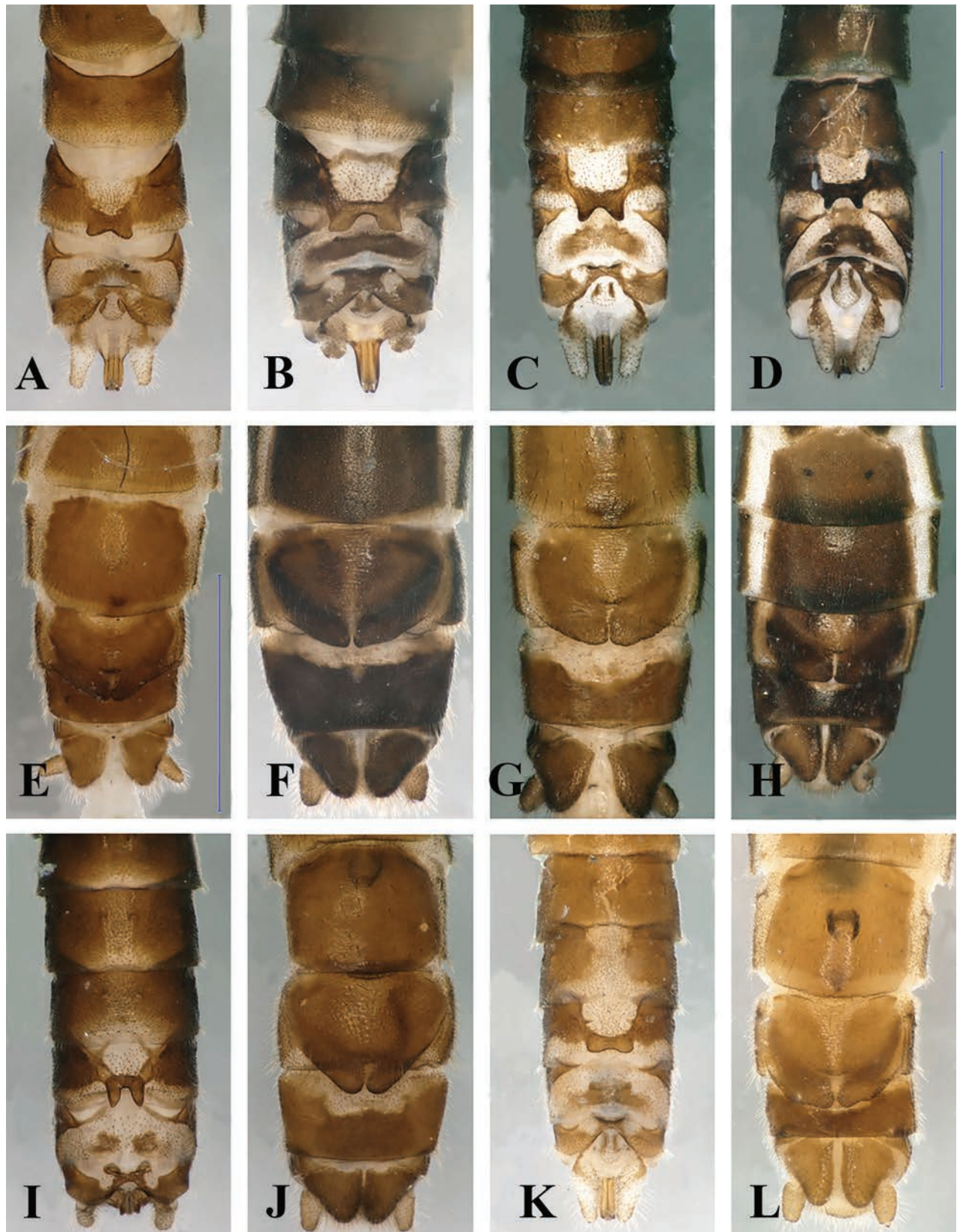
Figure 12. Terminalia of five Balkan members of the *Leuctra prima* group **A–D, I, K** male terminalia, dorsal view **E–H, J, L** female terminalia, ventral view **A, E** *L. puskasi* sp. nov., Kozara Mts, Bosnia & Herzegovina **B, F** *L. visitor* sp. nov., Visitor Mts, Montenegro **C, G** *L. dalmoni* Vinçon & Murányi, 2007, Visitor Mts, Montenegro **D, H** *L. dalmoni*, Golija Mts, Serbia **I–J** *L. prima* Kempny, 1899, Börzsöny Mts, Hungary **K–L** *L. pseudosignifera* Aubert, 1954, Poljana Mts, Slovakia. Scale bars: 1 mm (**D** for **A–D, I, K**; **E** for **E–H, J, L**).

wide V-shaped notch; sternite IX bears a vesicle much shorter than 1/2 segment length; specillum slightly longer than paraproct, tip blunt behind subterminal constriction. Female subgenital plate large, trapezoid, with an incision between the long lobes slightly widening towards the median bulge but not forming a triangular field; median bulge is wide in ventral view and distinctly raised in lateral view, with distinct, erect setation; spermathecal sclerite ring-shaped, with large and converging posterior teeth.

Description. Medium sized, robust species, both sexes brachypterous (Fig. 11A–C). Forewing length: holotype 3.2 mm, male paratypes 3.0–3.8 mm, female paratypes 4.2–5.2 mm; body length: holotype 6.2 mm, male paratypes 5.4–7.0 mm, female paratypes 6.8–9.0 mm. Setation generally short and dense. General colour dark brown to blackish. Head, antennae, and palpi dark brown. Pronotum dark brown, as wide as long and having rounded corners, rugosities distinct. Legs brown to dark brown. Wings brownish but hyaline, venation brown.

Male abdomen (Figs 10A–D, 12B): Tergite I membranous in its whole medial portion, tergite II membranous anteromedially behind antecosta. Transverse row of four pigmented spots distinct on terga I–VII. Terga II and III with medially divided antecosta, terga IV–VII with entire antecosta and full sclerotised, tergite VII with small posterior membranous portion. Tergite VIII: antecosta interrupted by a wide membranous area, each part ends in a small triangular plate, and the membranous area between them is bridged by a weakly sclerotised crossband; width of the membranous area is less than 1/2 the segment width, and reaches below 1/2 the segment length above the posteromedial process, posterior margin of the membranous portion nearly straight; the surrounding sclerotisation of the membranous area paler than remainder of the segment; posteromedial process paler than the lateral areas of the segment, not erect in side view and slightly overhangs the segment posterior edge, as wide as the membranous area above, bilobed with angular teeth slightly pointed laterad, the space between the teeth is deeply indented and concave; posterior margin between the posteromedial process and segment sides indented in a shallow, rounded membranous field but not lobed. Tergite IX mostly membranous, antecosta interrupted in the medial 1/2 of its length; posteromedial sclerite short but wide, medial areas usually slightly darker, the medial portion usually not narrowed. Anterior margin of tergite X bilobed anteriorly, posterior margin with deep, V-shaped notch, 1/2 as wide as tergite width. Epiproct large, posteriorly rounded, sclerotised only at its sides, stalk relatively long. Cercus short, covered with long setae. Sterna II–VIII simple, sternite IX bears a vesicle much shorter than 1/2 segment length, its width more than 1/2 its length; the area surrounding the vesicle is pale, posterior edge with two pale and weakly sclerotised areas. Paraproct with moderately wide base, abruptly narrowed after basal 1/3, apex gently curved in lateral view and tapering towards a sharp tip. Base of paraproct connected to a subrectangular lateral expansion with an apical, short, blunt triangular process. Specillum slightly longer than the paraproct, gently curved in lateral view and ending in a subterminally constricted, blunt tip.

Female abdomen (Figs 10E, F, 12F): Terga I–VIII with transverse row of four pigmented spots clearly visible; terga I–VIII mostly membranous but with lateral sclerites, terga II, III, and VI–VIII, sometimes also tergite V, bear a patch-like medial sclerite, largest on tergite VIII; tergite IX membranous only antero-laterally, tergite X fully sclerotised. Sterna I–VII simple, sterna II–VII with one

subrectangular median sclerite and two small anterior sclerites that are fused with the median sclerite on sternite VII. Subgenital plate of sternite VIII large and trapezoid, not fused with other sclerites. It has two large wide lobes, slightly darker brown than remainder of the plate; posterior margin convex, incision between the lobes is a membranous strip, slightly widened towards the median bulge near the centre of the plate but not forming a triangular field; median bulge is wide in ventral view, distinctly raised, nose-shaped in lateral view, with distinct erect setation. Sternite IX with wide but shallow anterior indentation. Paraproct, cercus, and epiproct simple. Spermathecal sclerite ring-shaped, with small anterior teeth and large, converging posterior teeth.

Affinities. The males are morphologically closest to *L. dalmoni* (compare with Fig. 12C, D) while the female is closest to *L. prima* (compare with Fig. 12J). Males can be distinguished from *L. dalmoni* on the basis of the following characters: a weak crossband on the membranous area of tergite VIII lacking in *L. dalmoni*, angular teeth of the posteromedial process of tergite VIII stronger than those of *L. dalmoni*; the posterior indentation of tergite X is V-shaped, while it is rounded in *L. dalmoni*; the ventral vesicle of sternite IX is shorter than 1/2 the segment length, while clearly longer than 1/2 the segment length in *L. dalmoni*. The males of the new species can be easily distinguished from *L. prima* and *L. pseudosignifera*: *L. pseudosignifera* is characterised by a pair of rounded sclerotised expansions, located between the posteromedial process and segment sides of tergite VIII (Fig. 12K); the posteromedial process of tergite VIII is erect in lateral view in *L. prima*; furthermore, this species has a divided posteromedial sclerite on tergite IX (Fig. 12I). Females can be distinguished from *L. prima* on the basis of the distinct, erect hairs of the subgenital plate as seen in lateral view, and the nose-shape of the bulge of the subgenital plate; the bulge is rounded in *L. prima* and the subgenital plate lacks distinct setation. The wide bulge of the subgenital plate (in ventral view), and the erect hairs (in lateral view) distinguish the new species from *L. dalmoni* and *L. pseudosignifera*; furthermore, *L. pseudosignifera* is characterised by a triangular membranous field at the end of the incision between the lobes of the subgenital plate (Fig. 12L). Distinction of both sexes from *L. puskasi* was described in detail above.

Distribution and ecology. The species was collected at three high-elevation brooks and spring outlets in the Visitor Mts of eastern Montenegro (Fig. 1). The Visitor is a mostly volcanic range of small area, with its highest peak reaching more than 2200 meters, surrounded by the notably higher limestone chains of the Prokletije Mts. The Visitor receives high precipitation and is covered with dense forest, resulting in a rich pattern of different waterflows. The streams where the new species was found are running in mixed forest or partly open meadows, the lentic parts usually with dense *Caltha* growth (Fig. 11D, E). The brooks have variable flow rates but are permanent streams, the substrate is stony mixed with mud and plenty of dead wood. The specimens were emerging together with *L. dalmoni* (Fig. 12C, G) and both species were present with many mating pairs in May, but we found no interbreeding couples (Fig. 11C). We visited the area three times: the new species was more numerous than *L. dalmoni* in early May 2023, both scarce in early June 2022, and both absent by late June 2023. In May, the upper site (1845 m) was not available, and even the lowest site (1515 m) was partly covered by snow, but all were snow-free by late June. We found a rich accompanying stonefly fauna at the lowest site: *Brachyptera helenica* (adults

and matured larvae, early June), *B. graeca* Berthélemy, 1971 (adults, late June), *B. seticornis* (adults, early June), *Capnia* s. l. *vidua rilensis* (adults, May and early June), *Leuctra nigra* (adults, May and June), *L. dalmoni* (adults, May and early June), *L. metsovonica* Aubert, 1956b (adults, early June), *Protonemura* cf. *auberti* Illies, 1954b (adults and matured larvae, early June), *Nemurella pictetii* (adults, May and June), *Nemoura cinerea cinerea* (adults, early June), *Nemoura marginata* (adults, May and early June), a yet unnamed *Nemoura* of the *marginata* group (adults, May and early June), *N. uncinata* Despax, 1934 (adults, May and early June), *Arcynopteryx dichroa* (McLachlan, 1872) (adults and matured larvae, June), a yet unnamed *Isoperla* related to *I. breviptera* Ikonomov, 1980 (adults and matured larvae, June), *I.* cf. *tripartita* Illies, 1954a (larvae, June), and unidentified larvae of *Siphonoperla* and *Chloroperla* (early June). Some of these were probably not developing in the same stream section since the site is placed at a junction of three different brooks. The type locality (sampled only in May) was inhabited by the new species, *L. nigra* (adults), *L. dalmoni* (adults), the unnamed *Nemoura* (adults and putative larvae), an unidentified *Protonemura* (larvae), and the unnamed *Isoperla* (larvae). At the highest site (sampled only in June), the new species was found together with *Leuctra nigra* (adults), *L. dalmoni* (adults), the unnamed *Nemoura* (adults), *Nemurella pictetii* (adults), *Arcynopteryx dichroa* (larvae), and the unnamed *Isoperla* (adults). *Capnia* s. l. *vidua rilensis*, *Leuctra dalmoni*, and *L. metsovonica* are new records for Montenegro.

Etymology. The name *visitor* is derived from the Visitor Mountains of Montenegro, where the new species was found and probably restricted to the high elevations of the range. Used as a noun, gender neutral.

Discussion

Four new, presumably microendemic, species are described from different regions of the western Balkans. *Leuctra enigma* is a morphologically isolated member of the *L. hippopus* group, found in a single mountain stream in central Albania. *Leuctra golija* is closely related to the Balkan endemics *L. hippopoides* and *L. pseudohippopus*, and was found in the higher region of the Golija Mts in southwestern Serbia. Two brachypterous members of the *L. prima* species complex were described from the Kozara Mts of Bosnia & Herzegovina and the Visitor Mts of Montenegro. Molecular studies are underway to clarify the composition of this species complex in the Balkans, but these two species are morphologically distinctive and their ecology supports their specific status: *L. puskasi* is the only member of the complex in the Kozara, while *L. visitor* co-exists with *L. dalmoni* in the Visitor but the two do not interbreed.

To date, there are 48 species and one subspecies of *Leuctra* reported from the Balkans, including the Aegean Isles. More than half of these taxa are endemic to the region (27 taxa), and their distributions and emergence periods are given in Table 1. Only ten of them have a wider distribution within the Balkan mainland. A further six are endemic to one or more of the Greek islands, and eleven (including the four new species described herein) are restricted to a single mountain chain. The mountain endemics are mostly of reduced or lost flight capability (three apterous, three micropterous to strongly brachypterous, two brachypterous); all others, including the island endemics, are macropterous.

Table 1. Balkan endemic *Leuctra*, with their emergence periods and distributions.

Species/subspecies	Emergence period	Distribution
fusca group		
L. aegaeica Pardo & Zwick, 1993	X–III	Andros, Euboea, Naxos (Greece)
L. candiae Zwick, 1978	IX–IV	Crete (Greece)
L. cretica Zwick, 1978	X–V	Crete (Greece)
L. graeca Zwick, 1978	IX–X	Albania, Greece, Montenegro, North Macedonia
L. kykladica Pardo & Zwick, 1993	X	Naxos (Greece)
L. minoica Pardo & Zwick, 1993	XII–II	Crete (Greece)
L. moreae Zwick, 1978	X–V	Greece
L. mortoni feheri Murányi, 2007	IX–X	Albania, Bulgaria
hippopus group		
L. enigma sp. nov.	X	Çermenikë Mts (Albania)
L. golija sp. nov.	V–VI	Golija Mts (Serbia)
L. hippopoides Kaćanski & Zwick, 1970	IV–V	Albania, Bosnia & Herzegovina, Greece *, Montenegro, Serbia
L. pavesii Vinçon, 2015	III	Cephalonia (Greece)
L. pseudohippopus Raušer, 1965	V–VII	Bulgaria, North Macedonia, Serbia
prima/signifera group		
L. hansmalickyi Graf, 2010	VI	Rila Mts (Bulgaria)
L. helenae Braasch, 1972	IX	Stara Planina (Bulgaria)
L. jahorinensis Kaćanski, 1972	X	Jahorina Mts (Bosnia & Herzegovina) **
L. joosti Braasch, 1970	IV–VI	Bulgaria, Turkey (European part)
L. kumanskii Braasch & Joost, 1977	X	Pirin Mts (Bulgaria)
L. olympia Aubert, 1956b	IV–V	Bosnia & Herzegovina, Greece, Montenegro, North Macedonia, Serbia
L. malcor Murányi, 2007	X	Prokletije Mts (Albania)
L. marani Raušer, 1965	IV–VIII	Bulgaria, Greece
L. papukensis Reding, Vinçon & Graf, 2023	X	Papuk Mts (Croatia)
L. puskasi sp. nov.	III	Kozara (Bosnia & Herzegovina)
L. visitor sp. nov.	V–VI	Visitor Mts (Montenegro)
inermis group		
L. aptera Kaćanski & Zwick, 1970	IV	Sutjeska (Bosnia & Herzegovina)
L. balcanica Raušer, 1965	V–VII	Bulgaria
L. metsovonica Aubert, 1956b	IV–VIII	Albania, Greece, Montenegro, North Macedonia ***

* Greek specimens of *L. hippopus* were reported to have intermediate characters towards *L. hippopoides* by Zwick (1978).
** records from Montenegro (Murányi 2011) needs confirmation.
*** records from Italy (Pardo and Zwick 1993) needs confirmation.

Acknowledgements

Additional information

Conflict of interest

Ethical statement

Funding

Author contributions

Dávid Murányi and Tibor Kovács: manuscript writing and review; Dávid Murányi: drawings; Tibor Kovács: figure editing.

Author ORCIDs

Dávid Murányi ● https://orcid.org/0000-0002-3907-5590
Tibor Kovács ● https://orcid.org/0000-0003-4577-0394

Data availability

All of the data that support the findings of this study are available in the main text.

References

Aubert J (1949) Plécoptère helvétiques: Notes morphologiques et systématiques. Mitteilungen der Schweizerischen Entomologischen Gesellschaft 22(2): 217–236. https://doi.org/10.5169/seals-401060

Aubert J (1954) Contribution à l'étude du genre *Leuctra* Stephens et description de quelques espèces nouvelles de ce genre. Mitteilungen der Schweizerischen Entomologischen Gesellschaft 27(2): 124–136. https://doi.org/10.5169/seals-401211

Aubert J (1956a) Synonymie et homonymi de quelques Plécoptères. Mitteilungen der Schweizerischen Entomologischen Gesellschaft 29(2): 92. https://doi.org/10.5169/seals-401269

Aubert J (1956) Contribution à l'étude des Plécoptères de Grèce. Mitteilungen der Schweizerischen Entomologischen Gesellschaft 29(2): 187–213. https://doi.org/10.5169/seals-401268

Aubert J (1962) Quelques *Leuctra* nouvelles pour l'Europe (Plécoptères Leuctridae). Mitteilungen der Schweizerischen Entomologischen Gesellschaft 35(1–2): 155–169. https://doi.org/10.5169/seals-401429

Berthélemy C (1971) Plécoptères de Grèce Centrale et d'Eubée. Biologia Gallo-Hellenica 3(1): 23–56.

Bilalli A, Musliu M, Ibrahimi H, Sivec I (2020) New records for the stonefly fauna (Insecta: Plecoptera) of Kosovo. Natura Croatica 29(1): 29–36. https://doi.org/10.20302/NC.2020.29.4

Bogoesco C, Tabacaru I (1960) Contribution à l'étude des *Leuctra* (Plécoptères) des Carpathes roumaines. Mitteilungen der Schweizerischen Entomologischen Gesellschaft 33(1–2): 91–96. https://doi.org/10.5169/seals-401378

Braasch D (1969) *Chloroperla russevi* n. sp. und *Chloroperla kosarovi* n. sp. aus Bulgarien. Mitteilungen der Deutschen Entomologischen Gesellschaft 28(5/6): 51–54.

Braasch D (1970) *Leuctra joosti* n. sp. (Plecoptera) aus Bulgarien. Entomologische Nachrichten 14(2): 20–22. https://www.zobodat.at/pdf/EntBer_14_0020-0022.pdf

Braasch D (1972) Neue Funde von Plecopteren in Bulgarien. Entomologische Nachrichten 16(7/8): 81–90. https://www.zobodat.at/pdf/EntBer_16_0081-0090.pdf

Braasch D, Joost W (1971) Zur Plecopterenfauna Bulgariens. Limnologica Berlin 8(2): 265–294. https://doi.org/10.1515/9783112531501-003

Braasch D, Joost W (1977) *Leuctra kumanskii* n. sp. – eine neue aptere Steinfliege (Plecoptera, Leuctridae) aus Bulgarien. Entomologisches Nachrichtenblatt (Vienna, Austria) 21(12): 183–185.

Darilmaz MC, Salur A, Murányi D, Vinçon G (2016) Contribution to the knowledge of Turkish stoneflies with annotated catalogue (Insecta: Plecoptera). Zootaxa 4074(1): 1–74. https://doi.org/10.11646/zootaxa.4074.1.1

Despax R (1934) Plécoptères pyrénéens. VII. Etude et description de quelques formes de Nemoures apparentées à *Nemoura marginata* (Pict.). Bulletin de la Société d'histoire Naturelle de Toulouse 66(2): 255–270.

DeWalt RE, Hopkins H, Neu-Becker U, Stueber G (2023) Plecoptera Species File. [Accessed 3 December 2023] https://plecoptera.speciesfile.org

Graf W, Bálint M (2010) *Leuctra hansmalickyi* (Insecta: Plecoptera), a new species from the Rila Mountains in Bulgaria. Denisia 29: 121–124. https://www.zobodat.at/pdf/DENISIA_0029_0121-0124.pdf

Graf W, Lorenz AW, Tierno de Figueroa JM, Lucke S, López-Rodriguez MJ, Davies C (2009) Distribution and ecological preferences of European freshwater organisms. Vol. 2: Plecoptera. Schmidt-Kloiber A, Hering D (Eds) Pensoft Publishers, Sofia-Moscow, 262 pp.

Graf W, Popijač A, Previšić A, Gamboa M, Kučinić M (2012) Contribution to the knowledge of *Siphonoperla* in Europe (Plecoptera: Chloroperlidae): *Siphonoperla korab* sp. n. Zootaxa 3164(1): 41–48. https://doi.org/10.11646/zootaxa.3164.1.4

Graf W, Pauls SU, Vitecek S (2018) *Isoperla vjosae* sp. n., a new species of the *Isoperla tripartita* group from Albania (Plecoptera: Perlodidae). Zootaxa 4370(2): 171–179. https://doi.org/10.11646/zootaxa.4370.2.5

Guérin-Méneville FE (1843) Genre *Perle*. In: Guérin-Méneville FE (Ed.) Iconographie de Règne Animal de G. Cuvier. Insectes. Baillière, Paris 393–395. https://www.biodiversitylibrary.org/item/88601#page/399/mode/1up

Hlebec D, Sivec I, Podnar M, Skejo J, Kučinić M (2021) Morphological and molecular characterisation of the Popijač's Yellow Sally, *Isoperla popijaci* sp. nov., a new stenoendemic stonefly species from Croatia (Plecoptera, Perlodidae). ZooKeys 1078: 85–106. https://doi.org/10.3897/zookeys.1078.66382

Ikonomov P (1980) Nouvelles espèces de Plécoptères (Insecta, Plecoptera) de Macedoine. II. Fragmenta Balcanica 11(4): 19–31.

Ikonomov P (1986) Plekopterite na Makedonija (Insecta, Plecoptera). Taksonomija i distribucija. Acta Musei Macedonici Scientiarum Naturalium 18(4): 81–124.

Illies J (1954a) *Isoperla tripartita* n. sp., eine neue Plekoptere aus dem Wienerwald. Österreichische Zoologische Zeitschrift 5(1/2): 118–122. https://www.zobodat.at/pdf/OEZ_05_0118-0122.pdf

Illies J (1954b) *Protonemura fumosa* Ris 1902 und *Pr. auberti* n. spec. (Plecoptera). Zoologischer Anzeiger 152: 235–239.

Kaćanski D (1972) *Leuctra signifera jahorinensis* n. ssp., eine neue Plecopteren-subspecies aus Jugoslawien. Mitteilungen der Schweizerischen Entomologischen

Gesellschaft 45(1−3): 37−41. https://www.e-periodica.ch/cntmng?pid=seg-001%3A1972%3A45%3A%3A348

Kaćanski D (1975) Plecoptera u području planine Zlatibor. In: Zbornik radova o entomo-fauni SR Srbije, knjiga I. Srpske Akademije Nauka I Umetnosti, Belgrade 237−245.

Kaćanski D (1979) Some characteristics of the Plecoptera fauna in Bosnia and Herze-govina (Yugoslavia). Gewässer und Abwässer 64: 49−55.

Kaćanski D, Zwick P (1970) Neue und wenig bekannte Plecopteren aus Jugoslaw-ien. Mitteilungen der Schweizerischen Entomologischen Gesellschaft 43(1): 1−16. https://www.e-periodica.ch/cntmng?pid=seg-001%3A1970%3A43%3A%3A14

Karaouzas I, Andriopoulou A, Kouvarda T, Murányi D (2016) An annotated check-list of the Greek Stonefly Fauna (Insecta: Plecoptera). Zootaxa 4111(4): 301−333. https://doi.org/10.11646/zootaxa.4111.4.1

Kazanci N (2015) *Brachyptera berkii* Kazanci 2001, a new record of Plecoptera (Taeni-opterygidae) species from Crete (Greece). Review of Hydrobiology 8(2): 101−104.

Kempny P (1898) Zur kenntniss der Plecopteren. II. Neue und ungenügend bekannte *Leuctra*−Arten. I. Theil. Verhandlungen der Zoologisch-Botanischen Gesellschaft in Wien 48: 213−221 + Pl. III. https://www.biodiversitylibrary.org/part/39234

Kempny P (1899) Zur kenntniss der Plecopteren. II. Neue und ungenügend bekannte *Leuctra*−Arten. II. und III. Theile. Verhandlungen der Zoologisch-Botanischen Ge-sellschaft in Wien 49: 9−15, 269−278. https://doi.org/10.5962/bhl.part.24102

Kis B (1964) *Nemoura longicauda* n. sp. und *Leuctra transsylvanica* n. sp., neue Ple-copteren aus Rumänien. Mitteilungen der Schweizerischen Entomologischen Gesellschaft 36(4): 330−332. https://doi.org/10.5169/seals-401463

Klapálek F (1900) Plekopterologické Studie. Rozpravy České Akademie Cisaře Františka Josefa pro Vĕdy. Slovesnost a Umĕni 9(20): 1−34. [+ Pl. I−II.]

Klapálek F (1902) Zur kenntniss der Neuropteroiden von Ungarn, Bosnien und Herzegovina. Természetrajzi Füzetek 25(1−2): 161−180. https://epa.oszk.hu/02300/02370/00061/pdf/EPA02370_termszetrajzif25magy_01-02_161-180.pdf

Kovács T, Murányi D (2013) New country data of some mayflies (Ephemeroptera) from Europe. Folia historico-naturalia Musei Matraensis 37: 15−19. http://www.nhmus.hu/sites/default/files/balkan/literature/Ephemeroptera/Kovacs_Muranyi_Fh-nMM_15_2013.pdf

Kovács T, Murányi D (2023) Data to the distribution of *Helenoperla malickyi* Sivec, 1997 (Plecoptera: Perlidae). Folia historico-naturalia Musei Matraensis 47: 45−53. https://matramuzeum.nhmus.hu/sites/default/files/nhmusfiles/kiadvanyok/folia/vol47/04_Kov%C3%A1cs_Mur%C3%A1nyi_Helenoperla_47.pdf

Kovács T, Vinçon G, Murányi D, Sivec I (2012) A new *Perlodes* species and its subspe-cies from the Balkan Peninsula (Plecoptera: Perlodidae). Illiesia 8(20): 182−192. https://www.zobodat.at/pdf/Illiesia_08_0182-0192.pdf

Linnaeus C (1758) Systema naturae per regna tria natur, secundum classes, ordines, genera, species, cum characteribus, differentiis, synonymis, locis. Tomus I. Editio dec-ima, reformata. Laurentii Salvii, Holmi, 824 pp. https://doi.org/10.5962/bhl.title.542

McLachlan MR (1872) Matériaux pour une Faune Névroptérologique de l'Asie Septentri-onale. Seconde partie. Non-Odonates. Annales de la Sociètè Entomologique Belgique 15: 47−77 [+ Pl I−II]. https://www.biodiversitylibrary.org/item/44639#page/345/mode/1up

Morton KJ (1894) Palaearctic *Nemourae*. Transactions of the Entomological Society of London 1894(23): 557−574 [Pl.XIII−XIV]. https://www.biodiversitylibrary.org/item/50996#page/599/mode/1up

Murányi D (2007) New and little-known stoneflies (Plecoptera) from Albania and the neighbouring countries. Zootaxa 1533(1): 1–40. https://doi.org/10.11646/zootaxa.1533.1.1

Murányi D (2009a) A Kárpát-medence és a Balkán álkérész (Plecoptera) faunájának taxonómiai problémái, állatföldrajzi vizsgálata. PhD Thesis, Eötvös Loránd University, Budapest, Hungary. https://edit.elte.hu/xmlui/handle/10831/45104

Murányi D (2009b) The genus *Brachyptera* Newport (Plecoptera: Taeniopterygidae) in the Peloponnes, Greece. Zootaxa 2977(1): 61–68. https://doi.org/10.11646/zootaxa.2977.1.3

Murányi D (2011) Balkanian species of the genus *Isoperla* Banks, 1906 (Plecoptera: Perlodidae). Zootaxa 3049(1): 1–46. https://doi.org/10.11646/zootaxa.3049.1.1

Murányi D, Kovács T (2013) Contribution to the Odonata fauna of Albania and Montenegro. Folia historico-naturalia Musei Matraensis 37: 29–41. http://www.nhmus.hu/sites/default/files/balkan/literature/Odonata/Muranyi_Kovacs_2013.pdf

Murányi D, Kovács T (2024) Contribution to the Plecoptera fauna of Serbia. Folia historico-naturalia Musei Matraensis 48. [in press]

Murányi D, Gamboa M, Orci KM (2014a) *Zwicknia* gen. n., a new genus for the *Capnia bifrons* species group, with descriptions of three new species based on morphology, drumming signals and molecular genetics, and a synopsis of the West Palaearctic and Nearctic genera of Capniidae (Plecoptera). Zootaxa 3812(1): 1–82. https://doi.org/10.11646/zootaxa.3812.1.1

Murányi D, Kovács T, Orci KM (2014b) New country records and further data to the stonefly (Plecoptera) fauna of southeast Macedonia. Ecologica Montenegrina 1(2): 1–14. https://doi.org/10.37828/em.2014.1.9

Murányi D, Kovács T, Orci KM (2016) Contribution to the taxonomy and biology of two Balkan endemic *Isoperla* Banks, 1906 (Plecoptera: Perlodidae) species. Zoosymposia 11: 73–88. https://doi.org/10.11646/zoosymposia.11.1.11

Oláh J, Kovács T (2012a) New records of Chaetopterygini species (Trichoptera: Linmephilidae). Folia historico-naturalia Musei Matraensis 36: 81–88. http://www.nhmus.hu/sites/default/files/balkan/literature/Trichoptera/Olah_Kovacs_Fh-nMM_81_2012.pdf

Oláh J, Kovács T (2012b) New species and records of autumnal Trichoptera form Albania. Folia historico-naturalia Musei Matraensis 36: 89–104. http://www.nhmus.hu/sites/default/files/balkan/literature/Trichoptera/Olah_Kovacs_Fh-nMM_89_2012.pdf

Oláh J, Kovács T (2013) New species and new records of Balkan Trichoptera II. Folia historico-naturalia Musei Matraensis 37: 109–121. http://www.nhmus.hu/sites/default/files/balkan/literature/Trichoptera/Olah_Kovacs_2013.pdf

Oláh J, Kovács T, Sivec I, Szivák I, Urbanič G (2012) Seven new species in the *Chaetopteryx rugulosa* species group: applying the phylogenetic species concept and the sexual selection theory (Trichoptera: Limnephilidae). Folia historico-naturalia Musei Matraensis 36: 51–79. http://www.nhmus.hu/sites/default/files/balkan/literature/Trichoptera/Olah_etal_2012.pdf

Olivier GA (1811) Némoure. Encyclopédie méthodique, ou par ordre de matiéres 8: 185–187. https://archive.org/details/encyclopdiemthod08oliv/page/186/mode/2up

Pardo I, Zwick P (1993) Contribution to the knowledge of Mediterranean *Leuctra* (Plecoptera: Leuctridae). Mitteilungen der Schweizerischen Entomologischen Gesellschaft 66(3–4): 417–434. https://doi.org/10.5169/seals-402536

Pešić V, Gadawski P, Gligorović B, Glöer P, Grabowski M, Kovács T, Murányi D, Płóciennik M, Šundić D (2018) The diversity of the zoobenthos communities of the Lake Skadar/Shkodra Basin. In: Pešić V, Karaman G, Kostianoy A (Eds) The Skadar/Shkodra Lake

environment. The handbook of environmental chemistry, Vol. 80. Springer, Cham 255–293. https://doi.org/10.1007/698_2017_234

Petrović A, Simić V, Milošević D, Paunović M, Sivec I (2014) Diversity and distributional patterns of stoneflies (Insecta: Plecoptera) in the aquatic ecosystems of Serbia (Central Balkan Peninsula). Acta Zoologica Bulgarica 66(4): 517–526.

Pictet FJ (1836) Description de quelques nouvelles espéces d'Insectes du Bassin du Léman. Memoires de la Société de physique et d'histoire naturelle de Genève 7(1): 173–190. https://www.biodiversitylibrary.org/item/39755#page/201/mode/1up

Pictet FJ (1841) Histoire naturelle générale et particulière des insects Névroptères. Famille des Perlides. Kessmann-Baillière, Genève-Paris, 423 pp. [+ Pl. I–LIII]. https://doi.org/10.5962/bhl.title.124172

Popijač A, Sivec I (2009a) First records of the Alpine stonefly species *Protonemura julia* Nicolai, 1983 (Insecta, Plecoptera) in Croatia. Natura Croatica 18(1): 83–89. https://hrcak.srce.hr/file/60470

Popijač A, Sivec I (2009b) Stoneflies (Insecta, Plecoptera) from museum collections in Croatia. Natura Croatica 18(2): 243–254. https://hrcak.srce.hr/file/70104

Raušer J (1956) K poznání československých larev rodu *Protonemura.* Acta Academiae Scientiarum Čechoslovenicae Basis Brunensis 28(9): 449–498.

Raušer J (1962) Plecoptera bulgarica – I. Acta Faunistica Entomologica Musei Nationalis Pragae 8(70): 67–82. https://www.aemnp.eu/data/article-91/72-8_0_67.pdf

Raušer J (1965) Plecoptera bulgarica – II. Acta Faunistica Entomologica Musei Nationalis Pragae 10(92): 125–138. https://www.aemnp.eu/data/article-113/94-10_0_125.pdf

Ravizza C (2002a) *Leuctra marani* Raušer, new for the Greek stonefly-fauna. Atti della Società italiana di Scienze naturali e del Museo civico di Storia naturale di Milano 143(2): 191–193. https://www.biodiversitylibrary.org/page/58443289#page/201/mode/1up

Ravizza C (2002b) Atlas of the Italian Leuctridae (Insecta, Plecoptera) with an appendix including Central European species. Lauterbornia 44: 1–42. https://www.zobodat.at/pdf/Lauterbornia_2002_45_0001-0042.pdf

Ravizza Dematteis E, Vinçon G (1994) *Leuctra ravizzai*, an orophilic new species of *Leuctra* from the Western Alps (Plecoptera). Aquatic Insects 16(2): 91–94. https://doi.org/10.1080/01650429409361541

Reding JPG, Vinçon G, Graf W (2023) Notes on *Leuctra signifera* Kempny, 1899 and *Leuctra austriaca* Aubert, 1954 (Plecoptera: Leuctridae), with the description of a new species. Zootaxa 5296(1): 1–15. https://doi.org/10.11646/zootaxa.5296.1.1

Retzius AJ (1783) Caroli de Geer genera et species insectorum. Cruse, Lipsiae, 220 pp. https://www.biodiversitylibrary.org/item/80958#page/68/mode/1up

Rostock M (1881) Verzeichniss der Neuropteren Deutschlands (1), Oesterreichs (2) und der Schweiz (3). Entomologische Nachrichten 7(15): 217–228. https://www.biodiversitylibrary.org/item/110225#page/221/mode/1up

Sánchez-Campaña C, Múrria C, Hermoso V, Sánchez-Fernández D, Tierno de Figueroa JM, González M, Millán A, Moubayed J, Ivković M, Murányi D, Graf W, Derka T, Mey W, Sipahiler F, Pařil P, Polášková V, Bonada N (2023) Anticipating where are unknown aquatic insects in Europe to imrove biodiversity conservation. Diversity & Distributions 29(8): 1021–1034. https://doi.org/10.1111/ddi.13714

Schmid F (1947) *Leuctra niveola* n. sp. et quelques Plécoptères printaniers des Alpes suisses. Mitteilungen der Schweizerischen Entomologischen Gesellschaft 20(7): 683–685. https://doi.org/10.5169/seals-401023

Sivec I (1980) Plecoptera. Catalogus Faunae Jugoslaviae 3(6): 1–30.

Sowa R (1970) Deux Plécoptères nouveaux de Bulgarie. Bulletin de l'Académie Polonaise des Sciences 18(12): 767–772.

Stephens JF (1836) Family II. – Perlidae, Leach. Illustrations of British Entomology 6: 134–145. https://doi.org/10.5962/bhl.title.8133

Tierno de Figueroa JM, Fochetti R (2001) Description of *Protonemura aroania* sp. n. and of the male of *Leuctra moreae* Zwick, 1978, with a contribution to the knowledge of the stonefly fauna of Greece (Insecta, Plecoptera). Aquatic Insects 23(3): 209–217. https://doi.org/10.1076/aqin.23.3.209.4889

Tyufekchieva V, Evtimova V, Murányi D (2019) First checklist of stoneflies (Insecta: Plecoptera) of Bulgaria, with application of the IUCN Red List Criteria at the national level. Acta Zoologica Bulgarica 71(3): 349–358. https://www.acta-zoologica-bulgarica.eu/downloads/acta-zoologica-bulgarica/2019/71-3-349-358.pdf

Vinçon G (2015) A new stonefly from Greece, *Leuctra pavesii* sp. n. (Plecoptera: Leuctridae). Mitteilungen der Schweizerischen Entomologischen Gesellschaft 88(1–2): 73–76. https://www.e-periodica.ch/digbib/view?pid=seg-001%3A2015%3A88%3A%3A6#82

Vinçon G, Murányi D (2007) *Leuctra dalmoni*, a new orophilic species with wide distribution in Europe (Plecoptera). Nouvelle Revue d'Entomologie 23(3): 237–248.

Vinçon G, Pardo I (1994) Contribution to the knowledge of Pyrenean stoneflies: *Leuctra joani* sp. n. and *L. clerguae* sp. n. (Insecta Plecoptera). Aquatic Insects 16(4): 205–212. https://doi.org/10.1080/01650429409361557

Zhiltzova LA (1960) K poznanyu vesnyanok (Plecoptera) Kavkaza. 4. Novye vidy Leuctridae. Entomologicheskoe Obozrenie 39(1): 156–171.

Zwick P (1978) Steinfliegen (Plecoptera) aus Griechenland und benachbarten Ländern - 2. Teil. Mitteilungen der Schweizerischen Entomologischen Gesellschaft 51(2–3): 213–239. https://doi.org/10.5169/seals-401879

ZooKeys

Research Article

Two new rove beetle genera in Staphylininae that reduce "*Heterothops*" and "*Quedius*" taxonomic wastebaskets (Coleoptera, Staphylinidae)

José L. Reyes-Hernández[1][ID], Alexey Solodovnikov[1][ID]

1 Natural History Museum of Denmark, University of Copenhagen, Zoological Museum, Universitetsparken 15, 2100, Copenhagen, Denmark
Corresponding author: José L. Reyes-Hernández (jl.reyeshdez@gmail.com)

Abstract

The here-provided description of the new genera *Chiquiticus* **gen. nov.** and *Nitidocolpus* **gen. nov.** was necessitated by a phylogenetic study of Staphylininae (to be published separately), which will be used for the proper characterization of their respective new suprageneric lineages in an upcoming update of the higher classification of this subfamily. Both new genera are erected for species that had been previously described but misplaced in the highly polyphyletic "taxonomic wastebasket" genera *Heterothops* (Amblyopinina) and *Quedius* (Quediina), resulting in the following new combinations: *Chiquiticus arizonicus* (Smetana, 1971), **comb. nov.** ex. *Heterothops*; *Chiquiticus campbelli* (Smetana, 1971), **comb. nov.** ex. *Heterothops*; †*Chiquiticus cornelli* (Chatzimanolis & Engel, 2013), **comb. nov.** ex. *Heterothops*; *Chiquiticus gemellus* (Smetana, 1971), **comb. nov.** ex. *Heterothops*; †*Chiquiticus infernalis* (Chatzimanolis & Engel, 2013), **comb. nov.** ex. *Heterothops*; *Chiquiticus occidentis* (Casey, 1886), **comb. nov.** ex. *Heterothops*; *Chiquiticus pusio* (LeConte, J. L., 1863), **comb. nov.** ex. *Heterothops*; *Chiquiticus rambouseki* (Blackwelder, 1943), **comb. nov.** ex. *Heterothops*; *Nitidocolpus aurofasciatus* (Bernhauer, 1917), **comb. nov.** ex. *Quedius*; *Nitidocolpus championi* (Sharp, 1884), **comb. nov.** ex. *Quedius*; *Nitidocolpus columbinus* (Bernhauer, 1917), **comb. nov.** ex. *Quedius*; *Nitidocolpus germaini* (Bernhauer, 1917), **comb. nov.** ex. *Quedius*; *Nitidocolpus illatus* (Sharp, 1884), **comb. nov.** ex. *Quedius*; *Nitidocolpus laeticulus* (Sharp, 1884), **comb. nov.** ex. *Quedius*; *Nitidocolpus triangulum* (Fauvel, 1891), **comb. nov.** ex. *Quedius*. Additionally, several more Neotropical *Quedius* species, which resemble *Nitidocolpus*, have been revised and transferred to the amblyopinine genus *Cheilocolpus* or the cyrtoquediine genus *Cyrtoquedius*, with the following new combinations: *Cheilocolpus forsteri* (Scheerpeltz, 1960), **comb. nov.** ex. *Quedius*; *Cheilocolpus speciosus* (Bernhauer, 1917), **comb. nov.** ex. *Quedius*; *Cheilocolpus viridulus* (Erichson, 1840), **comb. nov.** ex. *Quedius*; *Cyrtoquedius viridipennis* (Fauvel, 1891), **comb. nov.** ex. *Quedius*. The undescribed species diversity of the newly described genera is also highlighted.

Key words: *Cheilocolpus*, *Chiquiticus* gen. nov., *Cyrtoquedius*, Neotropical fauna, new combinations, new lineages, *Nitidocolpus* gen. nov., taxonomy

Introduction

During a large-scale systematic study of Staphylininae rove beetles (in the broad sense of Newton 2022), which integrates phylogenomic, morphological, and biogeographic evidence for the first time (Reyes-Hernández et al. in prep.), we discovered two new genera, *Chiquiticus* gen. nov. (Figs 1–3, 4A–C) and *Nitidocolpus* gen. nov. (Figs 5, 6A–C), both from the New World. These genera represent two previously unrecognized phylogenetic lineages within Staphylininae. The formal recognition of these lineages addresses a taxonomic gap, with further details to be presented in a forthcoming paper by Reyes-Hernández et al. (in prep.). Currently, both new genera are classified as Staphylininae *incertae sedis*.

Chiquiticus gen. nov. belongs to a newly recovered lineage that also includes the genus *Ctenandropus* Cameron, 1926 (now in the subtribe Amblyopinina of Staphylinini), the genus *Amazonothops* Jenkins Shaw, Orlov & Solodovnikov, 2020 (now Staphylinini *incertae sedis*), and a few extant and extinct (from Dominican amber) Nearctic and Neotropical species of the genus *Heterothops* Stephens, 1829 (now in the subtribe Amblyopinina). The small Australo-Asian genus *Ctenandropus* is morphologically and biogeographically peculiar and poorly known. *Amazonothops* is also a small Neotropical genus that was discovered only recently (Jenkins Shaw et al. 2020). *Chiquiticus* gen. nov. is erected for the few species of *Heterothops* that in fact do not belong to that genus and even to the subtribe Amblyopinina.

Nitidocolpus gen. nov. forms a monogeneric lineage comprising several Neotropical species of "*Quedius*" Stephens, 1829, primarily those related to *Q. columbinus* Bernhauer, 1917. The phylogenetic analysis of Reyes-Hernández et al. (in prep.) reveals that this lineage is distinct from true Quediina, as defined by Brunke et al. (2021). However, some species currently classified as *Quedius*, although superficially similar to *Q. columbinus* and its allies, were found to be more closely related to the genus *Cheilocolpus* Solier, 1849, both phylogenetically and morphologically. As a result, these species are transferred here to *Cheilocolpus*. Below, we present, justify, and discuss all these taxonomic novelties.

Material and methods

The studied specimens are deposited in the following collections: **AMNH** (American Museum of Natural History, New York, USA; D.A. Grimaldi and A. Pierwola), **CNC** (Canadian National Collection, Ontario, Canada; A. Brunke), **FMNH** (Field Museum of Natural History, Chicago, Illinois, USA; M. Turcatel, A.F. Newton, M.K. Thayer), **IRSNB** (Institut Royal des Sciences Naturelles de Belgique, Brussels, Belgium; W. Dekoninck), **NHM** (The Natural History Museum, London, United Kingdom; M. Barclay and D. Telnov), **MCZ** (Museum of Comparative Zoology, Harvard University, Cambridge, Massachusetts, USA; C. Maier), and **MFNB** (Museum für Naturkunde an der Humboldt Universität, Berlin, Germany; B. Jäger).

Specimens were examined with a Leica M125 dissecting microscope (Leica Microsystems, Switzerland). Photographs were captured using a Canon 5D

Mark III camera with a Canon MP-E 65mm f/2.8 1–5× macro lens (Canon, Japan) and a StackShot 3x (Cognisys, USA). Images were then stacked using Zerene Stacker (Zerene Systems, USA) with the PMax function. Further image processing, including cropping, lightening, drawing lines, and adding scales, was performed in Adobe Photoshop 2023.

Morphological terminology mainly follows Li and Zhou (2011), Brunke et al. (2019), and Reyes-Hernández et al. (2024), with the following modifications in prothorax and pterothorax terminology to align with that of Herman (2023). In the ventral view of the prothorax, what was formerly referred to as the basisternum and furcasternum, separated by the sternacostal ridge, is now termed the upper probasisternum (UBS, Fig. 1E) and lower probasisternum (LBS, Fig. 1E), respectively, separated by the intercoxal carina (ICC, Fig. 1E). In Staphylininae, the profurcasternum is a significantly reduced sclerite defined by an internal ridge connecting the apophyseal invaginations (Herman 2023). In the mesothorax (ventral view), the anterior margin is referred to as the external part of prepectus (EXPP, Fig. 1F), the sternopleural (anapleural) suture is termed as mesanapleural sutures (MNPS, Fig. 1F), and in the metathorax, the marginal carina of the mesocoxal acetabuli is called the pericoxal ridge. Regarding the frontoclypeal (epistomal) "suture", here we clarify that it represents the connection of the anterior tentorial arms (CATA, Fig. 4A) inside the head capsule, which is superficially visible externally as a dark line (Figs 2B, 3B; see also fig. 7D, E in Reyes-Hernández et al. 2024). This "suture" or ridge is more clearly visible in teneral or chemically clarified specimens, while in highly sclerotized species it appears as a shallow line on the surface as well. The supra-antennal ridge (SAR) is the term used here for a structure referred to as the supra-antennal carina in the figure legend of Brunke (2022: fig. 3A, B) but described as the suprantennal ridge in the main text. It represents the fold of the anterior or anterolateral margin of the supra-antennal tubercle which may or may not be carinated (Figs 4, 6). Additionally, new characters are introduced and illustrated here, such as the anterolateral clypeal punctures (ACP, Figs 4, 6), which are setiferous punctures laterally adjacent to the frontoclypeal punctures on the dorsal portion of the head. On the abdominal segments, the medial macroseta (MMA, Fig. 1D) and posteromarginal large macroseta (PMA, Fig. 1D) are also indicated. In certain Staphylininae species, the base of the paramere (on its outer side around the area of its attachment to the median lobe) exhibits an upward or forward projection that is most distinctly visible in lateral view (Fig. 6I, L, O).

Abbreviations for measurements are as follows: EYL (eye length in lateral view), HL (head length from the apex of the clypeus to the nuchal ridge, or when the latter is dorsally absent, then to a hypothetical line joining the sides of the nuchal ridge or the groove marking the nuchal constriction), HW (head width at the widest point, including eyes), GL (gena length), NW (neck width at the widest point), PL (pronotum length along the median line), PW (pronotum width at the widest point), and TL (total length from the anterior margin of the clypeus to the posterior margin of segment VIII). All measurements were taken in millimeters using an ocular micrometer on a dissecting microscope.

Results

Family Staphylinidae Latreille, 1802
Subfamily Staphylininae Latreille, 1802
Tribe incertae sedis

Genus *Chiquiticus* gen. nov.
https://zoobank.org/4BCF12DF-8231-4269-B13B-917E194D43B9
Figs 1−3, 4A−C

Type species. *Heterothops pusio* J.L. LeConte, 1863, here designated.

Included species. *Chiquiticus arizonicus* (Smetana, 1971), comb. nov. ex. *Heterothops* [holotype and 2 paratypes from CNC examined]; *Chiquiticus campbelli* (Smetana, 1971), comb. nov. ex. *Heterothops* [holotype, and 7 paratypes from CNC examined]; †*Chiquiticus cornelli* (Chatzimanolis & Engel, 2013), comb. nov. ex. *Heterothops* [photos of the holotype and one paratype from AMNH examined]; *Chiquiticus gemellus* (Smetana, 1971), comb. nov. ex. *Heterothops* [holotype from MCZ and 2 paratypes from CNC 2 examined]; †*Chiquiticus infernalis* (Chatzimanolis & Engel, 2013), comb. nov. ex. *Heterothops* [moved to *Chiquiticus* based on the data in the publication]; *Chiquiticus occidentis* (Casey, 1886), comb. nov. ex. *Heterothops* [holotype of *Heterothops mediocris* Fall, 1907, from MCZ examined, *H. mediocris* is a junior synonym of *H. occidentis* according to Smetana (1971) and non-type material identified by A. Smetana in CNC]; *Chiquiticus pusio* (LeConte, J. L., 1863), comb. nov. ex. *Heterothops* [1 presumed syntype or at least historical specimen examined, (MCZ) conspecific with the type material according to Smetana (1971) and non-type material identified by A. Smetana in CNC]; *Chiquiticus rambouseki* (Blackwelder, 1943), comb. nov. ex. *Heterothops* [1 syntype from NHM examined].

Diagnosis. Small Staphylininae mainly around 2.5−3.5 mm long (Fig. 1A, B) with subconical head with ventral basal ridge but without postgenal ridge (Fig. 1C); without supra-antennal punctures (Fig. 4A); pronotum transverse (PW/PL ≥ 1.1), with its maximum width in posterior half, with paired punctures on dorsal series widely separated from each other (Fig. 4B); mesanapleural sutures transverse not reaching or fusing with external part of prepectus (Fig. 1F); males with black combs on first mesotarsomeres, but without black combs on mesotrochanters; tergites VII and VIII without broader, foliose setae in addition to usual acuminate, simple setae; tergite X not fused to lateral tergal sclerites in males.

Description. Body small (TL = 2.3−3.9 mm). Head (Fig. 1C): frontoclypeal (epistomal) "suture" complete; head about as wide as long (HW/HL > 0.9 but < 1.1); neck from moderately (NW/HW > 0.75 but < 0.90) to distinctly wide (NW/HW ≥ 0.90); dorsal macrosetae: anterolateral clypeal punctures present; frontoclypeal punctures present; supra-antennal punctures absent; parocular punctures present as one on each side or absent; basal punctures present, single; posterior frontal punctures located posterior to temporal punctures; gular sutures separated, gula with distinct transverse basal impression; ventral basal ridge (VBR) present, postgenal ridge absent; postmandibular ridge (PMR) extended diagonally towards gula; infraorbital ridge extends to PMR; nuchal ridge absent or rudimentary, at most present as a linear impression but not a ridge; eye from medium large (EYL/HL ratio > 1/2 but < 3/4) to very small (EYL/HL ratio less than 3/10); antennomere 1 distinctly shorter than antennomeres 3 and

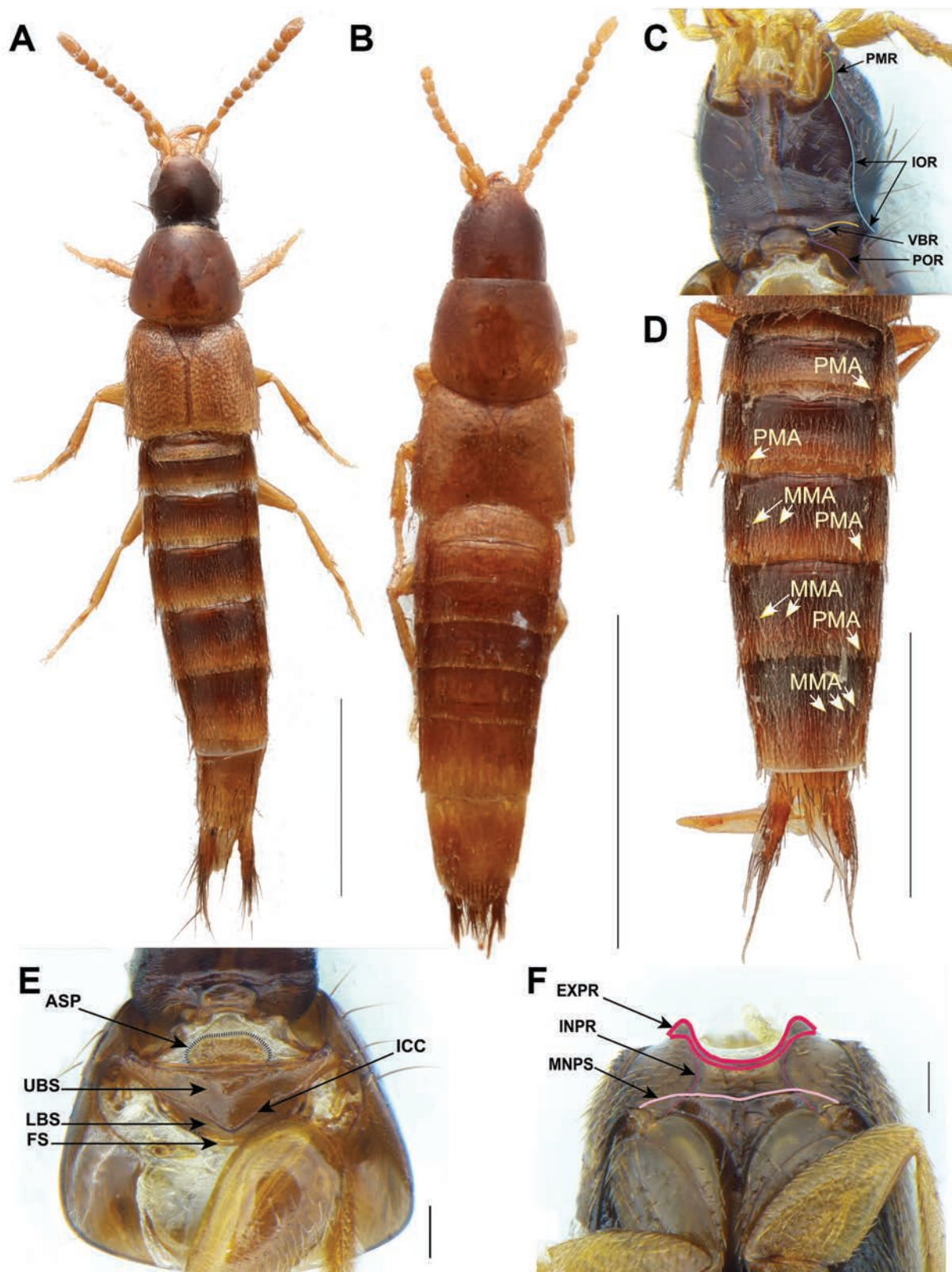**Figure 1.** Some *Chiquiticus* species and characters **A** *C*. sp. nr. *pusio* **B** *C. rambouseki* (Blackwelder, 1943) **C** *C. pusio* (Le-Conte, J. L., 1863), head ventral view **D** *C. pusio*, abdomen **E** *C. pusio*, prosternum **F** *C. pusio*, mesothorax. Abbreviations: ASP, antesternal plate; EXPR, external part of prepectus; FS, profurcasternum; ICC, intercoxal carina of the probasisternum; INPR, internal part of prepectus; IOR, infraorbital ridge; LBS, lower probasisternum; MMA, medial macroseta; MNPS, mesanapleural sutures; PMA, posteromarginal large macrosetae; PMR, postmandibular ridge; POR, postoccipital ridge; UBS, upper probasisternum; VBR, ventral basal ridge. Scale bars: 1 mm (**A, B, D**); 0.1 mm (**C, E, F**).

2 combined; male and female antennomere 11 at least two times longer than antennomere 10; left mandible with proximal, not bifid tooth; maxillary palps: palpomere 4 (apical) subulate, distinctly shorter than palpomere 2, palpomere 3 markedly dilated compared to palpomere 4; labial palps: palpomere 3 (apical) more or less cylindrical, distinctly narrower and longer than palpomere 2, parallel-sided and needle-shaped, palpomere 2 markedly dilated at apex.

Thorax (Fig. 1E, F): prothorax with slightly transverse pronotum (PW/PL ≥ 1.1) with one pair of setiferous punctures in dorsal series widely separated from each other, the distance between them being about equal to the distance between them and the lateral margin; sublateral setiferous punctures present or absent; sternacostal (transverse carina) ridge medially not protruding; antesternal membrane with distinct semisclerotized plate (Fig. 1E); pronotum and prosternum not fused in procoxal cavity, pronotosternal suture complete in cavity; pronotal hypomeron not setose, without postcoxal hypomeral process; upper probasisternum with or without pair of macrosetae. Mesothorax: mesoscutellum without posterior scutellar carina, without sub-basal ridge; elytron without humeral spines or spine-like setae, with evenly setiferous punctation on disc and epipleuron; mesanapleural sutures (Fig. 1F) transverse not reaching or fusing with external part of prepectus, medially fused or nearly touching each other; apex of mesobasisternal intercoxal process varies from sharply pointed to obtuse angle, without V-shaped projection medially; mesocoxal cavities contiguous; pericoxal ridge absent. Metathorax with wings present, with veins CuA and MP4 fused in one vein; metakatepisternal processes divided. Legs: protarsomeres expanded in both sexes; apical tarsomere of all legs with one empodial seta distinctly shorter than tarsal claws; protibial row of laterodorsal spines always present in females but maybe absent in males in some species; ventral tibial spur resting at base of apical excavation connected to tibial margin by thin membranous region; first segment of mesotarsi in males with black comb lateroventrally, without pale adhesive setae; mesotrochanters in both sexes without black comb.

Abdomen: tergites III–V with only anterior transverse basal carina; tergites III–VI with a large posteromarginal macroseta on each side (Fig. 1D); tergites VII and VIII without broader, foliose setae in addition to the usual acuminate, simple setae; anterior transverse basal carina of tergite VII not continuing to paratergites; lateral tergal sclerites IX cylindrical; male sternite VIII with medial apical emargination; male sternum IX symmetrical. Aedeagus with rounded apex.

Distribution. Nearctic region, Central America, the Caribbean. Introduced into Central Europe: *C. pusio* in Germany (Schülke and Renner 2020) and another species related to *C. pusio* collected in Austria with a car net.

Ecology. The North American species occur in various types of debris like leaf litter and similar substrates, with some species also occurring facultatively in mammal burrows or nests (*Neotoma* Say & Ord, 1825), especially in drier regions (Smetana 1971; Adam Brunke pers. comm.). In Europe, where they are introduced, they have been collected using car nets.

Comparison. *Chiquiticus* gen. nov. can be distinguished from all other genera of Staphylininae in broad sense (Newton 2022) by the combination of characters mentioned in the diagnosis. From species close to the type of *Heterothops*, it is distinguished by the paired setiferous macropunctures of the dorsal series being distinctly separated from each other, by a black comb on first mesotar-
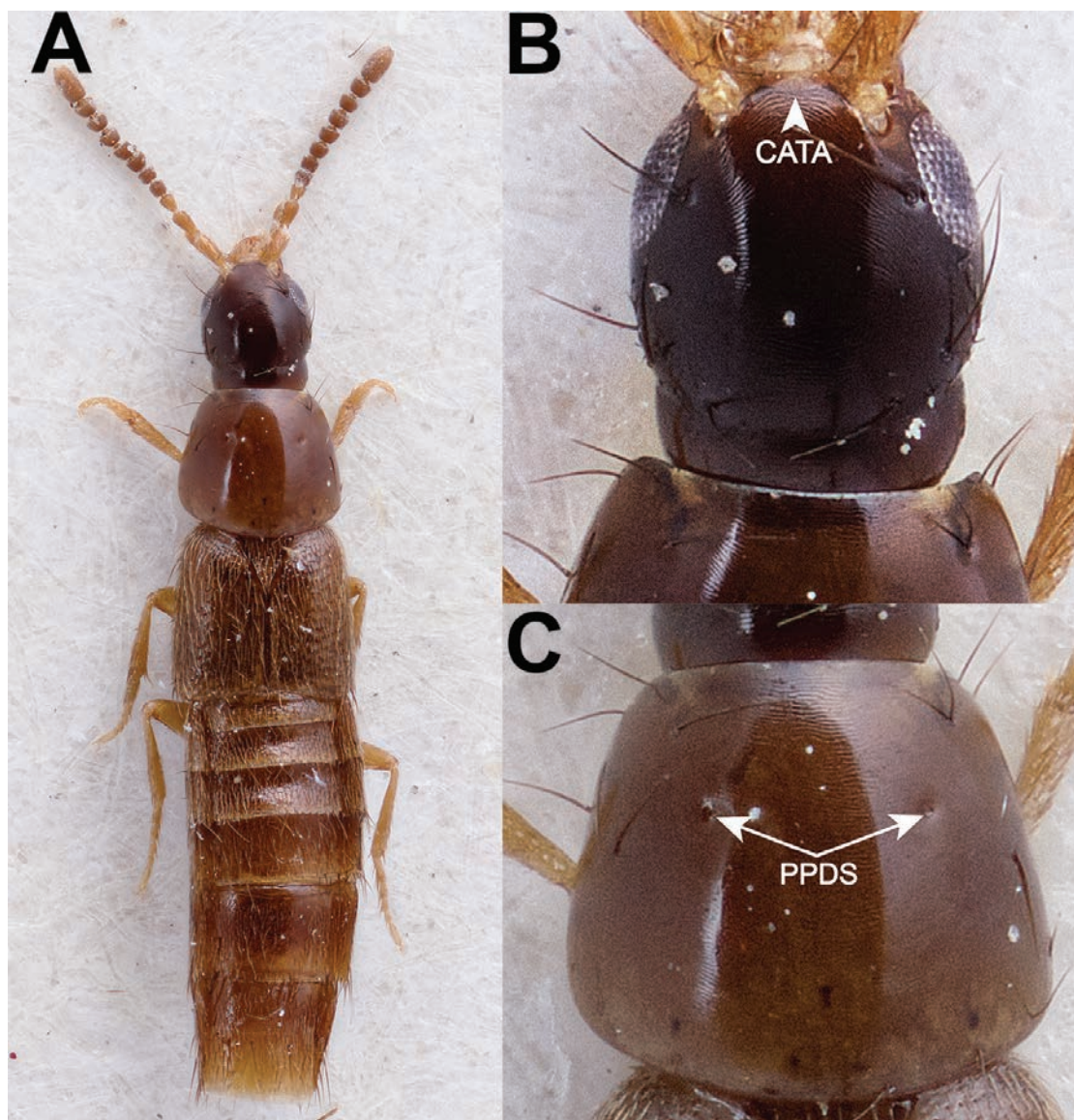
Figure 2. *Chiquiticus arizonicus* (Smetana, 1971) (Holotype #CNC935711) **A** dorsal habitus **B** head **C** pronotum. Abbreviations: CATA, connection of the anterior tentorial arms (frontoclypeal "suture"); PPDS, paired punctures on dorsal series. Photos of # CNC935711 (J. Buffam, Canadian National Collection of Insects, Arachnids and Nematodes).

somere of males, and by presence of only one posteromarginal macrosetae on each side of tergites III–VI. In species close to the type of *Heterothops*, the paired setiferous macropunctures of the dorsal series are close together, the distance between them being distinctly less than the distance between dorsal row and respective lateral margin of pronotum. Also, in the true *Heterothops*, males do not have a black comb on the first mesotarsomere and their pattern of posteromarginal large macrosetae on tergites III–VI is 1, 1, 2 and 2 per side. For more details on the differentiation between *Chiquiticus* gen. nov. and *Heterothops* species from Central Europe, see Schülke and Renner (2020). Presence of a frontoclypeal "suture" is a rare trait in Staphylininae, which in *Chiquiticus* gen. nov. is always visible. In Staphylininae this character is found in few basal lineages, like *Arrowinus* Bernhauer, 1935, several genera of Amblyopinina including *Loncovilius* Germain, 1903 (Reyes-Hernández et al. 2024), and in the relatives to *Chiquiticus*, *Amazonothops* (Jenkins Shaw et al. 2020), and *Ctenandropus*.
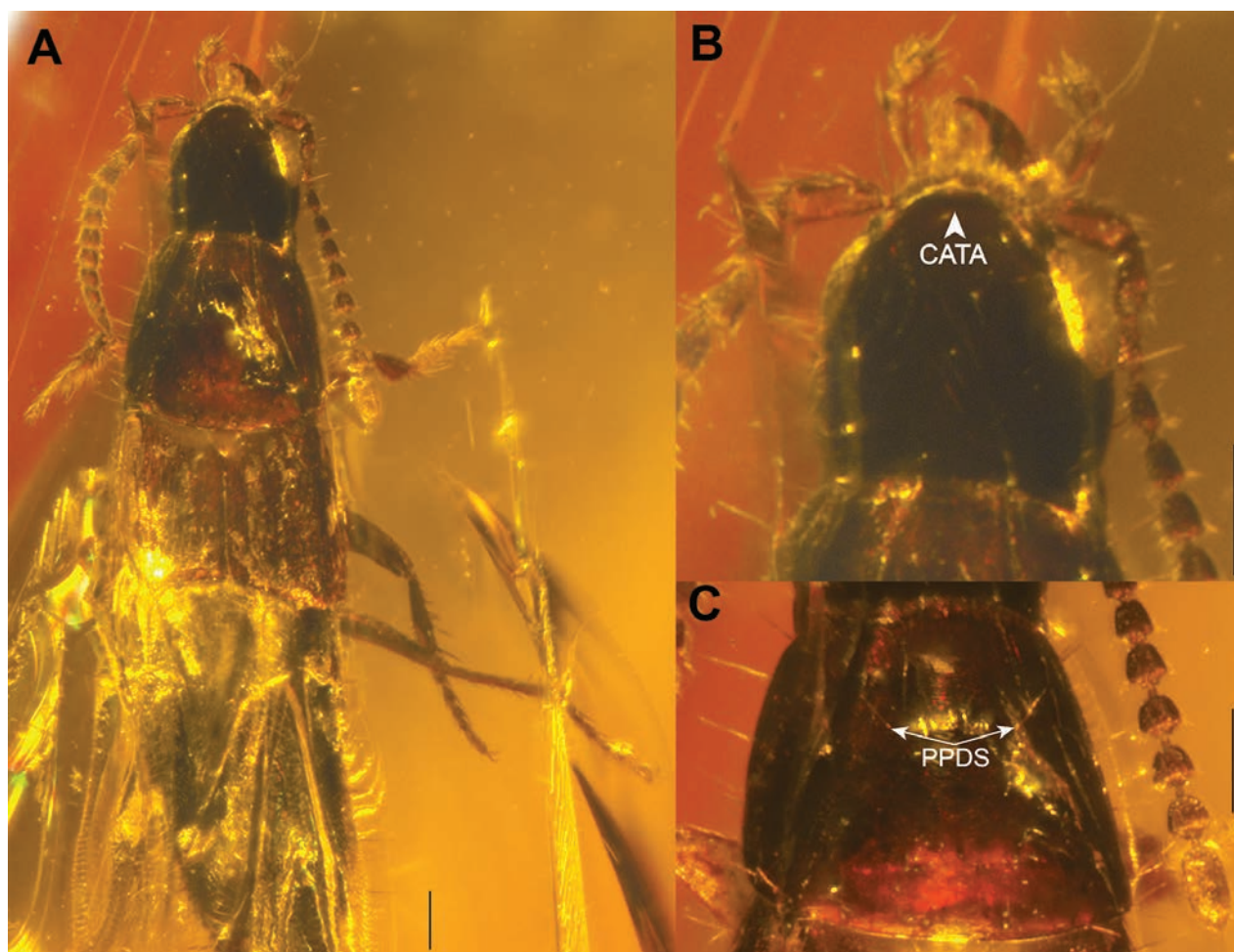
Figure 3. †*Chiquiticus cornelli* (Chatzimanolis & Engel, 2013) (paratype AMNH DR-10-1214) **A** dorsal habitus **B** head **C** pronotum. Abbreviations: CATA, connection of the anterior tentorial arms (frontoclypeal "suture"); PPDS, paired punctures on dorsal series. Photo of AMNH DR-10-1214 (A. Pierwola, American Museum of Natural History). Scale bars: 0.1 mm.

Additionally, *Chiquiticus* gen. nov. displays an antesternal plate, currently known as a unique character of groups such as *Arrowinus* and several tribes united in Xatholininae sensu Żyła and Solodovnikov (2020). However, this plate sometimes is also found in Amblyopinina among Staphylinini, for example in species that are close to the types of the currently non-monophyletic genera *Heterothops* and *Cheilocolpus* (Reyes-Hernández et al. 2024). Furthermore, *Chiquiticus* exhibits unique characters shared only with the related genera *Ctenandropus* and *Amazonothops*, such as the presence of transverse mesanapleural sutures distinctly separated from the external portion of the prepectus (Fig. 1F and fig. 3E in Jenkins Shaw et al. (2020) misinterpreted as "transvere ridge (TR)") and distinctly elongated protergal glands (fig. 3F in Jenkins Shaw et al. (2020)). *Chiquiticus* is distinguished from *Ctenandropus* by the subconical head with ventral basal ridge; the transverse pronotum (PW/PL ≥ 1.1) with its maximum width in the posterior half; usually by presence of intercoxal carina separating the upper probasisternum and lower probasisternum; and by tergites III–V lacking a posterior transverse carina. In *Ctenandropus*, the head is subquadrate, without postgenal ridge or ventral basal ridge; the pronotum is as long as wide (PW/PL > 0.9 but < 1.1), with its maximum width in the anterior half; without intercoxal carina separating the upper probasisternum and lower probasisternum; and
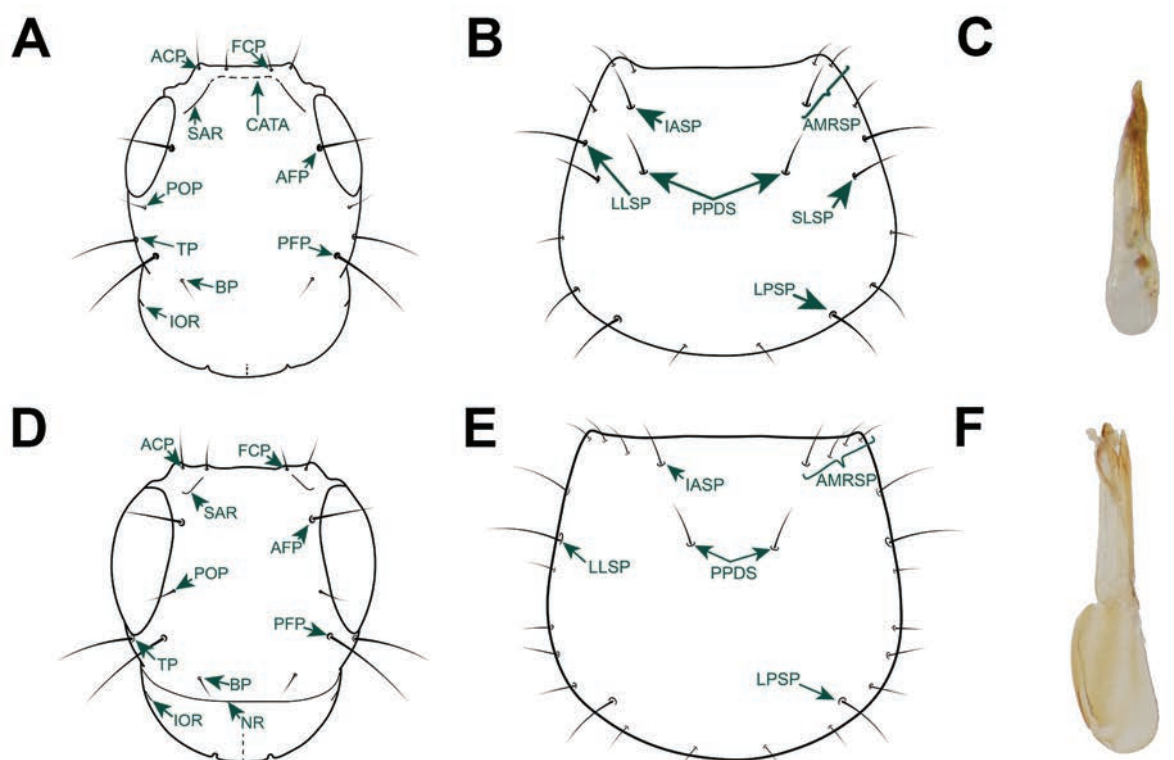
Figure 4. Morphological details of *Chiquiticus* and *Heterothops* **A–C** *Chiquiticus* sp. aff. *pusio* from Panama **D–F** *Heterothops* sp. undescribed from Costa Rica **A, D** head **B, E** pronotum **C, F** aedeagus in lateral view, the scale to the right is equal to 1 mm. Abbreviations: ACP, anterolateral clypeal puncture; AFP, anterior frontal; AMRS, anterior marginal row of setiferous punctures; BP, basal puncture; CATA, connection of the anterior tentorial arms (frontoclypeal "suture"); FCP, frontoclypeal puncture; IASP, internalmost setiferous puncture of the anterior margin; IOR, infraorbital ridge; LLSP, large lateral setiferous puncture; LPSP, large posterior setiferous puncture; NR, nuchal ridge; PFP, posterior frontal puncture; POP, parocular punctures; PPDS, paired punctures on dorsal series; SAR, supra-antennal ridge; SLSP, sublateral setiferous puncture; TP, temporal puncture.

tergites III–V have a posterior transverse carina. *Chiquiticus* is distinguished from *Amazonothops* by the absence of a black comb on the mesotrochanters of males and foliaceous setae on the tergites in both sexes, by distinctly short empodial setae, by the tergite X not fused to internal face of lateral sclerites and by paramere with rounded apex and short lateroapical setae.

Etymology. The name is derived from the Latinization of the word "Chiquitico", which is a term used in some Hispanophone countries to refer to very small things. The gender is masculine.

New combinations notes. The extinct species †*C. infernalis* from Dominican Amber is here restudied based on the original descriptions only. Many details important for the taxonomic placement of this species (e.g. pronotum and mesanapleural sutures) are not visible in the photos of this fossil there and probably they would be available only with the mCT examination. However, such visible features as habitus including small body size, as well as antennal bases located close to each other, very elongated last antennomere that is almost as long as the two preceding ones, oval and setose preapical maxillary palpomere that is clearly wider than the apical one, and wide neck allowed us to conclude that †*C. infernalis* is an extinct member of the new genus *Chiquiticus*. For †*C. cornelli*, in addition to the original description, we were able to examine better

photos of the holotype and paratype kindly made available at our request (Fig. 3). In these images, in addition to the characters previously described for †*C. infernalis*, the connection of the anterior tentorial arms (Fig. 3B) and the widely separated paired punctures in the dorsal series (Fig. 3C) are visible. It should be noted that both fossil species are known only from females. Also, two specimens of the extant *C. rambouseki* (Blackwelder, 1943) that we examined were females and not in the best condition; however, the combination of their visible characters allows the species to be placed in *Chiquiticus*.

Biogeographic note. As far as currently known, the Nearctic is the region with the greatest species diversity of *Chiquiticus*. However, the *Chiquiticus* fossils found in mid-Miocene Dominican amber (Chatzimanolis and Engel 2013) could suggest that Nearctic speciation took place after the genus dispersed there from the southern hemisphere where its closely related genera *Amazonothops* and *Ctenandropus* are also found (Reyes-Hernández et al. in prep.). Such dispersal may have occurred via the GAARlandia land bridge (Iturralde-Vinent 2006; Masonick et al. 2017; Iturralde-Vinent and MacPhee 2023).

Genus *Nitidocolpus* gen. nov.
https://zoobank.org/9BC238C3-B742-4E1E-8B59-48E8C83288DF
Figs 5, 6A−C

Type species. *Quedius columbinus* Bernhauer, 1917, here designated.
Included species. *Nitidocolpus aurofasciatus* (Bernhauer, 1917), comb. nov. ex. *Quedius* [1 syntype from FMNH examined]; *Nitidocolpus championi* (Sharp, 1884), comb. nov. ex. *Quedius* [1 syntype from FMNH examined]; *Nitidocolpus columbinus* (Bernhauer, 1917), comb. nov. ex. *Quedius* [2 syntypes from FMNH examined]; *Nitidocolpus germaini* (Bernhauer, 1917), comb. nov. ex. *Quedius* [1 syntype from FMNH examined]; *Nitidocolpus illatus* (Sharp, 1884), comb. nov. ex. *Quedius* [1 syntype from NHM examined]; *Nitidocolpus laeticulus* (Sharp, 1884), comb. nov. ex. *Quedius* [1 syntype from NHM examined]; *Nitidocolpus triangulum* (Fauvel, 1891), comb. nov. ex. *Quedius* [1 syntype from IRSNB examined].

Diagnosis. Supra-antennal punctures and paraocular punctures absent (Fig. 6A); pronotum without paired dorsal series of setiferous macropunctures (Fig. 6B); mesanapleural sutures transverse or nearly transverse but reaching the external part of prepectus (Fig. 5E); mesobasisternal intercoxal process with V-shaped projection medially (Fig. 5E); metatrochanters with apical spine (Fig. 5F).

Description. Small to medium-sized Staphylininae (TL = 4.5−10 mm) (Fig. 5A−D). Head: Frontoclypeal (epistomal) suture absent or distinct only laterally and only in teneral (or chemically cleared) specimens; head slightly transverse (HW/HL ≥ 1.1) without distinct posterior angles; disc smooth; frons with microsculpture as transverse waves, without distinct concavity between antennal insertions; neck moderately wide (NW/HW > 0.75 but < 0.90); dorsal macrosetae (Fig. 6A): anterolateral clypeal punctures present; frontoclypeal punctures present; supra-antennal punctures absent; parocular punctures absent; basal punctures present, single; ventral macrosetae: postocular punctures present; infraorbital punctures absent; postmandibular punctures present; submentum with two pairs of macrosetae; mentum with seta alpha only, seta beta absent;
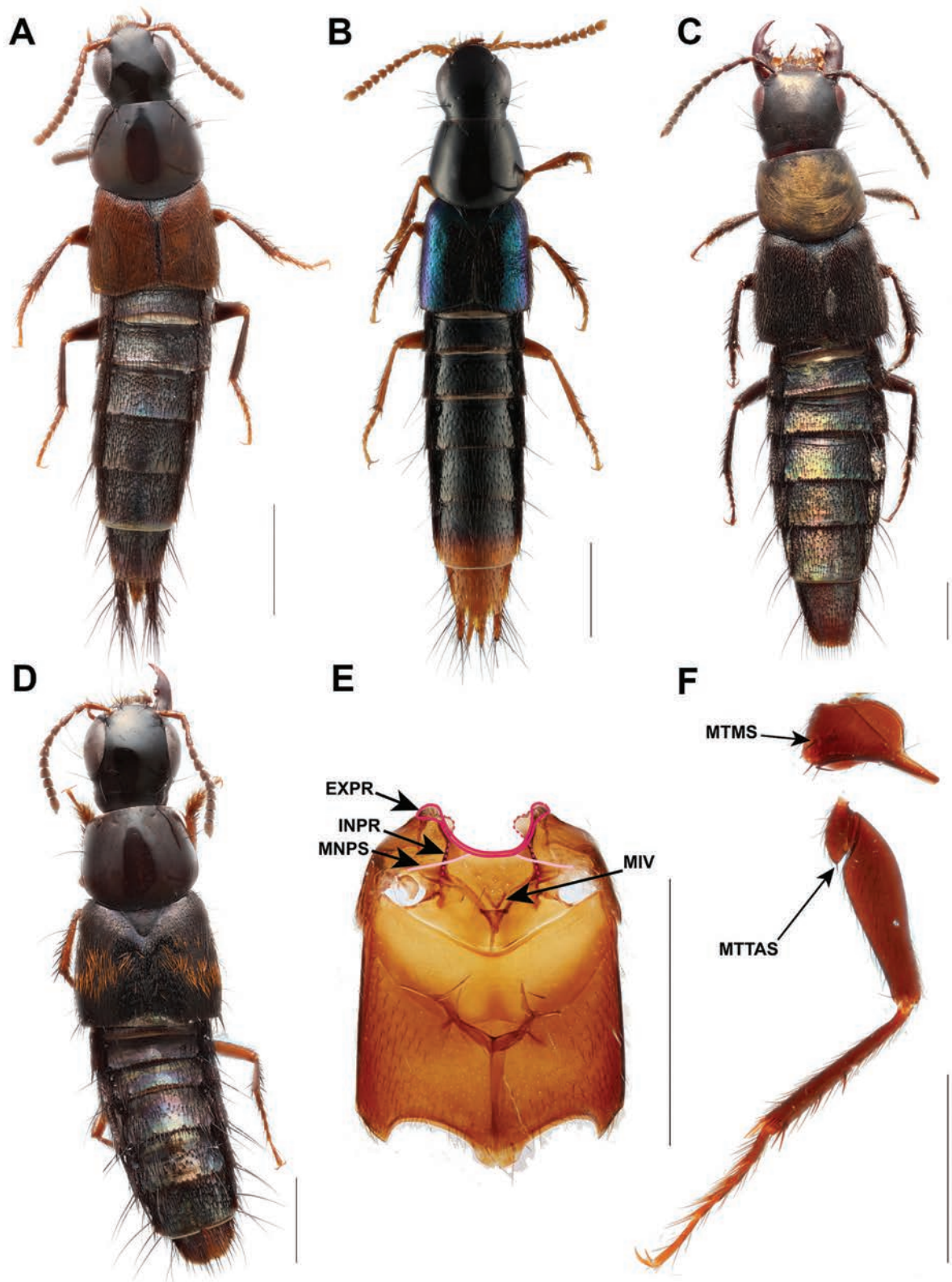
Figure 5. Some *Nitidocolpus* species and characters **A** *N. illatus* (Sharp, 1884) **B** *N. laeticulus* (Sharp, 1884) **C** *N. germaini* (Bernhauer, 1917) **D** *N. aurofasciatus* (Bernhauer, 1917) **E** *N. illatus*, pterothoraces **F** *N. columbinus* (Bernhauer, 1917), metacoxa and metatrochanter, dissected right leg in dorsal view (side faced to the abdomen). Abbreviations: EXPR, external part of prepectus; INPR, internal part of prepectus; MIV, mesobasisternal intercoxal process with V-shaped projection medially; MNPS, mesanapleural sutures; MTMS, metacoxa with dorsomedial spine; MTTAS, metatrochanter with dorsoapical spine. Photo B by J. Jenkins Shaw. Scale bars: 1 mm.

gular sutures separated from each other, gula with distinct transverse basal impression; ventral basal ridge present; postgenal ridge present; postmandibular ridge short, extended parallel to margin of eye, without fusion with any other ridge and distinctly separated from eye margin; infraorbital ridge merged with postgenal ridge; nuchal ridge missing dorsally, present laterally, merged with infraorbital ridge; eyes of medium size (EYL/HL ratio more than 1/2 but less than 3/4); gena short (GL/ETL < 0.5); tomentose pubescence begins from fourth antennomere, its density on fourth antennomere as on following antennomeres; setation of antennomere 3 almost evenly distributed; antennomere 11 with subapical rounded field, without subapical lateral pits; mandibles with dorso-lateral seta, without dorso-lateral groove, external edge with curved base and apex, straight in middle length; right mandible with proximal tooth and bifid distal tooth, apically deflexed ventrad at an angle of >20°; left mandible rather straight; labrum with transparent wide apical membrane, anterior margin emarginate at middle; maxillary palps: palpomere 4 (apical) subconical, with evenly narrowed apex, longer than palpomere 2 and weakly dilated compared to palpomere 3; labial palps: palpomere 3 (apical) more or less fusiform or subconical, distinctly longer than, and about as wide as, palpomere 2.

Thorax: Prothorax with slightly transverse pronotum (PW/PL ≥ 1.1), without dorsal or sublateral series of setiferous punctures; prosternum without longitudinal keel; antesternal membrane without distinct semisclerotized patch or patches; probasisternum triangular, with narrowed lateral arms and disc protruding medially, with pair of macrosetae on the upper probasiternum; with rounded postcoxal hypomeral process, interrupted by inferior line. Mesothorax: mesoscutellum without posterior scutellar carina, without sub-basal ridge; elytra with humeral spines or spine-like setae, with even setiferous punctation on disc and epipleuron (sometimes with various setose color patterns); with setiferous punctures at apical margin of elytral suture (underside); mesanapleural sutures transverse or nearly transverse but reaching and fusing with external part of prepectus; mesobasisternum with intercoxal process narrowly pointed into sharp angle, without V-shaped projection medially; mesocoxal cavities contiguous; pericoxal ridge present and complete. Metathorax: wings present, with veins CuA and MP4 fused; metakatepisternal processes divided; metascutellar mid-longitudinal internal suture well developed (only visible in chemically cleared specimens). Legs: apical tarsomere of all legs without dorsal setae, with one empodial seta distinctly shorter than tarsal claws; protarsomeres 1–3 distinctly wider than long in both sexes, with pale adhesive setae ventrally; procoxa with internal ridge running parallel along external ridge; mesotarsi in both sexes without black comb, sometimes in males ventral side of first mesotarsomere with pale adhesive setae; mesotibiae straight; metatarsomere 1 shorter than metatarsomere 5; metatarsi shorter than metatibiae; metatrochanter apically rounded, with strong straight dorsoapical spine; metacoxae with four or fewer spines on ventral posterolateral lobe, spines on dorsomedial disc also present; basal part of metacoxae distinctly wider and more convex than apical part.

Abdomen: protergal glands well manifested as rounded cuticular acetabula; tergites III–V in some species with posterior basal transverse carinae, in some species they are only with anterior carinae; on tergite VII anterior trans-
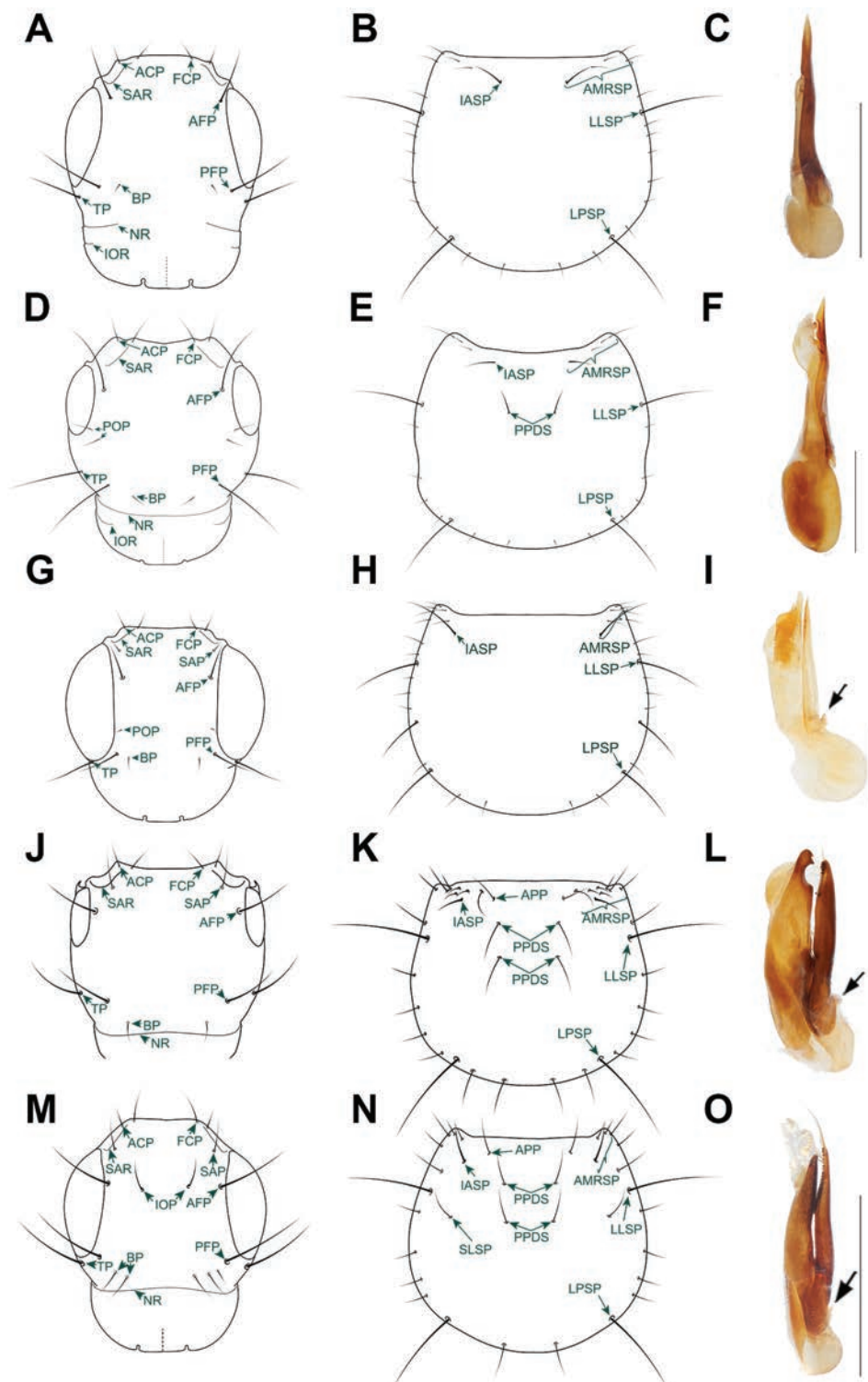
Figure 6. Morphological details of *Nitidocolpus* and other relevant genera of Staphylininae **A–C** *Nitidocolpus columbinus* **D–F** *Cheilocolpus viridulus* **G–I** *Cyrtoquedius* sp. **J–L** *Quedionuchus* nr. *impunctus* **M–O** *Quedius* nr. *advena*. **A, D, G, J, M** head **B, E, H, K, N** pronotum **C, F, I, L, O** aedeagus in lateral view, the black arrow pointing down indicates the basal projection of the paramere. Abbreviations: ACP, anterolateral clypeal puncture; AFP, anterior frontal; AMRSP, anterior marginal row of setiferous punctures; APP, additional paired punctures adjacent to AMRSP; BP, basal puncture; FCP, frontoclypeal puncture; IASP, internalmost setiferous puncture of the anterior margin; IOP, interocular punctures; IOR, infraorbital ridge; LLSP, large lateral setiferous puncture; LPSP, large posterior setiferous puncture; NR, nuchal ridge; PFP, posterior frontal puncture; POP, parocular punctures; PPDS, paired punctures on dorsal series; SAP, supra-antennal puncture; SAR, supra-antennal ridge; SLSP, sublateral setiferous puncture; TP, temporal puncture. Scale bars: 1 mm.

verse basal carina not continuing to paratergites; tergites III–VI with different patterns of posteromarginal large macroseta (PMM) on each side, IV–VI with more than one PMM per side; punctation of tergites in form of fine to moderate impressions, some species with wide glabrous areas; lateral tergal sclerites IX short and slightly laterally flattened; male sternite VIII with medial apical emargination. Aedeagus with paramere fused to median lobe only at base and very closely appressed to median lobe along entire length; base of the paramere flat medially, not projecting upwards in the middle; paramere strongly produced over apex of median lobe. Ovipositor with each second gonocoxite with one medial macroseta, without spine-like setae on outer lateral margin.

Distribution. Neotropical Realm: Mexican Transition Zone, Central America, and northern South America.

Ecology. This genus has been collected from a variety of microhabitats, including mushrooms (e.g., *Pleurotus* spp.), under decomposing logs, beneath bark, and in leaf litter found in cloud, oak, and pine forests. They are also frequently captured using flight-intercept and Malaise traps. Additionally, some species are associated with the inflorescences of plants from the families Arecaceae, Betulaceae, and Heliconiaceae.

Comparison. *Nitidocolpus* gen. nov. can be distinguished from all other genera of Staphylininae by the combination of characters mentioned in the diagnosis. *Nitidocolpus* is further distinguished from the superficially similar Quediina and Cytoquediina (Fig. 6) by the lack of supra-antennal punctures, the presence of a single carina on the mesoscutellar shield (posterior carina absent), by hind wings with fused CuA and MP4 veins, by a single empodial setae, and by the base of the paramere, which has no upward or forward projection in the middle. Compared to other Neotropical genera that resemble *Nitidocolpus*, such as *Cheilocolpus*, *Mimosticus* Sharp, 1884, and *Heterothops*, *Nitidocolpus* is distinguished by the absence of paraocular punctures on the head, the lack of setiferous punctures in or near the center of the pronotal disc, and the presence of postcoxal hypomeral processes. In some species of *Nitidocolpus*, such as *N. laeticulus* (Fig. 5B) and *N. aurofasciatus* (Fig. 5D), the basal punctures have shifted anteriorly and thus may be erroneously considered paraocular punctures. However, they can be easily distinguished as basal punctures, because they are the only punctures located near the posterior frontal punctures, aside from the temporal punctures. In other species of *Nitidocolpus*, such as *N. illatus* (Fig. 5A), the innermost macrosetae on the anterior margin maybe erroneously considered as a puncture of the dorsal row because it is located far from the anterior margin of pronotum.

Etymology. The name is derived from the Latin words "nitidus" and "colpus", which mean "shiny" and "hit", respectively. The name refers to the great clarity with which the head and pronotum punctures are seen. The gender is masculine.

New combinations in the genera *Cheilocolpus* Solier, 1849 and *Cyrtoquedius* Bernhauer, 1917

As shown above, describing the genus *Nitidocolpus* required careful examination of a number of the poorly known species of *Quedius*, some of which, as we should stress, do not belong to *Nitidocolpus*. They belong to neither *Quedius* nor Quediina. Our examination revealed that most of them belong to the ambly-
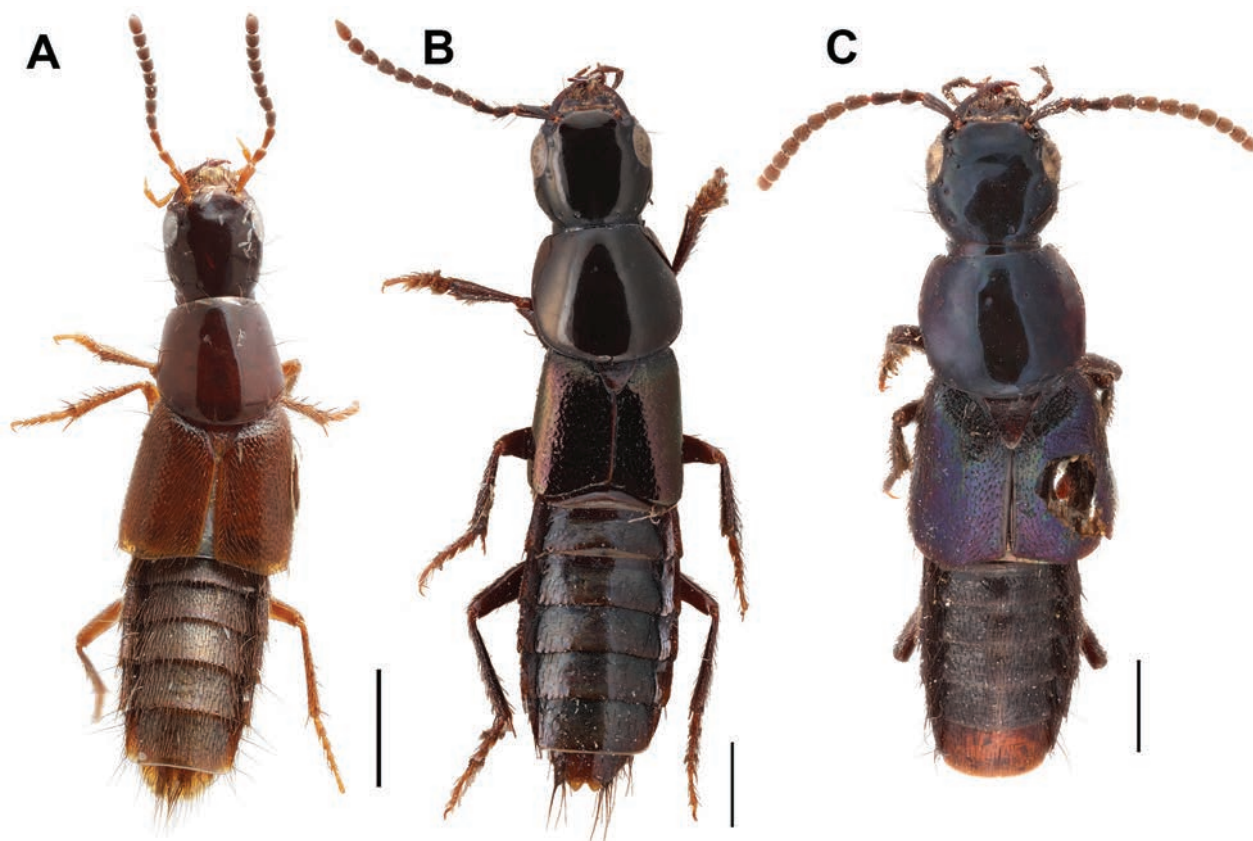
Figure 7. Some *Cheilocolpus* species **A** *Ch. pyrostoma* (Solier, 1849) **B** *Ch. speciosus* (Bernhauer, 1917) **C** *Ch. viridulus* (Erichson, 1840).

opinine genus *Cheilocolpus*, as it is defined in Coiffait and Sáiz (1966) and Sáiz (1971), with adjustments by Reyes-Hernández et al. (2024); i.e., they are close to the type species *Cheilocolpus pyrostoma* (Solier, 1849) (Fig. 7A). As a result, here we move these species as follows: *Cheilocolpus forsteri* (Scheerpeltz, 1960), comb. nov. ex. *Quedius* [although the type material was not examined, the detailed original description and distribution data provided by Scheerpeltz (1960) allow this species to be placed within *Cheilocolpus*; it has a combination of features typical for *Cheilocolpus* from the páramos: brachypterous habitus, entirely brownish-black body, rectangular head with transverse microsculpture and small convex eyes, paraocular punctures, and tergites III–V with posterior transverse basal carina]; *Cheilocolpus speciosus* (Bernhauer, 1917), comb. nov. ex. *Quedius* [1 syntype from FMNH examined (Fig. 7B)]; *Cheilocolpus viridulus* (Erichson, 1840), comb. nov. ex. *Quedius* [2 syntypes from MFNB examined (Fig. 7C)].

Furthermore, we propose the following new combination for the species *Cyrtoquedius viridipennis* (Fauvel, 1891), comb. nov. ex. *Quedius*. Although the type material was not examined, the original description and distribution data provided by Fauvel (1891) support placing this species within *Cyrtoquedius*, in accordance with the diagnosis by Brunke et al. (2016). Fauvel noted that it is closely related to *Cy. labiatus* (Erichson, 1840) but differs in coloration. He also described the elytra as having three rows of larger punctures, with the remaining punctures faint and vaguely marked, which are typical characteristics of this genus. This contrasts with *Nitidocolpus* and *Cheilocolpus*, where the elytra are evenly setose rather than mostly glabrous except for rows of macrosetae.

Discussion

The description of *Chiquiticus* gen. nov. and *Nitidocolpus* gen. nov. was necessitated due to the upcoming formal taxonomic embedding of the newly discovered lineages in Staphylininae in Reyes-Hernández et al. (in prep.). Also, it is a step towards badly needed taxonomic clean-up of the polyphyletic large wastebasket genera *Heterothops* (Amblyopinina) and *Quedius* (Quediina), especially for the New World fauna, because here we based our genus descriptions solely on the species earlier described in those genera. These are eight species of *Heterothops* (of which two are extinct) for *Chiquiticus* and eight species of *Quedius* for *Nitidocolpus*. Globally, many more non-related convergently similar species remain misplaced in both *Heterothops* and *Quedius*. In the American fauna, following the establishment of *Chiquiticus* and *Nitidocolpus*, the number of misclassified *Heterothops* species has significantly decreased. Moreover, in the course of this study we reclassified a number of the Neotropical *Quedius* species which superficially resemble *Nitidocolpus* but in fact, belong to the amblyopinine genus *Cheilocolpus* or the cyrtoquediine genus *Cyrtoquedius*. It should be noted that in both *Chiquiticus* and *Nitidocolpus* there are also several new species to be described; as well as in the genus *Cheilocolpus* and other genera of the former "southern quediines". Due to the above-mentioned pragmatic taxonomic purposes of the current generic descriptions, here we considered solely the described species based on the type material or their original descriptions if they displayed enough data to adequately identify them as either new genus. Descriptions of all new species as well as the update of the taxonomy including lectotype designations, redescriptions, summary of the distribution, and bionomics information on the earlier described species in both new and other involved genera will be provided in future revisionary work.

Acknowledgements

Additional information

Conflict of interest

The authors have declared that no competing interests exist.

Ethical statement

No ethical statement was reported.

Author contributions

Both authors have contributed equally.

Author ORCIDs

José L. Reyes-Hernández ⓘ https://orcid.org/0000-0002-4726-4439
Alexey Solodovnikov ⓘ https://orcid.org/0000-0003-2031-849X

Data availability

All of the data that support the findings of this study are available in the main text.

References

Brunke AJ (2022) A world generic revision of Quediini (Coleoptera, Staphylinidae, Staphylininae), part 1. Early diverging Nearctic lineages. ZooKeys 1134: 129–170. https://doi.org/10.3897/zookeys.1134.87853

Brunke AJ, Chatzimanolis S, Schillhammer H, Solodovnikov A (2016) Early evolution of the hyperdiverse rove beetle tribe Staphylinini (Coleoptera: Staphylinidae: Staphylininae) and a revision of its higher classification. Cladistics 32(4): 427–451. https://doi.org/10.1111/cla.12139

Brunke AJ, Żyła D, Yamamoto S, Solodovnikov A (2019) Baltic amber Staphylinini (Coleoptera: Staphylinidae: Staphylininae): a rove beetle fauna on the eve of our modern climate. Zoological Journal of the Linnean Society 187(1): 166–197. https://doi.org/10.1093/zoolinnean/zlz021

Brunke AJ, Hansen AK, Salnitska M, Kypke JL, Predeus AV, Escalona H, Chapados JT, Eyres J, Richter R, Smetana A, Ślipiński A, Zwick A, Hájek J, Leschen RAB, Solodovnikov A, Dettman JR (2021) The limits of Quediini at last (Staphylinidae: Staphylininae): a rove beetle mega-radiation resolved by comprehensive sampling and anchored phylogenomics. Systematic Entomology 46(2): 396–421. https://doi.org/10.1111/syen.12468

Chatzimanolis S, Engel MS (2013) The Fauna of Staphylininae in Dominican Amber (Coleoptera: Staphylinidae). Annals of Carnegie Museum 81(4): 281–294. https://doi.org/10.2992/007.081.0401

Coiffait H, Sáiz F (1966) Les Quediini du Chili (Col. Staphylinidae). Annales de la Société Entomologique de France (n. ser.) 2: 385–414.

Fauvel A (1891) Voyage de M. E. Simon au vénézuela (Décembre 1887–Avril 1888). 11e Mémoire. Revue d'Entomologie 10: 87–127.

Herman L (2023) Generic Revisions of the Scopaeina and the Sphaeronina (Coleoptera: Staphylinidae: Paederinae: Lathrobiini). Bulletin of the American Museum of Natural History 460(1): 1–194. https://doi.org/10.1206/0003-0090.460.1.1

Iturralde-Vinent M (2006) Meso-Cenozoic Caribbean paleogeography: implications for the historical biogeography of the region. International Geology Review 48(9): 791–827. https://doi.org/10.2747/0020-6814.48.9.791

Iturralde-Vinent MA, MacPhee RDE (2023) New evidence for late Eocene-early Oligocene uplift of Aves Ridge and paleogeography of GAARlandia. Geologica Acta 21.5: 1–10. https://doi.org/10.1344/GeologicaActa2023.21.5

Jenkins Shaw J, Orlov I, Solodovnikov A (2020) A new genus and species of Staphylininae rove beetle from the Peruvian Amazon (Coleoptera, Staphylinidae). ZooKeys 904: 103–115. https://doi.org/10.3897/zookeys.904.48592

Li L, Zhou HZ (2011) Revision and phylogenetic assessment of the rove beetle genus *Pseudohesperus* Hayashi, with broad reference to the subtribe Philonthina (Coleoptera: Staphylinidae: Staphylinini). Zoological Journal of the Linnean Society 163(3): 679–722. https://doi.org/10.1111/j.1096-3642.2011.00731.x

Masonick P, Michael A, Frankenberg S, Rabitsch W, Weirauch C (2017) Molecular phylogenetics and biogeography of the ambush bugs (Hemiptera: Reduviidae: Phymatinae). Molecular Phylogenetics and Evolution 114: 225–233. https://doi.org/10.1016/j.ympev.2017.06.010

Newton A (2022) StaphBase_2022-12-12_15:41:00_-0600. In: Bánki O, Roskov Y, Döring M, Ower G, Vandepitte L, Hobern D, Remsen D, Schalk P, DeWalt RE, Keping M, Miller J, Orrell T, Aalbu R, Abbott J, Adlard R, Adriaenssens EM, Aedo C, Aescht E, Akkari N, et al. (Eds) Catalogue of Life Checklist (Aug 2022). https://doi.org/10.48580/dg9ld-3gk

Reyes-Hernández JL, Hansen AK, Jenkins Shaw J, Solodovnikov A (2024) Phylogeny-based taxonomic revision and niche modelling of the rove beetle genus *Loncovilius* Germain, 1903 (Coleoptera: Staphylinidae: Staphylininae). Zoological Journal of the Linnean Society 202: zlad143. https://doi.org/10.1093/zoolinnean/zlad143

Sáiz F (1971) Sur les Quediini du Chili (Col. Staphylinidae). Bulletin de la Société d'Histoire Naturelle de Toulouse 106: 364–392.

Scheerpeltz O (1960) Zur kenntnis neotropischer staphyliniden (col.). Beitrage zur Neotropischen Fauna 2: 65–138. https://doi.org/10.1080/01650526009380624

Schülke M, Renner K (2020) *Heterothops* pusio Leconte, 1863 eine neue Adventivart aus Nordamerika in Deutschland (Coleoptera, Staphylinidae, Staphylininae, Amblyopinini). Linzer biologische Beiträge 52(1): 501–507.

Smetana A (1971) Revision of the tribe Quediini of America north of Mexico (Coleoptera: Staphylinidae). The Memoirs of the Entomological Society of Canada 103(S79): 1–303. https://doi.org/10.4039/entm10379fv

Żyła D, Solodovnikov A (2020) Multilocus phylogeny defines a new classification of Staphylininae (Coleoptera, Staphylinidae), a rove beetle group with high lineage diversity. Systematic Entomology 45(1): 114–127. https://doi.org/10.1111/syen.12382

Research Article

Four new species of leptonetid spiders (Araneae, Leptonetidae) from Anhui Province, China

Shuhui Li[1]*, Qiang Chen[2]*, Yanfeng Tong[1]

1 *College of Life Science, Shenyang Normal University, Shenyang 110034, China*
2 *Experimental Teaching Center, Shenyang Normal University, Shenyang 110034, China*
Corresponding author: Yanfeng Tong (tyf68@hotmail.com)

Abstract

Four new species of leptonetid spiders from Anhui Province, China are recognized: *Jingneta qishan* Tong, **sp. nov.** (♂♀), *Jingneta wukuishan* Tong, **sp. nov.** (♂), *Leptonetela jingde* Tong, **sp. nov.** (♂♀) and *Rhyssoleptoneta lishan* Tong, **sp. nov.** (♂♀). An identification key to leptonetid spiders from Anhui is provided.

Key words: Asia, biodiversity, identification key, *Jingneta*, *Leptonetela*, new taxa, *Rhyssoleptoneta*, taxonomy

Introduction

Members of the family Leptonetidae Simon, 1890 are tiny (1–3 mm) and typically have six eyes, with the posterior median eyes displaced behind the anterior lateral eyes and the posterior lateral eyes, and anterior median eyes have been lost. Most species live in moist habitats, such as leaf litter, under rocks and in caves (Ledford et al. 2021).

Leptonetidae includes 22 genera and 392 species from North America, the Mediterranean, and East and Southeast Asia (World Spider Catalog 2024). Currently, 145 species belonging to eight genera have been recorded in China (Wang et al. 2020; Liu and Zhang 2022; Yang et al. 2022; Hu and Liu 2023; Liu et al. 2024). Anhui Province, a provincial-level administrative region of China, is located in the Yangtze River Delta region of East China (Fig. 14). Four species belonging to three genera have been recorded in Anhui Province: *Jingneta maculosa* (Song & Xu, 1986), *J. tunxiensis* (Song & Xu, 1986), *Leptonetela microdonta* (Xu & Song, 1983) and *Longileptoneta shenxian* Wang & Li, 2020 (Xu and Song 1983; Song and Xu 1986; Wang et al. 2020).

In this study, four new species of leptonetid spiders from the Anhui Province of China are described and illustrated. An identification key is provided.

___
* These authors contributed equally to this work.

Materials and methods

Specimens used in this study were collected by sifting forest leaf litter and examined using a Leica M205 C stereomicroscope. Fine details were studied using an Olympus BX51 compound microscope. Female genitalia were cleared in lactic acid. Photomicroscope images were made with a Canon EOS 750D zoom digital camera (24.2 megapixels) mounted on an Olympus BX51 compound microscope. Photos were stacked with Helicon Focus ® (version 8.2.0) and processed in Adobe Photoshop CC 2020 ®. Scanning electron microscope images (SEM) were taken under high vacuum with a Hitachi S-4800 after critical-point drying and gold-palladium coating. Leg measurements are shown as: total length (femur, patella, tibia, metatarsus, tarsus) and, when missing, were coded as "−". All measurements were taken using an Olympus BX51 compound microscope and are in millimeters.

All specimens are preserved in 75% ethanol. The type material is deposited in the Shenyang Normal University (**SYNU**) in Liaoning, China (curator: Yanfeng Tong).

Terminology follows Wang et al. (2020) and Yang et al. (2022). The following abbreviations are used in the text and figures: AER = anterior eye row; ALE = anterior lateral eyes; at = atrium; emb = embolus; ma = median apophysis; mo = median outgrowth; ms = median sclerite; PER = posterior eye row; pl = prolateral lobe; PLE = posterior lateral eyes; PME = posterior median eyes; po = prolateral outgrowth; ps = prolateral sclerite; rl = retrolateral lobe; ro = retrolateral outgrowth; sc = scape; so = small outgrowth; sp = spermathecae; spr = short projection; ss = spermathecal stalk; ts = tarsal spur.

Taxonomy

Family Leptonetidae Simon, 1890

Genus *Jingneta* Wang & Li, 2020

Type species. *Leptoneta cornea* Tong & Li, 2008.
    Diagnosis. See Wang et al. (2020).
    Composition. Twelve species, including two described here.
    Distribution. China (Anhui, Beijing, Hebei).

***Jingneta qishan* Tong, sp. nov.**
https://zoobank.org/C77BF2C5-2968-4EAA-9F12-11D412A835DF
Figs 1–4, 13A, 14

Type material. *Holotype* CHINA • ♂ (SYNU-1168); Anhui, Chizhou City, Guichi District, Qishan Scenic Area; 30°38'19"N, 117°29'57"E, 70 m; 12.I.2022; H. Fu & K. Yang leg. *Paratype*: CHINA • ♀ (SYNU-1169), same data as holotype.
    Etymology. The specific name refers to the type locality and is a noun in apposition.
    Diagnosis. This new species is similar to *Jingneta exilocula* (Tong and Li 2008: fig. 2A–H) in the horn-shaped apophysis of palpal tibia, but can be distinguished by the chelicerae lacking a stridulatory file on the lateral margin
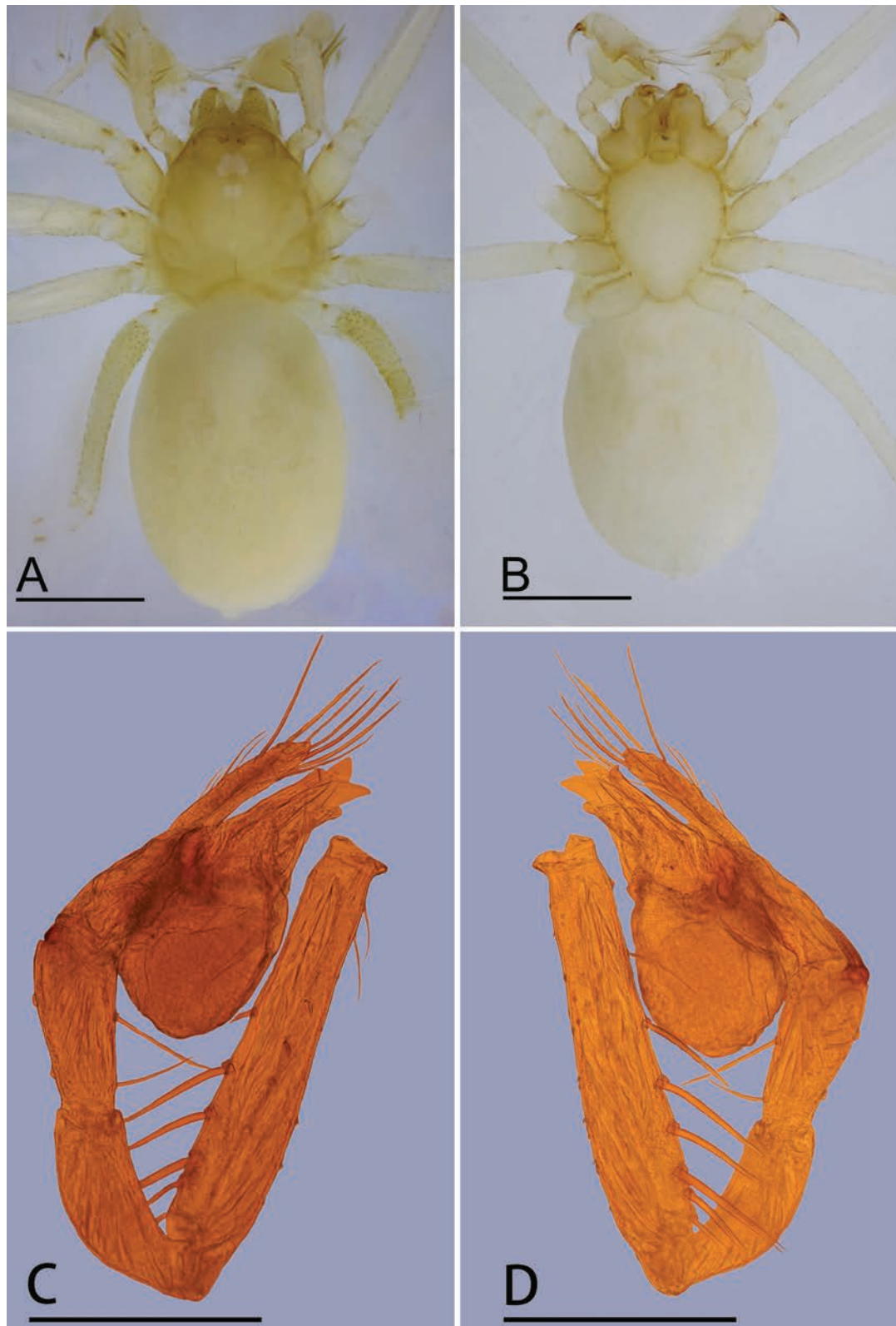
Figure 1. *Jingneta qishan* sp. nov., male **A, B** habitus, dorsal and ventral views **C, D** left palp, prolateral and retrolateral views. Scale bars: 0.4 mm (**A, B**); 0.3 mm (**C, D**).

(Fig. 13A) vs. with a stridulatory file, palpal femur with six long setae retrolaterally (Fig. 1D) vs. eight long setae, tip of bulb with a spine-like prolateral sclerite (Fig. 2A, C) vs. lacking and female genital area with a scape (Fig. 3C) vs. lacking.
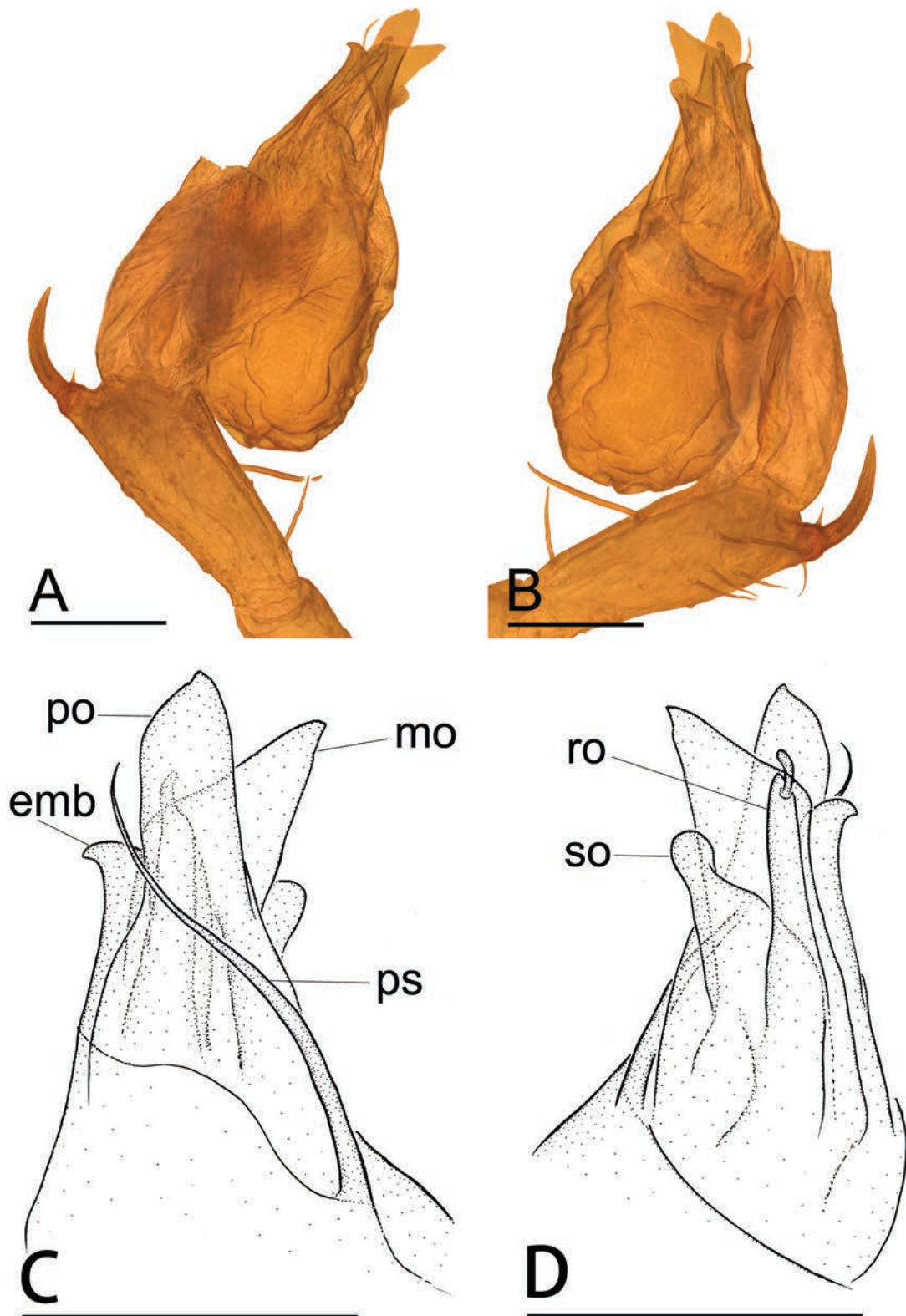
Figure 2. *Jingneta qishan* sp. nov. **A, B** left palpal bulb and tibia, prolateral and retrolateral views **C, D** distal part of bulb, prolateral and retrolateral views. Abbreviations: emb = embolus; mo = median outgrowth; po = prolateral outgrowth; ps = prolateral sclerite; ro = retrolateral outgrowth; so = small outgrowth. Scale bars: 0.1 mm.

Description. Male (holotype). Habitus as in Fig. 1A, B. Total length 1.55. Carapace 0.62 long, 0.59 wide. Abdomen 0.99 long, 0.68 wide. Eye sizes and interdistances: ALE 0.05, PLE 0.05, PME 0.04; ALE−PME 0.06, PLE−PLE 0.02, PLE−PME
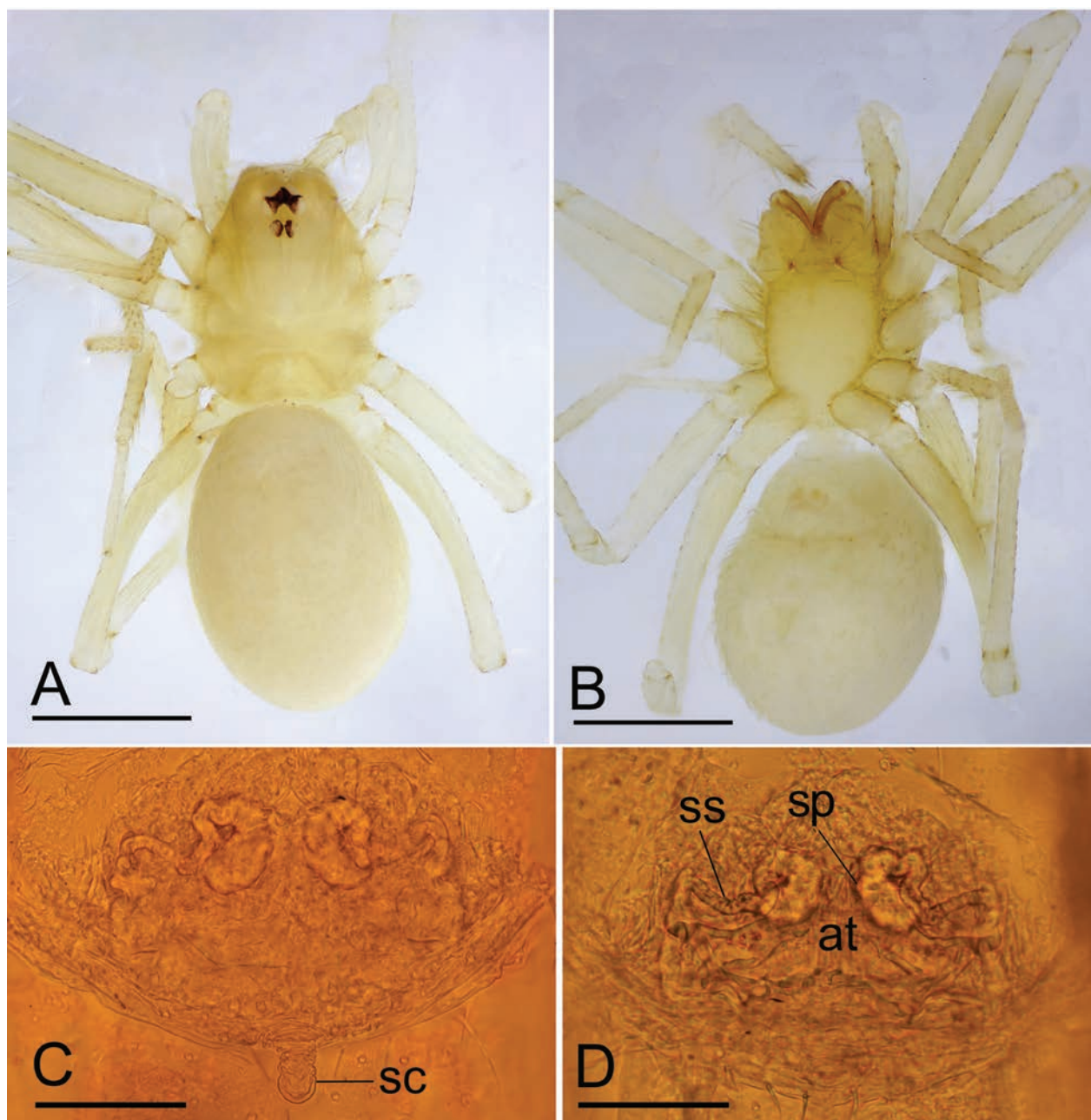
Figure 3. *Jingneta qishan* sp. nov., female **A, B** habitus, dorsal and ventral views **C, D** genitalia, ventral and dorsal views. Abbreviations: at = atrium; sc = scape; sp = spermathecae; ss = spermathecal stalk. Scale bars: 0.4 mm (**A, B**); 0.1 mm (**C, D**).

0.03; AER 0.08, PER 0.10. Carapace light yellow. Median groove, cervical grooves and radial furrows distinct. Chelicerae with eight large promarginal and five small retromarginal teeth. Labium rectangular; endites with serrula anterolaterally; sternum light yellow, longer than wide, heart shaped, smooth. Abdomen whitish, ovoid. Leg measurements: I - (1.15, 0.19, 1.16, 0.90, -); II - (0.94, 0.19, 0.95, 0.73, 0.59); III - (-, 0.19, 0.72, 0.64, 0.48); IV - (1.26, -, -, -, -). Metatarsus III with row of fine hairs ventrally (preening comb, arrow in Fig. 4H). Palp (Figs 1C–D, 2A–D, 4A–E): femur with six long setae retrolaterally; tibia with one horn-shaped apophysis distally; tip of bulb with triangular embolus, a spine-like prolateral sclerite and several outgrowths, including a leaf-shaped prolateral outgrowth, a median triangular outgrowth, a small outgrowth and a ribbon-shaped retrolateral outgrowth.
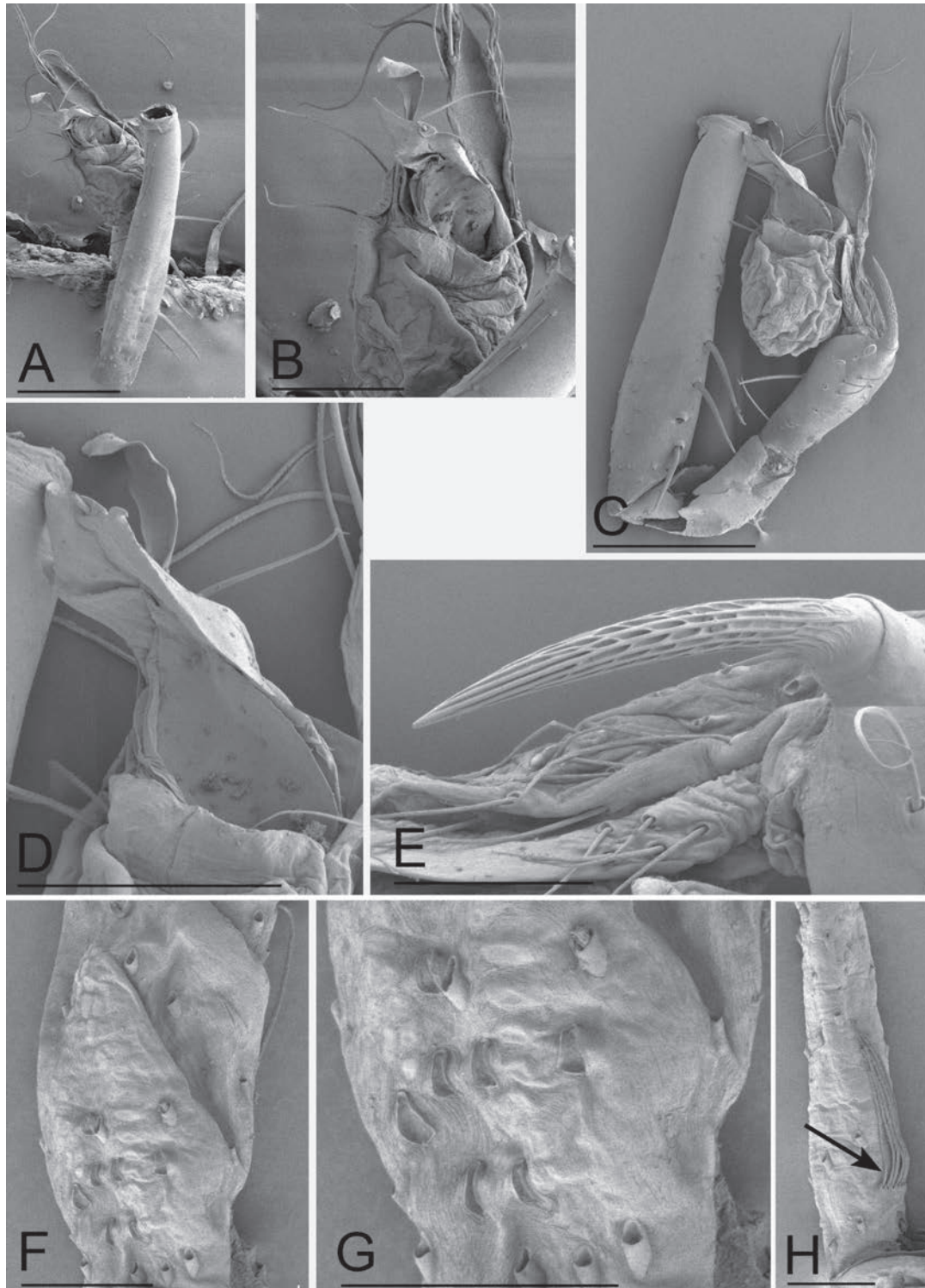
Figure 4. *Jingneta qishan* sp. nov., SEM **A, C** left palp, ventral and retrolateral views **B** bulb, ventral view **D** distal part of bulb, ventral view **E** detail of palpal tibial apophysis, lateral view **F** patella III, dorsal view **G** detail of patella III, dorsal view **H** metatarsus III, ventral view, arrow shows preening comb. Scale bars: 0.2 mm (**A, C**); 0.1 mm (**B, D**); 0.05 mm (**E–H**).

Female (paratype). Similar to male in general features. Habitus as in Fig. 3A, B. Total length 1.37. Carapace 0.61 long, 0.49 wide. Abdomen 0.77 long, 0.55 wide. Eye sizes and interdistances: ALE 0.05, PLE 0.05, PME 0.04; ALE–PME 0.10, PLE–PLE 0.03, PLE–PME 0.02; AER 0.08, PER 0.11. Leg measurements: I 2.19 (0.59, 0.21, 0.57, 0.45, 0.37); II 1.85 (0.50, 0.18, 0.46, 0.37, 0.34); III 1.64

(0.45, 0.18, 0.36, 0.35, 0.30); IV 2.38 (0.70, 0.18, 0.69, 0.46, 0.35). Genital area (Fig. 3C) with a scape on the posterior edge. Internal genitalia (Fig. 3D) with a pair of coiled spermathecae and sperm stalk; atrium oval.

Distribution. China (Anhui).

Jingneta wukuishan Tong, sp. nov.

https://zoobank.org/91782FAE-C3E8-4350-A294-5F2A0DAF7E2F
Figs 5, 6, 13C, 14

Type material. *Holotype* CHINA • ♂ (SYNU-1170); Anhui, Huangshan City, She County, Wukui Mountain; 29°51'0"N, 118°24'55"E, 138 m; 3.I.2022; W. Cheng, H. Fu & K. Yang leg. *Paratype:* CHINA • 1 ♂ (SYNU-1171), same data as holotype.

Etymology. The specific name refers to the type locality and is a noun in apposition.

Diagnosis. This new species is similar to *Jingneta maculosa* (Song and Xu 1986: fig. 2A–C) in the dark stripes of abdomen, but can be distinguished by the chelicerae with seven promarginal teeth (Fig. 13C) vs. ten promarginal teeth, palpal femur with six long setae retrolaterally and tibia lacking specialized setae (Fig. 5D) vs. nine setae and tibia with three short blunt spines.

Description. Male (holotype). Habitus as in Fig. 5A, B. Total length 1.52. Carapace 0.61 long, 0.54 wide. Abdomen 0.93 long, 0.62 wide. Eye sizes and interdistances: ALE 0.06, PLE 0.06, PME 0.05; ALE–PME 0.06, PLE–PLE 0.04, PLE–PME 0.02; AER 0.11, PER 0.12. Carapace yellow to dark brown. Median groove, cervical grooves and radial furrows indistinct. Chelicerae with seven large promarginal and seven small retromarginal teeth. Labium rectangular; endites with serrula anterolaterally; sternum yellow to brown, longer than wide, heart shaped, smooth. Abdomen light brown, darker on sides, ovoid. Leg measurements: I 2.96 (0.83, 0.21, 0.78, 0.65, 0.49); II - (-, -, -, -, -); III 2.73 (0.75, 0.21, 0.67, 0.61, 0.49); IV 3.93 (1.08, 0.21, 1.20, 0.88, 0.56). Palp (Figs 5C, D, 6A–E): femur with six long setae retrolaterally; cymbium constricted medially, attached to a small earlobe-shaped process retrolaterally; tip of bulb with a strong spine-like prolateral sclerite and several membranous outgrowths.

Female. Unknown.

Distribution. China (Anhui).

Genus *Leptonetela* Kratochvíl, 1978

Guineta Lin & Li, 2010: 6.
Qianleptoneta Chen & Zhu, 2008: 12.
Sinoneta Lin & Li, 2010: 82.

Type species. *Sulcia kanellisi* Deeleman-Reinhold, 1971.

Diagnosis. See Wang et al. (2017).

Composition. One hundred and twenty-three species, of which 9 species occur in Greece, 2 in Turkey, 1 in Azerbaijan and Georgia, 1 in Vietnam, and 110 species in China, including the one described here.

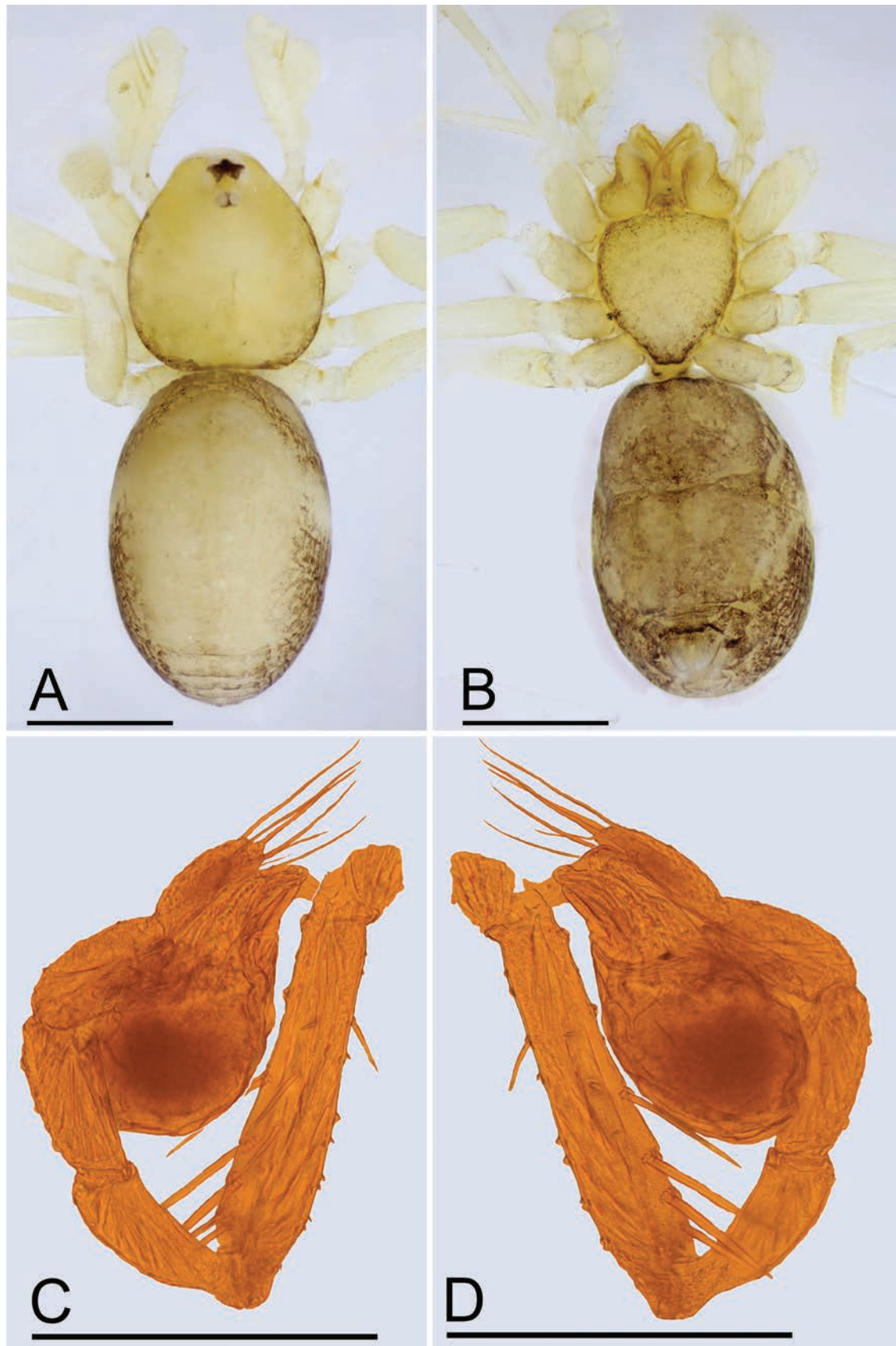**Distribution.** Azerbaijan, China, Georgia, Greece, Turkey and Vietnam.

Figure 5. *Jingneta wukuishan* sp. nov., male **A, B** habitus, dorsal and ventral views **C, D** left palp, prolateral and retrolateral views. Scale bars: 0.4 mm (**A, B**); 0.3 mm (**C, D**).
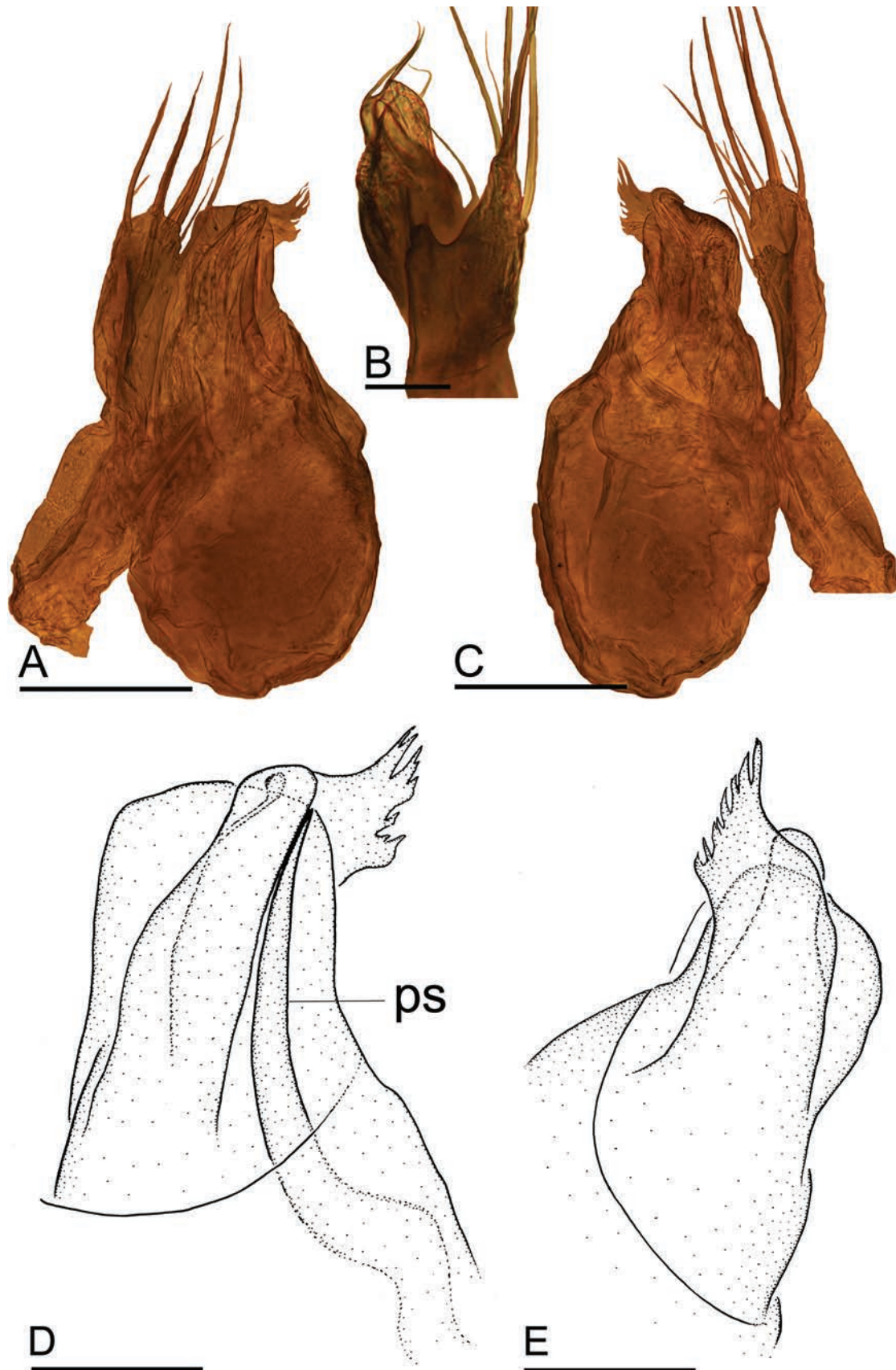
Figure 6. *Jingneta wukuishan* sp. nov. **A, B, C** left palp, prolateral, dorsal and retrolateral views **D, E** distal part of bulb, prolateral and retrolateral views. Abbreviation: ps = prolateral sclerite. Scale bars: 0.1 mm (**A, C**); 0.05 mm (**B, D, E**).

Leptonetela jingde Tong, sp. nov.

https://zoobank.org/E77EDBB0-8D15-4419-8036-F727BE934CC4
Figs 7–9, 13B, 14

Type material. *Holotype* CHINA • ♂ (SYNU-1172); Anhui, Xuancheng City, Jingde County, Tu'er Mountain; 30°18'23"N, 118°32'15"E, 240 m; 7.I.2022; W. Cheng, H. Fu & K. Yang leg. *Paratype:* CHINA • 4 ♂ 1 ♀ (SYNU-1173–1177), same data as holotype.

Etymology. The specific name refers to the type locality and is a noun in apposition.

Diagnosis. This new species is similar to *Leptonetela microdonta* (Wang and Li 2011: figs 28–31) in the long setae on palpal tibia, but can be distinguished by the chelicerae with seven promarginal teeth (Fig. 13B) vs. eight, palpal tibia with four long setae retrolaterally, the basal two thick (Fig. 7D) vs. six long setae, with the basal one thinner and the distal three thick, the prolateral sclerite spine-like (Fig. 8D) vs. fork-shaped, with five teeth distally and the abdomen with four dark chevron-shaped stripes (Figs 7A, 9A) vs. lacking.

Description. Male (holotype). Habitus as in Fig. 7A, B. Total length 1.25. Carapace 0.61 long, 0.59 wide. Abdomen 0.89 long, 0.73 wide. Eye sizes and interdistances: ALE 0.08, PLE 0.08, PME 0.07; ALE–PME 0.08, PLE–PLE 0.08, PLE–PME 0.03; AER 0.14, PER 0.17. Carapace light yellow. Median groove, cervical grooves and radial furrows distinct. Chelicerae with seven large promarginal and four small retromarginal teeth, with stridulatory file on the lateral margin. Labium rectangular; endites with serrula anterolaterally; sternum brown, shield shaped, smooth. Abdomen whitish, ovoid, with four dark chevron-shaped stripes. Leg measurements: I 2.66 (0.72, 0.17, 0.73, 0.57, 0.47); II 2.20 (0.62, 0.17, 0.55, 0.46, 0.40); III 1.97 (0.58, 0.18, 0.46, 0.46, 0.29); IV 2.45 (0.72, 0.17, 0.62, 0.54, 0.40). Palp (Figs 7C, D, 8A–E): femur without long setae retrolaterally; tibia with four long setae retrolaterally, the basal two thick; cymbium constricted medially, attached to a large earlobe-shaped process retrolaterally; tip of bulb with a short spine-like prolateral sclerite and leaf-shaped median apophysis.

Female (paratype). Similar to male in general features. Habitus as in Fig. 9A, B. Total length 1.36. Carapace 0.64 long, 0.58 wide. Abdomen 0.96 long, 0.80 wide. Eye sizes and interdistances: ALE 0.08, PLE 0.07, PME 0.07; ALE–PME 0.12, PLE–PLE 0.08, PLE–PME 0.02; AER 0.14, PER 0.17. Leg measurements: I - (0.73, 0.20, 0.67, 0.56, -); II 2.19 (0.62, 0.20, 0.52, 0.45, 0.40); III 1.97 (0.58, 0.18, 0.44, 0.45, 0.32); IV - (0.73, 0.21, 0.62, -, -). Internal genitalia (Fig. 9C, D) with sub-trapezoidal atrium, slightly swollen spermathecae, and convoluted spermathecal stalk including six coils.

Distribution. China (Anhui).

Genus *Rhyssoleptoneta* Tong & Li, 2007

Type species. *Rhyssoleptoneta latitarsa* Tong & Li, 2007.

Diagnosis. See Tong and Li (2007) and Wang et al. (2012).

Composition. Three species, including one described here.
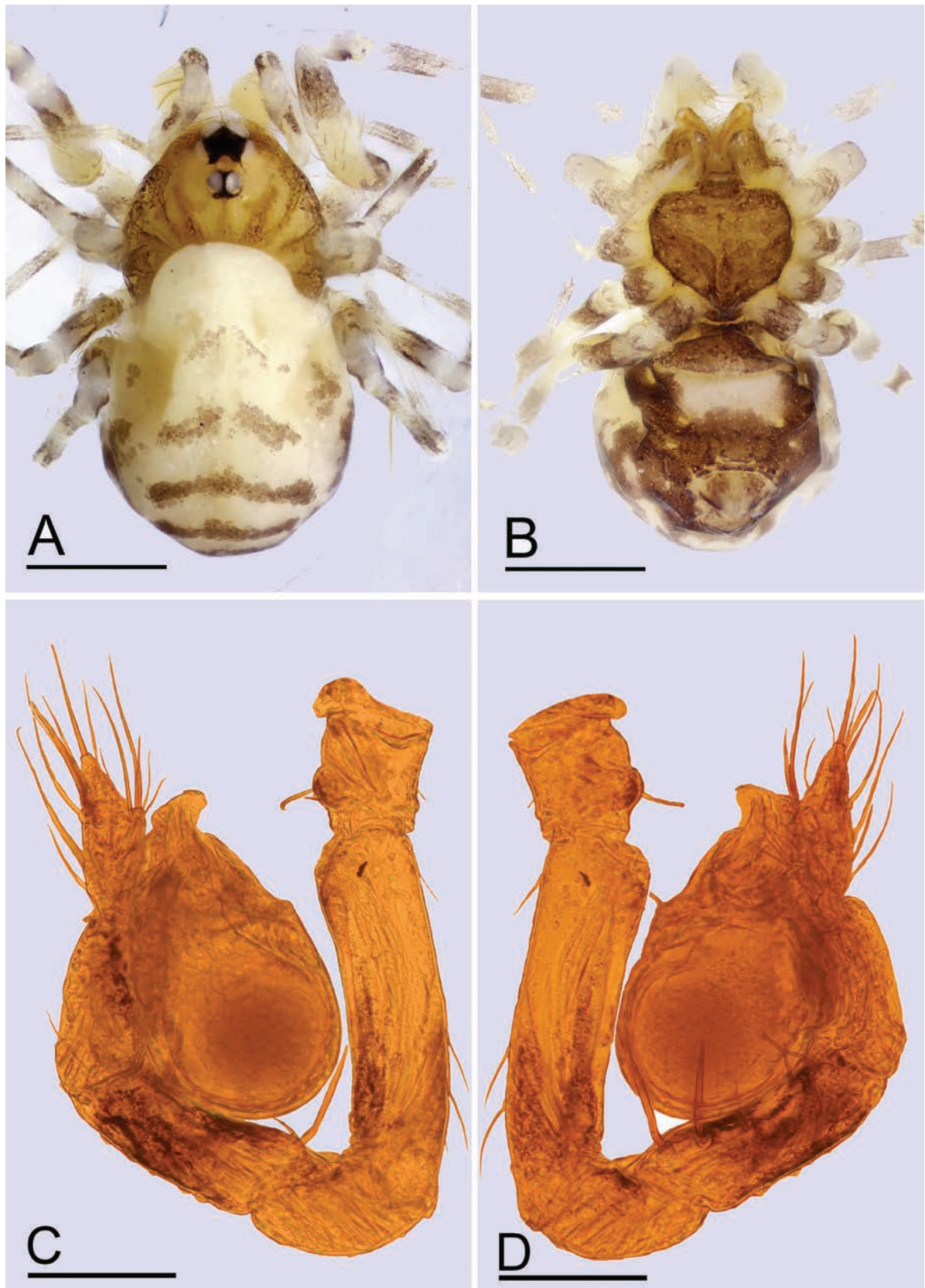
Distribution. China (Anhui, Beijing, Hebei).

Figure 7. *Leptonetela jingde* sp. nov., male **A, B** habitus, dorsal and ventral views **C, D** left palp, prolateral and retrolateral views. Scale bars: 0.4 mm (**A, B**); 0.1 mm (**C, D**).
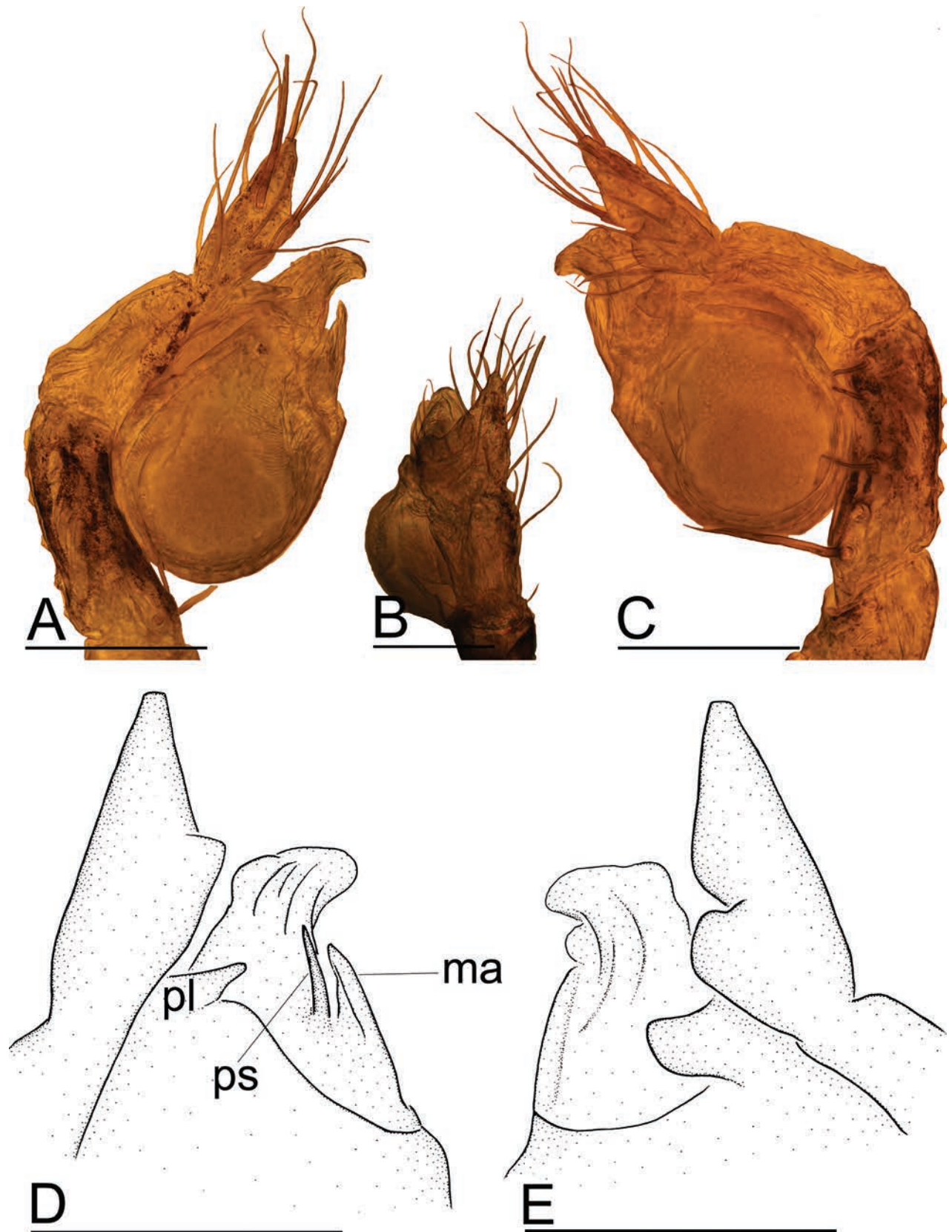
Figure 8. *Leptonetela jingde* sp. nov. **A, B, C** left palp, prolateral, dorsal and retrolateral views **D, E** detail of palpal bulb, prolateral and retrolateral views. Abbreviation: ma = median apophysis; pl = prolateral lobe; ps = prolateral sclerite. Scale bars: 0.1 mm.
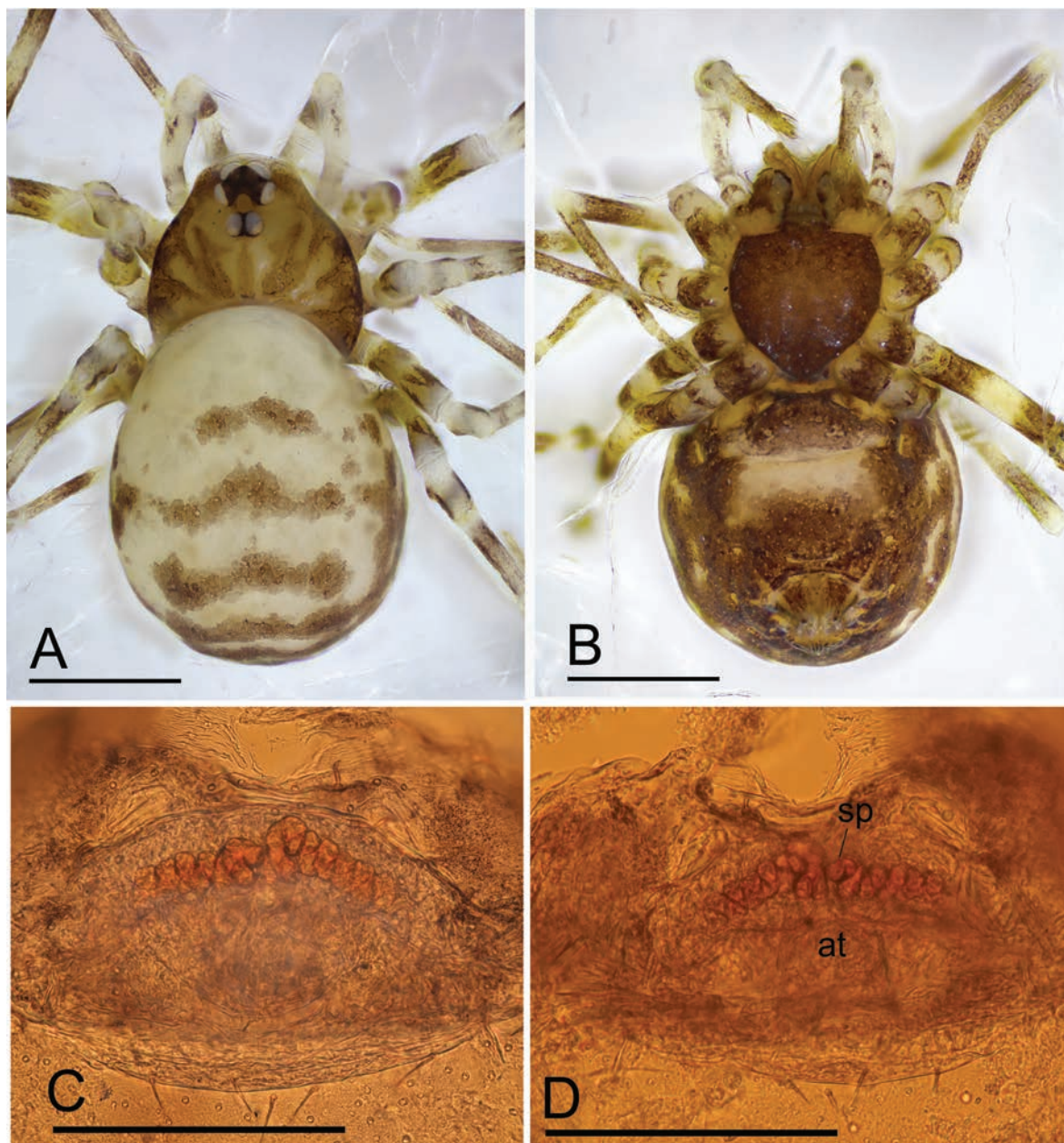
Figure 9. *Leptonetela jingde* sp. nov., female **A, B** habitus, dorsal and ventral views **C, D** genitalia, ventral and dorsal views. Abbreviations: at = atrium; sp = spermathecae. Scale bars: 0.4 mm (**A, B**); 0.2 mm (**C, D**).

Rhyssoleptoneta lishan Tong, sp. nov.

https://zoobank.org/DF212BC3-9B09-4A97-B11F-73669221EAF3

Figs 10–12, 13D, 14

Type material. *Holotype* CHINA • ♂ (SYNU-1163); Anhui, Chizhou City, Guichi District, Lishan Village; 30°36'28"N, 117°30'12"E, 20 m; 14.I.2022; H. Fu & K. Yang leg. *Paratype*: CHINA • 1 ♀ (SYNU-1164), same data as holotype.

Other material examined. CHINA • 3 ♀; Anhui, Chizhou City, Guichi District, Santaishan Park; 30°39'34"N, 117°28'21"E, 30 m; 13.I.2022; H. Fu & K. Yang leg.

Etymology. The specific name refers to the type locality and is a noun in apposition.
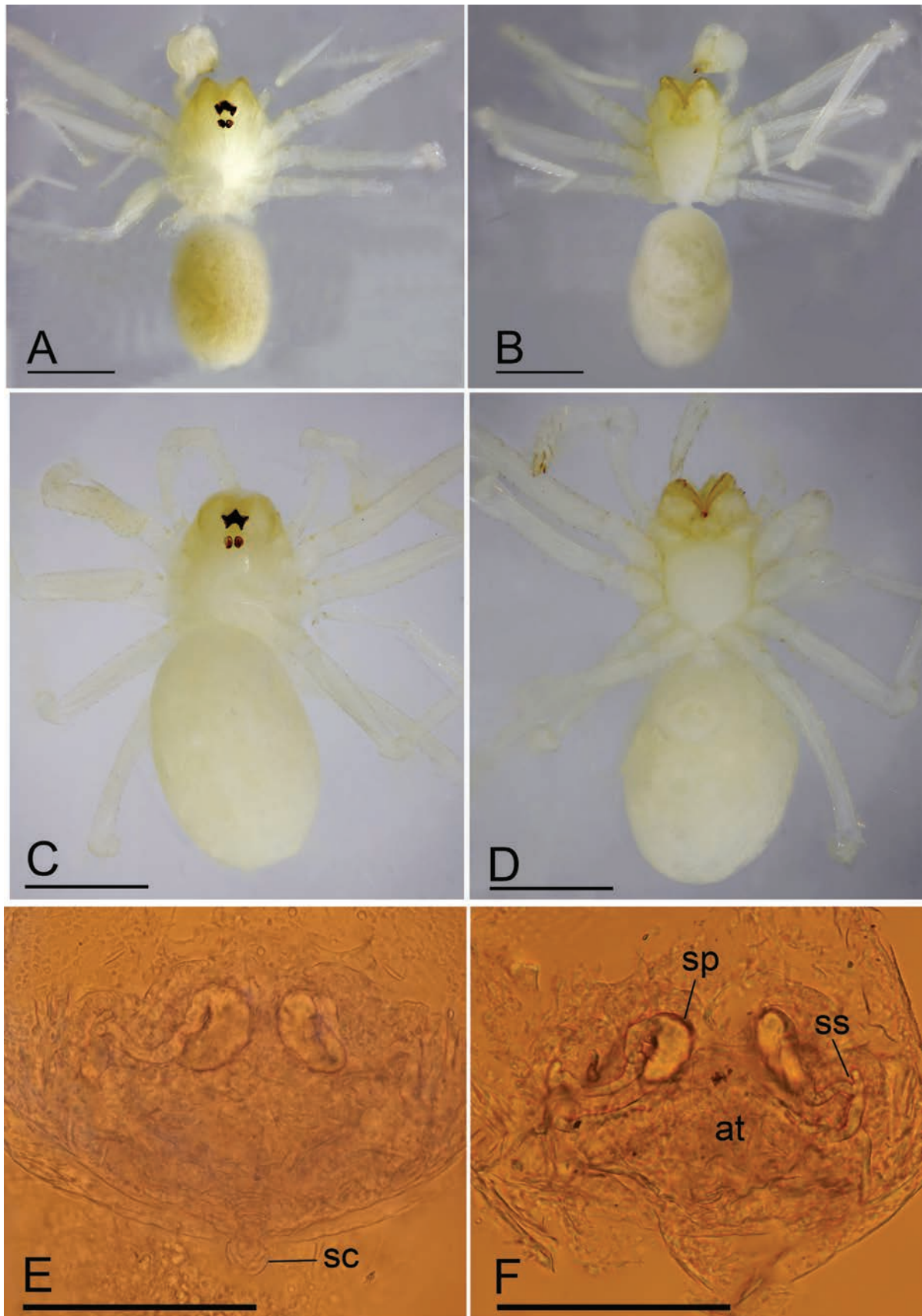
Figure 10. *Rhyssoleptoneta lishan* sp. nov. **A, B** male habitus, dorsal and ventral views **C, D** female habitus, dorsal and ventral views **E, F** genitalia, ventral and dorsal views. Abbreviations: at = atrium; sc = scape; sp = spermathecae; ss = spermathecal stalk. Scale bars: 0.4 mm (**A–D**), 0.1 mm (**E, F**).
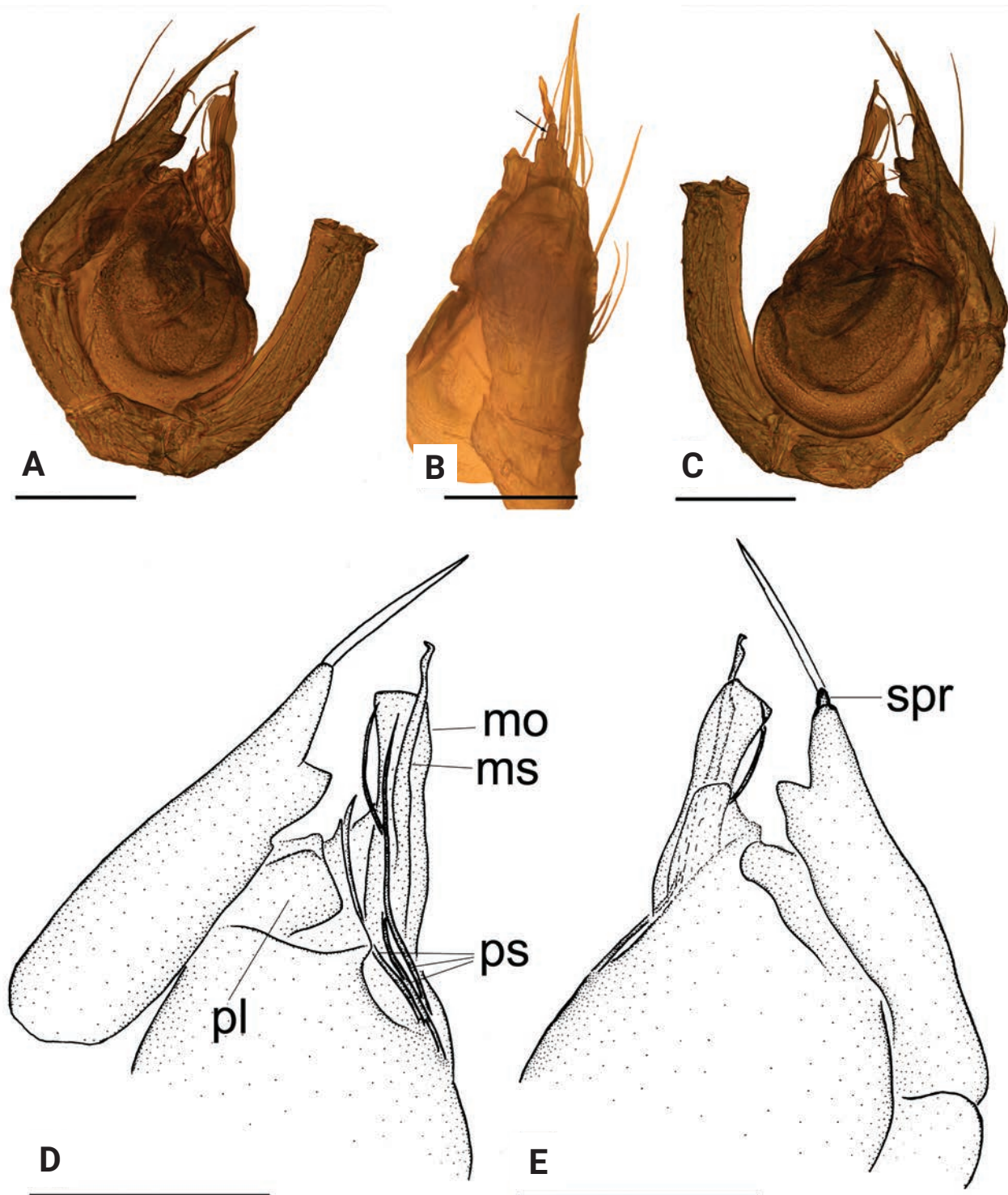
Figure 11. *Rhyssoleptoneta lishan* sp. nov. **A, B, C** left palp, prolateral, dorsal and retrolateral views, arrow shows the short projection **D, E** detail of palpal bulb, prolateral and retrolateral views. Abbreviations: mo = median outgrowth; ms = median sclerite; pl = prolateral lobe; ps = prolateral sclerite; spr = short projection. Scale bar: 0.1 mm.

Diagnosis. This new species is similar to *Rhyssoleptoneta aosen* (Zhu and Li 2021: figs 9A–D, 10A–C) in the scape of female genital area, but can be distinguished by the chelicerae with eight promarginal teeth and by the stridulatory file on the lateral margin (Fig. 13D) vs. seven promarginal teeth and lacking the stridulatory file, palpal bulb with membranous median outgrowth, without
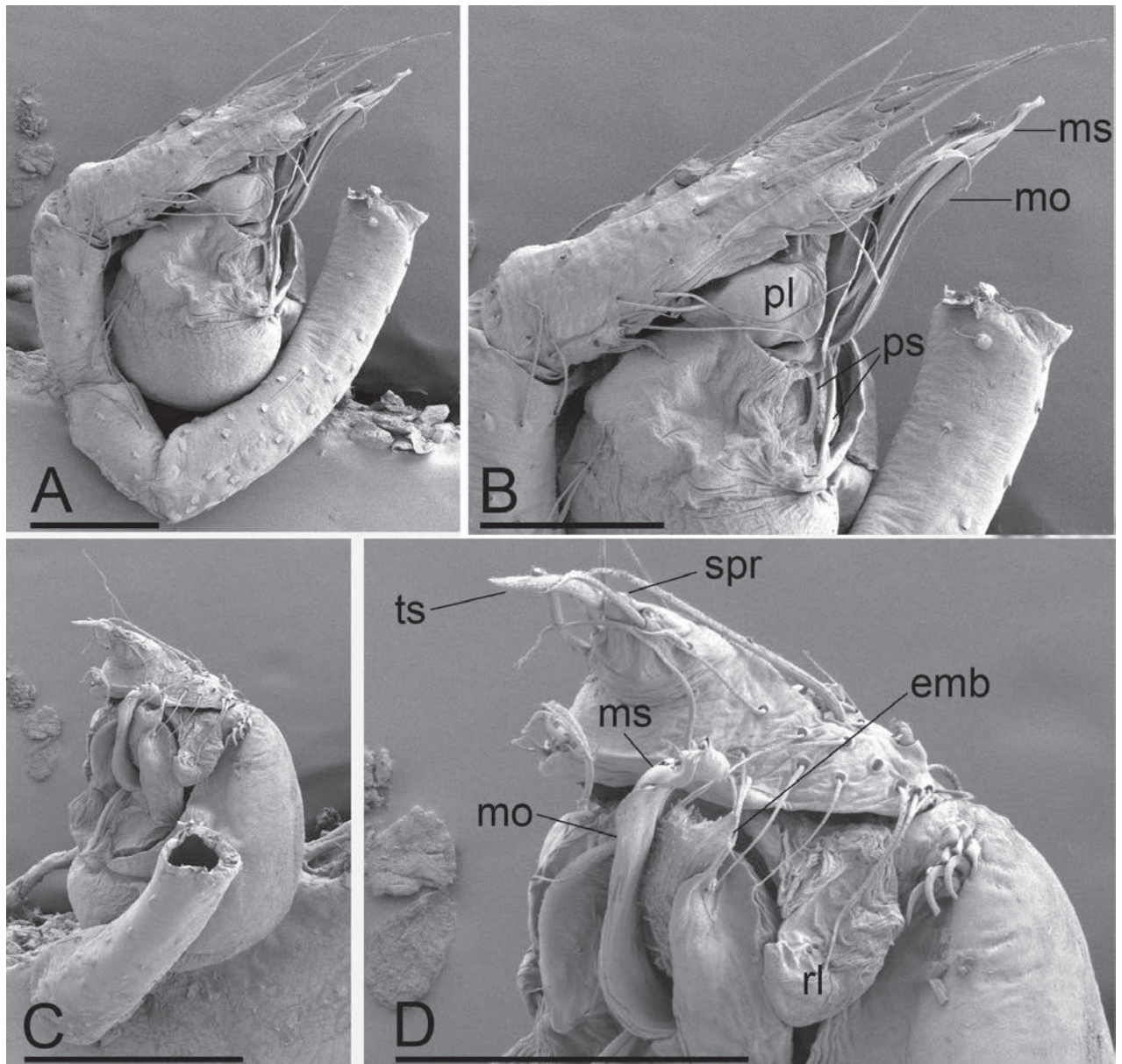
Figure 12. *Rhyssoleptoneta lishan* sp. nov., SEM **A, C** left palp, prolateral and dorsal views **B, D** detail of palpal bulb, prolateral and ventral views. Abbreviations: emb = embolus; mo = median outgrowth; ms = median sclerite; pl = prolateral lobe; ps = prolateral sclerite; rl = retrolateral lobe; spr = short projection; ts = tarsal spur. Scale bars: 0.1 mm.

tooth-shaped projections (Fig. 11D, E) vs. without median outgrowth but with three tooth-shaped projections, and the short projection of the palpal tarsus distally (Fig. 11E) vs. on the middle area.

Description. Male (holotype). Habitus as in Fig. 10A, B. Total length 1.31. Carapace 0.62 long, 0.50 wide. Abdomen 0.67 long, 0.45 wide. Eye sizes and interdistances: ALE 0.06, PLE 0.06, PME 0.04; ALE−PME 0.06, PLE−PLE 0.06, PLE−PME 0.02; AER 0.10, PER 0.12. Carapace light yellow. Median groove, cervical grooves and radial furrows indistinct. Chelicerae with eight large promarginal and four small retromarginal teeth, with stridulatory file on the lateral margin. Labium rectangular; endites with serrula anterolaterally; sternum whitish, longer than wide, heart shaped, smooth. Abdomen whitish, ovoid, with four dark chevron-shaped stripes.
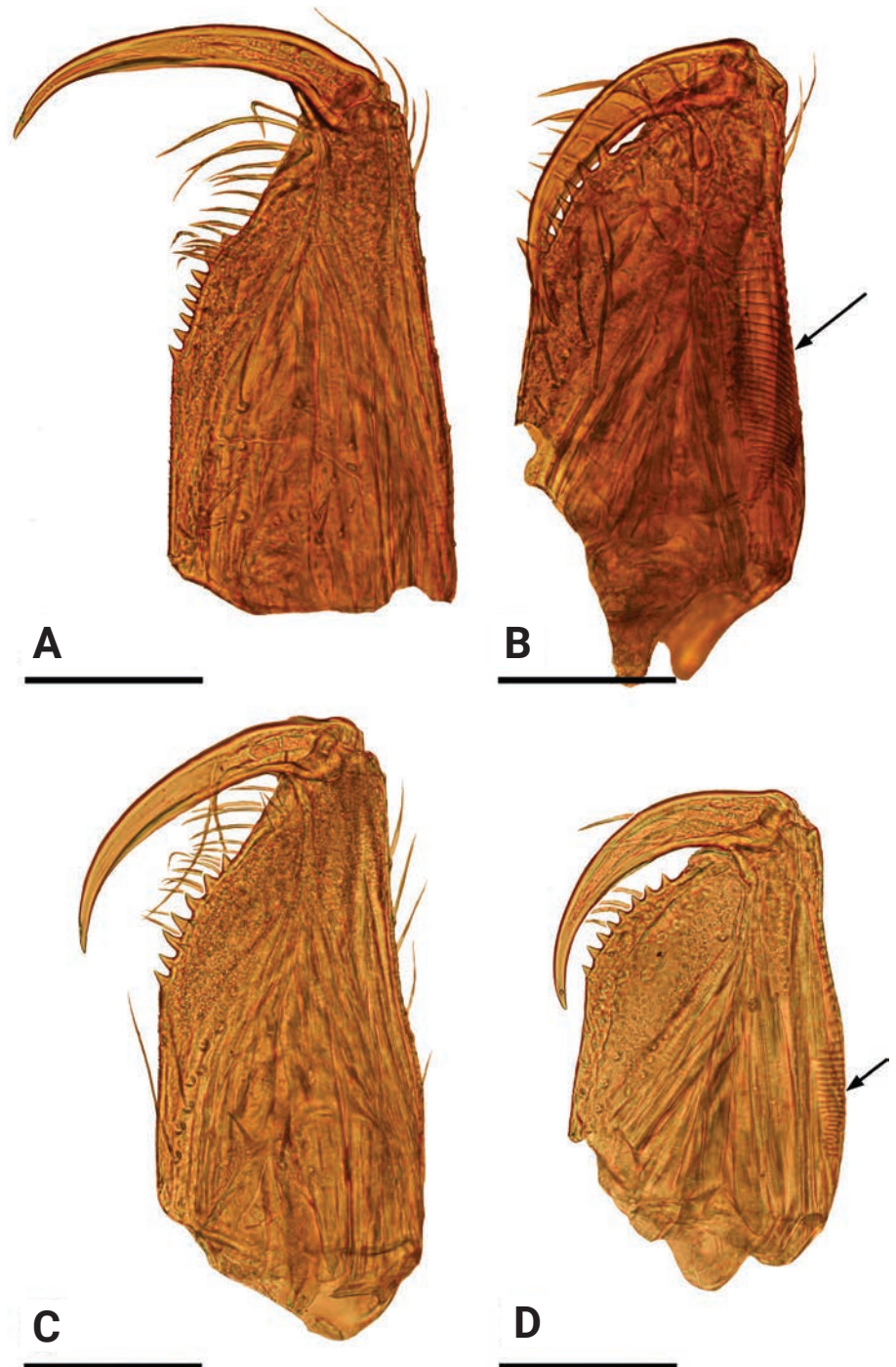
Figure 13. Male left chelicerae, posterior view **A** *Jingneta qishan* sp. nov. **B** *Leptonetela jingde* sp. nov. **C** *Jingneta wukuishan* sp. nov. **D** *Rhyssoleptoneta lishan* sp. nov. Arrows show the stridulatory file in B, D. Scale bars: 0.1 mm.

Leg measurements: I 2.51 (0.70, 0.19, 0.68, 0.55, 0.39); II 2.11 (0.59, 0.19, 0.53, 0.45, 0.35); III 1.80 (0.51, 0.17, 0.45, 0.40, 0.27); IV - (-, -, -, -, -). Male palp (Figs 11A–E, 12A–D): femur without long spines; tibia without special projection; tarsus wide, not branched distally, with a short projection and a long spur distally; bulb complex, wrinkled on prolateral surface, with 3 spine-like prolateral sclerites, with a membranous median outgrowth and belt-like median sclerite; embolus triangular.
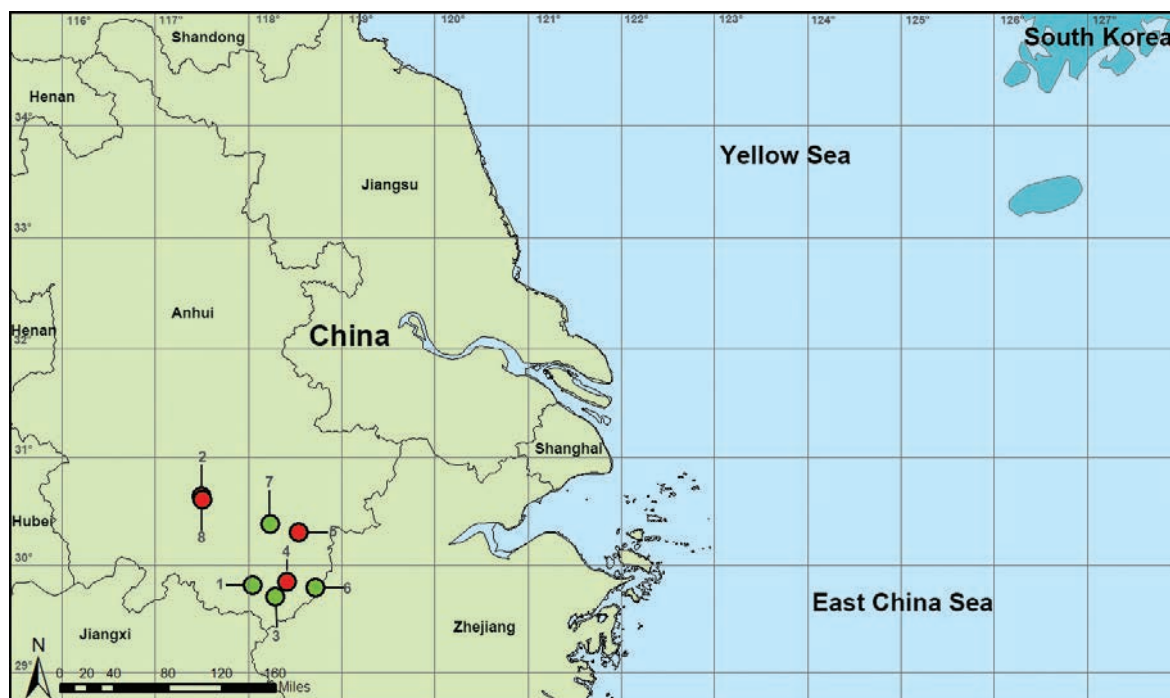
Figure 14. Distribution records of leptonetid spiders from Anhui, China, red circles refer to four new species, green circles indicate four known species **1** *Jingneta maculosa* **2** *Jingneta qishan* sp. nov. **3** *Jingneta tunxiensis* **4** *Jingneta wukuishan* sp. nov. **5** *Leptonetela jingde* sp. nov. **6** *Leptonetela microdonta* **7** *Longileptoneta shenxian* **8** *Rhyssoleptoneta lishan* sp. nov.

Female (paratype). Similar to male in general features. Habitus as in Fig. 10C, D. Total length 1.23. Carapace 0.54 long, 0.45 wide. Abdomen 0.80 long, 0.52 wide. Eye sizes and interdistances: ALE 0.05, PLE 0.05, PME 0.04; ALE−PME 0.06, PLE−PLE 0.05, PLE−PME 0.02; AER 0.09, PER 0.11. Leg measurements: I 1.95 (0.55, 0.15, 0.54, 0.38, 0.33); II 1.63 (0.43, 0.15, 0.44, 0.32, 0.29); III 1.44 (0.39, 0.15, 0.32, 0.31, 0.27); IV 2.11 (0.62, 0.16, 0.59, 0.43, 0.31). Genital area (Fig. 10E) with a scape on the posterior edge. Internal genitalia (Fig. 10F) with a pair of coiled spermathecae and sperm stalk; atrium triangular.

Distribution. China (Anhui).

Key to leptonetid spiders from Anhui Province, China

Females of *Jingneta wukuishan* are unknown.

1   Males...**2**
−   Females...**9**
2   Palpal femur with strong spines (Figs 1D, 5D) **3**
−   Palpal femur without strong spines (Figs 7D, 11A)....................................**7**
3   Eyes absent; palpal tibia with columnar apophyses; cymbium curved pro-laterally, with prolateral spine (Wang et al. 2020: fig. 12D).........................
    ....*Longileptoneta shenxian* **Wang & Li, 2020**
−   Eyes present; palpal tibia with one or two horn-shaped or spine-like apophyses; cymbium branched distally, without prolateral spine (Figs 1D, 2B) **4**
4   Body light yellow, abdomen without dark stripes (Fig. 1A).........................**5**
−   Body dark brown, abdomen with dark stripes (Fig. 5A) **6**

5 Male palpal tibia with one horn-shaped apophysis distally (Fig. 2B)...........
.... ***Jingneta qishan* sp. nov.**
– Male palpal tibia without horn-shaped apophysis (Song and Xu 1986: fig.
1C) .... ***Jingneta tunxiensis* (Song & Xu, 1986)**
6 Chelicerae with ten promarginal teeth; palpal femur with nine long setae
retrolaterally and tibia with three short blunt spines (Song and Xu 1986:
fig. 2C)... ***Jingneta maculosa* (Song & Xu, 1986)**
– Chelicerae with seven promarginal teeth (Fig. 13C); palpal femur with six
long setae retrolaterally and tibia lacking specialized setae (Fig. 5D) ....
.... ***Jingneta wukuishan* sp. nov.**
7 Palpal tibia without strong spines (Fig. 11A) ....
....***Rhyssoleptoneta lishan* sp. nov.**
– Palpal tibia with a row of strong spines (Fig. 7D) **8**
8 Abdomen with dark chevron-shaped stripes (Fig. 7A); chelicerae with sev-
en promarginal teeth (Fig. 13B); palpal tibia with four long setae retrolater-
ally, the basal two thick (Fig. 7D); prolateral sclerite spine-like (Fig. 8D).....
....***Leptonetela jingde* sp. nov.**
– Abdomen without dark chevron-shaped stripes; chelicerae with eight pro-
marginal teeth (Wang and Li 2011: figs 28A, 31C); palpal tibia with six long
setae retrolaterally, the basal one thinner and the distal three thick (Wang
and Li 2011: figs 28D, 30B); prolateral sclerite fork-shaped, with five teeth
distally (Wang and Li 2011: figs 28B, 31D) ....
.... ***Leptonetela microdonta* (Xu & Song, 1983)**
9 Abdomen with dark chevron-shaped stripes (Fig. 9A)...............................**10**
– Abdomen without dark chevron-shaped stripes **11**
10 Abdomen with four dark chevron-shaped stripes; spermathecal stalk in-
cluding six coils (Fig. 9D)...................................***Leptonetela jingde* sp. nov.**
– Abdomen with three dark chevron-shaped stripes; spermathecal stalk
straight, without coils (Song and Xu 1986: fig. 2B) ....
.... ***Jingneta maculosa* (Song & Xu, 1986)**
11 Eyes absent (Wang et al. 2020: fig. 13A) ....
.... ***Longileptoneta shenxian* Wang & Li, 2020**
– Eyes present **12**
12 Genital area with a scape (Fig. 3C) **13**
– Genital area without a scape...**14**
13 Scape enlarged distally; atrium triangular (Fig. 10F) ....
....***Rhyssoleptoneta lishan* sp. nov.**
– Scape not enlarged distally; atrium oval (Fig. 3D) .....***Jingneta qishan* sp. nov.**
14 Carapace with brown lateral margin; spermathecal stalk including six coils
(Wang and Li 2011: figs 29C, 30B)...
.... ***Leptonetela microdonta* (Xu & Song, 1983)**
– Carapace without brown lateral margin; spermathecal stalk straight, without
coils (Song and Xu 1986: fig. 1B).........***Jingneta tunxiensis* (Song & Xu, 1986)**

Acknowledgements

Additional information

Author ORCIDs

Shuhui Li https://orcid.org/0009-0000-0266-6859
Qiang Chen https://orcid.org/0009-0007-9722-1561
Yanfeng Tong https://orcid.org/0000-0002-4348-7029

Data availability

All of the data that support the findings of this study are available in the main text.

References

Chen H, Zhu M (2008) One new genus and species of troglobite spiders (Araneae, Leptonetidae) from Guizhou, China. Journal of Dali University 7(12): 11–14.

Hu C, Liu J (2023) The re-validation of *Leptonetela sublunata* (Chen, Jia & Wang, 2010) (Araneae, Leptonetidae). Acta Arachnologica Sinica 32(2): 110–117. https://doi.org/10.3969/j.issn.1005-9628.2023.02.009

Ledford J, Derkarabetian S, Ribera C, Starrett J, Bond J, Griswold C, Hedin M (2021) Phylogenomics and biogeography of leptonetid spiders (Araneae: Leptonetidae). Invertebrate Systematics 35(3): 332–349. https://doi.org/10.1071/IS20065

Lin Y, Li S (2010) Leptonetid spiders from caves of the Yunnan-Guizhou plateau, China (Araneae: Leptonetidae). Zootaxa 2587: 1–93. https://doi.org/10.11646/zootaxa.2587.1.1

Liu B, Zhang F (2022) A new eyeless Leptonetid spider from Beijing, China (Araneae, Leptonetidae). Acta Arachnologica Sinica 31(1): 44–48. https://doi.org/10.3969/j.issn.1005-9628.2022.01.007

Liu B, Yao Y, Jiang Z, Xiao Y, Liu K (2024) Midget cave spiders (Araneae, Leptonetidae) from Jiangxi and Fujian Province, China. ZooKeys 1189: 287–325. https://doi.org/10.3897/zookeys.1189.111041

Simon E (1890) Etudes arachnologiques. 22e Mémoire. XXXIV. Etude sur les arachnides de l'Yemen. Annales de la Société Entomologique de France 10(6): 77–124.

Song D, Xu Y (1986) Some species of oonopids and leptonetids from Anhui Province, China (Arachnida: Araneae). Sinozoologia 4: 83–88.

Tong Y, Li S (2007) Description of *Rhyssoleptoneta latitarsa* gen. nov. et sp. nov. (Araneae, Leptonetidae) from Hebei Province, China. Acta Zootaxonomica Sinica 32: 35–37.

Tong Y, Li S (2008) Six new cave-dwelling species of *Leptoneta* (Arachnida, Araneae, Leptonetidae) from Beijing and adjacent regions, China. Zoosystema 30: 371–386.

Wang C, Li S (2011) A further study on the species of the spider genus *Leptonetela* (Araneae: Leptonetidae). Zootaxa 2841: 1–90. https://doi.org/10.11646/zootaxa.2841.1.1

Wang C, Tao Y, Li S (2012) Notes on the genus *Rhyssoleptoneta*, with first report on the female of the type species (Araneae, Leptonetidae). Acta Zootaxonomica Sinica 37: 870–874.

Wang C, Xu X, Li S (2017) Integrative taxonomy of *Leptonetela* spiders (Araneae, Leptonetidae), with descriptions of 46 new species. Zoological Research 38(6): 321–448. https://doi.org/10.24272/j.issn.2095-8137.2017.076

Wang C, Li S, Zhu W (2020) Taxonomic notes on Leptonetidae (Arachnida, Araneae) from China, with descriptions of one new genus and eight new species. Zoological Research 41(6): 684–704. https://doi.org/10.24272/j.issn.2095-8137.2020.214

World Spider Catalog (2024) World Spider Catalog. Version 25.5. Natural History Museum Bern. http://wsc.nmbe.ch [Accessed on 5 September 2024] https://doi.org/10.24436/2

Xu Y, Song D (1983) A new species of the genus *Leptoneta* from China (Araneae: Leptonetidae). Journal of the Huizhou Teachers College 1983(2): 24–27.

Yang K, Li H, Tong Y, Bian D (2022) A new genus and species of leptonetid spiders (Araneae, Leptonetidae) from Guangdong Province, China. Biodiversity Data Journal 10(e80219): 1–8. https://doi.org/10.3897/BDJ.10.e80219

Zhu W, Li S (2021) Five new leptonetid spiders from China (Araneae: Leptonetidae). Zootaxa 4984(1): 281–299. https://doi.org/10.11646/zootaxa.4984.1.21

Research Article

Review of the wolf spider genus *Halocosa* Azarkina & Trilikauskas, 2019 from China (Araneae, Lycosidae)

Lu-Yu Wang[1], Muhammad Irfan[1,2], Yuri M. Marusik[3,4,5], Zhi-Sheng Zhang[1]

1 *Key Laboratory of Eco-environments in Three Gorges Reservoir Region (Ministry of Education), School of Life Sciences, Southwest University, Chongqing 400715, China*

2 *College of Plant Protection, Southwest University, Chongqing 400715, China*

3 *Institute for Biological Problems of the North RAS, Portovaya Str.18, Magadan 685000, Russia*

4 *Department of Zoology & Entomology, University of the Free State, Bloemfontein 9300, South Africa*

5 *Altai State University, Lenina Pr., 61, Barnaul, RF-656049, Russia*

Corresponding author: Zhi-Sheng Zhang (zhangzs327@qq.com)

Abstract

The wolf spider genus *Halocosa* Azarkina & Trilikauskas, 2019 from China is reviewed, including two species: *H. cereipes* (L. Koch, 1878) (♂♀) and *H. hatanensis* (Urita, Tang & Song, 1993) (♂♀). Both species are restricted to northern China, with *H. cereipes* recorded from China for the first time. *Halocosa jartica* (Urita, Tang & Song, 1993), **syn. nov.** is synonymized with *H. hatanensis* (Urita, Tang & Song, 1993). Detailed species descriptions, along with morphological photos, genitalia illustrations, SEM photos of the bulbs and photos of live specimens are also presented.

Key words: Distribution, Evippinae, Lycosinae, morphology, new record, redescription, synonym, taxonomy

Introduction

The wolf spider genus *Halocosa* is a small group within the subfamily Lycosinae, currently comprising three species: *H. cereipes* L. Koch, 1878 (generotype), *H. hatanensis* (Urita, Tang & Song, 1993) and *H. jartica* (Urita, Tang & Song, 1993) (WSC 2024) distributed in the Central Palearctic from the southern Ukraine (Azarkina and Trilikauskas 2019) to western Inner Mongolia (Li and Lin 2016). Of these, only the generotype is known for both sexes, and has been illustrated and described in detail, whereas the other two species, *H. hatanensis* and *H. jartica*, are only known for either female or male (WSC 2024).

While examining the materials from Xinjiang, Qinghai, Ningxia and Inner Mongolia, we found numerous female and male specimens that resembled *H. hatanensis* (male) and *H. jartica* (female). We conducted the present review to understand their taxonomic placement.

Materials and methods

Photos of living specimens were taken using an Olympus TG3 camera (Fig. 1A, B) and a Canon EOS 7D with an EF 100mm F2.8L lens (Fig. 1C, D). All specimens were preserved in 75% ethanol and examined, illustrated, photographed, and measured using a Leica M205A stereomicroscope equipped with a drawing tube, Leica DFC450 camera, and LAS software (ver. 4.6). Male palps and female epigynes were dissected for examination and illustration. Epigynes were cleared by immersing them in pancreatin (Álvarez-Padilla and Hormiga 2007). Scanning electron microscope (SEM) microphotographs were captured using a Zeiss Evo LS10 SEM. Eye sizes were measured as the maximum dorsal diameter. Leg measurements are provided as: total length (femur, patella and tibia, metatarsus, tarsus). All measurements are in millimeters. Specimens examined here are deposited in the Collection of Spiders, School of Life Sciences, Southwest University, Chongqing, China (SWUC).

Terminology follows Wang et al. (2015), except the word 'subspermathecae', which refers to a process attached on the lateral side of spermathecae.

Abbreviations used in the text: ALE, anterior lateral eye; AME, anterior median eye; PLE, posterior lateral eye; PME, posterior median eye.

Taxonomy

Family Lycosidae Sundevall, 1833

Halocosa Azarkina & Trilikauskas, 2019

Type species. *Lycosa cereipes* L. Koch, 1878 from Turkmenistan.

Diagnosis. This genus resembles *Xerolycosa* Dahl, 1908, another genus within subfamily Evippinae. Species of both genera lack a transverse depression on the carapace (Fig. 2A, B), tibia I and II with three pairs of ventral spines (Fig. 2E, F), and male palps with a bifid terminal apophysis (Fig. 2G, H). *Halocosa* can be distinguished by the presence of three retromarginal cheliceral teeth in *Halocosa* (Fig. 2C, D; vs. with two teeth in *Xerolycosa*); embolus lacking accompanied membrane (Fig. 2C, D; vs. present in *Xerolycosa*); strong or small tegular sclerite, bifid terminal apophysis (anterior arm strong and sclerotized, posterior arm thin and membranous) in *Halocosa* (Figs 3A, B, 4C–F, 5, 6A, B, 7E, F, 8; vs. both are membranous in *Xerolycosa*); wide square or rectangular septum covering whole atrium in *Halocosa* (vs. pear-shaped, partly covering atrium in *Xerolycosa*); slit-like copulatory openings, presence of accessory tube-like glands in *Halocosa* (Figs 3C, D, 4G, H, 6C, D, 7G, H; vs. glands absent in *Xerolycosa*).

Description. Medium sized (6.4–13.21) (Azarkina and Trilikauskas 2019) light colored. Carapace dirty brown with pattern formed by yellowish spots: butterfly like spot around fovea, pair of bean-shaped spots posteriorly from eye field and three pairs of marginal round spots; sternum brown; dorsum of abdomen with variegated pattern formed by numerous paired and unpaired spots on dirty brown background, venter uniformly yellow. Carapace very low (length/height ratio c. 4), furrow between cephalic and thoracic parts absent. Chelicera with three pro- and three retromarginal teeth. Leg formula: 4123 or

4132. Femora I–IV with three dorsal spines, patella with one dorsal, tibia and metatarsi III and IV with two dorsal spines (not indicated in tables). Within the intraspecific, the dorsal spines on tibia and metatarsus can be strong or weak, almost indistinguishable from large setae.

Palp with droplet-shaped cymbium, subtegulum (*St*) small, placed on prolateral side; tegulum large, going rather high on prolateral side with long ridge (*Tr*) on prolateral side that hold and hide part of embolus (*Em*); retrolateral part of tegulum with extension directed anteriorly, terminating by conductor, median part with tegular sclerite (*TS*); seminal duct thin, with "sharp" loop (*Sl*) on prolateral half; median apophysis located closer to retrolateral part of tegulum, without extensions, inner side of median apophysis with kind of pocket (or furrow) (*MA*), that holds tip of embolus and seems to serve as functional conductor; in retrolateral view median apophysis concave; embolic division with large sharply pointed terminal apophysis (*TA*) accompanied by membranous subterminal apophysis (*SA*); embolus long whip-like, smoothly rounded, slightly bent near tip, making almost whole circle, partly hidden by tegular ridge and median apophysis, base of embolus located in position of 2 o'clock.

Epigyne relatively small, one-fifth the width of the abdomen, densely covered with white setae to such extent that adult female could be considered as juvenile, especially in the field; fovea/atrium absent, totally covered with rectangular septum, septal stem absent, copulatory openings located in anterior part of epigynal plate, open into deep bulge which turns to wide, weakly sclerotized duct going straight down, near epigastral fold this duct turns up into strongly sclerotized, partly twisted, duct terminating by more or less clavate spermatheca; heavily sclerotized part of duct with finger-like or clavate accessorial gland (*Ag*).

Relationships. Azarkina and Trilikauskas (2019) placed this genus in Lycosinae due to "the latero-median origin of the embolus that is situated in a shallow and wide depression". This placement appears to be incorrect. All Lycosinae have palea (lacking in *Halocosa*), the median apophysis originates prolaterally and stretches horizontally (vs. originates retrolaterally and stretches parallel to cymbium axis), and the septum is not covered with setae (with exception of *Arctosa*) (vs. covered with setae). In addition, the carapace in *Halocosa* is very low, 3–4 times longer than high in comparison to Lycosinae (c. 2.4 longer than wide). To the best of our knowledge, the copulatory organs of this genus, as well as the flattened carapace, fit well with those known in Evippinae. Therefore, we consider *Halocosa* in Evippinae.

Composition. Two species: *H. cereipes* (L. Koch, 1878) and *H. hatanensis* (Urita, Tang & Song, 1993).

Biology. *Halocosa cereipes* is a dweller of saline places. It was collected around salt lakes (Iran, Azerbaijan, around the Aral Sea), and on the low seashore in the Crimea (personal data). The same habitats were reported by Azarkina and Trilikauskas (2019). Numerous spots on the carapace and abdomen, and leg annulation make the spiders very cryptic, and invisible if they are not moving.

Distribution. From southern Ukraine to western Inner Mongolia, south to Iran (Azarkina and Trilikauskas 2019; Nentwig et al. 2021). In China, known from Xinjiang, Ningxia, Qinghai and Inner Mongolia (present paper).

Halocosa cereipes (L. Koch, 1878)
Figs 1A, B, 2A, C, E, G, 3–5, 9
(角盐狼蛛)

Lycosa cereipes L. Koch, 1878: 68, pl. 2, fig. 6 (♂).
Pirata cereipes: Roewer 1955: 283.
Evippa apsheronica Marusik, Guseinov & Koponen, 2003: 52, figs 1–3 (♀); Ponomarev and Tsvetkov 2004: 86, figs 1–2 (♂♀).
Halocosa cereipes: Azarkina and Trilikauskas 2019: 557, figs 1–8, 15–18, 26–69 (♂♀, designated the neotype from the type locality).

Material examined. Cʜɪɴᴀ: **Xinjiang:** 1♀, Urumchi, Chaiwopu, 43°31.834'N, 087°53.695'E, 1097 m, 22 April 2014, L.Y. Wang & X.W. Meng leg. **Inner Mongolia:** 2♂ 2♀, Ejinaqi, Tiane Lake, 42°00.671'N, 101°35.242'E, 890 m, 5 June 2015, T. Lu and G.Q. Huang leg. • 3♂ 2♀, Ejinaqi, Juyanhai, 42°13.729'N, 101°04.404'E, 906 m, 5 June 2015, T. Lu and G.Q. Huang leg. • 9♂ 7♀, Ejinaqi, Juyanhai, 42°20.273'N, 101°15.020'E, 895 m, 5 June 2015, T. Lu and G.Q. Huang leg. • 4♂ 3♀, Alashanzuoqi, Jilantai Salt Lake, 39°43.281'N, 105°44.705'E, 1017 m, 7 June 2015, T. Lu and G.Q. Huang leg. • 10♂ 10♀, Alashanzuoqi, Jilantai, Dongshawo,

Figure 1. Photos of living specimens **A, B** *Halocosa cereipes* (L. Koch, 1878) (A female, B male) **C, D** *Halocosa hatanensis* (Urita, Tang & Song, 1993) (C female, D Same, male).
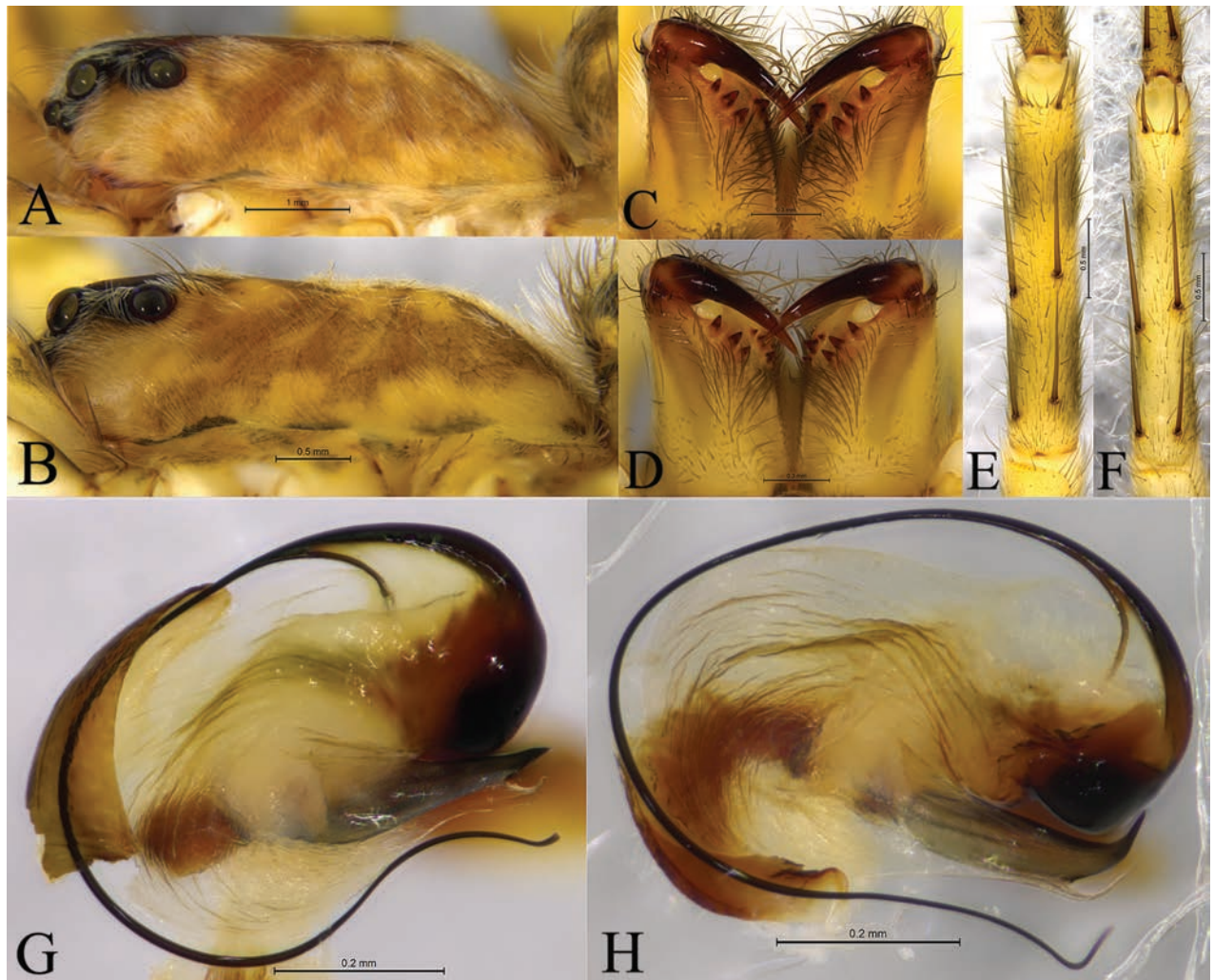
Figure 2. *Halocosa* spp. **A, C, E, G** *Halocosa cereipes* (L. Koch, 1878) **B, D, F, H** *Halocosa hatanensis* (Urita, Tang & Song, 1993) **A, B** carapace, lateral view **C, D** chelicerae, ventral view **E, F** tibia of leg I, ventral view **G, H** terminal apophysis and embolus, ventral view.

39°44.399'N, 105°46.484'E, elev. 1024 m, 7 June 2015, T. Lu and G.Q. Huang leg. • 1♂, Alashanzuoqi, Helan Mountain, Nan Temple, 38°39.918'N, 105°48.436'E, 1976 m, 9 June 2015, T. Lu and G.Q. Huang leg. • 1♂, Alashanzuoqi, Qinggele, 40°17.051'N, 105°51.200'E, 1165 m, 11 June 2015, T. Lu and G.Q. Huang leg. • 8♂ 17♀, Alashanzuoqi, Liutuan, Dongqing Lake, 40°30.288'N, 106°30.384'E, 1030 m, 11 June 2015, T. Lu and G.Q. Huang leg. • 1♂, Bayannur, Wulateqianqi, Eerdengbulage, Wuliangsuhai, 40°51.577'N, 108°50.906'E, 1025 m, 14 June 2015, T. Lu and G.Q. Huang leg.

Diagnosis. This species is similar to *H. hatanensis* (Figs 2B, D, F, H, 6–8), but differs by the dwarf tegular sclerite vs. large and almost square; the short, strong and flat terminal apophysis vs. long and crooked; the wide and short subterminal apophysis vs. long and thin; median apophysis not bifurcate and the end bent to conductor vs. bifurcate, ventral branches curved, dorsal branch straight and pointed (Figs 2G, 3A, B, 4C–F, 5); the arc-shaped copulatory openings, located on the anterior position of the septum vs. located below the septum; and the width of spermathecal head greater than the width of spermathecal stalk vs. width of spermathecal head almost the same as the width of spermathecal stalk (Figs 3C, D, 4G, H).
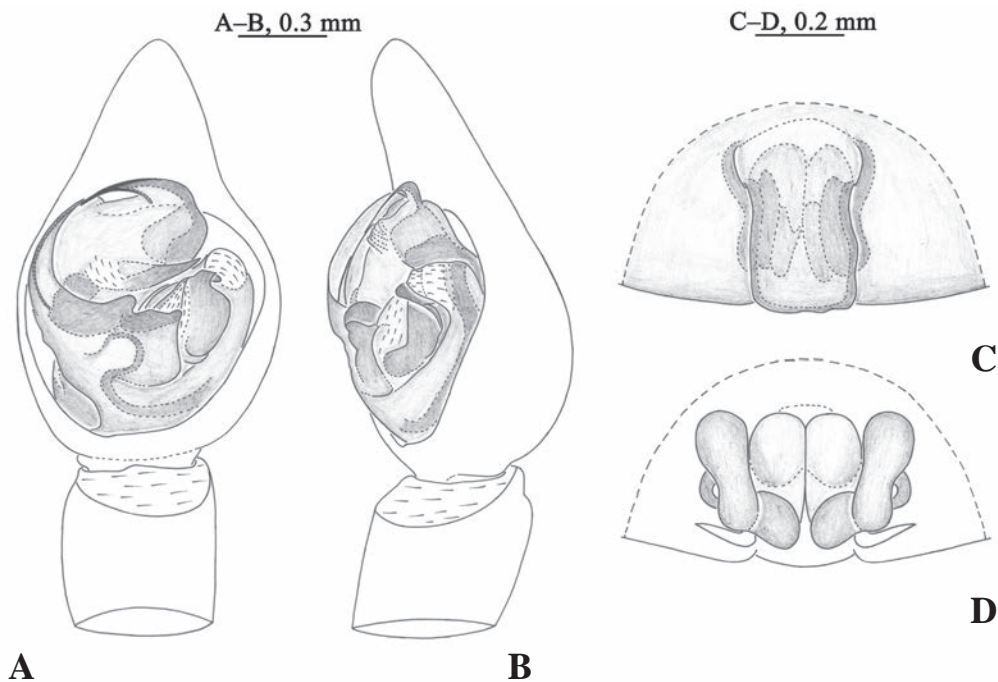
Figure 3. *Halocosa cereipes* (L. Koch, 1878) **A** left male palp, ventral view **B** same, retrolateral view **C** epigyne, ventral view **D** vulva, dorsal view.

Redescription. Males total length 7.65–10.19. One male (Figs 1B, 4A, from Dongqing Lake) total length 7.65, carapace 3.72 long, 3.69 wide; opisthosoma 4.11 long, 2.01 wide. Eye sizes and interdistances: AME 0.20, ALE 0.14, PME 0.35, PLE 0.33; AME–AME 0.10, AME–ALE 0.05, PME–PME 0.26, PME–PLE 0.31. Clypeus height 0.17. Leg measurements: I 11.68 (3.13, 3.93, 2.72, 1.90); II 10.62 (2.79, 3.47, 2.57, 1.79); III 10.53 (2.78, 3.15, 2.94, 1.66); IV 14.69 (3.69, 4.33, 4.44, 2.23).

Palp (Figs 2G, 3A, B, 4C–F, 5). Tip of cymbium 3 times shorter than cymbium; length/width ratio c. 1.7. The end of terminal apophysis short, strong and flat, subterminal apophysis membranous, as long as terminal apophysis. Median apophysis vertical, concave in lateral view. Tegular sclerite strongly sclerotized and dwarf. Embolus long and whip-like, smoothly rounded, slightly bent near tip, it makes almost whole circle, partly hidden by tegular ridge and median apophysis, base of embolus located in position of 2 o'clock. Conductor membranous.

Females total length 6.59–13.18. One female (Figs 1A, 4B, from Dongqing Lake) total length 6.59, prosoma 3.59 long, 2.47 wide; opisthosoma 2.99 long, 2.00 wide. Eye sizes and interdistances: AME 0.22, ALE 0.17, PME 0.37, PLE 0.32; AME–AME 0.12, AME–ALE 0.05, PME–PME 0.31, PME–PLE 0.35. Clypeus height 0.14. Leg measurements: I 11.41 (3.30, 3.86, 2.45, 1.80); II 10.84 (3.03, 3.63, 2.51, 1.67); III 10.76 (3.06, 3.16, 2.72, 1.82); IV 15.26 (4.09, 4.50, 4.50, 2.17).

Epigyne (Figs 3C, D, 4G, H). Septum 1.7 times longer than wide. Copulatory openings arc-shaped, located on the anterior position of the septum. Spermathecal heads slightly inflated, approaching to the anterior margins of spermathecal stalks. Spermathecal stalks as wide as heads. Accessorial gland arc-shaped, with a small and spherical head. Fertilization ducts hook-shaped.

Distribution. China (Xinjiang and Inner Mongolia, new records) (Fig. 9), southern Ukraine, northern Caucasus to southern part of West Siberia, Azerbaijan, Iran, Kazakhstan, Turkmenistan and Tajikistan.
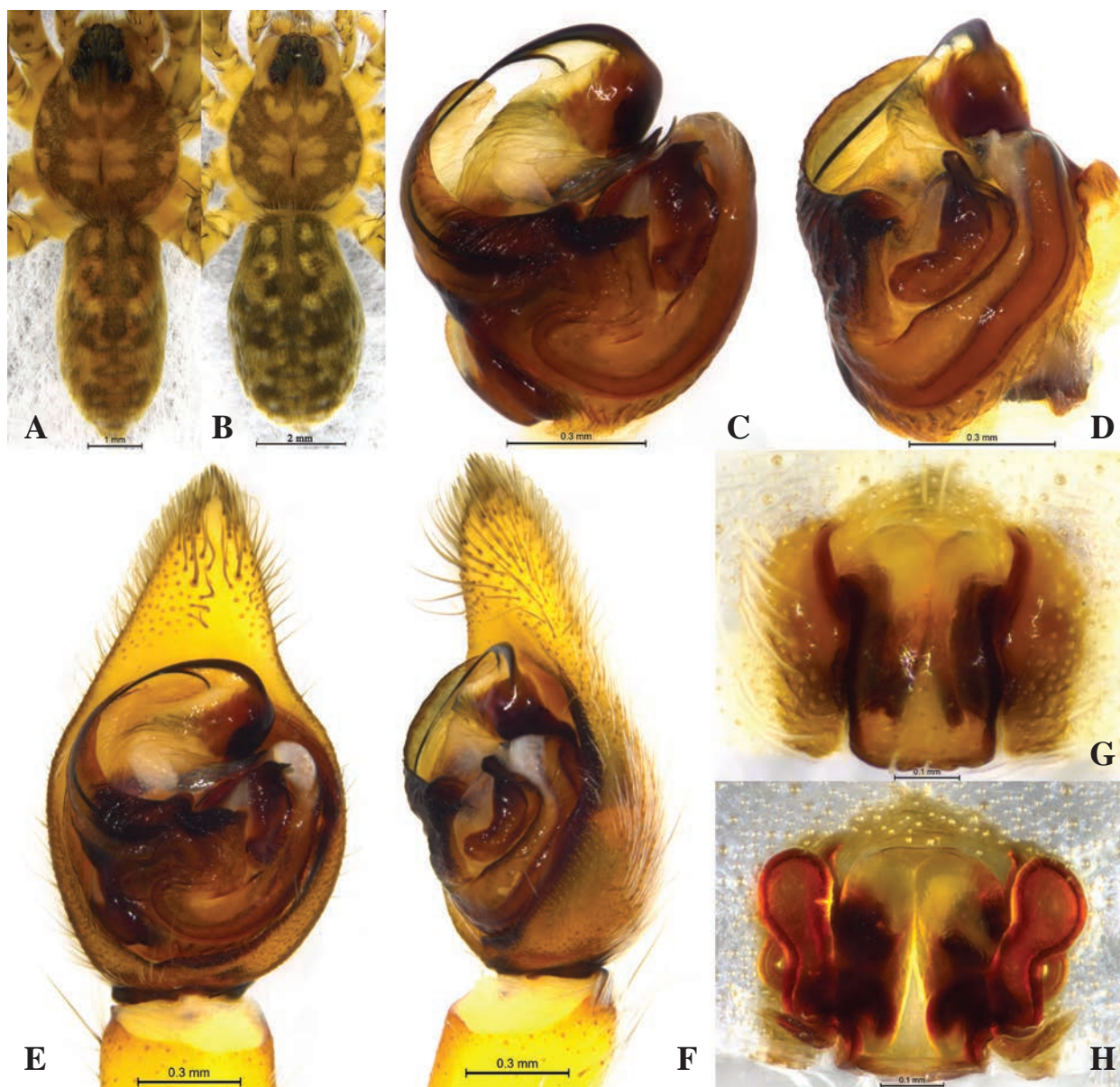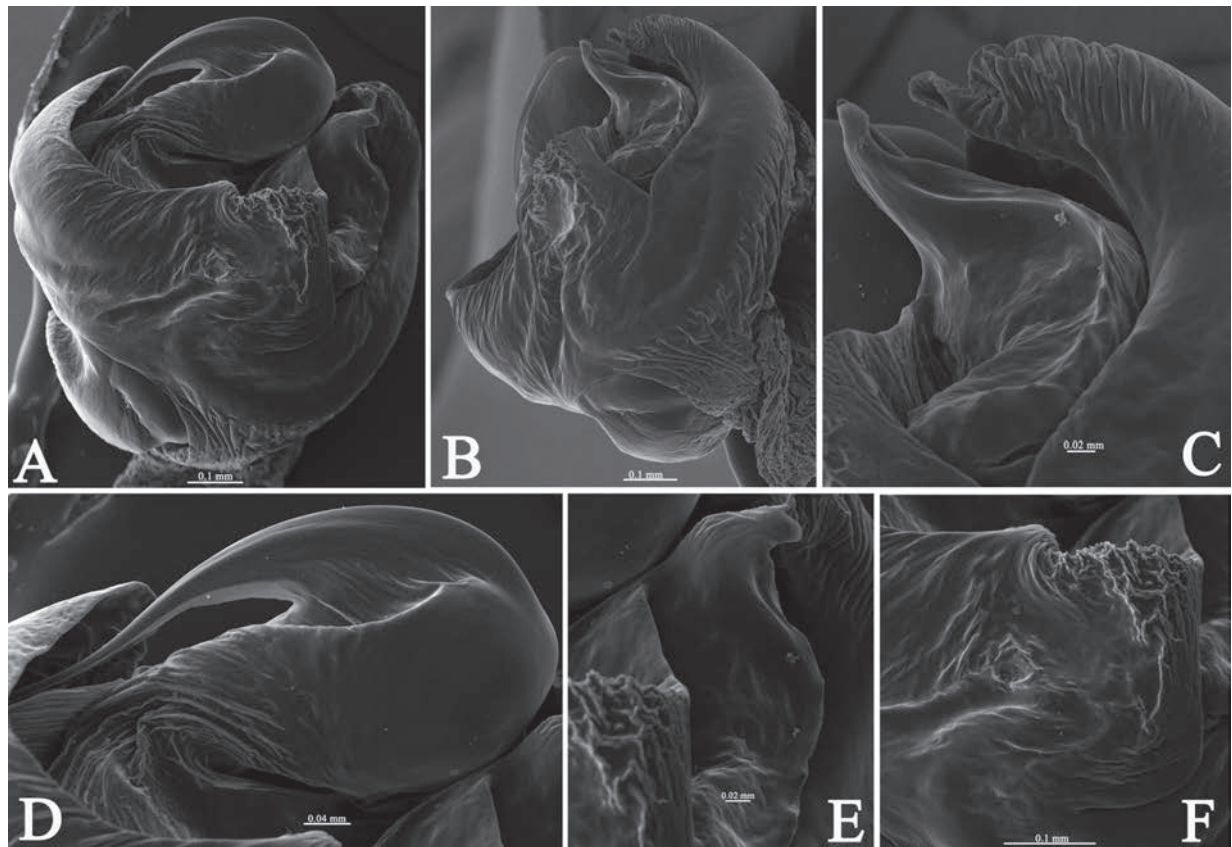
Figure 4. *Halocosa cereipes* (L. Koch, 1878) **A** male habitus, dorsal view **B** female habitus, dorsal view **C** left male palp, bulb, ventral view **D** same, retrolateral view **E** left male palp, ventral view **F** same, retrolateral view **G** epigyne, ventral view **H** vulva, dorsal view.

Halocosa hatanensis (Urita, Tang & Song, 1993)
Figs 1C, D, 2B, D, F, H, 6−9
(哈腾盐狼蛛)

Pardosa hatanensis Urita, Tang & Song, 1993: 46, figs 1A, B (holotype ♂ from Hatan Tohoi, Bayannur Meng, Inner Mongolia, China, deposited in Inner Magnolia Normal University, Hohhot, China, not examined).

Halocosa hatanensis: Azarkina and Trilikauskas 2019: 557 (transferred from *Pardosa*).

Pardosa jartica Urita, Tang & Song, 1993: 47, figs 2A, B (holotype ♀ from Jartai, Alxa Meng, Inner Mongolia China, deposited in Inner Magnolia Normal University, not examined). syn. nov.

Halocosa jartica: Azarkina and Trilikauskas 2019: 557 (transferred from *Pardosa*).

Figure 5. *Halocosa cereipes* (L. Koch, 1878) **A** left male pedipalp, bulb, ventral view **B** same, retrolateral view **C** median apophysis and conductor, retrolateral view **D** embolic base, ventral view **E** median apophysis, ventral view **F** tegular sclerite, ventral view.
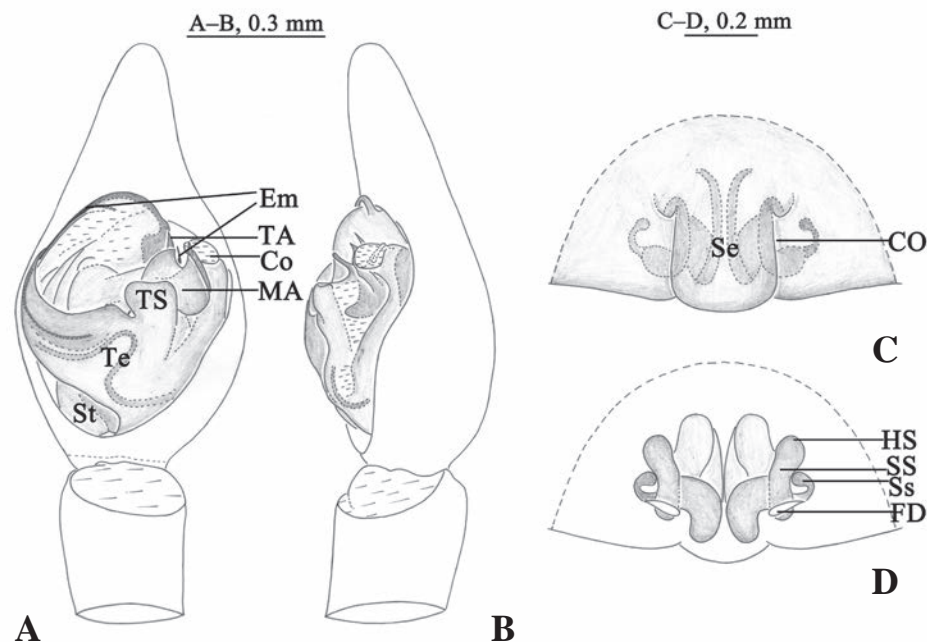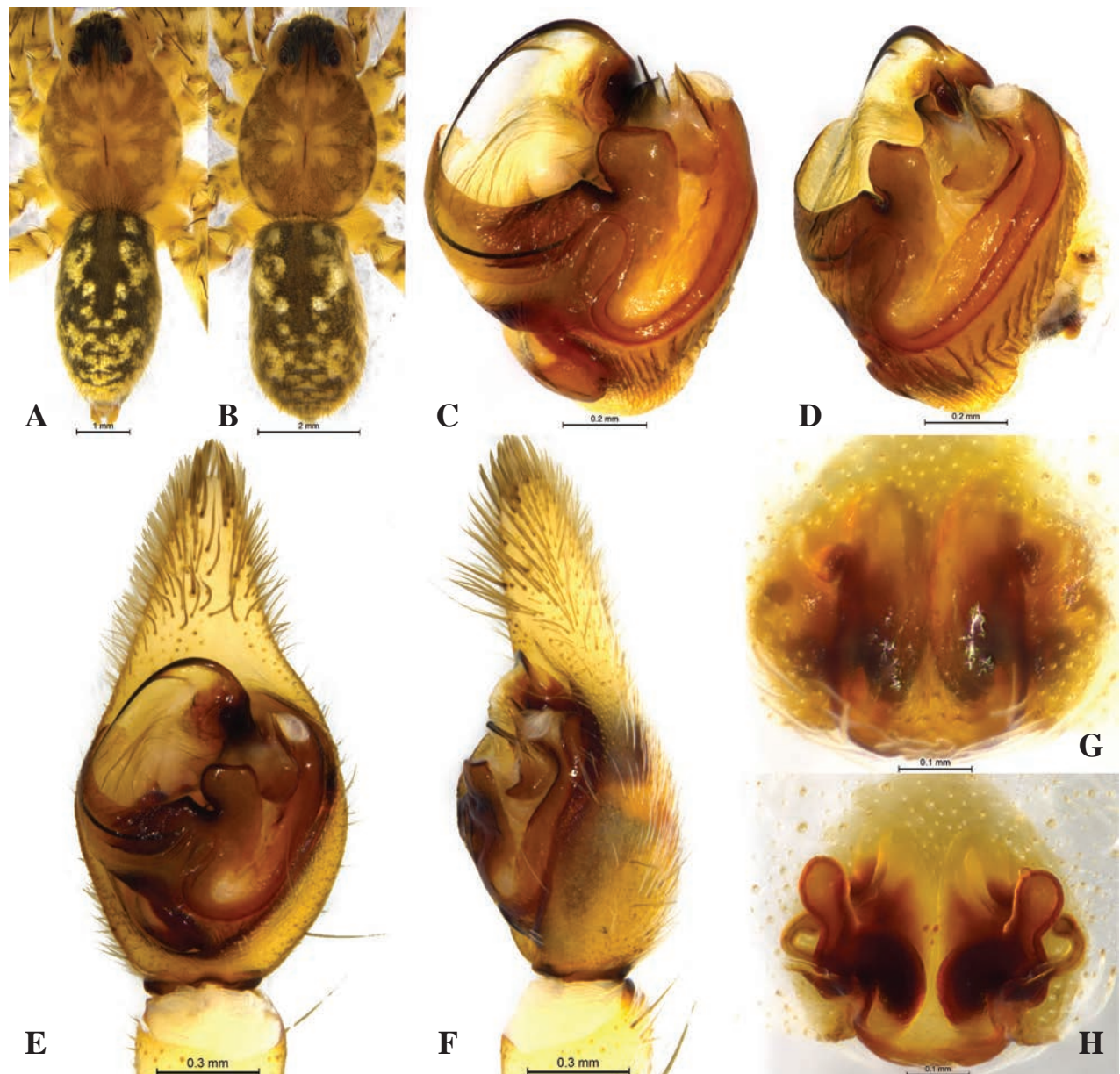

Figure 6. *Halocosa hatanensis* (Urita, Tang & Song, 1993) **A** left male pedipalp, ventral view **B** same, retrolateral view **C** epigyne, ventral view **D** same, dorsal view. Abbreviations: CO = copulatory opening; Co = conductor; Em = embolus; FD = fertilization duct; HS = head of spermatheca; MA = median apophysis; Se = septum; SS = stalk of spermatheca; St = subtegulum; TA = terminal apophysis; Te = tegulum; Ts = tegular sclerite.

Figure 7. *Halocosa hatanensis* (Urita, Tang & Song, 1993) **A** male habitus, dorsal view **B** female habitus, dorsal view **C** left male palp, bulb, ventral view **D** same, retrolateral view **E** left male palp, ventral view **F** same, retrolateral view **G** epigyne, ventral view **H** vulva, dorsal view.

Material examined. CHINA: **Xinjiang:** 1♀, Qiemo County, 31 July 2006, F. Zhang leg. • 1♂ 2♀, Korla City, Tashidian Town, 25 May 2009, D. Sun and Y.W. Zhao leg. • 2♀, Ruoqiang County, Taitema Lake, 39°28.309'N, 88°16.791'E, 789 m, 10 May 2013, L.Y. Wang leg. • 1♂, Qiemo County, 38°41.504'N, 86°53.235'E, 1029 m, 10 May 2013, L.Y. Wang leg. • 1♀, Yuli County, 41°06.476'N, 86°30.650' E, 868 m, 1 June 2014, L.Y. Wang and X.K. Jiang leg. • 7♂ 4♀, Yuli County, 40°43.939'N, 87°20.139'E, 863 m, 1 June 2014, L.Y. Wang and X.K. Jiang leg. • 1♂ 10♀, Ruoqiang County, Taitema Lake, 39°28.309'N, 88°16.791'E, 789 m, 1 June 2014, L.Y. Wang and X.K. Jiang leg. • 3♂ 2♀, Qiemo County, 38°41.536'N, 86°53.263'E, 1004 m, 2 June 2014, L.Y. Wang and X.K. Jiang leg. • 6♂, Qiemo County, Kalamilan River, 37°57.796'N, 84°26.794'E, 1260 m, 2 June 2014, L.Y. Wang & X.K. Jiang leg. • 1♀, Yutian County, Keliya River, 36°51.678'N, 81°42.622'E, 1382 m, 3 June
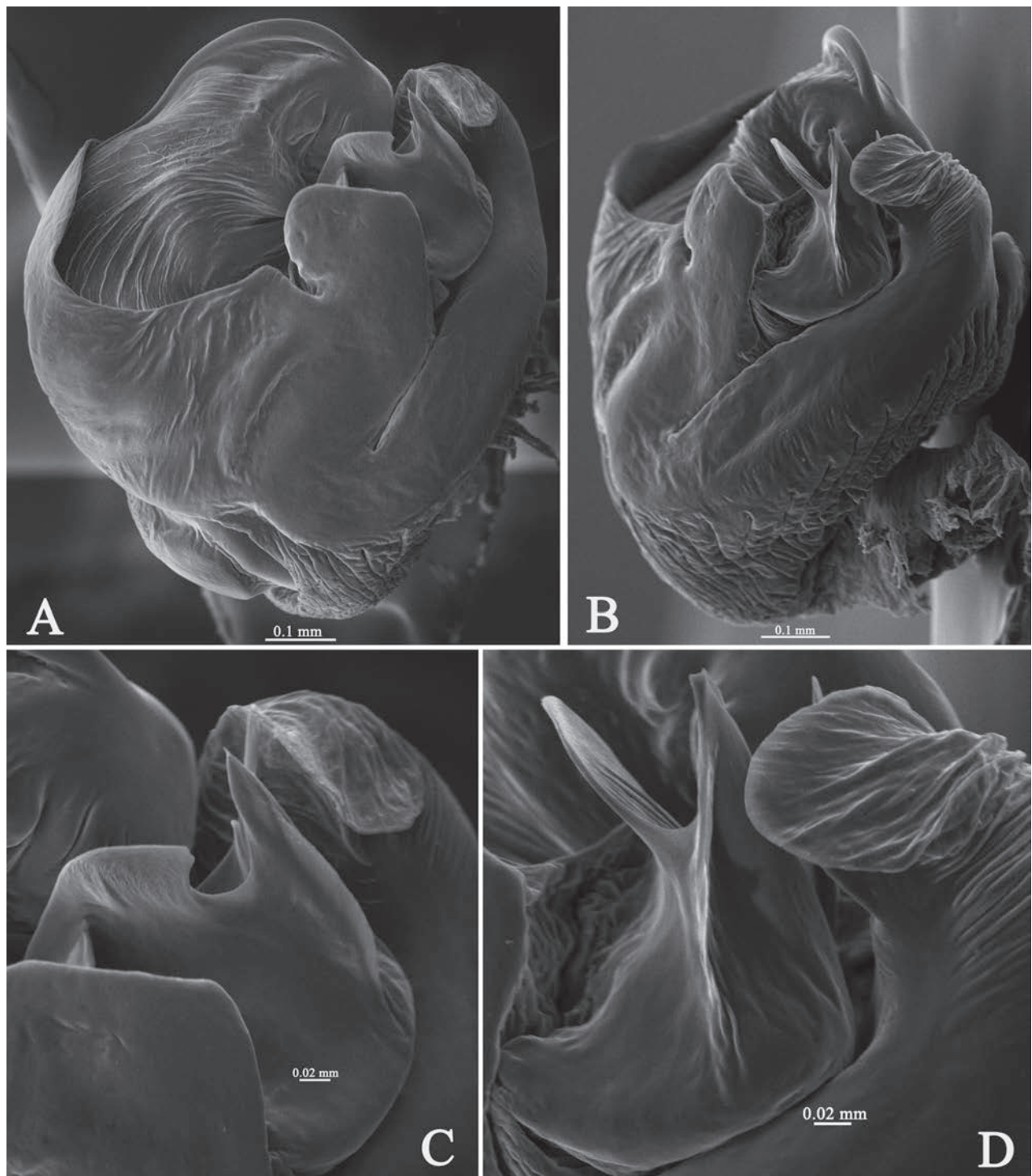
Figure 8. *Halocosa hatanensis* (Urita, Tang & Song, 1993) **A** left male pedipalp, bulb, ventral view **B** same, retrolateral view **C** median apophysis, ventral view **D** median apophysis and conductor, retrolateral view.

2014, L.Y. Wang and X.K. Jiang leg. **Qinghai:** 1♂, Geermu, 15 Septemper 2002, M.S. Zhu leg. **Inner Mongolia:** 3♂ 1♀, Alashanzuoqi, Jilantai (Jartai) Salt Lake, 39°43.281'N, 105°44.705'E, 1017 m, 7 June 2015, T. Lu and G.Q. Huang leg. • 1♂ 2♀, Bayannur, Wulateqianqi, Eerdengbulage, Wuliangsuhai, 40°51.577'N, 108°50.906'E, 1025 m, 14 June 2015, T. Lu and G.Q. Huang leg. **Ningxia:** 1♂ 1♀, Shizuishan City, Pingluo County, Sha Lake, 38°47.890'N, 106°20.934'E, 1104 m, L.Y. Wang, H.Y. Liu and K. Yu leg.
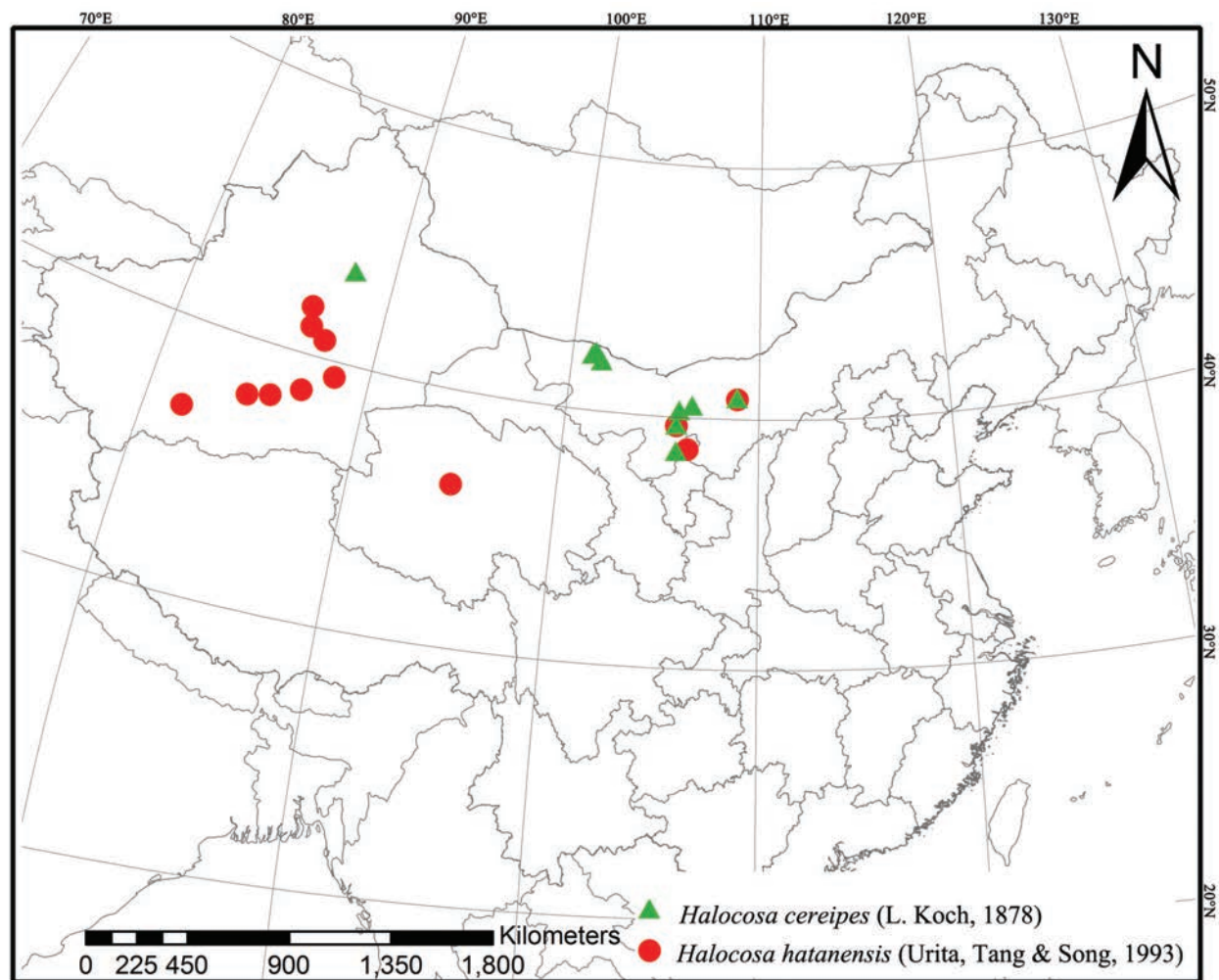
Figure 9. Distribution of *Halocosa* in China.

Diagnosis. This species is similar to *H. cereipes* (L. Koch, 1878) (Figs 2A, C, E, G, 3–5), but differs by the tall and almost square tegular sclerite vs. dwarf in *H. cereipes*; the long and crooked terminal apophysis vs. short, strong and flat; the long and thin subterminal apophysis vs. wide and short; the bifurcate median apophysis, ventral branches curved, dorsal branch straight and pointed vs. not bifurcate, end bent to conductor (Figs 2H, 6A, B, 7C–F, 8); the crack-shape copulatory openings and located below of the septum (vs. arc-shaped, located on the anterior position of the septum); and the width of spermathecal head almost the same as the width of spermathecal stalk (vs. width of spermathecal head greater than the width of spermathecal stalk) (Figs 6C, D, 7G, H).

Description. Males total length 7.52–10.36. One male (Figs 1D, 7A, from Qiemo County) total length 7.52: carapace 3.84 long, 2.73 wide; opisthosoma 3.82 long, 2.04 wide. Eye sizes and interdistances: AME 0.20, ALE 0.14, PME 0.36, PLE 0.32; AME–AME 0.13, AME–ALE 0.05, PME–PME 0.24, PME–PLE 0.30. Clypeus height 0.18. Leg measurements: I 11.82 (3.20, 4.03, 2.73, 1.86); II 11.52 (3.18, 3.81, 2.66, 1.86); III 11.58 (3.04, 3.55, 3.24, 1.75); IV 15.84 (4.00, 4.74, 4.83, 2.23).

Palp (Figs 2H, 6A, B, 7C–F, 8). Cymbium c. 1.9 times longer than wide. The end of terminal apophysis curving, subterminal apophysis thin and membranous, shorter than the length of terminal apophysis. Median apophysis vertical

and bifurcate, concave in lateral view. Tegular sclerite tall and almost square. Embolus long whip-like, smoothly rounded, slightly bent near tip, making almost whole circle, partly hidden by tegular ridge and median apophysis, base of embolus located in position of 2 o'clock. Conductor membranous.

Females total length 8.01–13.21. One female (Figs 1C, 7B, from Qiemo County) total length 8.01: carapace 4.03 long, 2.75 wide; opisthosoma 4.04 long, 2.45 wide. Eye sizes and interdistances: AME 0.23, ALE 0.15, PME 0.35, PLE 0.32; AME–AME 0.10, AME–ALE 0.04, PME–PME 0.27, PME–PLE 0.32. Clypeus height 0.19. Leg measurements: I 10.74 (3.05, 3.66, 2.29, 1.74); II 10.25 (2.88, 3.50, 2.20, 1.67); III 10.60 (2.90, 3.41, 2.63, 1.66); IV 14.62 (3.76, 4.55, 4.30, 2.01).

Epigyne (Figs 6C, D, 7G, H). Copulatory openings crack-shaped and located below of the septum. Spermathecal heads slightly inflated, approaching the anterior margins of spermathecal stalks. Spermathecal stalks as wide as heads. Accessorial gland arc-shaped, with a small and spherical head. Fertilization ducts small, crescent-shaped.

Distribution. China (Xinjiang, Qinghai, Ningxia and Inner Mongolia) (Fig. 9).

Remarks. Sample collected from the type locality of *H. jartica* contains specimens of both sexes. Comparison of these specimens with illustrations and descriptions of the *H. jartica* female and male of *H. hatanensis* reveals no differences, and therefore, we synonymized these names. The distance between the type localities is about 140 km. Although two species were described in the same paper, we consider *H. hatanensis* as the senior synonym because of page priority, and also because males have more diagnostic characters than females.

Acknowledgements

Additional information

Conflict of interest

The authors have declared that no competing interests exist.

Ethical statement

No ethical statement was reported.

Funding

Author contributions

All authors have contributed equally.

Author ORCIDs

Lu-Yu Wang ⬤ https://orcid.org/0000-0002-5250-3473
Muhammad Irfan ⬤ https://orcid.org/0000-0003-0445-9612
Yuri M. Marusik ⬤ https://orcid.org/0000-0002-4499-5148
Zhi-Sheng Zhang ⬤ https://orcid.org/0000-0002-9304-1789

Data availability

All of the data that support the findings of this study are available in the main text.

References

Álvarez-Padilla F, Hormiga G (2007) A protocol for digesting internal soft tissues and mounting spiders for scanning electron microscopy. Journal of Arachnology 35 (3): 538–542. https://doi.org/10.1636/Sh06-55.1

Azarkina GN, Trilikauskas LA (2019) *Halocosa* gen. n., a new genus of Lycosidae (Araneae) from the Palaearctic, with a redescription of *H. cereipes* (L. Koch, 1878). Zootaxa 4629(4): 555–570. https://doi.org/10.11646/zootaxa.4629.4.4

Koch L (1878) Kaukasische Arachnoiden. In: Schneider, O. (ed.) Naturwissenschaftliche Beiträge zur Kenntniss der Kaukasusländer auf Grund seiner Sammelbeute. Sitzungs-Berichte der naturwissenschaftlichen Gesellschaft Isis in Dresden 1878: 36–71, 159–160, [pl. 1–2].

Li SQ, Lin YC (2016) Species Catalogue of China, Vol. 2, Animals, Invertebrates (I), Arachnida: Araneae. Science Press, Beijing, 549pp.

Marusik YM, Guseinov EF, Koponen S (2003) Spiders (Arachnida: Aranei) of Azerbaijan. 2. Critical survey of wolf spiders (Lycosidae) found in the country with description of three new species and brief review of Palaearctoc *Evippa* Simon, 1885. Arthropoda Selecta 12: 47–65.

Nentwig W, Blick T, Bosmans R, Gloor D, Hänggi A, Kropf C (2021) Spiders of Europe. Version 08.2021. https://doi.org/10.24436/1 [accessed on August 25]

Ponomarev AV, Tsvetkov AS (2004) The generalized data on spiders (Aranei) of the Nature Research "Rostovski". Trudy Gosudarstvennogo Zapovednika "Rostovskii" 3: 84–104.

Roewer CF (1955) Katalog der Araneae von 1758 bis 1940, bzw. 1954. 2. Band, Abt. a (Lycosaeformia, Dionycha [excl. Salticiformia]). *2*. Band, Abt. b (Salticiformia, Cribellata) (Synonyma-Verzeichnis, Gesamtindex). Institut royal des Sciences naturelles de Belgique, Bruxelles, 1751 pp.

Urita, Tang GM, Song DX (1993) Two new species of the genus *Pardosa* from Inner Mongolia, China (Araneae, Lycosidae). Journal of Inner Mongolia Normal University (Natural Science Edition) 3: 46–49.

Wang LY, Li ZX, Zhou KX, Zhang ZS (2015) Redescription of three *Hippasa* species from China (Araneae: Lycosidae), with a proposed species group-division and diagnosis. Zootaxa 3974(2): 231–244. https://doi.org/10.11646/zootaxa.3974.2.7

WSC (2024) World Spider Catalog. Version 25.5. Natural History Museum Bern. https://doi.org/10.24436/2 [Accessed on: 2024-09-15]

ZooKeys

Research Article

Discovery of a new *Isonychia* species with distinctive characters from southwestern China, and preliminary exploration of its phylogenetic status (Ephemeroptera, Isonychiidae)

Pengxu Mu[1], Xiaolei Huang[1]

1 *State Key Laboratory of Ecological Pest Control for Fujian and Taiwan Crops, College of Plant Protection, Fujian Agriculture and Forestry University, Fuzhou 350002, China*
Corresponding authors: *Pengxu Mu (mupx927@fafu.edu.cn); Xiaolei Huang (huangxl@fafu.edu.cn)*

Abstract

The genus *Isonychia* Eaton, 1871 is widely distributed across the Holarctic and Oriental regions. However, no representatives of this genus have been reported from southwestern China, a region known for its high biodiversity. Here, we described and illustrated *Isonychia latias* **sp. nov.**, a new species recently collected from Guizhou Province, southwestern China, across all developmental stages. The imagos of this new species exhibit some uncommon characters within *Isonychia*, such as brown mid- and hindlegs, and pale stripes on the thorax. To explore the phylogenetic status of this new species within *Isonychia*, a multigene phylogenetic analysis was conducted.

Key words: *16S*, *COI*, mayfly, molecular phylogeny, taxonomy

Introduction

Isonychiidae is a monogeneric mayfly family represented by a single extant genus, *Isonychia* Eaton, 1871, which includes 16 species distributed in the Nearctic region and 21 species distributed in the Palaearctic and Oriental regions (Tiunova et al. 2004; Muthukatturaja et al. 2021; Huang et al. 2024; Qiang et al. 2024).

Kondratieff and Voshell (1983) conducted a comprehensive classification of the *Isonychia* species in North America. These authors established a new subgenus, *Prionoides* Kondratieff & Voshell, 1983 and divided the *Isonychia* s.s. into four species groups, including non-Nearctic species. McCafferty (1989) erected a new subgenus, *Borisonychia* McCafferty, 1989, for *I. diversa* Traver, 1934, the only representative of the *diversa* group sensu Kondratieff and Voshell (1983). Unfortunately, *I. diversa* has been declared extinct (McCafferty 2001), and no new members of this subgenus have been identified since then.

Before this study, a total of nine *Isonychia* species had been recognized from China (Qiang and Zhou 2023; Huang et al. 2024; Qiang et al. 2024), including three species from northeastern China (*I. sexpetala* Tiunova et al., 2004, *I. ussurica* Bajkova, 1970 and *I. vshivkovae* Tiunova et al., 2004), four species from eastern China (*I. formosana* (Ulmer, 1912), *I. guixiensis* Wu et al., 1992, *I. kiangsinensis* Hsu, 1936 and *I. taishunensis* Huang et al., 2024), and two species

from southern China (*I. ignota* (Walker, 1853) and *I. fuscimarginata* Qiang et al., 2024). Thus, the fauna of western China for this genus remains unknown.

Recently, we conducted a preliminary investigation of the mayfly fauna in Guizhou Province, southwestern China, and discovered an undescribed species of *Isonychia*. This species exhibits several uncommon characters within the genus. To determine its status within *Isonychia*, we performed a multigene phylogenetic analysis alongside adequate morphological studies.

Materials and methods

The adults and larvae of the new species were collected from the same site in Zunyi City, Guizhou Province, and were associated by DNA barcoding based on the mitochondrial cytochrome c oxidase subunit I (*COI*) gene. All imagos were reared from subimagos caught using a light trap, and the larval exuviae were found on rocks in a stream. All specimens used in this study are preserved in 95% ethanol and are deposited in the State Key Laboratory of Ecological Pest Control for Fujian and Taiwan Crops, College of Plant Protection, Fujian Agriculture and Forestry University (**FAFU**).

The specimens were examined and photographed using a computer-connected Nikon SMZ18 stereomicroscope. The photos were processed with Adobe Photoshop CC 2019. The SEM samples were dehydrated in 100% ethanol for 15 min and then coated with gold film in a vacuum.

To explore the status of our new species within *Isonychia*, we conducted a multigene phylogenetic analysis using the mitochondrial genes *COI* and 16S ribosomal RNA (*16S*). Total DNA was extracted from legs of larvae or adults using Trelief Hi-Pure Animal Genomic DNA Kit (Tsingke, Beijing, China). The mitochondrial genes *COI* and *16S* were PCR-amplified with the primers specified in Folmer et al. (1994) and Ogden and Whiting (2005), respectively. Optimized PCR conditions were as follows: 30 s of initial denaturation at 98 °C, a total of 35 cycles with denaturation at 98 °C for 10 s, annealing at 52 °C for 30 s and an extension at 72 °C for 30 s, and 2 min of final extension at 72 °C. The products of PCR were bidirectionally sequenced at Tsingke Biotechnology (Beijing, China). All sequences obtained in this study were assembled using BioEdit (Hall 1999) and deposited in GenBank. The accession numbers, along with the GPS coordinates of sample locations, are provided in Table 1. The nomenclature of gene sequences follows Chakrabarty et al. (2013). In addition to the sequences of our new species, we included sequences of five *Isonychia* species and two non-*Isonychia* species from GenBank for the phylogenetic analysis; the details of these sequences are shown in Table 2.

The phylogenetic analysis was conducted using the integrated platform PhyloSuite v. 1.2.3 (Xiang et al. 2023). Multiple sequence alignments were performed using MAFFT (Katoh and Standley 2013) in "Normal" alignment mode.

Table 1. Sequenced specimens of *Isonychia latias* sp. nov. ("-" indicates the same content as above).

Specimen voucher	Locality	Coordinates	Date	Stage	GenBank #	GenSeq nomenclature
GZZY01BaN011A1	Xishui, Guizhou	28.497144N, 106.410003E	21.V.2024	subimago	PP922980	genseq-2 COI
-	-	-	-	-	PQ289235	genseq-2 16S
GZZY01BaN011L2	-	-	-	larva	PP922981	genseq-2 COI

Table 2. Sequences of *Isonychia* spp. obtained from GenBank.

Species	Gene	GenBank #	Reference	Notes
I. (Prionoides) shima	*COI*	LC106878	Saito and Tojo 2016	–
I. (Prionoides) shima	*16S*	LC106655	Saito and Tojo 2016	–
I. (s.s.) japonica	*COI*	LC106699	Saito and Tojo 2016	As *I. valida*
I. (s.s.) japonica	*16S*	LC106476	Saito and Tojo 2016	As *I. valida*
I. (s.s.) ignota	*COI*	LC114396	Saito et al. 2016	–
I. (s.s.) ignota	*16S*	LC114375	Saito et al. 2016	–
I. (s.s.) ussurica	*COI*	LC114401	Saito et al. 2016	–
I. (s.s.) ussurica	*16S*	LC114379	Saito et al. 2016	–
I. (s.s.) kiangsinensis	*COI/16S*	MH119135	Ye et al. 2018	Derived from mitogenome
Chromarcys magnifica	*COI*	MG516472	Massariol et al. 2019	–
Chromarcys magnifica	*16S*	MG516460	Massariol et al. 2019	–
Paegniodes cupulatus	*COI/16S*	MW381300	Li et al. 2021	Derived from mitogenome

Further trimming of the *COI* and *16S* alignments was carried out using trimAl (Capella-Gutierrez et al. 2009) with default parameters before concatenation. The concatenated alignments were then imported into ModelFinder (Kalyaana-moorthy et al. 2017) to select the best-fit models for phylogenetic estimates using the "Edge-linked" partition mode. According to the Bayesian Information Criterion, the best fit models were TIM2+F+G4 for *COI* and TPM2u+F+G4 for *16S*. Maximum-likelihood (ML) phylogenetic tree reconstruction was conducted using IQ-TREE (Minh et al. 2020), with branch support analysis performed in "Ultrafast" mode with 5,000 bootstraps; other parameters were set to default. The phylogenetic tree was visualized using iTOL v. 6 (Letunic and Bork 2024).

Terminology for egg structure followed Koss and Edmunds (1974); the term "microlepides" was used according to Kluge and Novikova (2011); other terms were used according to Kluge (2004).

Results

Isonychia latias sp. nov.

https://zoobank.org/BDD9DBA9-82B4-4D68-BCF8-42F53CEC10A2
Figs 1−9
Chinese name: 比翼等蜉

Type material. *Holotype*: male imago, CHINA • **Guizhou Province,** Zunyi City, Xishui County, China Dan Xia Valley, Sanchahe River [贵州省遵义市习水县中国丹霞谷三岔河] (28.497144N, 106.410003E, alt. 880 m), 21.V.2024, leg. Pengxu Mu; in ethanol; FAFU. *Paratypes* • 8 male imagos, 8 female imagos, 12 male subimagos, 15 female subimagos, 12 larvae, 22 larval exuviae, same information as holotype; in ethanol; FAFU.

Description. Male imago. Forewing length 18.5−20.0 mm.

Coloration. General body color brown to reddish brown (Fig. 1A). Head capsule dark brown except anterior part pale; compound eyes gray (Fig. 2A). Pronotum dark brown except posterolateral parts pale; mesoscutum brown, and mesoscutellum and metanotum dark brown; pleura of pterothorax with
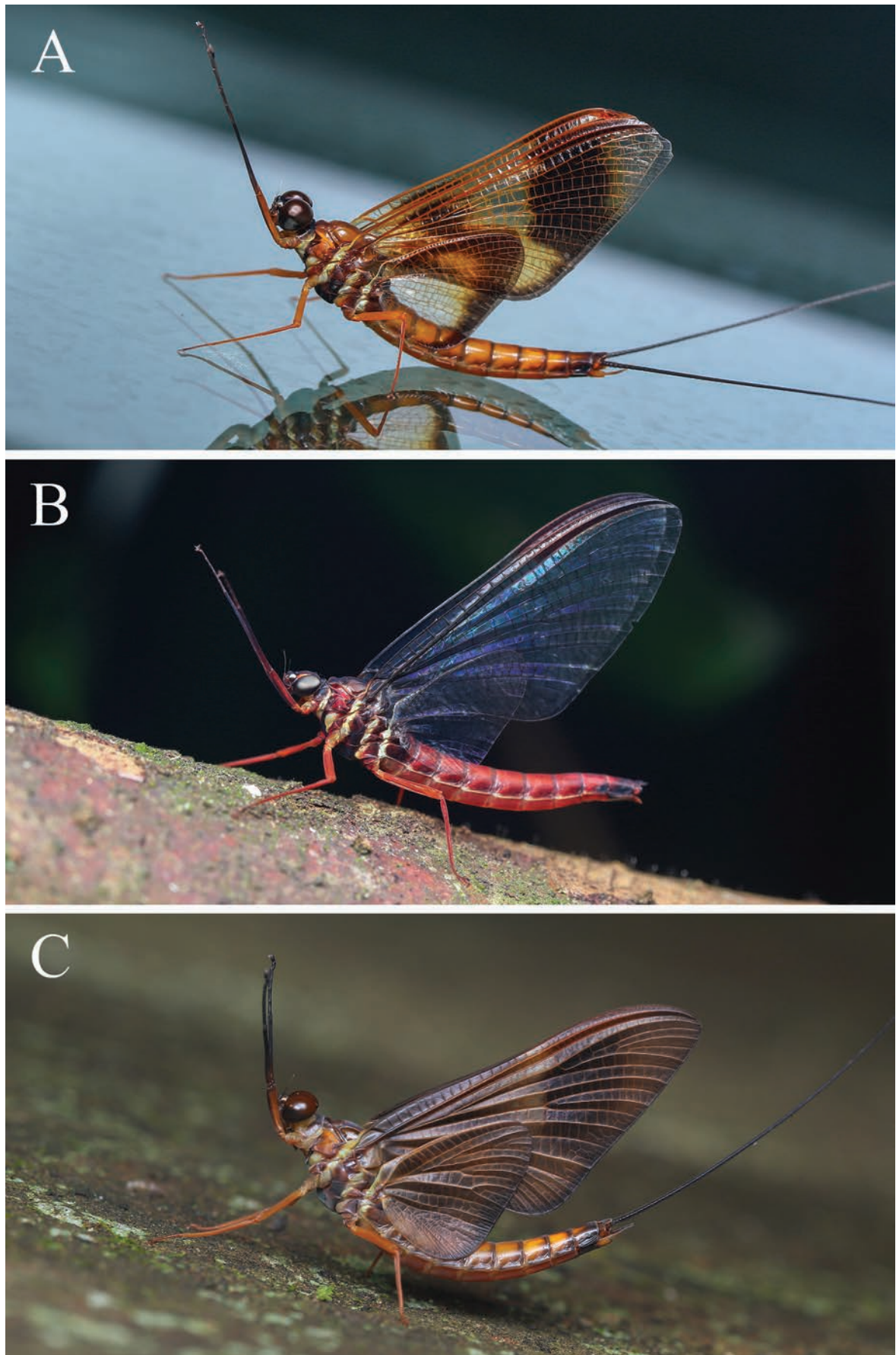
Figure 1. Adults of *Isonychia latias* sp. nov. **A** male imago **B** female imago **C** male subimago. (Photographed by Qianle Lu).

three yellowish stripes formed by pale conjunctivas; basisternum and furcasternum of mesothorax dark reddish brown, and basisternum of metathorax pale reddish (Fig. 2B, C). Forefemur brown, slightly shaded with dark brown apically; foretibia and foretarsus dark brown; mid- and hindlegs brown (Fig. 2G). Fore- and hindwings with distinct, dark brown coloration and pale yellowish shadings as in Fig. 3A; all veins of both wings pale brown. Abdominal terga I and X dark brown; terga II–VII pale brown, except lateral margins slightly shaded with dark brown; terga VIII–IX with anteromedian part pale brown and posterolateral part dark brown, and dark brown area of tergum IX larger than that of tergum VIII; terga II–IX with pair of dark, submedian, longitudinal, oblique stripes (Fig. 4A). Abdominal sterna reddish brown except sternum IX dark brown; sterna II–IX with pair of dark submedian longitudinal oblique stripes, and sterna II–VI with four dark dots situated in transverse line behind these stripes. Styliger and gonostyli pale brown, and penis dark brown (Fig. 4C). Cerci dark brown along their entire length.
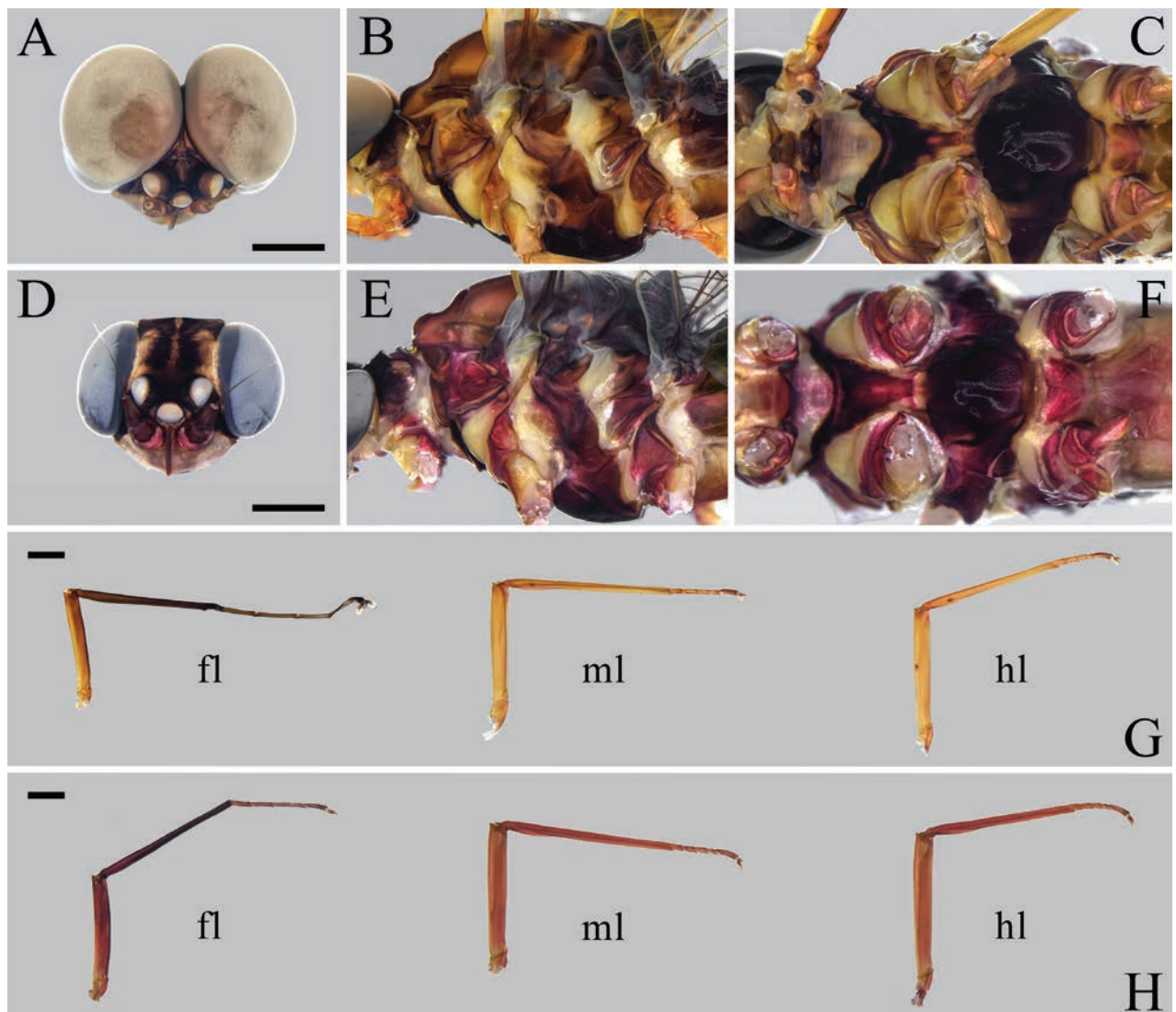

Figure 2. Imaginal structures of *Isonychia latias* sp. nov. **A–C** male imago **A** head **B** thorax, lateral view **C** thorax, ventral view **D–F** female imago **D** head **E** thorax, lateral view **F** thorax, ventral view **G, H** legs (fl: foreleg; ml: midleg; hl: hindleg) **G** male imago **H** female imago. Scale bars: 1.0 mm (**A, D, G, H**).
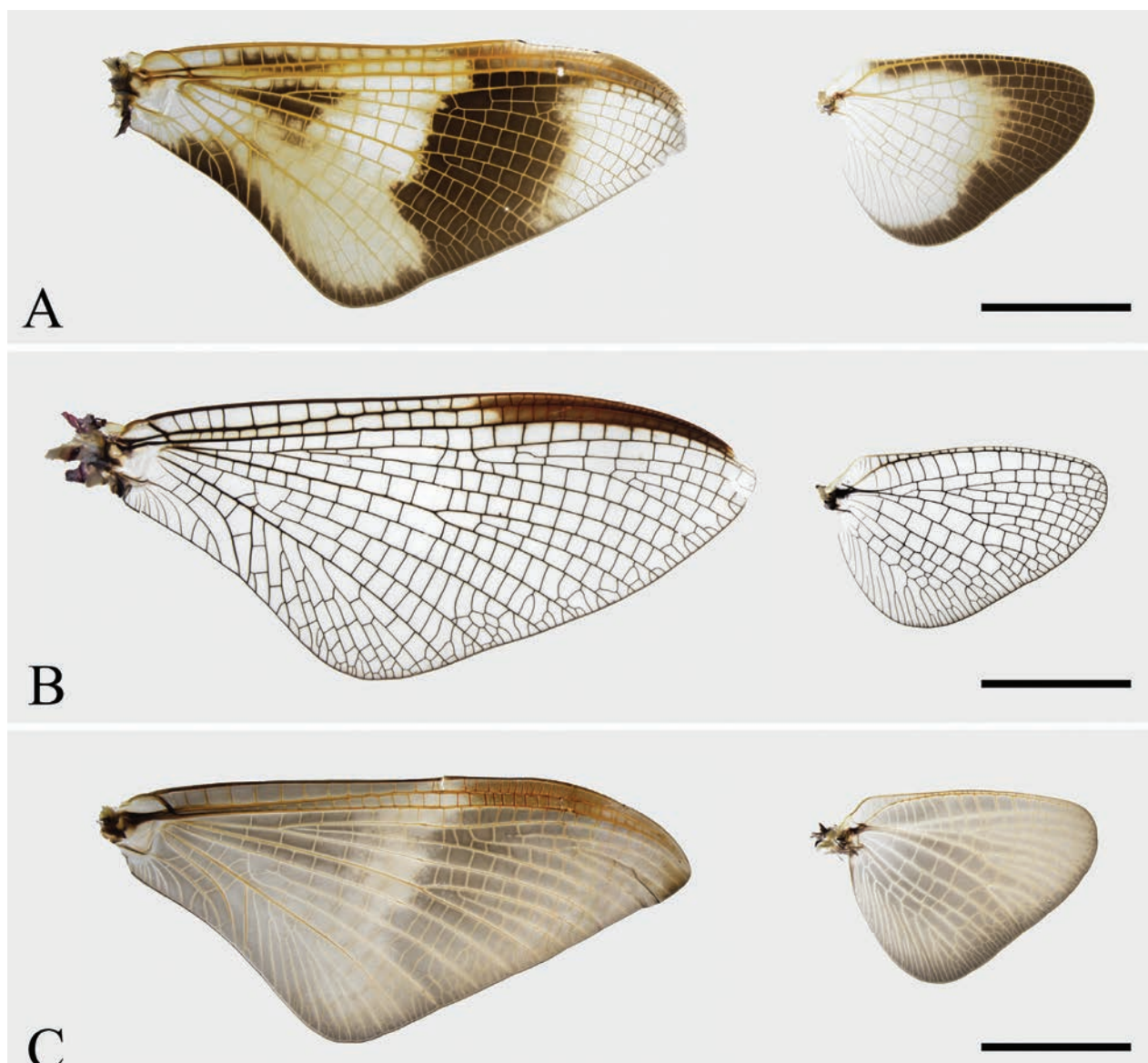
Figure 3. Wings of *Isonychia latias* sp. nov. **A** male imago **B** female imago **C** male subimago. Scale bars: 5.0 mm.

Legs (Fig. 2G). Foreleg: length ratio of femur (2.7 mm):tibia:tarsus 1.0:1.5:1.6, length ratio of tarsomeres from basal to apical 1.0:1.3:1.0:0.9:0.4. Midleg: length ratio of femur (3.2 mm):tibia:tarsus 1.0:1.4:0.6, tarsomeres arranged in decreasing order as 5, 2, 1, 3, 4. Hindleg: length ratio of femur (3.2 mm):tibia:tarsus 1.0:1.2:0.5, tarsomeres arranged in decreasing order as 5, 2, 1, 3, 4. Foreleg with both claws similar, blunt, and provided with a soft plate; mid- and hindlegs with both claws similar and pointed.

Wings (Fig. 3A). Forewing: number of crossveins relatively large, and pterostigmatic area with about 30 crossveins between C and Sc; MP forked asymmetrically, MP_2 strongly curved in proximal part; cubital field with two or three unforked and four forked veins gone from CuA to basitornal and tornoapical margins. Hindwing: length ratio of maximum length:width 1.4:1.0; costal projection round and with 4–5 crossveins; tornoapical margin slightly concave; RS forked about 1/2 of distance from base of vein to margin; MA forked slightly more apically than RS; MP forked about 3/4 of distance from base of vein to margin.
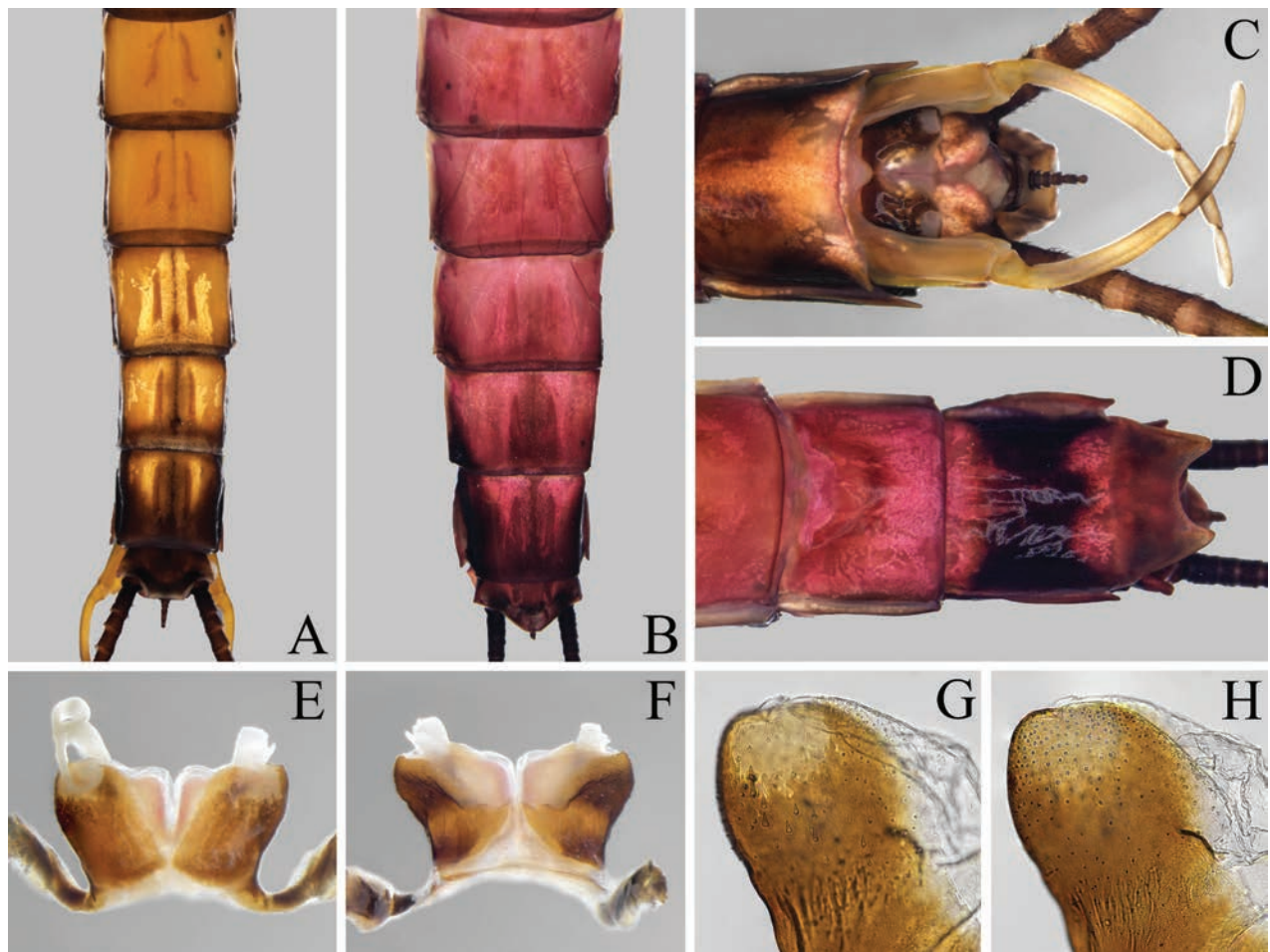
Figure 4. Imaginal structures of *Isonychia latias* sp. nov. **A, B** abdominal segments V–X, dorsal view **A** male **B** female **C, D** genital segments, ventral view **C** male **D** female **E–H** penis **E** ventral view **F** dorsal view **G** penis lobe enlarged, ventral view **H** penis lobe enlarged, dorsal view.

Genitals (Fig. 4C, E–H). Gonostyli pedestals relatively long with blunt ventral-apical-median angles. Gonostylus with length of segment II ca 2.0 of segment III length, and length of segment III ca 1.4 of segment IV length. Penis reaching to middle part of gonostyli pedestals; penis lobes deeply separated with apices strongly divergent, and stout spines only present on subapical area of ventral surface. Processes between styliger and penis absent.

Female imago. Forewing length 22.7–23.5 mm. Similar to male imago except the following:

Coloration. General body color reddish (Fig. 1B). Compound eyes blue-gray (Fig. 2D). Thoracic pattern similar to male imago but reddish in general (Fig. 2E, F). Forefemur reddish, slightly shaded with dark reddish apically; foretibia dark reddish; foretarsus, mid- and hindlegs reddish (Fig. 2H). Forewing with dark brown band occupying pterostigmatic area; hindwing colorless; all veins of both wings dark brown (Fig. 3B). Abdominal tergum I dark reddish; terga II–VII reddish; terga VIII–IX with anteromedian part reddish and posterolateral part black, and black area of tergum IX larger than that of tergum VIII (Fig. 4B). Abdominal sterna reddish brown, except sternum IX with large, transverse, dark brown band (Fig. 4D).

Legs (Fig. 2H). Foreleg: length ratio of femur (2.8 mm):tibia:tarsus 1.0:1.5:0.9, length ratio of tarsomeres from basal to apical 1.0:1.1:0.9:0.7:1.1. Midleg: length

ratio of femur (3.5 mm):tibia:tarsus 1.0:1.3:0.5. Hindleg: length ratio of femur (3.8 mm):tibia:tarsus 1.0:1.0:0.4. Both claws of all legs similar and pointed.

Wings (Fig. 3B). Hindwing: length ratio of maximum length:width 1.6:1.0; RS forked about 2/5 of distance from base of vein to margin; MA forked about 1/2 of distance from base of vein to margin; MP forked about 7/10 of distance from base of vein to margin.

Genitalia (Fig. 4D). Subgenital plate slightly elongated with rounded posterior margin. Subanal plate with deep posteromedian emargination.
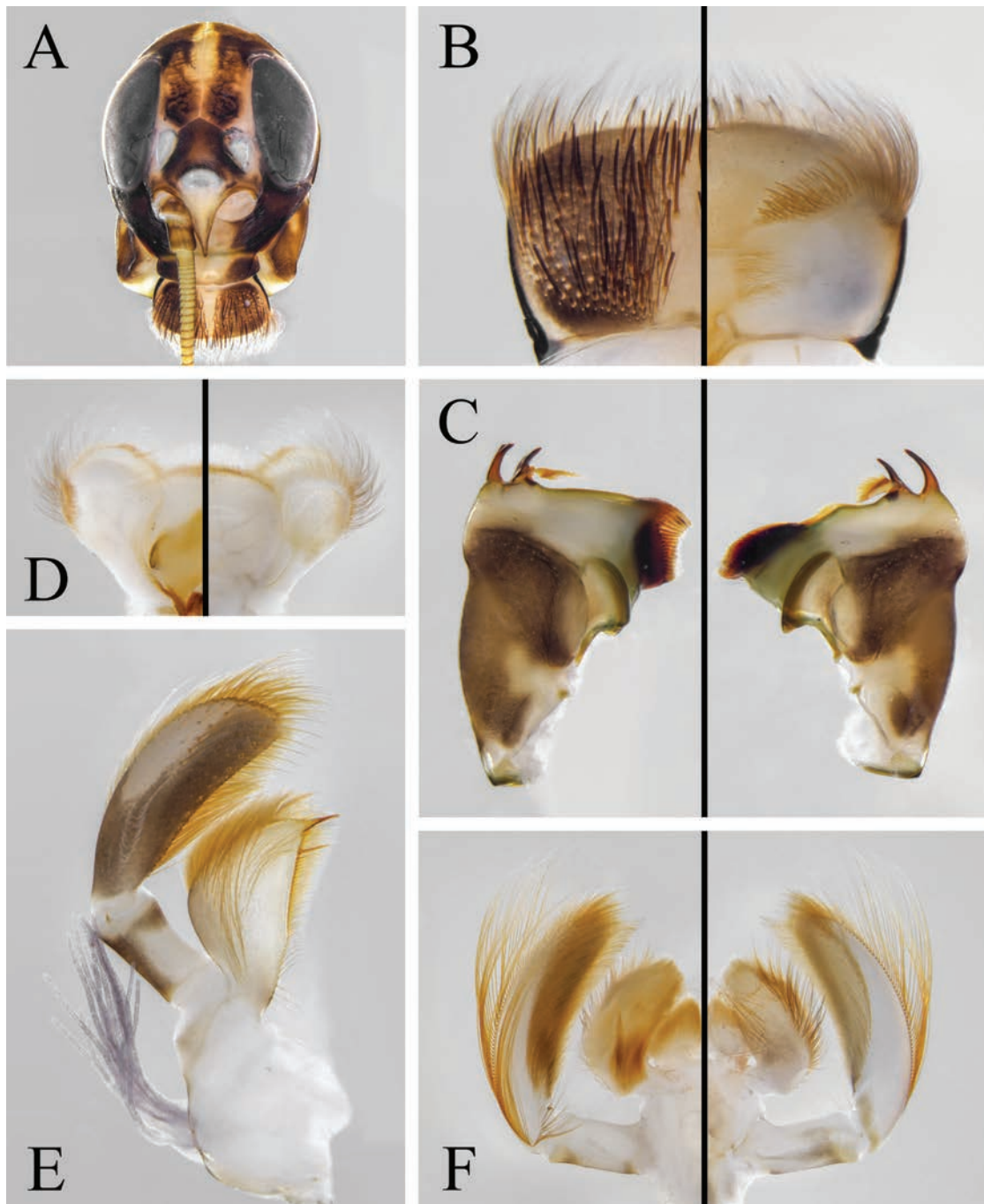

Figure 5. Larval structures of *Isonychia latias* sp. nov. **A** head, front view **B** labrum (left: dorsal view; right: ventral view) **C** mandible, dorsal view (left: left mandible right: right mandible) **D** hypopharynx (left: dorsal view right: ventral view) **E** maxilla, dorsal view **F** labium (left: dorsal view; right: ventral view).
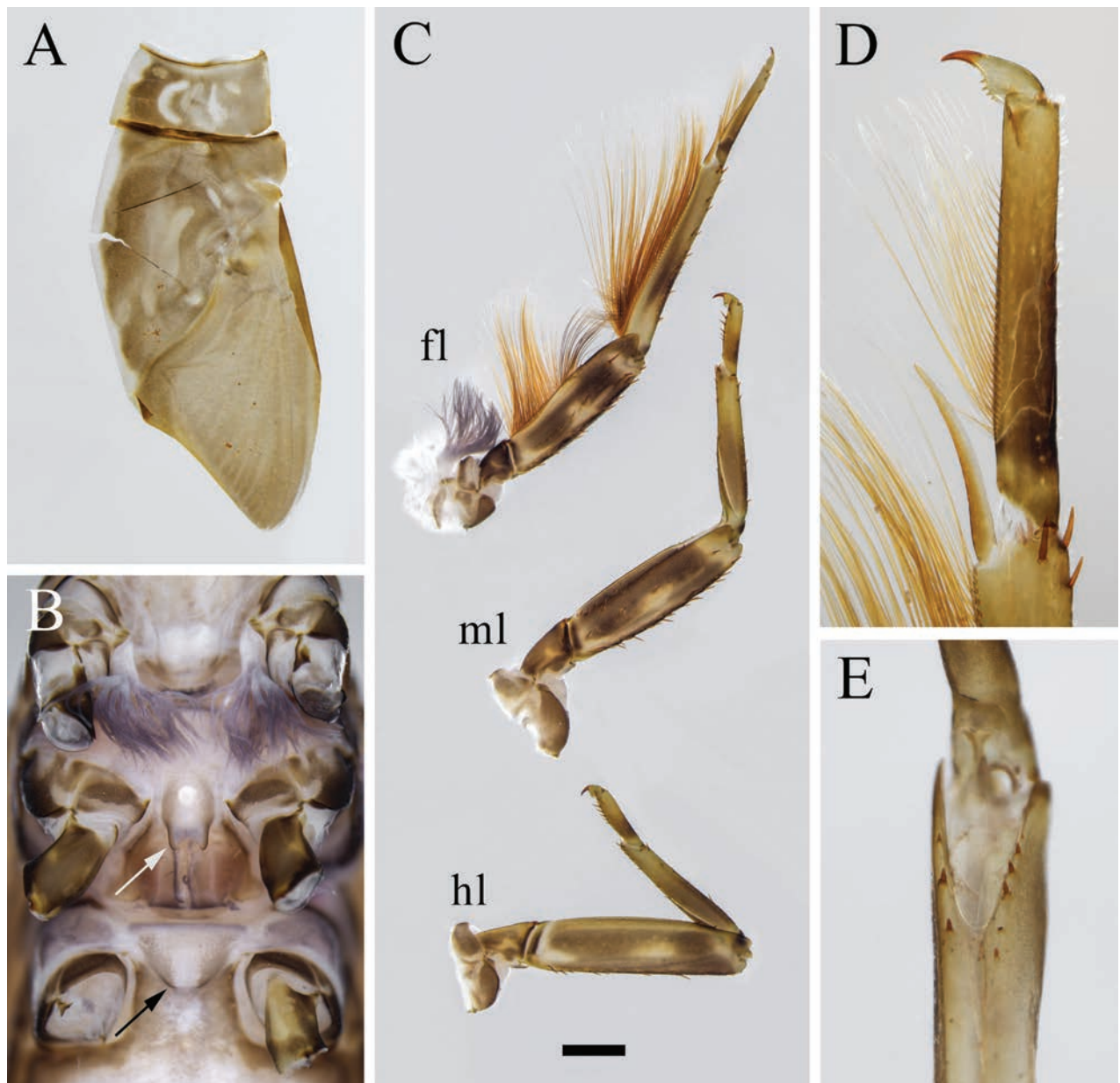
Figure 6. Larval structures of *Isonychia latias* sp. nov. **A** right half of pronotum and mesonotum **B** thorax, ventral view (white arrow shows projection on basisternum of mesothorax black arrow shows projection on basisternum of metathorax) **C** legs (fl: foreleg ml: midleg hl: hindleg) **D** apical part of foreleg **E** ventral cleft of hindfemur. Scale bar: 1.0 mm (**C**).

Male subimago. Similar to male imago except the following: Mesonotum with brown lateral pigmented area occupying submedioscutum and sublateroscutum back to posterior scutal protuberance (PSp); medioscutum and PSp pale. Foreleg: length ratio of femur (2.6 mm):tibia:tarsus 1.0:1.4:1.2, length ratio of tarsomeres from basal to apical 1.0:1.0:0.8:0.7:0.7. Tarsomeres of all legs covered with "U"-shape, blunt microlepides. Both claws of all legs similar and pointed. Wings brown to dark brown in general, coloration as in Fig. 3C.

Female subimago. Similar to male subimago except the following: Foreleg: length ratio of femur (2.9 mm):tibia:tarsus 1.0:1.4:0.9, length ratio of tarsomeres from basal to apical 1.0:1.1:0.9:0.7:1.1. Subgenital plate not elongated.

Larva. Body length: male 19.3–20.6 mm; female 23.7–26.1 mm.

Figure 7. Larval structures of *Isonychia latias* sp. nov. **A** tergalii (t1: tergalius I; t4: tergalius IV; t5: tergalius V; t7: tergalius VII) **B** thoracic sterna, lateral view (white arrow shows projection on basisternum of mesothorax black arrow shows projection on basisternum of metathorax) **C** abdominal terga I−X **D** abdominal sterna VIII−IX **E** caudalii. Scale bars: 1.0 cm (**A**); 2.0 mm (**C, E**).

Coloration. General body color dark brown. Head capsule dark brown, except frontal carina, and median parts of clypeus and vertex yellowish; scape and pedicel brown, flagella pale; dorsum of labrum dark brown with pale longitudinal line medially (Fig. 5A). Thoracic nota dark brown but with pale median longitudinal stripe and irregular pale markings (Fig. 6A). Forefemur with two transverse dark bands, foretibia with 1 transverse dark band medially, and foretarsus with 1 transverse dark band in proximal part; mid- and hindleg with similar coloration except femur with two transverse dark bands connected by dark stripe, and dark band on tibia more basally (Fig. 6C). Abdominal terga dark brown in general; terga I−VII with pale median longitudinal stripes (shorter and less pronounced posteriorly); terga II−IX with pair of pale submedian longitudinal stripes; tergum X with pair of light spots close to anterior margin (Fig. 7C). Abdominal sterna brown in general; sterna II−IX with pair of pale submedian longitudinal stripes,
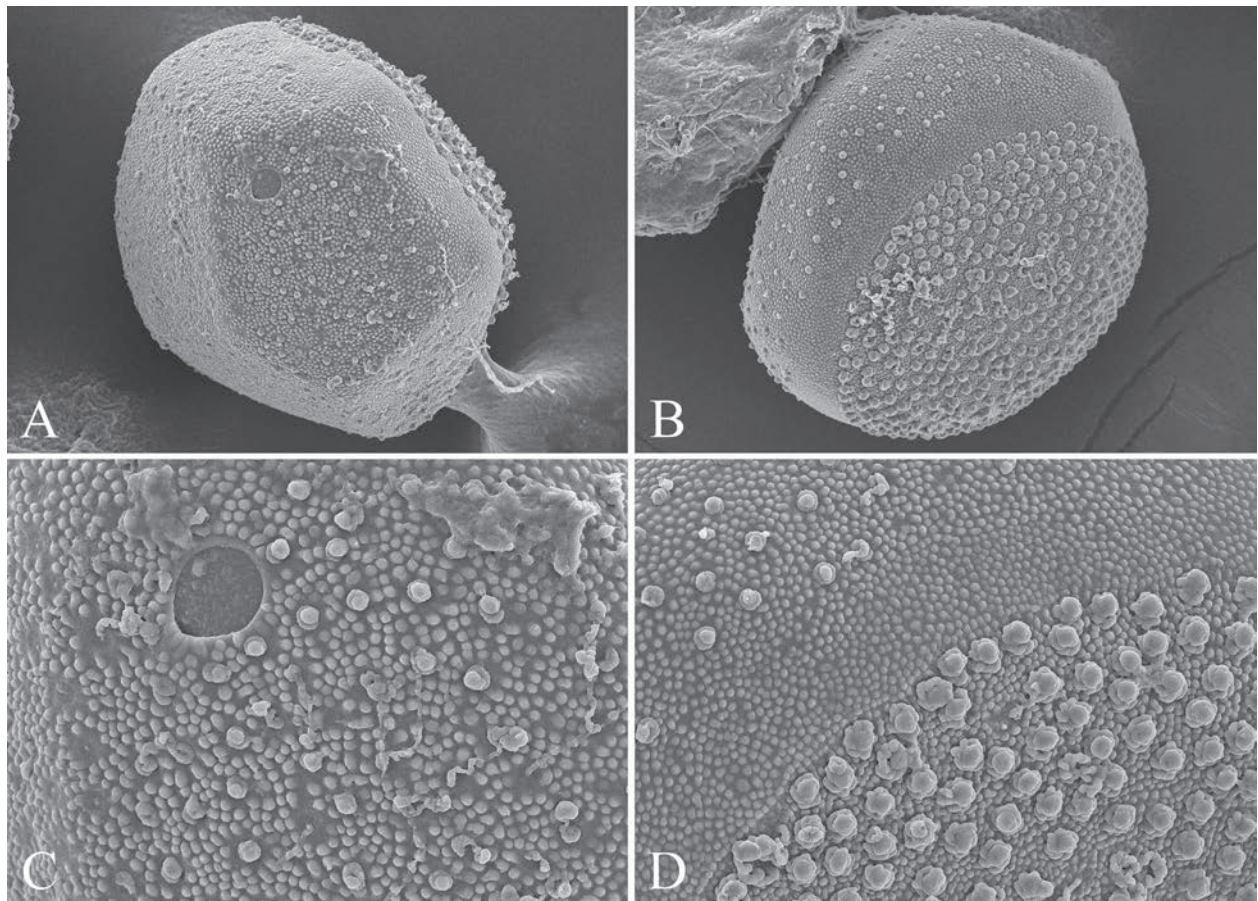
Figure 8. SEM photos of eggs of *Isonychia latias* sp. nov. **A, B** egg **C** micropyle enlarged **D** KCTs enlarged.

and sterna II−VIII with four dots situated in transverse line behind these stripes. Tergalii without distinct dots or markings (Fig. 7A). Caudalii brown basally and gradually paler towards apices without dark band medially.

Mouthparts (Fig. 5B−F). Typical of *Isonychia*, setal pattern consistent with other congeners in general. Labrum subquadrate, widest part about twice as long. Superlingua round, width ca 0.6 of lingua width. Distal dentiseta of maxilla strongly diminished, needle-like, distinctly shorter and slenderer than proximal dentiseta. Length of segment I of maxillary palp ca 0.4 of segment II length. Length of segment I of labial palp ca 0.5 of segment II length. Length of para-glossa ca 0.5 of glossa length.

Legs (Fig. 6C−E). Setal pattern typical of *Isonychia*. Ventral cleft of hind femur with 5−8 spines. All claws with 7−9 blunt denticles. Gill on joining of forecoxa with thorax well developed, tuft-like.

Thoracic sterna (Figs 6B, 7B). Bifurcate projection on basisternum of meso-thorax well developed; paired projections on basisternum of metathorax rela-tively weakly expressed.

Tergalii (Fig. 7A). Lamella of tergalius I distinctly smaller than other lamellae of tergalii, apical part of costal rib with 4−5 spine-like denticles; lamellae of ter-galii II−VII gradually larger posteriorly, each lamella usually with 5−7 spine-like denticles on apical part of costal rib and on apical part of posterior branch of anal rib (rarely beyond this range, and in tergalii III−VII mostly with 6 denticles), and no denticles present on apical margin between these two areas. Ventral fibrillose lobe well developed in all tergalii.

Figure 9. Habitat of *Isonychia latias* sp. nov. **A, B** Sanchahe River, Dan Xia Valley, China **C, D** mature larva of *Isonychia latias* sp. nov. about to emerge in natural environment.

Abdominal terga and sterna (Fig. 7C, D). Terga II–X with acute denticles along posterior margins. Sterna VI–VIII with acute denticles along posterior margins, and subanal plate with smaller and denser denticles on median part of posterior margin. Posterolateral spines well developed on segment VIII–IX.

Egg (Fig. 8A–D). Spherical; chorion densely covered with small tubercles, and without reticulation; KCTs dense in one hemisphere, and other area sparsely scattered with smaller KCTs.

Diagnosis. *Isonychia latias* sp. nov. can be readily distinguished from its congeners by the following combination of characters: For male imago: A) wings with distinct, dark brown coloration: on forewing occupying a large area of apical half as a transverse band, a small area around bifurcation point of Rs, and edges along basitornal margin and tornus, and on hindwing occupying almost whole apical part; B) mid- and hindlegs brown, nearly consistent with forefemur; C) pleura of pterothorax with three yellowish stripes formed by pale conjunctivas. For larvae: A) lamellae of all tergalii without spines on apical margin, and without distinct dots or markings; B) abdominal terga I–VII with pale median longitudinal stripes, terga II–IX with pair of pale submedian longitudinal stripes, and tergum X with pair of light spots close to anterior margin; C) caudalii brown basally and gradually paler towards apices without dark band medially. The larvae of *I. latias* sp. nov. resemble those of *I. fuscimarginata* Qiang et al., 2024, based on the similar coloration of abdominal terga. However, they can be differentiated by the following characters: A) each lamella of

tergalii of *I. fuscimarginata* with a large middle dark purple dot basally, while those of *I. latias* sp. nov. without dots; B) ventral fibrillose lobes of tergalii of *I. fuscimarginata* with fewer filaments than those of *I. latias* sp. nov.; C) *I. fuscimarginata* with submedian dark band on all caudalii and apical dark band on cerci, while all caudalii of *I. latias* sp. nov. without dark band along their entire length.

Distribution. China: Guizhou Province (Zunyi City, Sanchahe River).

Etymology. The new species is named after Latias, an alate Pokémon with red and white appearance. The specific epithet *latias* is treated as a noun in apposition to the generic name.

Biology. The larvae of *Isonychia latias* sp. nov. have so far been found only in the Sanchahe River in Guizhou Province. The collection site is located near a Danxia landform, characterized by a large amount of dark red rocks in the river (Fig. 9A, B). The larvae were primarily collected in rapid sections, and one mature larva about to emerge was found in a gravelly shallow area (Fig. 9C, D). The exuviae of the larvae were mainly found on stones 10–20 cm above the water surface, with the highest reaching more than 50 cm. The subimagos of both sexes moulted into imagos spending three nights after they were caught.

Genetics

We performed a multi-gene phylogenetic analysis using the mitochondrial genes *COI* and *16S*, including our new species, four *Isonychia* s.s. species, and one *Prionoides* species (Table 2). *Chromarcys magnifica* Navás, 1932 and *Paegniodes cupulatus* (Eaton, 1871) were used as outgroups. The topology of the ML tree shows that *Isonychia* (*Prionoides*) *shima* (Matsumura, 1931) is the first species to branch out, forming a sister group with the remaining species. Within the remaining species, our new species is the first to split off, forming a sister group with the other four *Isonychia* s.s. species, which form a monophyletic group (Fig. 10).
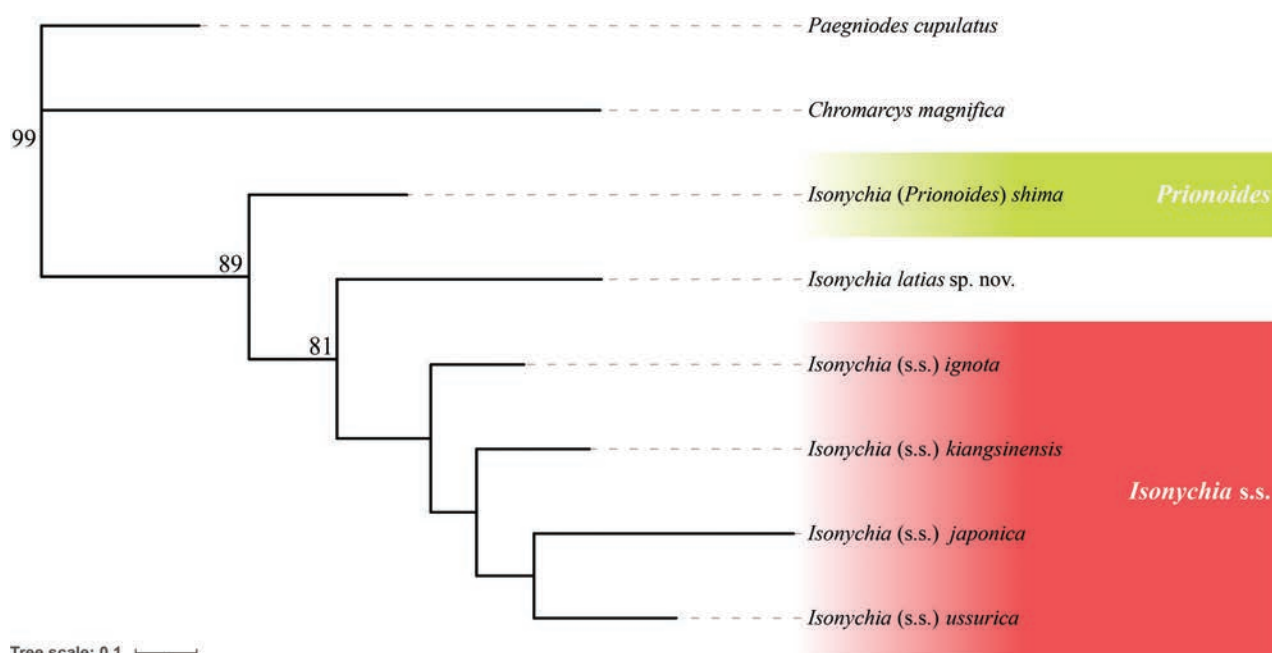

Figure 10. ML tree for *Isonychia* spp based on concatenated sequences of two genes (*COI* and *16S*) showing *Prionoides* (green) and *Isonychia* s.s. (red). ML bootstrap values above 70 are indicated next to the nodes.

Discussion

Tiunova et al. (2004) revised the *Isonychia* species of the Eastern Palaearctic region, reviewing the concept of *Isonychia* along with its two subgenera, *Isonychia* s.s. and *Prionoides*. In general, *I. latias* sp. nov. apparently morphologically belongs to *Isonychia* s.s., based on its spherical eggs, the strongly reduced styliger in male adults and the tuft-like forecoxal gills in larvae. This result is consistent with our molecular phylogenetic analysis, which shows that *I. latias* sp. nov. is grouped with four other *Isonychia* s.s. species, together forming a sister clade with *I.* (*P.*) *shima*.

However, it is worth mentioning that some of the reviewed characters given by Tiunova et al. (2004) do not apply to our new species. First, Tiunova et al. argued that forewing coloration could be present in male imagos of some *Isonychia* species but always absent in their female imagos. This is not the case in *I. latias* sp. nov., where the female imago has dark brown coloration occupying the pterostigmatic area. Such exceptions are also found in *I. formosana* (Ulmer, 1912) and *I. fuscimarginata* Qiang et al., 2024 (the female imago of the former has larger colored area than male on both wings; the female imago of the latter has similar wing coloration with male). Second, Tiunova et al. indicated that the first tarsomere is equal to or slightly longer than the second one in imagos of both sexes. In contrast, the first tarsomere of the male imago of *I. latias* sp. nov. is shorter than second one (length ratio of tarsomere I:II 1.0:1.3 in the holotype and 1.0:1.4 in one paratype).

Besides these two characters, the coloration of the legs and pleura of our new species is also uncommon in *Isonychia*. In most *Isonychia* species (at least in all well-studied *Isonychia* s.s. species), the mid- and hindlegs of imagos are distinctly paler than forelegs, and the coloration of pleura is relatively uniform. However, *I. latias* sp. nov. has brown to reddish brown mid- and hindlegs consistent with the forefemur, and its pleura of the pterothorax is more colorful. Notably, similar coloration was found in some *Prionoides* species, such as *I.* (*P.*) *shima* from Japan (Saito et al. 2020: fig. 1B). Correspondingly, the position of *I. latias* sp. nov. in our phylogenetic tree indicates its potential ancestral status within the *Isonychia* s.s clade. However, our molecular phylogenetic analysis did not include enough species to draw a definitive conclusion on the exact position of our new species within *Isonychia*. More research, especially of the Oriental fauna, is needed to fully understand the evolution of *Isonychia* and the systematic position of *I. latias* sp. nov. within the genus.

Acknowledgements

Additional information

Conflict of interest

The authors have declared that no competing interests exist.

Ethical statement

No ethical statement was reported.

Author contributions

Funding acquisition: XH. Investigation: PM. Visualization: PM. Writing - original draft: PM. Writing - review and editing: XH.

Author ORCIDs

Pengxu Mu ⓘ https://orcid.org/0000-0003-4906-0955
Xiaolei Huang ⓘ https://orcid.org/0000-0002-6839-9922

Data availability

All of the data that support the findings of this study are available in the main text.

References

Bajkova OY (1970) New and little-known species of mayflies (Ephemeroptera) from the basin of the Amur River. Entomologicheskoe Obozrenie I Revue d'Entomologie de l'URSS 49(1): 146−55. [In Russian]

Capella-Gutierrez S, Silla-Martínez JM, Gabaldón T (2009) trimAl: a tool for automated alignment trimming in large-scale phylogenetic analyses. Bioinformatics 25(15): 1972−1973. https://doi.org/10.1093/bioinformatics/btp348

Chakrabarty P, Warren M, Page LM, Baldwin CC (2013) GenSeq: an updated nomenclature and ranking for genetic sequences from type and non-type sources. ZooKeys 346: 29−41. https://doi.org/10.3897/zookeys.346.5753

Eaton AE (1871) A monograph on the Ephemeridae. The Transactions of the Entomological Society of London 2: 1−135.

Folmer O, Black M, Hoeh W, Lutz R, Vrijenhoek R (1994) DNA primers for amplification of mitochondrial cytochrome c oxidase subunit I from diverse metazoan invertebrates. Molecular Marine Biology and Biotechnology 3: 294−299.

Hall TA (1999) BioEdit: a user-friendly biological sequence alignment editor and analysis program for Windows 95/98/NT. Nucleic acids symposium series 41: 95−98.

Hsu YC (1936) New Chinese mayflies from Kiangsi Province (Ephemeroptera). Peking Natural History Bulletin 10(4): 319−325.

Huang D-D, Shen C-Y, Huang G-Y, Ye L-Y, Wu H-Y, Zhang S-S, Cheng H-Y (2024) A new species of *Isonychia* Eaton, 1871 (Ephemeroptera: Isonychiidae) from Taishun, China based on morphological characteristics and COX1 gene. Zootaxa 5437(4): 537−548. https://doi.org/10.11646/zootaxa.5437.4.6

Kalyaanamoorthy S, Minh BQ, Wong TKF, von Haeseler A, Jermiin LS (2017) Modelfinder: Fast model selection for accurate phylogenetic estimates. Nature Methods 14: 587−589. https://doi.org/10.1038/nmeth.4285

Katoh K, Standley DM (2013) MAFFT multiple sequence alignment software version 7: Improvements in performance and usability. Molecular Biology and Evolution 30: 772−780. https://doi.org/10.1093/molbev/mst010

Kluge NJ (2004) The phylogenetic system of Ephemeroptera. Kluwer Academic Publishers, Dordrecht, 442 pp. https://doi.org/10.1007/978-94-007-0872-3

Kluge NJ, Novikova EA (2011) Systematics of the mayfly taxon *Acentrella* (Ephemeroptera, Baetidae), with description of new Asian and African species. Russian Entomological Journal 20 (1): 1–56. https://doi.org/10.15298/rusentj.20.1.01

Kondratieff BC, Voshell Jr JR (1983) Subgeneric and species-group classification of the mayfly genus *Isonychia* in North America (Ephemeroptera: Oligoeuriidae). Proceedings of the Entomological Society of Washington 85(1): 128–138.

Koss RW, Edmunds Jr GF (1974) Ephemeroptera eggs and their contribution to phylogenetic studies of the order. Zoological Journal of the Linnean Society 55(4): 267–349. https://doi.org/10.1111/j.1096-3642.1974.tb01648.x

Letunic I, Bork P (2024) Interactive Tree of Life (iTOL) v6: recent updates to the phylogenetic tree display and annotation tool. Nucleic Acids Research 52(W1): W78–W82. https://doi.org/10.1093/nar/gkae268

Li R, Lei Z, Li W, Zhang W, Zhou C (2021) Comparative mitogenomic analysis of Heptageniid mayflies (Insecta: Ephemeroptera): conserved intergenic spacer and tRNA gene duplication. Insects 12(2): 1–15. https://doi.org/10.3390/insects12020170

Massariol F, Takiya DM, Salles FF (2019) Global classification and evolution of brush-legged mayflies (Insecta: Ephemeroptera: Oligoneuriidae): phylogenetic analyses of morphological and molecular data and dated historical biogeography. Zoological Journal of the Linnean Society 187(2): 378–412. https://doi.org/10.1093/zoolinnean/zlz031

Matsumura S (1931) 6000 Illustrated Insects of Japan Empire. Tokyo, 1497 pp. [In Japanese]

McCafferty WP (1989) Characterization and relationships of the subgenera of *Isonychia* (Ephemeroptera: Oligoneuriidae). Entomological News 100: 72–78.

McCafferty WP (2001) Notes on distribution and orthography associated with some poorly known North American mayflies (Ephemeroptera). Entomological News 112(2): 121–122.

Minh BQ, Schmidt HA, Chernomor O, Schrempf D, Woodhams MD, von Haeseler A, Lanfear R (2020) IQ-TREE 2: new models and efficient methods for phylogenetic inference in the genomic era. Molecular Biology and Evolution 37(5): 1530–1534. https://doi.org/10.1093/molbev/msaa015

Muthukatturaja M, Balasubramanian Ch, Rathikumar T, Sivaramakrishnan KG (2021) A new species of *Isonychia* Eaton, 1871 (Ephemeroptera: Isonychiidae) from Kapila River, Central Western Ghats, India. Zootaxa 4908(2): 283–291. https://doi.org/10.11646/zootaxa.4908.2.9

Navás L (1932) Insecta orientalia. X Series. Memorie dell'Accademia Pontifica dei Nuovi Lincei, Rome (2), 16: 921–949.

Ogden TH, Whiting MF (2005) Phylogeny of Ephemeroptera (mayflies) based on molecular evidence. Molecular Phylogenetics and Evolution 37: 625–643. https://doi.org/10.1016/j.ympev.2005.08.008

Qiang X-H, Zhou C-F (2023) A preliminary review of *Isonychia* Eaton, 1871 from Chinese mainland with a re-description of *I. kiangsinensis* Hsu, 1936 (Insecta, Ephemeroptera, Isonychiidae). ZooKeys 1178: 115–141. https://doi.org/10.3897/zookeys.1178.104619

Qiang X-H, Gong D-W, Zhou C-F (2024) A new mayfly species of *Isonychia* Eaton, 1871 (Ephemeroptera: Isonychiidae) with colourful wings from southern China. Aquatic Insects: 1–19. https://doi.org/10.1080/01650424.2024.2329539

Saito R, Tojo K (2016) Complex geographic- and habitat-based niche partitioning of an East Asian habitat generalist mayfly *Isonychia* japonica (Ephemeroptera:Isonychiidae) with reference to differences in genetic structure. Freshwater Science 35(2): 712–723. https://doi.org/10.1086/686564

Saito R, Jo J, Sekiné K, Bae YJ, Tojo K (2016) Phylogenetic analyses of the isonychiid mayflies (Ephemeroptera: Isonychiidae) in the northeast palearctic region. Entomological Research 46(4): 246–259. https://doi.org/10.1111/1748-5967.12168

Saito R, Jo J, Ito T (2020) Adult emergence patterns and body size of two mayfly species of *Isonychia* Eaton, 1871 from Hokkaido, Japan. Aquatic Insects 41(2): 145–156. https://doi.org/10.1080/01650424.2020.1730403

Tiunova TM, Kluge NJ, Ishiwata SI (2004) Revision of the East Palaearctic *Isonychia* (Ephemeroptera). Canadian Entomologist 136: 1–41. https://doi.org/10.4039/n02-108

Ulmer GH (1912) H. Sauter's Formosa-Ausbeute. Ephemeriden. Entomologische Mitteilungen 1: 369–375. https://doi.org/10.5962/bhl.part.25902

Walker F (1853) List of the specimens of neuropterous insects in the collection of the British Museum, Part III (Termitidae – Ephemeridae): 571–572.

Wu T, Gui H, Shi Z (1992) Two new species of genus *Isonychia* subgenus *Isonychia* sensu stricto (Ephemeriptera: Isonychiidae). Journal of Nanjing Normal University 15(2): 78–81.

Xiang C-Y, Gao F, Jakovlić I, Lei H-P, Hu Y, Zhang H, Zou H, Wang G-T, Zhang D (2023) Using PhyloSuite for molecular phylogeny andtree-based analyses. iMeta e87: 1–42. https://doi.org/10.1002/imt2.87

Ye Q-M, Zhang S-S, Cai Y-Y, Storey KB, Yu D-N, Zhang J-Y (2018) The complete mitochondrial genome of *Isonychia kiangsinensis* (Ephemeroptera: Isonychiidae). Mitochondrial DNA Part B 3(2): 541-542. https://doi.org/10.1080/23802359.2018.1467233

ZooKeys

Short Communication

Tachysurus taeniatus (Günther, 1873), a senior synonym of the congeneric species *T. ondon* (Shaw, 1934) (Teleostei, Bagridae) from eastern China

Wei-Han Shao[1], Jian-Li Cheng[2], E. Zhang[1]

1 Institute of Hydrobiology, Chinese Academy of Sciences, Wuhan, 430072, Hubei, China
2 School of Life Sciences and key laboratory of Jiangxi Province for Biological Invasion and Biosecurity, Jinggangshan University, Ji'an, 343009, Jiangxi, China
Corresponding author: Jian-Li Cheng (9920100038@jgsu.edu.cn)

OPEN ACCESS

Citation: Shao W-H, Cheng J-L, Zhang E (2024) *Tachysurus taeniatus* (Günther, 1873), a senior synonym of the congeneric species *T. ondon* (Shaw, 1934) (Teleostei, Bagridae) from eastern China. ZooKeys 1218: 153–166. https://doi.org/10.3897/zookeys.1218.135630

Abstract

Despite the current recognition of *Tachysurus taeniatus* and *T. ondon* as two separate valid species of China, neither species have been revised based on examination of their types and/or topotypical materials, nor have they genetically analyzed. In this study, examination of the holotype of *T. taeniatus* showed that it has a serrated anterior edge of the pectoral spine, a slightly emarginate caudal fin, and longer maxillary barbels extending beyond the base of the pectoral spine, the characters shared with specimens currently identified as *T. ondon*. Morphological comparisons and molecular analysis showed that specimens from mainland China, which are characterized by the three mentioned morphological features, represent a single species. According to the nomenclatural rule of priority, *T. taeniatus* is a senior subjective synonym of *T. ondon*. Within this concept, *T. taeniatus* is widely distributed in the lower reaches of Yangtze River and coastal rivers in Zhejiang and Fujian Province and closely related to *T. aurantiacus*, which is endemic to Japan. The morphological differences and species-level genetic distance between *T. taeniatus* and *T. aurantiacus* provide additional support for synonymization of *T. taeniatus* and *T. ondon*. The paper also describes ontogenetic color changes and coloration polymorphism in this species. Phylogeny of the *T. auranciatus* group, to which *T. taeniatus* belongs, is also discussed.

Key words: Coloration polymorphism, ontogenetic colouration change, original description, pectoral-fin spine, *T. auranciatus* group, taxonomy

Introduction

The bagrid genus *Tachysurus* is a species-rich group comprising more than seventy nominal species, widespread in the Far East to Southeast Asia (Shao and Zhang 2023). Currently, more than 30 of them are considered either invalid or questionable (Fricke et al. 2024). The majority of *Tachysurus* species, as listed by Ferraris (2007) were described more than a century ago. Original descriptions of some species were vague and/or inaccurate; thus, they are either out of modern taxonomic use or misleading when their diagnoses are ambiguous. Despite the recognition of some species as valid in the current taxono-

my of *Tachysurus*, they are only known from their original descriptions or by type specimens. One of them is *T. taeniatus*, a species originally described by Günther (1873) based on a single specimen six inches long (about 150 mm) collected from "Shanghai", without indicating an exact locality.

The original description of *T. taeniatus* mentioned a broad, blackish band along the side of the body and an adipose fin shorter than the anal fin in their basal lengths, both characters distinguishing it from all congeneric species with the rounded caudal fin. Although a recent examination (Watanabe and Kitabayashi 2001) of its holotype showed that the species has small serrations on the anterior margin of the pectoral spine similar to *T. ondon*, this character was not mentioned in the original description of *T. taeniatus*. Chinese researchers (Zheng and Dai 1999) did not have access to the type specimens of many species in their taxonomic revision of this genus. As a result, *T. taeniatus* is recognized as a valid species with a smooth anterior margin of the pectoral spine in the current taxonomy of Chinese *Tachysurus* species (Zheng and Dai 1999). Moreover, no additional specimens identified as *T. taeniatus* have been known from the type locality or adjacent areas since the original description. So, clarification of the taxonomic status of this species has been needed.

Tachysurus ondon was described by Shaw (1930) based on a single specimen of 77 mm SL captured from the Cao'e-Jiang, a coastal river that ultimately joins the Qiantang-Jiang before flowing into East China Sea, in Shing-Tsong (now Xinchang County in Zhejiang Province). It has so far been identified as a species with a serrated anterior edge of the pectoral spine, widely distributed in montane streams of Southeast China (Zheng and Dai 1999), despite no indication of this character in the original description. Our preliminary observations of Chinese *Tachysurus* species revealed that the anterior edge of the pectoral spine is smooth in all species with emarginate or rounded caudal fins except for *T. ondon* and *T. taeniatus*, as defined herein. Thus, given their similar morphology and proximate type localities, we undertook this study with the goal to clarify the taxonomic status of *T. ondon* and *T. taeniatus* based on morphological examination of the type and/or topotypical specimens integrating morphological and molecular evidence.

Materials and methods

Species collection and preservation

Four specimens of *Tachysurus taeniatus* were collected from an affluent of Taihu Lake in Huzhou City, Zhejiang Province. They are thus considered topotypical specimens as their collection site is very close (ca 50 km) to its type locality. Fourteen specimens of *T. ondon* were collected from the Cao'e-Jiang in Xinchang County (type locality), Zhejiang Province. In addition, 64 specimens identified as this species were captured from ten locations (Fig. 1) of coastal rivers in Zhejiang and Fujian Provinces. Captured specimens were stored in 10% formalin liquid after removal of right-side pelvic-fin clips. The extracted fin clips were kept in 95% ethyl alcohol and used for molecular analysis. The voucher specimens are preserved in the ichthyological collection at the Institute of Hydrobiology (**IHB**), Chinese Academy of Sciences, Wuhan. Careful morphological examination was made in this study on the holotype of *T. taeniatus*, currently stored in the Lake Biwa Museum, Japan (Fig. 2A, B).
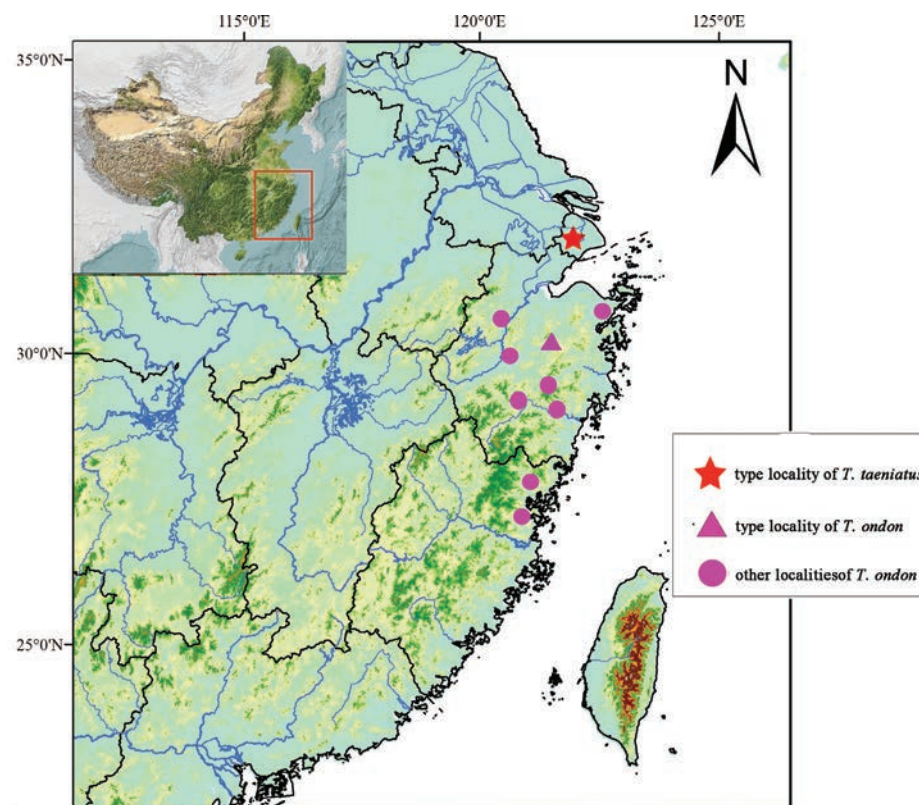
Figure 1. Map showing distributions of *Tachysurus taeniatus* and *T. ondon*.

Morphological analysis

Measurements were conducted using digital calipers, with data recorded to the nearest 0.1 mm. Whenever feasible, measurements were taken on the left side of each individual, following the techniques outlined by Cheng et al. (2008). Head length and measurements of other parts of the body are estimated as percentages of the standard length (SL). Subunits of the head are provided as percentages of the head length (HL). The number of rays in the dorsal and anal fins was determined following the method described by Watanabe (1995). Other fin rays were counted under a binocular dissecting microscope using transmitted light. Vertebral count was taken from X-ray photographs, with the five anteriormost vertebrae, namely the Weberian complex, not counted.

Morphometric data underwent principal component analysis (PCA) to reveal variations and assess relative contribution of specific variables to morphometric differences between the species. PCA was run with SPSS 16 (SPSS, Chicago, IL, USA). Before conducting the analysis, all measurements were standardized according to Reist (1985) to avoid effects of allometry.

Phylogenetic analysis

Phylogenetic analysis was performed using mtDNA *cyt-b* gene and the sequences have been uploaded to NCBI GenBank (Table 1). Twenty-seven *cyt-b* gene sequences amplified from 17 species of *Tachysurus* were used for molecular phylogenetic analysis. *Tachysurus trilineatus* was selected as the outgroup due to its identification as the basal lineage within the genus *Tachysurus* (Ku et al. 2007). The sequences were manually revised and then aligned using ClustalW

Table 1. GenBank accession numbers for molecular phylogenetic analysis.

	Taxon	Locality	Distribution	Accession number
Ingroup				
(1)	*Tachysurus aurantiacus*	Japan	Western Kyushu Island	LC533351
(2)	*Tachysurus brachyrhabdion*	Guizhou, China	Yuan-Jiang of middle Yangtze River	PP266650
(3)	*Tachysurus brevicorpus*	South Korea		NC_015625
(4)	*Tachysurus eupogon*	Hubei, China	Middle Yangtze River	PP266669
(5)	*Tachysurus gracilis*	Guangxi, China	Xiang-Jiang of middle Yangtze River	PP266654
(6)	*Tachysurus intermedius*	Hainan, China	Nandu-Jiang	PP266676
(7)	*Tachysurus koreanus*	South Korea		NC028434
(8)	*Tachysurus kyphus*	Guangxi, China	Fangcheng- Jiang	PP266671
(9)	*Tachysurus longispinalis*	Vietnam	Red River	PP266672
(10)	*Tachysurus nudiceps*	Japan	Central Honshu, Shikoku and eastern Kyushu Islands	LC664019
(11)	"*Tachysurus ondon*" NINGB37529	Zhejiang, China	Qiantang-Jiang	PQ497556
	"*Tachysurus ondon*" NINGB37531	Zhejiang, China	Qiantang-Jiang	PQ497557
	"*Tachysurus ondon*" NINGB37534	Zhejiang, China	Qiantang-Jiang	PQ497558
	"*Tachysurus ondon*" LIANJ30623	Fujian, China	Ao-Jiang	PQ497555
	"*Tachysurus ondon*" NINGD13612	Fujian, China	Jiao-Xi	PQ497559
	"*Tachysurus ondon*" NINGD13614	Fujian, China	Jiao-Xi	PQ497560
	"*Tachysurus ondon*" QINGT35898	Zhejiang, China	Ou-Jiang	PQ497561
	"*Tachysurus ondon*" XINC66761	Zhejiang, China	Cao'e-Jiang	PQ497562
	"*Tachysurus ondon*" XINC66762	Zhejiang, China	Cao'e-Jiang	PQ497563
(12)	*Tachysurus pratti*	Fujian, China	Upper Yangtze River	PP266656
(13)	*Tachysurus sinensis*	Sichuan, China	Middle Yangtze River	PP266674
(14)	*Tachysurus taeniatus* 1	Zhejiang, China	Taihu Lake	PQ497552
	Tachysurus taeniatus 2	Zhejiang, China	Taihu Lake	PQ497553
	Tachysurus taeniatus 3	Zhejiang, China	Taihu Lake	PQ497554
(14)	*Tachysurus tokiensis*	Japan	Eastern Honshu Island	AB054127
(15)	*Tachysurus truncatus*	Sichuan, China	Upper Yangtze River	PP266658
(16)	*Tachysurus virgatus*	Hainan, China	Jiajihe River	PP266673
Outgroup				
(17)	*Tachysurus trilineatus*	Guangdong, China	Dong-Jiang of Pearl River	PP266679

in MEGA7 (Kumar et al. 2016). Both Bayesian-inference (BI) and maximum-likelihood (ML) methods were used in the phylogenetic analysis. The optimal nucleotide substitution model was selected by ModelFinder (Kalyaanamoorthy et al. 2017) according to the Akaike Information Criterion. ML analysis was performed using IQ-tree (Nguyen et al. 2015), with the selected TIM3+F+I+G4 model and 1,000 non-parametric bootstrap replicates. Bayesian Inference was performed in MrBayes (Ronquist et al. 2012) under the selected GTR+F+I+G4 model. Two independent runs were carried out with four Monte Carlo Markov chains (three hot chains and one cold chain) for 20 million generations to calculate posterior probability. Trees were sampled every 1000 generations. The initial 25% of sampled trees were discarded as burn-in. Convergence of the runs was assessed by the average standard deviation of split frequencies (<0.01). The genetic distances, based on *cyt-b*, were computed in MEGA 7 using the Kimura-2-parameter (K2P) model (Kimura 1980).

Figure 2. *Tachysurus taeniatus*, holotype, BMNH 1873-7-30-73, 150 mm SL, from Shanghai, China **A** lateral view **B** dorsal view.

Results

Examination on the holotype of *T. taeniatus*

The holotype of *Tachysurus taeniatus*, currently stored in the British Museum of Natural History (BMNH), had not been examined by any Chinese investigators before this study. Our observation of this holotype (BMNH 1873-7-30-72; Fig. 2) coincides with its original description in the following characters: (1) maxillary barbels extending beyond the insertion of the pectoral fin, (2) nasal barbels extending beyond the posterior edge of the eye, (3) an adipose-fin shorter than the anal-fin in basal length, (4) a dorsal spine shorter than the body and head depth. However, the holotype has a slightly emarginate caudal fin with the upper lobe slightly longer than the lower lobe (Fig. 2B), rather than a rounded one as stated in its original description. Additionally, it also possesses small serrations on the anterior edge of the pectoral spine covered with skin, a character not mentioned in the original description but shared with the topotypical specimens of *T. ondon* (Fig. 3).

Note on type locality of *Tachysurus taeniatus*

The original description (Günther 1873: 240) is based on a specimen from a collection of freshwater fishes from China sent to the British Museum by Robert Swinhoe, H.M. Consul at Shanghai, who collected the fish "at that place" Günther 1873: 240); no specified localities are given. Though, some materials could be collected by Swinhoe during his trip upstream the Yangtze River in 1869 (Heok Hee Ng personal communication), we suppose that *Tachysurus taeniatus* was found in Shanghai or nearby area because of the following reasons. First, the species hasn't been collected from Shanghai in recent years due to urbanization; however, it still occurs in areas close to Shanghai, such as Huzhou City in Zhejiang Province. Second, and more important, *T. taeniatus* shows coloration polymorphism, and the coloration pattern described in the original publication—a continuous black stripe along the mid-body—is only
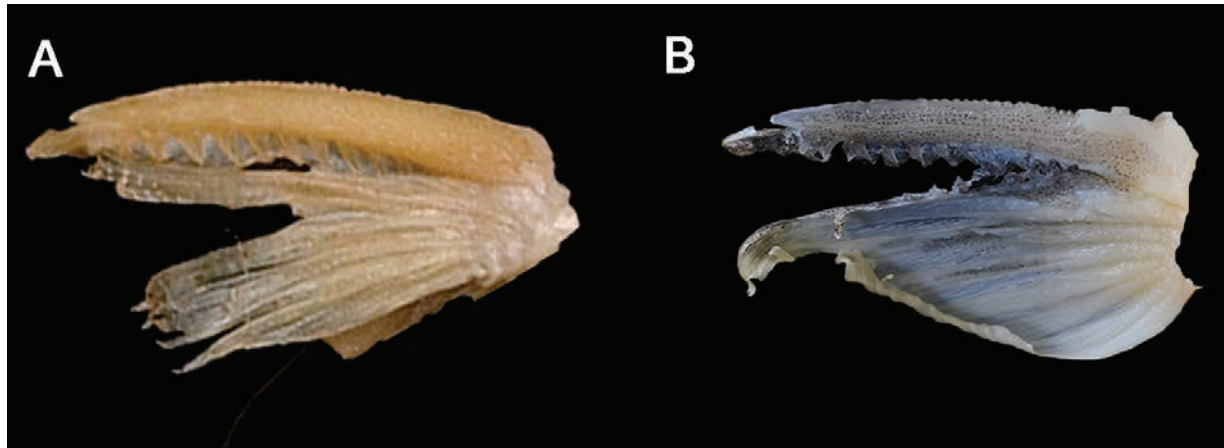
Figure 3. Serrations on the anterior edge of pectoral spine **A** holotype of *Tachysurus taeniatus* (BMNH 1873-7-30-73, 150 mm SL, from Shanghai, China) **B** topotype of *T. ondon* (IHB081570, 81.2 mm SL, from Xinchang County, Zhejiang Province).

found in Shanghai and some locations in adjacent Zhejiang Province (belonging to coastal rivers of southeast China); this particular coloration is absent in *T. taeniatus* from other parts of the Yangtze River.

Body coloration in topotypical specimens *Tachysurus taeniatus* and *T. ondon*

Brief accounts on the coloration pattern of the two species were provided in their original descriptions based only on a single specimen for each species, making it unfeasible to understand the intraspecific variations of coloration. In the *T. taeniatus* and *T. ondon* specimens examined in this study, ontogenetic changes in coloration were observed: the lateral blackish band or blotches found in small individuals becomes blurred in adult individuals exceeding 180 mm SL. Moreover, three coloration morphs exist in the juveniles and subadults of the specimens of these two species. One morph includes individuals which possess a yellowish body with three longitudinal blackish bands along the lateral body, of which the median band is continuous but the other two are interrupted to form three rectangular blotches (Fig. 4A). This coloration morph, as stated in the original description of *T. taeniatus* which reads "a broad blackish band along the side of the body", is only found in some topotypical specimens (Günther 1873). Despite the shared presence of three blackish bands, another coloration morph develops an uninterrupted median band. This is also present in the topotypical specimens of both *T. taeniatus* and *T. ondon* (Fig. 4B, C). Furthermore, one more morph was detected in the specimens identified as *T. ondon* from Ningde City, Fujian Province with three broad vertical brown blotches on the yellowish background of the body (Fig. 4D).

Morphometric and meristic comparisons between *Tachysurus taeniatus* and *T. ondon*

The specimens designated for comparative analysis were categorized into three groups: 1. topotypic *T. taeniatus*, 2. topotypic *T. ondon*, 3. other specimens primarily identified as *T. ondon*. The measurements of the examined specimens are summarized in Table 2. No discrete differences between these groups were
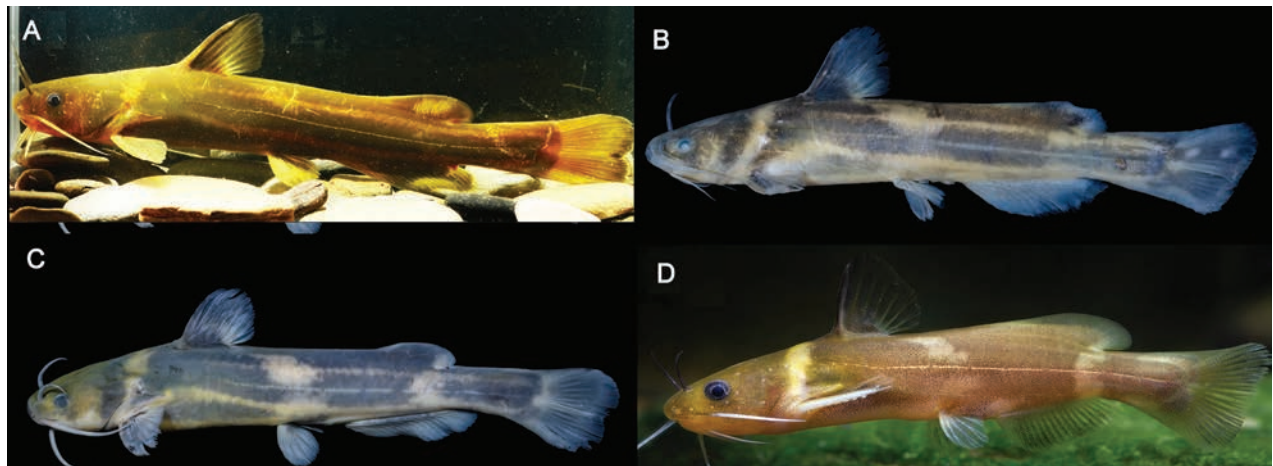
Figure 4. A color in life of adult of topotype of *Tachysurus taeniatus* **B** lateral view of *T. ondon*, topotype, IHB081570, 81.2 mm SL, Xinchang county, Zhejiang Province **C** lateral view of *T. taeniatus*, topotype, IHB202406066714, 74.4 mm SL, Huzhou city, Zhejiang Province **D** lateral view of a live specimen of *T. ondon* collected from Ningde City, Fujian Province.

Table 2. Morphomertric data for *Tachysurus taeniatus* and *T. ondon*.

| | T. taeniatus | | T. ondon | | | |
| | Topotypes (*n* = 4) | | Topotypes (*n* = 14) | | Other specimens (*n* = 64) | |
	Range	Mean ± SD	Range	Mean ± SD	Range	Mean ± SD
Standard length	66.9–149.9	106.4	43.1–118.3	80.5	55.79–142.2	87.9
In SL (%)						
Body depth at anus	13.6–17.3	15.4	14.7–18.0	16.1	12.5–17.8	15.3
Predorsal length	32.0–38.3	34.5	31.0–37.3	34.4	30.3–39.6	34.3
Pre-anal length	57.0–62.3	59.5	56.5–67.5	62.1	57.4–65.9	62.3
Prepelvic length	47.0–52.6	49.4	45.1–56.6	50.7	46.4–55.1	50.9
Length of dorsal-fin spine	12.6–18.2	15.7	10.4–18.4	14.5	13.3–18.6	16.8
Length of dorsal-fin base	12.1–14.5	13.4	10.1–15.1	11.9	12.7–15.0	13.8
Length of pectoral-fin spine	11.3–18.5	15.1	10.8–19.3	15.1	14.2–18.1	16.2
Length of anal-fin base	21.4–24.3	22.6	18.2–25.2	22.9	20.2–25.1	22.9
Adipose to caudal distance	16.1–17.3	16.9	14.1–18.4	15.9	14.6–19.1	16.9
Length of caudal peduncle	16.4–18.0	16.9	14.5–18.5	16.2	14.7–20.2	17.1
Depth of caudal peduncle	8.5–9.4	9.0	8.0–10.2	8.9	7.4–9.9	8.6
Head length at latera	22.9–25.2	24.0	24.5–30.7	26.5	22.3–28.2	24.8
In HL (%)						
Head depth	55.5–64.0	59.9	50.0–60.3	55.2	44.9–56.6	52.4
Head width	71.2–82.6	77.2	64.1–77.8	71.1	64.0–76.1	72.5
Snout length	23.1–31.0	27.5	22.9–33.6	26.9	25.8–32.7	27.9
Interorbital width	40.1–51.3	44.9	35.0–44.7	39.6	39.1–48.6	41.0
Eye diameter	14.8–21.7	18.3	14.2–25.8	19.9	14.6–22.5	17.7
Mouth width	52.5–60.4	56.5	47.0–57.3	50.7	46.5–58.7	50.1
Length of nasal barbel	43.6–57.2	51.3	41.0–54.8	47.0	41.5–57.3	49.5
Length of maxillary barbel	90.1–105.2	97.5	77.7–98.5	87.4	81.5–121.2	96.1
Length of inner mandibular barbel	44.0–54.4	48.2	41.7–55.9	48.1	35.1–55.3	44.1
Length of outer mandibular barbel	66.4–75.2	69.0	61.0–78.9	70.9	56.4–79.0	67.5

found by comparing the morphometric data. Meristic counts for the type specimens of *T. taeniatus* and *T. ondon*, and other specimens examined of *T. ondon* are given in Table 3. Three meristic characters have variable counts, namely anal and pelvic fins, and vertebrae. Counts of all three meristic characters are not significantly different with overlapping ranges among the three groups.

In a principal component analysis (PCA) performed on twenty-two morphometric characters, the combinations of PC1 against PC2 and PC3, along with PC2 against PC3, failed to separate the examined specimens of *T. ondon* and the topotypes of *T. taeniatus* (Fig. 5).

Table 3. Meristic counts (mean ± SD) for *Tachysurus taeniatus* and *T. ondon*.

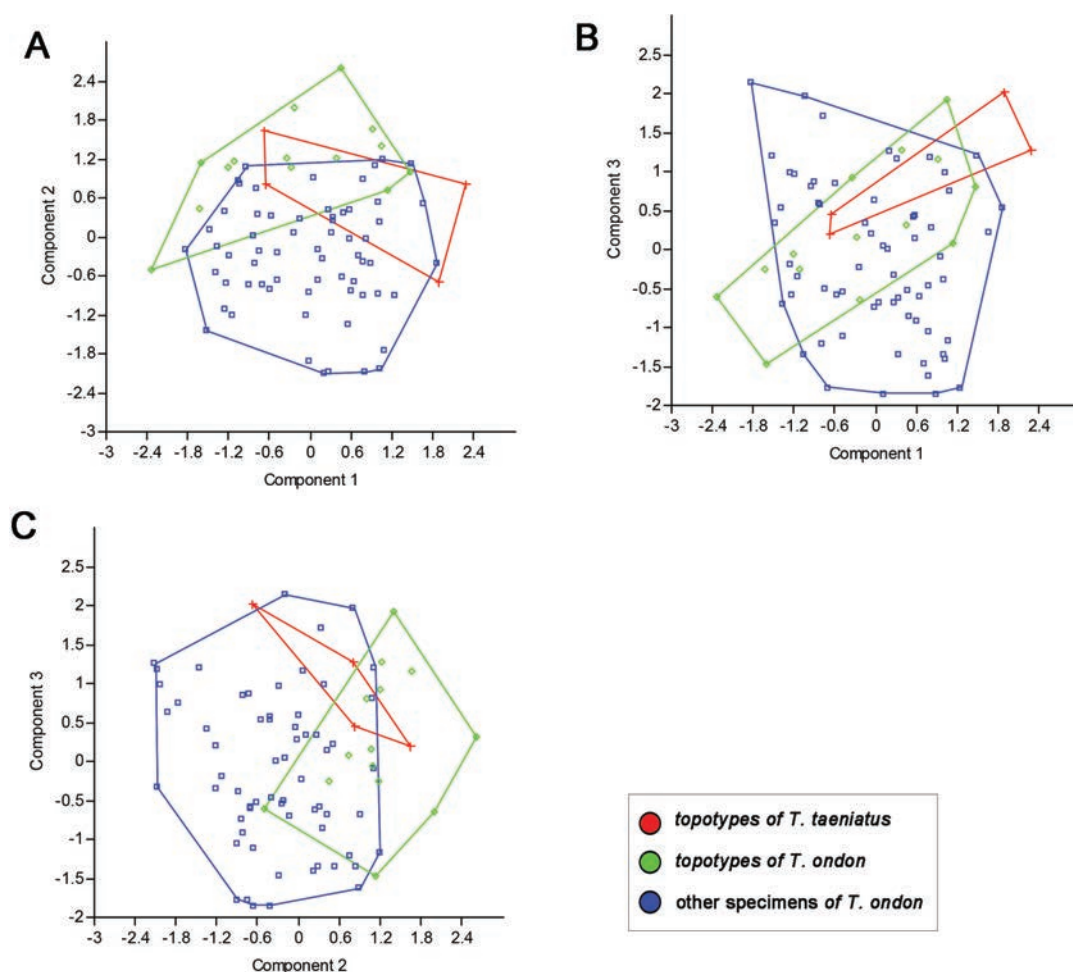| | *T. taeniatus* | *T. ondon* | |
	Topotypes	Tototypes	Other specimens
Soft rays			
Dorsal	7(7 ± 0.0)	7(7 ± 0.0)	7(7 ± 0.0)
Anal	17−19(18.5 ± 0.4)	18−20(19.2 ± 0.5)	16−20(18.1 ± 1.3)
Pectoral	7(7 ± 0.0)	7(7 ± 0.0)	7(7 ± 0.0)
Pelvic	6(6 ± 0.0)	6(6 ± 0.0)	6−7(6.2 ± 0.1)
Vertebrae	39−42(40.1 ± 1.8)	40−43(41.2 ± 1.1)	39−44(41.8 ± 2.1)

Figure 5. Scatter plots **A** PC1 against PC2 **B** PC1 against PC3 **C** PC2 against PC3 extracted from morphometric data for examined materials of *T. taeniatus* and *T. ondon*.

Molecular comparisons

A total of 1066 bps were included in the aligned dataset of the *cyt-b* gene, with 642 conservative sites, 424 variable sites, 242 parsim-informative sites and 94 singleton sites. The topologies of the phylogenetic trees were found to be similar between ML and BI methods (Fig. 6). The three topotypical specimens of *T. taeniatus* were found to be together with the specimens examined of *T. ondon* in a monophyletic group that was recovered with 100% posterior probabilities (pp) and 0.99 bs in ML and BI trees, respectively. This monophyly showed a phylogenetic affinity to the Japan endemic *T. aurantiacus*, within a clade containing *T. koreanus*, *T. nudiceps*, *T. brevicorpus*, *T. tokiensis*, *T. eupogon*, *T. sinensis* and *T. intermedius*, all of which were designated as belonging to the *T. aurantiacus* group by Shao and Zhang (2023).

The two closely related species of *T. taeniatus* and *T. aurantiacus* have a genetic distance of 1.5% and the distances between *T. taeniatus* and other members of the *T. aurantiacus* group are in the range of 6.4–10.0% (Table 4).

Table 4. K2P distances (%) for species within the *Tachysurus aurantiacus* group, based on the *cyt-*b gene.

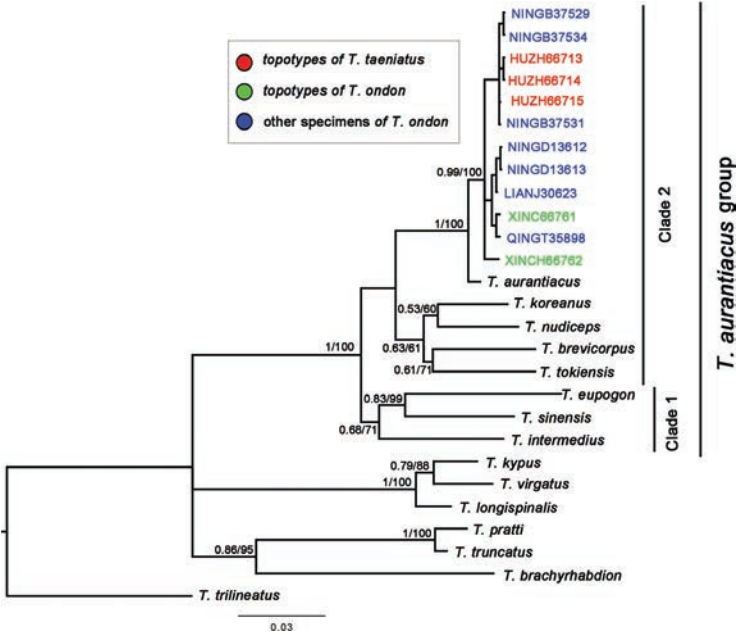|	1	2	3	4	5	6	7	8
1. T. taeniatus								
2. T. aurantiacus	1.5							
3. T. koreanus	6.5	5.9						
4. T. nudiceps	6.4	5.8	4.8					
5. T. brevicorpus	7.7	7.2	6.1	6.2				
6. T. tokiensis	6.9	6.9	5.8	6.0	6.9			
7. T. eupogon	10.0	9.6	9.3	9.4	8.9	11.0		
8. T. sinensis	8.1	7.8	8.5	8.6	8.8	8.2	8.2	
9. T. intermedius	8.0	7.4	8.2	7.3	9.8	7.8	9.1	8.1

Figure 6. Phylogenetic tree of *Tachysurus* species inferred from *cyt-b* using Bayesian-inference and maximum-likelihood methods. Bayesian posterior probabilities (>0.6) and maximum-likelihood bootstrap values (>60%) are shown, respectively. All members of the *T. aurantiacus* group (as defined by Shao and Zhang 2023), with the exception of *T. brevianalis*, were included in the phylogenetic tree.

Discussion

Identity of *Tachysurus taeniatus*

Main distinguishing characters of *Tachysurus taeniatus*, as herein diagnosed, include: (1) a serrated anterior edge of the pectoral spine; (2) a slightly emarginate caudal fin with the upper lobe slightly longer than the lower lobe; (3) longer maxillary barbels extending beyond the base of the pectoral spine; and (4) a shorter dorsal-fin spine than body depth. The first character was not mentioned in the original description. Our examination of the holotype confirmed observation by Watanabe and Kitabayashi (2001) that *T. taeniatus* has a serrated anterior edge of the pectoral spine (Fig. 3A). The statement of the second character (caudal-fin shape) in the original description of this species is inaccurate. According to our examination of the holotype, *T. taeniatus* has a slightly emarginate caudal fin with an upper lobe slightly longer than the lower lobe, in contrast with its original description that reads: "Caudal rounded". As far as is known, rounded caudal fins are only present in *T. tenuis*, *T. trilineatus*, *T. analis*, and *T. lani* (Cheng et al. 2021; Shao et al. 2021). Clearly, misled by the vagueness and inaccuracy of its original description and no accessibility to type materials, subsequent Chinese researchers (Zheng and Dai 1999) had a misconception that *T. taeniatus*, thus erroneously identify it as a species with a smooth anterior margin of the pectoral spine and a rounded caudal fin. This can reasonably explain why no additional specimens of *T. taeniatus* have been found from its type locality and nearby river systems since the original description.

Synonymization of *Tachysurus taeniatus* and *T. ondon*

Both *T. taeniatus* and *T. ondon* are currently assigned to the *T. aurantiacus* group which, thus, included eleven species (Shao and Zhang 2023). Four species, namely *T. nudiceps*, *T. sinensis*, *T. eupogon*, and *T. intermedius*, develop deeply forked caudal fins. A slightly emarginate caudal fin is found in the remaining seven species, viz., *T. aurantiacus*, *T. koreanus*, *T. tokiensis*, *T. brevianalis*, *T. brevicorpus*, *T. taeniatus*, and *T. ondon*. The last two species are known only from the mainland China, with the other species occurring in Korea Peninsula, Japan Archipelago, and Taiwan Island. However, our molecular phylogenetic analysis based on the *cyt-b* gene showed that all samples identified as these two species from Zhejiang and Fujian provinces of China, including those from the type locality of *T. ondon* and an affluent of Lake Taihu in proximity to the type locality of *T. taeniatus*, clustered together into a lineage sister to *T. aurantiacus*, a species endemic to western Kyushu of Japan (Watanabe and Maeda 1995).

Despite a 1.5% genetic distance between *T. taeniatus* (including *T. ondon*) and *T. aurantiacus*, they are clearly distinguishable by the snout length, 33–41% HL vs 23–33% (data for *T. aurantiacus* from Watanabe and Maeda (1995) and serration on the anterior edge of the pectoral spine which is better developed in *T. aurantiacus* incomparison with *T. taeniatus*. Although, the genetic distances between the two taxa are comparatively low, it lies within the range used for delineating currently described species of *Tachysurus*, for example, the genetic distance between *T. pratti* and *T. truncatus* is 1.4% and between *T. longispinalis* and *T. kyphus* is 1.6% (Ku et al. 2007). The relatively low genetic distance between closely related species within *Tachysurus* may be attributed to the significantly low substitution rate of the mitochondrial genes in the East Asian bagrids and

the recent estimated divergence time as supposed by Peng et al. (2002), Campbell and Piller (2017) and Shao et al. (2021). Besides, the two species have discontinuous distribution patterns. So, we treat them as two distinct species.

The genetic divergence among samples collected from coastal rivers of Zhejiang and Fujian provinces was 0.3−0.4%. No significant morphological variations were found among different geographic populations. All these findings suggest that the samples from mainland China, with a serrated anterior edge of the pectoral spine and a slightly emarginate caudal fin, represent a single species. According to International Code for Zoological Nomenclature, Art. 23.3 (International Commission on Zoological Nomenclature 1999), *T. taeniatus* should be considered a senior subjective synonym of *T. ondon*.

Coloration variation in *Tachysurus taeniatus*

In Chinese literature, a continuous black longitudinal stripe on the lateral body is viewed as the main diagnostic character for *T. taeniatus* (Zheng and Dai 1999). This body coloration pattern was utilized in this study to identify four specimens as *T. taeniatus* collected from an affluent of Lake Taihu, very close to the type locality. Ontogenetic changes in body coloration, though, were detected in *T. taeniatus*; there are conspicuous variations found between juveniles/sub-adults and adults. The blackish stripes or blotches on the flank become less distinct or disappear entirely in individuals of more than 180 mm SL, thus giving a uniformly brown body coloration. A similar ontogenetic change in body coloration has also been documented for closely related species, including *T. aurantiacus*, *T. tokiensis*, and *T. koreanus* (Lee and Kim 1990; Watanabe and Maeda 1995), all of them being members of the *T. aurantiacus* group. Recent studies of catfishes have inferred that ontogenetic coloration transformations are closely related to ontogenetic changes in daily activity period (Zanata and Prmitivo 2013; Vilardo et al. 2020; Costa et al. 2023). Juveniles and subadults exhibit heightened activity during the day, whereas adults display a preference for nocturnal behavior, necessitating a darker coloration phenotype. This explanation aligns with the field evidence presented in this study. Coloration polymorphism was also observed in the juveniles and sub-adults of *T. taeniatus* with three coloration morphs detected (Fig. 2). This implies that the body coloration of this species can vary not only due to ontogenetic changes but also in response to local environmental conditions and geographical distributions.

It is apparent that the existence of ontogenetic coloration changes and coloration polymorphism in *T. taeniatus* and closely related species argue against solely relying on body coloration for distinguishing species of *Tachysurus*. However, it is also incorrect to totally dismiss the taxonomic value of body coloration in *Tachysurus*. For example, *T. trillineatus* has three longitudinal brownish narrow bands running along its flank with the median band featuring a row of yellow spots along the lateral line, a unique body coloration separating it from all congeneric species (Shao and Zhang 2023). This unique body coloration has led to the designation of this species as a monotypic group, a classification supported by a molecular phylogenetic analysis (Ku et al. 2007). Body coloration should not be discarded a priori as evidence of species boundaries within *Tachysurus*. It is essential to reinforce species delineation hypotheses using additional morphological evidence such as morphometric characters or molecular data rather than relying solely on coloration.

Phylogenetic structure of *Tachysurus aurantiacus* group

The smoothness of the anterior edge of the pectoral-fin spine has been considered a significant diagnostic character in *Tachysurus* (Ku et al. 2007; Shao and Zhang 2023). The *T. aurantiacus* group, containing nine species (Fig. 6), can be distinguished from the congeners by the presence of a rough pectoral-fin spine (Shao and Zhang 2023). With the exception of *T. brevianalis*, which is endemic to Taiwan Island, all members of this group were included in the phylogenetic analysis in the present study that revealed its monophyly. The group is further subdivided into two clades (Fig. 6) different in some morphological features and ecological niches. Clade 1 includes *T. sinensis*, *T. intermedius*, and *T. eupogon*, distributed in mainland China and northern Vietnam. This clade is characterized by a forked caudal fin and a preference to inhabit the main stream of rivers. The remaining species of *T. aurantiacus* group form clade 2 (*T. taeniatus*, *T. aurantiacus*, *T. koreanus*, *T. nudiceps*, *T. brevicorpus*, *T. tokiensis*). Except for *T. nudiceps*, the members of this clade have round-tailed caudal fins and are adapted to fast-flowing montane streams (Krishnadas et al. 2018). All members of this clade, with the exception of *T. taeniatus*, are distributed in Japan or the Korean Peninsula. Since *T. taeniatus* appears to be the youngest lineage in clade 2, it is likely that the ancestor of clade 2 likely originated in Japan and/or the Korean Peninsula, subsequently dispersed to mainland China during interglacial periods (Zahiri et al. 2019) followed by subsequent isolation resulted in separation of *T. taeniatus* at the species level.

Acknowledgements

Additional information

Conflict of interest

The authors have declared that no competing interests exist.

Ethical statement

No ethical statement was reported.

Funding

Author contributions

Conceptualization: WHS. Data curation: JLC, WHS. Formal analysis: EZ, WHS. Funding acquisition: JLC, WHS. Supervision: EZ. Validation: EZ. Visualization: EZ. Writing - review and editing: JLC.

Author ORCIDs

E. Zhang ● https://orcid.org/0000-0002-6971-7160

Data availability

All of the data that support the findings of this study are available in the main text.

References

Campbell DC, Piller KR (2017) Let's jump in: a phylogenetic study of the great basin spring-fishes and poolfishes, *Crenichthys* and *Empetrichthys* (Cyprinodontiformes: Goodeidae). PloS ONE 12(10): e0185425. https://doi.org/10.1371/journal.pone.0185425

Cheng JL, Ishihara H, Zhang E (2008) *Pseudobagrus brachyrhabdion*, a new catfish (Teleostei: Bagridae) from the middle Yangtze River drainage, South China. Ichthyological Research 55(2): 112–123. https://doi.org/10.1007/s10228-007-0020-3

Cheng JL, Shao WH, Lopez JA (2021) *Tachysurus lani*, a new catfish species (Teleostei: Bagridae) from the Pearl river basin, south China. Ichthyological Exploration of Freshwaters 2021(4): 30. https://doi.org/10.23788/IEF-1156

Costa WJ, Mattos JLO, Amorim PF, Mesquita BO, Katz AM (2023) Chromatic polymorphism in *Trichomycterus albinotatus* (Siluriformes, Trichomycteridae), a mountain catfish from south-eastern Brazil and the role of colouration characters in trichomycterine taxonomy. Zoosystematics and Evolution 99(1):161–171. https://doi.org/10.3897/zse.99.98341

Ferraris CJ (2007) Checklist of catfishes, recent and fossil (Osteichthyes: Siluriformes), and catalogue of Siluriform primary types. Zootaxa 1418: 81–107. https://doi.org/10.11646/zootaxa.1418.1.1

Fricke R, Eschmeyer WN, Van der Laan R (2024) Eschmeyer's Catalog of Fishes: Genera, Species, References. http://researcharchive.calacademy.org/research/ichthyology/catalog/fishcatmain.asp [Accessed on 12 Aug 2024]

Günther A (1873) Report on a collection of fishes from China. Annals and Magazine of Natural History (Series 4) 12: 239–250. https://doi.org/10.1080/00222937308680749

International Commission on Zoological Nomenclature (1999) International code of zoological nomenclature, 4th edn. The International Trust for Zoological Nomenclature, London.

Kalyaanamoorthy S, Minh BQ, Wong TKF, von Haeseler A, Jermiin LS (2017) ModelFinder: Fast model selection for accurate phylogenetic estimates. Nature Methods 14(6): 587–589. https://doi.org/10.1038/nmeth.4285

Kimura M (1980) A simple method for estimating evolutionary rate of base substitutions through comparative studies of nucleotide sequences. Journal of Molecular Evolution 16(2): 111–120. https://doi.org/10.1007/BF01731581

Krishnadas A, Ravichandran S, Rajagopal P (2018) Analysis of biomimetic caudal fin shapes for optimal propulsive effeciency. Ocean Engineering 153: 132–142. https://doi.org/10.1016/j.oceaneng.2018.01.082

Ku X, Peng Z, Diogo R, He S (2007) MtDNA phylogeny provides evidence of generic polyphyleticism for East Asian bagrid catfishes. Hydrobiologia 579(1): 147–159. https://doi.org/10.1007/s10750-006-0401-z

Kumar S, Stecher G, Tamura K (2016) MEGA7: Molecular Evolutionary Genetics Analysis version 7.0 for bigger datasets. Molecular Biology and Evolution 33(7): 1870–1874. https://doi.org/10.1093/molbev/msw054

Lee CL, Kim IS (1990) A taxonomic revision of the family Bagridae (Pisces, Siluriformes) from Korea. Korean Journal of Ichthyology 2(2): 117–137.

Nguyen LT, Schmidt HA, von Haeseler A, Minh BQ (2015) IQ-TREE: a fast and effective stochastic algorithm for estimating maximum-likelihood phylogenies. Molecular Biology and Evolution 32(1): 268–274. https://doi.org/10.1093/molbev/msu300

Peng Z, He S, Zhang Y (2002) Mitochondrial cytochrome b sequence variations and phylogeny of the East Asian bagrid catfishes. Progress in Natural Science-Materials International 12(6): 421–425. [in Chinese]

Reist JD (1985) An empirical evaluation of several univariate methods that adjust for size variation in morphometric data. Canadian Journal of Zoology 63(6): 1429–1439. https://doi.org/10.1139/z85-213

Ronquist F, Teslenko M, van der Mark P, Ayres DL, Darling A, Höhna S, Larget B, Liu L, Suchard MA, Huelsenbeck JP (2012) MrBayes 3.2: efficient Bayesian phylogenetic inference and model choice across a large model space. Systematic Biology 61(3): 539–542. https://doi.org/10.1093/sysbio/sys029

Shao WH, Zhang E (2023) *Tachysurus latifrontalis*, a new bagrid species from the Jiulong-Jiang basin in Fujian Province, South China (Teleostei: Bagridae). Ichthyological Research 70(1): 110–122. https://doi.org/10.1007/s10228-022-00867-0

Shao WH, Cheng JL, Zhang E (2021) Eight in one: hidden diversity of the bagrid catfish *Tachysurus albomarginatus* s.l. (Rendhal, 1928) widespread in lowlands of south China. Frontiers in Genetics 12: 2195. https://doi.org/10.3389/fgene.2021.713793

Shaw TH (1930) Notes on some fishes from Ka-Shing and Shing-Tsong, Chekiang Province. Bulletin of the Fan Memorial Institute of Biology 1: 109–121.

Vilardo PJ, Katz AM, Costa WJEM (2020) Relationships and description of a new species of *Trichomycterus* (Siluriformes: Trichomycteridae) from the Rio Paraíba do Sul basin, south-eastern Brazil. Zoological Studies (Taipei, Taiwan) 59: 53. https://doi.org/10.6620/ZS.2020.59-53

Watanabe K (1995) *Pseudobagrus pratti* (Gunther, 1892), a senior synonym of *P. emarginatus* (Regan, 1913) (Siluriformes: Bagridae). Japanese Journal of Ichthyology 42(3–4): 321–324. https://doi.org/10.11369/jji1950.42.321

Watanabe K, Kitabayashi (2001) A fossil bagrid from the Pliocene Tsubusagawa Formation in Ajimu Basin, Oita Prefecture. Research report of the Lake Biwa Museum 18: 66–71. [in Japanese]

Watanabe K, Maeda H (1995) Redescription of two ambiguous Japanese bagrids, P*seudobagrus aurantiacus* (Temminck and Schlegel) and *P. tokiensis* Döderlein. Japanese Journal of Ichthyology 41(4): 409–420. https://doi.org/10.11369/jji1950.41.409

Zahiri R, Schmidt BC, Schintlmeister A, Yakovlev RV, Rindoš M (2019) Global phylogeography reveals the origin and the evolutionary history of the gypsy moth (Lepidoptera, Erebidae). Molecular Phylogenetics and Evolution 137: 1–13. https://doi.org/10.1016/j.ympev.2019.04.021

Zanata AM, Prmitivo C (2013) Natural history of *Copionodon pecten*, an endemic trichomycterid catfish from Chapada Diamantina in northeastern Brazil. Journal of Natural History 48(3–4): 203–228. https://doi.org/10.1080/00222933.2013.809168

Zheng BS, Dai DY (1999) Bagridae. In: Chu XL, Zheng BS, Dai DY (Eds) Fauna Sinica: Osteichthyes: Siluriforms. Science Press, Beijing, 35–73. [in Chinese]

The first record of the genus *Dichodontocis* Kawanabe, 1994 (Coleoptera, Ciidae) from China, with the description of a new species and its larva

Nan Li[1], Ji-Shan Xu[1,2]

1 College of Agriculture and Biological Science, Dali University, Dali, Yunnan 671003, China
2 Co-Innovation Center for Cangshan Mountain and Erhai Lake Integrated Protection and Green Development of Yunnan Province, Dali University, Dali, Yunnan 671003, China

Corresponding author: Ji-Shan Xu (xujishan001@163.com)

Abstract

The genus *Dichodontocis* Kawanabe, 1994 is newly recorded from China, and a new species, *Dichodontocis guangzhouensis* **sp. nov.** and its larva, is described and illustrated from Guangdong Province. We provide habitat and host fungi photos of the new species and a key to all described species of the genus.

Key words: Minute tree-fungus beetle, Ciini, morphology, taxonomy, Guangdong

Introduction

The genus *Dichodontocis* was described by Kawanabe (1994) based on a new species named *Dichodontocis uncinatus* (Kawanabe, 1994) from southwestern Japan, which has unique characteristics of the 10-segmented antennae, the bidentate apex and the serrated outer margin of protibiae, and the laminate prosternal process (Kawanabe 1994). It belongs to the tribe Ciini of the subfamily Ciinae because of the globulous procoxae and the presence of the metaventrital medio-longitudinal groove (Lawrence 1971; Kawanabe 1994). Then the genus *Dichodontocis* was redescribed and a new species named *D. queenslandicus* (Lawrence, 2016) was described by Lawrence in 2016. The genus *Dichodontocis* has the following main characteristics (Lawrence 2016): 1) dual vestiture consisting of bristles and fine hairs; 2) outer edge of protibia lined with fixed spines and bearing two teeth at the outer apical angle; 3) spinose meso- and metatibial apices; 4) short, weakly biconcave and subcarinate prosternum with laminate prosternal process; 5) dual, seriate elytral punctation; and 6) 10-segmented antennae.

In the present paper, a new species of the genus *Dichodontocis*, *D. guangzhouensis* sp. nov., and its larva are described and illustrated.

Material and methods

The type specimens of the new species described herein are deposited in the Biological Science Museum, Dali University, Yunnan, China.

Adults and larvae were examined under an Olympus SZX7 stereomicroscope (Olympus, Shinjuku, Japan). The adult genitalia were dissected, and then temporarily fixed on glass slides by glycerol. Specimens were photographed and measured using the Keyence VHX-7000 free-angle observation system (Keyence, Osaka, Japan). Adult specimens were pinned, and the genitalia were preserved in glycerol. Habitus images were taken using a digital camera (Canon EOS 60D). All figures were post-corrected with Adobe Photoshop CS6 software.

The terminology of adults follows Lawrence and Lopes-Andrade (2010) and Lawrence (1974, 2016). The structure terminology of hind wings follows Lawrence et al. (2021, 2022). The structure terminology of larvae follows Lawrence (1974). The following abbreviations are adapted (Lopes-Andrade and Grebennikov 2015): TL (total length, excluding head), PL (pronotal length along midline), PW (greatest pronotal width), EL (elytral length along the midline), EW (greatest width of both elytra), GD (greatest depth of body measured in lateral view), GW (greatest diameter of compound eye), BW (basal width of scutellar shield).

Taxonomy

Dichodontocis guangzhouensis sp. nov.

https://zoobank.org/163A1D96-3556-4578-A340-85D0291607EA
Figs 1–3
Chinese vernacular name: 广州双齿木覃甲

Type material. *Holotype*: CHINA • male, "China: Guangdong, Guangzhou (广州), Huangpu District (黄埔区), Tianlu Lake Forest Park (天鹿湖森林公园), 23°12'N, 113°25'E, 303 m, 05.XI.2023, leg. Da-Rui Mo". *Paratypes*: CHINA • 3 males, 6 females, same data as the holotype.

Diagnosis. This new species is similar to *D. uncinatus* from southern Japan. From the illustration of the holotype (Kawanabe 1994), the elytral setae appear to be more clearly seriate and ordered in that species than in *D. guangzhouensis* sp. nov., both anal veins of hind wings are absent, but in *D. guangzhouensis* sp. nov. the hind wings have apical color spots (Figs 1D, 3D) and the impression of the anterior margin of pronotum of *D. guanzhouensis* appears broadly and deeply impressed and extends posteriorly, distinctly beyond the bases of the horn, while in *D. uncinatus*, from the illustration of the holotype (Kawanabe 1994), the impression of the anterior margin of pronotum is only between the bases of the horn and much weaker than in *D. guanzhouensis* sp. nov.. The terminalia are somewhat different. In *D. uncinatus*, the eighth abdominal sternite has the posterior margin slightly emarginate at the middle, and the anterior margin strongly emarginate. In the new species, however, the eighth abdominal sternite with the posterior margin is broadly emarginate in the middle, anterior margin is not emarginate (Fig. 2I) in the middle. The tegmen is broad at the base and gradually narrower near the end in *D. uncinatus*. In the new species, the tegmen is broad at the base, from base 1/5–4/5, the sides are nearly parallel, and gradually narrower near the end, slightly curving.
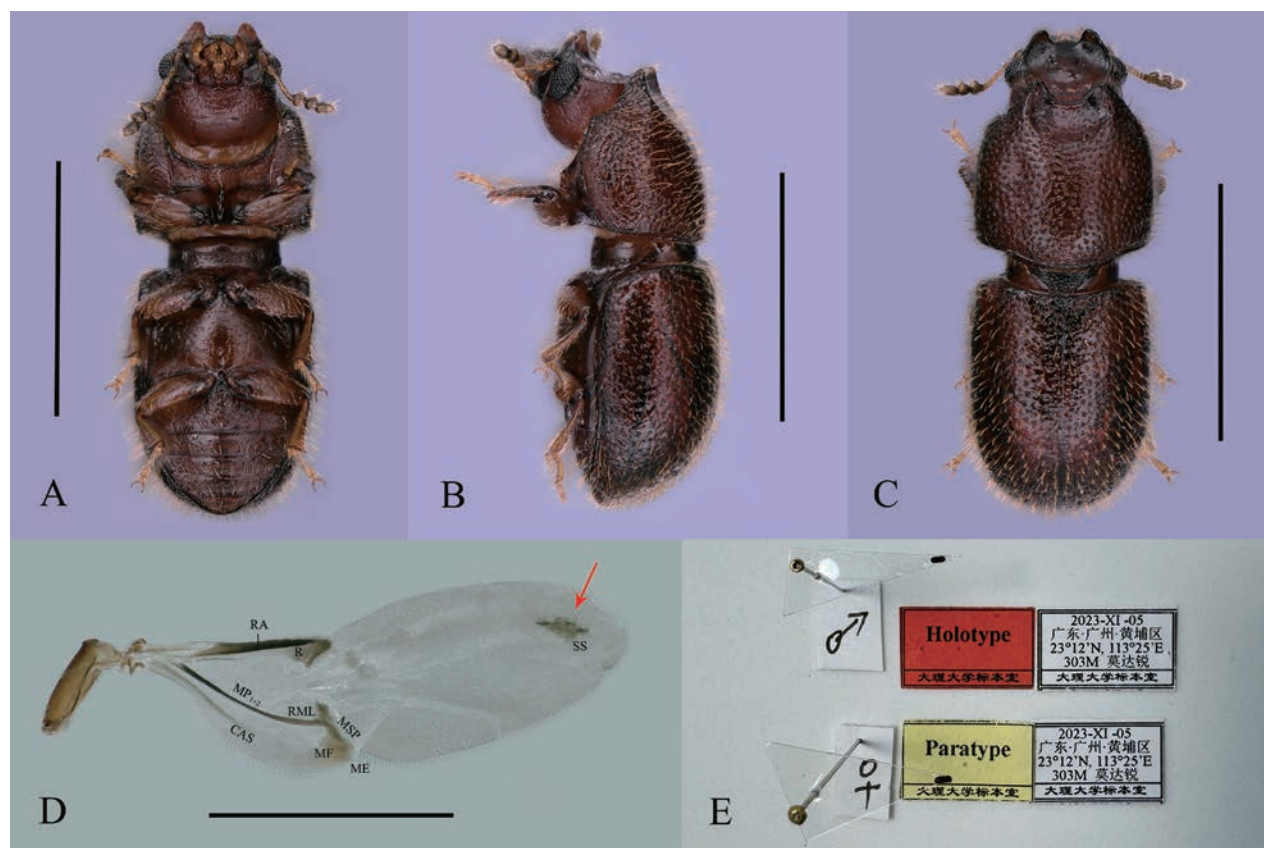
Figure 1. *Dichodontocis guangzhouensis* sp. nov. **A–C** holotype **D** male paratype **A–C** ventral, lateral and dorsal views, respectively **D** right hind wing of male, (dorsal view, RA: radius anterior, R: radial cell, MP$_{1+2}$: media posterior, branches 1 and 2, RML: radiomedial loop, MSP: medial spur, CAS: cubitoanal strut, MF: medial fleck, ME: medial embayment, SS: support sclerite) **E** labels of holotype and one paratype. Scale bars: 1 mm (**A–D**).

The new species is also similar to *D. queenslandicus* from northern Queensland. The size and dimensions of the two species are similar. But there are some differences between the two species. Head relatively and largely exposed, partially visible from above in *D. queenslandicus*. Head almost entirely exposed, visible from above in the new species. The impression of the anterior margin of the pronotum of *D. guanzhouensis* sp. nov. appears broadly and deeply impressed and extends posteriorly, distinctly beyond the bases of the horn, while in *D. queenslandicus*, from the illustration of the holotype (Lawrence 2016), the impression of the anterior margin of pronotum is slightly weaker and more in front than in *D. guanzhouensis* sp. nov. The tegmen of *D. queenslandicus* is 4 times as long as wide, and the pens is 4 times as long as wide. The tegmen of the new species is 6.4 times as long as wide, pens 8.0 times as long as wide. The sternite VIII of the *D. queenslandicus* is the posterior margin slightly emarginate in the middle, the eighth abdominal sternite of the new species with the posterior margin is broadly emarginate in the middle, anterior margin is not emarginate (Fig. 2I) in the middle.

Description of the adult. With the characters of the genus. Male. Fully pigmented adult. Measurements in mm: TL 1.511, PL 0.678, PW 0.695, EL 0.833, EW 0.717, GD 0.636. Ratios: PL/PW 0.98, EL/EW 1.16, EL/PL 1.23, GD/EW 0.89, TL/EW 2.11.
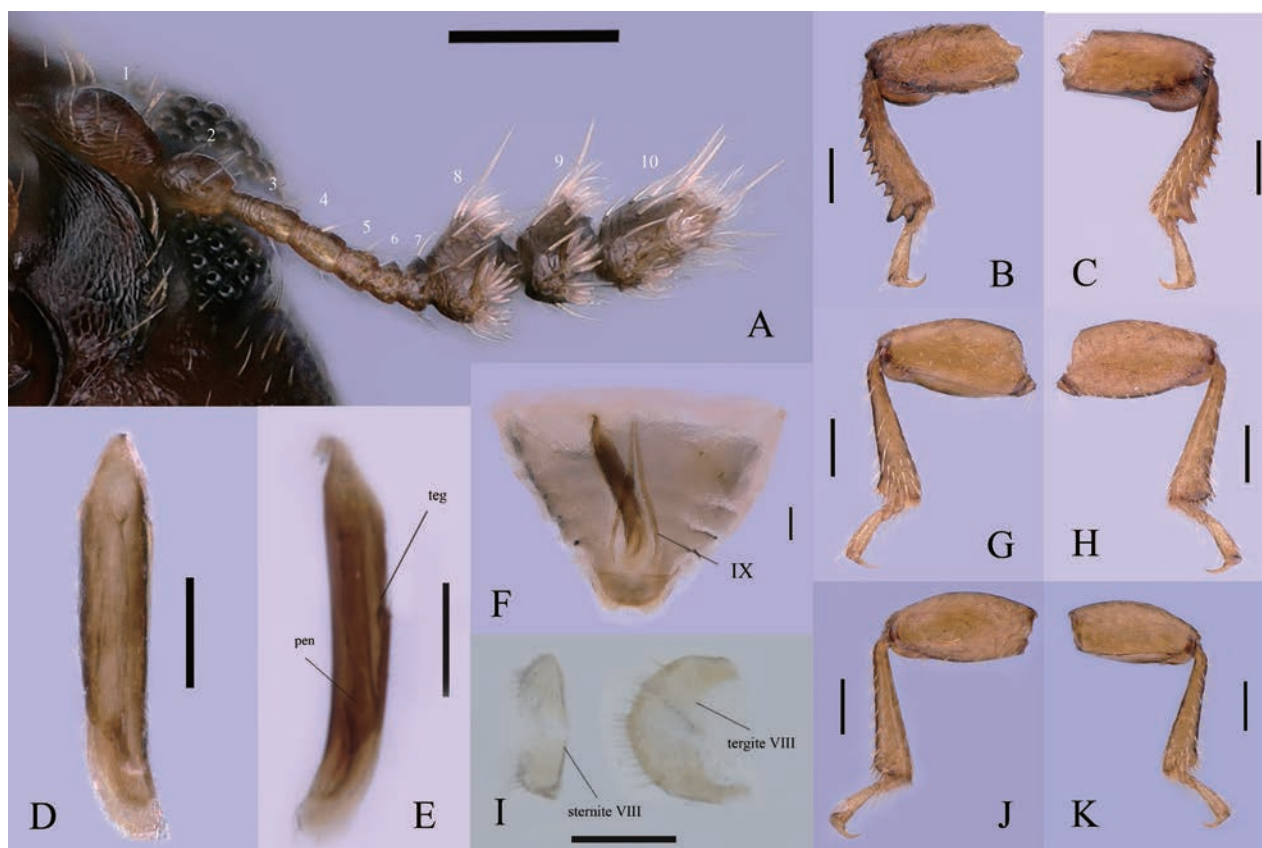
Figure 2. *Dichodontocis guangzhouensis* sp. nov., male paratypes **A** antenna **B** protibia, ventral view **C** protibia, dorsal view **D** tegmen and penis, dorsal view **E** tegmen (teg) and penis (pen), lateral view **F** terminal segments of the abdomen, including the aedeagus and pregenital segments, the abdominal ventrites have been removed, leaving only the eighth sternite, ventral view **G** mesotibia, ventral view **H** mesotibia, dorsal view **I** sternite VIII, ventral view, and tergite VIII, dorsal view **J** metatibia, ventral view **K** metatibia, dorsal view. Scale bars: 0.1 mm (**A–K**).

Body (Fig. 1C) elongate, convex, reddish brown to dark brown; dorsal setae, tarsi, antennae (except club), maxillary palpus and labial palpus are pale yellow; dorsal vestiture dual, consisting of long and short erect setae.

Head wider slightly than long, partially visible from above, with sparse punctures and dual setae, frontoclypeal strongly elevated forming a pair of broad-based, reflexed at each side subtriangular plates, behind eyes. Compound eyes are finely facetted and suboval, each bearing approximately 70 ommatidia; GW 0.17 mm. Antennae (Fig. 2A) bearing 10 antennomeres with the following lengths (in mm): 0.07, 0.05, 0.04, 0.03, 0.02, 0.02, 0.02, 0.05, 0.05, 0.08. Mandibles are asymmetrical (misaligned), with well-developed, transversely ridged molae.

Pronotum (Fig. 1C) is as long as broad and parallel-sided, which is slightly raised in the middle with shallow and fine punctures bearing short and long dual setae, erect. Punctures are separated by a distance equal to one to two diameters. Lateral margins (Fig. 1B, C) are narrow, and not visible for their entire lengths from above. Anterior edge produced forward and upturned into two small lateral projections. The anterior edge deeply and broadly emarginate in the middle just like a horseshoe, and the impression of the anterior margin of the pronotum extends posteriorly, distinctly beyond the bases of the horn. Anterior angles (Fig. 1B) obtuse. Posterior margin (Fig. 1B) feebly bisinuous posterior angles rounded.

Scutellar shield developed, with a few punctures and setae; subtriangular, BW 0.13 mm.

Elytra (Fig. 1C) 1.2 times as long as broad, 1.3 times as long as pronotum; punctures rough; setae dual short and long, inclined and suberect; sides subparallel in basal 2/3, then gradually convergent apical.

Hind wings (Fig. 1D) are fully developed, nearly pellucid. The venation type is folding patterns. Strongly reduced venation patterns of the clavus, anal vein absent. A medial field with one vein and a small fleck, a medial embayment, a small support sclerite near the wing apex; with a distinct cubitoanal strut and radiomedial loop. The hind wings are 3.3 times as long as broad, the widest part is in the middle, shrinking to the sides.

Protibia (Fig. 2B, C) expanded to the apex, outer apical angle with 2 acute teeth and dentate along the outer edge which are shorter near the base and gradually becoming longer towards the apex. Meso-and metatibia (Fig. 2G, H, J, K) expanded forming a rounded lobe lined with socketed spines.

Prosternum (Fig. 1A) is weakly biconcave and subcarinate; the prosternal process is flaked and slender somewhat slightly broadened near the apex, slightly higher than the procoxae (best seen in lateral view).

Metaventrite (Fig. 1A) is convex but slightly emarginate in the middle, with sparse punctuation and bristles; discrimen nearly one-fourth length of ventrite. Abdominal ventrites (Fig. 1A) with fine setae and shallow puncture, the surface between them microreticulate; the first abdominal ventrite is 2.2 times as long as 2nd, the ventrites bearing a small, circular, not obvious and marginally pubescent fovea. The length of the ventrites (in mm) is as follows: 0.202, 0.093, 0.077, 0.072, 0.078.

Aedeagus 4.9 times as long as ventrite 5. Tegmen (Fig. 2D, E) is slender 6.4 times as long as the widest, widest at the base and gradually narrower near the apex with the basal end subacute like a hook; narrowed gradually from base to apex; apex slightly bent. Penis (Fig. 2E) is shorter and narrower than the tegmen, 8.0 times as long as the widest, with a subacute apex and moderately long, sides parallel from basal to four fifth, then just like the rhombus near the end. The basal piece is weakly sclerotized, much longer than a broad, like a narrow horseshoe. The sternite VIII (Fig. 2I) with the posterior margin broadly emarginate in the middle, with several short hairs on each side, anterior margin not emarginate. The tergite VIII (Fig. 2I) with the posterior margin not emarginate in the middle, anterior margin strongly emarginate.

Female (Fig. 3). Similar to male, except for the following points: frontoclypeal without strongly subtriangular plates; pronotum with anterior edge broadly rounded, without projections; first abdominal ventrites without a sex patch. The eighth abdominal sternite of females is different from males. The posterior margin is not emarginate in the middle which is flat and the anterior margin is strongly emarginate in the female. Female genitalia (Fig. 3E, F) is as long as wide, widest at the middle; paraprocts (Fig. 3E) is 0.85 times as long as gonocoxites.

Measurements. Males (*n* = 3, including the holotype; mm): TL 1.48−1.51 (1.50 ± 0.02); PL 0.66−0.68 (0.67 ± 0.01); PW 0.70−0.71 (0.70 ± 0.01); EL 0.83−0.84 (0.87 ± 0.01); EW 0.70−0.72 (0.71 ± 0.01); GD 0.63−0.64 (0.64 ± 0.01).

Females (*n* = 6; mm): TL 1.18−1.48 (1.33 ± 0.10); PL 0.46−0.60 (0.55 ± 0.06); PW 0.51−0.65 (0.59 ± 0.06); EL 0.72−0.90 (0.78 ± 0.07); EW 0.58−0.70 (0.65 ± 0.44); GD 0.56−0.74 (0.67 ± 0.08).
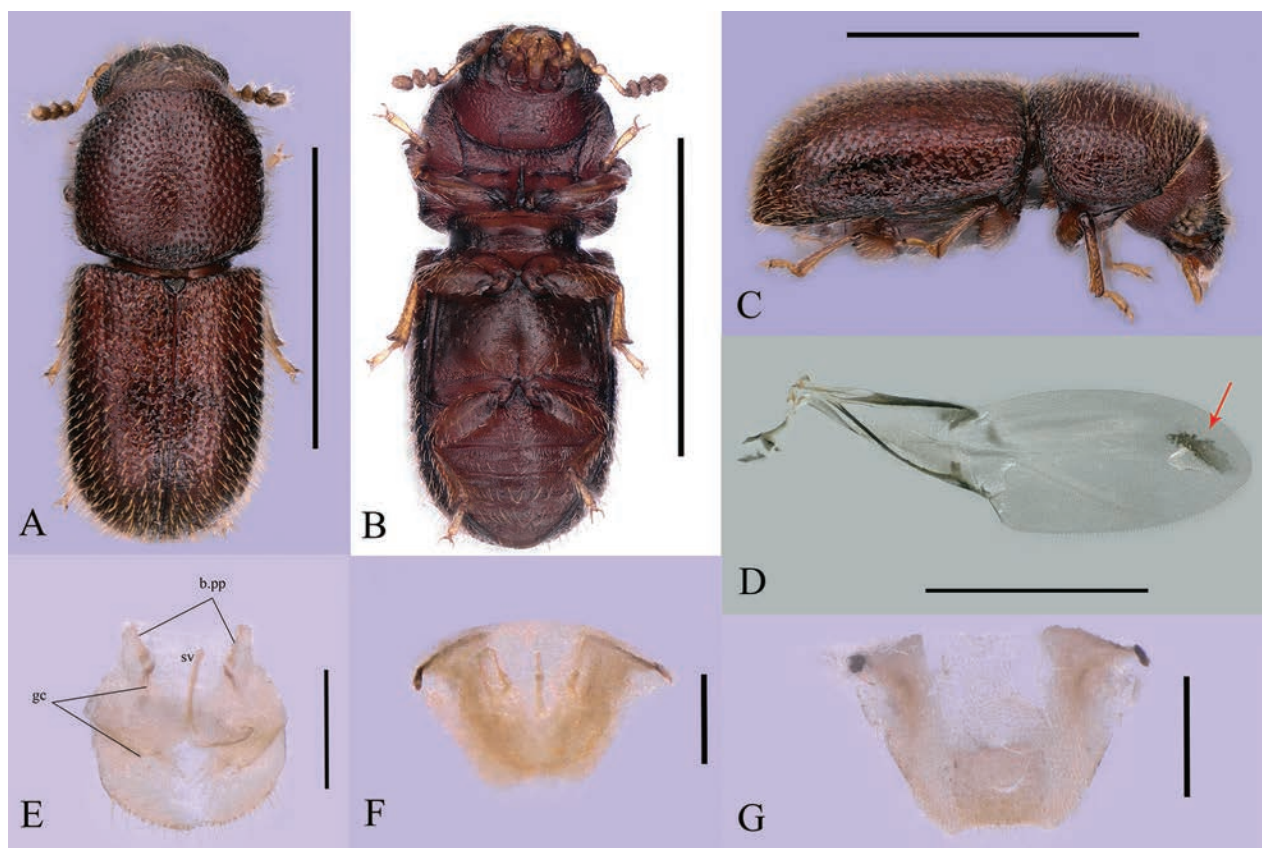
Figure 3. *Dichodontocis guangzhouensis* sp. nov., female paratype **A–C** dorsal, ventral, and lateral views, respectibly **D** right hind wing of female, dorsal view **E** female genitalia (ventral view, b.pp = paraproctal baculi; gc = gonocoxites; sv = spiculum ventral) **F** female genitalia, dorsal view **G** tergite VIII, dorsal view. Scale bars: 1 mm (**A–D**); 0.1 mm (**E–G**).

Distribution. Tianlu Lake Forest Park, Guangzhou, Guangdong, China.

Host fungi. Unidentified Polyporaceae (Fig. 6).

Etymology. The specific name *guangzhouensis* is taken from the type locality, Guangzhou.

Description of larva. Figs 4, 5. *Larva material*. "China: Guangdong, Guangzhou (广州), Huangpu District (黄埔区), Tianlu Lake Forest Park (天鹿湖森林公园), 23°12'N, 113°25'E, 303 m, 05.XI.2023, leg. Da-Rui Mo". We are sure that the polypore basidiomes contain only one species of insect, after rearing the larvae in the laboratory, it was found that they developed into adults of the new species successfully; however, their stadiums were not accurately recorded.

This description is based on a later instar larva (Fig. 4); 1.69 mm long, 0.35 mm broad, head-capsule of 0.31 mm wide. The body is opal and translucent except for the head, pretarsus (claw) and pygidium, which are light yellow to dark brown.

Body elongate, more or less parallel-sided, subcylindrical, slightly curved ventrally. Surfaces are relatively smooth except for the mouth frame and tips of urogomphi, rarely with light tergal plates on most segments, smooth with vestiture of scattered long and short setae.

Head subspherical, protracted and moderately to strongly declined (hypognathous); posterior edge not emarginate. The epicranial stem (Fig. 5D) is long with median endocarina (Fig. 5D) beneath it; frontal arms (Fig. 5D) are Y-shaped, with five stemmata on each side.
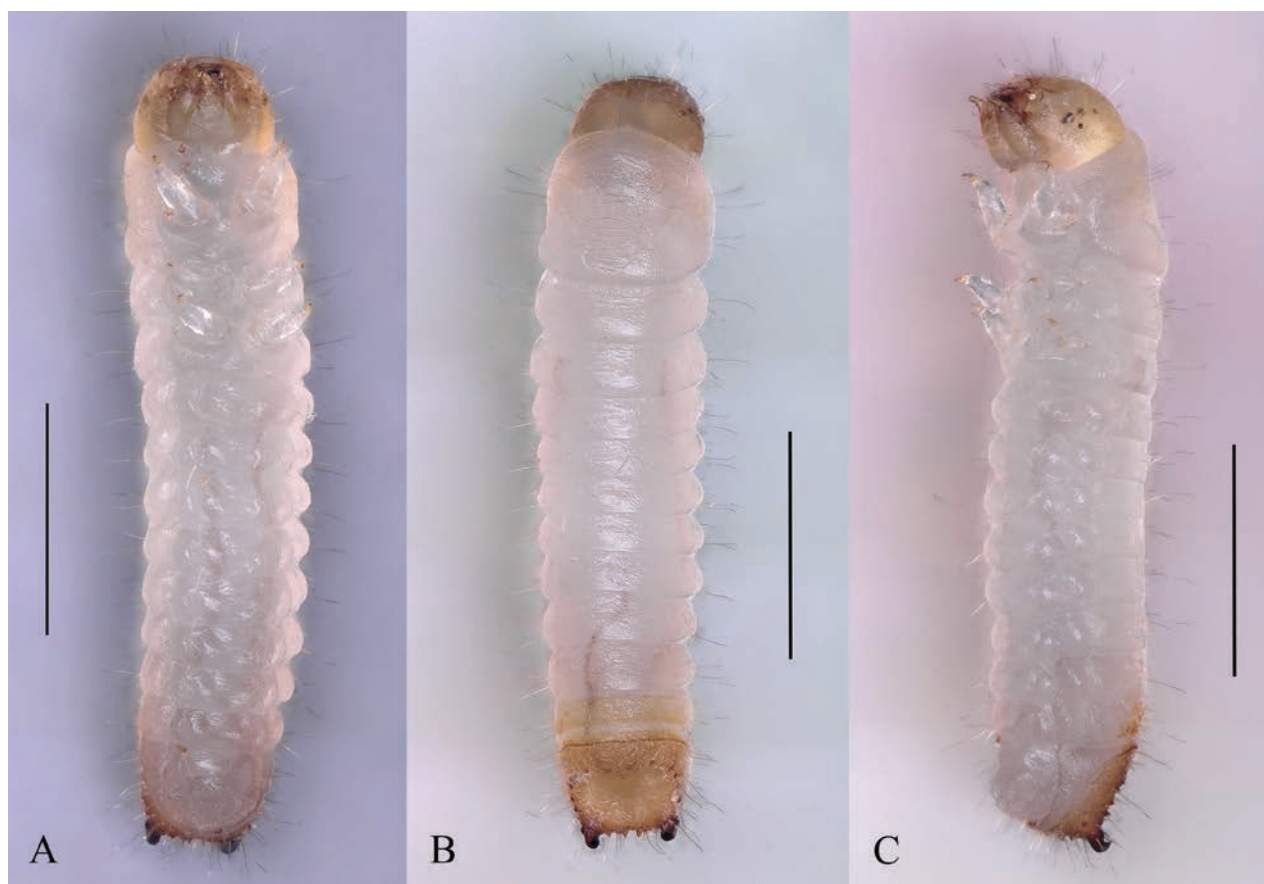
Figure 4. Larva of *Dichodontocis guangzhouensis* sp. nov. **A** ventral view **B** dorsal view **C** lateral view. Scale bars: 1 mm (**A–C**).

Antennal (Fig. 5H) insertion is a well-developed and concealed maxillary articulatory membrane. Antennae are very short with 2 segments which have a sensorium on the first segment and a long seta on the apical antennomere. The 1st segment is wider and shorter than the 2nd.

Mandibles (Fig. 5B, C) are large, robust, asymmetrical, and bidentate (one is large and the other is small), with a simple and transversely cutting edge.

Ventral mouthparts (Fig. 5A) retracted; stipes longer than wide; maxillary articulating area (Fig. 5A) reduced; galea (Fig. 5A, E, F) rounded; lacinia (Fig. 5E) represented by a short, truncate, subapical, lobe on the dorsal surface (ventral side not visible); palp (Fig. 5A) 3-segmented.

Labium (Fig. 5A) with submentum, mentum, bearing short ligula and 2-segmented palps. Hypopharyngeal sclerome absent.

Hypostomal rods absent; ventral epicranial ridges present.

Gula (Fig. 5A) is wider than long, fused to the submentum.

Thoracic terga without transverse carinae or rows of asperities. Prothorax (Fig. 4) is only slightly larger than meso- or metathorax.

Prosternum without special armature. Thoracic legs (Fig. 5J) are short and broad, subequal; 5-segmented with pretarsus (claw), bearing a few setae; coxae relatively close together.

The length of the abdomen is more than twice as long as thorax; terga and sterna without patches.
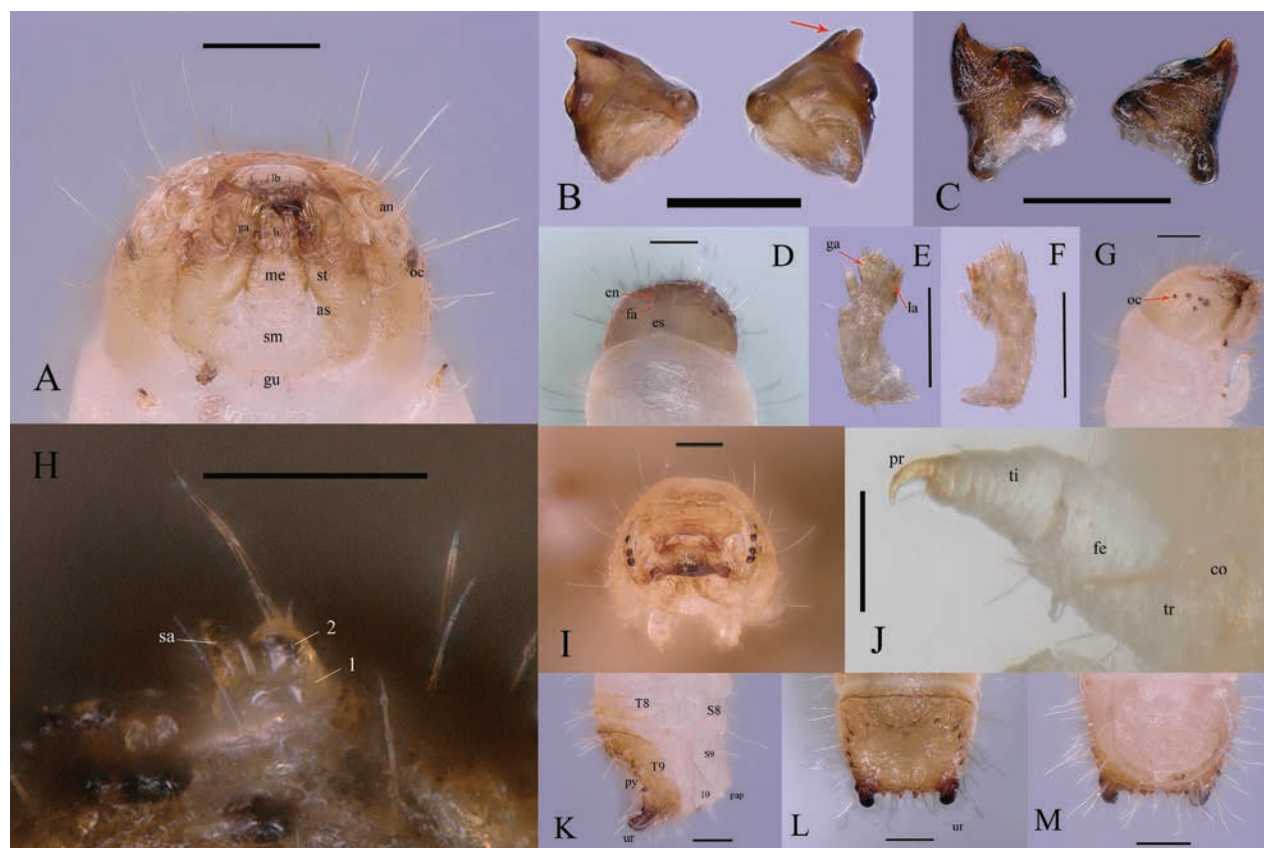
Figure 5. Details of the larva of *Dichodontocis guangzhouensis* sp. nov. **A** head and mouthparts (ventral view, lb: labrum, li: ligula, ga: galea, an: antenna, me: mentum, sm: submentum, gu: gula, st: stipes, as: articulating sclerite, oc: ocelli) **B** mandibles, ventral view **C** mandibles, dorsal view **D** head (dorsal view, en: endocarina, es: epicranial stem, fa: frontal arms) **E** maxillary (dorsal view, ga: galea, la: lacinia) **F** maxillary, ventral view **G** head (lateral view, oc: ocelli) **H** antenna (sa: sensory appendix) **I** head, frontal view **J** leg (co: coxa, tr: trochanter, fe: femur, ti: tibiotarsus, pr: pretarsus) **K** apex of abdomen (lateral view, T8: tergum 8, S8: sternite 8, T9: tergum 9, S9: sternite 9, ur: urogomphi, py: pygidium, pap: papillae) **L** apex of abdomen (dorsal view, ur: urogomphi) **M** apex of abdomen, ventral view. Scale bars: 0.1 mm (**A–G, I, K–M**); 0.05 mm (**H, J**).

Terga IX (Fig. 5K, L) is slightly transverse and longer and has variously modified, with concave and heavily sclerotized disc and with a pair of upturned urogomphi whose color is deepened from brown to black. There are 4–6 dark-colored, small protrusions between the urogomphi. There are also five protrusions on each side of the terga. Segment X (Fig. 5K) is transverse, posteroventrally oriented. It is only about ½ as long as terga IX; anal opening transverse. Spiracles are annular.

Measurements. Later instar larva (*n* = 5, mm): TL 1.33–1.75 (1.61 ± 0.17); Wide 0.31–0.35 (0.34 ± 0.02).

Comments. Currently, there are only three species of *Dichodontocis* known in the world. The type species, *D. uncinatus* is distributed in southwestern Japan (Yakushima island). *Dichodontocis queenslandicus* occurs in a rainforest in Australia (Queensland). The new species is known from Guangzhou (Tianlu Lake Forest Park), China. As they are distributed in hot, rainy environments, more *Dichodontocis* species may eventually be found in tropical areas of Asia and Australia.
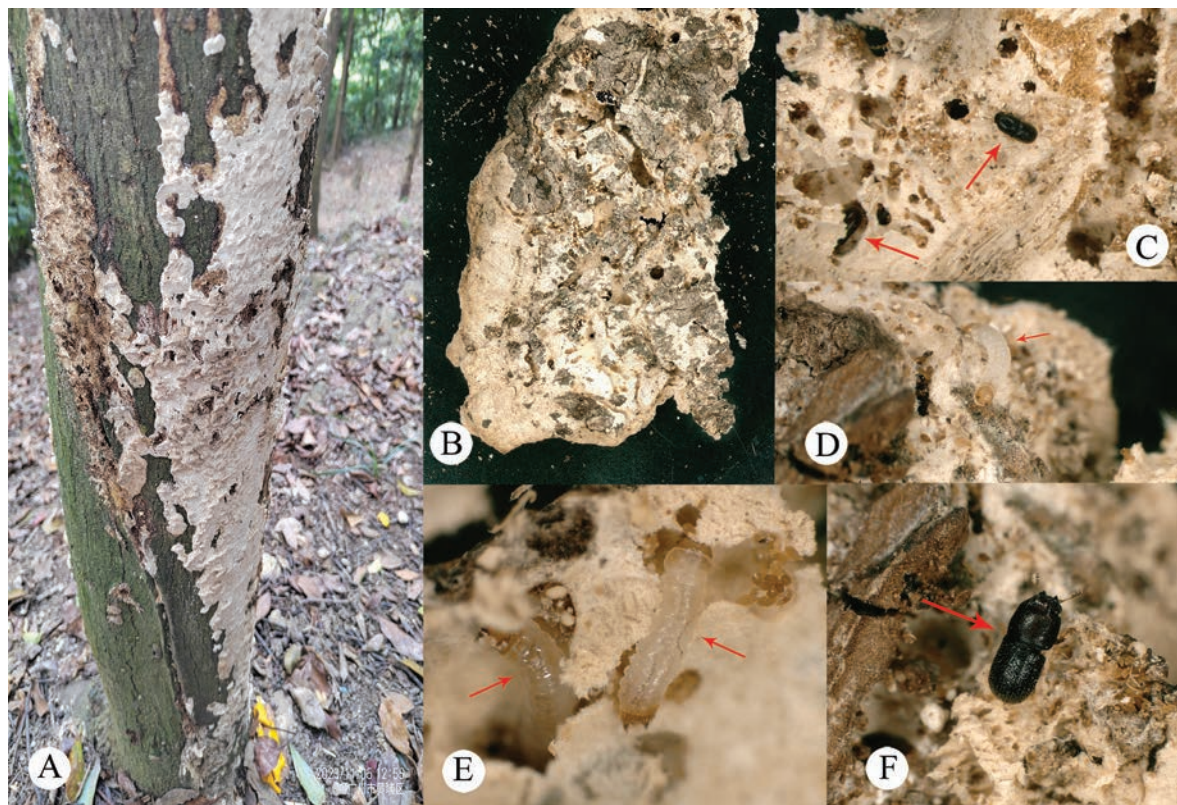
Figure 6. Habitat of *Dichodontocis guangzhouensis* sp. nov. **A** trunk with polypore basidiomes **B** host fungi, unidentified Polyporaceae **C−F** Live specimen containing larvae and adults of *D. guangzhouensis* sp. nov. on the surface of a polypore basidiome.

Key to the described *Dichodontocis* species

Based on Kawanabe 1994 and Lawrence 2016.

1   Elytral vestiture is clearly seriate, the impression of the anterior margin of pronotum is weak and only between the bases of the horn, the sternite VIII has the posterior margin slightly emarginate at the middle, and the anterior margin strongly emarginate .... ***D. uncinatus***
–   Elytral vestiture is slightly irregular, The impression of the anterior margin of pronotum is deeper and broader and extends posteriorly, distinctly beyond the bases of the horn **2**
2   The posterior edge of sternite VIII is slightly narrowly emarginate in the middle .... ***D. queenslandicus***
–   The eighth abdominal sternite with the posterior margin broadly emarginate in the middle.. ***D. guangzhouensis*** **sp. nov.**

Acknowledgements

Additional information

Author ORCIDs

Nan Li https://orcid.org/0009-0001-0013-6536
Ji-Shan Xu https://orcid.org/0000-0001-8903-0078

Data availability

All of the data that support the findings of this study are available in the main text.

References

Kawanabe M (1994) A new genus and species of the family Ciidae (Coleoptera) from southwest Japan. Japanese Journal of Entomology 62: 186–192.

Lawrence JF (1974) The larva of *Sphindocis denticollis* fall and a new subfamily of Ciidae (Coleoptera: Heteromera). Breviora 424: 1–14.

Lawrence JF (2016) The Australian Ciidae (Coleoptera: Tenebrionoidea): a preliminary revision. Zootaxa 4198(1): 1–208. https://doi.org/10.11646/zootaxa.4198.1.1

Lawrence JF, Zhou Y-L, Lemann C, Sinclair B, Ślipiński A (2021) The hind wing of Coleoptera (Insecta): morphology, nomenclature and phylogenetic significance: part 1. General discussion and Archostemata–Elateroidea. Annales Zoologici 71(3): 421–606. https://doi.org/10.3161/00034541ANZ2021.71.3.001

Lawrence JF, Zhou Y-L, Lemann C, Sinclair B, Ślipiński A (2022) The hind wing of Coleoptera (Insecta): morphology, nomenclature and phylogenetic significance: part 2. Further discussion, Histeroidea, Bostrichoidea to Curculionoidea. Annales Zoologici 72(3): 433–755. https://doi.org/10.3161/00034541ANZ2022.72.3.004

Lawrence JF, Lopes-Andrade C (2010) Ciidae Leach in Samouelle, 1819. In: Leschen RAB, Beutel RG, Lawrence JF (Eds) Handbuch der Zoologie/Handbook of Zoology. Band/Volume IV Arthropoda: Insecta teilband/ Part 38. Coleoptera, Beetles. Vol. 2. Morphology and Systematics (Elateroidea, Bostrichiformia, Cucujiformia partim). DeGruyter, Berlin, 504–514. https://doi.org/10.1515/9783110911213.504

Lopes-Andrade C, Grebennikov VV (2015) First record and five new species of Xylographellini (Coleoptera: Ciidae) from China, with online DNA barcode library of the family. Zootaxa 4006(3): 463–480. https://doi.org/10.11646/zootaxa.4006.3.3

ZooKeys

Research Article

Desert diversification: revision of *Agroecotettix* Bruner, 1908 (Orthoptera, Acrididae, Melanoplinae) with descriptions of sixteen new species from the United States and Mexico

JoVonn G. Hill[1]

1 Mississippi Entomological Museum, Department of Molecular Biology, Biochemistry, Entomology, and Plant Pathology, Mississippi State University, Starkville, USA
Corresponding author: JoVonn G. Hill (jgh4@msstate.edu)

Abstract

In this study, a morphological revision was conducted of *Agroecotettix* Bruner, a group of grasshoppers inhabiting open xeric desert scrub, shrublands, and plains, spanning central Texas to central Mexico. The genus was originally described by Bruner in 1908, with two taxa added by Hebard in 1922. *Agroecotettix* has remained unrevised despite numerous collections. This exploration, spurred by a novel discovery of significant male genitalia variation in *Agroecotettix aristus aristus*, suggests undescribed species. Through morphological specimen comparisons, sixteen new species are described from biologically rich regions of the South Texas Plains, Chihuahuan Desert, and Sierra Madre Oriental. The new taxa described here are *A. silverheelsi* **sp. nov.**, *A. xiphophorus* **sp. nov.**, *A. glochinos* **sp. nov.**, *A. texmex* **sp. nov.**, *A. cumbres* **sp. nov.**, *A. burtoni* **sp. nov.**, *A. moorei* **sp. nov.**, *A. chiantiensis* **sp. nov.**, *A. dorni* **sp. nov.**, *A. chisosensis* **sp. nov.**, *A. turneri* **sp. nov.**, *A. quitmanensis* **sp. nov.**, *A. vaquero* **sp. nov.**, *A. forcipatus* **sp. nov.**, *A. idic* **sp. nov.**, and *A. kahloae* **sp. nov.** This discovery sheds light on desert biodiversity and hints at a Pleistocene radiation akin to other melanoplines, urging further exploration to enrich our understanding of this fascinating lineage and unravel the biogeographic history within these arid landscapes.

Key words: Aridland scrub jumpers, Big Bend National Park, biodiversity, Chihuahuan Desert, Sierra Madre Oriental, Trans Pecos region

Citation: Hill JG (2024) Desert diversification: revision of *Agroecotettix* Bruner, 1908 (Orthoptera, Acrididae, Melanoplinae) with descriptions of sixteen new species from the United States and Mexico. ZooKeys 1218: 177–230. https://doi.org/10.3897/zookeys.1218.133703

Introduction

Agroecotettix Bruner, 1908 are commonly found in open shrublands, plains, and xeric desert scrub from central Texas to southeastern New Mexico, south to central Mexico. Bruner (1908) established the genus with the description of *Agroecotettix modestus* based on a female collected from Ciudad Lerdo, Coahuila, Mexico. Hebard (1922) added *Agroecotettix aristus aristus* and *Agroecotettix aristus crypsidomus* from Uvalde and Marathon, Texas, USA respectively, resulting in three described taxa.

Despite the passage of time since Hebard's work, species hypotheses in *Agroecotettix* have not been tested. Numerous collections have provided a wealth of material for study over the years, including those of Dr. Ted Cohn

from Mexico and recent efforts by the Mississippi Entomological Museum from Texas. During examination of specimens collected from Texas in 2020, a notable variation in the male genitalia of *A. aristus*, was suggestive that an undescribed species was present. Characters of the male genitalia have long been used for species hypotheses of Melanoplinae, and those hypotheses have withstood testing by molecular analyses (Hubbell 1932; Otte 2012; Hill 2015; Woller 2017; Huang et al. 2020).

Upon gathering numerous specimens of *Agroecotettix*, it became evident that the genus is distributed across several biologically diverse regions, including the Edwards Plateau, the South Texas Plains, the Chihuahuan Desert, and the Sierra Madre Oriental. Given the recent description of cryptic diversity in other melanopline grasshoppers in these areas (Otte 2012; Barrientos-Lozano et al. 2013a; Otte 2019; Hill 2023), it is likely that further explorations will unveil additional species of *Agroecotettix*.

Materials and methods

Most specimens examined in this study were borrowed from the University of Michigan Museum of Zoology (**UMMZ**) and the Academy of Natural Sciences of Drexel University (**ANSP**). Other specimens were collected by staff of the Mississippi Entomological Museum (**MEM**) during the summers of 2018–2023. Specimens were obtained by capturing them with a standard insect net. The captured individuals were placed into a jar containing potassium cyanide, for pinning, or 100% ethanol for molecular work. Specimens from New Mexico were borrowed from Brigham Young Arthropod Museum (**BYUC**) and the University of Kansas Natural History Museum (**SEMC**). All type specimens of newly described species are deposited in the MEM. Nomenclature follows Cigliano et al. (2024). Specimens collected by the MEM have been databased in the Symbiota Collection of Arthropods Network.

Internal male genitalia, which are typically concealed within the terminalia, were either exposed upon pinning fresh specimens, or the specimen was relaxed by soaking in warm water, then the genital mass was either extruded or dissected and examined in a manner similar to Gurney and Brooks 1959. Terminology for external morphology and male genitalia follows Carbonell (2007) and Eades (2000). Habitus and internal genitalia images were produced using a Leica DFC 495 digital camera mounted on a Leica Z16 microscope with motorized z-stepping. Image stacks were merged using Leica Application Suite V 4.1.0 with the Montage Module. Images were edited using Adobe Photoshop CS6 software. A green label stating "Measured by JGH" was added to the specimens measured in this study. Measurements were made with a Leica MZ 12.5 stereomicroscope with a reticule in the following ways:

- Body length — Dorsally from the fastigium verticis to the distal end of the genicular lobe of the hind femur in a parallel plane with the abdomen
- Pronotum length — Dorsally, along the median carina
- Male cercus length — Laterally, maximum measurement of the left cercus
- Male cercus basal width — Laterally, along the point of attachment from the dorsal to ventral margin
- Male mid cercus width — Laterally, at the mid-length of the left cercus

- Male cercus ventral branch length — Laterally, from beginning of the fork to the apex
- Male cercus ventral branch apex width — Laterally, along the distal end
- Male cercus dorsal branch length — Laterally, from beginning of the fork to the apex
- Male cercus dorsal branch apex width — Laterally, along the distal end
- Female dorsal ovipositor valve — Laterally, from the base to the apex
- Female ventral ovipositor valve — Laterally, from the base to the apex

Taxonomic account

Agroecotettix Bruner 1908

Diagnosis. A genus of medium-sized (18–31.1 mm) brachypterous grasshoppers (Fig. 1). Head large and as broad or slightly broader than the prozona; vertex between the eyes slightly wider than the basal antennomere; fastigium
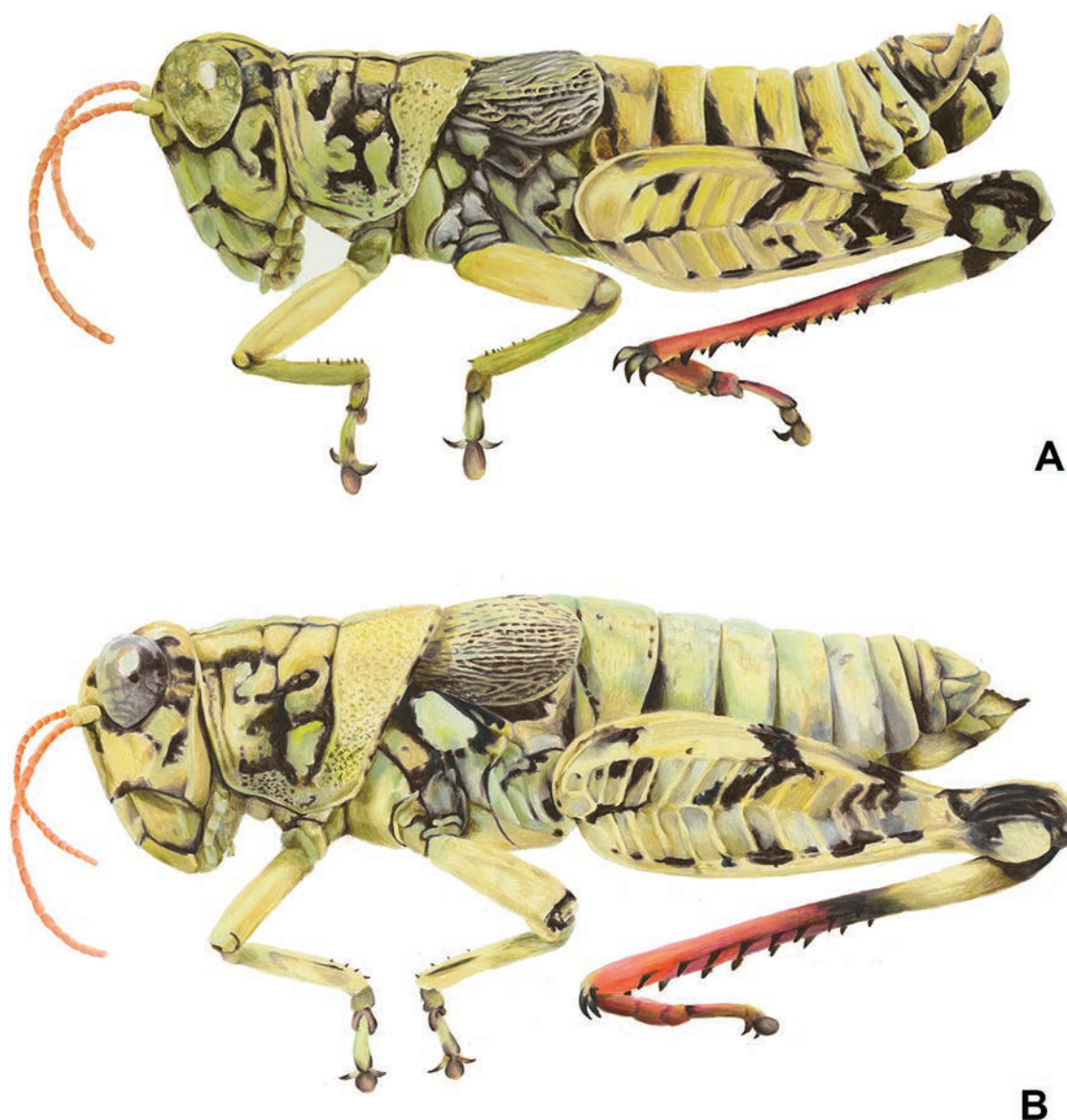

Figure 1. Habitus illustrations of *Agroecotettix aristus* **A** male **B** female. Created by Ashley Baker.

broadly rounded being more pronounced dorsally than ventrally, with a shallow medial depression throughout. Eyes somewhat prominent, especially in males. Three ocelli present. Antennae filiform, usually with 23 flagellomeres, but occasionally 24 or 25; nearly cylindrical, but slightly flattened dorso-ventrally; equal in width throughout, except two basal articles. **Thorax** with prosternal spine well-developed; subquadrate basally and acutely pointed distally. Pronotum slightly convex, anterior and caudal margins sub-truncate, lateral margins sub parallel. Prozona mostly smooth, with light punctation along the apical margin, then smooth throughout; lateral lobes quadrate (more so in females) with parallel lateral margins and the ventral margin sloping ventrally caudally. Metazona punctate throughout, with humeral margins rounded, slightly diverging posteriorly in dorsal view. Median carina low, but distinct throughout, except where the sulci cross it. Anterior, median, and posterior sulci are apparent due to their black coloration, and all dissect the median carina and nearly reach the ventral margin of the lateral lobes. Lateral pronotal margins broadly rounded on the prozona and slightly angular on the metazona. Interspace between mesosternal lobes nearly twice as long as broad. Tegmina broadly oval; dorsal margins only slightly separated dorsally; strongly veined; extending little past the anterior margin of the first abdominal tergite. Pro and meso thoracic legs robust, inflated, and bowed. Hind femur enlarged with basal end bi-lobed. Hind tibia with 11 or 12 pairs of spines, but typically 11. Tympanum present under tegmina, appearing as an opaque whitish disk. Abdomen cylindrical with distal portion distinctly, but not greatly enlarged. **Terminalia of male** with bifurcate cerci (Figs 2A–T, 3A, B), longer than wide, but the length and angle of the branches varies between species, the dorsal branch is rounded distally and flattened ventrally, the ventral branch is produced as straight and slender spike. Subgenital plate with a low but even margin. Furcula (Fig. 3A) typically broadly rounded protuberances, projecting slightly beyond the end of the segment from which they originate; well separated. Supra-anal plate (Fig. 3A, B) of male broadly triangular, length equal to the width of the base, with the median groove anteriorly distinct with elevated sides that fade caudally; with a small median tubercule lateral to the groove. Pallium evident, sometimes prominent (Fig. 7B) and covering the dorsally projecting internal genitalia. **Phallic structures** (Fig. 3C–F). The valves of the aedeagus are quite variable between species, but in *Agroecotettix* the dorsal and ventral valves appear to be fused into a single structure that when paired bilaterally form a central channel. In the *aristus* group, the sheath of the aedeagus is produced as thickened, fleshy projections on the dorsal side of the valves (Figs 4A–F, 5A–F). The valves in the *aristus* group are entire in lateral profile (Fig. 5A–F). In the *crypsidomus* group, the sheath of the aedeagus is produced as thin projections on the dorsal side of the valves (Figs 4G–R, 5G–R). The valves of most species in the *crypsidomus* group are often lobate or undulate in lateral profile, though some are entire (Fig. 5G–R). The epiphallus is of the typical melanoploid shape, having lophi, ancorae, and an undivided bridge, but more precisely, members of *Agroecotettix* have a concave bridge, broadly rounded lophi, convexly curved lateral plates that are subdeltate in shape with a rounded anterior lobe and an acuminate caudal tip, and ancorae that are triangular, often tapering to a point (Fig. 3C, D).
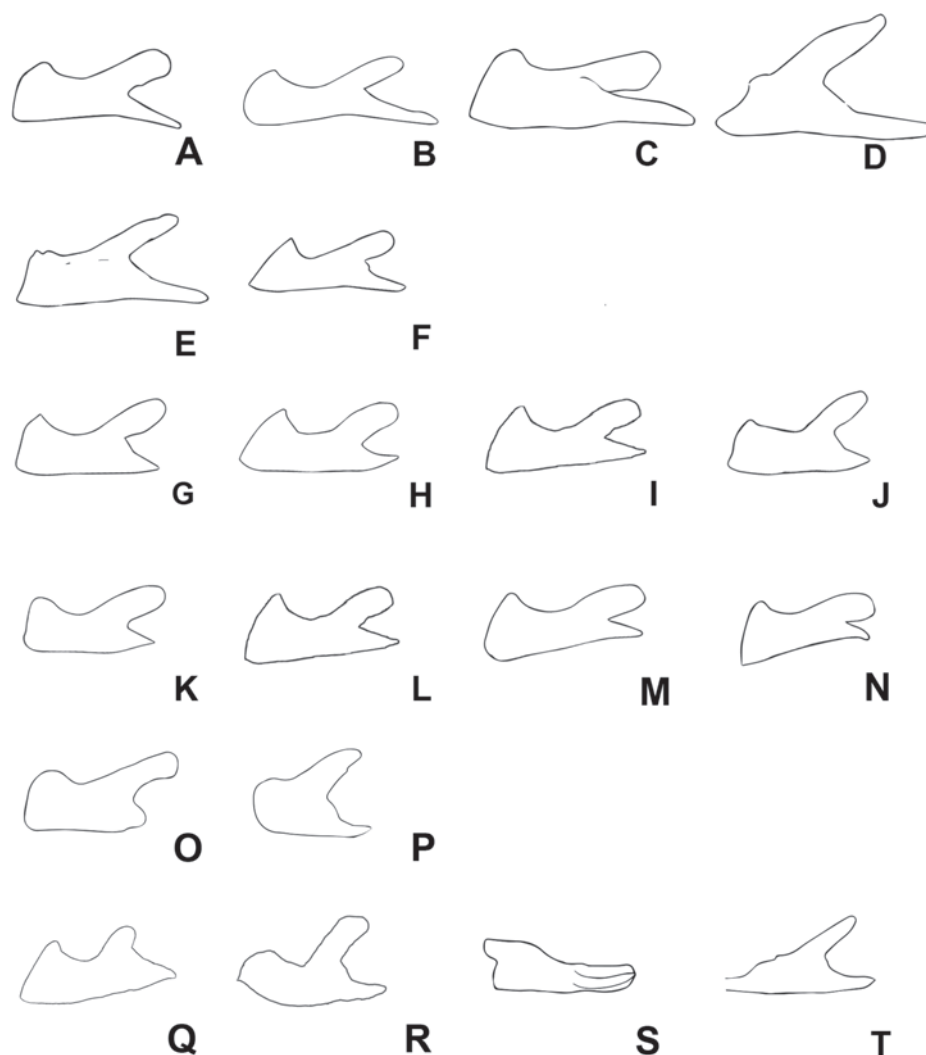
Figure 2. *Agroecotettix* cerci in lateral view unless noted otherwise **A** *A. aristus* **B** *A. silverheelsi* **C** *A. xiphophorus* **D** *A. xiphophorus* ventral view **E** *A. texmex* **F** *A. cumbres* **G** *A. crypsidomus* **H** *A. chisosensis* **I** *A. dorni* **J** *A. burtoni* **K** *A. turneri* **L** *A. quitmanensis* **M** *A. moorei* **N** *A. chiantiensis* **O** *A. vaquero* **P** *A. forcipatus* **Q** *A. kahloae* **R** *A kahloae* ventral view **S** *A. idic* lateral view **T** *A. idic* dorsal.

Females are similar to the males, but differ in being larger, more robust, with proportionately broader tegmina, and in the shape of the terminalia (Figs 1B, 6, 15C, E, 16D, 17E, F, 18G, H, 19D, 21C). **Terminalia of female** with triangular cerci and ovipositor valves that are subequal in length. The dorsal valves with their dorsum being nodose to slightly serrate proximally and concave and upcurving to a tip distally. The ventral valves with their ventral margins straight basally and then arching distally (Fig. 6).

Coloration. Ochraceous (brownish yellow) overall, with individual variation that can be either a tawny or cinereous hue (see Figs 26–35), with a conspicuous round, lighter tawny spot laterad on the metathorax near the bast of the tegmina. Head with black markings, including a band along the dorsum, flecks on the genae and a post-ocular stripe. Pronotum with the post-ocular stripe continuing onto the prozona and mesosoma and then disappearing on the metazona; median carinae and sulci black. The wings are
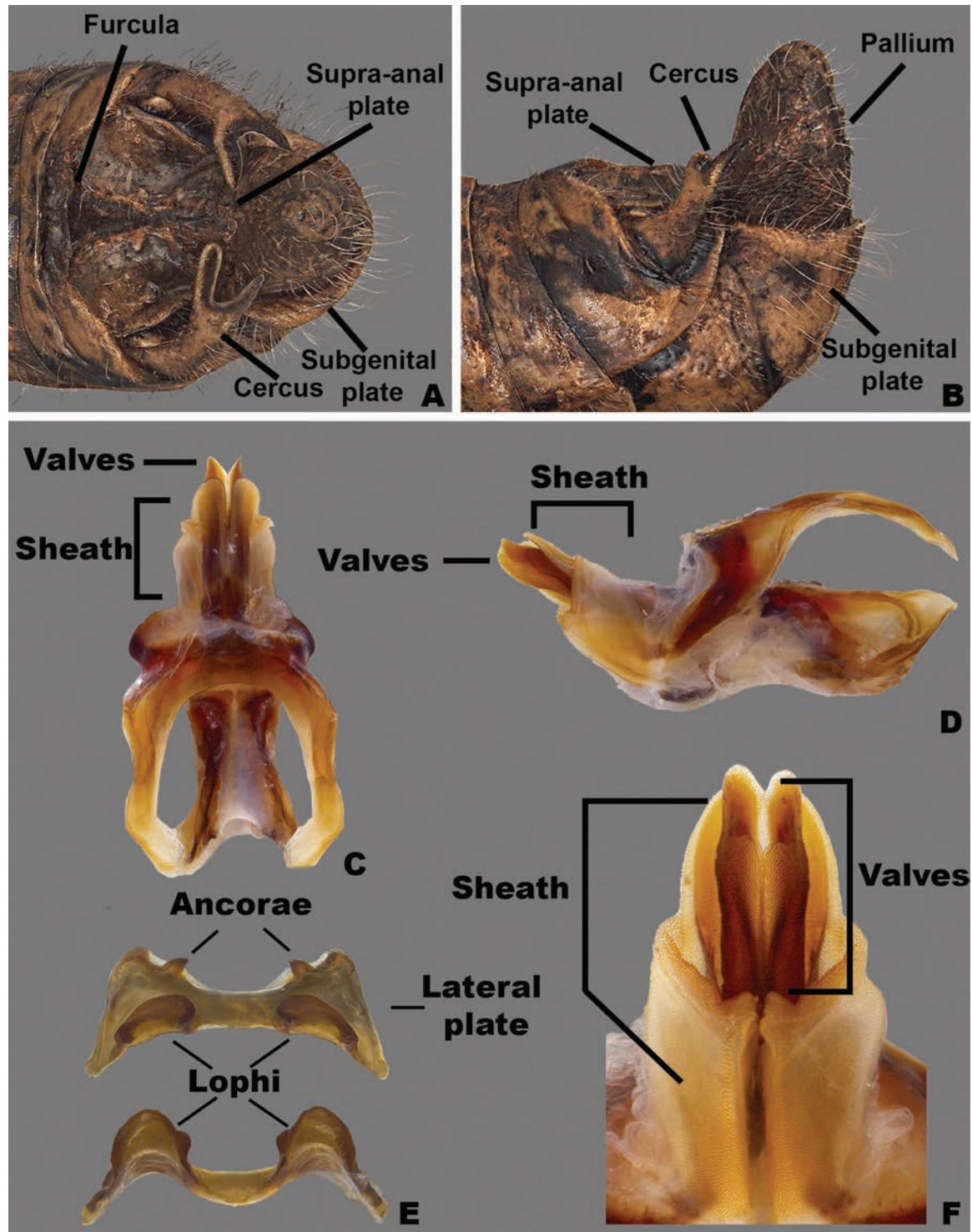
Figure 3. Morphology of the male terminalia and phallic complex of *Agroecotettix* used in this work **A** dorsal view of male terminalia **B** Lateral view of the male terminalia **C** dorsal view of the phallic complex **D** lateral view of the phallic complex **E** epiphallus dorsal and caudal views **F** caudal view of the aedeagus.

dark brown with a network of ochraceous veins. Abdomen with proximal tergites suffused with black spots. Ventral surface of the body pale with black sutures between the sternites. Male subgenital plate with a medial black spot. The fore and middle legs unmarked. The hind femur with two thick transverse bands laterally and suffused with black dorsally; genicular

Figure 4. Caudal view of the aedeagus of *Agroecotettix* **A**. *A. silverheelsi* **B** *A. aristus* **C** *A. xiphophorus* **D** *A. glochinos* **E** *A. texmex* **F** *A. cumbres* **G** *A. crypsidomus* **H** *A. burtoni* **I** *A. moorei* **J** *A. chiantiensis* **K** *A. forcipatus* **L** *A. quitmanensis* **M** *A. dorni* **N** *A. chisosensis* **O** *A. turneri* **P** *A. vaquero* **Q** *A. idic* **R** *A. kahloae*. Scale bars: 1.0 mm.

area black with ochraceous lobes; inner face bright yellow, and coral-red ventrally and crossed by black bands distally. Hind tibia with the first third ochraceous proximally, then with a ring of black, remaining two-thirds bright coral red with black tipped spines.

Etymology. *Agro* Latin = open country, *eco* Greek home, *tettix* Greek grasshopper.

Suggested common name. Aridland scrub jumpers. In reference to the arid habitat and plant community in which these grasshoppers are found.

Figure 5. Lateral view of the aedeagus of *Agroecotettix* **A** *A. silverheelsi* **B** *A. aristus* **C** *A. xiphophorus* **D** *A. glochinos* **E** *A. texmex* **F** *A. cumbres* **G** *A. crypsidomus* **H** *A. burtoni* **I** *A. moorei* **J** *A. chiantiensis* **K** *A. forcipatus* **L** *A. quitmanensis* **M** *A. dorni* **N** *A. chisosensis* **O** *A. turneri* **P** *A. vaquero* **Q** *A. idic* **R** *A. kahloae*.

Agroecotettix superficially resemble *Phaulotettix*, but can be differentiated as follows:

Agroecotettix
1. Tegmina broad and oval; attingent, nearly touching dorsally
2. Metathorax with a pale-colored spot

3. Cerci bifurcated
4. Hind tibia gray or yellow proximately, turning bright red distally
5. Inside of hind femur red
6. Furculae short and broad, and well separated from each other

Phaulotettix
1. Tegmina linear; their dorsal margins widely separated dorsally
2. Metathorax with a pale-colored stripe
3. Cerci falcate, simple
4. Hind tibia blue proximately, turning red distally
5. Inside of hind femur not red
6. Furculae short, obvious, linear; attingent or touching

Key to Agroecotettix

1 Male cerci with ventral branch longer than dorsal branch as in Fig. 2A–F; sheath of aedeagus produced as thickened fleshy lobes dorsal to the valves as in Figs 4A–F, 5A–F ....*A. aristus* group 3
– Male cerci with ventral branch equal, subequal, or shorter than the dorsal branch as in Fig. 2G–T; sheath of aedeagus not produced as thickened fleshy lobes dorsal to the valves (Figs 4G–R, 5G–R) **8**
2 Occurring north of the Rio Grande River in the United States......................**3**
– Occurring south of the Rio Grande River in Mexico....................................**5**
3 Valves of aedeagus shorter than the sheath in lateral view; and with broadly rounded apices (Figs 4B, 5B); found in the South Texas Plains (Fig. 25A)....
....*A. silverheelsi* **sp. nov.**
– Valves of aedeagus longer, extending well beyond the sheath in lateral view (Fig. 4A) **4**
4 In caudal view, the valves of the aedeagus are relatively narrower and forming parallel dorsal and ventral arches that are narrowly rounded at their apices as in Fig. 4B; in lateral view; the distal edge of the valves are broadly rounded as in Fig. 5B; found across central west Texas to southern New Mexico (Fig. 25A) ....*A. aristus* **Hebard**
– In caudal view, the valves of the aedeagus are relatively more wider and form distally diverging arches that are more broadly rounded at their apices as in Fig. 4E; In lateral view, the distal edge of the valves forming an acute point dorsally, but with a broadly rounded ventral edge (Fig. 5E); found in extreme southern Texas in the vicinity of Jim Hogg County (Fig. 25A).........
....*A. texmex* **sp. nov.** (in part)
5 Male cerci with branches widely separated and with the ventral branch much longer than the dorsal branch as in Fig. 2C, D; valves of the aedeagus with their dorsal margin somewhat bilobed and the ventral margin broadly rounded and with their distal apices diverging laterally as in Figs 4C, 5C; found in west-central Nuevo Leòn, Mexico (Fig. 25A, C) ....*A. xiphophorus* **sp. nov.**
– Male cerci with branches not widely separated and with the ventral branch only slightly longer than the dorsal branch as in Fig. 2E, F; valves of the aedeagus with their dorsal margin not bilobed **6**

6 Valves of the aedeagus with their lateral margins greatly expanded centrally and with the dorsal apices forming acute parallel points and the ventral apices forming rounded parallel arches in caudal view as in Fig. 4D; in lateral view the valves are directed apically (Fig. 5D); found in the vicinity of Galeana, MX (Fig. 25A, C) ....*A. glochinos* **sp. nov.**

– Valves of the aedeagus with their apices diverging distally in caudal view as in Fig. 4D, E; in lateral view the valves are directed more caudally as in Fig. 5D–F..**7**

7 In caudal view, the valves of the aedeagus relatively narrower (Fig. 4E); in lateral view, the ventral edge of the valves are broadly rounded at their apices (Fig. 5E); found in the vicinity northern Nuevo León, Mexico (Fig. 25A) . ...*A. texmex* **sp. nov.** (in part)

– In caudal view, the valves of the aedeagus are very broad (Fig. 4F); and are more broadly rounded at their apices (Fig. 4F) and in lateral view with their distal edge forming an acute point dorsally and the ventral edge truncated (Fig. 5F); found in the vicinity of Galeana, Mexico (Figs 25A, 26B)................ ....*A. cumbres* **sp. nov.**

8 In lateral view, the valves of the aedeagus are lobate as in Fig. 5G–J ....*A. crypsidomus* **group 9**

– In lateral view, the valves of the aedeagus are falcate or quadrate laterally as in Fig. 5K–R...**13**

9 In lateral view, the distal lobes of the aedeagus valves are more widely incised and the basal lobes are small or absent as in as in Fig. 5G, H, and in caudal view the dorsal valve is deeply undulate as in Fig. 4G, H **11**

10 In lateral view, the apical lobes of the aedeagus valves are narrowly, but deeply incised resulting in the basal lobe being more pronounced and obvious as in Fig. 5I, J **12**

11 In lateral view, basal lobe of aedeagus valves extending much beyond the sheath (Fig. 4G); dorsal lobes projected laterally in caudal view (Fig. 5G); Marathon, Texas (Figs 25, 26A) .... *A. crypsidomus* **Hebard**

– In lateral view, basal lobe of aedeagus valves not extending much beyond the sheath (Fig. 5H); dorsal lobe almost vertical or curving medially (Fig. 5H); Big Bend region of Texas (Figs 25, 26A)........... *A. burtoni* **sp. nov.**

12 In lateral view, the valves of the aedeagus are shallowly incised with a broad distal lobe that is truncated apically, and the basal lobe is shorter (Fig. 5I); in caudal view the valves of the aedeagus are concave as in Fig. 4I; Found in the vicinity of Sanderson, Texas (Figs 25, 26A) .... *A. moorei* **sp. nov.**

– In lateral view, the valves of the aedeagus are deeply incised with a narrower and slightly acute distal lobe, and a longer basal lobe as in Fig. 5J; in caudal view the valves of the aedeagus are convex as in Fig. 4J; found in the Chianti Mountains of southern Texas (Figs 25, 26A).............................. ....*A. chiantiensis* **sp. nov.**

13 Occurring north of the Rio Grande River in the United States....................**14**
– Occurring south of the Rio Grande River in Mexico...................................**17**

14 In lateral view, the apices of the valves of the aedeagus point caudally as in Fig. 5M, found in the vicinity of western Brewster County, Texas (Figs 25, 26A) ....*A. turneri* **sp. nov.**

– In lateral view, the apices of the valves of the aedeagus curve apically as is Fig. 5L–O...**15**

15 In lateral view, the apical edge of the valves of the aedeagus are thicker finger-like projections as in Fig. 5L; found in the vicinity of the Quitman Mountains in Hudspeth County, Texas (Figs 25, 26A) ....***A. quitmanensis* sp. nov.**

– In lateral view, the apical edge of the valves of the aedeagus are thin blade-like projections as in Fig. 5M, N) **16**

16 In lateral view, the valves of aedeagus thinly falcate, long and sword-like as in Figs 5M, and in caudal view the lateral margins extend well beyond the rest of the valves and their apical margins are slightly curved distally as in 4M; found in the southern Big Bend region of Texas (Figs 25, 26A, B)..........
....***A. dorni* sp. nov.**

– In lateral view, the valves of aedeagus broad as in Fig. 5N, and in caudal view the lateral margins do not extend well beyond the rest of the valves and their apical margins are curved medially as in Fig. 4N; endemic to the Chisos Mountains of the Big Bend region of Texas (Figs 25, 26A)......***A. chisosensis* sp. nov.**

17 Male cerci with the ventral branch reduced and rounded as in Fig. 2O; in lateral view, the sheath of the aedeagus is well developed and expanded laterally around the valves; in lateral view, the aedeagus valves are wide with their apices broadly curved (Fig. 5P); in caudal view the valves or greatly narrowed in their apical third as in Fig. 4P; found in northern Coahuila, Mexico (Fig. 25) ....***A. vaquero* sp. nov.**

– Male cerci longer with both dorsal and ventral branches well produced.......**18**

18 Male cerci short and not curved medially as in Fig. 2P; in lateral view, the valves of the aedeagus are acutely pointed apically and are greatly widened in their lower half; in caudal view the apical margins of the valves are slightly curved distally as in Fig. 4O; found southern Coahuila, Mexico in the vicinity of the Sierra de la Gloria (Fig. 25) ....***A. forcipatus* sp. nov.**

– Male cerci longer (Fig. 2Q–T); dorsal and lower branches subequal in length...**19**

19 Male cercus gently curved medially (Fig. 2Q, R); in lateral view the valves of the aedeagus are narrowly quadrate with the distal apices truncate apically as in Figs 4Q, 5Q; in caudal view the valves are also quadrate with the apical margin truncate as in Figs 4R, 5R; found in the vicinity of Saltillo, Mexico (Figs 25, 26B) ....***A. idic* sp. nov.**

– Male cercus strongly curved medially (Fig. 2S, T); in lateral view, the valves of the aedeagus are broad and arching with the distal apices rounded (Fig. 5R); in caudal view, valves acuminate; Arteaga, Mexico (Figs 25, 26B)
....***A. kahloae* sp. nov.**

Agroecotettix species checklist

Incertae sedis

1. *Agroecotettix modestus* Brunner, 1908, stat. nov. — Figs 6, 25

A. aristus group

2. *Agroecotettix silverheelsi* sp. nov. — Figs 2B, 4A, 5A, 7A–J, 23A–C, 25, 26A
3. *Agroecotettix aristus* Hebard, 1922, stat. nov. — Figs 2A, 4B, 5B, 8A–J, 25, 26A, 28A–E, 29A–E

4. *Agroecotettix xiphophorus* sp. nov. — Figs 2C, D, 4C, 5C, 9A–J, 25, 26B

5. *Agroecotettix glochinos* sp. nov. — Figs 4D, 5D, 10A–J, 25, 26B

6. *Agroecotettix texmex* sp. nov. — Figs 2E, 4E, 5E, 11A–J, 25, 26B

7. *Agroecotettix cumbres* sp. nov. — Figs 2F, 4F, 5F, 12A–J, 25, 26B

A. crypsidomus group

8. *Agroecotettix crypsidomus* Hebard, 1922, stat. nov. — Figs 2G, 4G, 5G, 13A–J, 25, 26A, 31A–F

9. *Agroecotettix burtoni* sp. nov. — Figs 2J, 4H, 5H, 14A–J, 25, 26A, 31A–D

10. *Agroecotettix moorei* sp. nov. — Figs 2M, 4I, 5I, 15A–J, 25, 26A, 32A–D

11. *Agroecotettix chiantiensis* sp. nov. — Figs 2N, 4J, 5J, 16A–J, 25, 26A, 33A–C

12. *Agroecotettix dorni* sp. nov. — Figs 2I, 4M, 5M, 17A–J, 25, 26A, 34A–D

13. *Agroecotettix chisosensis* sp. nov. — Figs 2H, 4N, 5N, 18A–J, 25, 26A, 36A–E

14. *Agroecotettix turneri* sp. nov. — Figs 2K, 4K, 5K, 19A–J, 25, 26A, 36A–D

15. *Agroecotettix quitmanensis* sp. nov. — Figs 2L, 4P, 5P, 20A–J, 25, 26A

16. *Agroecotettix vaquero* sp. nov. — Figs 2T, 4P, 5P, 21A–J, 25

17. *Agroecotettix forcipatus* sp. nov. — Figs 2O, 4O, 5O, 22A–J, 25

18. *Agroecotettix idic* sp. nov. — Figs 2S, 4Q, 5Q, 23A–J, 25, 26B

19. *Agroecotettix kahloae* sp. nov. — Figs 2Q, 4R, 5R, 24A–J, 25, 26B

Species accounts

Agroecotettix modestus Bruner, 1908, stat. nov.
Figs 6, 25

Agroecotettix modestus Bruner, L., 1908. Biologia Centrali-Americana 2: 312.
Agroecotettix modestus modestus Bruner, 1908: Fontana et al. 2008: 155.
Agroecotettix modestus modestus Bruner, 1908: Barrientos-Lozano et al. 2013b: 211–212.

Diagnosis. None of the diagnostic characters used here or typically in the Melanoplinae for species level diagnosis are available as this species is known only from the female type.

Figure 6. Habitus of type specimen of *Agroecotettix modestus*.

Female measurements (mm. (*n* = 1) Body length 28.7; pronotum length 6.9; tegmen length 5.0; hind femur length 15.5; dorsal ovipositor valve length 2.0; ventral ovipositor valve length 2.0.

Holotype examined. • 1♀, Mexico, Durango, Lerdo, November. Deposited in the Academy of Natural Sciences of Drexel University.

Habitat. Bruner (1908) did not report any habitat or environmental data, but it is likely desert scrub as with other members of the genus.

Distribution. Known only from the type locality (Fig. 25).

Note. Given that the only known specimen of this species is female, and it is a distributional outlier with other species occurring between its distribution and that of its subspecies, *A. modestus* is raised to species level.

Etymology. *modestus* Latin = modest.

Suggested common name. Modest aridland scrub jumper.

Agroecotettix silverheelsi sp. nov.

https://zoobank.org/27EE581C-3C87-4296-A82B-536AAC187499

Figs 2B, 4A, 5A, 7A–J, 25, 23A–C, 25, 26A

Diagnosis. Differentiated from the other species in the group based on the male cerci that have the ventral branch longer than the dorsal branch and by the male aedeagus that has a thickened sheath, and the valves of that are shorter than the sheath with broadly rounded apices (Figs 4A, 5A). Most similar to *A. aristus* and *A. texmex* but differs from those by the shape of the male genitalia which in caudal view, has the valves of the aedeagus relatively shorter and broader than in *A. aristus* (Figs 4B, 5B) and by the having valves that that are parallel (Figs 4A, 5A) as opposed to diverging apically as in *A. texmex*. (Figs 4D, 5D); in lateral view, the distal edge of the valves is broadly rounded.

Male measurements (mm). (*n* = 7) Body length 20.6–24.5 (mean = 22.7); pronotum length 4.4–5.5 (mean = 5.2); tegmen length 2.9–4.0 (mean = 3.4); hind femur length 10.4–12.4 (mean = 11.6); cerci length 1.4–1.7 (mean = 1.6); basal width of cercus 0.5–0.6 (mean = 0.6); mid-cercal width 0.4 (mean = 0.4); cerci dorsal fork length 0.4–0.5 (mean = 0.5); cerci dorsal fork apex width 0.2 (mean = 0.2); cerci ventral fork length 0.6–0.8 (mean = 0.6); cerci ventral fork apex width 0.1 (mean = 0.1).

Phallus measurements (mm). (*n* = 3) Length 0.7–0.8 (mean = 0.8); apex width 0.4–0.5 (mean = 0.4); middle width 0.5–0.8 (mean = 0.7); basal width 0.6–0.7 (mean = 0.6); lateral apex width 0.2–0.4 (mean = 0.3); lateral medial width 0.3–0.4 (mean = 0.3); lateral basal width 05–0.7 (mean = 0.6).

Female measurements (mm). (*n* = 3) Body length 25.2–27.2 (mean = 26.2); pronotum length 6.5–7.2 (mean = 6.8) tegmen length 4.5–5.1 (mean = 4.8); hind femur length 13.2–15.2 (mean = 14.2); dorsal ovipositor valve length 1.2–2.1 (mean = 1.8); ventral ovipositor valve length 1.2–2.1 (mean = 1.8).

Holotype. • 1♂, USA, Texas, Dimmit Co., Asherton, 28.4559, -99.7778, 19 July 2020, J.G. Hill; open grassland with *Opuntia*, *Cylindropuntia*, and *Prosopis*. Deposited in the Mississippi Entomological Museum.

Specimens examined. USA, **Texas:** • Dimmit Co., Asherton, 28.4559, -99.7778, 19 July 2020, J.G. Hill (1♂, 1♀). • Maverick Co., 1.8 mi E Eagle Pass, 18 August 1961, I.J. Cantrall and T.J. Cohn (5♂, 2♀).
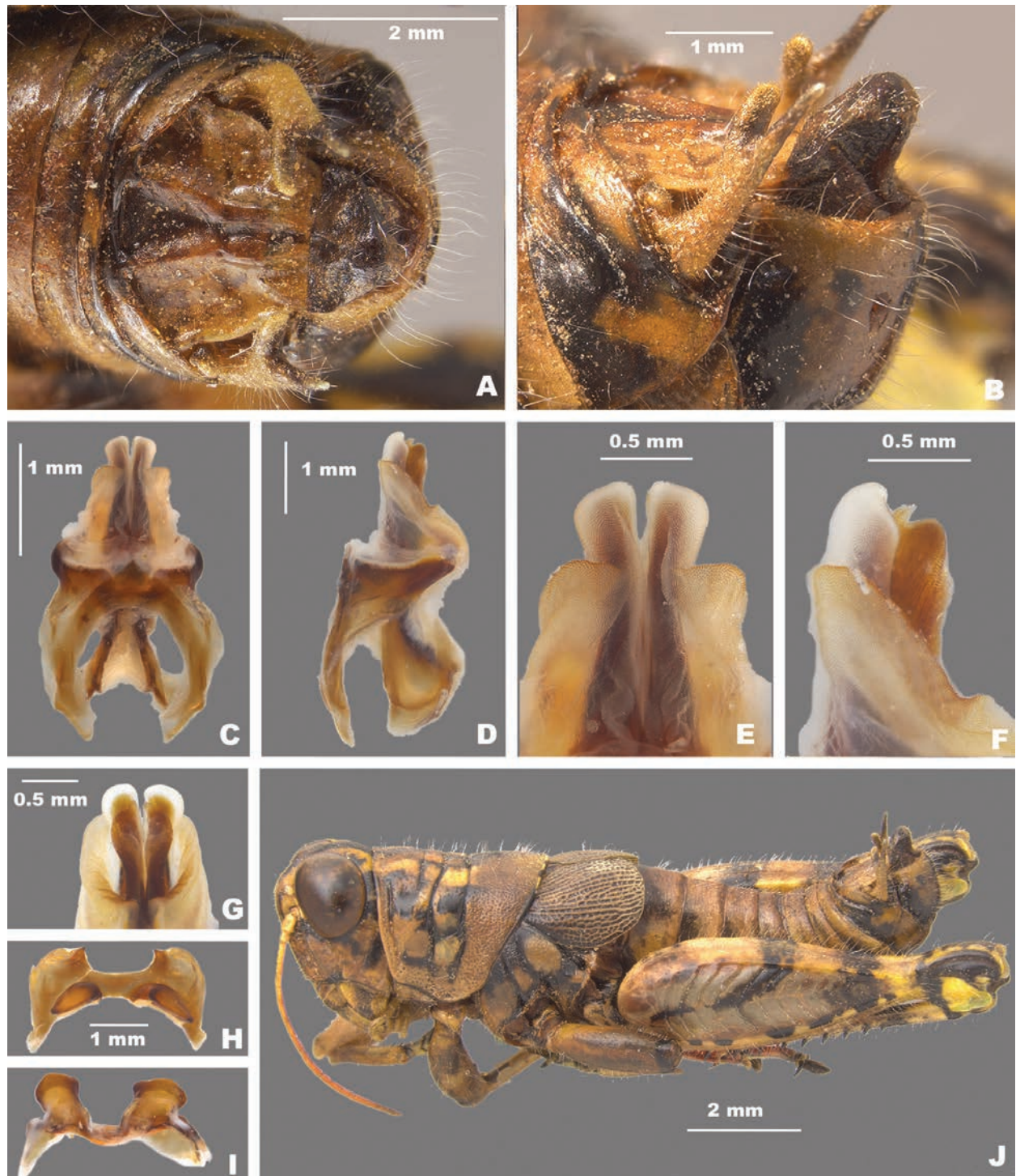
Figure 7. *Agroecotettix silverheelsi* **A** dorsal view of male terminalia **B** lateral view of male terminalia **C** dorsal view of phallic complex **D** lateral view of phallic complex **E** dorsal view of aedeagus **F** lateral view of aedeagus **G** caudal view of the aedeagus **H** dorsal view of epiphallus **I** caudal view of epiphallus **J** habitus.

Habitat. On *Vachellia* branches in an open grassland with *Opuntia*, *Cylindropuntia*, and *Prosopis* (Fig. 26C).

Distribution. Known only from the northwestern South Texas Plains region of Texas (Fig. 25).

Etymology. The name *silverheelsi* is a patronym honoring Jay Silverheels. a Native American athlete and actor who most famously portrayed the fictional

character Tonto in "The Lone Ranger" television series from 1949–1957. Silverheels was one of the first Native American actors to portray a major Indigenous character on a television series. Throughout his career, Silverheels advocated for more inclusion of Indigenous people in media and founded the Indian Actors Workshop in Los Angeles during the 1960's. This naming honors Silverheels' cultural impact and the Texas landscapes where the series was set.

Suggested common name. Silverheels' aridland scrub jumper.

Agroecotettix aristus Hebard, 1922, stat. nov.
Figs 2A, 4B, 5B, 8A–J, 25, 26A, 28A–E, 29A–E

Agroecotettix modestus aristus Hebard, 1922. Trans. Amer. Entomol. Soc. 48(1): 49.

Diagnosis. Differentiated from other species in the genus by the combination of male cerci that have the lower branch longer than the dorsal branch and the male aedeagus that has a thickened sheath and valves that are longer than the sheath and have narrowly rounded apices (Figs 4B, 5B). Most similar to *A. silverheelsi* and *A. texmex* but differ from those by the shape of the male genitalia which in caudal view, has the valves of the aedeagus longer and narrower than in *A. silverheelsi* (Figs 4A, 5A) and parallel and narrowly rounded apices as opposed to the broad, latterly diverging apices of *A. texmex* (Figs 4D, 5D). In lateral view, the distal edge of the valves is broadly rounded as in Fig. 5B.

Male measurements (mm). (n = 16) Body length 19.5–24.9 (mean = 22.4); pronotum length 4.4–6.2 (mean = 5.2); tegmen length 2.7–4.6 (mean = 3.4); hind femur length 10.4–14.0 (mean = 11.7); cerci length 1.2–1.7 (mean = 1.5); basal width of cercus 0.5–0.7 (mean = 0.6); mid-cercal width 0.4–0.5 (mean = 0.4); cerci dorsal fork length 0.3–0.5 (mean = 0.4); cerci dorsal fork apex width 0.1–0.3 (mean = 0.2) cerci ventral fork length 0.4–0.6 (mean = 0.5); cerci ventral fork apex width 0.1 (mean = 0.1).

Phallus measurements (mm). (n = 16) Length 0.6–0.8 (mean = 0.7); apex width 0.3–0.5 (mean = 0.3); middle width 0.4–0.6 (mean = 0.5); basal width 0.5–0.8 (mean = 0.6); lateral apex width 0.2–0.3 (mean = 0.3); lateral medial width 0.3–0.4 (mean = 0.4); lateral basal width 0.5–0.6 (mean = 0.5).

Female measurements (mm). (n = 9) Body length 25.5–27.6 (mean = 26.9); pronotum length 6.5–7.3 (mean = 7.0) tegmen length 3.3–6.5 (mean = 4.4); hind femur length 13.3–15.5 (mean = 14.7); Dorsal ovipositor valve length 1.5–2.0 (mean = 1.8); ventral ovipositor valve length 1.5–2.0 (mean = 1.8).

Holotype. • 1♂, USA, Texas, Uvalde, 22 August 1912, Rehn and Hebard, 1000–1100 ft.

Specimens examined. USA, **New Mexico:** • Eddy Co., Sitting Bull Falls, 22 August 1985, B. Ruish, Whiting, (1♂) • Lincoln National Forest, Sitting Bull Falls, 32.2461, -104.6979, 27 September 2024, J.G. Hill (2♂, 1♀). **Texas:** • Culberson Co., Frijole, 4–16 July 1935, J.M. Brennan (1♂) • Jeff Davis Co., Davis Mountains State Park, 30.5992, -103.9075, 16 July 2023, J.G. Hill (1♂, 1♀) • Kimble Co., 5 mi SW Junction, 5 August 1955, T.J. Cohn, 1750 ft (1♂) • Kinney Co., 2 mi S Brackettville, 30 July 1959, T.J. Cohn, 1100 ft (1♂) • Mitchell Co., 1 mi W Colorado City, 9 July 1956, T.J. Cohn, E. Matthews, 2100 ft

Figure 8. *Agroecotettix aristus* **A** dorsal view of male terminalia **B** lateral view of male terminalia **C** dorsal view of phallic complex **D** lateral view of phallic complex **E** dorsal view of aedeagus **F** lateral view of aedeagus **G** caudal view of the aedeagus **H** dorsal view of epiphallus **I** caudal view of epiphallus **J** habitus.

(2♂) • Odessa Co., Sheffield, 23 October 1931, L. Seaton (1♂, 1♀) • Sterling Co., 7 mi NE Sterling City, 27 June 1967, T.J. Cohn (1♂) • Upton Co., 8.8 mi W. Rankin, 31.1533, -102.0650, 16 July 2023, J.G. Hill, J.L. Seltzer (1♂) • Terrell Co., 18 mi S Sheffield, 1 June 1949, W.F. Blair (1♂, 1♀) • Uvalde Co., Concan, 6 July 1936, R.H. Beamer (1♂) • Pecos Co., 6 mi W Ft. Stockton, 8 August

1956, T.J. Cohn 3000 ft. (2♂) • Uvalde, 22 August 1912, Rehn and Hebard, 1000−1100 ft (Paratypes) (1♂, 1♀) • 21 mi N Uvalde, 29.4636, -100.01389, 29 July 2020, M.J. Thorn, J.G. Hill (1♂, 2♀) • Val Verde Co., 6.5 mi SE Comstock, 23 August 1956, T.J. Cohn, 1400 ft (1♂) • 22 mi NW (rd.) Loma Alta, 31 August 1958 T.J. Cohn (1♂) • Pecos River x HWY 90, 29.705, -101.35084, 24 July 2020, J.G. Hill (1♂, 1♀).

Habitat. Often found on or associated with thorny leguminous shrubs. On the Edwards Plateau in Texas, this species is often found on stunted, low shrubs growing just above ground level amongst the limestone rocks (Fig. 28A−F). In the Davis Mountains and the northern Chihuahuan Desert, this species was observed on the interior branches of larger (> 2 m tall) *Vachellia* species (Fig. 29A−E).

Distribution. Found across central and west Texas to southeastern New Mexico (Figs 25, 26A).

Note. Given that the only known specimen of *A. modestus* is female and it is a distributional outlier, with other species occurring between its distribution and that of its subspecies, *A. modestus* was raised to species level above. Additionally, due to the differences in the internal male genitalia, *A. aristus* and *A. crypsidomus* are each raised to species level.

Etymology. Hebard (1922) did not indicate the etymology in the description of this species, but it is likely from Latin *arista* in reference to the aristate or awn-like point of the male cerci in this genus.

Suggested common name. Aristate aridland scrub jumper.

Agroecotettix xiphophorus sp. nov.

https://zoobank.org/D5ABD4CA-455E-4C03-8C3A-F6BF29A1147C

Figs 2C, D, 4C, 5C, 9A−J, 25, 26B

Diagnosis. Easily differentiated from other species in the genus by the combination of male cerci with branches widely separated and with the ventral branch much longer than the dorsal branch (Figs 2C, D, 9A, B), the male aedeagus that has a thickened sheath and valves with somewhat bilobed dorsal margins and broadly rounded ventral margins that have with their distal apices diverging laterally (Figs 4C, 5C). Most like *A. idic* and *A. kahloae* but is distinguished from those species by the shape of the male cerci, which in *A. idic* and *A. kahloae* are smaller with the dorsal and ventral branches of similar length, and by the shape of the male phallic complex (Figs 9C−G, 23C−G, 24C−G).

Male measurements (mm). (*n* = 8) Body length 21.8−27.5 (mean = 24.8); pronotum length 5.0−6.7 (mean = 5.9); tegmen length 3.5−4.6 (mean = 4.1); hind femur length 11.7−14.1 (mean = 12.9); cerci length 2.0−2.5 (mean = 2.3); basal width of cercus 0.5−0.7 (mean = 0.6); mid-cercal width 0.3−0.7 (mean = 0.6); cerci ventral arm length 1.2−1.7 (mean = 1.5); cerci ventral arm apex width 0.1 (mean = 0.1) cerci dorsal arm length 0.6−0.9 (mean = 0.8); cerci dorsal arm apex width 0.2−0.4 (mean = 0.3).

Phallus measurements (mm). (*n* = 5) Length 0.7−1.0 (mean = 0.8); apex width 0.4−0.5 (mean = 0.5); middle width 0.9−1.0 (mean = 0.9); basal width 0.6−0.7 (mean = 0.7); lateral apex width 0.2−0.4 (mean = 0.3); lateral medial width 0.4−0.6 (mean = 0.5); lateral basal width 0.5−0.9 (mean = 0.7).
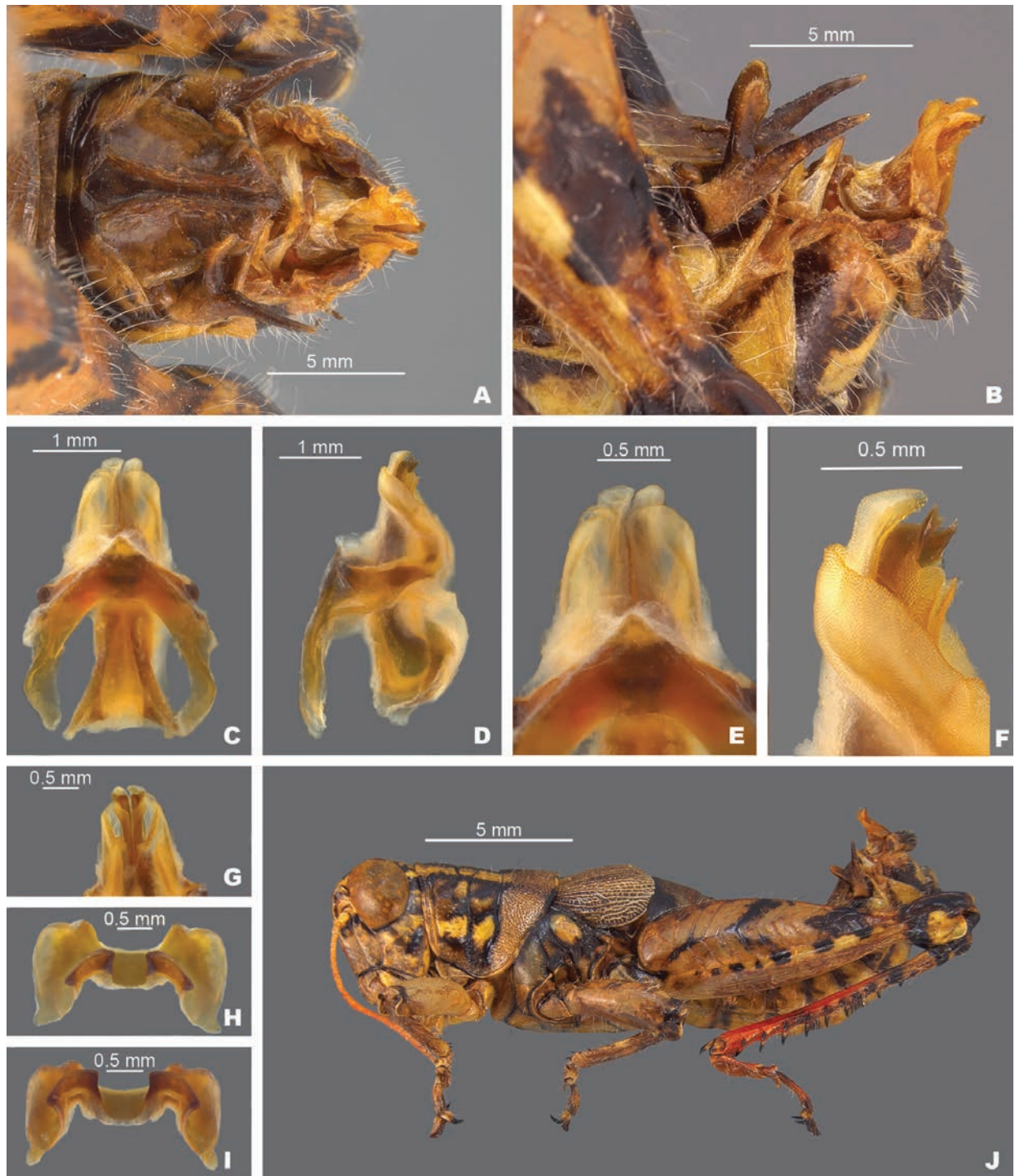
Figure 9. *Agroecotettix xiphophorus* **A** dorsal view of male terminalia **B** lateral view of male terminalia **C** dorsal view of phallic complex **D** lateral view of phallic complex **E** dorsal view of aedeagus **F** lateral view of aedeagus **G** caudal view of the aedeagus **H** dorsal view of epiphallus **I** caudal view of epiphallus **J** habitus.

Female measurements (mm). (*n* = 7) Body length 24.0–31.3 (mean = 27.5); pronotum length 6.7–8.8 (mean = 7.5); tegmen length 4.1–5.3 (mean = 4.7); hind femur length 14.4–16.7 (mean = 15.5) Dorsal ovipositor valve length 1.6–2.5 (mean = 2.0); ventral ovipositor valve length 1.6–2.5 (mean = 2.0).

Holotype. • 1♂, Mexico, Nuevo Leòn, 1.7 mi W Santa Caterina. 8 August 1959, T.J. Cohn, 2380 ft, #155. Deposited in the Mississippi Entomological Museum.

Specimens examined. Mexico, **Nuevo Leòn:** • Monterrey airport, 14 July 1964, T.J. Cohn (2♂, 1♀) • 5 mi W Monterrey, 16 July 1936, H.R. Roberts, 3000 ft. (2♂, 2♀) • Villa de Garcia, 28−29 August 1966, J. Mathieu (4♂, 3♀).

Habitat. Cohn (1959) lists the habitat at the type locality as a fair patch of roadside weeds, especially a tall sticky composite and blue flowered solanaceous plant with spaced out low trees of Acacia and mesquite.

Distribution. Found west-central Nuevo Leòn, Mexico (Figs 25, 26B).

Etymology. *xiphos* Greek = sword; *phorus* Greek = bearing:. reference to the long sword-like ventral projection of the male cerci.

Suggested common name. Sword-tailed aridland scrub jumper.

Agroecotettix glochinos sp. nov.

https://zoobank.org/AEE452D0-59FA-4F1F-B50B-51EA3630666B
Figs 4D, 5D, 10A−J, 25, 26B

Diagnosis. Easily differentiated from other species in the genus by the combination of male cerci that have the lower branch longer than the dorsal branch (Fig. 10A, B) and the male aedeagus with a thickened sheath, valves that are longer than the sheath, and in caudal view the valves of the aedeagus are widen laterally in their mid-section, and abruptly narrow apically such that the dorsal apieces form acute parallel points; the ventral apices of the valves are broadly rounded (Figs 4D, 10C−G). In lateral view the valves are directed apically instead of dorsally as in all other *Agroecotettix* species (Figs 5D, 10C−G).

Male measurements (mm). (n = 2) Body length 13.3−18.7 (mean = 16); pronotum length 2.9−4.1 (mean = 3.5); tegmen length 2.2−3.0 (mean = 2.6); hind femur length 7.3−10.0 (mean = 8.7); cerci length 0.8−1.1 (mean = 1.0); basal width of cercus 0.4−0.5 (mean = 0.5); mid-cercal width 0.2−0.3 (mean = 0.3); cerci dorsal fork length 0.1−0.3 (mean = 0.2); cerci dorsal fork apex width 0.1−0.2 (mean = 0.2); cerci ventral fork length 0.2−0.4 (mean = 0.3); cerci ventral fork apex width 0.1 (mean = 0.1).

Phallus measurements (mm). (n = 1) Length 0.8; apex width 0.3; middle width 0.4; basal width 0.6; lateral apex width 0.5; lateral medial width 0.7; lateral basal width 0.7.

Female measurements (mm). (n = 3) Body length 21.3−23.3 (mean = 22.0); pronotum length 4.7−5.1 (mean = 4.9) tegmen length 3.5−3.8 (mean = 3.7); hind femur length 10.8−11.7 (mean = 11.2); dorsal ovipositor valve length 1.3−1.5 (mean = 1.3); ventral ovipositor valve length 1.3−1.5 (mean = 1.4).

Holotype. • 1♂, Mexico, Nuevo Leòn, 7 mi SE Galeana, 11 August 1959, 5350', T.J. Cohn, #166. Deposited in the Mississippi Entomological Museum.

Specimens examined. Mexico, **Nuevo Leòn:** • 7 mi SE Galeana, 11 August 1959, T.J. Cohn, 5350' (1♂, 3♀).

Habitat. Cohn (1959) does not include a habitat description for the single locality from which this species is known.

Distribution. Known only from the type locality at this time (Figs 25, 26B).

Etymology. *glochinos* Greek = point of an arrow, in reference to the pointed, arrowhead-like shape of the aedeagus.

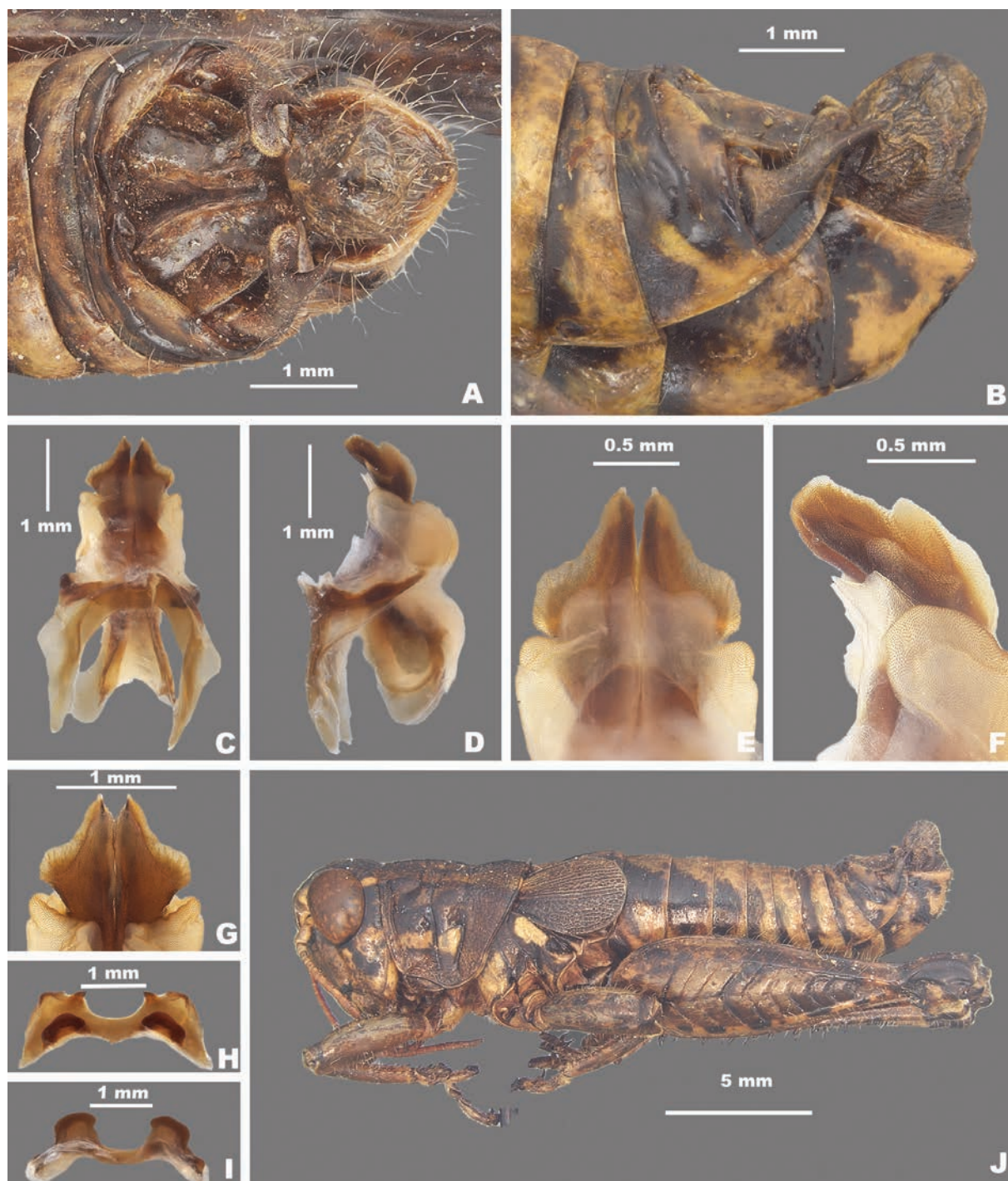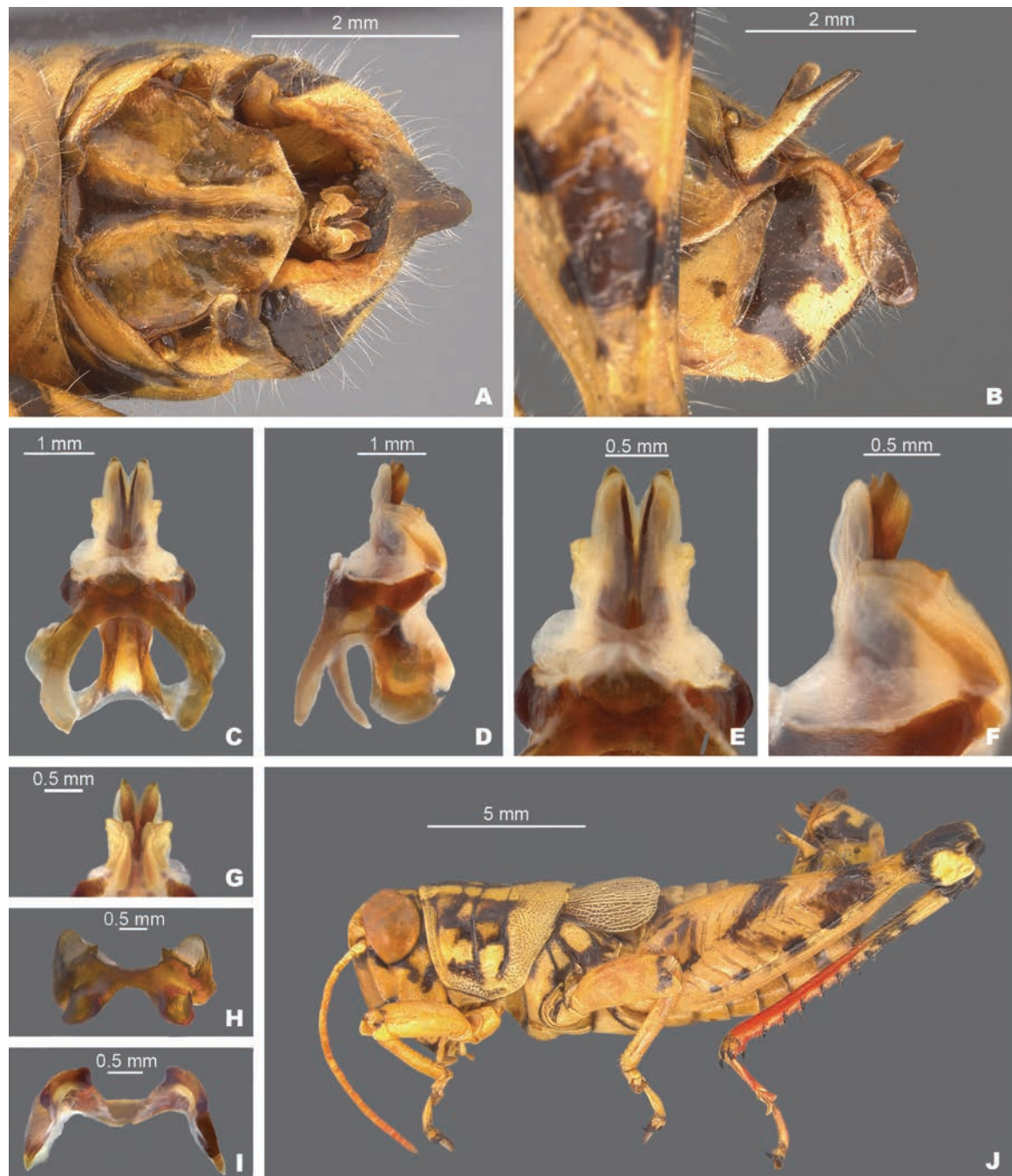**Suggested common name.** Arrowhead aridland scrub jumper.

Figure 10. *Agroecotettix glochinos* **A** dorsal view of male terminalia **B** lateral view of male terminalia **C** dorsal view of phallic complex **D** lateral view of phallic complex **E** dorsal view of aedeagus **F** lateral view of aedeagus **G** caudal view of the aedeagus **H** dorsal view of epiphallus **I** caudal view of epiphallus **J** habitus.

Agroecotettix texmex **sp. nov.**
https://zoobank.org/04E23B25-B968-450D-9988-E6D7FE14622E
Figs 2E, 4E, 5E, 11A–J, 25, 26B

Diagnosis. Differentiated from other species in the genus by the combination of male cerci that have the lower branch longer than the dorsal branch (Figs 2E, 11A, B) and the male aedeagus that has a thickened sheath and valves that are

Figure 11. *Agroecotettix texmex* **A** dorsal view of male terminalia **B** lateral view of male terminalia **C** dorsal view of phallic complex **D** lateral view of phallic complex **E** dorsal view of aedeagus **F** lateral view of aedeagus **G** caudal view of the aedeagus **H** dorsal view of epiphallus **I** caudal view of epiphallus **J** habitus.

longer than the sheath, and narrow valves that diverge in lateral view (Figs 4E, 5E, 11C–G). Most similar to *A. aristus*, *A. glochinos*, and *A. silverheelsi*. Differs from *A. aristus* by that species by having valves that diverge laterally in caudal view and are broader in lateral view (Figs 4C, D, 5C, D) and from *A. glochinos* by having narrower valves (Figs 4D, E, 5D, E). Differs from *A. silverheelsi* by having a narrower and folded caudal edge of the sheath as opposed to an unfolded and open edge as in *A. silverheelsi*.

Male measurements (mm). (*n* = 7) Body length 22.2–24.0 (mean = 23.1); pronotum length 4.6–6.5 (mean = 5.4); tegmen length 3.3–4.1 (mean = 3.6);

hind femur length 11.5–13.5 (mean = 12.6); cerci length 1.6–1.8 (mean = 1.7); basal width of cerci 0.4–0.7 (mean = 0.6); mid-cercal width 0.4–0.6 (mean = 0.5); cerci dorsal fork length 0.4–0.7 (mean = 0.5); cerci dorsal fork apex width 0.1–0.3 (mean = 0.2); cerci ventral fork length 0.4–1.0 (mean = 0.7); cerci ventral fork apex width 0.1 (mean = 0.1).

Phallus measurements (mm). (*n* = 2) Length 0.6–0.7 (mean = 0.7); apex width 0.4–0.5 (mean = 0.5); middle width 0.5–0.6 (mean = 0.6); basal width 0.3 (mean = 0.3); lateral apex width 0.2–0.4 (mean = 0.3); lateral medial width 0.2–0.5 (mean = 0.4); lateral basal width 0.2–0.6 (mean = 0.4).

Female measurements (mm). (*n* = 7) Body length 25.2–29.8 (mean = 27.3); pronotum length 6.5–7.5 (mean = 6.9) tegmen length 4.1–5.1 (mean = 4.7); hind femur length 14.0–16.2 (mean = 15.1); dorsal ovipositor valve length 1.5–2.0 (mean = 1.7); ventral ovipositor valve length 0.6–2.0 (mean = 1.6).

Holotype. • 1♂, USA, Texas, Jim Hogg Co., 26 mi S Hebronville, 19 August 1955, 5–700 ft., T.J. Cohn. Deposited in the Mississippi Entomological Museum.

Specimens examined. Mᴇxɪᴄᴏ, **Tamaulipas:** • 12 mi S Nuevo Laredo, 9 July 1936, H.R. Roberts (1♂, 1♀) • Nuevo Leòn, 34 miles S Sabinas Hildalgo, 12 IX 1958, 1700 ft, T.J. Cohn (1♂, 1♀) • Mamulique Pass, 10 July 1936, 1800 ft, H.R. Roberts (2♀); 19 mi W Santa Catarina, 9 August 1959, T.J. Cohn (♂) • 6 mi SE Santiago, 29 September 1958.T.J. Cohn, 1550 ft (1♂, 1♀) • Villa de Santiago, 4 July 1964, T.J. Cohn (1♂).

Habitat. Cohn (1959) states the habitat at 19 mi W of Santa Catarina was above an arroyo in an area with large smooth margined leaved oaks and a variety of low bushes, succulents, broadleaf blackberry, and sparse but good weeds in clumps. The habitat at Villa de Santiago was rolling country in spined bushes that were fairly thick and more than 8 feet tall (Cohn 1964).

Distribution. Southern Texas and northeastern Mexico (Figs 25, 26B).

Etymology. The name *texmex* is a portmanteau of Texas and Mexico as this is the only known species of *Agroecotettix* that occurs in both countries.

Suggested common name. Texmex aridland scrub jumper.

Agroecotettix cumbres sp. nov.

https://zoobank.org/FEE97243-6929-491A-9BC4-7020291EAFD4
Figs 2F, 4F, 5F, 12A–J, 25, 26B

Diagnosis. Differentiated from other species in the genus by the combination of male cerci that have the lower branch longer than the dorsal branch (Figs 2F, 12A, B) and the male aedeagus that has a thickened sheath, valves that are longer than the sheath, and broad valves that have their distal half angled caudally (Figs 4F, 5F, 12C–G). Most similar to *A. texmex* but differs by having valves that are broader than that species both in lateral and caudal view (Figs 4D, E, 5D, E).

Male measurements (mm). (*n* = 4) Body length 21.3–23.5 (mean = 22.5); pronotum length 4.7–5.5 (mean = 5.0); tegmen length 3.2–4.2 (mean = 3.7); hind femur length 11.1–12.2 (mean = 11.8); cerci length 1.7–1.9 (mean = 1.8); basal width of cercus 0.5–0.6 (mean = 0.6); mid-cercal width 0.4–0.5 (mean = 0.5); cerci dorsal fork length 0.5–0.7 (mean = 0.6); cerci dorsal fork apex width 0.5–0.7 (mean = 0.6); cerci ventral fork length 0.7–0.9 (mean = 0.8); cerci ventral fork apex width 1.0 (mean = 1.0).
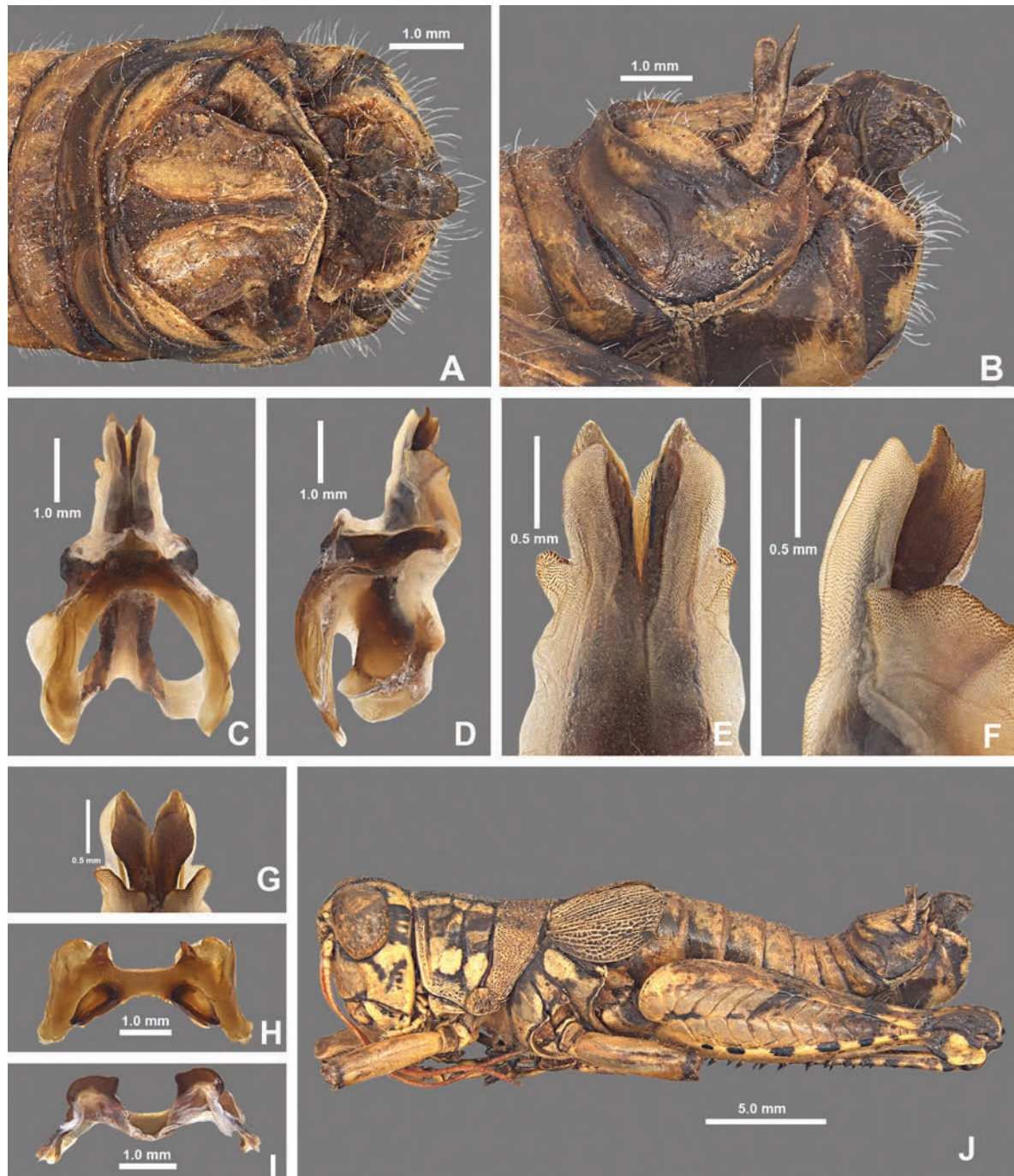
Figure 12. *Agroecotettix cumbres* **A** dorsal view of male terminalia **B** lateral view of male terminalia **C** dorsal view of phallic complex **D** lateral view of phallic complex **E** dorsal view of aedeagus **F** lateral view of aedeagus **G** caudal view of the aedeagus **H** dorsal view of epiphallus **I** caudal view of epiphallus **J** habitus.

Phallus measurements (mm). (*n* = 4) Length 0.6−0.8 (mean = 0.8); apex width 0.3−0.4 (mean = 0.4); middle width 0.5−0.6 (mean = 0.6); basal width 0.5 (mean = 0.5); lateral apex width 0.2−0.3 (mean = 0.3); lateral medial width 0.4−0.5 (mean = 0.5); lateral basal width 0.6 (mean = 0.6).

Female measurements (mm). (*n* = 11) Body length 24.1−28.0 (mean = 25.7); pronotum length 5.5−7.0 (mean = 6.4) tegmen length 4.0−5.0 (mean = 4.4); hind femur length 12.1−15.5 (mean = 14.3); dorsal ovipositor valve length 1.4−2.0 (mean = 1.7); ventral ovipositor valve length 1.4−2.0 (mean = 1.7).

Holotype. • 1♂, Mexico, Nuevo Leòn, 500–800 m. 24 mi NW Montemorelos, 3 Sept. 1955, T.J. Cohn. Deposited in the Mississippi Entomological Museum.

Specimens examined. Mexico, **Nuevo Leòn:** • 10 mi NW Montemorelos, 29 September 1958, T.J. Cohn, 2000 ft (1♂, 1♀) • 24 mi NW Montemorelos, 3 September 1955, T.J. Cohn (11♂, 2♀) • 5 mi SW Santiago, Horse Tail Falls, 29 September 1958. T.J. Cohn (1♂) • 6 mi SW Villa Santiago, 29 September 1958. T.J. Cohn (1♂, 3♀).

Distribution. Area to the south of Monterrey, Mexico and in and east of Monterrey Peaks (Figs 25, 26B).

Habitat. Cohn (1955) describes the locality at 24 mi NW Montemorelos as a rocky hillside with a draw and thorny bushes and at 6 mi SW Villa de Santiago as rolling as country in heavy spiney bushes, fairly thick and more than 8 ft tall. Cohn (1964) describes the locality at the Monterrey airport as badly overgrazed range, but with a good variety of green, thick, bushes, including fair-sized mesquite and other leguminous trees, soil sloped.

Etymology. The specific epithet *cumbres* is the Spanish word for summits and is in reference to the Parque Nacional Cumbres de Monterrey and the mountain summits near where this species found.

Suggested common name. Cumbres aridland scrub jumper.

Agroecotettix crypsidomus Hebard, 1922, stat. nov.
Figs 2G, 4G, 5G, 13A–J, 25, 26A, 31A–F

Agroecotettix modestus crypsidomus Hebard, 1922. Trans. Amer. Entomol. Soc. 48(1): 53.

Diagnosis. Differentiated from other species in the genus by the combination of male cerci with ventral branch equal or subequal in length to dorsal branch as in Fig. 2G; thin and lightly sclerotized sheath (Fig. 5H); valves of the aedeagus that are lobate with the basal lobe more produced in lateral view, extending beyond the sheath as in Fig. 4G, and with the dorsal lobe projected laterally in caudal view as in Fig. 5G.

Male measurements (mm). (n = 11) Body length 18.0–21.5 (mean = 23.8); pronotum length 4.2–5.5 (mean = 4.7); tegmen length 2.8–3.9 (mean = 3.3); hind femur length 9.6–11.7 (mean = 11.0); cerci length 1.2–1.5 (mean = 1.4); basal width of cercus 0.5–0.7 (mean = 0.6); mid-cercal width 0.3–0.5 (mean = 0.4); cerci dorsal fork length 0.4–0.6 (mean = 0.5); cerci dorsal fork apex width 0.2 (mean = 0.2) cerci ventral fork length 0.3–0.5 (mean = 0.4); cerci ventral fork apex width 0.1 (mean = 0.1).

Phallus measurements (mm). (n = 11) Length 1.0–1.1 (mean = 1.1); apex width 0.3–0.7 (mean = 0.5); middle width 0.4–0.5 (mean = 0.4); Basal width 0.6–0.7 (mean = 0.7); lateral apex width 0.4–0.6 (mean = 0.6); lateral medial width 0.5–0.6 (mean = 0.5); lateral basal width 0.5–0.7 (mean = 0.6).

Female measurements (mm). (n = 14) Body length 21.0–25.7 (mean = 23.8); pronotum length 4.9–6.7 (mean = 5.8) tegmen length 3.1–4.5 (mean = 3.9); hind femur length 11.3–14.8 (mean = 13.2); Dorsal ovipositor valve length 0.9–2.0 (mean = 1.6); ventral ovipositor valve length 0.9–2.0 (mean = 1.6).
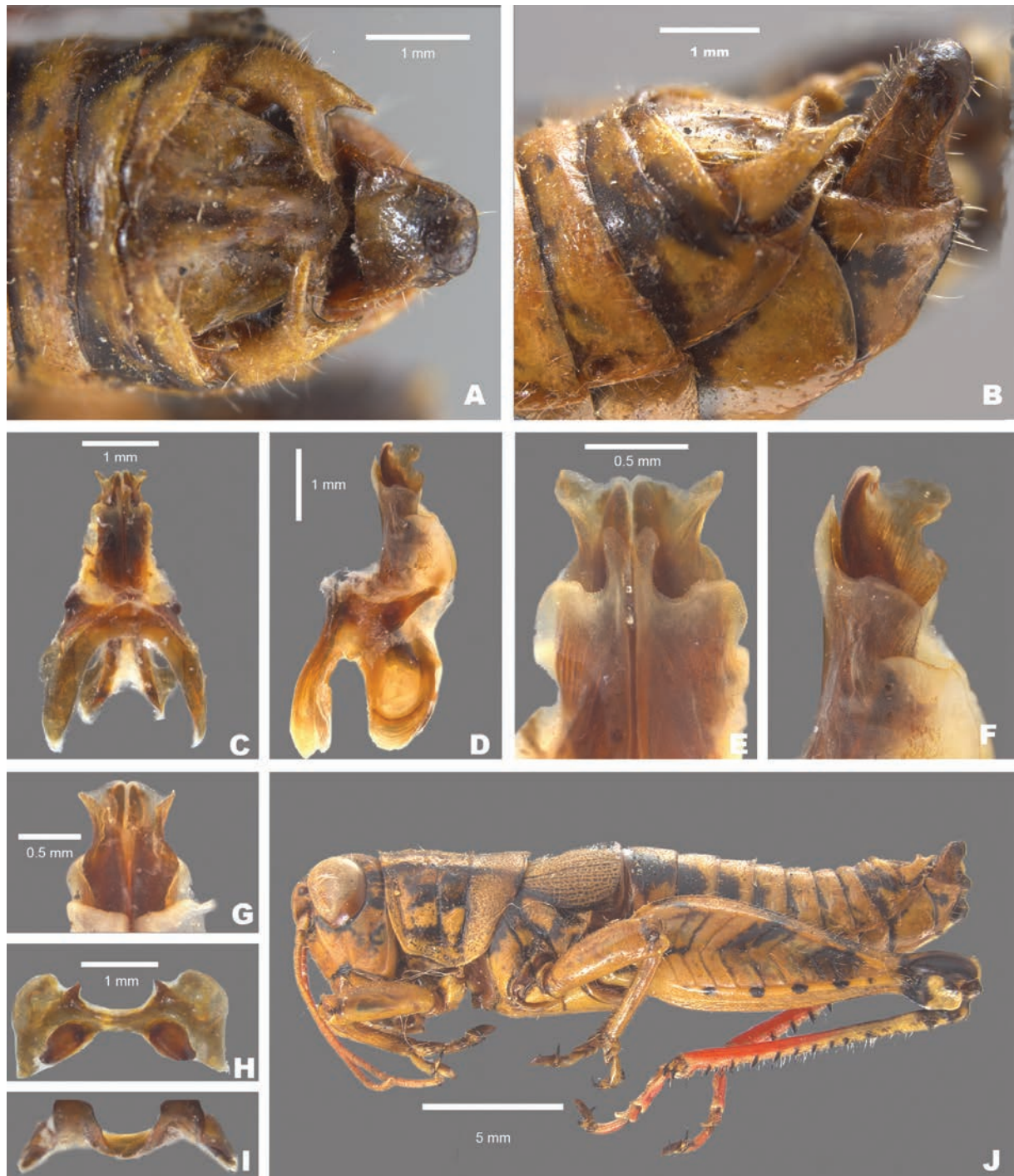
Figure 13. *Agroecotettix crypsidomus* **A** dorsal view of male terminalia **B** lateral view of male terminalia **C** dorsal view of phallic complex **D** lateral view of phallic complex **E** dorsal view of aedeagus **F** lateral view of aedeagus **G** caudal view of the aedeagus **H** dorsal view of epiphallus **I** caudal view of epiphallus **J** habitus.

Holotype examined. • 1♂, USA, Texas, Marathon, Brewster Co., Sept. 12–13, 1912, Rehn and Hebard, 2000–4160 ft. Deposited in the Academy of Natural Sciences of Drexel University.

Specimens examined. USA, **Texas:** • Garden Springs, 2 September 1912, Rehn and Hebard (1♂, 1♀) • 4 mi S Marathon, 11 October 1952, M.J.D. White (3♀) • 4.3 mi S Marathon, 30.1530, -103.2865, 13 July 2023, J.G. Hill, J.L. Seltzer (2♂, 2♀) • Marathon, 12–13 September 1912, Rehn and Hebard (9♂, 9♀).

Habitat. Chihuahuan Desert scrub, often associated with thorny shrubs such as *Acacia* (Fig. 31A–F).

Distribution. Found in the vicinity of Marathon, Texas and the Marathon basin (Figs 25, 26A).

Note. Given that the only known specimen of *A. modestus* is female and it is a distributional outlier, with other species occurring between its distribution and that of its subspecies, *A. modestus* was raised to species level above. Additionally, due to the differences in the internal male genitalia, *A. aristus* and *A. crypsidomus* are each raised to species level.

Etymology. *crypsi* Greek = hidden, *domus* Latin = home: in reference to the cryptic nature of the species living in the inner branches of thorny shrubs.

Suggested common name. Seclusive aridland scrub jumper.

Agroecotettix burtoni sp. nov.

https://zoobank.org/3021D508-7E34-41ED-8AE8-1E18BC603211
Figs 2J, 4H, 5H, 14A–J, 25, 26A, 31A–D

Diagnosis. Differentiated from other species in the genus by the combination of male cerci with ventral branch equal or subequal in length to dorsal branch (Figs 2J, 14A, B), a thin and lightly sclerotized sheath of aedeagus (Figs 5H, 14C–G); valves of the aedeagus lobate in lateral view with the basal lobe not produced much beyond the sheath in lateral view (Figs 5H, 14D, F) and with the valves not projected laterally in caudal view, being almost vertical or curving medially (Fig. 5H, 14G).

Male measurements (mm). (*n* = 10) Body length 19.5–24.0 (mean = 21.6); pronotum length 4.0–5.0 (mean = 4.6); tegmen length 3.0–4.0 (mean = 3.5); hind femur length 10.5–12.4 (mean = 11.3); cerci length 1.0–1.3 (mean = 1.2); basal width of cercus 0.5–0.6 (mean = 0.6); mid-cercal width 0.3–0.5 (mean = 0.4); cerci ventral projection length 0.3–0.4 (mean = 0.3); cerci ventral projection apex width 0.1 (mean = 0.1) cerci dorsal projection length 0.3–0.4 (mean = 0.3); cerci dorsal projection apex width 0.2–0.3 (mean = 0.2).

Phallus measurements (mm). (*n* = 3) Length 1.1 (mean = 1.1); apex width 0.5 (mean = 0.5); middle width 0.5 (mean = 0.5); Basal width 0.7 (mean = 0.7); lateral apex width 0.5–0.6 (mean = 0.6); lateral medial width 0.4–0.5 (mean = 0.4); lateral basal width 0.4–0.5 (mean = 0.5).

Female measurements (mm). (*n* = 6) Body length 24.0–29.9 (mean = 25.9); pronotum length 5.5–6.5 (mean = 5.8); tegmen length 3.5–4.5 (mean = 4.1); hind femur length 13.0–14.5 (mean = 13.9) dorsal ovipositor valve length 1.5–2.0 (mean = 1.7); ventral ovipositor valve length 1.5–2.0 (mean = 1.7).

Holotype. • 1♂, USA, Texas, Brewster Co., Big Bend N.P., 29.3178, -103.3942, 15 July 2023, J.G. Hill; Collected in Chihuahuan Desert scrub. Deposited in the Mississippi Entomological Museum.

Specimens examined. USA, **Texas:** • Brewster Co., Big Bend N.P., 29.3988, -103.2029, 14 July 2023, J.G. Hill, R.C. Seltzer-Hill (1♂) • Big Bend N.P., 29.3178, -103.3942, 15 July 2023, J.G. Hill (2♀) • 1.4 mi NE Government Springs Junction Big Ben Park, 12 June 1961, T.J. and J.W. Cohn (2♂) • Basin, 8 September 1951, T.J. Cohn (1♂) • Glenn Spring, 1 August 1928, F.M. Gaige (6♂, 3♀).
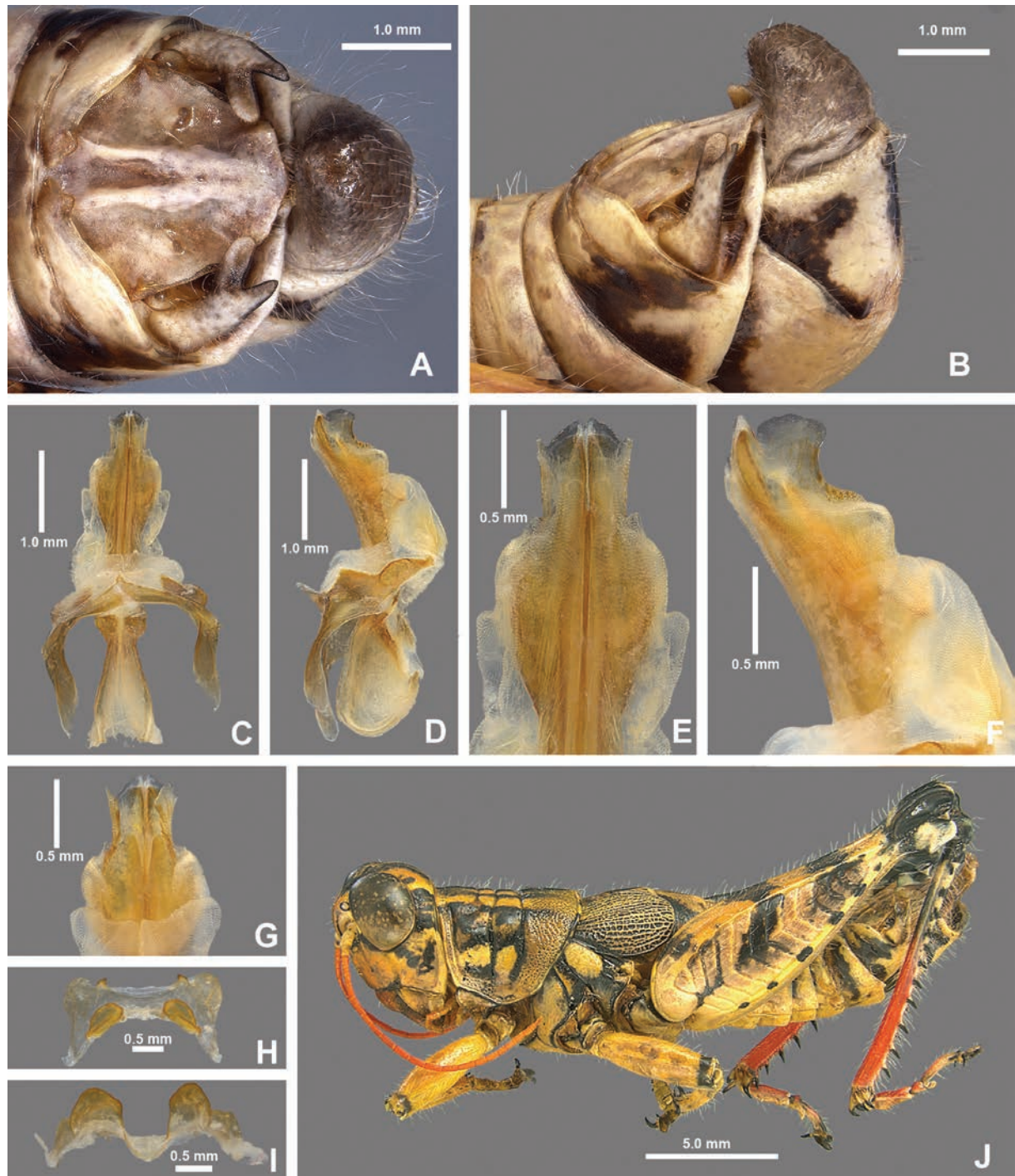
Habitat. Chihuahuan Desert Scrub (Fig. 31A).

Figure 14. *Agroecotettix burtoni* **A** dorsal view of male terminalia **B** lateral view of male terminalia **C** dorsal view of phallic complex **D** lateral view of phallic complex **E** dorsal view of aedeagus **F** lateral view of aedeagus **G** caudal view of the aedeagus **H** dorsal view of epiphallus **I** caudal view of epiphallus **J** habitus.

Distribution. Endemic to the Chihuahuan desert and more specifically to the southern big bend region of Texas (Figs 25, 26A). At present, all known populations occur within Big Bend National Park.

Etymology. The species name *burtoni* is a patronym honoring LeVar Burton, an iconic American actor, director, and children's television host renowned for his influential work in promoting literacy and education, particularly through his long-running role as the host of "Reading Rainbow." Additionally, Burton is

celebrated for his inspirational portrayal of Lieutenant Commander Geordi La Forge in "Star Trek: The Next Generation" and its spin-offs. His contributions to education and his advocacy for intellectual and cultural enrichment make him a fitting namesake for a species that thrives in the Big Bend region of Texas where deep history, nature, and vast starry skies come together in a unique American landscape.

Suggested common name. Burton's aridland scrub jumper.

Agroecotettix moorei sp. nov.

https://zoobank.org/9A4847D5-CC4C-4F38-98FA-34CDB373A25C

Figs 2M, 4I, 5I, 15A−J, 25, 26A, 32A−D

Diagnosis. Differentiated from other species in the genus by the combination of male cerci with ventral branch equal or subequal in length to dorsal branch (Figs 2L, 15A, B); sheath of aedeagus thin and lightly sclerotized (Fig. 5I); valves of the aedeagus are lobate and in lateral view, are shallowly incised with a broad distal lobe that is truncated apically, and the basal lobe is shorter (Figs 5I, 15D, F); in caudal view the valves of the aedeagus are concave as in Fig. 4I. Most like *A. crypsidomus* but differs in shape of the dorsal valves of the male aedeagus which with the broad distal lobe being distinctive for *A. moorei*. Furthermore, when viewed from above the inner margins of the valves of *A. moorei* form a right angle as opposed to being broadly rounded in *A. crypsidomus*.

Male measurements (mm). (*n* = 8) Body length 18.5−24.0 (mean = 20.2); pronotum length 4.3−5.0 (mean = 4.6); tegmen length 2.6−3.5 (mean = 3.0); hind femur length 10.0−12.1 (mean = 10.8); cerci length 1.2−1.3 (mean = 1.3); basal width of cercus 0.5 (mean = 0.5); mid-cercal width 0.3−0.5 (mean = 0.4); cerci dorsal fork length 0.3−0.5 (mean = 0.4); cerci dorsal fork apex width 0.2−0.3 (mean = 0.6) cerci ventral fork length 0.3−0.5 (mean = 0.4); cerci ventral fork apex width 0.1 (mean = 0.1).

Phallus measurements (mm). (*n* = 5) Length 0.9−1.0 (mean = 0.9); apex width 0.5−0.6 (mean = 0.5); middle width 0.4−0.5 (mean = 0.5); Basal width 0.7 (mean = 0.7); lateral apex width 0.4−0.6 (mean = 0.5); lateral medial width 0.5−0.8 (mean = 0.6); lateral basal width 0.6−0.7 (mean = 0.6).

Female measurements (mm). (*n* = 4) Body length 16.2−27.0 (mean = 22.1); pronotum length 4.8−6.5 (mean = 5.6) tegmen length 3.0−4.3 (mean = 3.6); hind femur length 10.8−14.2 (mean = 12.5); Dorsal ovipositor valve length 1.2−1.4 (mean = 1.3); ventral ovipositor valve length 1.2−1.4 (mean = 1.3).

Holotype. • 1♂, USA, Texas, Terrel Co., Sanderson, 30.1485, -102.3977, 30 Jul 2021, J.G. Hill, Collected in Chihuahuan desert. Deposited in the Mississippi Entomological Museum.

Specimens examined. USA, **Texas**: • Terrell Co. Sanderson, 25 August 1912, Rehn and Hebard, 2750−3180′ (4♂, 4♀) • Sanderson, 30.1458, -102.3977, 30 July 2021, Z.D. Brown, (1♂, 1♀).

Habitat. Chihuahuan desert scrub (Fig. 32D).

Distribution. Apparently, a narrow range endemic species that is restricted to the area around Sanderson, Texas in the Chihuahuan Desert (Figs 25, 26A).
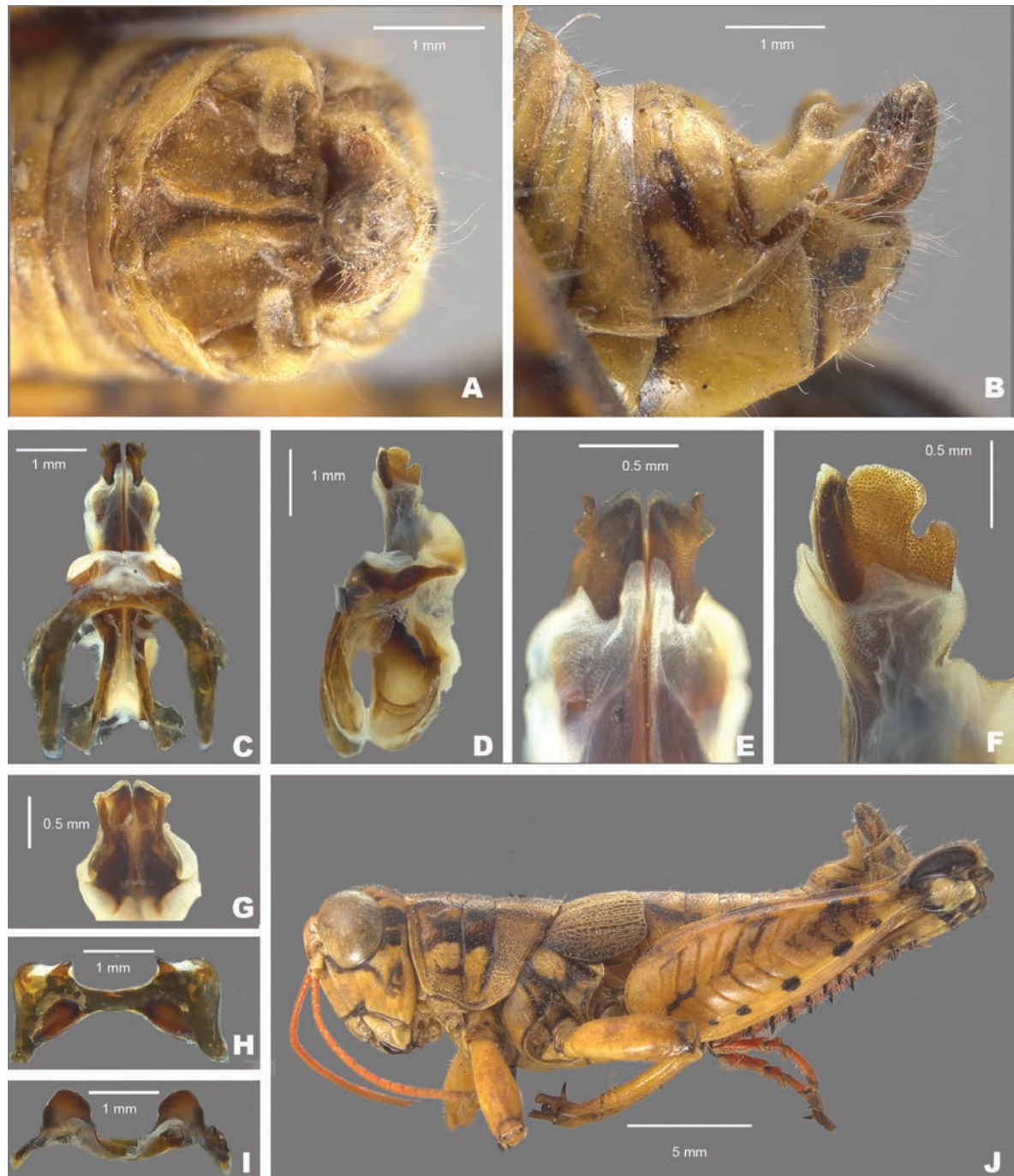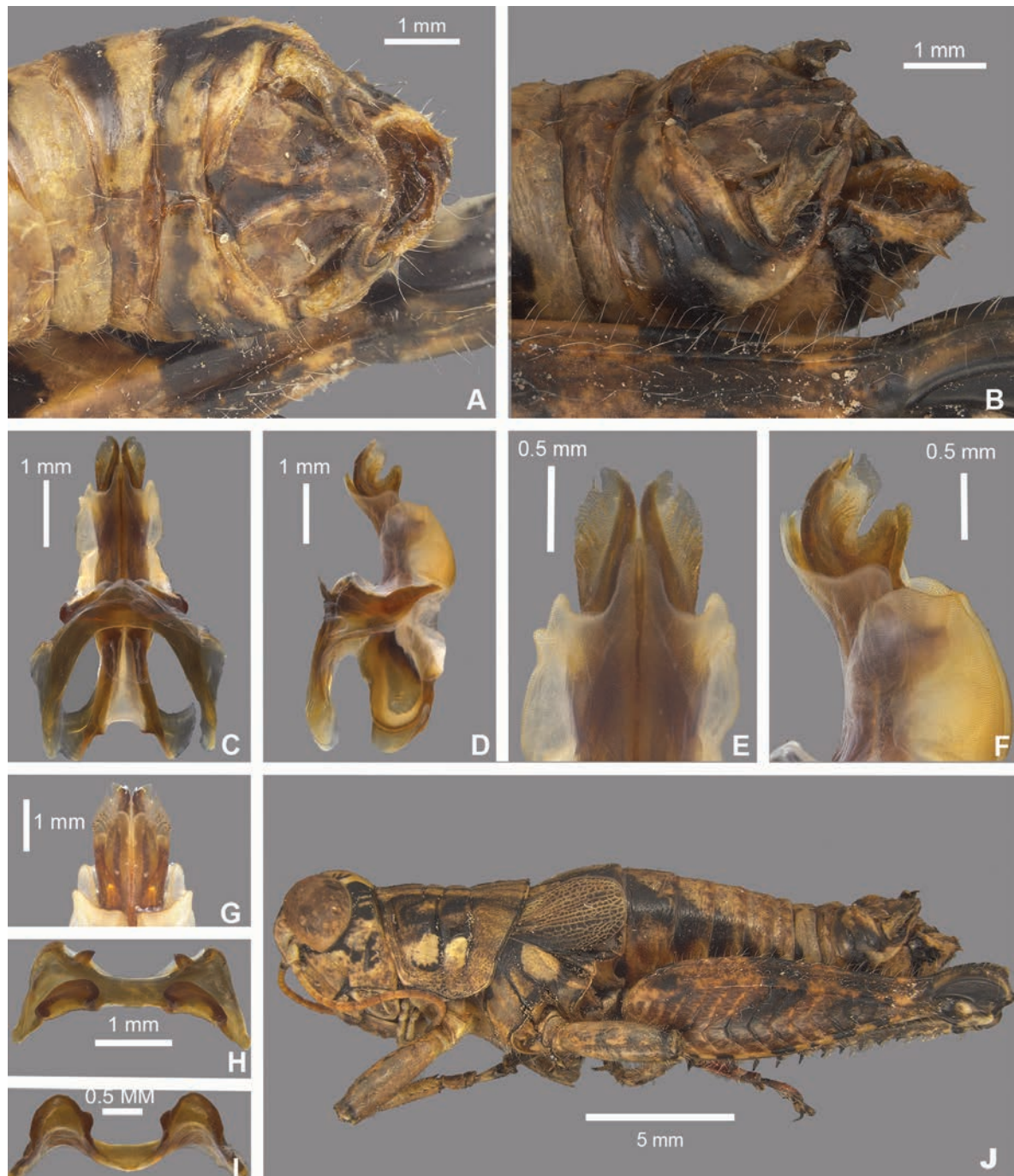
Figure 15. *Agroecotettix moorei* **A** dorsal view of male terminalia **B** lateral view of male terminalia **C** dorsal view of phallic complex **D** lateral view of phallic complex **E** dorsal view of aedeagus **F** lateral view of aedeagus **G** caudal view of the aedeagus **H** dorsal view of epiphallus **I** caudal view of epiphallus **J** habitus.

Etymology. The species name *moorei* is a patronym honoring Clayton Moore, the American actor who most famously starred as a fictional Texas Ranger in "The Lone Ranger" television series from 1949–1957. Moore's portrayal of the character embodied qualities of justice, bravery, and a deep connection to the American West. This naming honors Moore's cultural impact and the desert landscapes that inspired Moore's legendary character.

Suggested common name. Moore's aridland scrub jumper.

Agroecotettix chiantiensis sp. nov.

https://zoobank.org/0F102A87-0418-4C34-BB5B-EBF28D8CC9DE
Figs 2N, 4J, 5J, 16A–J, 25, 26A, 33A–C

Diagnosis. Differentiated from other species in the genus by the combination of male cerci with ventral branch equal or subequal in length to dorsal branch (Figs 2N, 15A, B); sheath of aedeagus thin and lightly sclerotized (Fig. 5J); valves of the aedeagus are lobate, and in lateral view, are deeply incised with

Figure 16. *Agroecotettix chiantiensis* **A** dorsal view of male terminalia **B** lateral view of male terminalia **C** dorsal view of phallic complex **D** lateral view of phallic complex **E** dorsal view of aedeagus **F** lateral view of aedeagus **G** caudal view of the aedeagus **H** dorsal view of epiphallus **I** caudal view of epiphallus **J** habitus.

a narrower and slightly acute distal lobe and a longer basal lobe as in Figs 5J, 16D, F); in caudal view the valves of the aedeagus are convex as in Figs 4J, 15G).

Male measurements (mm). (*n* = 1) Body length 20.5; pronotum length 4.2; tegmen length 3.2; hind femur length 11.2; cerci length 1.1; basal width of cercus 0.5; mid-cercal width 0.4; cerci dorsal fork length 0.3; cerci dorsal fork apex width 0.2; cerci ventral fork length 0.2; cerci ventral fork apex width 1.

Phallus measurements (mm). (*n* = 1) Length 1; apex width 0.4; middle width 0.4; basal width 0.6; lateral apex width 0.5; lateral medial width 0.7; lateral basal width 0.7.

Female measurements (mm). (*n* = 1) Body length 25.1; pronotum length 6.2; tegmen length 3.7; hind femur length 15.1; dorsal ovipositor valve length 2; ventral ovipositor valve length 2.

Holotype. • 1♂, USA, Texas, Presidio Co., 32 mi SW Marfa, 30.0488, -104.4663, 15 July 2023, J.G. Hill, thorny shrub in Chihuahuan Desert, Chianti Mountains. Deposited in the Mississippi Entomological Museum.

Specimens examined. USA, **Texas:** • Presidio Co.; Chianti Mountains, 30 September 1928, E.R. Tinkham, (1♀) • 2.3 mi S Shafter, 23 July 1956, T.J. Cohn, B. Mathews (1♂) • Shafter cemetery, 29.8112, -104.3058, 28 September 2024, J.G. Hill, J.L. Seltzer (1♀).

Habitat. Chihuahuan Desert Scrub (Fig. 33C) on leguminous shrubs and *Yucca*. Cohn (1956) describes the habitat at 2.3 mi S Shafter as "rocky foothills of the Chiantis on Spanish bayonet [*Yucca* sp.]".

Distribution. Known only from the Chianti Mountains of southwest Texas (Figs 25, 26A).

Etymology. The species name *chiantiensis* is derived from the Chianti Mountains where the species is apparently endemic to and the suffix "-ensis" (Latin) meaning "originating from" or "inhabiting". This name reflects the endemic nature of the species and hopefully draws attention to the importance of conservation of the unique biodiversity in this understudied mountainous region.

Suggested common name. Chianti aridland scrub jumper.

Agroecotettix dorni sp. nov.

https://zoobank.org/B2B38F60-80C4-4F45-8339-3A0C370D2655
Figs 2I, 4M, 5M, 17A–J, 25, 26A, 34A–D

Diagnosis. Differentiated from other species in the genus by the combination of male cerci with ventral branch equal or subequal in length to dorsal (Figs 2I, 17A, B); sheath of aedeagus thin and lightly sclerotized (Figs 5M, 17C–F); valves of the aedeagus are lobate, and in lateral view, the valves are thinly falcate, long and sword-like (Figs 5M, 17D, F), and in caudal view the lateral margins extend well beyond the rest of the valves and their apical margins are slightly curved distally (Figs 4M, 17G).

Male measurements (mm). (*n* = 4) Body length 18.5–19.9 (mean = 19.2); pronotum length 4.1–4.5 (mean = 4.3); tegmen length 2.5–3.0 (mean = 2.8); hind femur length 10.7–11.0 (mean = 10.9); cerci length 1.2 (mean = 1.2); basal width of cercus 0.5–0.6 (mean = 0.6); mid-cercal width 0.4 (mean = 0.4); cerci dorsal fork length 0.3 (mean = 0.3); cerci dorsal fork apex width 0.3 (mean = 0.3) cerci ventral fork length 0.3 (mean = 0.3); cerci ventral fork apex width 0.2 (mean = 0.2).
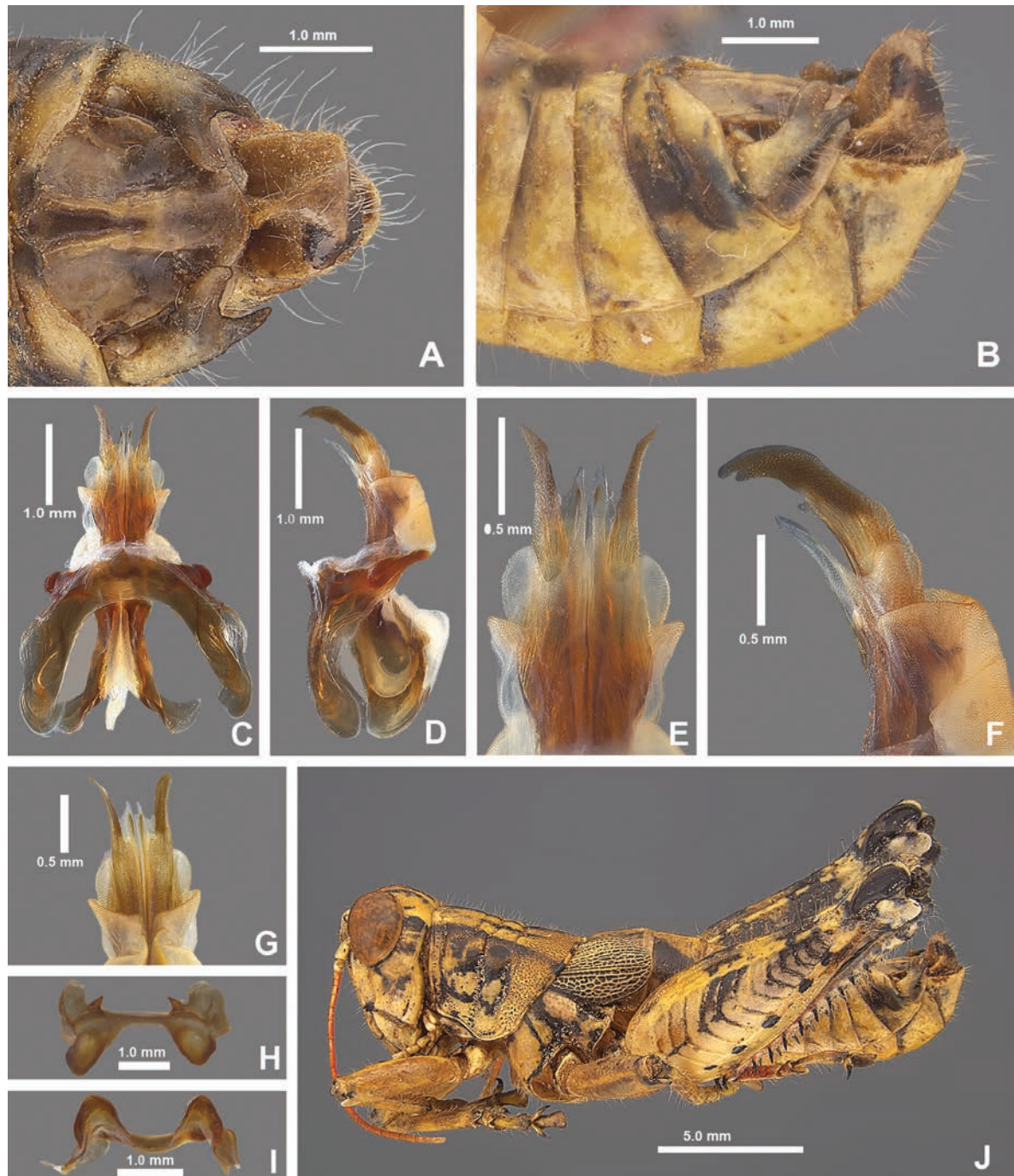
Figure 17. *Agroecotettix dorni* **A** dorsal view of male terminalia **B** lateral view of male terminalia **C** dorsal view of phallic complex **D** lateral view of phallic complex **E** dorsal view of aedeagus **F** lateral view of aedeagus **G** caudal view of the aedeagus **H** dorsal view of epiphallus **I** caudal view of epiphallus **J** habitus.

Phallus measurements (mm). (*n* = 2) Length 1.0 (mean = 1.0); apex width 0.4 (mean = 0.4); middle width 0.4 (mean = 0.4); Basal width 0.6−0.7 (mean = 0.7); lateral apex width 0.3 (mean = 0.3); lateral medial width 0.4 (mean = 0.4); lateral basal width 0.5 (mean = 0.5).

Female measurements (mm). (*n* = 4) Body length 22.0−25.5 (mean = 24.1); pronotum length 5.1−6.0 (mean = 5.7) tegmen length 3.4−4.2 (mean = 3.8); hind femur length 12.2−15.0 (mean = 14.0); Dorsal ovipositor valve length 1.3−1.7 (mean = 1.5); ventral ovipositor valve length 1.3−1.7 (mean = 1.5).

Holotype. • 1♂, USA, Texas, Brewster Co., Big Bend National Park, 29.1970, -102.9276, 14 July 2023, J.G. Hill, J.L. Seltzer; On shady side of sotol in mid-day heat, Boquillas Canyon. Deposited in the Mississippi Entomological Museum.

Specimens examined. USA, **Texas:** • Brewster Co., Big Bend National Park, 29.1970, -102.9276, 14 July 2023, J.G. Hill, J.L. Seltzer (2♂, 4♀) • Big Bend National Park, Boquillas Ranger Station, 28−30 July 1956, T.J. Cohn and Mathews (1♀) • same data as previous, except 9 June 1961, T.J. and J.W. Cohn (1♀).

Habitat. Chihuahuan Desert scrub (Fig. 33E). In July 2023 at the type locality, I observed this species roosting on the underside of *Dasylirion* leaves during the mid-day hours with *Netrosoma* and *Phaulotettix* species (Fig. 34A−D).

Distribution. Endemic to the Chihuahuan Desert and more specifically to the southern big bend region of Texas (Figs 25, 26A). At present, all known populations occur within Big Bend National Park.

Etymology. The species name *dorni* is a patronym honoring Michael Dorn, an American actor and narrator born in Texas who is most famous for portraying the Star Trek character Worf in the television series "Star Trek: The Next Generation" and its spin-offs. The name highlights a unique morphological characteristic of the species, drawing a creative parallel between the blade like aedeagus valves of the male genitalia and the form of the kur'leth, a traditional Klingon weapon used by Worf.

Suggested common name. Dorn's aridland scrub jumper.

Agroecotettix chisosensis **sp. nov.**
https://zoobank.org/8E0B8267-E724-4B1B-8B73-71676E40E530
Figs 2H, 4N, 5N, 18A−J, 25, 26A, 36A−E

Diagnosis. Differentiated from other species in the genus by the combination of male cerci with ventral branch equal or subequal in length to dorsal branch (Figs 2H, 18A, B); sheath of aedeagus thin and lightly sclerotized, (Fig. 5N); valves of the aedeagus are lobate, and in lateral view, the valves of aedeagus broad (Figs 5N, 18D, F) and in caudal view the lateral margins do not extend well beyond the rest of the valves and their apical margins are curved medially (Figs 4N, 18G).

Male measurements (mm). (n = 8) Body length 18.7−21.3 (mean = 19.9); pronotum length 4.5−4.9 (mean = 4.6); tegmen length 3.0−3.6 (mean = 3.2); hind femur length 10.3−11.5 (mean = 10.8); cerci length 1.1−1.2 (mean = 1.2); basal width of cercus 0.6−0.7 (mean = 0.6); mid-cercal width 0.3−0.4 (mean = 0.4); cerci dorsal fork length 0.4−0.5 (mean = 0.4); cerci dorsal fork apex width 0.2 (mean = 0.2) cerci ventral fork length 0.3 (mean = 0.3); cerci ventral fork apex width 0.1 (mean = 0.1).

Phallus measurements (mm). (n = 4) Length 0.9−1.1 (mean = 1.1); apex width 0.3−0.5 (mean = 0.4); middle width 0.4−0.6 (mean = 0.5); basal width 0.6 (mean = 0.6); lateral apex width 0.3−0.5 (mean = 0.4); lateral medial width 0.4−0.5 (mean = 0.4); lateral basal width 0.5 (mean = 0.5).

Female measurements (mm). (n = 5) Body length 23.5−26.8 (mean = 25.1); pronotum length 5.5−6.2 (mean = 5.8) tegmen length 3.5−4.5 (mean = 4.0); hind femur length 12.9−13.9 (mean = 13.5); Dorsal ovipositor valve length 1.5−2.0 (mean = 1.8); ventral ovipositor valve length 1.5−2.0 (mean = 1.8).
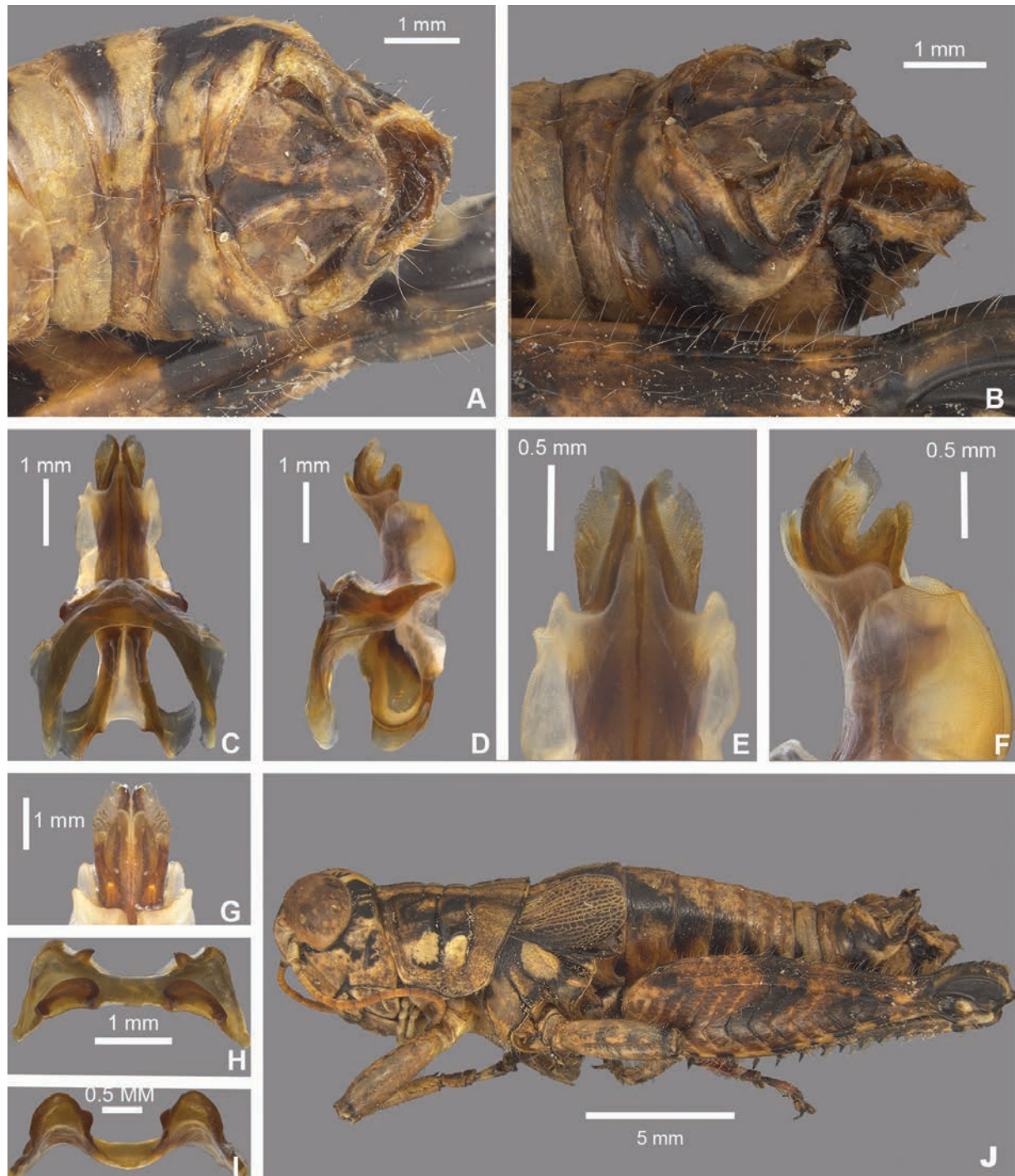
Figure 18. *Agroecotettix chisosensis* **A** dorsal view of male terminalia **B** lateral view of male terminalia **C** dorsal view of phallic complex **D** lateral view of phallic complex **E** dorsal view of aedeagus **F** lateral view of aedeagus **G** caudal view of the aedeagus **H** dorsal view of epiphallus **I** caudal view of epiphallus **J** habitus.

Holotype. • 1♂, USA, Texas, Brewster Co., Big Bend National Park, 29.2706, -103.3017, 14 July 2023, J.G. Hill; Chisos Mountain desert scrub, eating *Dasylirion* pollen. Deposited in the Mississippi Entomological Museum.

Specimens examined. USA, **Texas:** • Brewster Co., Big Bend National Park, 29.2706, -103.3017, 14 July 2023, J.G. Hill (3♂, 1♀) • Juniper Canyon, Chisos Mts, 16 July 1928, F.M. Gaige (2♀) • Canyon behind Pulliam Bluff, Chisos Mts., 7 September 1912, Rehn and Hebard, 4000−5000 ft (2♂, 2♀) • Chisos Mts, 12

August 1940, Rehn and Hebard (1♂, 1♀) • Neville Springs, 8 September 1912, Rehn and Hebard (1♂).

Habitat. Chihuahuan Desert scrub (Fig. 35F) in the Chisos Mountains. In July 2023 I observed the species eating *Dasylirion* pollen (Fig. 35D, E).

Distribution. Endemic to the Chisos Mountains in the Big Bend region of Texas (Figs 25, 26A).

Etymology. The species name *chisosensis* is derived from the Chisos Mountains where the species is apparently endemic to and the suffix "-ensis" (Latin) meaning "originating from" or "inhabiting". This name reflects the endemic nature of the species and hopefully draws attention to the importance of conservation of the unique biodiversity in this mountainous region.

Suggested common name. Chisos aridland scrub jumper.

Agroecotettix turneri sp. nov.

https://zoobank.org/C09F938B-B081-42DD-A82D-7A1A193957C9

Figs 2K, 4K, 5K, 19A–J, 25, 26A, 36A–D

Diagnosis. Differentiated from other species in the genus by the combination of male cerci with ventral branch equal or subequal in length to dorsal branch (Figs 2K, 19A, B); sheath of aedeagus thin and lightly sclerotized (Fig. 5M), and in lateral view, the valves of the aedeagus are entire (not lobate) with apices of point caudally (Figs 5K, 19D, F). In caudal view, lateral margins converge medially, giving a more pointed appearance (Figs 4N, 18G).

Male measurements (mm). (n = 3) Body length 14.3–19.3 (mean = 17.7); pronotum length 3.2–4.5 (mean = 4.0); tegmen length 2.3–4.5 (mean = 4.0); hind femur length 7.9–10.7 (mean = 9.8); cerci length 0.8–1.2 (mean = 9.8); basal width of cercus 0.5–0.6 (mean = 0.6); mid-cercal width 0.3–0.4 (mean = 0.4); cerci dorsal fork length 0.3 (mean = 0.3); cerci dorsal fork apex width 0.1 (mean = 0.1) cerci ventral fork length 0.3–0.4 (mean = 0); cerci ventral fork apex width 0.2 (mean = 0.2).

Phallus measurements (mm). (n = 3) Length 1.1 (mean = 1.1); apex width 0.3 (mean = 0.3); middle width 0.6 (mean = 0.6); Basal width 0.5–0.6 (mean = 0.6); lateral apex width 0.4 (mean = 0.4); lateral medial width 0.4 (mean = 0.4); lateral basal width 0.5 (mean = 0.5).

Female measurements (mm). (n = 6) Body length 17.1–26.5 (mean = 23.2); pronotum length 4.4–6.5 (mean = 5.6) tegmen length 2.2–4.4 (mean = 3.7); hind femur length 9.7–15.0 (mean = 12.9); Dorsal ovipositor valve length 0.9–2.5 (mean = 1.7); ventral ovipositor valve length 0.9–2.1 (mean = 1.5).

Holotype. • 1♂, USA, Texas, Brewster Co., 22 mi S of Alpine, 30.045026, -103.573517, 15 July 2023, J.G. Hill; Collected in Chihuahuan Desert scrub. Deposited in the Mississippi Entomological Museum.

Specimens examined. USA, **Texas:** • Brewster Co., Alpine, 21 August 1939, F.B. Isely (1♂, 4♀) • 22 mi S of Alpine, 30.045026, -103.573517, 15 July 2023, J.G. Hill (1♀) • "Big Bend" 23 June 1947, R.H. Beamer (1♂, 1♀).

Habitat. Chihuahuan Desert scrub on *Vachellia* sp. (Fig. 36D).

Distribution. Found in the area between Big Bend National Park and Alpine, Texas (Figs 25, 26A).

Etymology. The species name *turneri* is a patronym honoring Robert Edward "Ted" Turner III, an American media mogul and philanthropist renowned for his
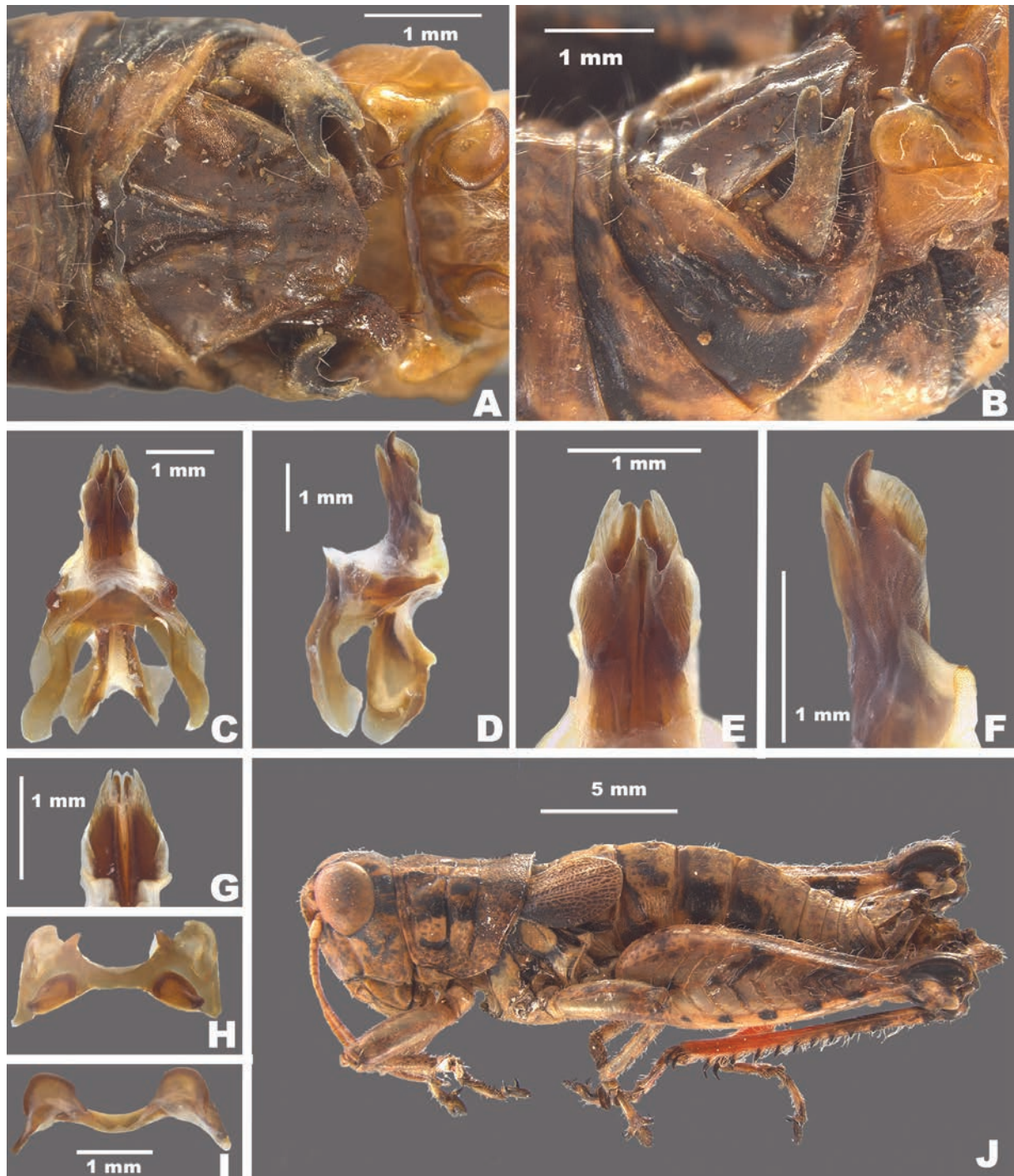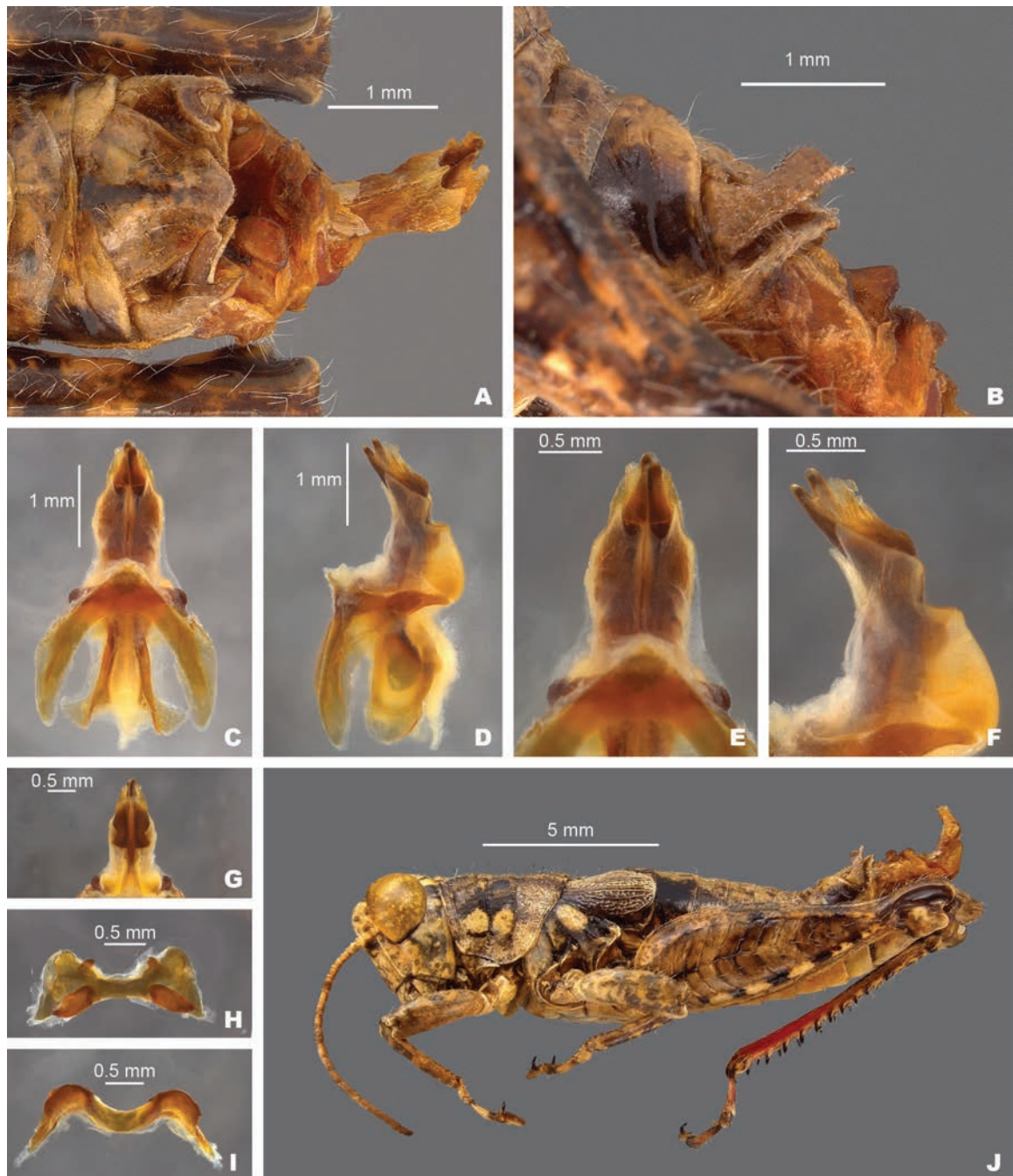
Figure 19. *Agroecotettix turneri* **A** dorsal view of male terminalia **B** lateral view of male terminalia **C** dorsal view of phallic complex **D** lateral view of phallic complex **E** dorsal view of aedeagus **F** lateral view of aedeagus **G** caudal view of the aedeagus **H** dorsal view of epiphallus **I** caudal view of epiphallus **J** habitus.

extensive contributions to environmental conservation. Turner, the founder of CNN and a major philanthropist, has been instrumental in numerous initiatives aimed at protecting the environment and biodiversity. His establishment of the Turner Endangered Species Fund and his efforts in large-scale land conservation have provided critical support for the preservation of diverse ecosystems, including those that likely sustain a great diversity of grasshopper species.

Suggested common name. Turner's aridland scrub jumper.

Agroecotettix quitmanensis sp. nov.

https://zoobank.org/8A91A6D1-09C0-4758-A4C7-C6B36C77ECEE
Figs 2L, 4P, 5P, 20A–J, 25, 26A

Diagnosis. Differentiated from other species in the genus by the combination of male cerci with ventral branch equal or subequal in length to dorsal branch as in Fig. 2; sheath of aedeagus thin and lightly sclerotized, as in Fig. 5L. In lateral view, the apical edge of the valves of the aedeagus are thickened finger-like projections that curve apically as in Fig. 5L.

Figure 20. *Agroecotettix quitmanensis* **A** dorsal view of male terminalia **B** lateral view of male terminalia **C** dorsal view of phallic complex **D** lateral view of phallic complex **E** dorsal view of aedeagus **F** lateral view of aedeagus **G** caudal view of the aedeagus **H** dorsal view of epiphallus **I** caudal view of epiphallus **J** habitus.

Male measurements (mm). (*n* = 1) Body length 17.4; pronotum length 4.0; tegmen length 2.7; hind femur length 9.7; cerci length 1.2; basal width of cercus 0.6; mid-cercal width 0.4; cerci dorsal fork length 0.4; cerci dorsal fork apex width 0.3; cerci ventral fork length 0.4; cerci ventral fork apex width 0.1.

Phallus measurements (mm). (*n* = 1) Length 1.2; apex width 0.4; middle width 0.6; basal width 0.8; lateral apex width 0.2; lateral medial width 0.4; lateral basal width 0.4.

Female measurements (mm). (*n* = 1) Body length 20.6; pronotum length 3.0; tegmen length 3.8; hind femur length 11.7; Dorsal ovipositor valve length 1.6; ventral ovipositor valve length 1.6.

Holotype examined. • 1♂, USA, Texas, Quitman Mountains, El Paso Co., Sept. 14, 1912, H.[ebard], 4800–5100 ft. Deposited in the Mississippi Entomological Museum.

Habitat. Unknown, but likely desert scrub as other species of the genus.

Distribution. Found in the vicinity of the Quitman Mountains of southwest Texas (Fig. 25A).

Etymology. The species name *quitmanensis* is derived from the Quitman Mountains where the species is apparently endemic to and the suffix "-ensis" (Latin) meaning "originating from" or "inhabiting". This name reflects the endemic nature of the species and hopefully draws attention to the importance of conservation of the unique biodiversity in this understudied mountainous region.

Suggested common name. Quitman aridland scrub jumper.

Agroecotettix vaquero sp. nov.

https://zoobank.org/FA1E3188-352E-4EEB-966E-02FBF0C56D0E
Figs 2T, 4P, 5P, 21A–J, 25

Diagnosis. Differentiated from other species in the genus by the combination of male cerci with the ventral branch reduced and rounded as in Fig. 2S; in lateral view, the sheath of the aedeagus is well developed and expanded laterally around the valves; the aedeagus valves are wide with their apices broadly curved in lateral view as in Fig. 5P; in caudal view the valves or greatly narrowed in their apical third as in Fig. 4P.

Male measurements (mm). (*n* = 17) Body length 21.2–25.2 (mean = 23.5); pronotum length 4.7–6.0 (mean = 5.4); tegmen length 2.7–4.1 (mean = 3.4); hind femur length 10.9–13.2 (mean = 12.1); cerci length 1.0–1.7 (mean = 1.3); basal width of cercus 0.5–0.7 (mean = 0.6); mid-cercal width 0.4–0.6 (mean = 0.5); cerci dorsal fork length 0.4–0.6 (mean = 0.5); cerci dorsal fork apex width 0.2–0.4 (mean = 0.3); cerci ventral fork length 0.1–0.3 (mean = 0.2); cerci ventral fork apex width 0.1 (mean = 0.1).

Phallus measurements (mm). (*n* = 4) Length 0.8–1.0 (mean = 1.0); apex width 0.3 (mean = 0.3); middle width 0.5 (mean = 0.5); basal width 0.6–0.7 (mean = 0.6); lateral apex width0.3–0.4 (mean = 0.4); lateral medial width 0.5–0.6 (mean = 0.5); lateral basal width 0.5 (mean = 0.5).

Female measurements (mm). (*n* = 17) Body length 24.5–29.9 (mean = 26.6); pronotum length 5.9–7.2 (mean = 6.5) tegmen length 3.1–4.8 (mean = 3.9); hind femur length 13.0–15.4 (mean = 14.3); dorsal ovipositor valve length 1.3–2.2 (mean = 1.7); ventral ovipositor valve length 1.2–2.2 (mean = 1.7).
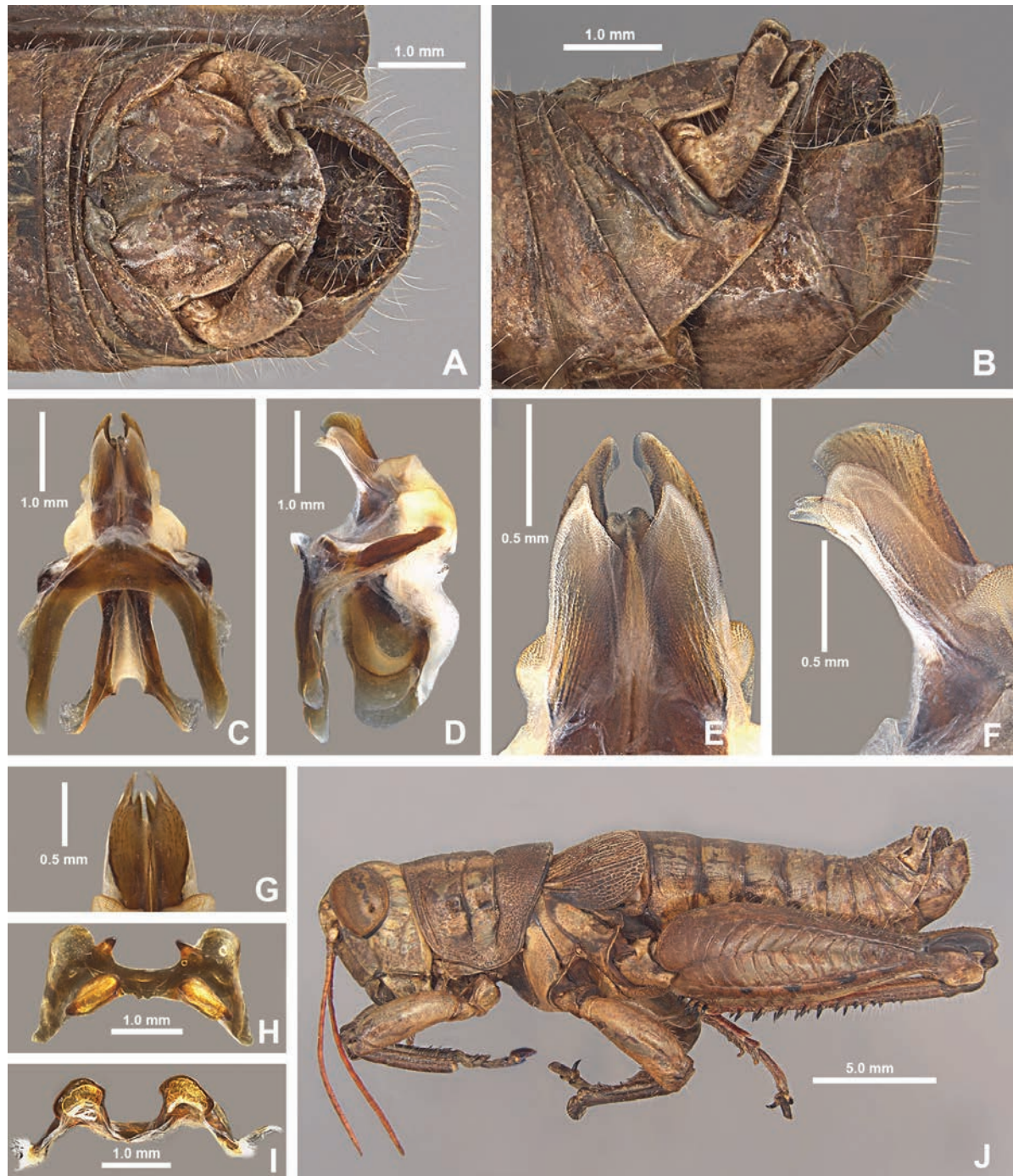
Figure 21. *Agroecotettix vaquero* **A** dorsal view of male terminalia **B** lateral view of male terminalia **C** dorsal view of phallic complex **D** lateral view of phallic complex **E** dorsal view of aedeagus **F** lateral view of aedeagus **G** caudal view of the aedeagus **H** dorsal view of epiphallus **I** caudal view of epiphallus **J** habitus.

Holotype. • 1♂, Mexico, Coahulla, 11 mi NW Muzquiz, 31 July 1959, 1550 ft, T.J. Cohn, #126, UMMZI-0058033. Deposited in the Mississippi Entomological Museum.

Specimens examined. Mexico: **Coahuila:** • 5.8 mi S Castaños, 20 August 1965, T.J. Cohn, 2700 ft, (3♂, 1♀) • 2 mi NW Hermanas, 19 September 1958 13−1400' T.J. Cohn (1♂) • 5 mi S Hermanas, 1 August 1959, T.J. Cohn, 1350 ft (1♂, 1♀) • 2 mi SE Muzquiz, 14 September 1958, T.J. Cohn, 3700 ft (3♂, 5♀) • 4 mi E Muzquiz, 1 August 1959, T.J. Cohn, 1600 ft (2♂, 2♀) • 2 mi SE Muzquiz, 14

September 1958, T.J. Cohn, 3700 ft. (2♂, 2♀) • 11 mi NW Muzquiz, 31 July 1959, T.J. Cohn, 1550 ft (3♂, 2♀) • San Juan de Sabinas-Rosita, 15–16 September 1958, T.J. Cohn, 1200 ft (5♂, 4♀).

Habitat. Cohn (1965) described the habitat at 5.8 mi S Castanos as low Mesquite, Creosote, *Vachellia rigidula*, and *Agave lechuguilla*.

Distribution. Found in northern Coahuila, Mexico (Fig. 25A).

Etymology. The species name *vaquero* is the Spanish word for cowboy.

Suggested common name. Vaquero aridland scrub jumper.

Agroecotettix forcipatus sp. nov.

https://zoobank.org/97EE7BEC-3C6A-44E2-B54D-EF09C9727251

Figs 2O, 4O, 5O, 22A–J, 25

Diagnosis. Differentiated from other species in the genus by the combination of male cerci with dorsal and ventral branches that are short but equal or subequal in length and widely separated as in Fig. 2N; sheath of aedeagus thin and lightly sclerotized (Fig. 5O); in lateral view, the valves of the aedeagus are acutely pointed apically and are greatly widened in their lower half; in caudal view the apical margins of the valves are slightly curved distally as in Fig. 4O.

Male measurements (mm). (*n* = 12) Body length 21.0–23.5 (mean = 22.1); pronotum length 4.3–5.5 (mean = 4.8); tegmen length 2.5–4.1 (mean = 3.3); hind femur length 10.6–12.2 (mean = 11.4); cerci length 1.2–1.5 (mean = 1.3); basal width of cercus 0.6–0.8 (mean = 0.7); mid-cercal width 0.3–0.5 (mean = 0.4); cerci dorsal fork length 0.3–0.4 (mean = 0.4); cerci dorsal fork apex width 0.2–0.3 (mean = 0.3); cerci ventral fork length 0.3–0.5 (mean = 0.4); cerci ventral fork apex width 0.1 (mean = 0.1).

Phallus measurements (mm). (*n* = 4) Length 1.3–1.4 (mean = 1.4); apex width 0.4–0.5 (mean = 0.5); middle width 0.5–0.6 (mean = 0.5); basal width 0.9–1.0 (mean = 1.0); lateral apex width 0.3–0.4 (mean = 0.3); lateral medial width 0.6 (mean = 0.6); lateral basal width 0.6–0.8 (mean = 0.7).

Female measurements (mm). (*n* = 10) Body length 24.0–27.5 (mean = 25.2); pronotum length 5.1–6.2 (mean = 5.6) tegmen length 3.5–4.2 (mean = 3.8); hind femur length 12.0–14.2 (mean = 13.3); dorsal ovipositor valve length 1.5–2.0 (mean = 1.6); ventral ovipositor valve length 1.5–2.0 (mean = 1.6).

Holotype. • 1♂, Mexico, Coahuila, 22.6 mi S Castaños, (11.2 mi N of San Lazaro), 19 August 1961, I.J. Cantrall, T.J. Cohn. UMMZI-00057993. Deposited in the Mississippi Entomological Museum.

Specimens examined. Mᴇxɪᴄᴏ, **Coahuila:** • 25 mi S Castaños, 3 August 1959, T.J. Cohn 3150 ft (8♂, 9♀) • 5 mi S Monolova, 2 August 1959, T.J. Cohn, 2300 ft (6♂, 2♀).

Habitat. Cohn (1959) described the habitat at 5 mi S. Monolova as rich lush desert, with very little grass consisting of a few species, but many types of succulent stem bushes in abundance along with leguminous bushes and broad leaf black berries.

Distribution. Found southern Coahuila, Mexico in the vicinity of the Sierra de la Gloria (Fig. 25A)

Etymology. *forceps* Latin = forceps, pincers and *atus* Latin = "provided with".

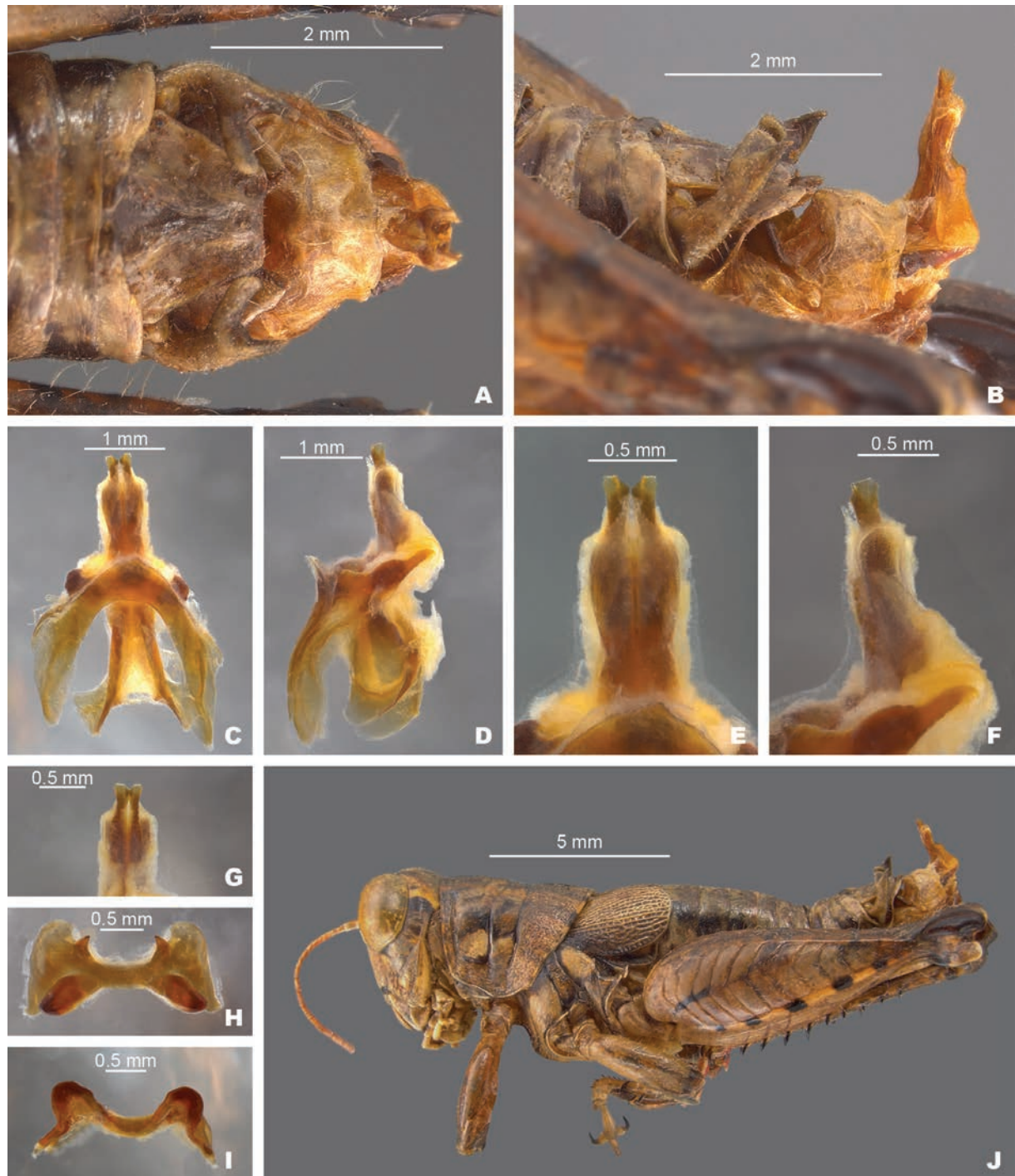**Suggested common name.** Pincered aridland scrub jumper.

Figure 22. *Agroecotettix forcipatus* **A** dorsal view of male terminalia **B** lateral view of male terminalia **C** dorsal view of phallic complex **D** lateral view of phallic complex **E** dorsal view of aedeagus **F** lateral view of aedeagus **G** caudal view of the aedeagus **H** dorsal view of epiphallus **I** caudal view of epiphallus **J** habitus.

Agroecotettix idic **sp. nov.**

https://zoobank.org/D4BF1146-CC49-4EFB-8C3A-C30C111200B5

Figs 2S, 4Q, 5Q, 23A–J, 25, 26B

Diagnosis. Differentiated from other species in the genus by the combination of male cerci that curve medially (Fig. 2Q) and with dorsal and ventral branches that are short but equal or subequal in length and widely separated as in Fig. 2R; in

Figure 23. *Agroecotettix idic* **A** dorsal view of male terminalia **B** lateral view of male terminalia **C** dorsal view of phallic complex **D** lateral view of phallic complex **E** dorsal view of aedeagus **F** lateral view of aedeagus **G** caudal view of the aedeagus **H** dorsal view of epiphallus **I** caudal view of epiphallus **J** habitus.

lateral view, the sheath of the aedeagus is thin and shorter than the valves; the aedeagus valves are the most diminutive of the genus and are rectangular in shape, the distal edge is edge truncate in lateral (Fig. 4Q) and in caudal view (Fig. 5Q).

Male measurements (mm). (*n* = 1) Body length 18.5; pronotum length 4.4; tegmen length 3.0; hind femur length 10.0; cerci length 1.5; basal width of cercus 0.6; mid-cercal width 0.5; cerci dorsal fork length 0.3; cerci dorsal fork apex width 0.3; cerci ventral fork length 0.5; cerci ventral fork apex width 0.1.

Phallus measurements (mm). (*n* = 1) Length 1.5; apex width 0.2; middle width 0.5; basal width 0.4; lateral apex width 0.2; lateral medial width 0.3; lateral basal width 0.4.

Female measurements (mm). (*n* = 1) Body length 24.2; pronotum length 5.7; tegmen length 3.5; hind femur length 12.5; dorsal ovipositor valve length 2.0; ventral ovipositor valve length 2.0.

Holotype. • 1♂, Mexico, Higueros, Coah., Mex. Bet. Monterrey and Saltillo, 4000', IX 14 1936, H.R. Roberts. Deposited in the Mississippi Entomological Museum.

Habitat. Unknown, but likely desert scrub as other species of the genus.

Distribution. Known only from the type locality (Fig. 25A, C).

Etymology. The species epithet *idic* references the IDIC principle from the Star Trek television series. IDIC stands for "Infinite Diversity in Infinite Combinations," a Vulcan philosophy celebrating the richness and complexity of the universe. This name pays homage to the Star Trek principle of embracing diversity and complexity and highlights the rich biodiversity found in Mexico, the native land of this grasshopper. It is hoped that this name encourages appreciation and protection of the diverse forms of life that coexist on our planet.

Suggested common name. Idic aridland scrub jumper.

Agroecotettix kahloae sp. nov.

https://zoobank.org/EAA95587-C4F7-4E95-83B3-42B6EFD80515

Figs 2Q, 4R, 5R, 24A–J, 25, 26B

Diagnosis. Differentiated from other species in the genus by the combination of male cerci that strongly curve medially as in Fig. 2Q, R; and with dorsal and ventral branches that are short but equal or subequal in length and widely separated (Fig. 2R); sheath of aedeagus thin and lightly sclerotized, as in Fig. 5R; in lateral view the valves of the aedeagus are broad and arching with the distal apices rounded as in Fig. 5R; in caudal view the valves are acuminate.

Male measurements (mm). (*n* = 1) Body length 18.5; pronotum length 4.2; tegmen length 2.7; hind femur length 9.9; cerci length 1.3; basal width of cercus 0.4; mid-cercal width 0.5; cerci dorsal fork length 0.4; cerci dorsal fork apex width 0.2; cerci ventral fork length 0.5; cerci ventral fork apex width 0.1.

Phallus measurements (mm). (*n* = 1) Length 1.2; apex width 0.2; middle width 0.5; basal width 0.8; lateral apex width 0.3; lateral medial width 0.4; lateral basal width 0.6.

Holotype. • 1♂, Mexico, Coahuila, 29 rd, mi SE Arteaga, 10 August 1959, 6150 ft., T.J. Cohn, #164. Deposited in the Mississippi Entomological Museum.

Habitat. None recorded.

Distribution. Known only from the type locality (Fig. 25A, C).

Etymology. The species name *kahloae* patronym honoring Frida Kahlo (1907–1954), the iconic Mexican painter known for her vivid deeply personal and symbolic artwork. Her enduring connection to Mexican culture makes her an apt figure to be commemorated through this species, which is endemic to Mexico. In naming a species in her honor I celebrate her artistic legacy and underscore the importance of preserving the biodiversity of her homeland.

Suggested common name. Kahlo's aridland scrub jumper.

Figure 24. *Agroecotettix kahloae* **A** dorsal view of male terminalia **B** lateral view of male terminalia **C** dorsal view of phallic complex **D** lateral view of phallic complex **E** dorsal view of aedeagus **F** lateral view of aedeagus **G** caudal view of the aedeagus **H** dorsal view of epiphallus **I** caudal view of epiphallus **J** habitus.

Discussion

The discovery of sixteen new species of *Agroecotettix*, predominantly comprising endemics of the Chihuahuan Desert, Sierra Madre Occidental, and the South Texas Plains, presents a significant advancement in our knowledge of desert biodiversity and the ecological complexity of this unique region. However, without population level genetic data, it is challenging to definitively pinpoint
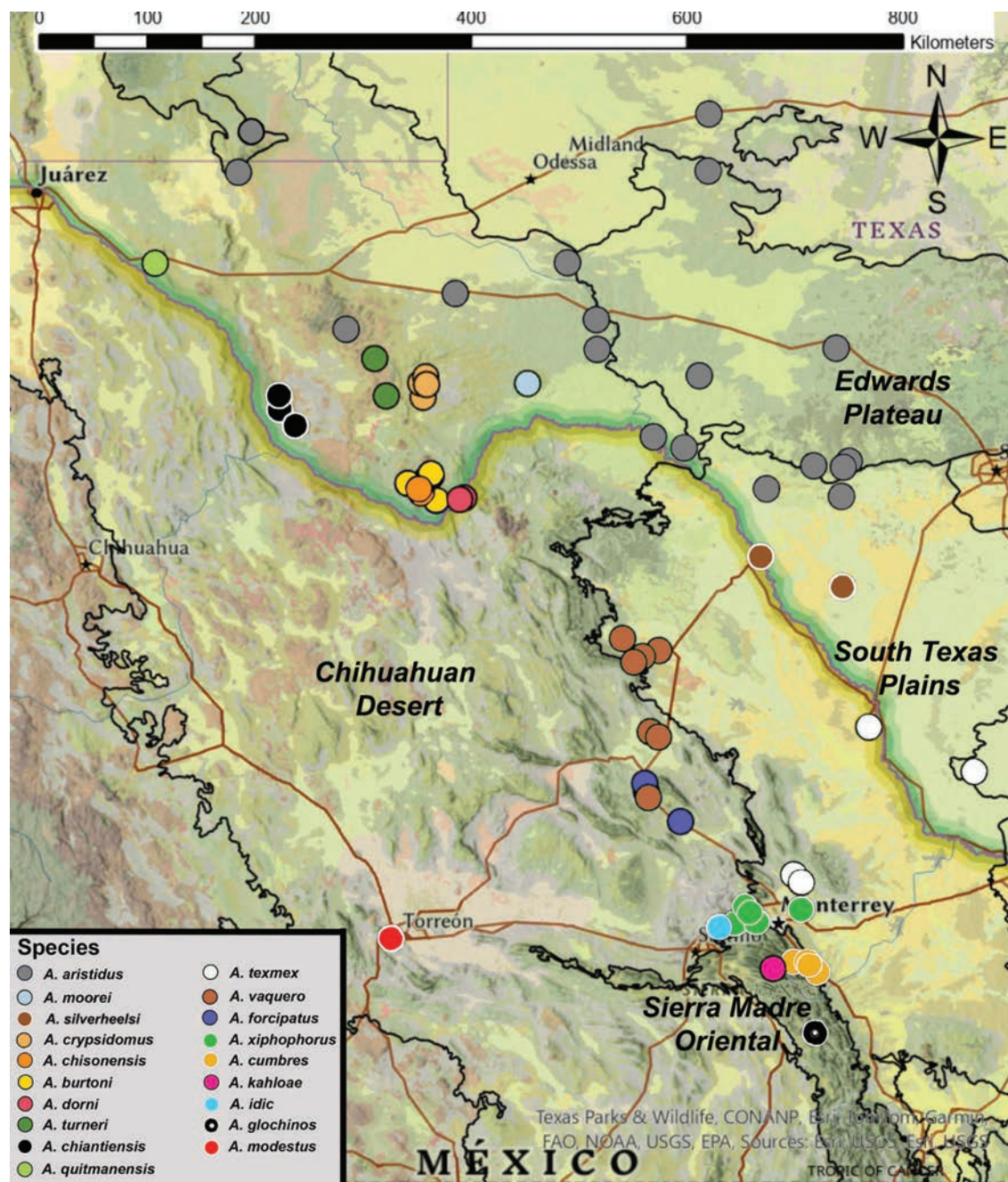
Figure 25. Distribution of *Agroecotettix* species.

the factors that led to the diversification and biogeographic patterns observed here. Evolution of other brachypterous groups of North American melanoplines were influenced by Pleistocene glacial cycles that impacted river flow, mountain ecosystems, and the isolation of islands/sand ridges, which resulted in population cycles of contraction, isolation, divergence, expansion, and secondary contact processes. (Knowles 2007; Woller 2017; Huang et al. 2020). Indeed, this may be case for *Agroecotettix* as well.

The Chihuahuan Desert (Fig. 25) stands out as the center of diversity for *Agroecotettix*, with eleven of the nineteen species inhabiting this area, nine of which are endemic. This desert, known for its biological diversity and vast expanse, hosts a rich variety of plant and animal life, including numerous en-
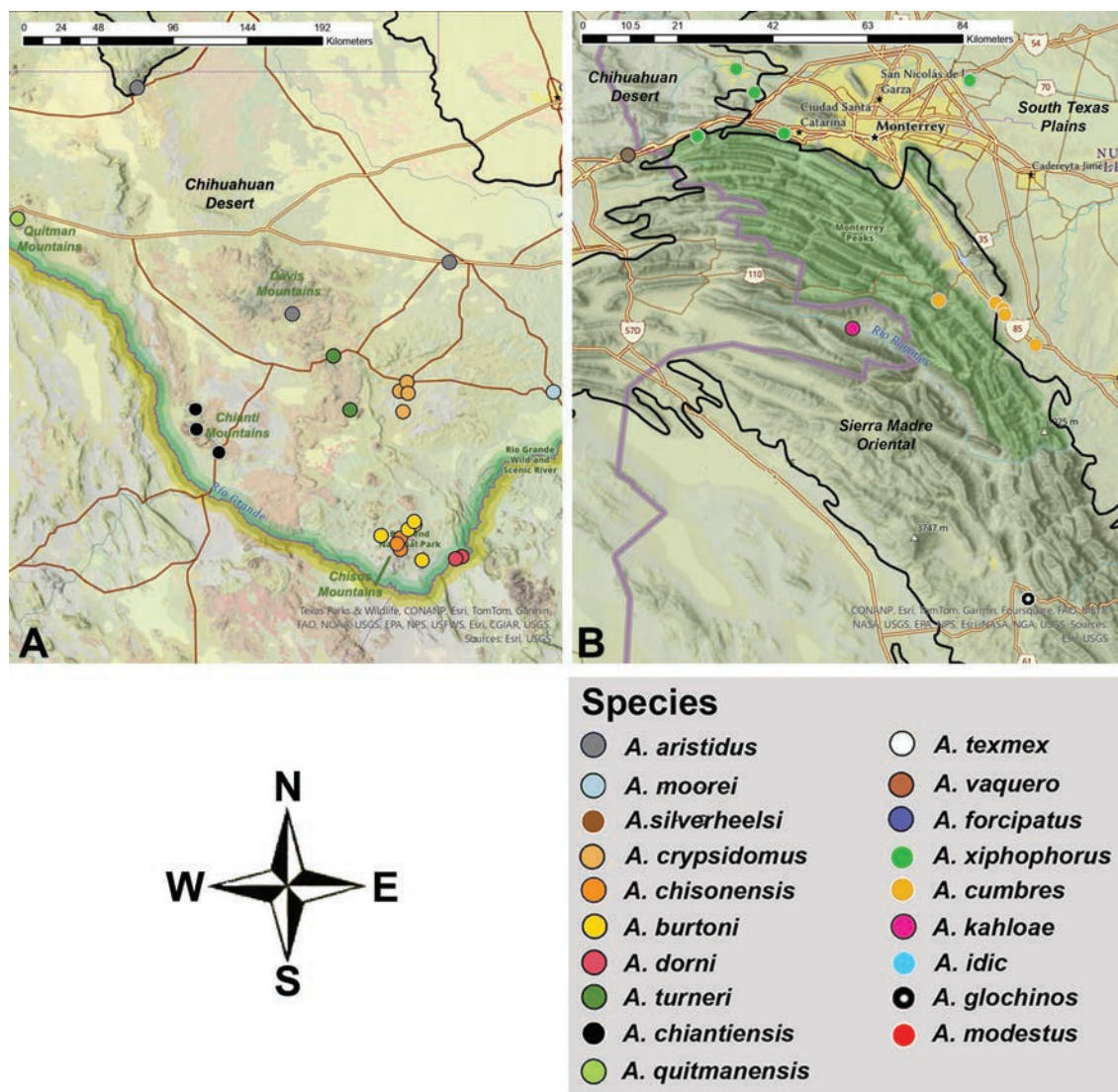
Figure 26. Distribution of *Agroecotettix* species **A** Big Bend region of Texas **B** zoom in on the area around Monterrey, Mexico at the convergence of the Chihuahuan Desert, Sierra Madre Oriental, and South Texas Plains ecoregions.

demics specially adapted to its arid conditions (Medellin-Leal 1982; Toledo and Ordóñez 1993; Villarreal-Quintanilla et al. 2017; Scheinvar et al. 2020).

Today, this desert is inhabited by a myriad of specialized plants and animals, including cacti, yuccas, reptiles, mammals, and a diverse array of invertebrates. However, during the Pleistocene, especially the Late Wisconsin (27,000–11,000 yr B.P.), the Chihuahuan Desert was a very different place. During that time, the area around Big Bend and the New Mexico/Arizona borderline were dominated by a woodland of paper-shell pinyon and juniper, and the Mapimian region vegetation assemblages were dominated by coniferous/juniper forest. The microphyllous Desertic Brushwood system that *Agroecotettix* is today associated with such as *Acacia* and sotol (*Dasylirion* spp.) as well as other characteristic Chihuahuan desert elements such as lechuguilla (*Agave lechuguilla*), and prickly pears (*Opuntia* spp.) was much rarer (Betancourt et al. 1990; Scheinvar et al. 2020). Establishment of Chihuahuan desert scrub as a dominant element was not recorded until 8,000–9,000 yr B.P. (Betancourt et al. 1990; Holmgren et al. 2003).
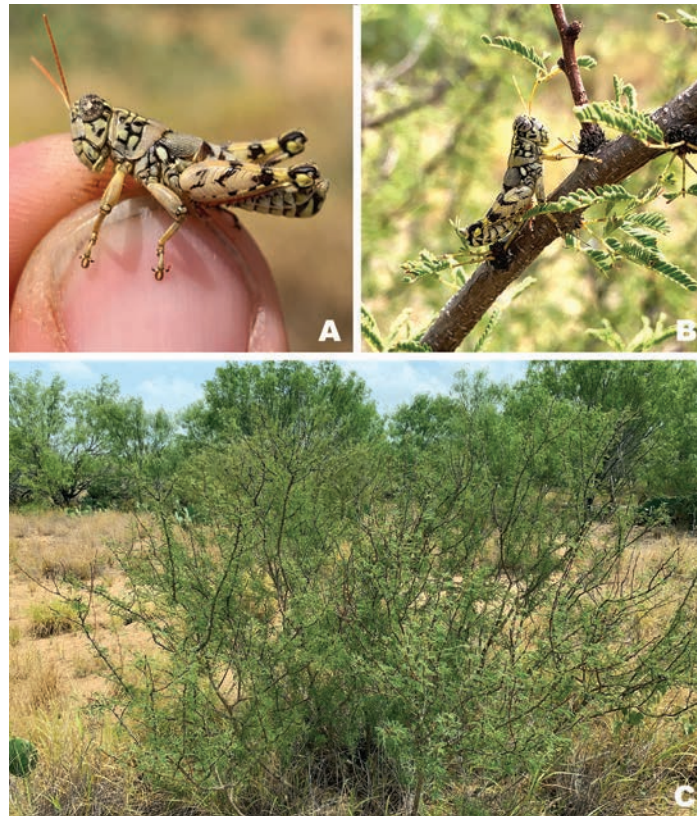
Figure 27. *Agroecotettix silverheelsi* from Dimmit Co, TX **A** male **B** male on interior *Vachellia* branch **C** *Vachellia* plant and habitat where the type specimen was collected.
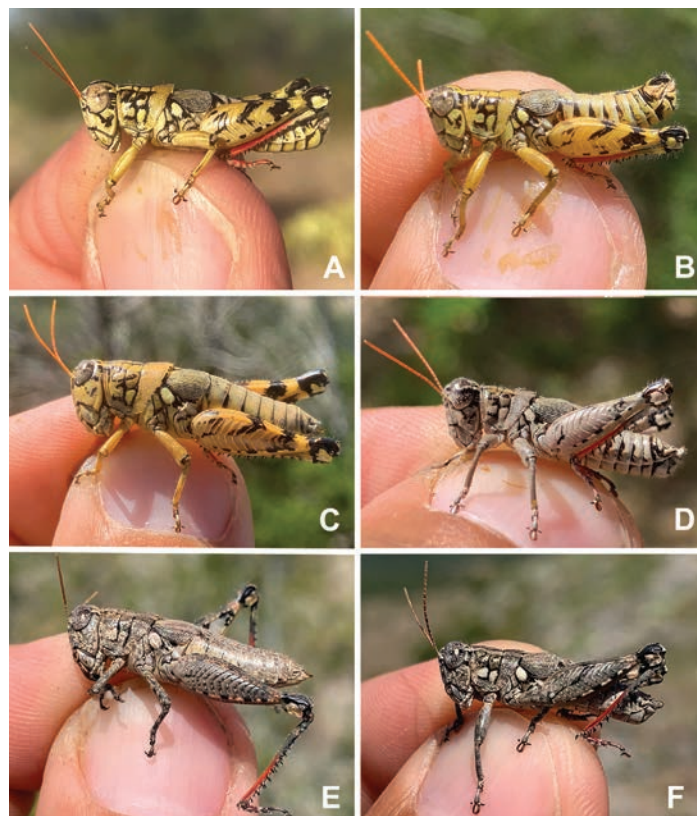
Figure 28. *Agroecotettix aristus* **A** male, Upton Co, TX **B** male, Edwards Co., TX **C** female, Edwards Co., TX **D** male Edwards Co., TX **E** female, Edwards Co., TX **F** male, Uvalde, Co., TX.
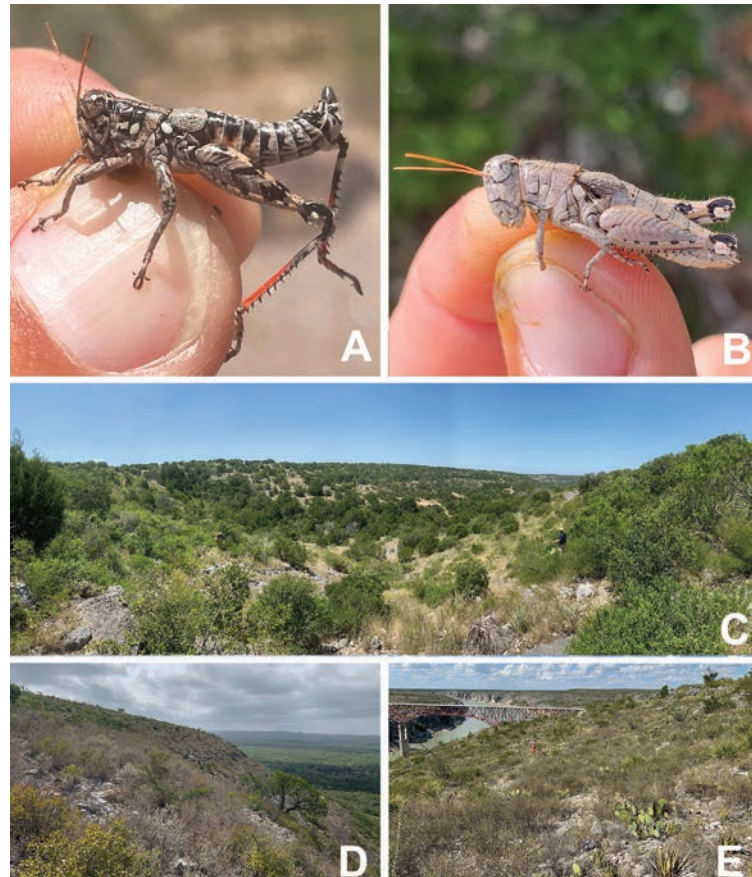
Figure 29. *Agroecotettix aristus* **A** male, Jeff Davis Co., TX **B** female Edwards Co., TX **C** habitat in Edwards Co., TX **D** habitat in Uvalde Co, TX **E** habitat in Val Verde Co., TX.

Figure 30. *Agroecotettix crypsidomus* from Brewster Co., Texas **A** male **B** male on *Vachellia* **C** male **D** male **E** female **F** female on *Vachellia*.

Figure 31. *Agroecotettix burtoni* from Brewster Co., Texas **A** habitat view in Big Bend National Park **B** male **C** male **D** male.

Figure 32. *Agroecotettix moorei* Terrel Co., Texas **A** male **B** male **C** male **D** habitat view near Sanderson, TX.
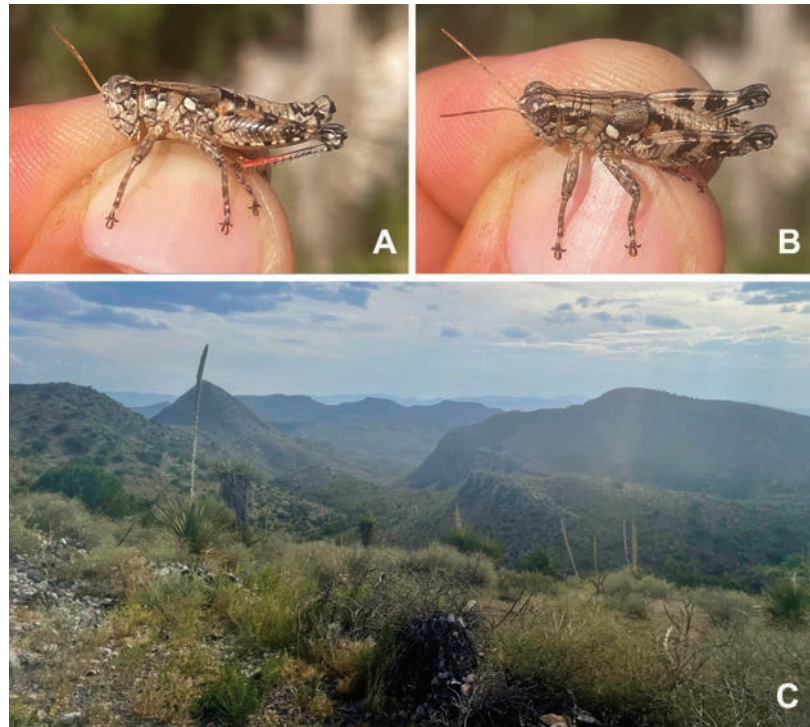
Figure 33. *Agroecotettix chiantiensis* from Presidio Co., Texas **A** male in lateral view **B** male is semi-dorsal view **C** habitat view.
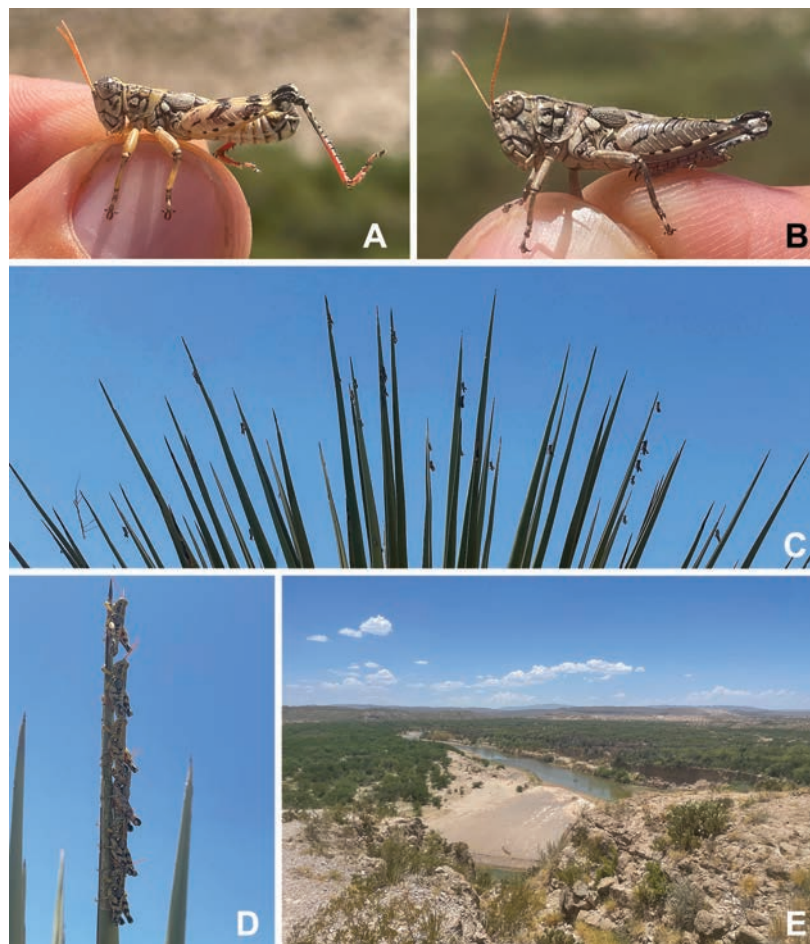
Figure 34. *Agroecotettix dorni* from Brewster Co., Texas **A** male in lateral view **B** female in lateral view **C** Individuals roosting during the heat of the day on *Dasylirion* leaves **D** habitat view.
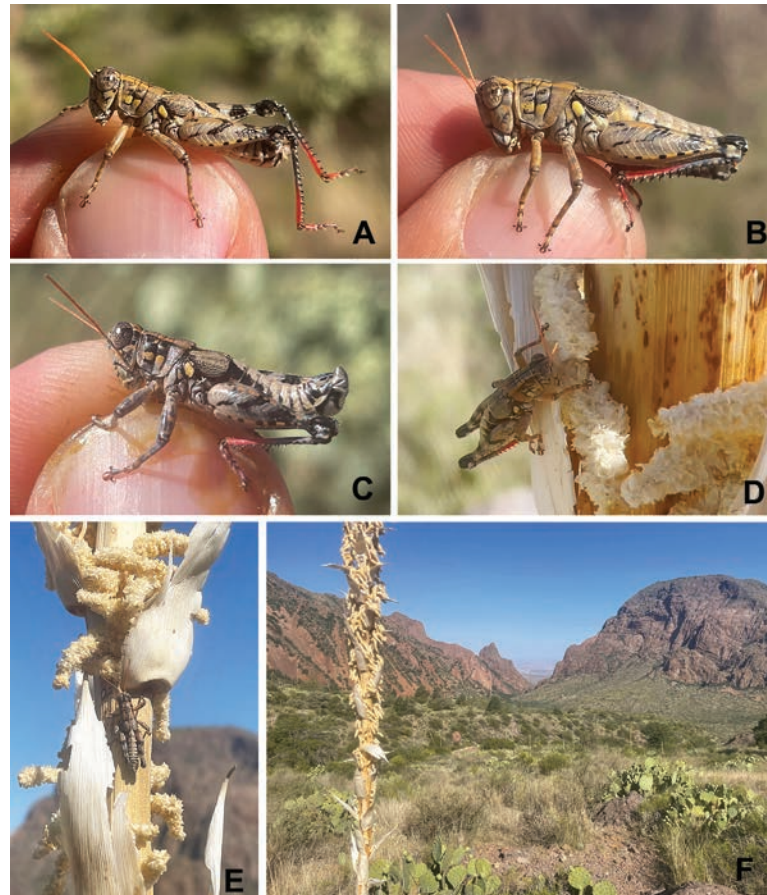
Figure 35. *Agroecotettix chisosensis* from Brewster Co., Texas **A** male in lateral view **B** female in lateral view **C** male in lateral view **D** male feeding on *Dasylirion* flowers **E** male feeding on *Dasylirion* flowers **F** habitat view.
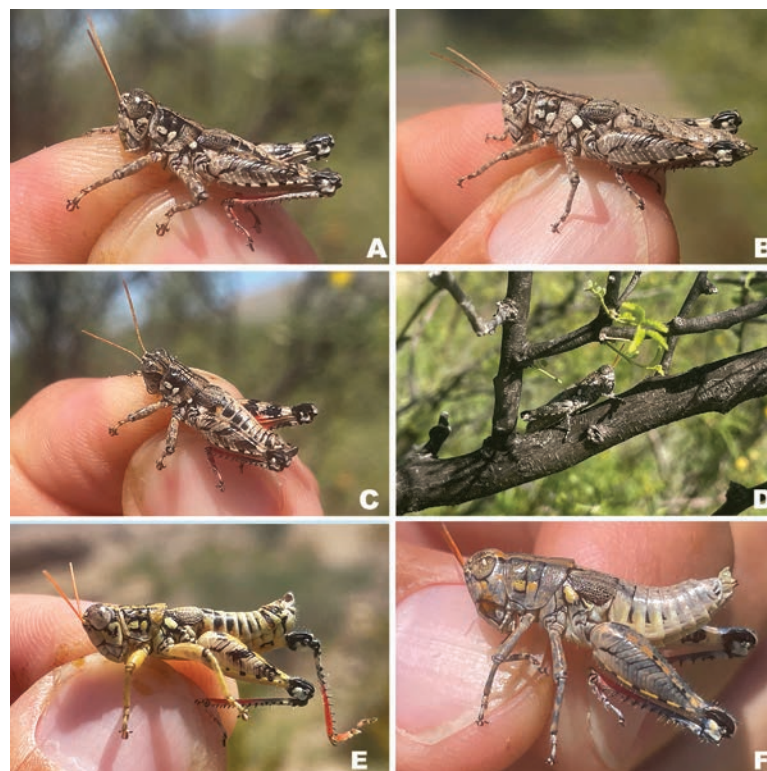
Figure 36. *Agroecotettix turneri* from Brewster Co., Texas **A** male **B** female **C** male **D** female on *Vachellia*.

Similarly, Toomey et al. (1993) described the environment of the Edwards Plateau (Fig. 25) during the late Pleistocene (ca 20–14,000 yr B.P.) as having much of the uplands covered in a deep reddish-clay soil and open mixed tall and short grass savanna. Drying conditions during the Holocene (10,500–2,500 yr B.P.) resulted in diminished vegetation cover which caused the gradual degradation of soil mantles and a shift to short grasses and scrub plant communities (Toomey et al. 1993. The Edwards Plateau and surrounding areas, in contrast to the Chihuahuan Desert, host the most widespread *Agroecotettix*, namely, *A. aristus*. This distribution suggests that the species and genus might have originated in the south and spread to their current range during a more recent arid period.

Specimens from my fieldwork in the United States have recently been sent for sequencing, but there are still large collecting gaps in Mexico, and little genetic data currently available for specimens there. It is hoped that this article will stir interest in searching for more *Agroecotettix* species to help tell the story of the biogeographic history of this interesting region.

Acknowledgements

Additional information

Conflict of interest

The author has declared that no competing interests exist.

Ethical statement

No ethical statement was reported.

Funding

Author contributions

JoVonn Hill, wrote the manuscript, conducted the data collection, and aquired the funding for the project.

Author ORCIDs

JoVonn G. Hill https://orcid.org/0000-0002-1892-7117

Data availability

All of the data that support the findings of this study are available in the main text.

References

Barrientos-Lozano, L, Rocha-Sánchez AY, Horta-Vega J (2013a) Two new species of *Melanoplus* Stål, 1873 (Orthoptera: Acrididae) from northeastern Mexico. Zootaxa 3669: 261–286. https://doi.org/10.11646/zootaxa.3669.3.4

Barrientos-Lozano L, Rocha-Sánchez AY, Buzzetti FM, Méndez-Gómez BR, Horta-Vega JV (2013b) In Saltamontes y esperanzas del noreste de México (Insecta: Orthoptera). Guía ilustrada. Miguel Ángel Porrúa, Ciudad de México, 388 pp.

Betancourt JL, Van Devender TR, Martin PS, Paul S (1990) Packrat middens: the last 40,000 years of biotic change. University of Arizona Press, Tucson, AZ, 478 pp.

Bruner L (1908) Orthoptera. The Acrididae. Biologia Centrali-Americana 2: 249–342.

Carbonell CS (2007) The genus *Zoniopoda* Stål 1873 (Acridoidea, Romaleidae, Romaleinae). Journal of Orthoptera Research 16(1): 1–33. https://doi.org/10.1665/1082-6467(2007)16[1:TGZSAR]2.0.CO;2

Cigliano MM, Braun H, Eades DE, Otte D. (2024) Orthoptera Species File. http://orthoptera.speciesfile.org/ [Accessed 22 July 2024]

Cohn TJ (1955) UMMZI-FN358. [Accessed online at] https://quod.lib.umich.edu/cgi/i/image/image-idx?id=S-INSECT1IC-X-401%5DUMMZI-FN358_001 [Accessed 14 May 2024]

Cohn TJ (1956) UMMZ-FN294. [Accessed online at] https://quod.lib.umich.edu/cgi/i/image/image-idx?id=S-INSECT1IC-X-348%5DUMMZI-FN294_001 [accessed 15 May 2024]

Cohn TJ (1959) UMMZ-FN298. [Accessed online at] https://quod.lib.umich.edu/cgi/i/image/image-idx?id=S-INSECT1IC-X-352%5DUMMZI-FN298_001 [accessed 15 May 2024]

Cohn TJ (1964) UMMZ-FN300. [Accessed online at] https://quod.lib.umich.edu/cgi/i/image/image-idx?id=S-INSECT1IC-X-354%5DUMMZI-FN300_001 [accessed 15 May 2024]

Cohn TJ (1965) UMMZ-FN301. [Accessed online at] https://quod.lib.umich.edu/cgi/i/image/image-idx?id=S-INSECT1IC-X-355%5DUMMZI-FN301_001 [accessed 15 May 2024]

Eades DC (2000) Evolutionary relationships of phallic structures of Acridomorpha (Orthoptera). Journal of Orthoptera Research 9: 181–210. https://doi.org/10.2307/3503648

Fontana P, Buzzetti FM, Mariño-Pérez R (2008) Chapulines, Langostas, Grillos y Esperanzas de México. Guía fotográfica - Grasshoppers, Locusts, Crickets & Katydids of Mexico. Photographic guide. World Biodiversity Association, Verona, Italy, 272 pp.

Gurney AB, Brooks AR (1959) Grasshoppers of the *Mexicanus* Group, Genus *Melanoplus* (Orthoptera: Acrididae). Proceedings of the United States National Museum 110: 1–93. https://doi.org/10.5479/si.00963801.110-3416.1

Hebard M (1922) New genera and species of Melanopli found within the United States and Canada (Orthoptera: Acrididae): Part IV. Transactions of the American Entomological Society 48: 49–66.

Hill JG (2015) Revision and Biogeography of the *Melanoplus scudderi* Species group (Orthoptera: Acrididae: Melanoplinae) with a Description of 21 New Species and Establishment of the Carnegiei and Davisi Species Groups. Transactions of the American Entomological Society 141: 252–350. https://doi.org/10.3157/061.141.0201

Hill JG (2023) Diversification deep in the heart of Texas: seven new grasshopper species and establishment of the *Melanoplus discolor* species group (Orthoptera:

Acrididae: Melanoplinae). ZooKeys 1165: 101–136. https://doi.org/10.3897/zookeys.1165.104047

Holmgren CA, Peñalba MC, Rylander KA, Betancourt JL (2003) A 16,000 14C yr B.P packrat midden series from the USA-Mexico borderlands. Quaternary Research 60: 319–329. https://doi.org/10.1016/j.yqres.2003.08.001

Huang JP, Hill JG, Ortego J, Knowles LL (2020) Paraphyletic species no more—genomic data resolve Pleistocene radiation and validate morphological species of the *Melanoplus scudderi* species complex (Insecta: Orthoptera). Systematic Entomology 45(3): 594–605. https://doi.org/10.1111/syen.12415

Hubbell TH (1932) A revision of the *Puer* Group of the North American genus *Melanoplus*, with remarks on the taxonomic value of the concealed male genitalia in the Cyrtacanthacrinae (Orthoptera, Acrididae). University of Michigan Museum of Zoology Miscellaneous Publication 23, 64 pp.

Knowles LL (2007) Tests of Pleistocene speciation in montane Grasshoppers (Genus *Melanoplus*) from the sky islands of western North America. Evolution 54: 1337–1348. https://doi.org/10.1111/j.0014-3820.2000.tb00566.x

Medellin-Leal F (1982) The Chihuahuan Desert. In: Bender GL (Ed.) Reference handbook on the Deserts of North America. Greenwood Press, Westport, CT, 321–381. [594 pp]

Otte D (2012) Eighty new *Melanoplus* species from the United States (Acrididae: Melanoplinae). Transactions of the American Entomological Society 138: 73–167. https://doi.org/10.3157/061.138.0103

Otte D (2019) Revision of the genus *Paraidemona* Bruner Von Wattenwyl 1893 (Acrididae: Melanoplinae). Transactions of the American Entomological Society 145: 435–535. https://doi.org/10.3157/061.145.0308

Scheinvar E, Gámez N, Moreno-Letelier A, Aguirre E, Eguiarte, LE (2020) Phylogeography of the Chihuahuan Desert: Diversification and Evolution Over the Pleistocene. In: Mandujano M, Pisanty I, Eguiarte LE (Eds) Plant Diversity and Ecology in the Chihuahuan Desert: Emphasis on the Cuatro Ciénegas Basin. Springer, Cham, 19–44. https://doi.org/10.1007/978-3-030-44963-6_2

Toledo VM, Ordóñez MJ (1993) The biodiversity scenario of Mexico: a review of terrestrial habitats. In: Ramamoorthy TP, Bye RA, Lot A, Fa J (Eds) Biological diversity of Mexico: origins and distribution. Oxford University Press, New York, NY, 757–777.

Toomey III RS, Blum MD, Valastro Jr S (1993) Late Quaternary climates and environments of the Edwards Plateau, Texas. Global and Planetary Change 7: 299–320. https://doi.org/10.2993/0278-0771-33.2.170

Villarreal-Quintanilla JA, Bartolomé-Hernández JA, Estrada-Castillón E, Ramírez-Rodríguez H, Martínez-Amador SJ (2017) El elemento endémico de la flora vascular del Desierto Chihuahuense. Acta Botánica Mexicana 118: 65–96. https://doi.org/10.21829/abm118.2017.1201

Woller D (2017) Xerophilic Flightless Grasshoppers (Orthoptera: Acrididae: Melanoplinae: *Melanoplus*: The Puer Group) of the Southeastern U.S.A.: An Evolutionary History. Texas A&M Dissertation, 341 pp.

Research Article

Revision of the Tomoderinae (Coleoptera, Anthicidae). Part V. Three new *Macrotomoderus* Pic, 1901 from continental China and an updated key to the Palaearctic species

Dmitry Telnov[1,2,3]

1   *Coleopterological Research Center, Institute of Life Sciences and Technology, Daugavpils University, Vienības iela 13, LV–5401, Daugavpils, Latvia*

2   *Department of Life Sciences, Natural History Museum, Cromwell Road, SW7 5BD, London, UK*

3   *Institute of Biology, University of Latvia, O. Vācieša iela 4, LV-1004, Rīga, Latvia*

Corresponding author: Dmitry Telnov (anthicus@gmail.com)

Abstract

Descriptions of the following three new species of *Macrotomoderus* Pic, 1901 from continental China are provided: *M. blinsteini* **sp. nov.**, *M. hirsutus* **sp. nov.**, and *M. turpiculus* **sp. nov.** The available identification key to the Palaearctic *Macrotomoderus* species is supplemented and updated.

Key words: Ant-like flower beetles, identification, morphology, taxonomy

Introduction

This is the fifth work devoted entirely to the study of the species of *Macrotomoderus* Pic, 1901 and the fourth restricted to the Palaearctic species (see Telnov 1998, 2007b, 2018, 2022). *Macrotomoderus* is the second most speciose among the six genera of Tomoderinae Bonadona, 1961 (Chandler 2010; Telnov 2022; Telnov and Gusakov 2023). *Macrotomoderus* was originally erected to include a species from the Greater Sunda Islands, Sumatra (Pic 1901). Numerous species were described under the name of *Derarimus* Bonadona, 1978 which is now considered a junior synonym of *Macrotomoderus* (Bonadona 1978; Telnov 2007a). The distinctive morphological features of *Macrotomoderus* were re-defined by Telnov (2007a). The geographical distribution of *Macrotomoderus* is vast and stretches from the Indo−Australian Archipelago (the Greater Sunda Islands southwards including Java), mainland SE Asia (Uhmann 1993, 1994a, 1994b, 1994c, 1996a, 1996b, 1998, 1999; Telnov 2004, 2007a), the Philippine Archipelago (Uhmann 1994a; Telnov 2023) towards the Indian Subcontinent (Bonadona 1978), China, Japanese and Taiwan archipelagos (Telnov 2020, 2022). One hundred and forty-six species are currently attributed to *Macrotomoderus*, of which 96 are Oriental and 50 Palaearctic (author's unpublished checklist and references herein). Additional species are described in the present paper.

The aim of the current paper is to present descriptions and illustrations of three *Macrotomoderus* species new to science from continental China and to provide an updated key to the Palaearctic species of the genus.

Material and methods

All taxa are listed in alphabetical order (except in the key) since a phylogenetic arrangement is not yet possible. Paired morphological structures are generally treated as singular in text. For morphological studies, a Leica S6D binocular stereomicroscope (Leica Microsystems, Wetzlar, Germany) was used. Habitus images were produced with a Canon EOS 5D SLR camera (Canon Co., Tokyo, Japan) and a Canon MP-E 65 mm macro lens (Canon Co., Tokyo, Japan). Genitalia were relaxed in KOH solution, mounted on microscope slides, and fixed in dimethyl hydantoin formaldehyde (DMHF) for study and imaging; after the study, genitalia were mounted on the same slides with corresponding specimens and fixed in DMHF. Genitalia were studied and imaged using an AmScope BH 200 light microscope (AmScope Co., Los Angeles, U.S.A.) with an attached external Sony DSC−WX100 (Sony Co., Tokyo, Japan) digital camera for imaging. Helicon Focus 7 software (Helicon Soft, Kharkiv, Ukraine) was used for image stacking. Further image manipulations were done using GNU Image Manipulation Program (GIMP).

Label text is reproduced verbatim and enclosed in double quotation marks. Labels, if more than one on the same specimen, are separated by a double slash. All type specimens of the new species are provided with a black framed label on red paper with "HOLOTYPUS" or "PARATYPUS". Author's comments are given in square brackets.

Acronyms for scientific collections:

DTC   Collection Dmitry Telnov, Rīga, Latvia;
IBC   Working collection Igor Belousov, Saint Petersburg, Russia;
NME   Naturkundemuseum Erfurt, Erfurt, Germany.

Results

Taxonomic account

Class Insecta Linnaeus, 1758
Order Coleoptera Linnaeus, 1758
Suborder Polyphaga Emery, 1886
Superfamily Tenebrionoidea Latreille, 1802
Family Anthicidae Latreille, 1819
Subfamily Tomoderinae Bonadona, 1961

Genus *Macrotomoderus* Pic, 1901

= *Derarimus* Bonadona, 1978: 655, synonymy introduced by Telnov (2007a).
   Type species: *Derarimus carinatus* Bonadona, 1978: 655 original designation.

Type species. *Macrotomoderus latipennis* Pic, 1901: 741 by monotypy.

Macrotomoderus blinsteini sp. nov.

https://zoobank.org/7A41AD57-09C9-4A48-A0E5-80CE83C7B47F

Figs 1, 2

Type material designated. *Holotype* • ♂ NME: "CHINA: Shaanxi/Sichuan Daba Shan, pass 20 km SSE Zhenping ~1750 m leg. Schülke 12.7.2001" [printed]. *Paratype* • 1♀ DTC: "CHINA: Shaanxi: Dabashan; 20 km SSE Zhenping 1700 m leg. Stary 26.6.2002" [printed].

Measurements. Holotype, total body length 3.9 mm; head including exposed part of cranial 'neck' 0.8 mm long, across eyes 0.8 mm wide, pronotum 1 mm long, maximum width 0.8 mm, minimum width 0.3 mm, elytra 2.1 mm long, combined width 1.4 mm. Paratype ♀ 4 mm long.

Description. Holotype, male. Dorsum and venter uniformly brown, head comparatively slightly darker. Mouthparts, antennae, palps, and legs brownish testaceous. Head transversely ovoid, glossy dorsally and ventrally, with rather small, distinctly ovoid compound eyes which are not protruding beyond lateral or dorsal outline of head. Head rounded in broad arc posterior to eyes. Head dorsal punctures minute and inconspicuous but rather deep. Intervening spaces 4–6 × as wide as diameter of punctures. Head dorsal setae inconspicuous, moderately dense, whitish to yellowish. Antenna reach base of pronotum when directed posteriad. Antennomere 3 subequal in length to antennomere 2, antennomeres 6 and 7 approximately as long as wide, 8–10 transverse, of which 9–10 strongly so. Terminal antennomere strongly asymmetrically triangular with rounded apex, ~ 1.5–1.6 × as long as penultimate antennomere. Terminal maxillary palpomere securiform. Pronotum stout, moderately glossy dorsally and laterally, narrower than head across compound eyes, with broad, medially distinctly notched (in dorsal view) postmedian lateral constriction. Front margin of anterior lobe very broadly rounded, dorsally without modifications and anterior rim. Anterior lobe barely convex in lateral view (Fig. 1B). Lateral constriction barely continues onto pronotal disc in lateral view (Fig. 1B). Lateral pronotal fovea moderately broad at lower (lateroventral) extent of laterally strongly declivous pronotal disc, somewhat widens upwards towards pronotal disc in lateral view, lateral edges of fovea carinate, narrowly separated (all in lateral view), denticle-like in dorsal view. In lateral view anterior and posterior edge of pronotal fovea covered with bristle of short golden setae except at their lower extent. Cavity in lateral wall of pronotum between lateral denticles moderate, deep. In dorsal view, lateral pronotal fovea moderately wide, anterior and posterior denticle poorly visible, glabrous. Pronotal punctures on disc similar to those on head dorsum; lateral constriction dorsally with dense, large, irregularly circular punctures with corrugate backgrounds separated by much less than puncture diameters. Dorsal pronotal setae similar to those on head dorsum, denser on lateral sides of pronotum. Few longer erect tactile setae on lateral sides of anterior lobe. Scutellar shield minute, apically rounded, glabrous, and glossy. Elytra moderately glossy, dorsally elliptical, slightly convex in lateral view, strongly widened laterally around midlength, lateral margins broadly rounded, humerus obsolete (apterous species). Elytral punctures much stronger and larger than those on dorsal forebody, more or less regularly circular, smaller, and less coarse than dorsal punctures on pronotal constriction. Punctures flatter but not much sparser on apical third of elytra. Intervening spaces ~ 1.5–2 × as wide as diameter of punctures. Elytral setae long and sparse, suberect, yellowish.
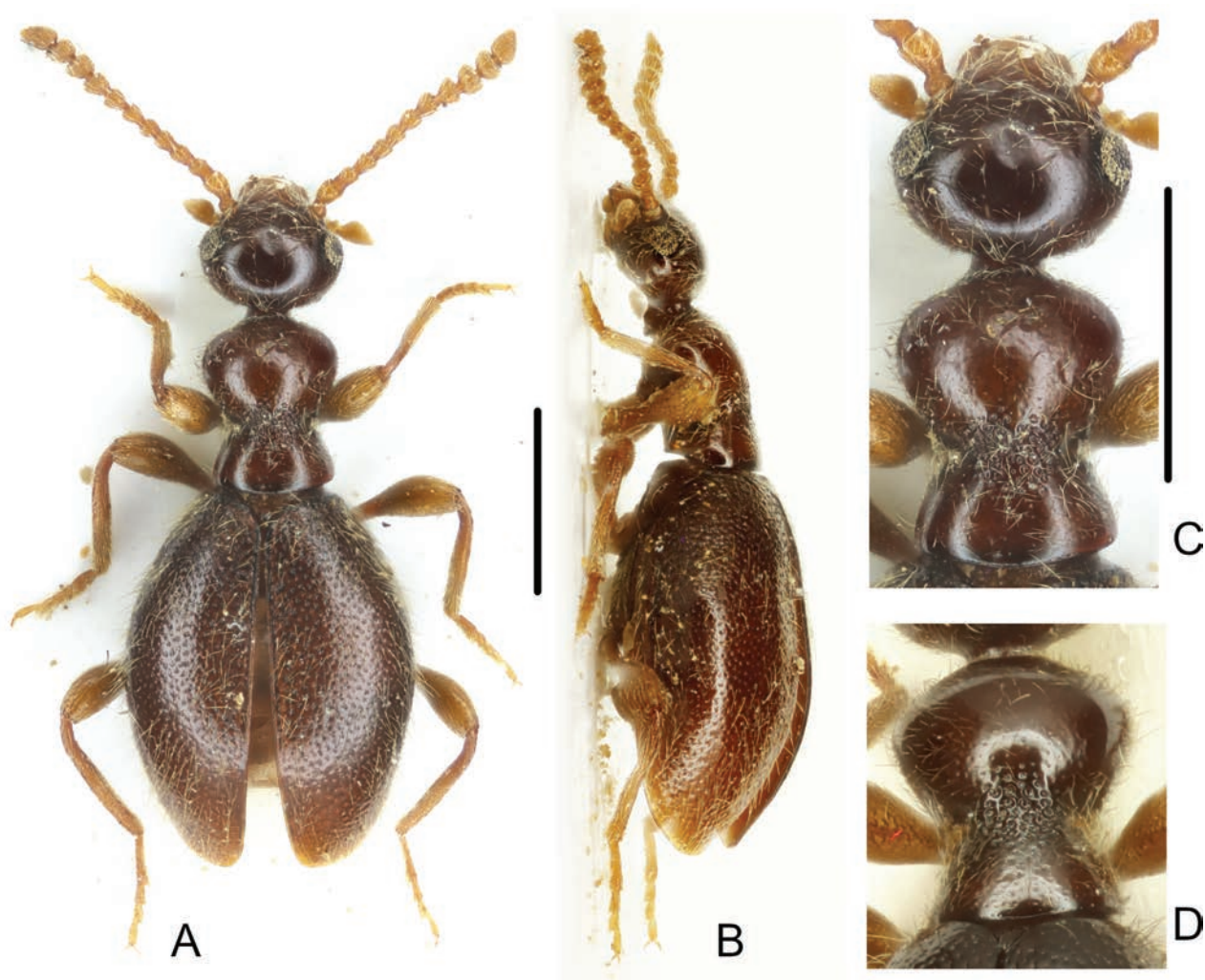
Figure 1. *Macrotomoderus blinsteini* sp. nov. **A** holotype ♂, habitus, dorsal view **B** ditto, lateral view **C** ditto, dorsal forebody **D** paratype ♀, pronotum, posterodorsal view. Scale bars: 1 mm.

Male tergite and sternite VII broadly rounded at posterior margin. Sternite IX rodlike, strongly sinuous (Fig. 2A). Aedeagus as in Fig. 2B–H, thick and bulbous in basal portion, narrowing towards subtruncate apex. Endophallic armature of numerous minute, peculiarly tack-shaped spines in apical part and, in basal portion, with large, pebble-like sclerites arranged in a kind of garland and intermixed with dense spines filling intervening spaces between sclerites (Fig. 2B–E).

Sexual dimorphism. Female tergite and sternite VII broadly rounded at posterior margin, pronotum comparatively slenderer and elytra somewhat stronger constricted towards apex than in male.

Differential diagnosis. This species falls in a group of species from continental China including, for example, *M. hartmanni* Telnov, 2022 and *M. korolevi* Telnov, 2022 (both from Yunnan) with the lateral constriction area of the pronotum densely and roughly but ordinary punctate and sparsely to moderately densely setose dorsally, lacking the longitudinal carinae, sulci or elongate pores. The aedeagus is differently shaped in *M. blinsteini* sp. nov., the endophallic armature is smaller, thinner and peculiarly tack-shaped, and the elytral punctures are comparatively coarser and deeper.

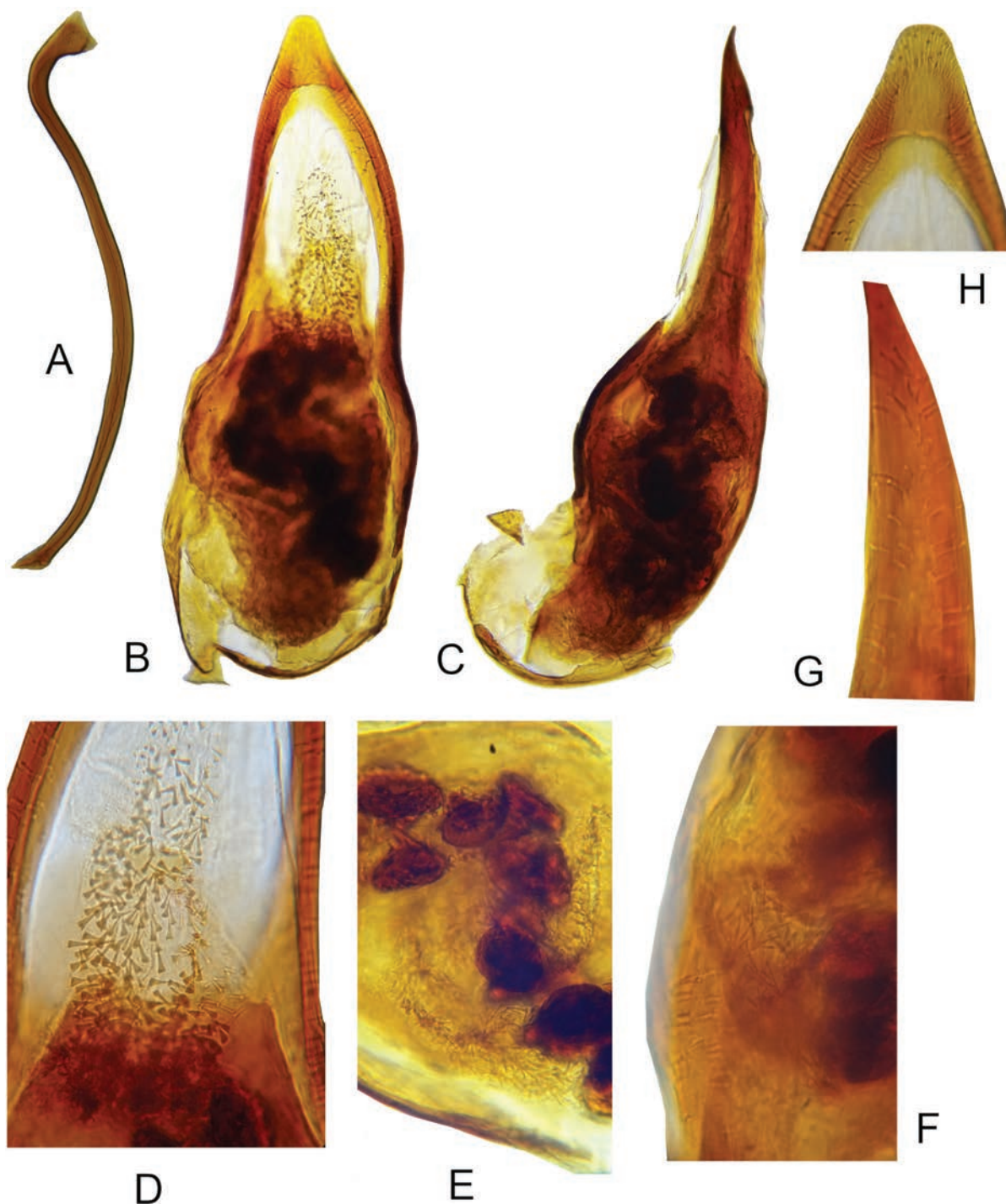**Ecology.** Collected at ~ 1700–1750 m a.s.l.

Figure 2. *Macrotomoderus blinsteini* sp. nov. holotype ♂, terminalia and aedeagus **A** sternite IX, lateral view **B** aedeagus, ventral view **C** ditto, lateral view **D** ditto, endophallic armature in median portion of aedeagus **E** ditto, endophallic armature in basal portion of aedeagus **F** ditto, different portion of basale **G** ditto, lateral view of apical portion with endophallic armature **H** ditto, ventral view of apex [not to scale].

Distribution. Known from the Daba Mountains in southern Shaanxi Province along boundary with Sichuan, central China.

Etymology. Patronymic. This species named for Semen Blinstein (Dortmund, Germany; previously Odessa, Ukraine) – a well-known coleopterist who possesses a valuable beetle collection from southern Ukraine and is the author of some Anthicidae species from the region.

Macrotomoderus hirsutus sp. nov.

https://zoobank.org/1D16E28A-F43F-40E5-88C6-82CCAB013AB1

Figs 3, 4

Type material designated. *Holotype* • ♂ NME: "CHINA: Hubei: Dabashan; 13 km NW Muyuping 1900 m leg. Stary 16.7.2002" [printed].

Measurements. Holotype, total body length 3.8 mm; head including exposed part of cranial 'neck' 0.9 mm long, across eyes 0.9 mm wide, pronotum 1.1 mm long, maximum width 0.9 mm, minimum width 0.35 mm, elytra 2.3 mm long, 1.7 mm combined wide.

Description. Holotype, male. Head and pronotum brown, elytra pale brown. Mouthparts, antennae, palps, and legs pale brownish–testaceous. Head ovoid, moderately glossy dorsally and ventrally, with moderate, nearly circular compound eyes which are slightly protruding beyond lateral outline of head. Head rounded in broad arc posterior to eyes. Head dorsal punctures minute but rather deep, denser on occiput and vertex. Intervening spaces 2–4 × as wide as punctures. Head dorsal setae yellowish, inconspicuous on most of head dorsum but long and dense, forming a subconical bristle (in dorsal view) at head base and therefore concealing median part of anterior pronotal margin. Apical portions of these long head–base setae are curled and in part tangled (Fig. 3B, C). Antenna exceeds slightly beyond base of elytra when directed posteriad. Antennomere 3 subequal in length to antennomere 2, antennomeres 6–10 transverse, of which 8–10 strongly so. Terminal antennomere asymmetrically triangular with rounded apex, ~ 1.6 × as long as penultimate antennomere. Terminal maxillary palpomere securiform. Pronotum stout, moderately glossy dorsally and laterally, approximately as wide as head across compound eyes, with broad, medially strongly notched (in dorsal view) postmedian lateral constriction. Anterior lobe much wider than posterior, its front margin broadly rounded, dorsally without modifications and anterior rim. Anterior lobe nearly flat in lateral view (Fig. 3B). Lateral constriction does not continue onto disc in lateral view (Fig. 3B). Lateral pronotal fovea wide at lower (lateroventral) extent of laterally strongly declivous pronotal disc, not widens upwards towards pronotal disc in lateral view, lateral edges of fovea carinate, moderately separated and densely setose (all in lateral view), in dorsal view denticle-like. In lateral view anterior and posterior edge of pronotal fovea completely covered with bristle of short golden setae. Cavity in lateral wall of pronotum moderate. In dorsal view, lateral pronotal fovea wide, anterior and posterior denticle clearly visible, dense brush-like setose (Fig. 3A, C). Pronotal punctures on disc similar to those on head dorsum, intervening spaces 3–7 × as wide as punctures; lateral constriction dorsally with irregularly shaped and variably dense and deep, generally moderately to strongly elongated punctures; median ones particularly large and elongate, groove-like. Dorsal pronotal setae moderately dense, but much denser on lateral sides of pronotum, especially in constriction area where setation effectively conceals shape of lateral pronotal denticles. Several longer erect tactile setae on lateral sides of anterior lobe. Scutellar shield minute, apically rounded, glabrous, and glossy. Elytra moderately glossy, dorsally elongate elliptical, slightly convex in lateral view, widened laterally around midlength, lateral margins broadly rounded, humerus obsolete (apterous species). Elytral punctures stronger and larger than those on dorsal forebody, more or less regularly circular, smaller than dorsal punctures on lateral pronotal constriction. Punctures becoming more flat
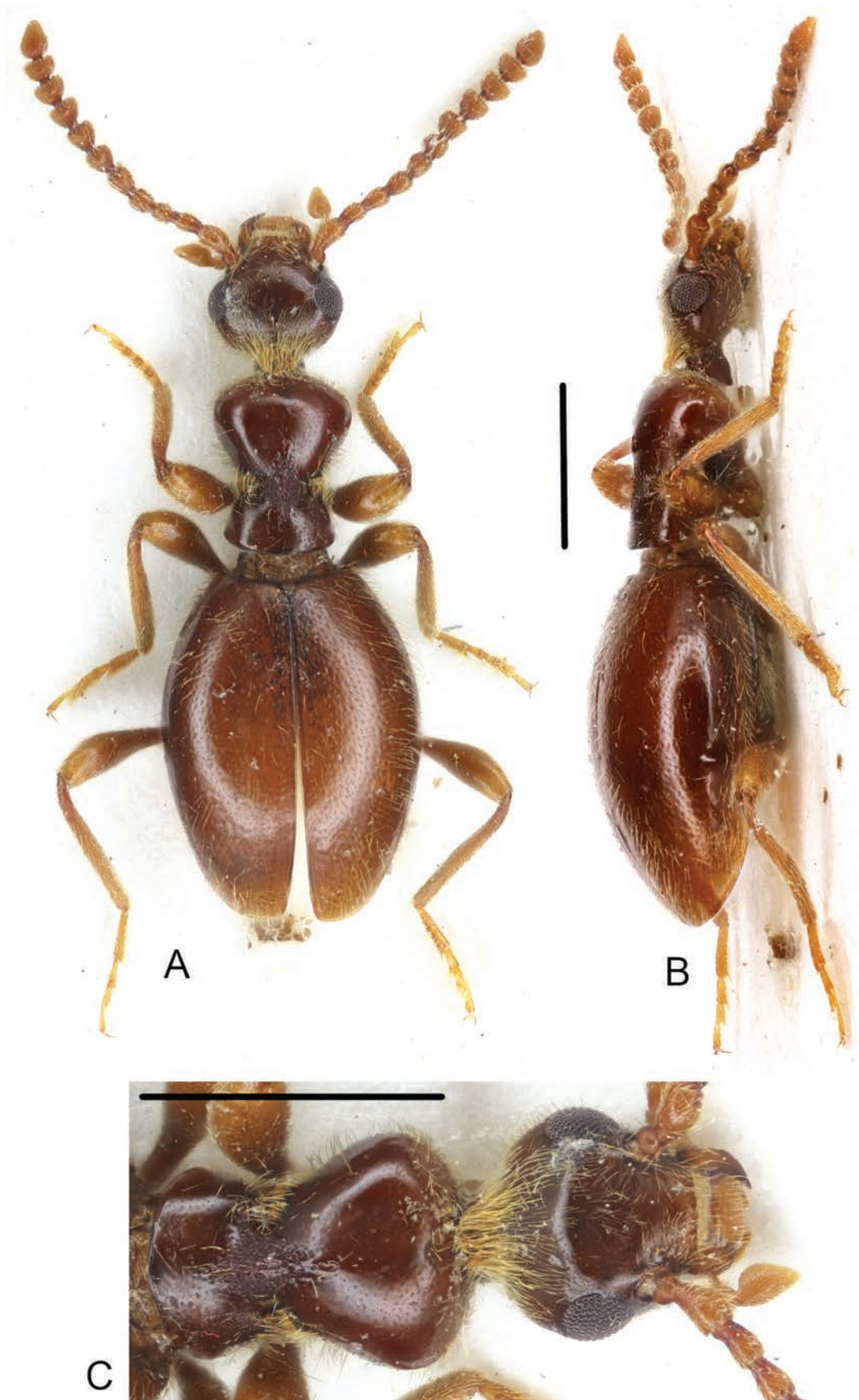
Figure 3. *Macrotomoderus hirsutus* sp. nov. holotype ♂ **A** habitus, dorsal view **B** ditto, lateral view **C** dorsal forebody. Scale bars: 1 mm.

Figure 4. *Macrotomoderus hirsutus* sp. nov. holotype ♂, terminalia and aedeagus **A** sternite IX, lateral view **B** aedeagus, ventral view **C** ditto, lateral view **D** ditto, median portion, endophallic armature **E** ditto, basal portion, endophallic armature **F** ditto, endophallic armature, lateral view of basal portion **G** ditto, ventral view of apex [not to scale].

and somewhat sparser on apical third of elytra. Intervening spaces ~ 3–5 × as wide as diameter of punctures. Elytral setae long and sparse, suberect, yellowish. Male tergite and sternite VII broadly rounded at posterior margin. Sternite IX rod–

like, slightly bisinuate (Fig. 4A). Aedeagus as in Fig. 4B–G, elongate, narrows apically, apex somewhat subspatulate, widened and rounded. Endophallic armature of numerous large peculiarly spike/nail-shaped spines (Fig. 4B–F).

Sexual dimorphism. Female is unknown.

Differential diagnosis. This species is readily recognized due to the presence of the dense clump of setae on male head base in the combination with the peculiar, spike/nail-like endophallic armature of the aedeagus. The shape of the aedeagus somewhat resembles that of *M. dali* Telnov, 2022 (Yunnan, China), *M. muli* Telnov, 2022 (Sichuan, China), and *M. wudu* Telnov, 2022 (Gansu, China), but all three have entirely different endophallic armatures. The head base with more or less dense setation is present in *M. conus* Telnov, 2018, *M. gracilis* Telnov, 2018, *M. microscopicus* Telnov, 2018, *M. monstrificabilis* Telnov, 2018, *M. perforatus* Telnov, 2018, and *M. schuelkei* Telnov, 2018 (all from Yunnan, China), but other morphological features and the endophallic armature are quite different.

Ecology. Collected at 1900 m a.s.l.

Distribution. Known from Daba Mountains in western part of Hubei Province, central China.

Etymology. From Latin *hirsutus* – shaggy, hairy, bristly, referring to the bristle of setae on the head base of this species.

Macrotomoderus turpiculus sp. nov.

https://zoobank.org/CB509362-B8B8-47A9-9586-315EF586829B

Figs 5, 6

Type material designated. *Holotype* • ♂ IBC: "CH, S Sichuan, S of Xichang, E slope of Mt. ´4282´ (NE of Dechang) 3200–2800 m, 6.05.2001 Belousov & Korolev leg." [printed] // "Macrotomoderus sp.? n. aff. monstrificabilis [handwritten] A. Kovalev det. 20 [printed] 19" [handwritten] [label with black frame]. The holotype will be donated to a local public institution (I. Belousov, pers. comm. viii.2021). *Paratype* • 1♂ DTC: same labels as holotype.

Measurements. Holotype, total body length 4.1 mm; head 0.8 mm long, across eyes 0.8 mm wide, pronotum 1.2 mm long, maximum width 1 mm, minimum width 0.25 mm, elytra 2.2 mm long, 1.5 mm combined wide. Paratype ♂ 4 mm long.

Description. Holotype, male. Dorsum and venter brown, posterior lobe of pronotum slightly paler. Mouthparts, antennae, palps, and legs brownish testaceous. Head subtriangular, moderately glossy dorsally and ventrally, with moderate, slightly ovoid compound eyes which are slightly protruding beyond lateral outline of head. Tempus short, constricted towards head base, temporal angle rounded. Head base truncate, declivous. Head dorsal punctures minute and inconspicuous, flat. Intervening spaces much wider than punctures. Head dorsal setae yellowish, short, moderately dense. Head base medially with somewhat longer, apically curled golden setae. Antenna exceeds slightly beyond base of elytra when directed posteriad. Antennomere 3 ~ 2 × as long as antennomere 2, asymmetrical, distal edge obliquely emarginate to accommodate shortened and only slightly longer than wide antennomere 4, antenna appears somewhat bent at area of antennomeres 3–5 (Fig. 5A, B, F). Antennomeres 8–10 transverse, of which antennomere 10 strongly so. Terminal antennomere strongly asymmetrically triangular with rounded apex, ~ 1.8–1.9 × as long as penultimate antennomere. Terminal
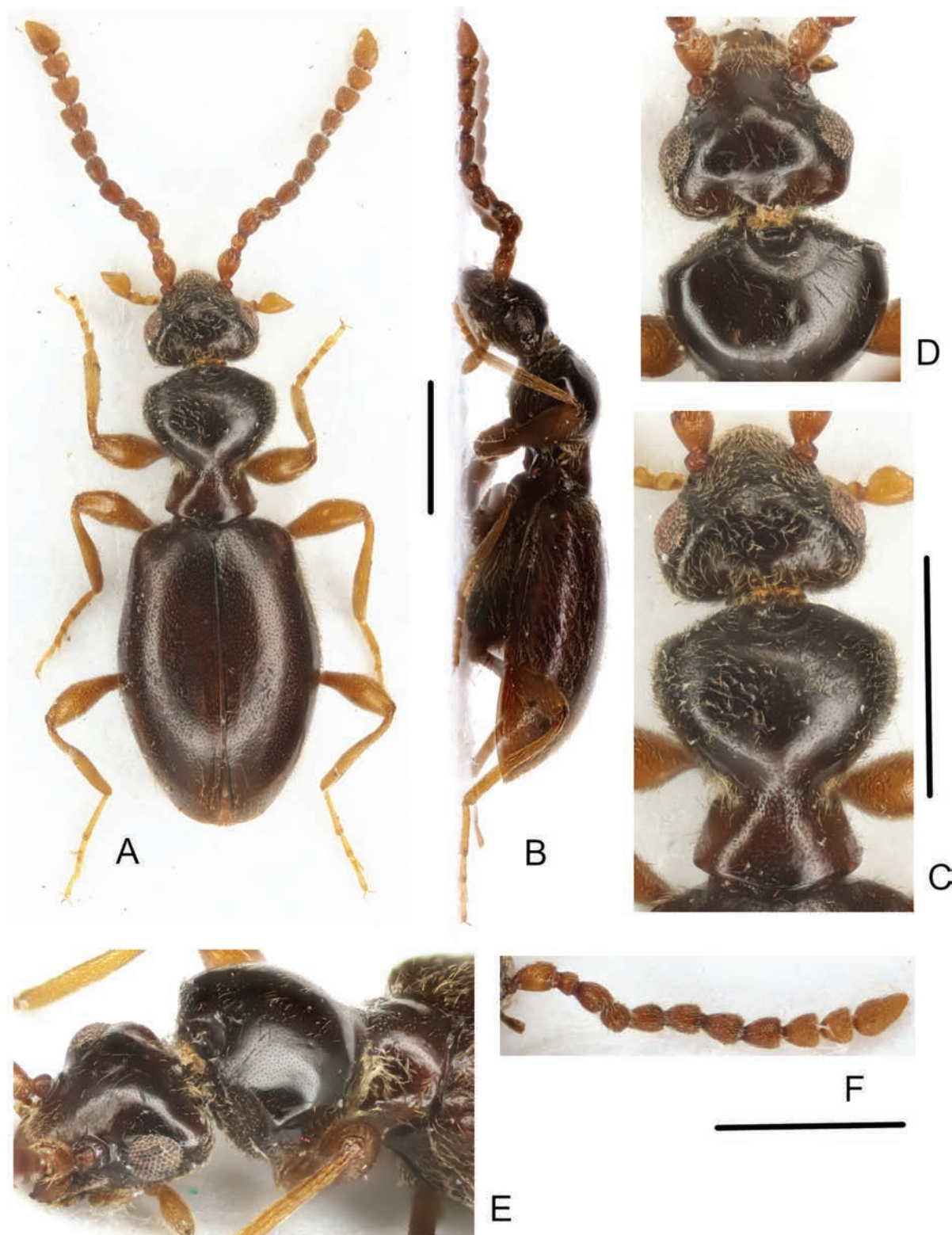
Figure 5. *Macrotomoderus turpiculus* sp. nov. ♂ **A** holotype, habitus, dorsal view **B** ditto, lateral view **C** ditto, dorsal forebody **D** paratype, forebody, anterodorsal view **E** ditto, latero-dorsal view **F** holotype, right antenna. Scale bars: 1 mm.

maxillary palpomere securiform. Pronotum stout, moderately glossy dorsally and laterally, much wider than head across compound eyes, with moderately broad, medially strongly notched (in dorsal view) postmedian lateral constriction. Anterior lobe much wider than posterior, its front margin medially subtruncate, without
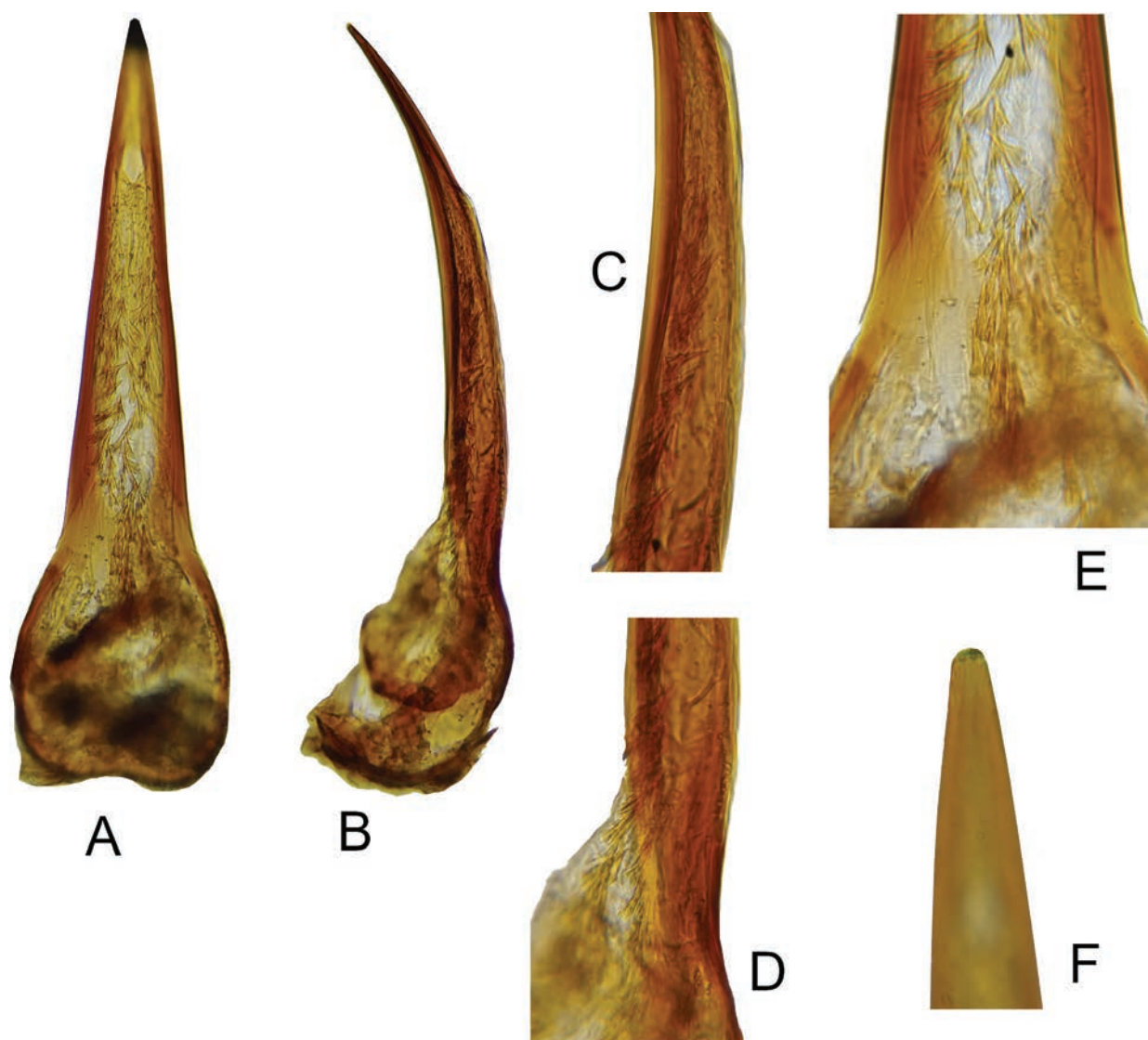
Figure 6. *Macrotomoderus turpiculus* sp. nov. holotype ♂, aedeagus **A** ventral view **B** lateral view **C** median portion, lateral view **D** basal portion, lateral view **E** basal portion, endophallic armature, ventral view **F** apical portion [not to scale].

anterior rim, with moderate mesal impression and transverse median ridge covered with dense golden setae which are directed antero-dorsally (Fig. 5C–E). Pronotum flattened anteroventrally each side of subtruncate median part of its anterior margin (Fig. 5D, E). Anterior lobe convex in lateral view (Fig. 5B). Lateral constriction barely continues onto disc in lateral view (Fig. 5B). Lateral pronotal fovea broad at lower (lateroventral) extent of laterally strongly declivous pronotal disc, not or barely widens upwards towards pronotal disc, lateral edges of fovea carinate, narrowly separated, nearly glabrous (all in lateral view), in dorsal view denticle-like. In lateral view anterior and posterior edge of pronotal fovea covered with a bristle of moderately long whitish setae. In dorsal view, lateral pronotal fovea wide, anterior and posterior denticle clearly visible, in part setose (Fig. 5A, C). There is an inconspicuous trace of short dorsal median longitudinal carina in lateral constriction area. Pronotal punctures on disc small and sparse, intervening spaces 5–8 × as wide as diameter of punctures; lateral constriction dorsally with irregularly ovoid and variably dense, deep punctures. Intervening spaces among punctures in laterally constricted area vary from much narrower than to twice

as wide as punctures. Dorsal pronotal setae short and dense, much longer and denser at lateral pronotal fovea, in part concealing its structure in dorsal view. Few longer erect tactile setae on lateral sides of anterior lobe. Scutellar shield minute, apically rounded, moderately glossy. Elytra moderately glossy, dorsally elongate elliptical, moderately convex in lateral view, widened laterally around midlength, lateral margins broadly rounded, humerus broadly rounded. Metathoracic wings fully developed (functional). Elytral punctures stronger and larger than those on dorsal forebody, nearly as large as those on lateral constriction area, more or less regularly circular. Punctures becoming more flat and somewhat sparser on apical third of elytra. Intervening spaces ~ 2.5−4 × as wide as diameter of punctures. Elytral setae long and moderately dense, suberect, yellowish. Male tergite and sternite VII broadly rounded at posterior margin. Aedeagus as in Fig. 6, elongate and narrow, narrows and acutely angulate apically. Endophallic armature of numerous basally multifurcate spines (Fig. 6A−E).

Sexual dimorphism. Female is unknown.

Differential diagnosis. This species falls into a group of species from mainland China with strongly widened, apically subtruncate anterior margin of pronotum, long heavy antennae, and slender, dagger-shaped aedeagus: *M. imitator* Telnov, 2022, *M. monstratus* Telnov, 2018, and *M. monstrificabilis* Telnov, 2018 (all from Yunnan). *Macrotomoderus turpiculus* sp. nov. is peculiar due to the absence of the large elongate median projection on head base (large projection present in *M. monstrificabilis*, only small projection in *M. turpiculus* sp. nov.; cf. Fig. 5A, C, E), the truncate and declivous head base (the head base broadly rounded in the similar species, not declivous), the differently modified anterior pronotal margin (see the description) especially the anteroventrally flattened pronotum, the asymmetrical antennomere 3 and the shortened antennomere 4 (both not modified in *M. monstratus*), the wide head (the head is narrower than the pronotum in *M. imitator*), and the peculiar endophallic armature not like in other congeners.

Ecology. Collected between 2800−3200 m a.s.l.

Distribution. Known only from southern part of Sichuan Province, southwestern China.

Etymology. From Latin *turpiculus* – misshaped, ugly, referring to the unusual body shape of this species.

Updated key to the Palaearctic species of *Macrotomoderus*

Female features alone are generally insufficient for species delimitation; therefore, the present key is mainly based on male features. For most confident identification, the original descriptions of each species must be consulted. The present key is an update to Telnov (2022) and covers all *Macrotomoderus* taxa from the zoogeographic area as defined in the latest edition on the Palaearctic catalogue for tenebrionoid beetles (Iwan and Löbl 2020).

1   Head base distinctly constricted, tapered ....**M. conus Telnov, 2018**
–   Head rounded, subtruncate, truncate or emarginate (concave) posterior to compound eyes (species with median conical projection on generally rounded to subtruncate head base should be included here) **2**

2 Male metafemur with conspicuous, large, apically acutely pointed spine at posterior margin ....***M. femoridens* Telnov, 2022**

– Posterior margin of metafemur in both sexes without modifications **3**

3 Head base in male with median projection, small or distinct, sometimes concealed beneath dense setae and difficult to observe **4**

– Head base in male without median projection...**7**

4 Head base in male truncate, head base declivous; anterior margin of pronotum with shallow median emargination and mesally with transverse ridge covered with dense antero-dorsally pointed setae; anteroventral part of pronotum flattened each side of median area (Fig. 6); endophallic armature of numerous basally multifurcate spines........................***M. turpiculus* sp. nov.**

– Head base rounded, not declivous; anterior margin of pronotum without modifications or modification is different (e.g., laterally angulate median impression with transverse ridge or simple shallow median impression), not flattened anteroventrally; endophallic armature not as above...............**5**

5 Anterior margin of male pronotum with broad mesal emargination facing median part of head base, anterolateral margins of emarginated area moderately raised in dorsal aspect, appear angulate; anterior edge of pronotum in front of emargination in male forms median transverse ridge that is covered with conspicuous, in part curved, anterodorsally pointed setae............
....***M. lapidarius* Telnov, 2022**

– Anterior margin of pronotum, if impressed, with margins of impression not angular **6**

6 Anterior margin of male pronotum truncate, with shallow mesal impression; tapered projection of head base large; head with distinct tempora, compound eye twice as long as tempus; head base subtruncate ....
....***M. monstrificabilis* Telnov, 2018**

– Anterior margin of male pronotum broadly rounded, not impressed; projection of head base less conspicuous, smaller; head rounded in broad arc posterior to eyes, tempora not delimited ....***M. mirabilis* Telnov, 2018**

7 Head base in male truncate when observed strictly from above, temporal angle present, obtuse; anterior margin of male pronotum with broad mesal impression facing median part of head base, anterolateral margins of impressed area slightly raised in dorsal aspect, appearing obtuse angular; anterior edge of male pronotum in front of anterior impression forms thin, low, transverse median ridge covered with conspicuous, in part curved, anterodorsally pointed setae ....***M. truncatulus* Telnov, 2022**

– Combination of features different; male head base rounded, subtruncate, or truncate but temporal angle never appearing angular.................................**8**

8 Total body length ≤ 2 mm **9**

– Total body length ≥ 2.5 mm **10**

9 Species from Okinawa, Ryukyu Islands; anterior lobe of pronotum dorsally with inconspicuous median longitudinal carina; anterior margin of male pronotum without modifications, rounded ....***M. satoi* (M. Saitô, 2003)**

– Species from Yunnan, continental China; pronotum dorsally not carinate; anterior margin of male pronotum with mesal impression that holds small frontal projection ....***M. microscopicus* Telnov, 2018**

10 Anterior margin of male pronotum with modifications – mesally impressed or projected anteriorly or provided with conspicuous, grouped, dense setae..**11**

– Anterior margin of male pronotum evenly rounded, subtruncate or truncate, without modifications or group(s) of conspicuous setae, at most slightly impressed mesally **28**

11 Anterior lobe of pronotum distinctly wider than head across eyes...........**12**

– Anterior lobe of pronotum nearly as wide as or narrower than head across eyes **16**

12 Head base truncate; compound eyes conspicuously large and laterally convex; tempus distinct, much shorter than dorsal eye length ....
....***M. boops* Telnov, 2022**

– Head rounded in broad arc posterior to comparatively small, more or less strongly flattened compound eyes; tempus not delimited (rounded) but not much shorter than dorsal eye length **13**

13 Male occiput not declivous or impressed posterodorsally (above insertion of cranial 'neck'); anterior margin of male pronotum slightly impressed both sides of median projection; male antenna comparatively shorter, not exceeding median third of elytra ....***M. hengduan* Telnov, 2022**

– Male occiput slightly declivous posterodorsally or shallowly impressed posterodorsally above insertion of cranial 'neck'; male antenna extending or nearly extending beyond median third of elytra **14**

14 Male occiput slightly declivous posterodorsally; anterior margin of pronotum without median projection......................................***M. dali* Telnov, 2022**

– Male occiput shallowly impressed posterodorsally above insertion of cranial 'neck'; anterior margin of pronotum with distinct, median triangular projection..**15**

15 Anterior margin of pronotum truncate; lateral constriction area of pronotum dorsally with inconspicuous, short, median longitudinal carina, densely and roughly punctured both sides of it, intervening spaces much smaller than punctures ....***M. imitator* Telnov, 2022**

– Anterior margin of pronotum subtruncate; lateral constriction area of pronotum dorsally not carinate, with rather large and sparse punctures and wide, glossy, and glabrous intervening spaces...
.... ***M. monstratus* Telnov, 2018**

16 Lateral foveae of pronotum not or marginally visible in dorsal view, not forming deep notches in pronotal constriction in dorsal aspect; denticles of lateral foveae of pronotum not or only partially visible in dorsal view.......**17**

– Lateral foveae of pronotum clearly visible in dorsal view in a form of variably deep notches in sides of pronotum at constriction area; denticles of lateral foveae of pronotum generally well visible in dorsal view **20**

17 Lateral constriction of pronotum dorsally with more or less prominent median longitudinal carina...***M. chingpo* Telnov, 2018**

– Lateral constriction of pronotum dorsally not carinate **18**

18. Anterior margin of male pronotum without modifications, broadly rounded, with a group of C-like shaped (curled posteriad) posteriad-pointed setae; head base without bunch of setae ....***M. angelinii* Telnov, 2022**

– Anterior margin of pronotum in male medially elevated and projecting anteriad; head base with or without group of longer setae................................**19**

19 Anterior projection of pronotum with a group of ɣ-like shaped (bent anteriad) anteriad-pointed setae; head base medially with a bunch of dense setae; pronotum slender, elongate, narrower than head across eyes................
....***M. gracilis* Telnov, 2018**
– Anterior margin of pronotum without bent or curved setae; pronotum rather broad, approx. the width of head across eyes............ ***M. kawa* Telnov, 2018**
20 Dorsum of anterior lobe of pronotum or its lateral constriction area or both medially longitudinally carinate..**21**
– Pronotum not carinate dorsally **25**
21 Anterior lobe of pronotum dorsally with median longitudinal carina (almost complete but not touching its anterior margin or restricted to posterior half of anterior lobe), projecting or not on lateral constriction area.................**22**
– Pronotum only carinate on lateral constriction area; anterior lobe of pronotum without dorsal carina **24**
22 Anterior margin of male pronotum not excavated, mesally with group of dense, strongly Ɔ-like shaped (curled anteriad) anteriad-pointed setae.......
....***M. wudu* Telnov, 2022**
– Anterior margin of male pronotum excavated, without median group of dense, curved setae..**23**
23 Aedeagus with strongly widened, bulbous basal portion, apically narrowly rounded to subacute in dorsal and ventral view; apex of aedeagus straight in lateral view .... ***M. transitans* Telnov, 2022**
– Aedeagus with moderately wide, non-bulbous basale, apically clearly rounded in dorsal and ventral view; apex of aedeagus slightly curved in lateral view .... ***M. bordonii* Telnov, 2022**
24 Lateral constriction area of pronotum tricarinate dorsally, of which both lateral carinae less prominent and shorter than median carina; lateral pronotal foveae in dorsal view comparatively shallower and less broadly notched; dorsal setae on pronotum moderately long .... ***M. yunnanus* (Telnov, 1998)**
– Lateral constriction area of pronotum dorsally unicarinate along midline; lateral pronotal foveae in dorsal view deeply and broadly notched; dorsal setae on pronotum longer...................................***M. perforatus* Telnov, 2018**
25 Anterior margin of male pronotum without modifications, broadly rounded, medially with a bunch of rather short and dense, apically C-shaped (curved) posteriad-pointed setae ....***M. tenuis* Telnov, 2022**
– Anterior margin of male pronotum with median emargination or projection
....**26**
26 Anterior margin of male pronotum truncate, with small and shallow median emargination; anterior transverse ridge in this impression with a group of ɣ-like shaped (bent anteriad), antero-dorsally pointed setae raised from one pore... ***M. schuelkei* Telnov, 2018**
– Anterior margin of male pronotum rounded to broadly rounded, of different structure..**27**
27 Anterior margin of male pronotum with paired bunch of long, strongly Ɔ-like shaped (curled anteriad) anteriad-pointed setae touching cranial 'neck' and head base; occiput slightly declivous posterodorsally; head base broadly rounded ....***M. bicrispus* Telnov, 2022**
– Anterior margin of male pronotum mesally emarginated; anterior margin of this cavity laterally with some long, apically curved, erect setae which are

meeting apically in П-like shaped arc over anterior wall of pronotum...........
....***M. similis* Telnov, 2022**

28 Lateral constriction of pronotum dorsally with two rather large, elongate ovoid notch-like pores and 2 or 3 obtuse, transverse sulci ....***M. negator* Telnov, 2007**
– Dorsal sculpture of lateral pronotal constriction different..........................**29**

29 Head base with bristle of long posteriad-directed setae of subconical appearance; aedeagus as in Fig. 4, endophallic armature of peculiar, spike-nail-shaped spines...***M. hirsutus* sp. nov.**
– Head base without subconical-like bristle of long posteriad-directed setae; shape of aedeagus and endophallic armature different.............................**30**

30 Setae conspicuously dense in pronotal constriction area, in dorsal view effectively concealing structure of constriction, its lateral notches, and its denticles...**31**
– Setae more or less sparse in pronotal constriction, its structure, notches, and denticles clearly visible through setae in dorsal view..........................**32**

31 Aedeagus comparatively stronger elongate, basale not bulbous, apical portion strongly sinuous in lateral view; tempus rather long, slightly constricted posteriad, temporal angle broadly rounded; distribution – Sichuan Province, China ....***M. muli* Telnov, 2022**
– Aedeagus shorter and stouter, basale strongly bulbous, apical portion slightly sinuous in lateral view; head posterior to compound eyes evenly broadly rounded in arc; distribution – Zhejiang Province, China....................
....***M. makarovi* Telnov, 2018**

32 Lateral constriction of pronotum dorsally more or less distinctly medially longitudinally carinate (sometimes only visible by sufficient light!); median carina projected or not to anterior lobe...**33**
– Lateral constriction of pronotum dorsally more or less distinctly punctate or rugulose, not carinate **39**

33 Dorsal median longitudinal carina of pronotal constriction projected to anterior lobe of pronotum for approx. half-length of lobe **34**
– Dorsal median longitudinal carina of pronotal constriction restricted to lateral constriction area or (at maximum) also its anterior and posterior slope.......**36**

34 Basal half of elytra strongly punctate; pronotum paler than dark brown head and elytra; basal portion of aedeagus bulbous in lateral view ....
....***M. andibani* Telnov, 2007**
– Basal half of elytra comparatively less strongly punctate; dorsal body uniformly brown; aedeagus basally bulbous or not **35**

35 Male antennomeres 9 and 10 less strongly transverse (cf. Telnov 2022: fig. 3D); anterior lobe of pronotum convex in lateral view; clypeus emarginate anterodorsally; elytra comparatively longer, elytron apically rounded ....
....***M. belousovi* Telnov, 2022**
– Male antennomeres 9 and 10 strongly transverse (cf. Telnov 2022: fig. 24D); anterior lobe of pronotum flattened in lateral view; clypeus truncate anterodorsally; elytra comparatively shorter, elytron apically subtruncate ...
....***M. kabaki* Telnov, 2022**

36 Terminal antennomere broadly subtriangular, apically rounded; head darker than rest of body; pronotum comparatively slender; aedeagus apically

unevenly rounded in dorsal and ventral view (Telnov 2018: fig. 100) ....
....***M. bukejsi* Telnov, 2018**

– Terminal antennomere elongate triangular, apically pointed; head not darker than rest of body; pronotum comparatively less slender; aedeagus apex different in dorsal and ventral view **37**

37 At least elytra dark brown; sternite IX distinctly sinuous; in dorsal view; lateral constriction area of pronotum with dense, rough punctures continue to sides (slopes) of lateral fovea; aedeagus thick, basal portion bulbous, endophallic armature without pebble-like sclerites ....
....***M. spurisi* Telnov, 2018**

– Dorsum uniformly pale brown, elytra not darker than rest of body; sternite IX arched or slightly sinuous; in dorsal view sides (slopes) of lateral fovea of lateral constriction area of pronotum smooth, not densely punctured; aedeagus if thick with bulbous bosal portion than also pebble-like sclerites present in endophallic armature..**38**

38 Basale of aedeagus strongly bulbous; anterior margin of pronotum broadly rounded; lateral pronotal fovea dorsally deep and broad, lateral denticles prominent, well visible dorsally.............................***M. jiuhuanus* Telnov, 2007**

– Basale of aedeagus slightly bulbous, aedeagus distinctly slenderer; anterior margin of pronotum subtruncate; lateral pronotal fovea dorsally rather narrow, lateral denticles less conspicuous, not prominent, poorly visible in dorsal view .... ***M. periclitatus* Telnov, 2018**

39 Lateral fovea of pronotal constriction in dorsal view on each edge with two pairs of lateral denticles (anterior and posterior, upper and lower) **40**

– Lateral fovea of pronotal constriction in dorsal view on each edge with one pair of lateral denticles (anterior and posterior)..**41**

40 Upper posterior denticle of lateral fovea of pronotal constriction with a brush of short, dense setae (in lateral and dorsal view); lateral constriction continues onto pronotal disc, rather deep in lateral view; compound eye moderately large.. ***M. sichuanus* (Telnov, 1998)**

– No brush of setae on denticles in lateral fovea; lateral constriction vaguely continues onto disc, flat in lateral view; compound eye small ....
....***M. darrenmanni* Telnov, 2018**

41 Species from Japanese Archipelago (Honshu, Shikoku)................................
.... ***M. clavipes* (Champion, 1890)**

– Species from Taiwan...................................***M. nigripennis* (Uhmann, 1994)**

– Species from mainland China...**42**

42 Denticles of lateral pronotal fovea not visible in dorsal view; basal portion of endophallic armature of two subparallel rows of dense spines ....
....***M. daxiangling* Telnov, 2022**

– Denticles of lateral pronotal fovea clearly visible in dorsal view; endophallic armature different...**43**

43 Transition of lateral constriction fovea to pronotal disc is gradual; transverse section across constriction area is arc-shaped **45**

– Transition of lateral constriction fovea to the disc of pronotum is delimited by dorso–lateral expansion of pronotal disc; transverse section across constriction area is similar to T-shape **44**

44　Terminal antennomere elongate; pronotal constriction area comparatively wider (in dorsal view); elytra comparatively shorter; aedeagus without apical projection, apex pointed............................***M. wuliangshan* Telnov, 2018**

–　Terminal antennomere small; pronotal constriction area comparatively narrower (dorsal view); elytra comparatively more elongate; aedeagus with step-like apical projection, apex subtruncate ....
.... ***M. silvicolus* Telnov, 2018**

45　At least one denticle of lateral pronotal fovea (anterior or posterior, as visible in dorsal view) with brush of very dense, short setae...........................**46**

–　Denticles of lateral pronotal fovea glabrous or with sparse, long setae.....**47**

46　Species from Hubei, China; anterior pronotal lobe dorsally minutely punctured; lateral pronotal fovea in dorsal view rather short and narrow; lateral pronotal constriction comparatively less deep (Telnov 2018: fig. 40)...........
....***M. kurbatovi* (Telnov, 1998)**

–　Species from Guangdong, China; anterior pronotal lobe dorsally with sparse but large and deep punctures; lateral pronotal fovea in dorsal view broad and deep; lateral pronotal constriction deeper and broader (Telnov 2022: fig. 16) .... ***M. hajeki* Telnov, 2022**

47　Lateral constriction area of pronotum dorsally smooth and glossy, none or only tracks of sculpture present.........................***M. uhmanni* (Telnov, 1998)**

–　Lateral constriction area of pronotum dorsally distinctly punctured, glossy or subopaque..**48**

48　Anterior margin of pronotum medially truncate, slightly declivous anteriorly; aedeagus stout and bulbous, strongly bi-gibbose in lateral view...................
.... ***M. palaung* Telnov, 2022**

–　Anterior margin of pronotum broadly rounded to subtruncate, not declivous anteriorly; aedeagus different in lateral view..**49**

49　Dorsal body dark brown; endophallic armature garland-like (Telnov 2022: fig. 19) ....***M. hartmanni* Telnov, 2022**

–　Dorsal body dark or pale brown; endophallic armature distinctly different...
....**50**

50　Lateral constriction area of pronotum dorsally with large, elongate, median longitudinal notch; dorsal punctures on lateral constriction area of pronotum comparatively smaller and less rough; aedeagus strongly constricted towards narrowly rounded apex (Telnov 2022: fig. 43)..................................
....***M. usitatus* Telnov, 2022**

–　Lateral constriction area of pronotum dorsally without median longitudinal notch, punctate; dorsal punctures on lateral constriction area of pronotum comparatively larger and rougher; aedeagus not strongly constricted towards apex..**51**

51　Endophallic armature of apical portion of aedeagus small, peculiarly tack-shaped (Fig. 2B, D); elytral punctures comparatively coarser and deeper ....
.... ***M. blinsteini* sp. nov.**

–　Endophallic armature of apical portion of aedeagus not tack-shaped; punctures on posterior half of elytron comparatively less dense and flatter ....
....***M. korolevi* Telnov, 2022**

References

Bonadona P (1978) Les Tomoderini subendogés d'Afrique centrale et de l'Inde méridionale (Col. Anthicidae). Revue suisse de Zoologie 85(3): 645–656. https://doi.org/10.5962/bhl.part.82253

Chandler DS (2010) 11.26. Anthicidae Latreille, 1819. In: Leschen RAB, Beutel RG, Lawrence JF (Eds) *Coleoptera*, *Beetles*. Vol. 2: Morphology and systematics (Elateroidea, Bostrichiformia, Cucujiformia partim). Arthropoda Insecta. Handbook of zoology. De Gruyter, Berlin-New York, 729–741. https://doi.org/10.1515/9783110911213.729

Iwan D, Löbl I (2020) Catalogue of Palaearctic Coleoptera. Volume 5. Revised and Updated 2nd edn. Tenebrionoidea. Brill, Leiden-Boston, [xxiv +] 945. https://doi.org/10.1163/9789004434998

Pic M (1901) Hylophilidae de la Malaisie et nouveau genre d'Anthicidae de Sumatra. Annali del Museo Civico di Storia Naturale "Giacomo Doria" 2(40): 737–742.

Telnov D (1998) Anthicidae (Coleoptera) der Sammlung Sergej Kurbatov, mit Beschreibung von sechs neuen Arten aus der Orientalis. Bulletin de la Société royale Belge d'Entomologie 134(1): 81–100.

Telnov D (2004) Neue und wenig bekannte Anthicidae (Coleoptera) von dem malayischen Borneo. Entomologische Zeitschrift 114(5): 209–222.

Telnov D (2007a) Revision der Tomoderinae. Die *Macrotomoderus gracilicollis*-Artengruppe (Coleoptera: Anthicidae). Mitteilungen des Internationalen Entomologischen Vereins e.V. 32(1–2): 1–25.

Telnov D (2007b) Zur Kenntnis asiatischer Anthicidae, IV (Insecta: Coleoptera). Mitteilungen des Internationalen Entomologischen Vereins e.V. 32(3–4): 89–105.

Telnov D (2018) Revision of the Tomoderinae (Coleoptera: Anthicidae). Part II. *Macrotomoderus* Pic, 1901 species from China and Taiwan. Annales zoologici 68(3): 463–492. https://doi.org/10.3161/00034541ANZ2018.68.3.008

Telnov D (2020) Family Anthicidae Latreille, 1819. In: Iwan D, Löbl I (Eds) Catalogue of Palaearctic Coleoptera. Vol. 5. Revised and Updated Second Edition. Tenebrionoidea. Brill, Leiden-Boston, 575–625.

Telnov D (2022) Revision of the Tomoderinae (Coleoptera: Anthicidae). Part III. New species and records of *Macrotomoderus* Pic, 1901 from China and a key to the Palaearctic species. European Journal of Taxonomy 797: 1–100. https://doi.org/10.5852/ejt.2022.797.1667

Telnov D (2023) Revision of the Tomoderinae Bonadona, 1961 (Coleoptera: Anthicidae). Part IV. First review of the Philippine Archipelago species. Tijdschift voor Entomologie 166: 125–162. https://doi.org/10.1163/22119434-bja10026

Telnov D, Gusakov AA (2023) Rediscovery of *Tomosomus* Motschulsky, 1855 (Coleoptera: Anthicidae) with redescription of the genus, a new genus-rank synonym, and a key to species. Zootaxa 5293(3): 541–556. https://doi.org/10.11646/zootaxa.5293.3.6

Uhmann G (1993) Anthiciden aus Sabah (Borneo) aus dem Naturhistorischen Museum in Genf (Coleoptera, Anthicidae). Revue suisse de Zoologie 110(2): 373–404. https://doi.org/10.5962/bhl.part.79867

Uhmann G (1994a) Neue Anthicidae aus Borneo, Malaysia, von den Philippinen und aus Zambia (Coleoptera). Entomologische Zeitschrift 104(11): 210–217.

Uhmann G (1994b) Die von Rudolf Schuh in Asien gefundenen Anthiciden. Entomofauna 15(35): 405–416.

Uhmann G (1994c) Südostasiatische Anthiciden aus dem Naturhistorischen Museum in Genf, 4 (Coleoptera, Anthicidae). Revue suisse de Zoologie 101(3): 655–676. https://doi.org/10.5962/bhl.part.79922

Uhmann G (1996a) Anthiciden aus dem Naturhistorischen Museum in Wien (Coleoptera, Anthicidae). Entomologische Blätter 92(1–2): 19–36.

Uhmann G (1996b) Indo-australische Anthicidae (Coleoptera) im Naturhistorischen Museum in Genf. Revue suisse de Zoologie 103(3): 737–748. https://doi.org/10.5962/bhl.part.79971

Uhmann G (1998) Beschreibung von vier neuen Arten der Gattung *Derarimus* (Coleoptera, Anthicidae) aus Malaysia. Revue suisse de Zoologie 15(2): 493–497. https://doi.org/10.5962/bhl.part.80048

Uhmann G (1999) Neue Anthicidae aus der Sammlung von Jürgen Wiesner (Coleoptera, Anthicidae). Entomologische Blätter 95(2–3): 145–156.

New taxonomic and faunistic data on the funnel-weavers (Araneae, Agelenidae) of Turkiye and the Caucasus, with five new species

Alireza Zamani[1], Rahşen S. Kaya[2], Yuri M. Marusik[3,4,5]

1   *Zoological Museum, Biodiversity Unit, FI-20014 University of Turku, Turku 20500, Finland*
2   *Department of Biology, Faculty of Arts and Science, Bursa Uludağ University, TR-16059, Bursa, Turkiye*
3   *Department of Zoology & Entomology, University of the Free State, Bloemfontein 9300, South Africa*
4   *Altai State University, Lenina Pr., 61, Barnaul, RF-656049, Russia*
5   *Institute for Biological Problems of the North, Portovaya Str. 18, Magadan 685000, Russia*

Corresponding author: Alireza Zamani (zamani.alireza5@gmail.com)

Citation: Zamani A, Kaya RS, Marusik YuM (2024) New taxonomic and faunistic data on the funnel-weavers (Araneae, Agelenidae) of Turkiye and the Caucasus, with five new species. ZooKeys 1218: 251–286. https://doi.org/10.3897/zookeys.1218.135249

Abstract

New taxonomic and faunistic data on the agelenid spiders of Turkiye and the Caucasus are provided. Five species are described as new to science: *Maimuna antalyensis* **sp. nov.** (♂♀; Turkiye: Antalya), *Tegenaria ballarini* **sp. nov.** (♂♀; Turkiye: Antalya), *T. beyazcika* **sp. nov.** (♂; Turkiye: Antalya), *T. egrisiana* **sp. nov.** (♂♀; Georgia: Imereti), and *T. hoeferi* **sp. nov.** (♂♀; Armenia: Kotayk). *Tegenaria lazarovi* Dimitrov, 2020, **syn. nov.** is proposed as a new junior synonym of *T. averni* Brignoli, 1978. *Persiscape caucasica* (Guseinov, Marusik & Koponen, 2005) is newly reported from Armenia, and *T. chumachenkoi* Kovblyuk & Ponomarev, 2008 is reported for the first time from Turkiye. New distribution records for *T. dalmatica* Kulczyński, 1906, *T. hamid* Brignoli, 1978, *T. longimana* Simon, 1898 and *T. percuriosa* Brignoli, 1972, and topotype material for *T. tekke* Brignoli, 1978 are reported. The record of *Eratigena fuesslini* (Pavesi, 1873) from Turkiye is found to be based on a misidentification, and is herein attributed to *T. hamid*. The presence of an embolic spine, unknown in any other species of *Tegenaria*, is documented in *T. anhela* Brignoli, 1972 for the first time. Photographs are provided for all treated species.

Key words: Anatolia, Armenia, Georgia, *Maimuna*, new record, new synonymy, *Persiscape*, *Tegenaria*

Introduction

Agelenidae C.L. Koch, 1837 is a large family of spiders, encompassing 1,405 extant species across 96 genera worldwide (WSC 2024). Commonly known as "funnel-weavers," the family has been relatively well-studied in the Palaearctic (e.g., de Blauwe 1980; Levy 1996). In the Western Palaearctic, Turkiye has the highest recorded diversity of Agelenidae, with 74 species documented (Danışman et al. 2024). Other areas within the Western Palaearctic remain largely under-studied. For example, in the Caucasus, Otto (2022) lists 36 species in ten genera of Agelenidae, yet only three species have been reported from Armenia and 18 from Georgia to date. This highlights the limited understanding of agelenid diversity in this region (Zarikian et al. 2022).

While examining spiders from Turkiye, Georgia, and Armenia, we had the opportunity to study several agelenid specimens from these countries. In this paper, we present the following findings: the descriptions of four new species of *Tegenaria* Latreille, 1804 and of one new species of *Maimuna* Lehtinen, 1967; the synonymization of *T. lazarovi* Dimitrov, 2020; the presence of an embolic spine in *T. anhela* Brignoli, 1972; and several new faunistic data for agelenids in Turkiye and Armenia.

Materials and methods

Photographs of specimens and their copulatory organs were obtained using an Olympus Camedia E-520 camera attached to an Olympus SZX16 stereo-microscope at the Zoological Museum of the University of Turku, Finland. Digital images of different focal planes were stacked with Helicon Focus™ 8.1.1. Illustrations of vulvae were made after digesting tissues off in a 10% KOH aqueous solution. Body measurements exclude the chelicerae and spinnerets. Leg segments were measured on the dorsal side. Measurements of legs are listed as: total (femur, patella, tibia, metatarsus, tarsus). All measurements are given in millimeters.

Abbreviations used in the text and figures

Eyes: **ALE**—anterior lateral eye, **AME**—anterior median eye, **PLE**—posterior lateral eye, **PME**—posterior median eye.

Leg segments: **Fe**—femur, **Pa**—patella, **Ta**—tarsus, **Ti**—tibia.

Male palp: **Eb**—embolus base, **Em**—embolus, **Es**—embolic spine, **Cc**—claw-like projections of the conductor, **Cn**—conductor, **Cp**—basal process of the cymbium, **Ma**—median apophysis, **Mp**—median process, **Rd**—retrodorsal tibial apophysis, **Rl**—retrolateral tibial apophysis, **Rv**—retroventral tibial apophysis, **Ts**—tooth of the retrolateral tibial apophysis, **Vc**—retroventral crest.

Epigyne: **Cd**—copulatory duct, **Co**—copulatory opening, **Fo**—fovea, **Mr**—membranous part of the receptacle, **Rs**—sclerotized part of the receptacle, **Sl**—longitudinal scuta.

Depositories: **MHNG**—Muséum d'histoire naturelle, Genève, Switzerland (L. Monod); **ZMUT**—Zoological Museum of the University of Turku, Finland (V. Vahtera); **ZMMU**—Zoological Museum of the Moscow State University, Russia (K.G. Mikhailov); **ZMUU**—Zoological Museum of the Bursa Uludağ University, Turkiye (R.S. Kaya).

Taxonomy

Family Agelenidae C.L. Koch, 1837
Subfamily Ageleninae C.L. Koch, 1837

Tribe Agelenini C.L. Koch, 1837

Comment. For the diagnosis and composition, see Lehtinen (1967), Bolzern et al. (2013), and Zamani and Marusik (2020).

Persiscape caucasica (Guseinov, Marusik & Koponen, 2005)
Figs 1C, 2D, E

Agelescape caucasica Guseinov et al., 2005: 157, figs 9−12, 69−71, 105 (♀).
Persiscape caucasica: Zamani and Marusik 2020: 376, fig. 12M−O (♀).

Material. Armenia: Kotayk Prov.: • 1 ♀ (ZMUT), env. of Geghadir, 40°09'N, 44°38'E, 15.05.2021 (Y.M. Marusik).

    Comment. The male of this species is currently unknown.

    Distribution. Previously known from Greece, Turkiye, Georgia, and Azerbaijan (WSC 2024). A new record for Armenia.

Tribe Textricini Lehtinen, 1967

Comment. For the diagnosis and composition, see Kaya et al. (2023).

Maimuna antalyensis sp. nov.
https://zoobank.org/3A871504-2F88-4DF2-9053-90DFF4238122
Figs 1A, B, 2A−C, 3A−D, 4A−D

Type material. *Holotype* • ♂ (ZMUT), Turkiye: Antalya Prov.: Alanya, env. Kestel, Dim Valley, 36°32'34.5"N, 32°06'17.5"E, 110 m, pine and oak forest, 2.01.2013 (Y.M. Marusik). *Paratypes*: • 5 ♀ (ZMUT), same data as for the holotype; • 1 ♀ (ZMUT), Asmaca, 36°36'32.3"N, 32°03'12.4"E, 686 m, pine and oak forest, 3.01.2013 (Y.M. Marusik); • 2 ♀ (ZMUT), Elikesik rd., 36°33'55.6"N, 31°55'30.3"E, 24 m, maquis on S exposed slope, 8.01.2013 (Y.M. Marusik); • 2 ♀ (ZMUT), slopes of Alanya Castle, Damlataş side, 36°32'11.6"N, 31°59'30.3"E, 50 m, pine forest, under stones and in litter, 7.01.2013 (Y.M. Marusik).

    Comparative material. *Maimuna vestita* (C.L. Koch, 1841): Turkiye: Bursa Prov.: • 1 ♀ (ZMUU), Bursa Uludağ University campus area, 30.11.1999 (R.S. Kaya); • 2 ♀ (ZMUU), same, 16.05.2000 (R.S. Kaya); • 1 ♀ (ZMUU), same, 3.03.2003 (R.S. Kaya); • 1 ♀ (ZMUU), same, 10.09.2005 (R.S. Kaya); • 1 ♂ 1 ♀ (ZMUU), same, 20.04.2012 (R.S. Kaya); • 1 ♂ 1 ♀ (ZMUU), same, 21.05.2012 (R.S. Kaya); • 5 ♀ (ZMUU), same, 4.05.2023 (R.S. Kaya); • 2 ♂ 3 ♀ (ZMUU), same, 4.01.2024 (R.S. Kaya); • 1 ♂ 2 ♀ (ZMUU), same, 11.07.2024 (R.S. Kaya); • 5 ♀ (ZMUU), Lake Uluabat, Halilbey Island, 8.04.2001 (R.S. Kaya); • 1 ♂ 3 ♀ (ZMUU), Lake Uluabat, Terzioğlu Island, 14.10.2004 (R.S. Kaya); • 5 ♀ (ZMUU), same, 25.04.2005 (R.S. Kaya); • 1 ♂ 2 ♀ (ZMUU), Lake Uluabat, Manastır Island, 28.09.2005 (R.S. Kaya); • 1 ♂ (ZMUU), same, 29.09.2005 (R.S. Kaya); • 2 ♂ 1 ♀ (ZMUU), Lake Uluabat, Halilbey Island, 15.12.2005 (R.S. Kaya); • 1 ♀ (ZMUU), Karacabey, Boğaz, 4.05.2005 (R.S. Kaya); • 3 ♀ (ZMUU), same, 8.08.2007 (R.S. Kaya); • 2 ♀ (ZMUU), same, 5.06.2018 (R.S. Kaya); • 2 ♀ (ZMUU), same, 11.06.2021 (R.S. Kaya); • 1 ♂ 1 ♀ (ZMUU), Kaplıkaya, 29.03.2007 (R.S. Kaya); • 2 ♂ 2 ♀ (ZMUU), same, 10.12.2008 (R.S. Kaya); • 1 ♀ (ZMUU), Görükle Vill., 20.04.2012 (R.S. Kaya); • 1 ♀ (ZMUU), Nilüfer Metro station, 26.05.2012 (R.S. Kaya); • 1 ♂ (ZMUU), Orhangazi Dist., 4.05.2014 (R.S. Kaya); Çanakkale Prov.: • 1 ♀ (ZMUU), Gökçeada Island, Lake salt area, 4.05.2004 (R.S. Kaya).

Figure 1. Habitus of *Maimuna antalyensis* sp. nov. (**A, B**), *Persiscape caucasica* (**C**), and *Tegenaria hamid* (**D**), dorsal view. **A** male **B–D** females.

Diagnosis. The new species is similar to *M. cariae* Brignoli, 1978 in the overall shape of its copulatory organs. The male differs by having a shorter tip of the cymbium (as long as the palpal tibia, vs longer), and by a different shape of the conductor and the median process (cf. Fig. 3B–D and Dimitrov 2022: fig. 26). The female of the new species has a hexagonal epigynal fovea, in contrast to the subtriangular fovea of *M. cariae* (cf. Fig. 2A, B and Dimitrov 2022: fig. 17).
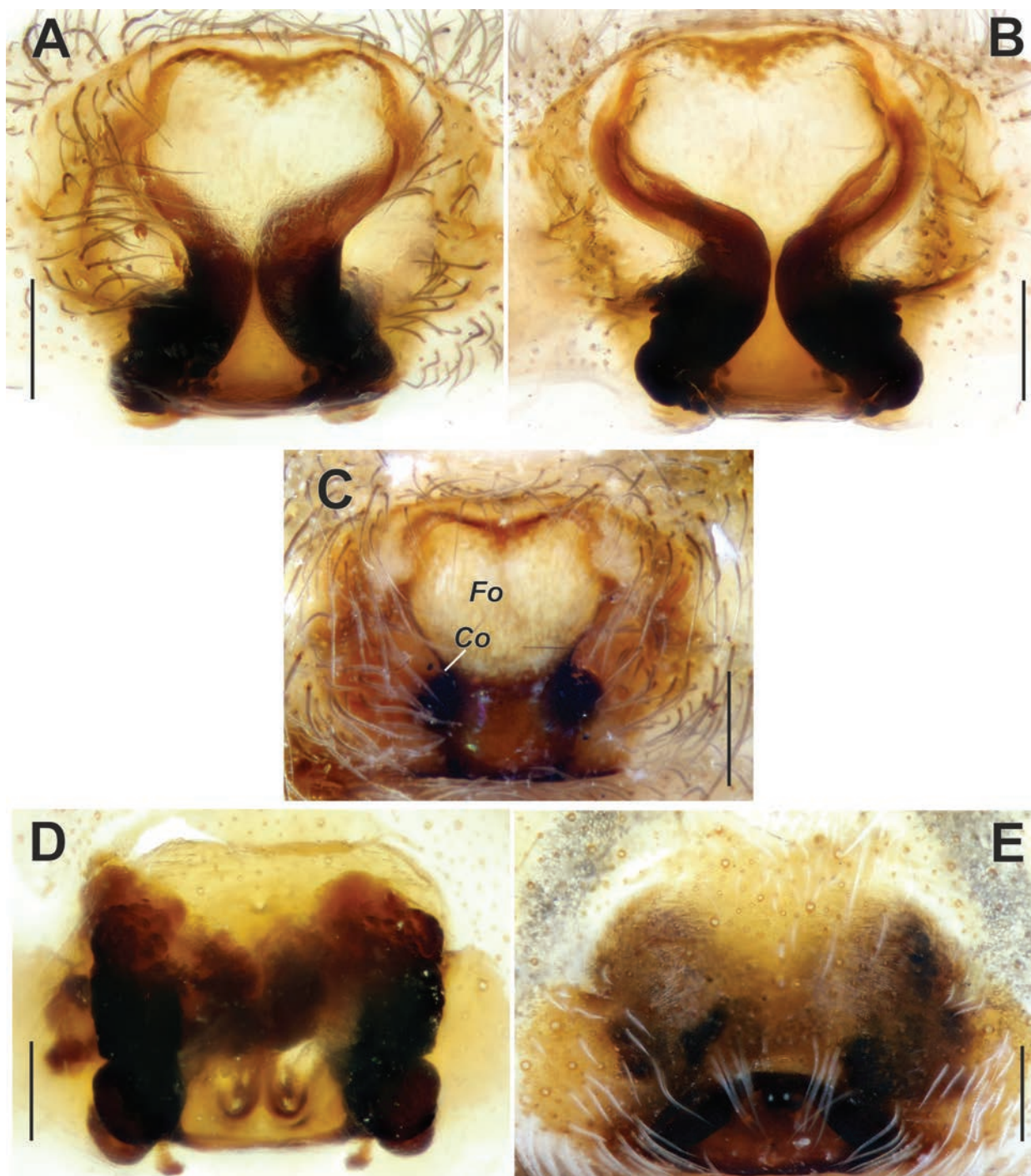
Figure 2. Epigyne of *Maimuna antalyensis* sp. nov. (**A–C**) and *Persiscape caucasica* (**D, E**). **A** macerated, ventral view **B, D** vulva, dorsal view **C, E** intact, ventral view. Abbreviations: *Co* – copulatory opening, *Fo* – fovea. Scale bars: 0.2 mm.

Description. Male. Habitus as in Fig. 1A. Total length 5.40. Carapace 2.60 long, 1.90 wide. Eye sizes: AME: 0.10, ALE: 0.13, PME: 0.18, PLE: 0.13. Carapace, sternum, labium, and maxillae pale brown; carapace with darker submedian bands; ocular region black. Legs yellowish brown, with annulations. Abdomen dorsally dark greyish with paler chevrons, pale greyish ventrally. Spinnerets pale greyish, darker basally. Measurements of legs: I: 5.81+missing Ta (1.74, 0.82, 1.43, 1.82, missing), II: 6.73 (1.77, 0.82, 1.37, 1.73, 1.04), III: 6.64 (1.74, 0.76, 1.34, 1.74, 1.06), IV: 8.53 (2.19, 0.85, 1.80, 2.55, 1.14).
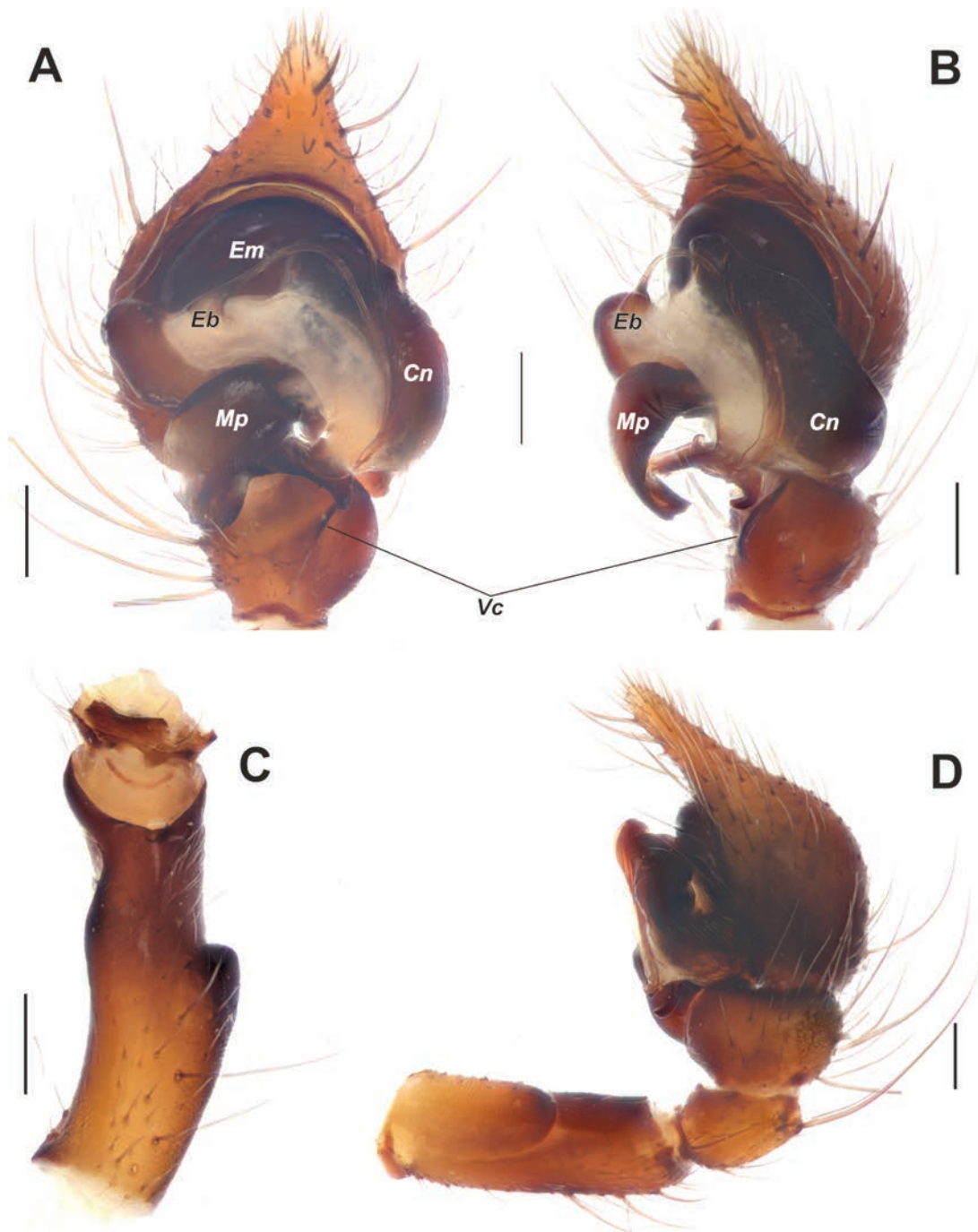
Figure 3. Male palp of *Maimuna antalyensis* sp. nov. **A** ventral view **B** retroventral view **C** femur, ventral view **D** retrolateral view. Abbreviations: *Eb* – base of the embolus, *Em* – embolus, *Cn* – conductor, *Mp* – median process, *Vc* – retroventral crest of the tibia. Scale bars: 0.2 mm.

Palp as in Figs 3A–D, 4A–D; femur modified – with retroventral bump in mid part, ~ 3× longer than wide, shorter than cymbium; dorsal length of patella same as in tibia; tibia ~ 1.4× wider than long (Fig. 3C, D), lacking prominent apophysis but with retroventral crest (*Vc*) (Fig. 3A, B); cymbium ~ 1.4× longer than wide, with tip ~ 1/3 of cymbial length; bulb as long as wide; conductor (*Cn*) massive, strongly sclerotized prolateral arm lacking, terminal part with two claw-like projections (*Cc*; Fig. 4D); median process (*Mp*) massive, roundly bent in lateral view (Fig. 4B, C); embolus (*Em*) filiform, weakly sclerotized, with small base (*Eb*).
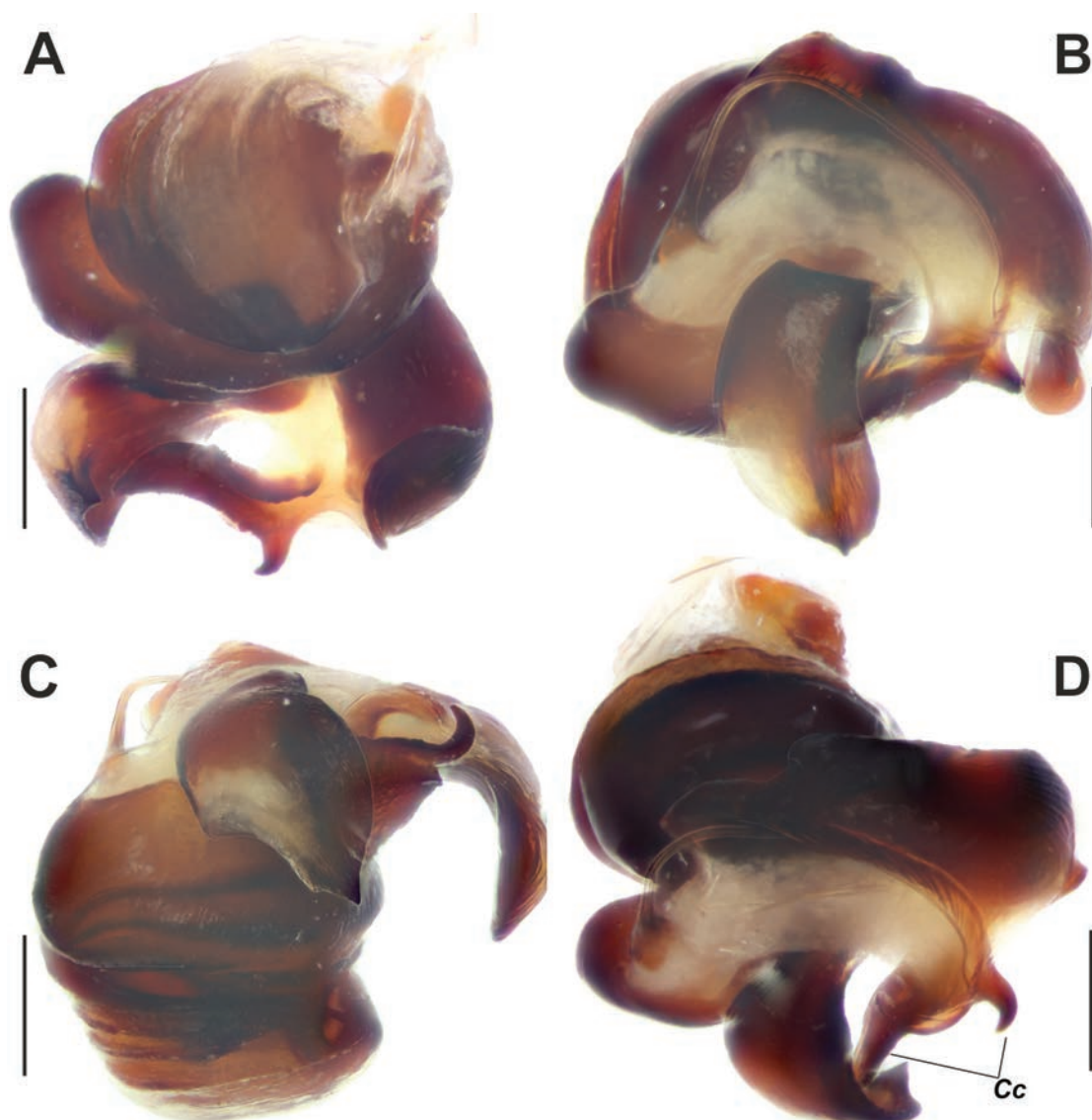
Figure 4. Dissected bulb of *Maimuna antalyensis* sp. nov. **A** proximal view **B** ventral view **C** proventral view **D** retroventral view. Abbreviation: *Cc* – claw-like projections of the conductor. Scale bars: 0.2 mm.

Female. Habitus as in Fig. 1B. Total length 7.50. Carapace 3.28 long, 2.07 wide. Eye sizes: AME: 0.12, ALE: 0.17, PME: 0.20, PLE: 0.15. Coloration as in male. Measurements of legs: I: 7.25 (1.94, 1.02, 1.44, 1.76, 1.09), II: 7.24 (1.85, 1.05, 1.47, 1.73, 1.14), III: 7.37 (2.00, 0.96, 1.42, 1.94, 1.05), IV: 9.58 (2.45, 1.11, 2.13, 2.66, 1.23).

Epigyne as in Fig. 2A–C; epigynal plate slightly wider than long; fovea (*Fo*) hexagonal, approximately as long as wide, located anteriorly (Fig. 2C); copulatory ducts gradually turning to receptacles and approximately as wide as receptacles; copulatory ducts converging and contiguous, receptacles diverging (Fig. 2A, B).

Comment. In the examined comparative female specimens of *M. vestita*, we observed noticeable variation in both body size and epigyne morphology. In particular, in smaller individuals, the shape of the epigynal fovea can vary significantly. A similar pattern is observed in *M. antalyensis* sp. nov., where smaller females also exhibit variation in the shape of the epigynal fovea, ranging from hexagonal to nearly circular in some specimens.
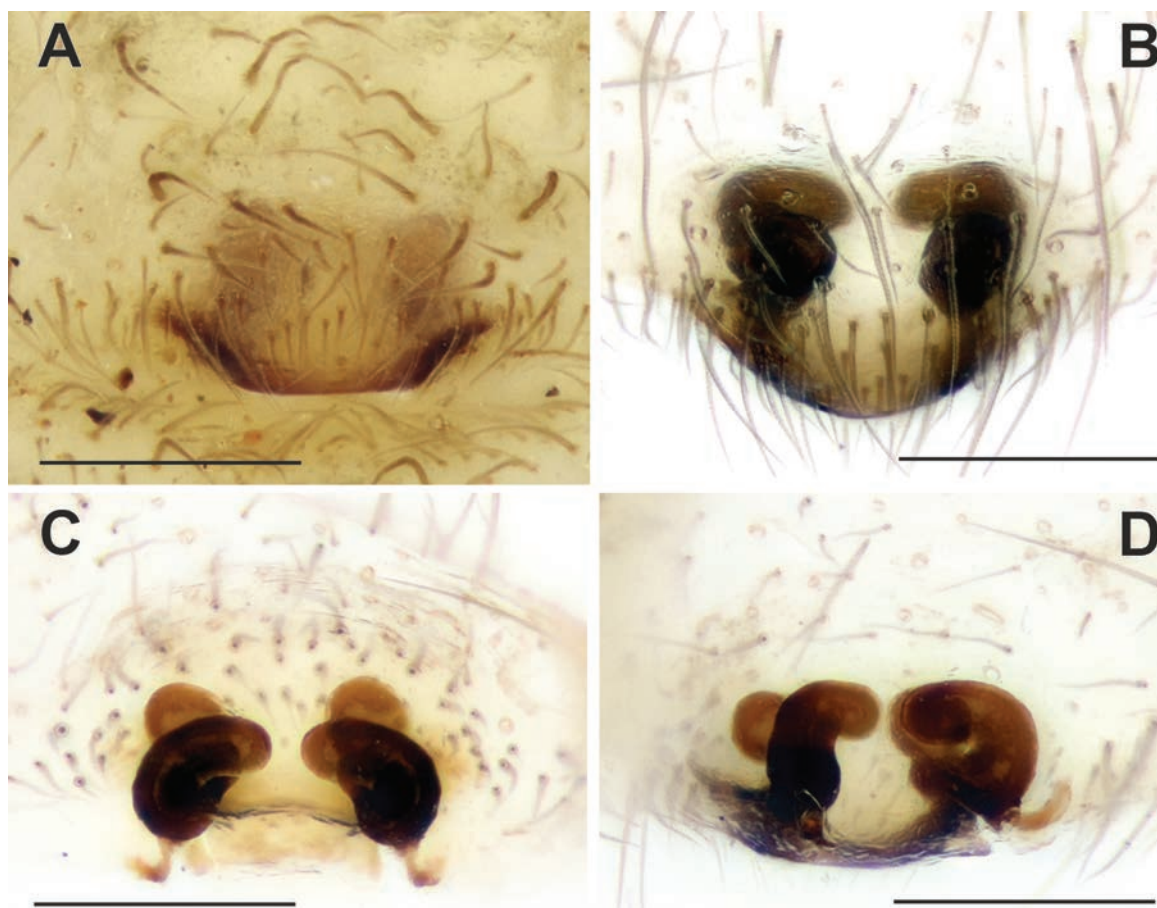
Figure 5. Epigyne of *Tegenaria hamid*. **A** intact, ventral view **B** macerated, anteroventral view **C** vulva, dorsal view **D** vulva, anterodorsal view. Scale bars: 0.2 mm.

Note. For comments on the homology of the structure referred to here as the "median process," see Kaya et al. (2023).

Distribution. Known from the listed localities in Antalya Province, southwestern Turkiye.

Etymology. The specific epithet refers to the type locality of the species in Antalya, Turkiye.

Tribe Tegenariini Lehtinen, 1967

Comment. For the diagnosis and composition, see Bolzern et al. (2010).

***Tegenaria anhela* Brignoli, 1972**
Figs 6A, B, 7A–D, 8A–C, 20B

Tegenaria anhela Brignoli, 1972: 173, figs 24–27 (♂♀).
Malthonica anchela: Guseinov et al. 2005: 164 (lapsus).
Tegenaria anhela: Bolzern et al. 2013: 846.

Material. Turkiye: Antalya Prov.: • 1 ♂ 1 ♀ (ZMUT), Döşemealtı, 37°01'N, 30°36'E, 4.08.2009 (R.S. Kaya, C. Kaya); • 1 ♂ 1 ♀ (ZMUU). same data; • 2 ♀ (ZMUU), Döşemealtı, Karain Cave (R.S. Kaya, C. Kaya).
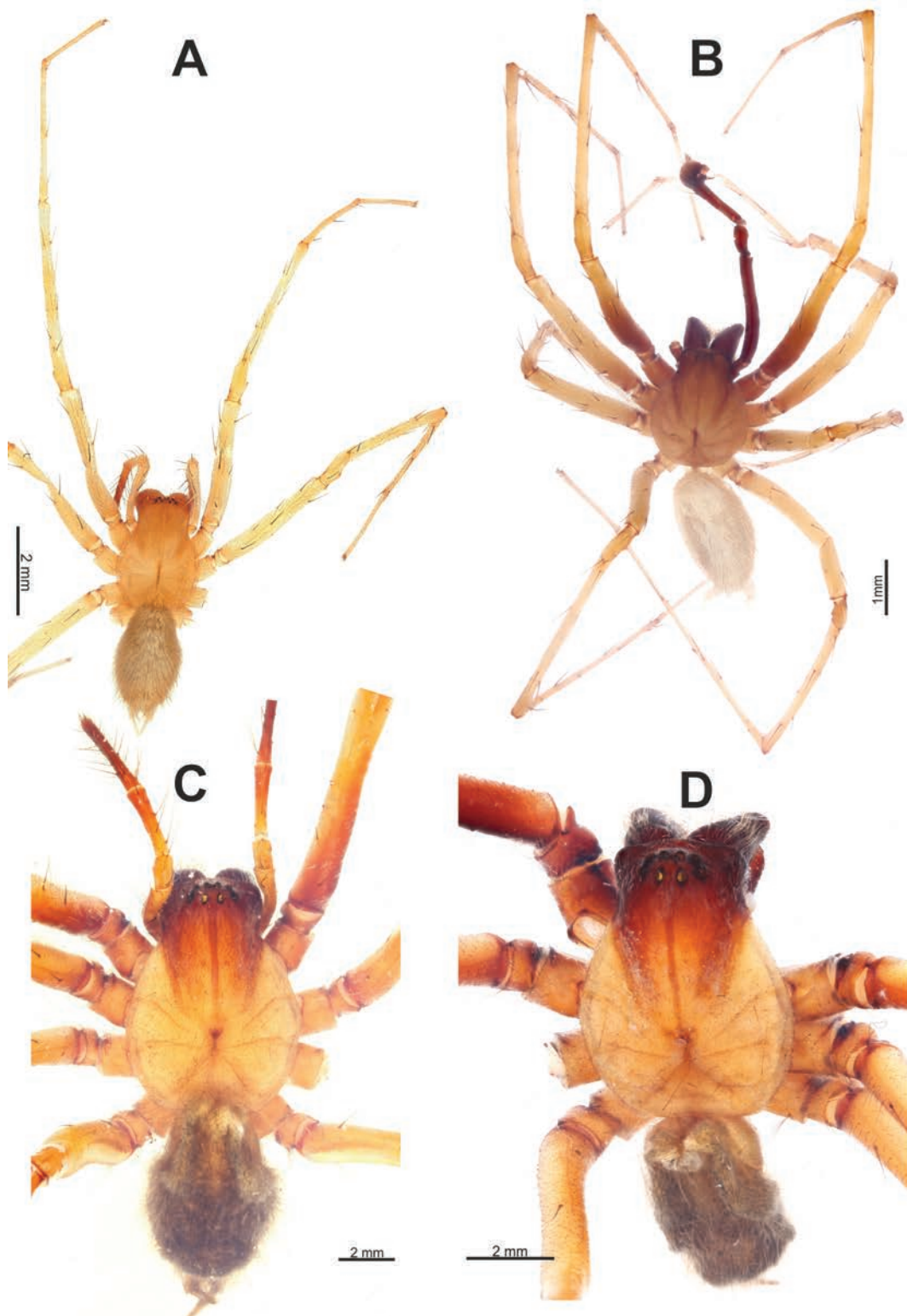
Figure 6. Habitus of *Tegenaria anhela* (**A, B**) and *Tegenaria ballarini* sp. nov. (**C, D**). **A, C** females **B, D** males.

Comments. *Tegenaria anhela* was described based on material collected from Karain Cave in Antalya (Brignoli 1972). Later, it was recorded from Mustan Ini Cave, which is located near the type locality (Brignoli 1978a). Although the original description includes informative illustrations, it lacks detailed explanations of the palpal structures. During the examination of our material, we
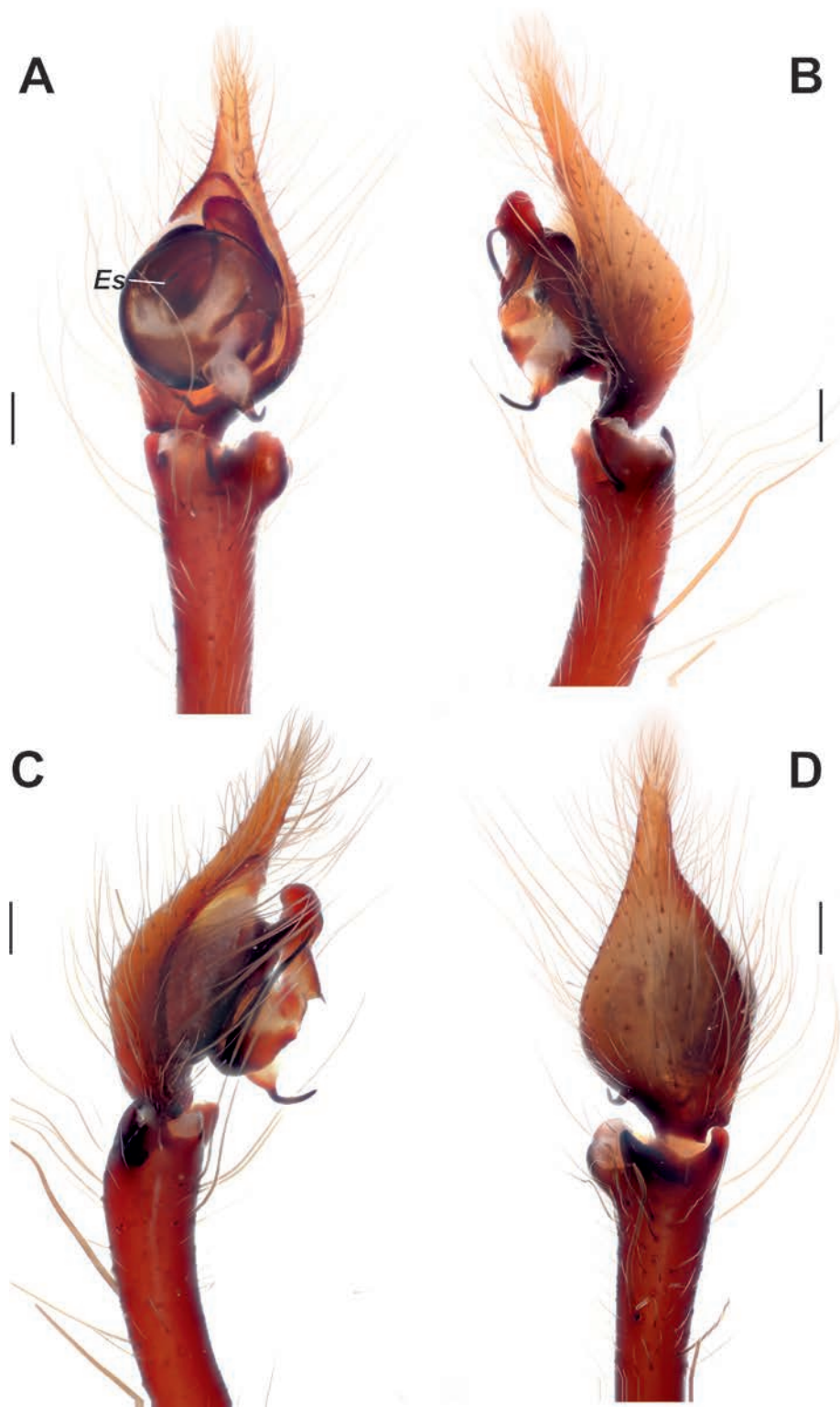
Figure 7. Male palp of *Tegenaria anhela*. **A** ventral view **B** retrolateral view **C** prolateral view **D** dorsal view. Abbreviation: *Es* – embolic spine. Scale bars: 0.2 mm.

observed a unique structure, which we term the "embolic spine" (*Es*; Fig. 7A). This structure, the homology of which remains unclear, is situated between the base of the embolus and the conductor, and it has not been reported in any other *Tegenaria* species to date.

Distribution. Known only from Antalya Province, southwestern Turkiye.

Tegenaria averni Brignoli, 1978
Figs 8D, E, 13A–D

Tegenaria averni Brignoli, 1978a: 50, fig. 10 (♀).
Tegenaria lazarovi Dimitrov, 2020: 48, figs 1–12 (♂♀). Syn. nov.

Material. Turkiye: Mersin Prov.: • 2 ♂ 2 ♀ (ZMUT), Silifke, Cennet Cave, 36°26'12"N, 34°06'22"E, 20.09.2010 (Y.M. Marusik).

Comments. *Tegenaria averni* was described based on a single female from Cennet Cave in Mersin (Brignoli 1978a). In his review of the *ariadnae* species-group, Dimitrov (2020) described *T. lazarovi* based on material of both sexes collected in a cave in Mersin. Although the type locality of *T. lazarovi* is only 65 km away from that of *T. averni*, and both are in the same provincial district, *T. averni* is not mentioned in Dimitrov (2020) at all, likely due to a lack of males. Collection of material of both sexes at the type locality of *T. averni* revealed that these two populations are conspecific. Therefore, *T. lazarovi* syn. nov. is proposed as a junior synonym of *T. averni*.

Distribution. Known only from two caves in Mersin Province, southern Turkiye.

Tegenaria ballarini sp. nov.
https://zoobank.org/BB2AE92D-4A0E-4BFD-9FC5-8F2434070636
Figs 6C, D, 9A–D, 10A, B, 12A–C

Type material. *Holotype* • ♂ (ZMUU), Turkiye: Antalya Prov.: Bozyaka, Köprülü Canyon National Park, 37°11'51"N, 31°11'03"E, 243 m, 15.05.2008 (R.S. Kaya). *Paratypes*: • 1 ♂ 2 ♀ (ZMUT), same data as for the holotype; • 7 ♀ (ZMUU), same data as for the holotype.

Comparative material. *Tegenaria vankeerorum* Bolzern, Burckhardt & Hänggi, 2013 (Figs 10C, D, 11A–D): Turkiye: Muğla Prov.: • 1 ♂ 1 ♀ (ZMUT), Yatağan, Orman İşletme, 37°20'N, 28°08'E, 18.05.2011 (R.S. Kaya).

Diagnosis. The new species is closely related to *T. vankeerorum* and has very similar copulatory organs, especially the male palp. The male of *T. ballarini* sp. nov. differs from the similar species by having relatively longer palpal tibia and a retrolateral apophysis (*RI*) located in the distal half of the tibia, rather than at the midpoint (cf. Figs 9C, 10B, 11B). The female of the new species differs from all other species of *Tegenaria* by having a pair of longitudinal scuta (*Sl*) anterior to the epigynal plate and a straight posterior margin of the epigyne (Fig. 12C). Additionally, the vulva of the new species differs from that of *T. vankeerorum* by having relatively longer copulatory ducts that almost reach the anterior margin of the receptacle (vs reaching only the mid part of the receptacle; cf. Figs 12A, B, 10D, E).

Description. Male. Habitus as in Fig. 6D. Total length 10.75. Carapace 6.75 long, 4.65 wide. Eye sizes: AME: 0.25, ALE: 0.25, PME: 0.22, PLE: 0.25. Pars cephalica, sternum, labium, maxillae, and Fe I brown; pars thoracica and remaining leg segments yellowish brown; chelicerae dark reddish brown. Legs without annulations. Abdomen dark grey, without patterns. Spinnerets uniformly greyish brown. Measurements of legs: I: 48.87+missing Ta (14.28, 2.82, 14.60, 17.17, missing), II: 44.00 (12.00, 2.72, 11.50, 14.28, 3.50), III: 36.83 (9.98, 2.45, 8.65, 12.65, 3.10), IV: 44.36 (11.56, 2.50, 10.88, 15.82, 3.60).
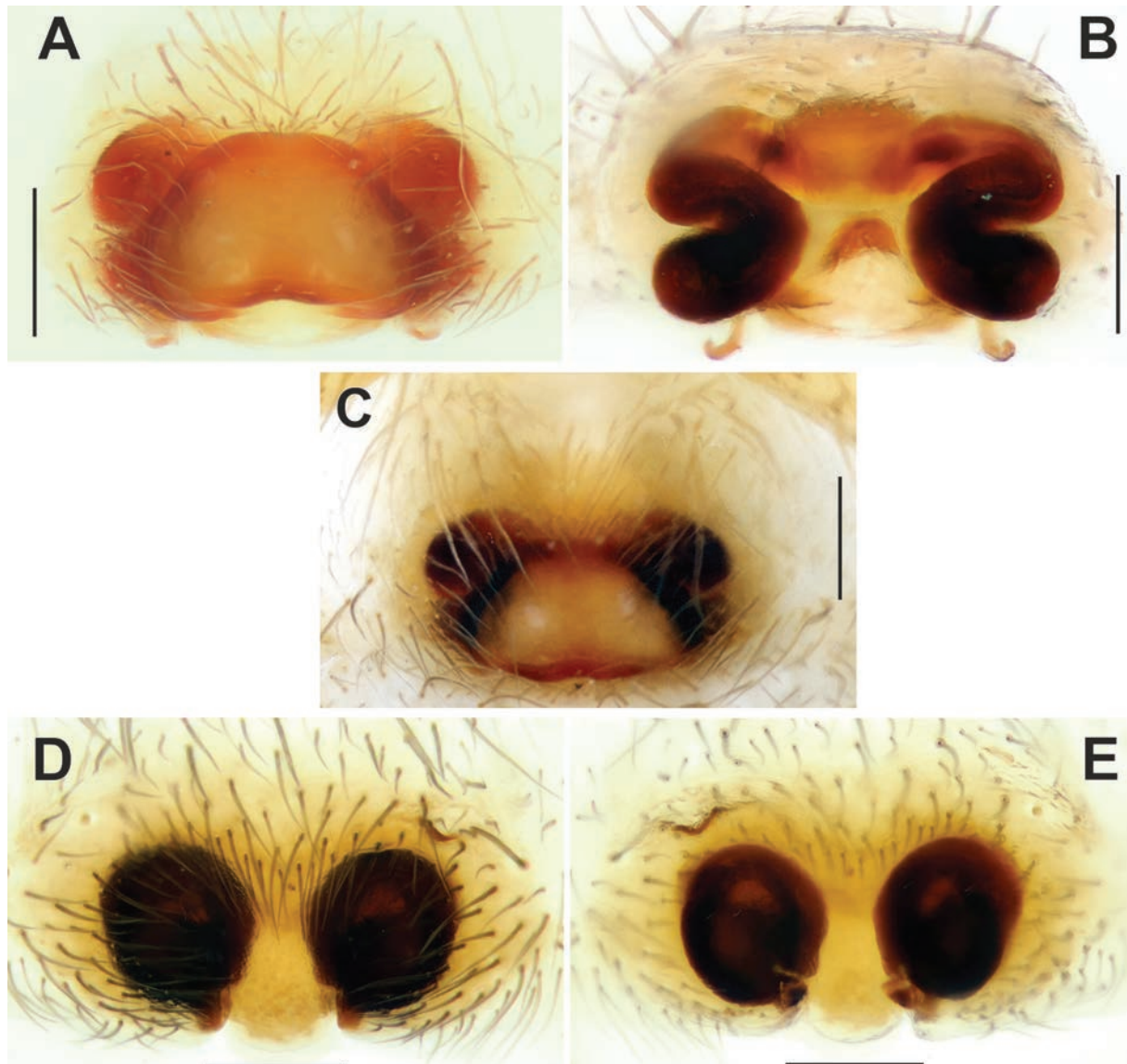
Figure 8. Epigyne of *Tegenaria anhela* (**A–C**) and *T. averni* (**D, E**). **A, D** macerated, ventral view **B, E** vulva, dorsal view **C** intact, ventral view. Scale bars: 0.2 mm.

Palp as in Figs 9A–D, 10A, B; femur 5× longer than wide and ~ 1.8× longer than tibia; patella ~ 1.9× longer than wide; tibia long, ~ 3.5× longer than wide, with three apophyses: retrolateral (*Rl*), retroventral (*Rv*) and retrodorsal (*Rd*) (Fig. 9A–C); retrolateral apophysis located in distal 1/3 of tibia, spine-like, directed antero-retrolaterally, with small tooth (*Ts*) (Fig. 9B); cymbium long, 2.6× longer than wide, tip as long as bulb (Fig. 10B); bulb as long as wide (accounting conductor), tegulum oval, bent prolaterally, and distal part extending embolus; conductor (*Cn*) with rounded distal arm and gradually tapering proximal arm with claw-like tip, terminated at ~ 3 o'clock position; embolus originates at 9 o'clock position, thick basally, roundly bent (Fig. 10A).

Female. Habitus as in Fig. 6C. Total length 14.15. Carapace 8.20 long, 6.15 wide. Eye sizes: AME: 0.25, ALE: 0.27, PME: 0.28, PLE: 0.31. Coloration as in male. Measurements of legs: I: 42.17 (11.61, 3.40, 11.17, 12.34, 3.65), II: 37.29 (10.48, 2.98, 9.36, 11.12, 3.35), III: 33.05 (9.40, 2.75, 7.70, 10.20, 3.00), IV: Fe: 11.03, Pa: 2.98, Ti: 10.03, remaining segments missing.
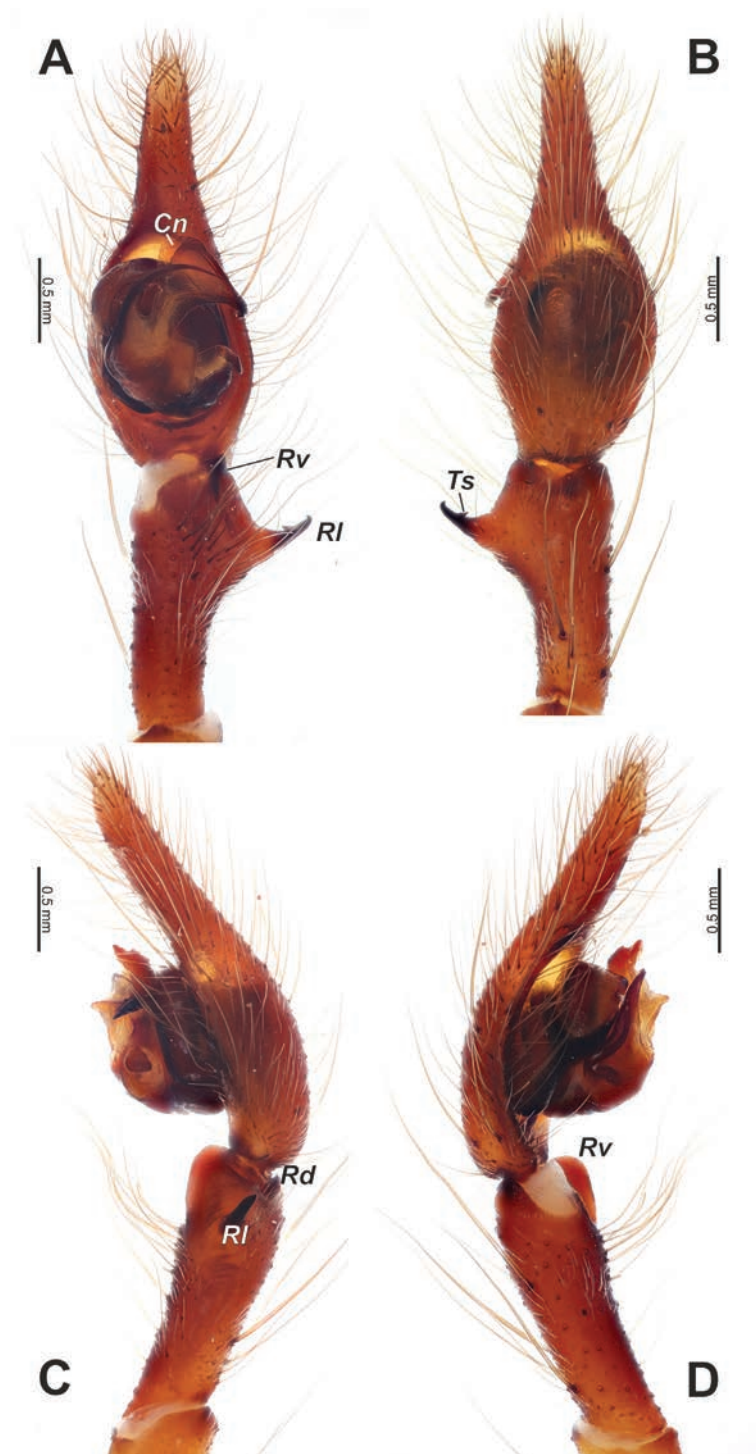
Figure 9. Male palp of *Tegenaria ballarini* sp. nov. **A** ventral view **B** dorsal view **C** retrolateral view **D** prolateral view. Abbreviations: *Cn* – conductor, *Rd* – retrodorsal apophysis, *Rl* – retrolateral apophysis, *Rv* – retroventral apophysis, *Ts* – small tooth of the retrolateral apophysis.

Epigyne as in Fig. 12A–C; epigynal plate > 2× wider than long, with straight and heavily sclerotized posterior margin; area anteriorly from plate with pair of elongate scuta (*Sl*) (Fig. 12C); receptacles subdivided into two parts, anterior pear-shaped membranous part (*Mr*) and heavily sclerotized posterior parts (*Rs*) (Fig. 12B); copulatory ducts well sclerotized, thin, contiguous, terminating near anterior edges of receptacles.
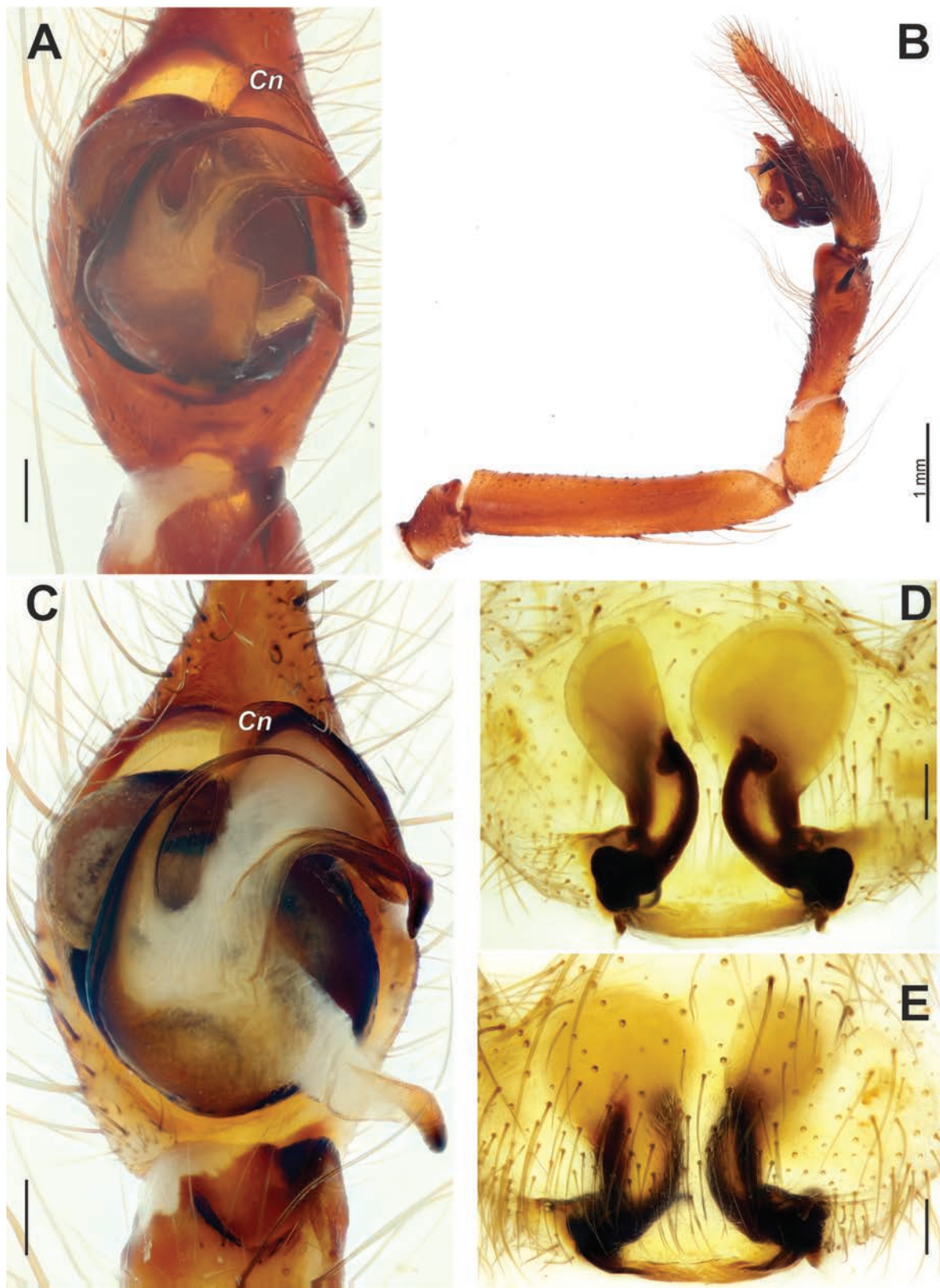
Figure 10. Copulatory organs of *Tegenaria ballarini* sp. nov. (**A, B**) and *T. vankeerorum* (**C–E**). **A, C** palp, ventral view **B** full palp, retrolateral view **D** vulva, dorsal view **E** macerated epigyne, ventral view. Abbreviation: *Cn* – conductor. Scale bars: 0.2 mm, unless otherwise indicated.

Figure 11. Male palp of *Tegenaria vankeerorum*. **A** ventral view **B** retrolateral view **C** dorsal view **D** prolateral view.
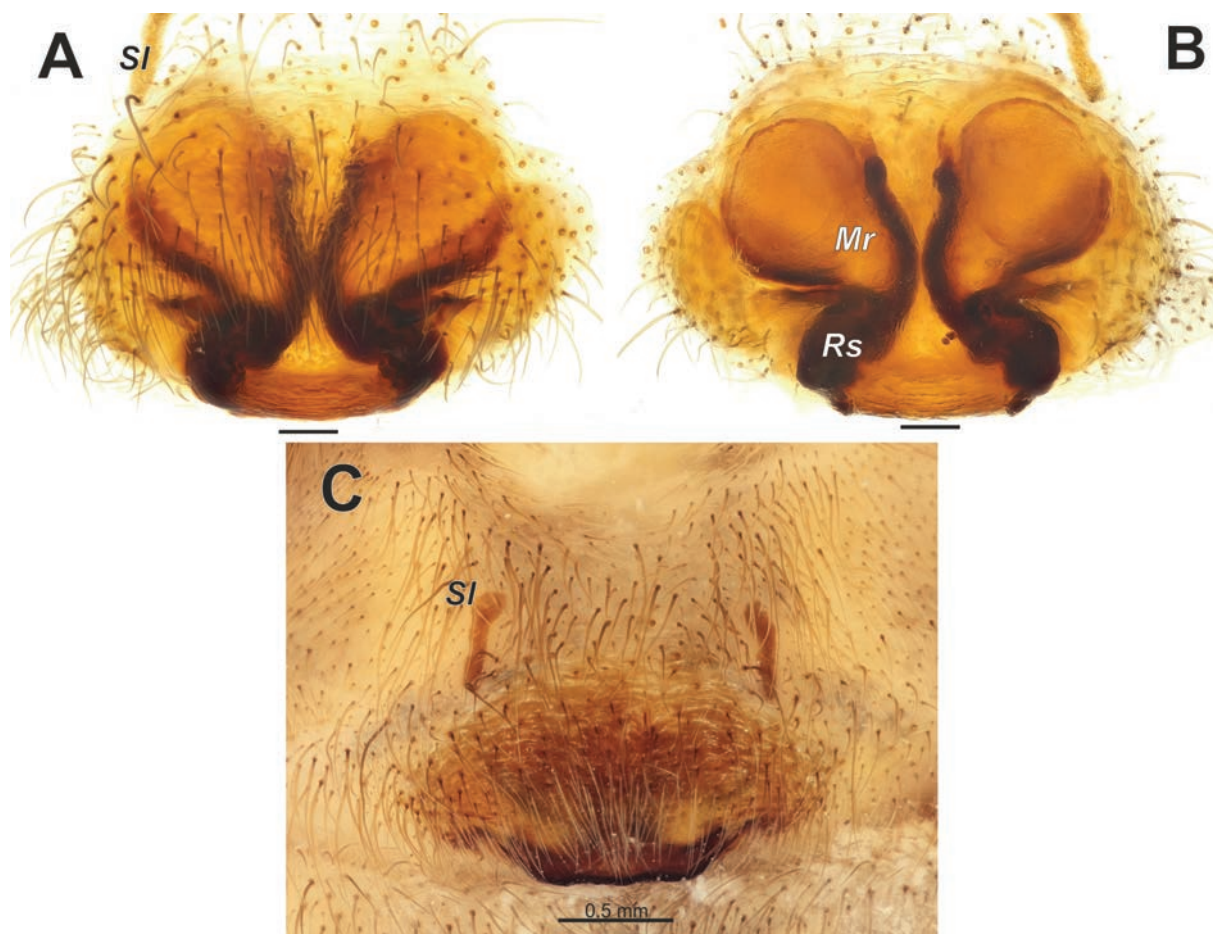
Figure 12. Epigyne of *Tegenaria ballarini* sp. nov. **A** macerated, ventral view **B** vulva, dorsal view **C** intact, ventral view. Abbreviations: *Mr* – membranous part of the receptacle, *Rs* – sclerotized part of the receptacle, *Sl* – longitudinal scutum of the epigynal plate. Scale bars: 0.2 mm, unless otherwise indicated.

Distribution. Known only from the type locality in Antalya Province, southwestern Turkiye.

Etymology. The new species is named in honor of our colleague Francesco Ballarin (Tokyo, Japan), in recognition of his assistance to the second author during her visit to the Brignoli collection in Verona, Italy.

Tegenaria beyazcika sp. nov.

https://zoobank.org/2EEF98AE-7348-4DEA-AE26-AE050EFBA76A
Figs 14A–D, 18D

Type material. *Holotype* • ♂ (ZMUT), Turkiye: Antalya Prov.: Alanya, env. Kestel, Dim Valley, 36°32'34.5"N, 32°06'17.5"E, 110 m, pine and oak forest, 2.01.2013 (Y.M. Marusik). *Paratypes*: • 4 ♂ (ZMUT), same data as for the holotype.

Diagnosis. The new species belongs to the *ariadnae* species-group and is most similar to *T. averni*. The male of the new species differs from that of *T. averni* by having thickened male palpal femur with four strong dorsal spines (Fig. 14B), an almost straight embolus on the prolateral half (vs roundly bent), a relatively shorter tibia with a length/width ratio of 2.5 (vs 2.9), and a conductor with subequal arms (vs a distal arm that is longer than the proximal arm; cf. Figs 14A, 13A).
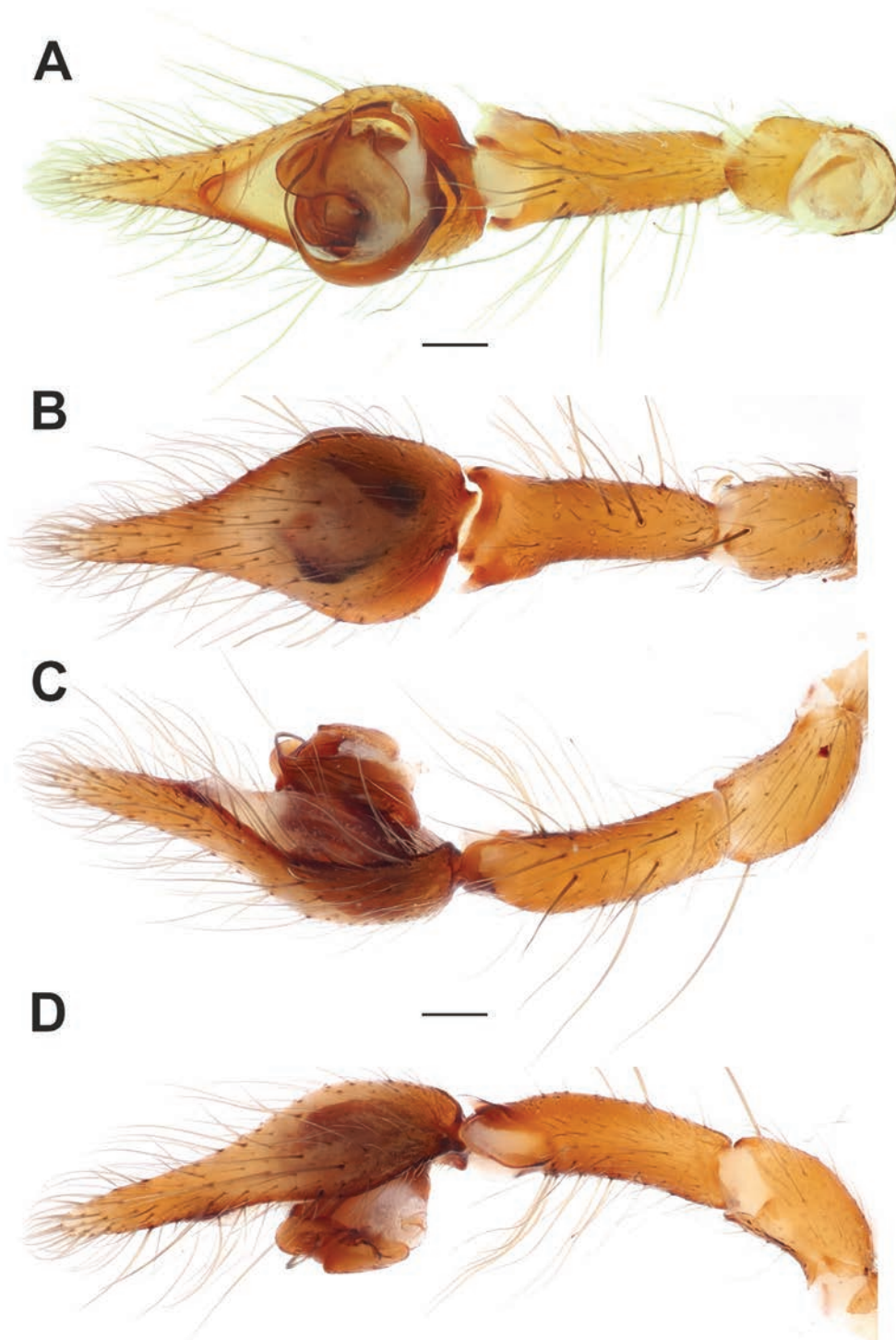
Figure 13. Male palp of *Tegenaria averni*. **A** ventral view **B** dorsal view **C** prolateral view **D** retrolateral view. Scale bars: 0.2 mm.

Description. Male. Habitus as in Fig. 18D. Total length 4.00. Carapace 1.95 long, 1.55 wide. Eye sizes: AME: 0.04, ALE: 0.07, PME: 0.06, PLE: 0.07. Pars cephalica, chelicerae, labium, maxillae, and Fe I and II pale brown, Fe II paler than I; pars thoracica, sternum, and remaining leg segments pale brown. Legs without annulations. Fe I, and to lesser degree Fe II, with ventral coating of long setae. Abdomen pale beige, without patterns. Spinnerets uniformly pale beige. Measurements of legs: I: 9.00 (2.36, 0.78, 2.24, 2.24, 1.38), II: 7.95 (2.16, 0.74, 1.85, 1.93, 1.27), III: 7.39 (1.93, 0.67, 1.65, 2.00, 1.14), IV: 9.78 (2.55, 0.75, 2.36, 2.74, 1.38).
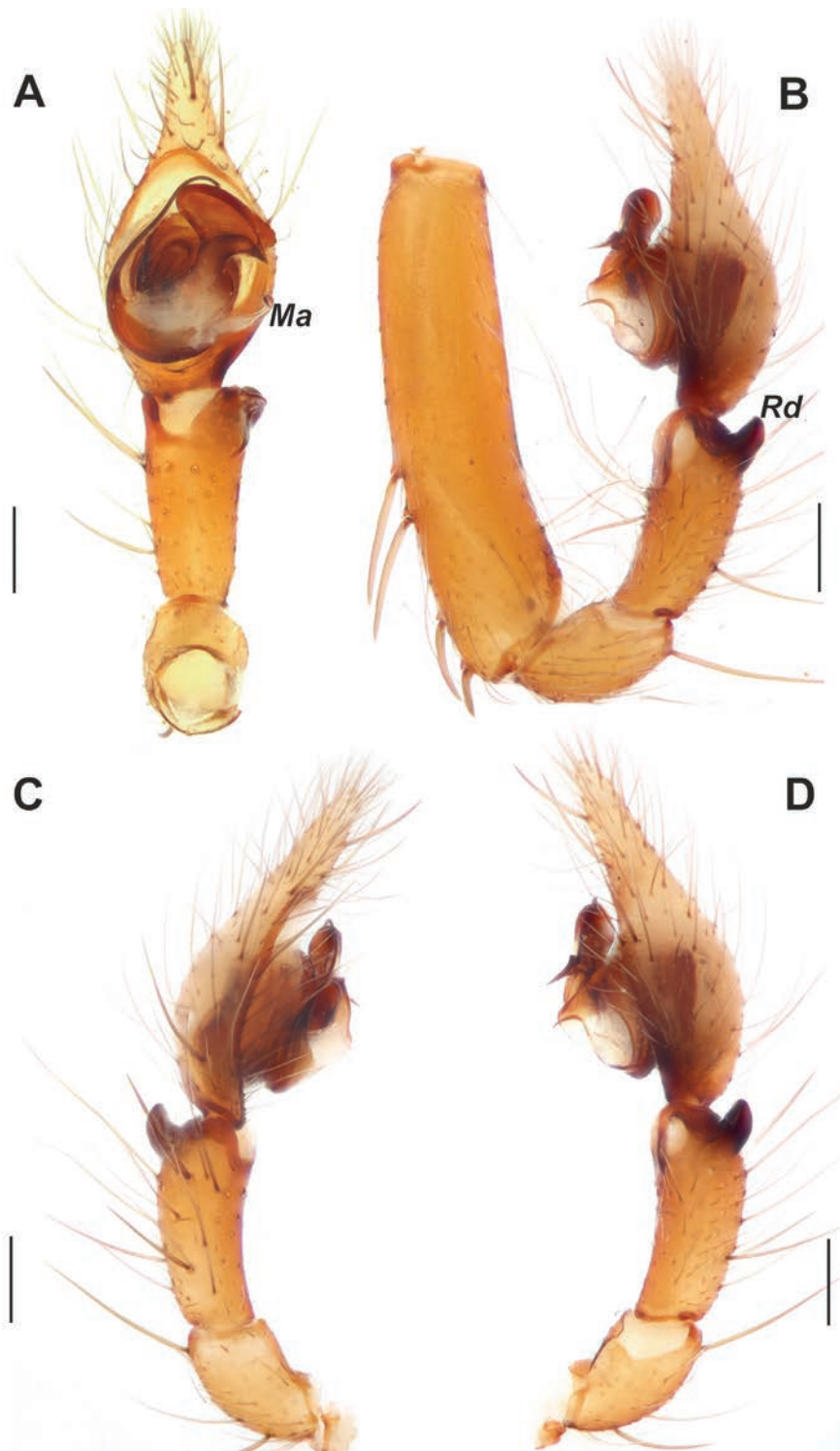
Figure 14. Male palp of *Tegenaria beyazcika* sp. nov. **A** ventral view **B** full palp, retrolateral view **C** prolateral view **D** retrolateral view. Abbreviations: *Ma* – median apophysis, *Rd* – retrodorsal apophysis. Scale bars: 0.2 mm.

Palp as in Fig. 14A–D; femur 4× longer than wide, longer than cymbium, 1.5× wider than tibia, with 4 strong spines in distal 1/2 (Fig. 14B); patella 2× longer than wide; tibia 2.25× longer than wide, with retroventral (*Rv*) and retrodorsal (*Rd*) apophyses (Fig. 14B); cymbium > 2× longer than wide, tip approximately as long as cymbium wide, with two strong macrosetae (= spines) on retrolateral

1/2; bulb as long as wide; median apophysis (*Ma*) long, approximately as long as width of tibia, originating at ~ 5 o'clock position (Fig. 14A); conductor fungiform, with both arms of equal length and width; embolus originating at ~ 8 o'clock position, straight in prolateral 1/2 of bulb and strongly roundly bent proximally at retrolateral side.

Female. Unknown.

Comments. Although the specimens of both *T. hamid* and *T. beyazcika* sp. nov. (known only from females and males, respectively) were collected from the same locality, we consider them to belong to different species due to noticeable differences in size and coloration. Additionally, *T. hamid* has a different conformation of the copulatory organs compared to those of the species in the *ariadnae* group, thus belonging to a different species-group than *T. beyazcika* sp. nov. Given the pale coloration of this species, the relatively elongated legs, and the dense ventral coating of long setae on femora I and II, it seems that the collection locality mentioned on the label is slightly off. It is more likely that the species was collected from a cave, such as the nearby Dim Cave.

Distribution. Known only from the type locality in Antalya Province, southwestern Turkiye.

Etymology. The specific epithet is derived from the Turkish word "beyaz", meaning pale, combined with the suffix -cik, meaning little. This refers to the relatively small size and pale coloration of this species.

Tegenaria chumachenkoi Kovblyuk & Ponomarev, 2008
Fig. 15A–D

Tegenaria chumachenkoi Kovblyuk & Ponomarev, 2008: 147, figs 18–21 (♀).
Tegenaria chumachenkoi: Ponomarev and Shmatko 2022: 212, figs 5–10 (♂♀).
  – Seropian et al. 2023: 147, suppl.: 5 fig. (♂).

Material. Turkiye: Artvin Prov.: • 1 ♂ (ZMUT), Şavşat Dist., env. of Meydancık Town, Erikli Vill., 41°27'13.1"N, 42°13'23.8"E, 1141 m, 12.06.2009 (Y.M. Marusik).

Distribution. Previously known from Azerbaijan, Georgia, and northern Caucasus (Ponomarev and Shmatko 2022). A new record for Turkiye.

Tegenaria dalmatica Kulczyński, 1906
Figs 16A–C, 18C

Malthonica dalmatica: Kovblyuk and Nadolny 2007: 19, figs 1–10 (♂♀).
Tegenaria dalmatica: Bolzern et al. 2013: 793, figs 1G, H, 2A, B, D, 15K, L, O, Q (♂♀).

Note. For a full list of 14 taxonomic entries, see WSC (2024).

Material. Turkiye: Izmir Prov.: • 6 ♀ (ZMUT), Kemalpaşa, Vişneli Vill., Fetrek-2 Cave, 38°20'N, 27°25'E, 311 m, 5.06.2009 (Y.M. Marusik); Bursa Prov.: • 1 ♂ (ZMUU), Lake Uluabat, Terzioğlu Island, 21.11.2003 (R.S. Kaya); • 1 ♀ (ZMUU), Lake İznik, Göllüce Vill., 14.10.2016, (R.S. Kaya).

Figure 15. Male palp of *Tegenaria chumachenkoi*. **A** ventral view **B** retrolateral view **C** dorsal view **D** prolateral view. Abbreviation: *Ma* – median apophysis. Scale bars: 0.2 mm.

Comment. The only previous record of this species from Turkiye was by Bolzern et al. (2013), although lacking further locality data.

Distribution. From Iberian Peninsula to Turkiye, south to northern Africa (Nentwig et al. 2024; WSC 2024).
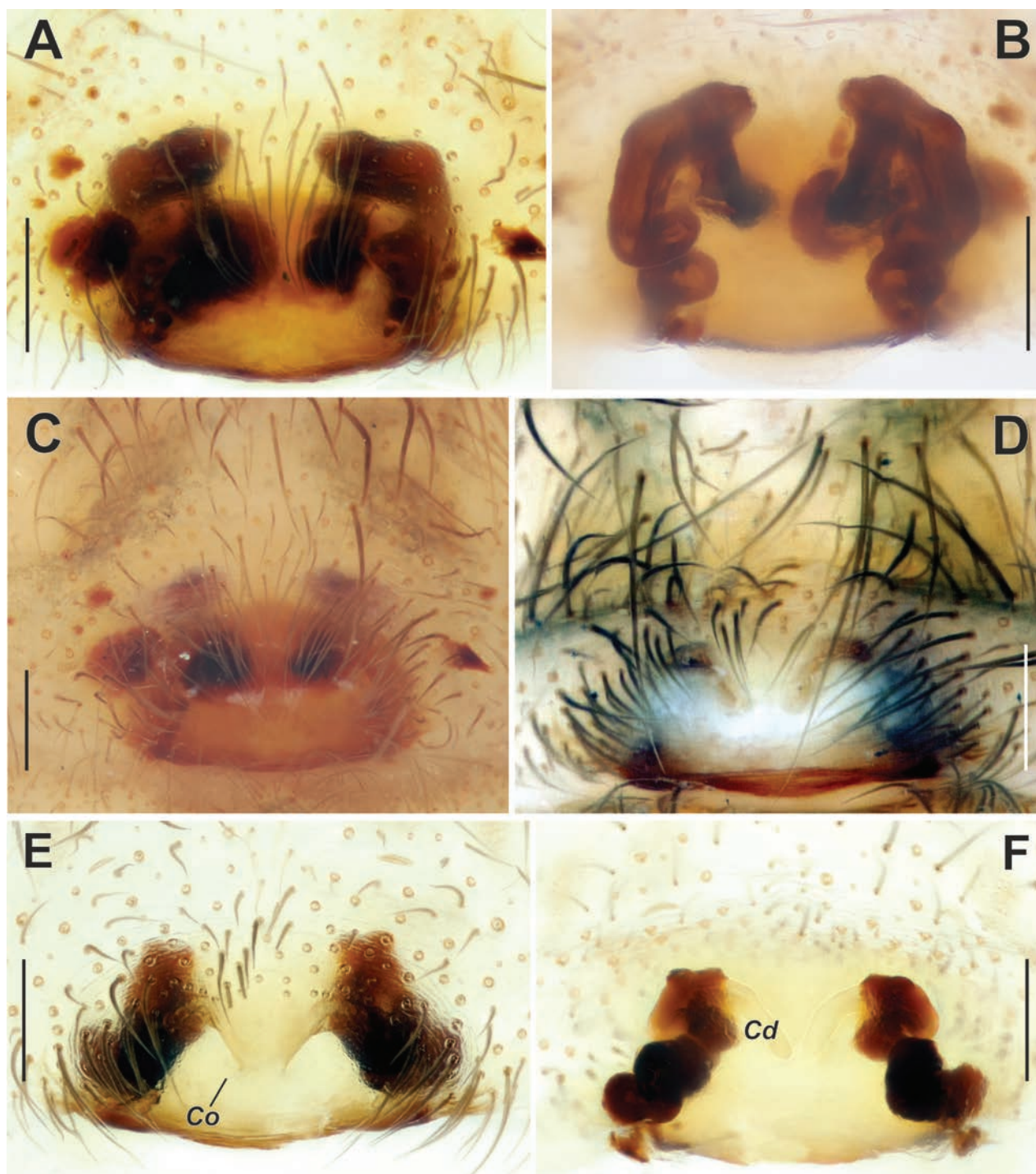
Figure 16. Epigyne of *Tegenaria dalmatica* (**A–C**) and *T. egrisiana* sp. nov. (**D–F**). **A, E** macerated, ventral view **B, F** vulva, dorsal view **C, D** intact, ventral view. Abbreviations: *Cd* – copulatory duct, *Co* – copulatory opening. Scale bars: 0.2 mm.

***Tegenaria egrisiana* sp. nov.**
https://zoobank.org/45CD9A9F-8B0B-47DD-B0A7-145458C6B6BE
Figs 16D–F, 17A–D, 18A, B, 20C

Type material. *Holotype* • ♂ (ZMMU), Georgia: Imereti Prov.: cave between Gumbrini and Khamali, 42°18'56.4"N, 42°38'09.4"E, 161 m, 19.07.2012 (Y.M. Marusik). ***Paratypes***: • 1 ♂ 1 ♀ (ZMUT), 2 ♀ (ZMMU), same data as for the holotype.
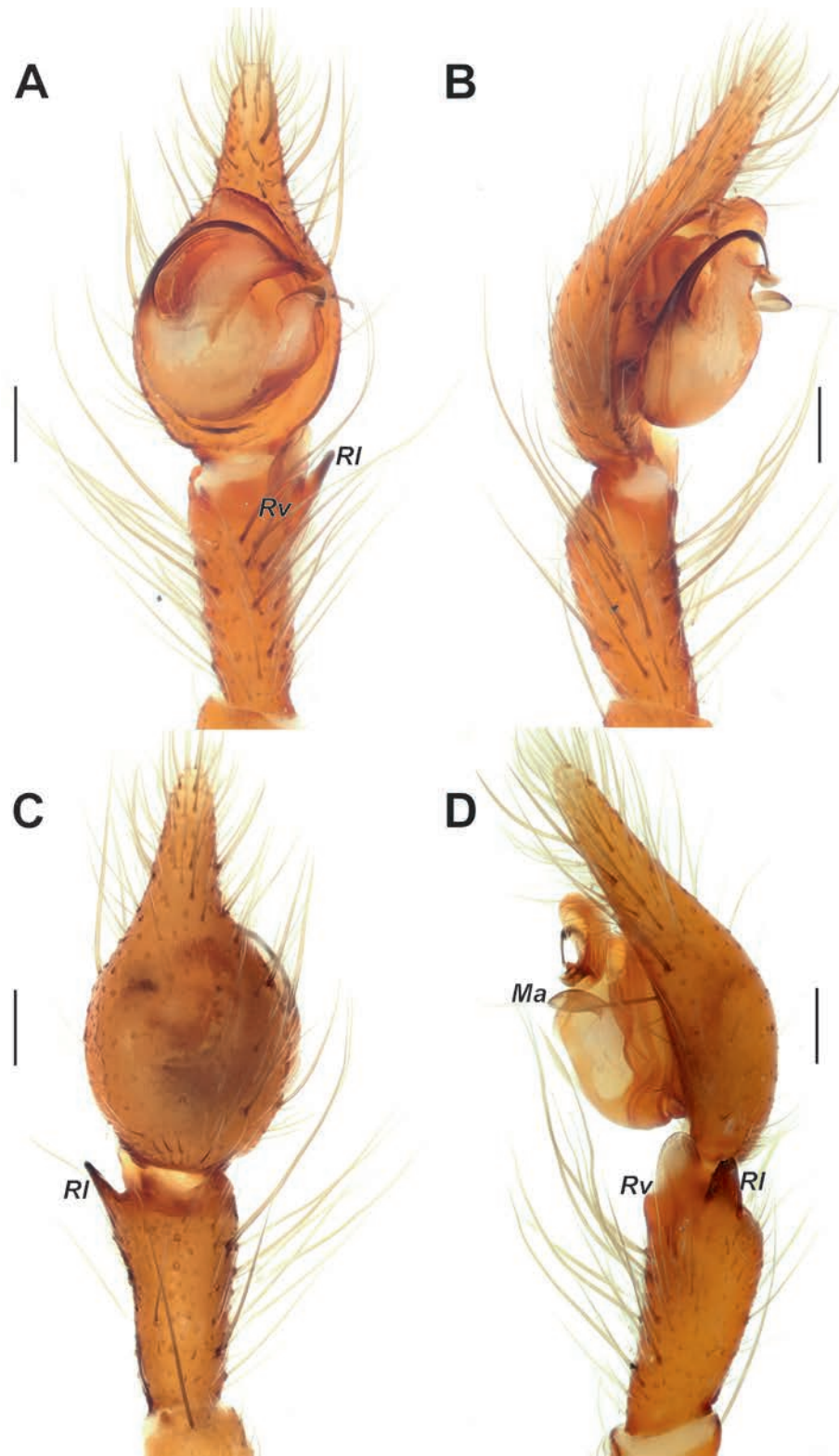
Figure 17. Male palp of *Tegenaria egrisiana* sp. nov. **A** ventral view **B** prolateral view **C** dorsal view **D** retrolateral view. Abbreviations: *Ma* – median apophysis, *Rl* – retrolateral apophysis, *Rv* – retroventral apophysis. Scale bars: 0.2 mm.

Diagnosis. *Tegenaria egrisiana* sp. nov. is very similar to *T. pallens* Zamani & Marusik, 2023 from Iran in the overall shape of the copulatory organs. However, the male differs from *T. pallens* in the shorter tip of the cymbium, ~ 0.7 the length of the palpal tibia (Fig. 17A–D, 20C; vs as long as the palpal tibia), the
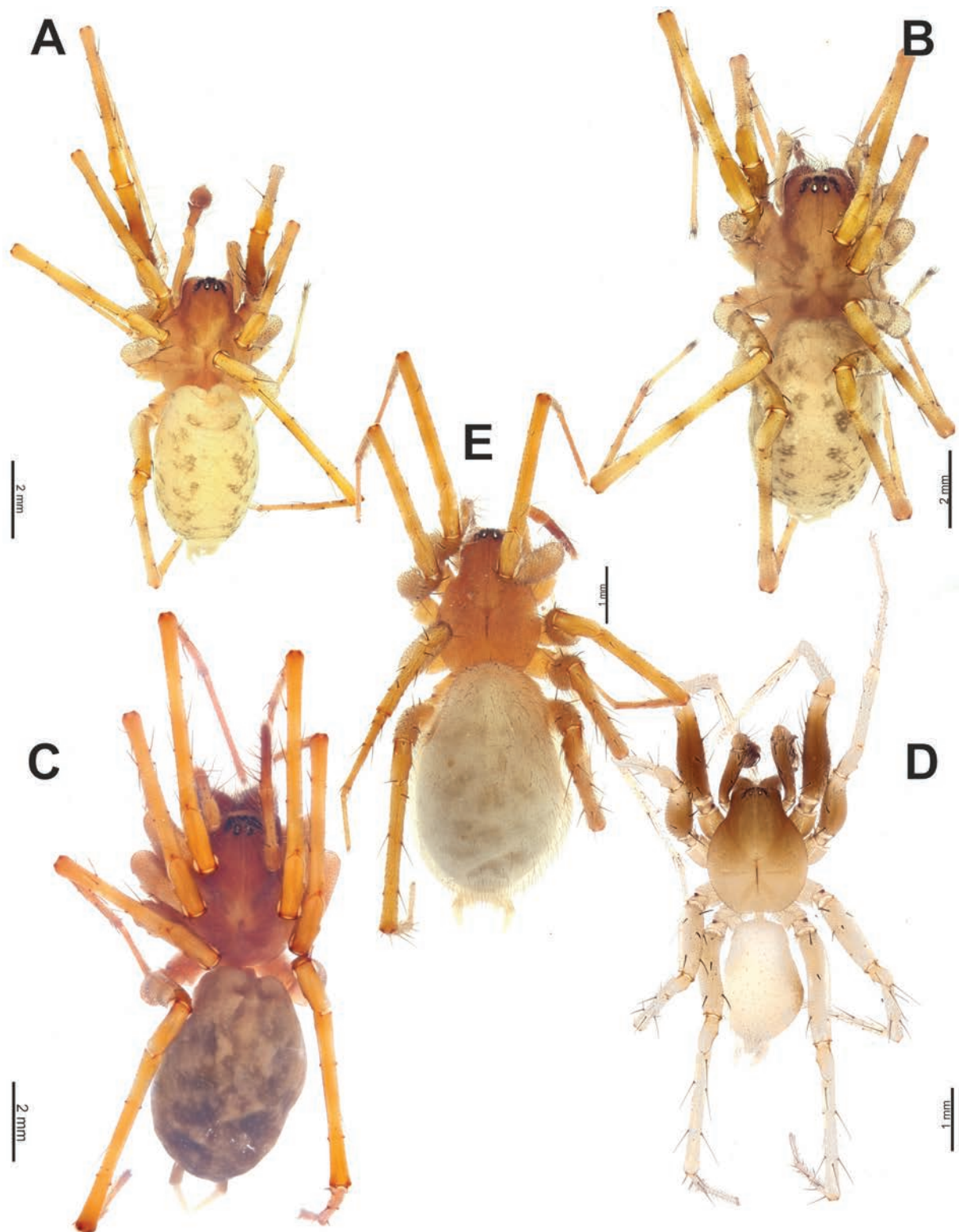
Figure 18. Habitus of *Tegenaria egrisiana* sp. nov. (**A, B**), *T. dalmatica* (**C**), *T. beyazcika* sp. nov. (**D**), and *T. tekke* (**E**), dorsal view. **A, D** males **B, C, E** females.

blunt tip of the conductor (vs pointed and curved; Zamani et al. 2023: fig. 2A), the embolus base positioned at the 9:00 o'clock position (vs 8:30 o'clock), the tip of the embolus terminating at ~ 2:00 o'clock position (Fig. 17A; vs 1:00 o'clock), and the median apophysis (*Ma*) with a different shape. The female of
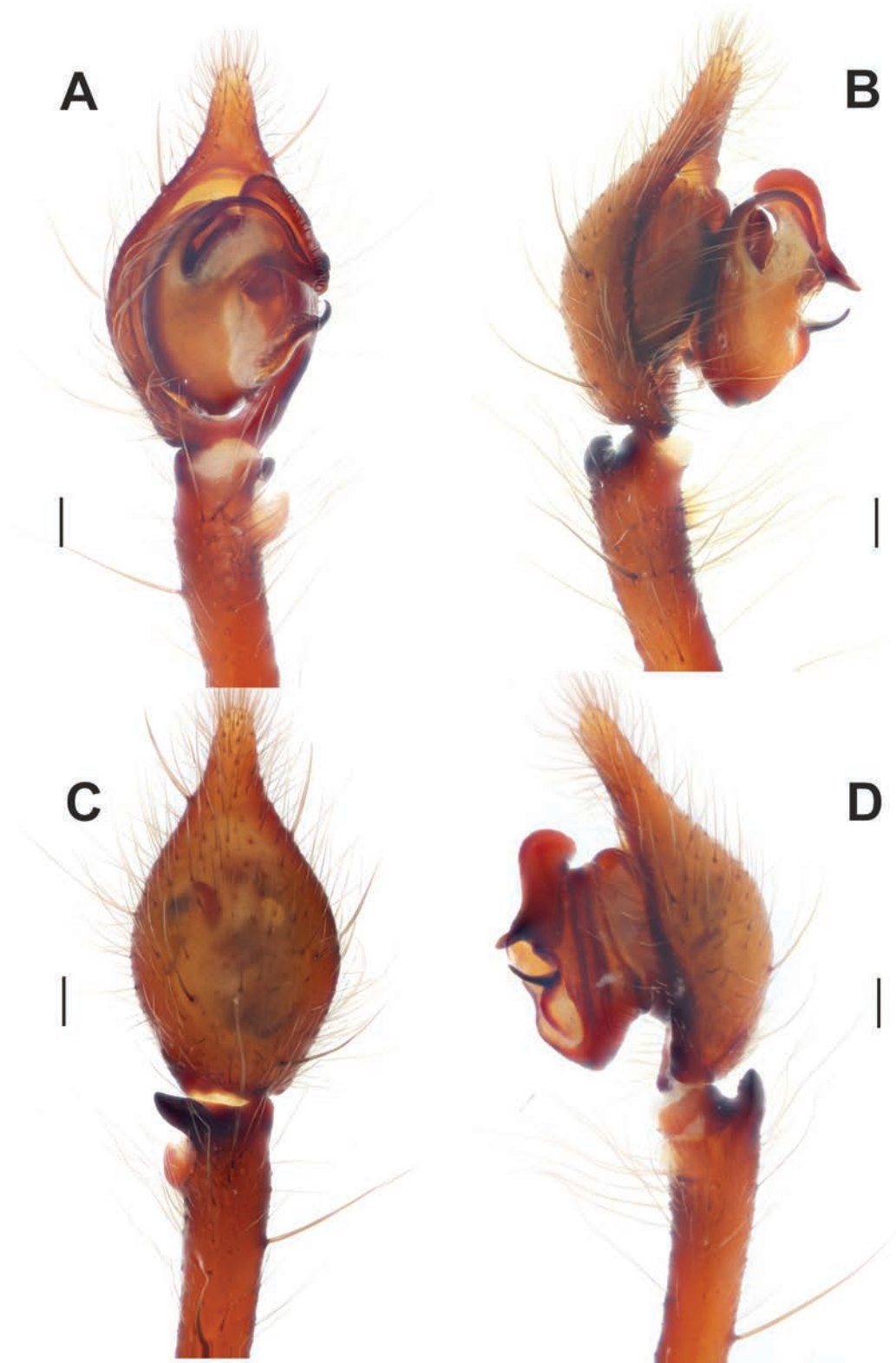
Figure 19. Male palp of *Tegenaria longimana*. **A** ventral view **B** prolateral view **C** dorsal view **D** retrolateral view. Scale bars: 0.2 mm.

the new species differs from that of *T. pallens* in the epigynal plate nearly twice as wide as it is long (vs > 3× wider than long; cf. Fig. 16D and Zamani et al. 2023: fig. 3C), in having a distinct median plate (vs absent), and a small rectangular fovea (vs oval; cf. Fig. 16D, E and Zamani et al. 2023: fig. 3A, B).
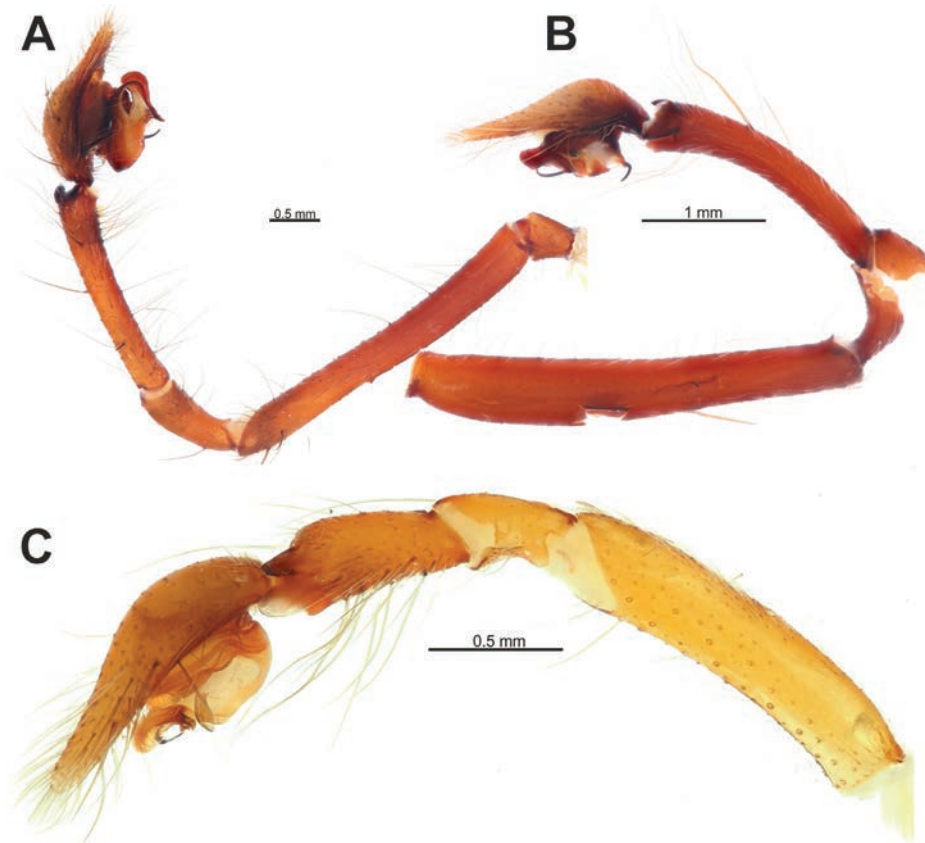
Figure 20. Full male palp of *Tegenaria longimana* (**A**), *T. anhela* (**B**), and *T. egrisiana* sp. nov. (**C**). **A** prolateral view **B, C** retrolateral view.

Description. Male. Habitus as in Fig. 18A. Total length 7.10. Carapace 3.23 long, 2.37 wide. Eye sizes: AME: 0.12, ALE: 0.17, PME: 0.14, PLE: 0.18. Carapace, labium, and maxillae pale brown; carapace with darker submedian bands; chelicerae reddish brown; sternum greyish brown, with yellow median band and six spots. Legs pale brown, with very faint annulations; Fe with long ventral setae at basal 1/2. Abdomen pale beige, with greyish dots, patches, and stripes. Spinnerets uniformly pale beige. Measurements of legs: I: 22.92 (6.12, 1.44, 6.26, 6.50, 2.60), II: 19.02 (5.05, 1.28, 4.96, 5.50, 2.23), III: 16.90 (4.63, 1.15, 4.15, 5.15, 1.82), IV: 20.79 (5.50, 1.28, 5.24, 6.65, 2.12).

Palp as in Fig. 17A–D; femur longer than patella+tibia; femur ~ 2.2× longer than tibia (Fig. 20C); patella 2× longer than wide; cymbium ~ 1.8× longer than tibia; tibia ~ 2× longer than wide, with two apophyses: large and membranous retroventral apophysis (*Rv*) and conical retrolateral apophysis (*Rl*) with a notched blunt tip (Figs 17D, 20C); retrolateral apophysis shorter than ventrolateral one; cymbium 2× longer than wide; bulb longer than wide; median apophysis (*Ma*) large and wide, originating at ~ 4 o'clock position; conductor as long as wide, with a spatula-like tip; embolus filiform, roundly bent, originating at ~ 9:00 o'clock position (Fig. 17A).

Female. Habitus as in Fig. 18B. Total length 8.68. Carapace 4.25 long, 2.95 wide. Eye sizes: AME: 0.12, ALE: 0.20, PME: 0.18, PLE: 0.20. Coloration as in male. Measurements of legs: I: 22.80 (6.13, 1.65, 6.00, 6.30, 2.72), II: 19.81 (5.53, 1.57, 4.96, 5.47, 2.28), III: 18.03 (5.07, 1.44, 4.32, 5.22, 1.98), IV: 22.57 (6.18, 1.47, 5.63, 7.00, 2.29).
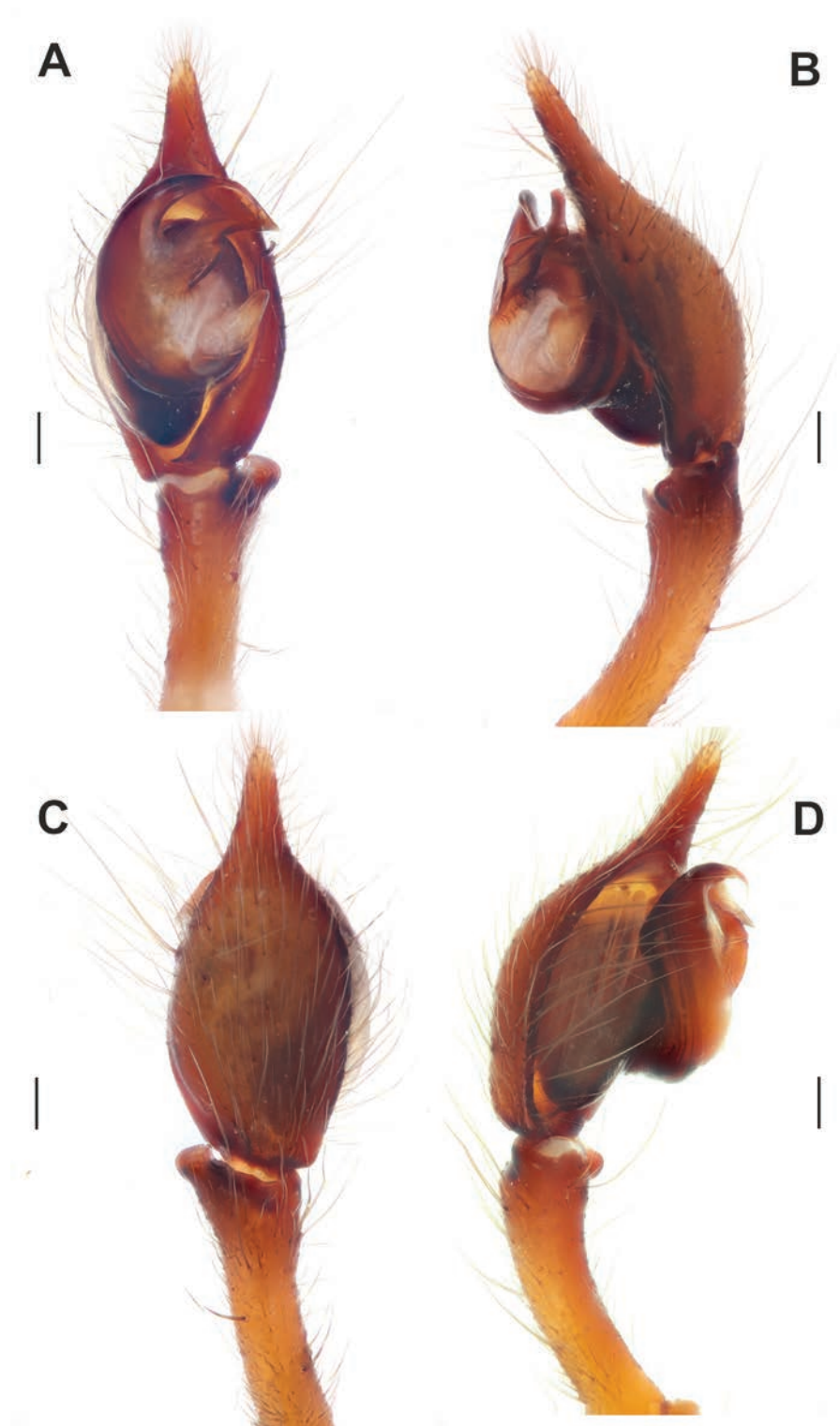
Figure 21. Male palp of *Tegenaria percuriosa*. **A** ventral view **B** prolateral view **C** dorsal view **D** retrolateral view. Scale bars: 0.2 mm.

Epigyne as in Fig. 16D–F; epigynal plate ~ 2× wider than long with two sclerotized and barely visible teeth; fovea small and almost rectangular; copulatory openings (*Co*) located on anterior edges of holes (Fig. 16D, E); copulatory ducts (*Cd*) with a membranous anterior part and a widened slightly sclerotized posterior part; receptacles tubular and twisted along their axis (Fig. 16F).
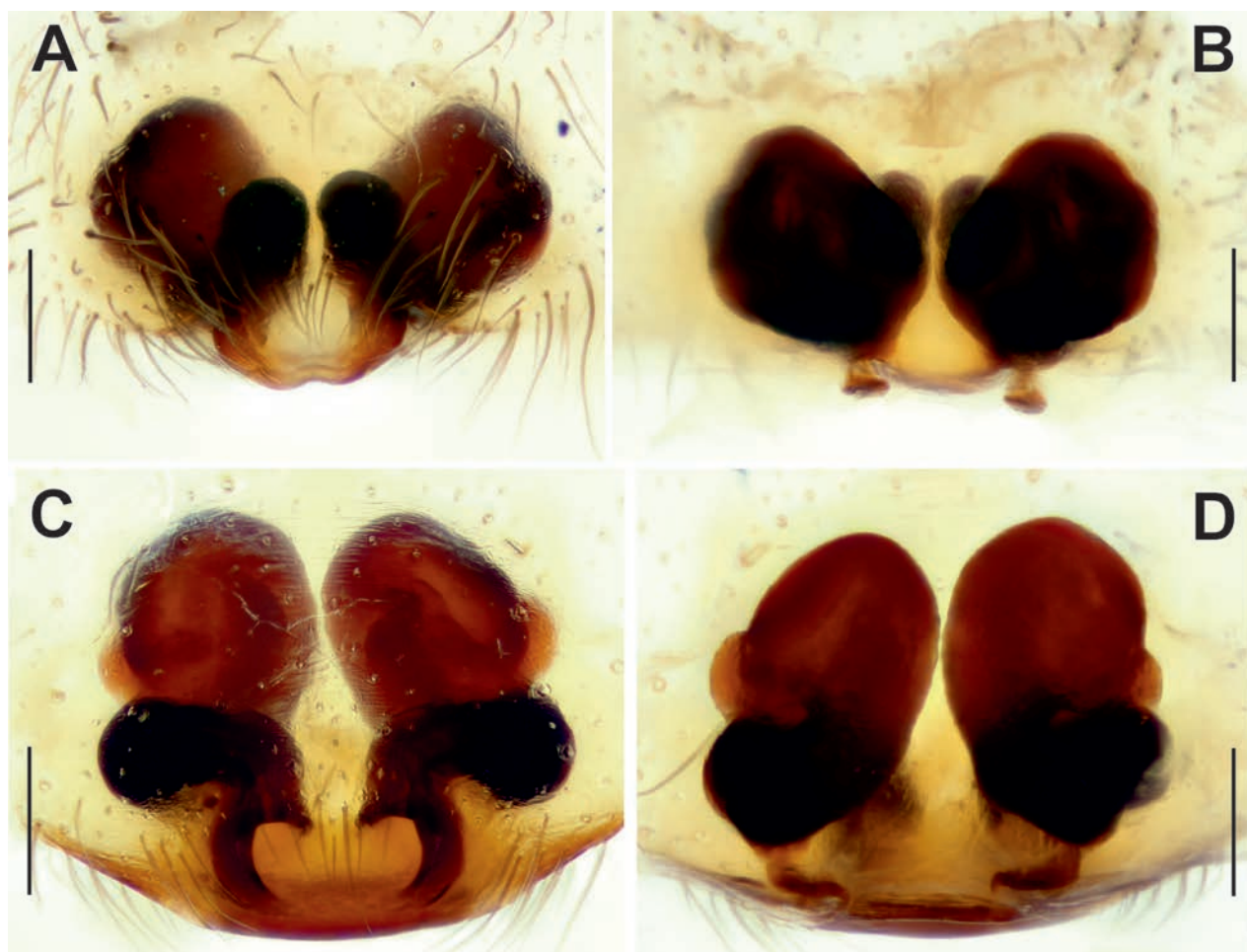
Figure 22. Epigyne of *Tegenaria percuriosa* (**A, B**) and *T. longimana* (**C, D**). **A, C** macerated, ventral view **B, D** vulva, dorsal view. Scale bars: 0.2 mm.

Distribution. Known only from the type locality in Imereti Province, central-western Georgia.

Etymology. The specific epithet refers to the historical Georgian polity of Egrisi, which was centered in present-day western Georgia.

Tegenaria hamid **Brignoli, 1978**
Figs 1D, 5A–D

Tegenaria hamid Brignoli, 1978b: 515, fig. 96 (♀).
Eratigena fuesslini: Topçu and Demircan 2018: 20, fig. 1 (♀).

Type material. *Holotype* • ♀ (MHNG), Turkıye: Isparta Prov.: Egridir, 18.04.1973 (P. Brignoli). [examined]

Other material. Turkıye: Antalya Prov.: • 2 ♀ (ZMUT), Alanya, env. Kestel, Dim Valley, 36°32'34.5"N, 32°06'17.5"E, pine and oak forest, 2–9.01.2013 (Y.M. Marusik); • 1 ♀ (ZMUT), Asmaca, 36°36'32.3"N, 32°03'12.4"E, 686 m, pine and oak forest, 3.01.2013 (Y.M. Marusik).

Comment. This species was previously known only from its original description. The single figure of the vulva provided by Brignoli (1978b) is rather

schematic and not depicted from an exact dorsal view. Therefore, we present additional figures from various angles based on newly collected material from Antalya. Additionally, upon checking the record of *Eratigena fuesslini* (Pavesi, 1873) from Turkiye by Topçu and Demircan (2018), it became evident that the figure presented corresponds to the anteroventral view of the macerated epigyne of *T. hamid*, rather than *E. fuesslini*. Consequently, the record of *E. fuesslini* is hereby removed from the list of Turkish spiders.

Distribution. Known only from Isparta and Antalya provinces, southwestern Turkiye.

Tegenaria hoeferi sp. nov.

https://zoobank.org/3606E8DA-51F1-4AB9-81F1-6354AAA1456C
Figs 23A–D, 24A–C, 25A–C

Type material. *Holotype* • ♂ (ZMUT), ARMENIA: Kotayk Prov.: env. Aghveran, 40°29'54"N, 44°35'24"E, 7–8.05.2021 (Y.M. Marusik). *Paratypes*: • 1 ♂ 3 ♀ (ZMUT, ZMMU), same data as for the holotype.

Diagnosis. The new species belongs to the *abchasica* species-group and is most similar to *T. chumachenkoi*. The male of the new species differs from that of *T. chumachenkoi* by the shape of the median apophysis, bulging proximally and widely pointed retrolaterally (vs straight proximally and sharply pointed retrolaterally in *T. chumachenkoi*; cf. Figs 23A, 15A). The female of the new species differs from that of *T. chumachenkoi* by having an oval median plate that is ~ 2× as wide as it is long (vs the median plate is not oval and is approximately as long as it is wide; cf. Fig. 25A and Ponomarev and Shmatko 2022: fig. 10).

Description. Male. Habitus as in Fig. 24B. Total length 8.40. Carapace 4.10 long, 3.20 wide. Eye sizes: AME: 0.20, ALE: 0.21, PME: 0.17, PLE: 0.19. Carapace, chelicerae, labium, and maxillae pale brown; carapace with black submedian and marginal bands; sternum greyish brown, with yellow median lobulated band and six spots. Legs pale brown, with distinct annulations. Abdomen dark greyish, with numerous beige dots, patches, and stripes. Anterior spinnerets greyish basally and pale beige apically, posterior ones uniformly pale beige. Measurements of legs: I: 17.48 (4.56, 1.62, 4.06, 4.91, 2.33), II: 17.14 (4.40, 1.63, 4.07, 4.71, 2.33), III: 15.86 (4.29, 1.47, 3.57, 4.48, 2.05), IV: 19.60 (5.16, 1.52, 4.58, 6.08, 2.26).

Palp as in Figs 23A–D, 24C; femur roundly bent, ~ 4× longer than wide; patella swollen, approximately as wide as long with long dorsal seta almost as long as tibia; tibia ~ 1/2 as long as femur (not counting apophyses) (Fig. 24C); retrodorsal apophysis (*Rd*) approximately as long as tibia wide distally, with strong spine directed proximoventrally (Fig. 23B); retroventral apophysis (*Rv*) small (Fig. 23C, D); cymbium 1.8× longer than wide, tip ~ 1/3 of cymbial length, lacking distinct spine, with basal process (*Cp*); bulb as long as wide; median apophysis (*Ma*) large (Fig. 23A), bent prolaterally; conductor with long and thin distal arm not reaching prolateral 1/2 of cymbium; embolus with large base, free part originating at 9 o'clock position, thin, roundly bent.

Female. Habitus as in Fig. 24A. Total length 10.28. Carapace 4.00 long, 3.00 wide. Eye sizes: AME: 0.18, ALE: 0.20, PME: 0.16, PLE: 0.18. Coloration as in male. Measurements of legs: I: 16.95 (4.33, 1.69, 4.18, 4.55, 2.20), II: 15.92
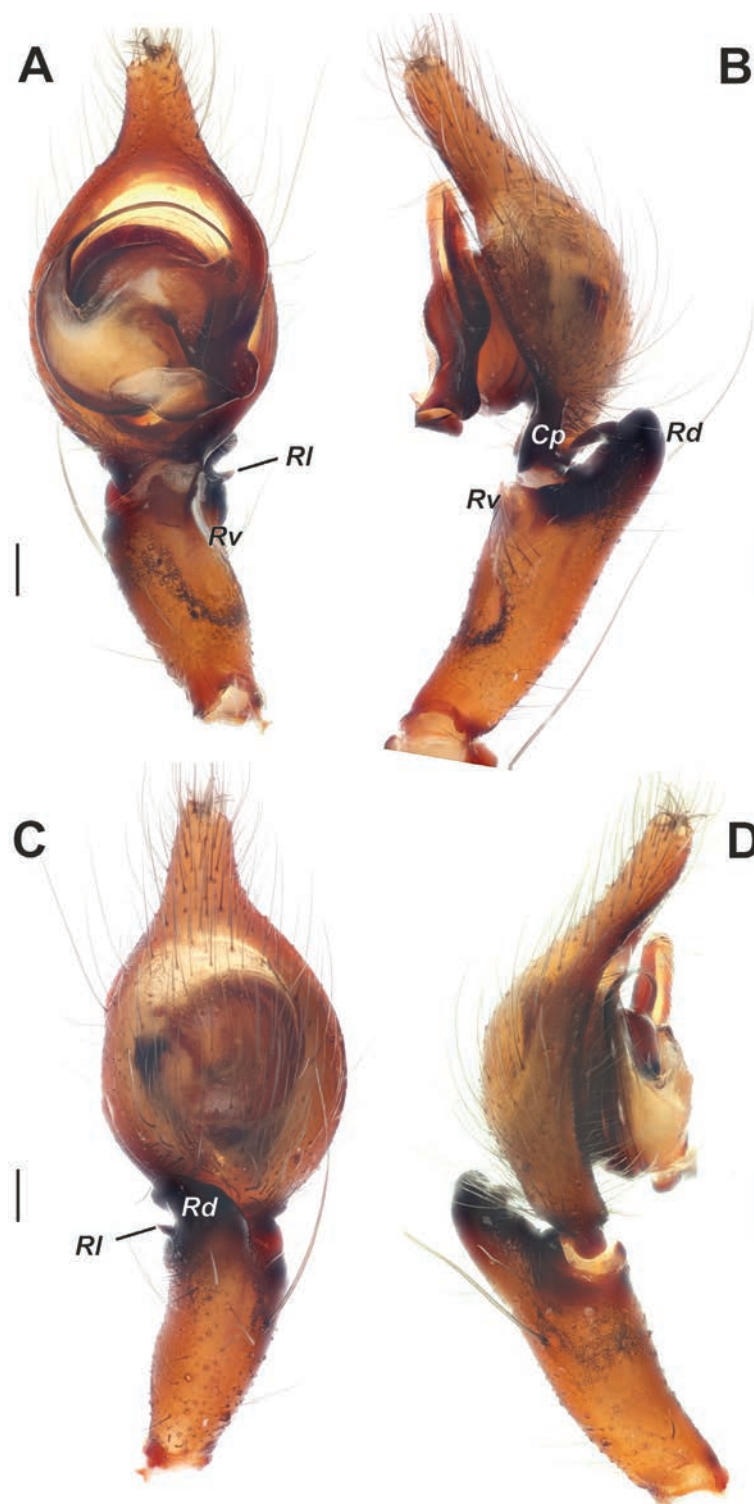
Figure 23. Male palp of *Tegenaria hoeferi* sp. nov. **A** ventral view **B** retrolateral view **C** dorsal view **D** prolateral view. Abbreviations: *Cp* – basal process of the cymbium, *Rd* – retrodorsal apophysis, *Rl* – retrolateral apophysis, *Rv* – retroventral apophysis. Scale bars: 0.2 mm.

(4.20, 1.63, 3.65, 4.15, 2.29), III: 14.43 (3.94, 1.43, 3.23, 4.00, 1.83), IV: 17.89 (4.74, 1.58, 4.21, 5.29, 2.07).

Epigyne as in Fig. 25A–C; plate 2× wider than long, median plate oval, wider than long (Fig. 25A, B); copulatory ducts and receptacles lacking distinct limits, contiguous (Fig. 25C).
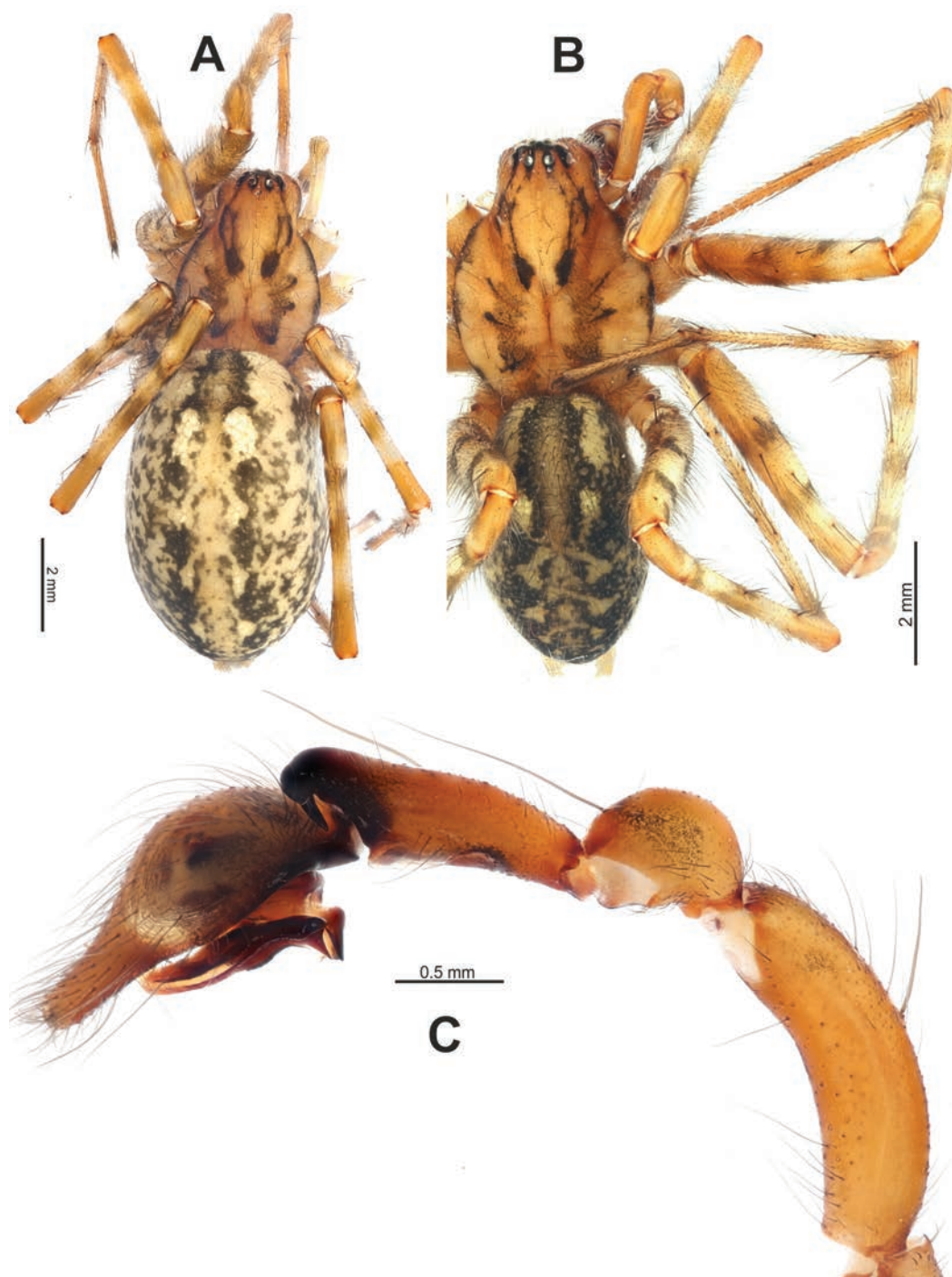
Figure 24. *Tegenaria hoeferi* sp. nov. **A, B** habitus, dorsal view **C** full palp, retrolateral view. **A** female **B, C** male.

Distribution. Known only from the type locality in Kotayk Province, central Armenia.

Etymology. This species is named after Hubert Höfer (Karlsruhe, Germany), a German arachnologist. He is the Curator of Invertebrates and head of Biosciences at the State Museum of Natural History Karlsruhe. He has made significant contributions to the study of spiders in both South America and Germany, leading numerous projects and helping to compile the largest dataset on distributions of spiders in Germany.

Tegenaria longimana Simon, 1898
Figs 19A–D, 20A, 22C, D

Tegenaria longimana: Ponomarev et al. 2024: 279, figs 29–33 (♂♀).

Note. For a full list of seven taxonomic entries, see WSC (2024).

Material. GEORGIA: Imereti Prov.: • 1 ♂ 4 ♀ (ZMUT), env. of Tskhaltubo, Khomuli Vill., Tetra Cave, 42°19'49.3"N, 42°37'00.9"E, 454 m, 18.07.2012 (Y.M. Marusik); • 1 ♀ (ZMUT), Bzvani Vill., deep cave, near the entrance, 42°03'01.3"N, 42°36'04.5"E, 402 m, 20.07.2012 (Y.M. Marusik).

Comment. This species was described from Batumi, the capital of the Georgian republic of Adjara.

Distribution. Known from Turkiye, Georgia, and northern Caucasus (Otto 2022; WSC 2024).

Tegenaria percuriosa Brignoli, 1972
Figs 21A–D, 22A, B

Tegenaria percuriosa: Dimitrov et al. 2022: 3, figs 1, 2, 7–13, 40, 41 (♂♀).

Note. For a full list of five taxonomic entries, see WSC (2024).

Material. TURKIYE: Antalya Prov.: • 1 ♀ 3j. (ZMUT), Alanya, env. Kestel, Dim Cave, 36°32'22.1"N, 32°06'34.4"E, 225 m, 4.01.2013 (Y.M. Marusik); Bursa Prov.: • 1 ♂ 1 ♀ (ZMUT), Uludağ, Göynükbelen rd., 39°59'N, 29°02'E, 14.05.2006 (R.S. Kaya); • 2 ♂ 2 ♀ (ZMUT), İnegöl, Great Oylat Cave, 39°56'N, 29°35'E, 519 m, 3.06.2009 (Y.M. Marusik); • 1 ♂ 1 ♀ (ZMUU), Uludağ Mountain, Baraklı Pond, 27.05.2003 (R.S. Kaya); • 1 ♂ (ZMUU), same, 8.05.2005 (R.S. Kaya); • 1 ♂ (ZMUU), same, 10.05.2010 (R.S. Kaya); • 1 ♂ (ZMUU), same, 1270 m, 16.05.2016 (R.S. Kaya); • 1 ♀ (ZMUU), Uludağ Mountain, Soğukpınar Valley, 40°03'N, 29°09'E, 5.06.2003 (R.S. Kaya); • 1 ♀ (ZMUU), Uludağ Mountain, Alaçam Forest, 30.08.2009 (R.S. Kaya); • 1 ♀ (ZMUU), Uludağ Mountain, Kocayayla Plateau, 25.09.2010 (R.S. Kaya); • 1 ♂ 14 ♀ (ZMUU), Uludağ Mountain, National Park, 40°06'N, 29°05'E, 2.06.2010 (R.S. Kaya); • 1 ♂ 2 ♀ (ZMUU), Kazanpınar Cave, 2.06.2009 (R.S. Kaya); • 2 ♂ 10 ♀ (ZMUU), same, 6.06.2009 (R.S. Kaya); • 2 ♂ 3 ♀ (ZMUU), Ayvaini Cave, 14.10.2012 (R.S. Kaya); • 1 ♀ (ZMUU), Oylat Cave, 15.10.2016 (R.S. Kaya); • 2 ♂ 2 ♀ (ZMUU), Mustafakemalpaşa Dist., Suuçtu Waterfall, 24.06.2012 (R.S. Kaya); Balıkesir Prov.: • 1 ♀ (ZMUU), Alaçam Mountain, 39°25'N, 38°35'E, 4.07.2012 (R.S. Kaya); Eskişehir Prov.: • 1 ♀ (ZMUU), Çatacık Forest, 39°57'N, 31°08'E, 1.08.2012 (R.S. Kaya); Isparta Prov.: • 1 ♀ (ZMUU), Zindan Cave, 21.05.2007 (R.S. Kaya); İstanbul Prov.: • 1 ♀ (ZMUU), Aydos Forest, 40°56'N, 29°14'E, 874 m, 30.04.2016 (R.S. Kaya).

Comment. In our male specimens, the tip of the apical part of the median apophysis is widened (Fig. 21A), which is different from that of the specimens illustrated by Dimitrov et al. (2022). This is herein considered an intraspecific variation.

Distribution. Known from Western Anatolia (Dimitrov et al. 2022).

Tegenaria tekke Brignoli, 1978
Figs 18E, 25D–F

Tegenaria tekke Brignoli, 1978b: 516, fig. 98 (♀).

Material. Turkiye: Antalya Prov.: • 3 ♀ (ZMUU), Kaş Dist., Kaş-Elmalı rd., 916 m, *Pinus brutia* and *Quercus* sp. forest, 20.05.2012 (R.S. Kaya); • 2 ♀ (ZMUT), same.
Comment. This species was previously known only from its original description.
Distribution. Known only from Antalya Province, southwestern Turkiye.

Discussion

As a result of this study, new taxonomic and faunistic data on the agelenid spiders of Turkiye, Georgia, and Armenia were provided. Turkiye is one of the most diverse countries in regards to Agelenidae, with 77 currently known species (including the results of the present study). This diversity is indeed higher compared to several other countries and regions, for example, the entire Caucasus (48 species), Greece (49 species), Bulgaria (44 species), Italy (58 species), France (41 species), and Spain (41 species) (Nentwig et al. 2024).

In this paper, four new species of *Tegenaria* were described, including two from Turkiye and one each from Georgia and Armenia. There are now 39 known species of this genus in Turkiye (Danışman et al. 2024; present study), and 32 from the Caucasus (Otto 2022; Ponomarev et al. 2024). The number of *Tegenaria* species recorded in each Caucasian subregion/country is as follows: Adygea (8), Armenia (1), Azerbaijan (15), Chechnya (3), Dagestan (7), Georgia (9 or 10), Ingushetia (1), Kabardino-Balkaria (0), Karachay-Cherkessia (3), Krasnodar Krai (13), North Ossetia-Alania (3), South Ossetia (3), and Stavropol Krai (6) (Otto 2022; Ponomarev et al. 2024).

Turkiye has been relatively well studied in terms of its Tegenariini, although new species and records continue to be discovered regularly. In the present study, all newly described species from Turkiye were collected from the Taurus Mountain range, a biodiversity hotspot located between the Mediterranean coastal region and the central Anatolian Plateau (Noroozi et al. 2019). The Taurus Mountains feature high altitudes, diverse valley slopes, depressions, and rugged karstic landforms, which create a variety of microhabitats and localized ecological conditions (Atalay et al. 2014). These mountain ranges in Anatolia, especially those divided by numerous valleys in the south, play a significant role in speciation and define various biogeographical subregions and provinces. From a zoological perspective, the Anatolian Taurus exhibits a very high degree of endemism and restricted local distributions (Çıplak 2003). This pattern of distribution underscores the importance of topography and microhabitat diversity in the evolution and distribution of *Tegenaria* in Anatolia. Many Anatolian species of *Tegenaria* are endemics, with most having limited, localized ranges primarily found in mountainous regions (Kaya et al. 2010). For instance, the fact that the two closely related species *T. bayrami* Kaya, Kunt, Marusik & Uğurtaş, 2010 and *T. ballarini* sp. nov. were both collected sympatrically from the same habitat further highlights the role of this region in speciation of this group. The Tegenariini of Georgia and Armenia remain less studied compared to Turkiye, although the region's diverse habitats and topography suggest that many undocumented species are still waiting to be discovered.
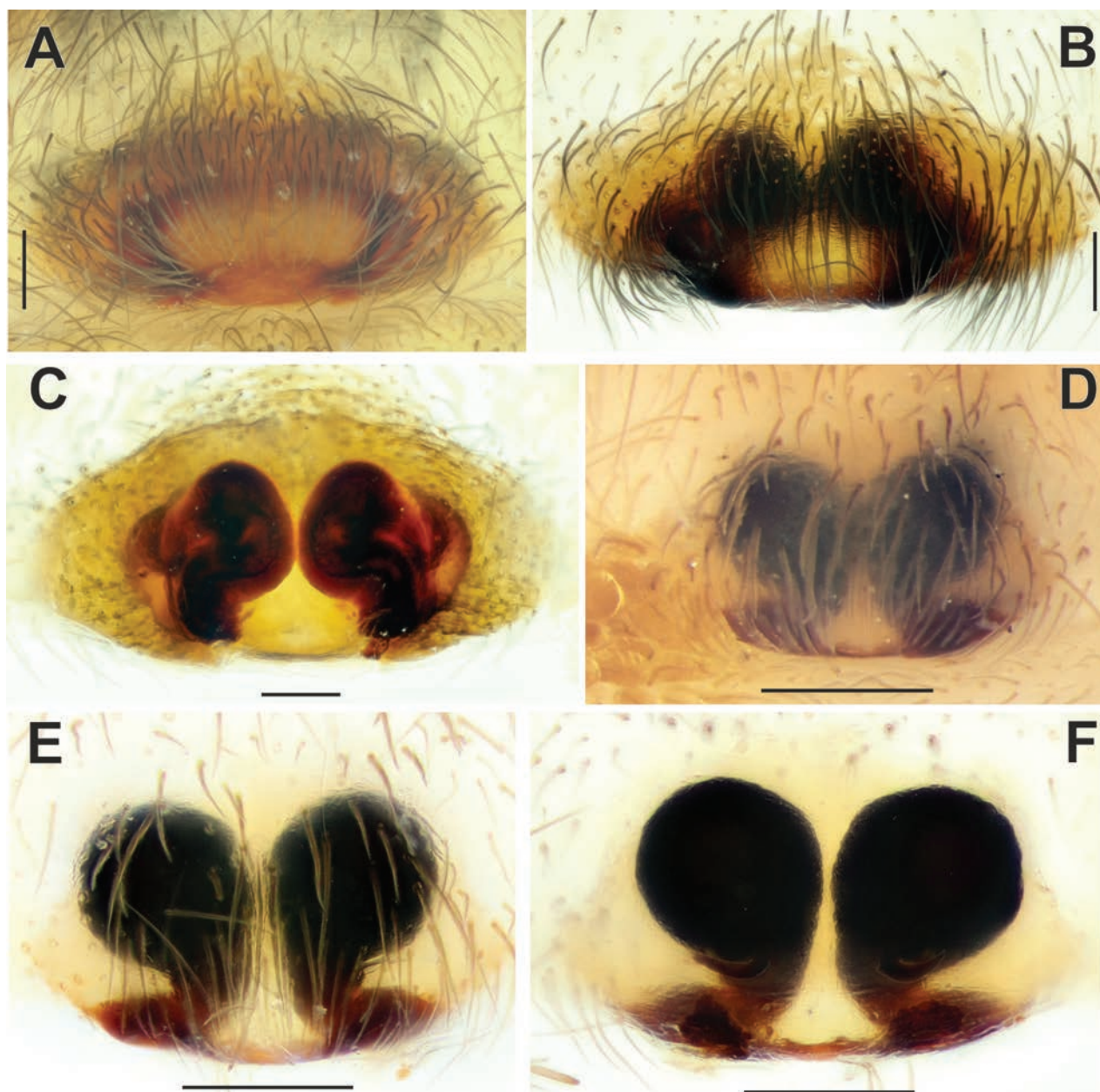
Figure 25. Epigyne of *Tegenaria hoeferi* sp. nov. (**A–C**) and *T. tekke* (**D–F**). **A, D** intact, ventral view **B, E** macerated, ventral view **C, F** vulva, dorsal view. Scale bars: 0.2 mm.

Acknowledgments

Additional information

Conflict of interest

The authors have declared that no competing interests exist.

Ethical statement

No ethical statement was reported.

Author contributions

All authors have contributed equally.

Author ORCIDs

Alireza Zamani ● https://orcid.org/0000-0002-8084-9666
Rahşen S. Kaya ● https://orcid.org/0000-0002-3769-9105
Yuri M. Marusik ● https://orcid.org/0000-0002-4499-5148

Data availability

All of the data that support the findings of this study are available in the main text.

References

Atalay I, Efe R, Öztürk M (2014) Effects of topography and climate of the ecology of Taurus Mountains in the Mediterranean Region of Turkey. Procedia – Social and Behavioral Sciences 120: 142–156. https://doi.org/10.1016/j.sbspro.2014.02.091

Bolzern A, Hänggi A, Burckhardt D (2010) *Aterigena*, a new genus of funnel-web spider, shedding some light on the *Tegenaria-Malthonica* problem (Araneae: Agelenidae). Journal of Arachnology 38(2): 162–182. https://doi.org/10.1636/A09-78.1

Bolzern A, Burckhardt D, Hänggi A (2013) Phylogeny and taxonomy of European funnel-web spiders of the *Tegenaria-Malthonica* complex (Araneae: Agelenidae) based upon morphological and molecular data. Zoological Journal of the Linnean Society 168(4): 723–848. https://doi.org/10.1111/zoj.12040

Brignoli PM (1972) Terzo contributo alla conoscenza dei ragni cavernicoli di Turchia (Araneae). Fragmenta Entomologica 8: 161–190.

Brignoli PM (1978a) Ragni di Turchia IV. Leptonetidae, Dysderidae ed Agelenidae nuovi o interessanti di grotte della Turchia meridionale (Araneae). Quaderni di Speleologia, Circolo Speleologico Romano 3: 37–54.

Brignoli PM (1978b) Ragni di Turchia V. Specie nuove o interessanti, cavernicole ed epigee, di varie famiglie (Araneae). Revue Suisse de Zoologie 85(3): 461–541. https://doi.org/10.5962/bhl.part.82243

Çıplak B (2003) Distribution of Tettigoniinae (Orthoptera, Tettigoniidae) bush-crickets in Turkey: The importance of the Anatolian Taurus Mountains in biodiversity and implications for conservation. Biodiversity and Conservation 12(1): 47–64. https://doi.org/10.1023/A:1021206732679

Danışman T, Kunt KB, Özkütük RS, Coşar İ (2024) The Checklist of the Spiders of Turkey. Version 2024. http://www.spidersofturkey.info [Accessed on 13.08.2024]

de Blauwe R (1980) Révision de la famille des Agelenidae (Araneae) de la région Méditerranéene (2e partie). Bulletin de l'Institut Royal des Sciences Naturelles de Belgique 52(1): 1–54.

Dimitrov D (2020) Description of a new *Tegenaria* Latreille, 1804 from southern Turkey with remarks on the *Tegenaria ariadnae* species-complex (Arachnida, Araneae). Zoo-Keys 935: 47–55. https://doi.org/10.3897/zookeys.935.52089

Dimitrov D (2022) A review of the genus *Maimuna* Lehtinen, 1967 (Araneae, Agelenidae) in Turkey, with a description of a new species. Zootaxa 5124(3): 383–390. https://doi.org/10.11646/zootaxa.5124.3.7

Dimitrov D, Bolzern A, Arnedo MA (2022) Bringing *Tegenaria boitanii* stat. rev. back to life with a review of the *Tegenaria percuriosa*-complex (Araneae: Agelenidae), description of a new species and insight into their phylogenetic relationships and evolutionary history. Systematics and Biodiversity 20(1): 1–18. https://doi.org/10.1080/14772000.2021.2012297

Guseinov E, Marusik YM, Koponen S (2005) Spiders (Arachnida: Aranei) of Azerbaijan 5. Faunistic review of the funnel-web spiders (Agelenidae) with the description of a new genus and species. Arthropoda Selecta 14(2): 153–177.

Kaya RS, Kunt KB, Marusik YM, Uğurtaş İH (2010) A new species of *Tegenaria* Latreille, 1804 (Araneae, Agelenidae) from Turkey. ZooKeys 51: 1–16. https://doi.org/10.3897/zookeys.51.467

Kaya RS, Zamani A, Yağmur EA, Marusik YM (2023) A new genus of Textricini Lehtinen, 1967 (Araneae, Agelenidae) from Anatolia. ZooKeys 1151: 31–45. https://doi.org/10.3897/zookeys.1151.100430

Kovblyuk MM, Nadolny AA (2007) *Malthonica dalmatica* (Kulczyński, 1906) from the Crimea, a spider new to the former Soviet Union (Aranei: Agelenidae). Arthropoda Selecta 16: 19–22.

Kovblyuk MM, Ponomarev AV (2008) New and interesting spiders (Aranei: Agelenidae, Corinnidae, Gnaphosidae, Nemesiidae, Thomisidae) from the west Caucasus. Caucasian Entomological Bulletin 4: 143–154. https://doi.org/10.23885/1814-3326-2008-4-2-143-154

Lehtinen PT (1967) Classification of the cribellate spiders and some allied families, with notes on the evolution of the suborder Araneomorpha. Annales Zoologici Fennici 4: 199–468.

Levy G (1996) The agelenid funnel-weaver family and the spider genus *Cedicus* in Israel (Araneae, Agelenidae and Cybaeidae). Zoologica Scripta 25(2): 85–122. https://doi.org/10.1111/j.1463-6409.1996.tb00154.x

Nentwig W, Blick T, Bosmans R, Gloor D, Hänggi A, Kropf C (2024) Spiders of Europe. Version 8.2024. https://www.araneae.nmbe.ch [accessed on 20.8.2024] https://doi.org/10.24436/1

Noroozi J, Zare G, Sherafati M, Mahmoodi M, Moser D, Asgarpour Z, Schneeweiss GM (2019) Patterns of endemism in Turkey, the meeting point of three global biodiversity hotspots, based on three diverse families of vascular plants. Frontiers in Ecology and Evolution 7: 1–12. https://doi.org/10.3389/fevo.2019.00159

Otto S (2022) Caucasian Spiders. A faunistic database on the spiders of the Caucasus. Version 02.2022. https://caucasus-spiders.info/

Ponomarev AV, Shmatko VY (2022) A review of the spider genus *Tegenaria* Latreille, 1804 (Aranei: Agelenidae) of the Russian Caucasus and Ciscaucasia. I. Species close to *Tegenaria abchasica* Charitonov, 1941. Caucasian Entomological Bulletin 18(2): 211–221. https://doi.org/10.23885/181433262022182-211221

Ponomarev AV, Mikhailov KG, Shmatko VY (2024) Review of spiders of the genus *Tegenaria* Latreille, 1804 (Aranei: Agelenidae) of Ciscaucasia and the Russian Caucasus III. New data on fauna and distribution, with material from neighbouring regions. Arthropoda Selecta 33(2): 273–287. https://doi.org/10.15298/arthsel.33.2.15

Seropian A, Otto S, Bulbulashvili N (2023) Picking pearls from the Silk Road: insights into the spider (Arthropoda, Araneae) diversity in Georgia from the CaBOL project. Part I. Caucasiana 2: 143–159. [& Suppl.] https://doi.org/10.3897/caucasiana.2.e107049

Topçu A, Demircan N (2018) New records of family Agelenidae for the spider fauna of Turkey (Araneae: Agelenidae). Indian Journal of Arachnology 6: 20–22.

WSC (2024) World Spider Catalog. Version 25.0. Natural History Museum Bern. http://wsc.nmbe.ch [accessed on 18.06.2024] https://doi.org/10.24436/2

Zamani A, Marusik YM (2020) A review of Agelenini (Araneae: Agelenidae: Ageleninae) of Iran and Tajikistan, with descriptions of four new genera. Arachnology 18(4): 368–386. https://doi.org/10.13156/arac.2020.18.4.368

Zamani A, Darvishnia H, Marusik YM (2023) New data on cave spiders (Arachnida: Araneae) of Iran, with new species and records. Zootaxa 5361(3): 345–366. https://doi.org/10.11646/zootaxa.5361.3.3

Zarikian NA, Propistsova EA, Marusik YM (2022) On spider families (Arachnida: Araneae) new to Armenia. Israel Journal of Entomology 51(2021): 103–117. https://doi.org/10.5281/zenodo.6466083

Research Article

Two new species and one new record of the genus *Torodora* Meyrick (Lepidoptera, Lecithoceridae) from China

Shuai Yu[1,2], Lin Liu[1], Xueqing Li[1], Shuxia Wang[2]

1   *College of Agriculture and Biology, Liaocheng University, Liaocheng 252000, China*
2   *College of Life Sciences, Nankai University, Tianjin 300071, China*
Corresponding author: Shuxia Wang (*shxwang@nankai.edu.cn*)

Abstract

Two new species of the genus *Torodora* Meyrick, 1894 are described from China: *T. lichi* **sp. nov.** and *T. mici* **sp. nov.** Additionally, *T. silvatica* Park, 2007 is newly recorded for China. Images of the adults and their genitalia are provided.

Key words: Gelechioidea, morphology, taxonomy, Torodorinae

Introduction

Torodora Meyrick, 1894 is the largest and type genus of the subfamily Torodorinae (Lecithoceridae). It is distributed in the Oriental, Palearctic, Ethiopian, and Australian region, and comprises more than 230 species (Park et al. 2022). Eighty-eight species of *Torodora* are recorded in China. The genus is characterized by having the following combination of characters: forewing with M_1 and M_2 free, M_3 separated or stalked with R_{4+5}, R_4 and R_5 stalked; M_1, M_2, and M_3 free; CuA_1 and CuA_2 stalked; hindwing with M_2 present; M_3 and CuA_1 stalked or coincident; genitalia morphologically varied and abdominal tergites with zones of spiniform setae. Here, we describe two new species of *Torodora*, as well as the first report of *T. silvatica* Park, 2007 from China.

Materials and methods

The specimens were collected at the locations indicated below. Each image was collected using GYZ 450 W high-pressure mercury lamps (Yaming, China). Morphological terminology in the descriptions was in accordance with Gozmány (1978). The wingspan was measured from the tips of the left and right forewings of fully well spread specimens. Slides of genitalia were prepared following Li (2002). Photographs of adults were taken using an M205A stereomicroscope, and photographs of genitalia were taken using a DM750 microscope with Leica Application Suite software version 4.6 (all from Leica, Germany). All photographs were manipulated in Photoshop CC (Adobe, USA).

The examined materials, including the type series of the new species, are deposited at Liaocheng University (**LCU**), Liaocheng, China.

Taxonomic accounts

Torodora Meyrick, 1894

Torodora Meyrick, 1894: 16. Type species: *Torodora characteris* Meyrick, 1894, by original designation.

Habrogenes Meyrick, 1918: 102. Type species: *Habrogenes eupatris* Meyrick, 1918, by original designation.

Panplatyceros Diakonoff, 1951: 76. Type species: *Panplatyceros serpentina* Diakonoff, 1951, by monotypy.

Toxotarca Wu, 1994: 123. Type species: *Toxotarca parotidosa* Wu, 1994, by monotypy.

Torodora lichi Yu & Wang, sp. nov.

https://zoobank.org/084DF877-08EC-4580-B044-11AFEF6951F6

Figs 1A, B, 2A

Type materials. *Holotype*: CHINA • ♂; Yunnan Prov., Menghai County, Nabanhe; 22.243°N, 100.599°E; 810 m elev.; 2 Aug. 2022; Shuai Yu & Kaijian Teng leg.; slide no. YUS004, in LCU.

Diagnosis. *Torodora lichi* is externally similar to the Thailand's species, *T. epicharis* Park, 2002. It can be distinguished by the forewing absent of a postmedian line, in the male genitalia by the foot-shaped cucullus, and the juxta with a triangular median process below the posterior margin; *T. epicharis* has a postmedian line in the forewing and has an ovate cucullus and a juxta lacking the median process (Park 2002: 156).

Description. Wingspan 15.0 mm (Fig. 1A). Head pale yellow. Antennae pale yellow, scape apically dark brown. Labial palpus with second palpomere white, roughly scaled ventrally; third palpomere white dorsally, dark brown ventrally, as long as second palpomere. Patagium white. Thorax and tegula white, mixed with pale, orange-yellow scales. Forewing with a slightly arched costal margin, apex triangularly produced, termen concave; ground color pale orange-yellow, with three white spots along the distal half of the costal margin; basal 1/4 with two straight, white lines running from the costal margin to the dorsum; a large black patch before the middle, mixed with white scales, anteriorly reaching below the costal margin of the forewing, posteriorly reaching the dorsum; outer margin sinuate; median line white, extending from the costal margin of the forewing along the outer margin of the patch to the dorsum; a crescent pale yellow spot at the distal 2/3 anterior of M_2; area between median line and termen brown along posterior 2/3; fringe pale orange yellow; venation with R_3, R_4, and R_5 stalked, M_1, M_2, and M_3 free, and CuA_1 and CuA_2 stalked. Hindwing and fringe pale, greyish brown; fringe with a pale-yellow basal line; venation with M_3 and CuA_1 stalked basally, distant from CuA_2 at base (Fig. 1B).

Male genitalia (Fig. 2A). Uncus elongated and triangular. Gnathos with median process wide at base, slightly narrowed toward the distal 2/5 where it curves and sharply tapers to a pointed apex. Valva wide basally, narrowed medially; cucullus foot-shaped, widened basally, narrowing toward a narrowly rounded apex; outer margin concave, ventral margin round, produced distally; costa deeply concave broadly; sacculus band-shaped. Vinculum U-shaped. Juxta rectangular,
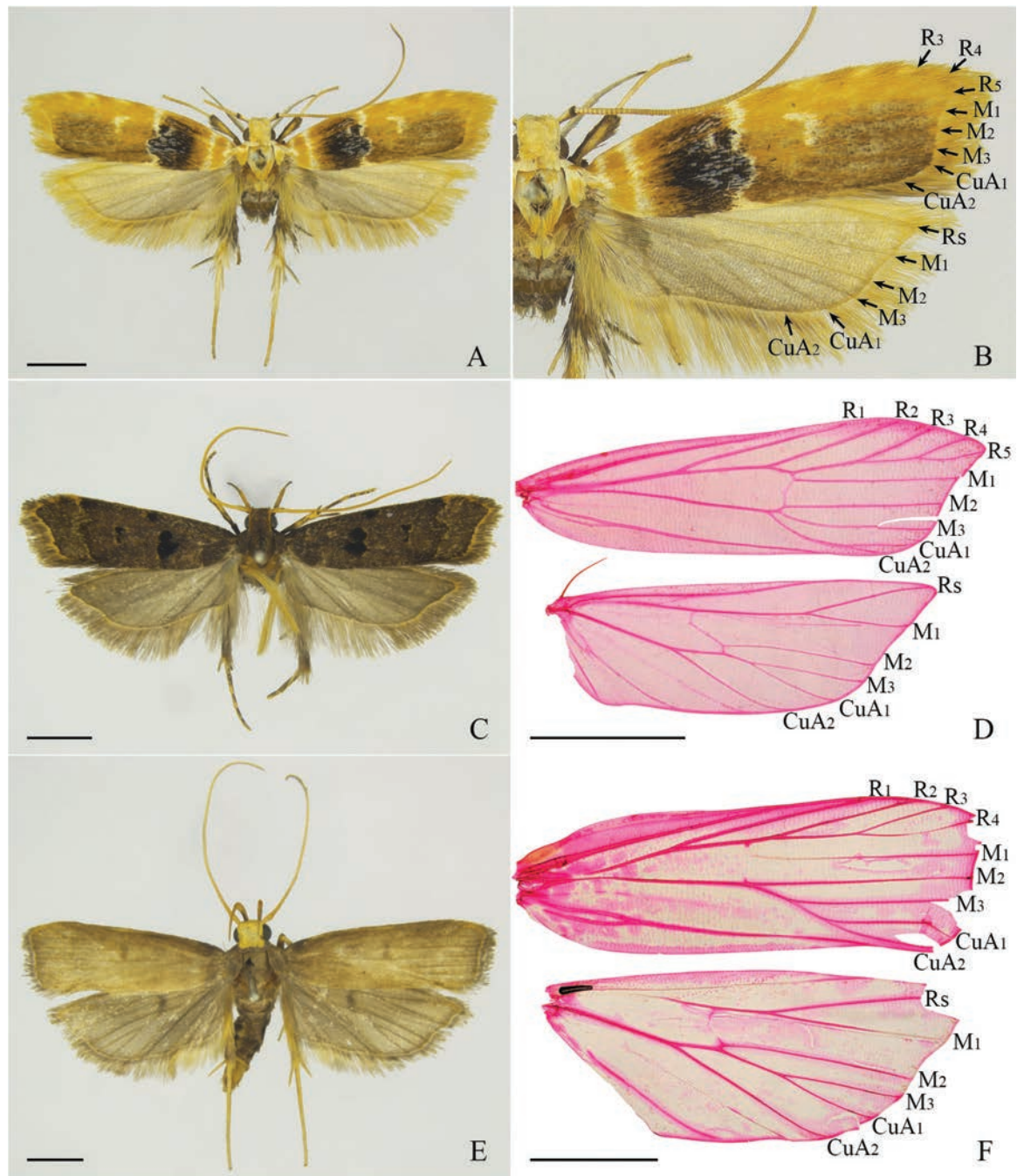
Figure 1. External features and wing venation of *Torodora* spp. **A** external features of *T. lichi* Yu & Wang, sp. nov., holotype, male, slide No. YUS004 **B** right wing venation of *T. lichi* Yu & Wang, sp. nov., holotype, male, slide No. YUS004 **C** external features of *T. mici* Yu & Wang, sp. nov., paratype, male, LCU204 **D** right wing venation of *T. mici* Yu & Wang, sp. nov., paratype, male, LCU033 **E** external features of *T. silvatica* Park, 2007, male, slide No. LCU218 **F** right wing venation of *T. silvatica* Park, 2007, male, slide No. LCU217. Scale bars: 2.0 mm.

longer than wide, with a heavily sclerotized, triangular median process along the posterior margin; posterolateral lobes elongated, horn-shaped; posterior lobes near the posterolateral lobes, weakly sclerotized, digitate, setose; anterior margin with an imbricate process near middle. Phallus wide at the base, gradually narrowing toward a blunt apex, curved; cornuti located distally, consisting of two small spinose plates, with two elongate spiculose bars.

Female. Unknown.

Distribution. China (Yunnan Province).

Etymology. The specific epithet is derived from Mandarin *li* (beautiful) and *chi* (wing), referring to the colorful forewing.

Torodora mici Yu & Wang, sp. nov.

https://zoobank.org/A7BB5155-311A-4E8E-8106-269201037072
Figs 1C, D, 2B, D

Type materials. *Holotype:* CHINA • ♂; Xizang Autonomous Region [Tibet], Motuo County [Mêdog], Beibengxiang; 29.242°N, 95.171°E; 1239 m elev.; 14 Jun. 2023; Shuai Yu leg.; slide no. LCU034, in LCU. *Paratypes:* 3 ♂ 1 ♀; same data as holotype; slide nos. LCU033♂, LCU204♂, LCU219♀, in LCU.

Diagnosis. *Torodora mici* is similar to *T. reniformis* Yu & Wang, 2022 in the male genitalia. It can be distinguished by the blackish brown forewing, the juxta reaching near posterior margin of the tegumen, and the cornutus an elongate bar; *Torodora reniformis* has a forewing that is dark brown on the basal 3/4 and orange white on the distal 1/4 (Yu et al. 2022: 16), the juxta reaches far from the posterior margin of the tegumen, and the cornuti consists of needle-like spines (Yu et al. 2022: 24).

Description. Wingspan 13.5–14.0 mm (Fig. 1C). Head dark brown, orange-yellow along lateral surfaces. Antennae yellow. Labial palpus dark brown, distally yellow on second palpomere; third paplomere slender, as long as the second. Thorax and tegula dark brown. Forewing with costal margin nearly straight, slightly curved distally, apex slightly down-curved, termen slightly concave; ground color dark brown, mixed with scattered yellow scales, distal 1/4 of the costal margin yellow; discal stigma rounded, black, outer margin edged with yellow scales; plical stigma nearly rounded, black, anteriorly extending toward discal stigma, outer margin edged with yellow scales; discocellular stigma small, paired, located one above another, with a yellow outer margin; subterminal line yellow, extending from 1/4 of the costal margin sinuated to the distal 1/5 of the dorsum; fringe dark brown, with a yellow basal line; venation with R_1, R_2 free, R_3, R_4, and R_5 stalked, R_5 extending to apex, M_1, M_2, M_3 free, CuA_1 and CuA_2 stalked distally. Hindwing greyish brown; fringe greyish brown, with a yellow basal line; venation with M_2 free, M_3 and CuA_1 stalked basally, CuA_2 distant from M_3+CuA_1 at the base (Fig. 1D).

Male genitalia (Fig. 2B). Uncus elongated with widened base. Gnathos with basal plate rounded on posterior margin, median process absent. Valva wide at the base, gradually narrowing to cucullus; cucullus extending obliquely dorsad, apical margin broadly rounded, costal margin nearly straight throughout length, abruptly curved upwards forming inner margin of cucullus; sacculus wide, elongate, densely spiculose. Vinculum U shaped, nearly straight on anterior margin. Juxta rectangular, longer than wide, with a longitudinal median line; posterolateral lobes digitate, reaching near the posterior margin of the tegumen, apex narrowly rounded, setose. Phallus shorter than the valva, straight, uniformly wide basally, narrowing apically; vesica densely granulate; cornutus an elongate bar near apex of vesica.

Female genitalia (Fig. 2D). Eighth abdominal sternite medially concave on posterior margin, forming two lateral parts broadly rounded posteriorly. Apophyses posteriores longer than apophyses anteriores. Antrum cup-shaped and membranous. Ductus bursae nearly wide throughout length, bearing sparse spines; ductus seminalis slender, arising from approximately the posterior 1/4
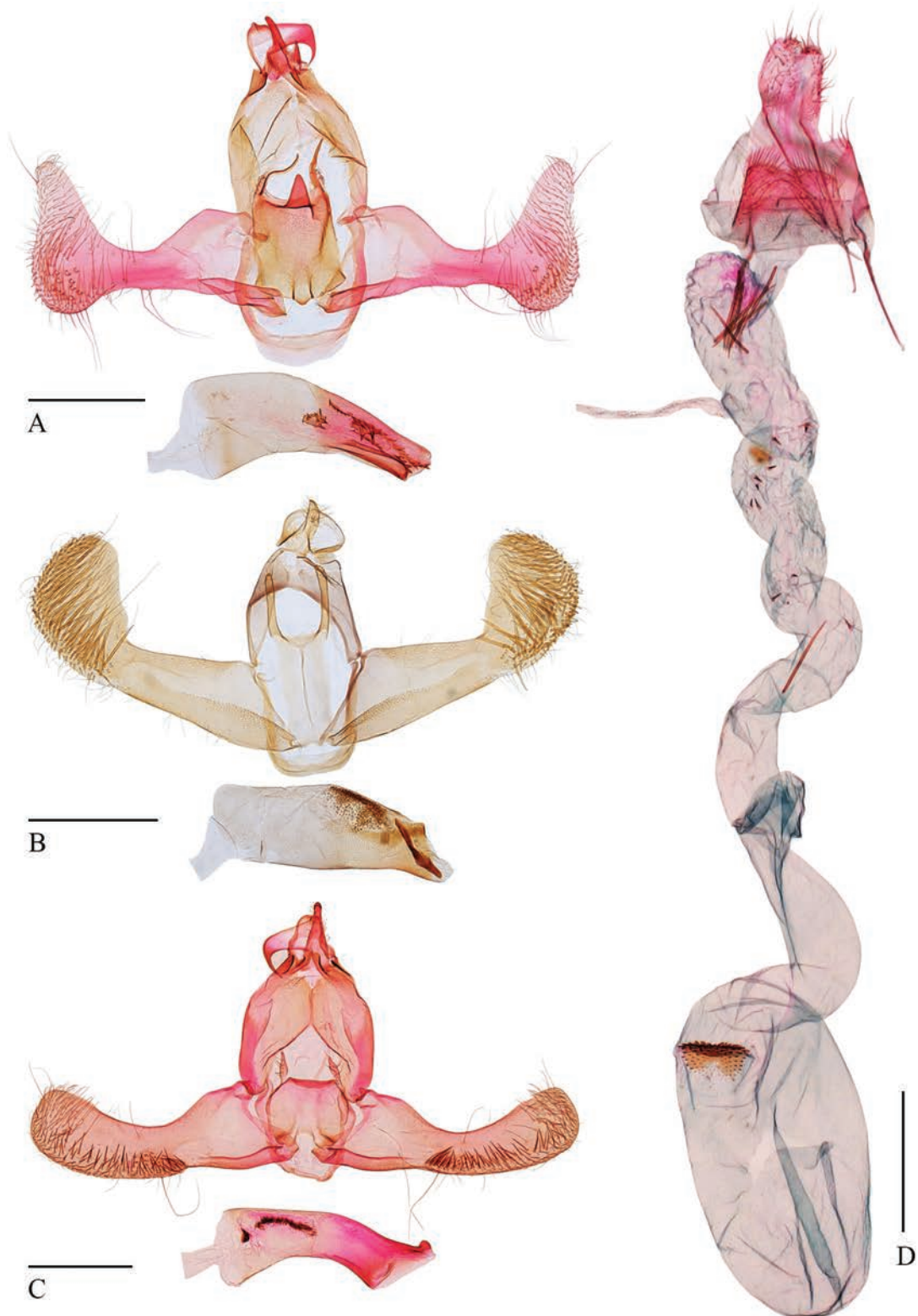
Figure 2. Genitalia of *Torodora* spp. **A** male genitalia of *T. lichi* Yu & Wang, sp. nov., holotype, slide No. YUS004 **B** male genitalia of *T. mici* Yu & Wang, sp. nov., holotype, slide No. LCU034 **C** male genitalia of *T. silvatica* Park, 2007, slide No. LCU217 **D** female genitalia of *T. mici* Yu & Wang, sp. nov., paratype, slide No. LCU219. Scale bars: 0.5 mm.

of ductus bursae, with dense spinules on the inner wall. Corpus bursae elliptical; signum on posterior end, a transverse plate, bearing dense spinules.

Distribution. China (Xizang Autonomous Region [Tibet]).

Etymology. The specific epithet is derived from the Mandarin *mi* (dense) and *ci* (spine), referring to the densely spined sacculus of the male genitalia.

Torodora silvatica Park, 2007
Figs 1E, F, 2C

Torodora silvatica Park, 2007: 23. Holotype male collected in Thailand, deposited at the University of Osaka Prefecture, Osaka, Japan (OPU).
Thubana silvatica (Park): Park et al. 2013: 312.
Thubana seimaensis Park, 2013: 312. Holotype male collected in Cambodia, deposited at the University of Incheon, Incheon, South Korea (UIK).

Specimens examined. CHINA • 1 ♂; Yunnan Prov., Menghai County, Nabanhe; 22.243°N, 100.599°E; 810 m elev.; 2–3 Aug. 2022; Shuai Yu & Kaijian Teng leg., in LCU • 1 ♂; Yunnan Prov., Jinghong City, Mt. Jinuo; 21.982°N, 100.889°E; 1425 m elev.; 6–7 Aug. 2022; Shuai Yu & Kaijian Teng leg.; slide no. LCU218, in LCU • 1 ♂; Yunnan Prov., Jinghong City, Yexianggu; 22.100°N, 100.520°E; 852 m elev.; 8 Aug. 2022; Shuai Yu & Kaijian Teng leg.; slide no. LCU217, in LCU.

Description. Adult wingspan 16.0–16.5 mm (Fig. 1E).

Distribution. China (Yunnan Province, new record), Cambodia, Thailand.

Remarks. Park (2007) firstly described *T. silvatica* from Thailand, and he later transferred the species to *Thubana* Walker, 1864 (Park et al. 2013). Park et al. (2022) transferred *Th. silvatica* back to *Torodora*. An explanation for this reversal is given: "the venation of forewing differs from that of the type species of *Torodora*, having M_3 and CuA_{1+2} on a common stalk, as well as that of *Thubana* Walker, but it is no doubt that the forewing color pattern and the male genital characters are closer to the genus *Torodora*" (Park et al. 2022: 368). We follow Park et al.'s treatment and concur with the taxonomic status of *Torodora silvatica*.

Acknowledgements

Additional information

Conflict of interest

The authors have declared that no competing interests exist.

Ethical statement

No ethical statement was reported.

Funding

Author contributions

Author ORCIDs

Shuai Yu ⬤ https://orcid.org/0000-0003-3670-2701
Shuxia Wang ⬤ https://orcid.org/0000-0002-9316-6661

Data availability

All of the data that support the findings of this study are available in the main text.

References

Diakonoff A (1951)[1952] Entomological results from the Swedish expedition 1934 to Burma and British India. Lepid. Microlepidoptera I. Arkiv för Zoologi 3(6): 59–94.

Gozmány L (1978) Lecithoceridae. In: Amsel HG, Reisser H, Gregor F (Eds) Microlepidoptera Palaearctica, 5. Georg Fromme & Co., Vienna, 1–306.

Li HH (2002) The Gelechiidae of China (I) (Lepidoptera: Gelechioidea). Nankai University Press, Tianjin, 504 pp.

Meyrick E (1894) On a collection of Lepidoptera from Upper Burma. Transactions of the Royal Entomological Society of London 1894: 1–29.

Meyrick E (1918) Exotic Microlepidoptera II. Thornhanger, Marlborough, Wilts, 640 pp.

Park KT (2002) Taxonomic review of the genus *Torodora* Meyrick in Thailand, with descriptions of fifteen new species (Lepidoptera: Lecithoceridae). Insecta Koreana 19(2): 147–166.

Park KT (2007) Three new species of *Torodora* Meyrick, 1894 from Thailand (Lepidoptera: Lecithoceridae). SHILAP Revista de Lepidopterología 35(137): 23–28.

Park KT, Bae YS, Kim S (2013) Three new species of *Thubana* Walker, 1864 from Cambodia and Malaysian Borneo (Lepidoptera: Lecithoceridae), SHILAP Revista de Lepidopterología 41(163): 311–316.

Park KT, Cho S, Koo JM (2022) The subfamily Torodorinae of the world (Lepidoptera: Lecithoceridae). National Institute of Biological Resources, Incheon, 584 pp.

Walker F (1864) List of the Specimens of Lepidopterous Insects in the Collection of the British Museum. Order of Trustees 29: 562–835.

Wu CS (1994) The Lecithoceridae (Lepidoptera) of China with descriptions of new taxa. Sinozoologia 11: 123–154.

Yu S, Zhu YM and Wang SX (2022) Eighteen new species and fifteen new records of the genus *Torodora* Meyrick (Lepidoptera: Lecithoceridae) from China. Zootaxa 5133(1): 1–39. https://doi.org/10.11646/zootaxa.5133.1.1

Research Article

A new species of *Rhyacophila* Pictet, 1834 (Trichoptera, Rhyacophilidae) from Corsica with the genomic characterization of the holotype

Ernesto Rázuri-Gonzales[1], Wolfram Graf[2], Jacqueline Heckenhauer[1,3], Julio V. Schneider[1],
Steffen U. Pauls[1,3,4]

1   Senckenberg Research Institute and Natural History Museum Frankfurt, Frankfurt, Germany
2   Institute of Hydrobiology and Aquatic Ecosystem Management (IHG), University of Natural Resources and Life Sciences, Vienna, Austria
3   LOEWE Centre for Translational Biodiversity Genomics (LOEWE-TBG), Frankfurt, Germany
4   Institute of Insect Biotechnology, Justus-Liebig University, Gießen, Germany

Corresponding author: Ernesto Rázuri-Gonzales (ernesto.razuri-gonzales@senckenberg.de, lerazuri@gmail.com)

Abstract

We describe a new species in the *Rhyacophila tristis* group, *Rhyacophila lignumvallis* Graf & Rázuri-Gonzales, **sp. nov.**, from the island of Corsica (France) based on a single male specimen. In addition to the morphological differences between the new species and the most similar species in the group, we also provide a phylogenetic tree based on the mitochondrial cytochrome *c* oxidase subunit I (mtCOI), including sequences from 16 out of the 28 currently recognized species in the group. These data, together with conspecific larval sequences, support the status of the new species and shed light on an additional potential new species near *Rhyacophila pubescens*. Using a low-cost next-generation sequencing approach, we generated the mito- and draft nuclear genome assembly of the holotype of *R. lignumvallis* **sp. nov.** as well as that of *R. tsurakiana*. This genetic data represents an important additional characterization to the description of morphological features and is valuable for future investigations, such as population or phylogenomic studies.

Key words: Caddisflies, holotype genomics, mitogenome, taxonomy

Introduction

The genus *Rhyacophila* Pictet 1834, with 814 extant and 30 fossil species, is the largest caddisfly genus in the world (Valladolid et al. 2023). These caddisflies are primarily distributed in the northern hemisphere, but they also occur in temperate and tropical India and southeastern Asia (Holzenthal et al. 2007). Given the sheer size of the genus, many species groups have been proposed based on the morphological characteristics of the larvae (Döhler 1950) and the male genitalia (Ross 1956; Schmid 1970). However, the groups and subgenera proposed by different authors do not correspond to each other. For example, some of the larval characters for the subgenera of Döhler are found in several of the groups of Schmid. Phylogenetic studies of different groups proposed by

Schmid (1970) seem to showcase the overall utility of his system, even if rearrangements are sometimes needed (Coppa et al. 2012).

One of the groups proposed by Schmid is the *Rhyacophila tristis* group in the *R. invaria* branch. It is mainly characterized by a large segment IX without an apical dorsal lobe, a simple and oblique segment X, with fairly large anal sclerites, which can be joined or partially fused to each other and fused to segment X, very large phallotheca with a simple or complex dorsal arm, a simple chitinous aedeagus, simple lobe-like parameres, and lacking a ventral lobe, among other characteristics (Schmid 1970). Currently, the species group contains 28 species in two subgroups: the *tristis* and the *pubescens* subgroups (Schmid 1970, Suppl. material 1). The *tristis* subgroup is further characterized by the complex shape of the dorsal arm of the phallotheca and the presence of fairly large parameres fused to the aedeagus. The *pubescens* subgroup, on the other hand, has a simpler dorsal arm of the phallotheca and elongated free parameres. Species of the *R. tristis* species group (i.e., both subgroups) generally occur in headwaters to medium-sized, fast-flowing streams at middle elevations throughout Europe (excluding the British Isles, Northern Europe, and Russia) and Western Asia (i.e., Turkey and Iran) (Schmid 1970; Coppa et al. 2012; Suppl. material 1).

Only two species in the *R. tristis* group were previously known on the island of Corsica (France): *R. pubescens* Pictet, 1834 and *R. tristis* Pictet, 1834. Both species were initially recorded by Mosely (1930, 1932). More recently, Engelhardt (2009) assessed the phylogenetic relationships in the *R. tristis* group and the phylogeography of *R. pubescens* throughout its distributional range. Engelhardt showed that the larval specimens of *R. pubescens* from the island were significantly divergent from all the other populations. Moreover, the Corsican specimens formed a highly supported clade, separate from all other *R. pubescens* (Engelhardt et al. 2011).

In the present paper, we confirm the genetic and morphological distinctness of adult males of the Corsican lineage to represent a new species and describe it as *Rhyacophila lignumvallis* sp. nov. in the *pubescens* subgroup of the *R. tristis* group. Additionally, we present an annotated draft genome from the holotype and its complete mitogenome, adding valuable genetic information to the holotype description. Finally, we also include a draft genome and the mitogenome for a second species in the *Rhyacophila tristis* species group, *R. tsurakiana* Malicky, 1984 from Albania. We hope these genomic resources stimulate research on this group of insects, especially since their diversity is high in this area and they seem to be restricted to specific mountain ranges, as suggested by Oláh et al. (2022).

Material and methods

Specimen collection

The specimen was swept from the riparian vegetation using a hand net.

DNA extraction, library preparation, and whole genome sequencing

A pair of legs from the holotype of *R. lignumvallis* sp. nov. were removed, and the tissue was incubated overnight in 60 µl TNES lysis buffer (100 mM Tris-HCl, 25 mM NaCl, 10 mM EDTA, 1% SDS) and 8 µl Proteinase K (20 mg/ml). For DNA

binding and cleanup, 75 µl custom speed-bead suspension was added (Sera-Mag SpeedBeads Carboxylate, hydrophobic, Cytiva; see Rohland and Reich 2012), incubated for 15 min on a rotating shaker, and the beads were washed twice with 75% ethanol after the supernatant had been removed and discarded. The DNA was eluted in 1X TE.

DNA sequences were generated for the cytochrome *c* oxidase subunit I barcoding region (mtCOI, 658 bp) using primers LCO1490-L and HCO2198-L (Nelson et al. 2007). Polymerase chain reactions (PCR) were run on a Mastercycler Pro S (Eppendorf, Hamburg, Germany) in reactions containing 1X MyTaq Reaction Buffer, 0.4 µM of each forward and reverse primer, 0.5 U MyTaq DNA Polymerase, 1 µl DNA and nuclease-free water to fill up to a total volume of 10 µl. Reaction conditions were 1 min at 95 °C for initial denaturation followed by 35 cycles of 20 s at 95 °C (denaturation), 30 s at 45 °C (annealing), and 30 s at 72 °C (extension). The reaction ended with a final extension for 5 min at 72 °C. PCR products were visualized on agarose gels and purified using a modified ExoSAP protocol with Exonuclease I (20U/µl) and Fast AP Themosensitive Alkaline Phosphatase (1U/µl; both ThermoFisher Scientific, Vilnius, Lithuania). DNA sequences were generated at the Laboratory Centre of the Senckenberg Biodiversity and Climate Research Centre using a 3730XL DNA Analyzer (Applied Biosystems).

Genomic DNA was taken from the above DNA isolates, quantified using a Qubit 4.0 fluorometer with a 1x dsDNA HS Assay Kit (ThermoFisher Scientific, Waltham, USA), and sheared to a target fragment size of 350 bp using a Bioruptor Pico (Diagenode, Seraing, Belgium). Genomic libraries were prepared from 27.4 ng sheared gDNA using the NEBNext Ultra II DNA Library Preparation Kit for Illumina (New England Biolabs, Ipswich, MA, USA), following the manufacturer's manual. Adapters were diluted 1:10 as recommended for low input libraries, and size selection was omitted due to the low DNA amount. A dual indexing PCR was run for 7 cycles on a Mastercycler (Eppendorf, Germany) using NEBNext Multiplex Oligos for Illumina (Dual Index Primers Set 1; New England Biolabs, Ipswich, MA, USA). After cleanup, library integrity was verified on a 2200 TapeStation with a High Sensitivity D1000 Tape (Agilent, Santa Clara, CA, USA), and shipped for 150 bp paired-end sequencing (ordering 30 Gbp output) on a partial lane of an Illumina NovaSeq 6000 platform (San Diego, CA) at Novogene (Cambridge, UK).

Raw reads are deposited in the National Center for Biotechnology Information's Sequence Read Archive (NCBI SRA) under the accession number SRR22799047 under Bioproject PRJNA899095.

DNA barcoding and phylogenetic analysis

The final mtCOI alignment included 71 sequences: 68 sequences from 16 species and 2 morphospecies in the *Rhyacophila tristis* group. *Rhyacophila italica* Moretti, 1981, *Himalopsyche kuldschensis* (Ulmer, 1927), and *H. triloba* (Hwang, 1958) were included as outgroups. All sequences were generated for this manuscript, except *R. bosnica* Schmid, 1970 (MK211322), *H. kuldschensis* (KX143534), and *H. triloba* (KX295339), which were retrieved from GenBank. The barcode region is 658 bp in length. However, some of our sequences were incomplete, and their lengths were between 576 and 658 bp. Therefore, the final alignment was completed with Ns on both ends, reaching 3.69% of missing data. Sequence specimen data and GenBank accession numbers are summarized in Table 1.

Table 1. Sequence specimen data, with GenBank accession numbers, of the studied *Rhyacophila* species and the outgroups *Himalopsyche kuldschensis* (Ulmer, 1927) and *H. triloba* (Hwang, 1958).

Species	Country*	Locality	Latitude, Longitude	Accession No.
Himalopsyche kuldschensis	KG	Kalay Makhmud valley between Or-Mazan-Suu and Ala Malden	39.683, 70.8833	KX143534
Himalopsyche triloba	CN	Sichuan, near Jiuzhaigou	30.45, 102.50	KX295339
R. akutila	BG	Prava Marica stream at Zavracica mountain hut	42.16789, 23.64139	PP515197
R. aquitanica	FR	Ruisseau de Chousse, upper tributary; between Arrette & La Pierre Saint-Martin	43.00757, -0.73572	PP515198
R. aquitanica	FR	Ruisseau de Chousse, upper tributary; between Arrette & La Pierre Saint-Martin	43.00757, -0.73572	PP515199
R. aquitanica	FR	Ruisseau de Chousse, upper tributary; between Arrette & La Pierre Saint-Martin	43.00757, -0.73572	PP515200
R. aquitanica	FR	Ruisseau de Chousse, upper tributary; between Arrette & La Pierre Saint-Martin	43.00757, -0.73572	PP515201
R. aquitanica	ES	tributaries to the Barranco de Urdiceto, above Embalse de Urdiceto	42.67832, -0.2772	PP515202
R. bosnica	BA	Vareš municipality, Rajčevački stream	–	MK211322
R. carpathica	RO	Galeş Lake	45.38650, 22.90914	PP515204
R. carpathica	RO	Galeş Lake	45.38650, 22.90914	PP515205
R. carpathica	RO	Galeş Lake	45.38650, 22.90914	PP515206
R. carpathica	RO	Galeş Lake	45.38650, 22.90914	PP515207
R. carpathica	RO	Caraş-Severin, Iauna Mare stream	45.51636, 22.59017	PP515208
R. carpathica	RO	Caraş-Severin, Poiana Mărului	45.39583, 22.53422	PP515209
R. cibinensis	RO	unnamed stream near Păltiniş	45.63878, 23.92540	PP515210
R. cibinensis	RO	unnamed stream near Păltiniş	45.63878, 23.92540	PP515211
R. cibinensis	RO	unnamed stream near Păltiniş	45.63878, 23.92540	PP515212
R. cibinensis	RO	Lotru river	45.38, 23.62	PP515213
R. italica	IT	Purello	43.32, 12.77	PP515214
R. lignumvallis sp. nov.	FR	Corsica, Tributary to the Tavignano	42.25639, 9.20583	PP515216
R. lignumvallis sp. nov.	FR	Corsica, Tributary to the Tavignano	42.25639, 9.20583	PP515217
R. lignumvallis sp. nov.	FR	Corsica, Tributary to the Tavignano	42.25639, 9.20583	PP515218
R. lignumvallis sp. nov.	FR	Corsica, bridge over the river Vecchio near the confluence with the river Tavignano	42.2275, 9.24306	PP515215
R. margaritae	BG	Lower left tributary to Zavodna, above Ribaritsa village and below Vezhen peak	42.76, 24.37	PP515219
R. margaritae	BG	Lower left tributary to Zavodna, above Ribaritsa village and below Vezhen peak	42.76, 24.37	PP515220
R. margaritae	BG	Lower left tributary to Zavodna, above Ribaritsa village and below Vezhen peak	42.76, 24.37	PP515221
R. obtusa	BG	Zavodna river, upstream of the confluence with the Beli Vit at the Ribaritsa village	42.812, 24.371	PP515222
R. obtusa	BG	Zavodna river, upstream of the confluence with the Beli Vit at the Ribaritsa village	42.791, 24.377	PP515223
R. orghidani	RO	right-side inflow of Leşu artificial lake	46.80981, 22.58948	PP515224
R. orghidani	RO	right-side inflow of Leşu artificial lake	46.80981, 22.58948	PP515225
R. orghidani	RO	Băişoara	46.53287, 23.28078	PP515226
R. orghidani	RO	Băişoara	46.53287, 23.28078	PP515227
R. pirinica	BG	24.5 km NNW from Gotse Delchev	41.63156, 23.44628	PP515228
R. pirinica	BG	24.5 km NNW from Gotse Delchev	41.63156, 23.44628	PP515229
R. pirinica	BG	24.5 km NNW from Gotse Delchev	41.63156, 23.44628	PP515230
R. producta	AT	Nockberge	46.85, 13.76	PP515231
R. producta	AT	Nockberge	46.85, 13.76	PP515232
R. pubescens	CH	La Motte above Ocourt	47.35, 7.06	PP515233

Species	Country*	Locality	Latitude, Longitude	Accession No.
R. pubescens	CH	La Motte above Ocourt	47.35, 7.06	PP515234
R. pubescens	FR	Ravin de Chambiéres	43.93278, 6.63694	PP515235
R. pubescens	FR	Ravin de Chambiéres	43.93278, 6.63694	PP515236
R. pubescens	FR	La Condamine-Châtelard	44.451, 6.741	PP515237
R. pubescens	FR	La Condamine-Châtelard	44.451, 6.741	PP515238
R. pubescens	FR	La Condamine-Châtelard	44.451, 6.741	PP515239
R. pubescens	IT	Tributary of Fiume Tescio	43.09722, 12.67556	PP515240
R. pubescens	IT	Tributary of Fiume Tescio	43.09722, 12.67556	PP515241
R. pubescens	IT	Tributary of Fiume Tescio	43.09722, 12.67556	PP515242
R. pubescens	IT	Nameless brook near Rezzo	44.02583, 7.86667	PP515243
R. pubescens	IT	Valle di Pietra	44.07722, 7.80639	PP515244
R. pubescens	IT	Valle di Pietra	44.07722, 7.80639	PP515245
R. sarplana	AL	Tropojë, open stream on Mt. Callumit, above town	42.49862, 20.12443	PP515203
Rhyacophila sp., *tristis* grp.	AT	Carinthia, Gail river at Kötschach-Mauthen town	46.67, 12.98	PP515255
Rhyacophila sp., *tristis* grp.	IT	Lombardia, Valle del Ferro	45.77277, 9.98996	PP515256
Rhyacophila sp., *tristis* grp.	IT	Trentino-Alto Adige/Südtirol, Camposilvano	45.75988, 11.14189	PP515257
Rhyacophila sp., *tristis* grp.	FR	Ruisseau de Chousse, upper tributary; between Arrette & La Pierre Saint-Martin	43.00757, -0.73572	PP515258
R. trescavicensis	ME	Ali-pašini springs	42.54706, 19.83240	PP515246
R. trescavicensis	ME	Ali-pašini springs	42.54706, 19.83240	PP515247
R. trescavicensis	ME	Ali-pašini springs	42.54706, 19.83240	PP515248
R. trescavicensis	ME	Ali-pašini springs	42.54706, 19.83240	PP515249
R. tristis	RO	Hunedoara, Câmpu lui Neag	45.30227, 22.97388	PP515250
R. tristis	RO	Hunedoara, Câmpu lui Neag	45.30227, 22.97388	PP515251
R. tristis	RO	Covasna, Comandău	45.81488, 26.32934	PP515252
R. tristis	RO	Harghita, Voşlăbeni	46.6815, 25.6738	PP515253
R. tristis	RO	Vâlcea, Voineasa, Lotru river	45.463, 23.62	PP515254
R. tsurakiana	AL	river Shushica at the village of Brataj	40.26622, 19.67198	PP515259
R. vranitzensis	BA	Sljeme	43.9403, 18.5122	PP515260
R. vranitzensis	BA	Sljeme	43.9403, 18.5122	PP515261
R. vranitzensis	BA	Sljeme	43.9403, 18.5122	PP515262
R. vranitzensis	BA	Skakavac waterfall	43.94238, 18.44196	PP515263
R. vranitzensis	BA	Skakavac waterfall	43.94238, 18.44196	PP515265

* Country codes in the ISO 3166-1 alpha-2 standard

The maximum likelihood tree was produced using IQ-TREE v.2.1.3 (Minh et al. 2020), using the command *iqtree2 -s RhyacophilaLignumvalleMS_658bp. fasta -B 1000 -bnni -alrt 1000 --prefix RhyacophilaLignumvalleMS_658bp*. The TIM2+F+I+G4 nucleotide substitution model was selected using ModelFinder (Kalyaanamoorthy et al. 2017). Statistical support for the tree topology was assessed with the ultrafast bootstrap approximation (UFboot) (Hoang et al. 2017). Clades with UFboot ≥ 95% are considered well-supported. Additionally, each bootstrap tree was optimized with a hill-climbing nearest neighbor interchange (NNI) search (flag -bnni in the command above) based on the corresponding bootstrap alignment to prevent overestimating UFboot branch support values, as recommended by Hoang et al. (2017).

The consensus tree was visualized and edited in TreeViewer v.2.2.0 (Bianchini and Sánchez-Baracaldo 2024). Additional aesthetic edits were made in Adobe Illustrator CS6.

Holotype mitogenome and nuclear genome assembly

After quality control with FastQC v.0.11.9 (Andrews 2019), raw reads were trimmed for low-quality regions, adapter sequences, and overrepresented *k-mers* using autotrim.pl v.0.6.1 (Waldvogel et al. 2018) and Trimmomatic v.0.39 (Bolger et al. 2014) with the adapter_all.fa of Trimmomatic and the following settings ILLUMINACLIP:2:30:10:8:true, SLIDINGWINDOW:4:20, MINLEN:50, and TOPHRED33. Unpaired reads were discarded and paired reads were checked for contamination using Kraken v.2.0.9 (Wood and Salzberg 2014).

Genome size was estimated using a method based on *k-mer* distribution. For this, *k-mers* were counted with JELLYFISH v.2.3.0 (Marçais and Kingsford 2011) using *jellyfish count -C -s 1000000000 -F 2* and a *k-mer* length of 21 based on the raw sequence reads. A histogram of *k-mer* frequencies was created with *jellyfish histo* and used for analysis with the online web tool GenomeScope v.2.0 (Ranallo-Benavidez et al. 2020) using the following parameters: *k-mer* length = 21, ploidy = 2, max *k-mer* coverage = 10000.

The mitochondrial genomes were first assembled with the raw reads using NOVOplasty v.4.2 (Dierckxsens et al. 2016) using the following parameters: type = mito, genome range = 12000–22000, *k-mer* = 33, max memory = 100, read length = 150, insert size = 300, platform = illumina, paired = PE, insert size auto = yes. The partial sequence of the cytochrome *c* oxidase subunit I (COX1) gene of *Rhyacophila fasciata* Hagen, 1859 (MT559357.1) was used as seed input. All other parameters were kept as default. In addition, we used a second mitogenome assembler MitoZ v.2.3 (Meng et al. 2019). For this purpose, the raw data was subsampled to 10,000,000 reads using seqk and then used as input for *MitoZ assemble* with the following parameters: genetic_code 5, clade Arthropoda, fastq_read_length 150, insert_size 300, run_mode 2, filter_taxa_method 1, requiring_taxa 'Arthropoda'. Annotation of tRNAs, rRNAs, and protein-coding genes was done for the best mitogenome assembly of each species with MitoZ v.2.3 using the module annotate with genetic_code 5 and clade Arthropoda. Both mitogenome assemblies were aligned to the complete mitogenome of *R. quadrifida* Sun & Yang, 1995 (OL678049.1) and *R. kando* Schmid, 1970 (OL678048.1) with MAFFT in Geneious Prime v.2022.1.1 (Biomatters Ltd.) to set the correct start position and manually curate the control-region. The mitochondrial genome assembly was deposited in GenBank under the accession OQ984043.

Nuclear genome assembly was conducted in Spades v.3.14.1 (Bankevich et al. 2012) with the default settings. Scaffolds smaller than 500 bp and those with blast hits to the mitochondrial genome assembly were filtered out. Assembly statistics were calculated with Quast v.5.0.2 (Gurevich et al. 2013) and completeness was assessed via screening for single-copy orthologs with BUSCO v.5.2.2 (Manni et al. 2021) using the endopterygota_odb10 dataset. As an additional quality control, trimmed reads were mapped back to the assembly with bwa-mem v.0.7.17-r1188 (Li 2013) with parameters -a -c 10000, and the back-mapping rate was calculated with qualimap v.2.2.1 (Okonechnikov et al. 2015). To check for potential contamination, taxon-annotated GC-coverage (TAGC) plots were generated with BlobTools v.1.1.1 (Laetsch and Blaxter 2017). For this purpose, the bam file resulting from the back-mapping analysis was converted to a blobtools readable cov file with *blobtools map2cov*. Taxonomic

assignment for BlobTools was conducted with blastn v.2.10.0+ (Camacho et al. 2009) using -task megablast and -e-value 1e-25. The blobDB was created and plotted with the cov file and blast hits. The nuclear draft genome assembly was deposited in GenBank under accession JAPMAE000000000. The DNA barcode region was extracted from the genome assembly and aligned to the traditionally sequenced mtCOI sequences and showed 100% identity to the larvae included by Engelhardt et al. (2011).

Genomic methods were identical for *R. tsurakiana* (see Suppl. material 3).

Morphological examination

The holotype specimen was prepared and examined following standard methods for ethanol-preserved material (Blahnik and Holzenthal 2004; Blahnik et al. 2007). Forewing length was measured from base to apex with a microscale (BioQuip Products, Rancho Dominguez, California, USA).

The abdomen was removed from the specimen, soaked in 85% lactic acid, and heated to 99 °C for 60 min to dissolve internal soft tissues. The macerated tissues were then flushed out of the abdomen with a syringe. The holotype was examined on an Olympus SZX10 stereomicroscope, and pencil sketches of the genitalia were prepared using a Leitz Dialux 20 compound microscope outfitted with a drawing tube. Pencil sketches were scanned and placed in an Adobe Illustrator CS6 document as a template for vector illustrations. Morphological terminology follows Schmid (1970) for the male genitalia, Holzenthal et al. (2007) for wing venation, and Ivanov (1990) for setal warts.

Results

Phylogenetic analysis

After collapsing clades with less than 70% bootstrap support, the species in the *Rhyacophila tristis* group were placed in a polytomy, and sister to *R. italica* (Fig. 2). The first clade of the polytomy includes *R. pubescens*, *R. tsurakiana*, and the new species. The holotype specimen (marked with an asterisk in Fig. 2) was included in a highly supported clade (100% bootstrap support) with three *Rhyacophila* larvae from Corsica. Based solely on larval identification, these were originally considered to be *R. pubescens* (Engelhardt 2009; Engelhardt et al. 2011). It now seems clear that these are larvae of *R. lignumvallis* sp. nov.

The second clade in the polytomy includes several species from the *tristis* subgroup (*R. orghidani* Botosaneanu, 1952, *R. cibinensis* Botosaneanu & Marinkovic-Gospodnetic, 1967, *R. margaritae* Kumanski, 1998, *R. bosnica*, and *R. obtusa* Klapalek, 1894), and two species from the *pubescens* subgroup (*R. pirinica* Kumanski, 1980 and *R. producta* McLachlan, 1879). These specimens were collected in Albania, Austria, Bulgaria, and Romania. The third clade in the polytomy exclusively includes species from the *tristis* subgroup (*R. aquitanica* McLachlan, 1879, *R. carpathica* Botosaneanu, 1995, *R. trescavicensis* Botosaneanu, 1960, *R. tristis* Pictet, 1834, *R. vranitzensis* Botosaneanu & Marinkovic-Gospodnetic, 1967, and *Rhyacophila* sp.). These specimens were collected in Austria, Bosnia and Herzegovina, Bulgaria, France, Italy, Montenegro, Romania, and Spain.

Figure 1. Type locality of *Rhyacophila lignumvallis* sp. nov. on the island of Corsica (France).

Whole genome sequencing and genome characterization of *R. lignumvallis* sp. nov.

Illumina sequencing resulted in 212,866,450 raw reads with a data amount of 31.9 Gbp for *R. lignumvallis* sp. nov. After trimming and contamination filtering, 173,132,236 reads (22.2 Gbp) were kept. The Genomescope2 analysis revealed a genome size of 699,853,381 bp and heterozygosity of 20% (see Suppl. material 2).

The NOVOplasty mitogenome assembly resulted in three contigs (18,087 bp, 1,404 bp, 238 bp) that could not be circularized. Therefore, the 15,623 bp long contig obtained by MitoZ was chosen for annotation. The annotation of the mitogenome revealed all expected 13 protein-coding genes and both rRNAs and 23 tRNAs.

The nuclear genome assembly of *R. lignumvallis* sp. nov. contains 206,802 scaffolds with a total length of 644 Mb, an N50 of 5.6 kb, and a GC of 30%. The BUSCO search with 2,124 Endopterygota orthologs resulted in 82.5% BUSCOs; of these, 47.9% were complete (47.4% single, 0.5% duplicated), and 34.6% were fragmented. 96.3% of the reads were mapped back to the original assembly. Blobtools detected no contamination in the assembly for *R. lignumvallis* sp. nov. (see Suppl. material 2). However, some contamination was detected by NCBI using the improved FCS-GX screen according to https://github.com/ncbi/fcs (see Suppl. material 2).

The genomic characterization of *R. tsurakiana* is included in Suppl. material 3.

Figure 2. Phylogenetic relationships in the *Rhyacophila tristis* group based on the mtCOI barcode region and estimated by maximum likelihood, as implemented in IQ-TREE v.2.1.3 (Minh et al. 2020). Nodal support was calculated using the ultrafast bootstrap (UFboot) approximation (Hoang et al. 2017); nodes with UFboot values greater than 95% are considered well supported. Branches with support values of less than 70% were collapsed. Branch lengths are measured in nucleotide substitutions per site (see scale bar for reference). The branch leading to *Rhyacophila* was shortened (total branch length was 0.12 substitutions per site). Numbers in parentheses correspond to GenBank accession numbers. The holotype and the Corsican larvae are shaded.

Species description

Rhycophila lignumvallis Graf & Rázuri-Gonzales, sp. nov.
https://zoobank.org/5A58EBFA-E945-4032-917A-877444F5DA2B

Holotype. France • ♂; Corsica, bridge over the river Vecchio near the confluence with the river Tavignano; 42.2275°N, 9.24306°E; 195 m a.s.l.; 25 Jul. 2019; col. W. Graf leg.; in ethanol; SMF (SMFTRI00018634).

    Diagnosis. *Rhyacophila lignumvallis* sp. nov. (Figs 4, 5A, B) belongs to the *Rhyacophila tristis* species group (Schmid 1970). It is most similar to *R. pubescens* (Fig. 5C, D), *R. tsurakiana* (Fig. 5E, F), *R. ligurica* Oláh & Vinçon, 2021 (in Oláh et al. 2021, figs 55−57 therein), *R. harmasa* Oláh & Vinçon, 2021 (in Oláh et al. 2021, figs 52−54 therein), and *R. abruzzica* Oláh & Vinçon, 2021(in Oláh et al. 2021, figs 49−51 therein), but *R. lignumvallis* sp. nov. is distinguishable from these species by the shape of tergum X, the dorsal arm of the phallic apparatus in lateral and ventral views, the shape of the aedeagus and parameres, and the second segment of the inferior appendages.

The dorsal surface of segment X is convex in all these species but narrower and higher in the new species, *R. tsurakiana*, and *R. harmasa*. In dorsal view, however, the new species has a slightly membranous, mesally notched, and inflated segment X, while segment X in *R. tsurakiana* appears flatter. Additionally, the dorsal branch of tergum X is rounded and broader in the new species, while it is narrower in *R. tsurakiana* and *R. harmasa*.

The dorsal appendix of the phallic apparatus in the new species is longer than the aedeagus and the parameres (Fig. 4D). This also occurs in *R. harmasa*, *R. ligurica*, *R. pubescens*, and *R. tsurakiana* but not in *R. abruzzica*. However, the shape of the dorsal appendix in lateral view in the new species is digitate and slightly curved dorsad, whereas *R. harmasa* has a slightly wider apical half, *R. ligurica* has a low bump mesally on its dorsal surface, and *R. tsurakiana* has a straight and flat dorsal appendix. In *R. abruzzica*, the dorsal appendage is broad and medially widened in lateral view. In comparison to *R. lignumvallis* sp. nov. (Figs 4D, 5A, B), *R. tsurakiana*, and *R. abruzzica*, the dorsal appendix of the phallic apparatus is much longer and clearly exceeds segment X in dorsal view in *R. harmasa*, *R. pubescens*, and *R. ligurica*. In ventral view, the dorsal appendix is straight and rounded apically in the new species (Fig. 4E), slightly inflated on the apical half and rounded apically in *R. harmasa*, almost straight and truncate apically in *R. ligurica*, constricted basally and truncate apically in *R. tsurakiana*, and rectangular in *R. abruzzica*.

The aedeagus and parameres in *R. lignumvallis* sp. nov. are most similar to *R. pubescens*. However, in lateral view, the tip of the aedeagus in the new species is slenderer and slightly more curved apically than in *R. pubescens*. In lateral view, the parameres in the new species are broader than in *R. pubescens*. In ventral view, the parameres in the new species are club-shaped and curved mesad, while in *R. pubescens*, the parameres are digitate and directed posterad.

The second segment of the inferior appendages in the new species is triangular, with a straight dorsal margin, while all the other species have a concave dorsal margin (Fig. 4A, 5B).

Description. *Adult male.* Specimen in ethanol, mostly denuded; dorsally brown, ventrally light brown. Legs light brown with slightly darker tibial spurs. Head with frontal setal wart triangular; antennal setal wart subtriangular and smaller than frontal setal wart; posterior setal warts oval and connected to ocellar setal warts via a raised cuticular "bridge" (see Schmid, 1970; pl. I, fig. 1). Forewing length (8.8 mm, N = 1) mostly denuded, with sparse, very short light brown setae and golden brown microtrichia. Hind wings also mostly denuded, with slightly longer light brown setae. Forewing (Fig. 3A) with crossveins connecting costal (C) and subcostal (Sc) veins; subcostal (Sc) and first radial (R_1) veins, first (R_1) and second radial (R_2) veins (r), fifth radial (R_5) and first medial (M) veins (r-m), first medial (M) and first cubital (Cu1) veins (m-cu), and first cubital (Cu1) and second cubital (Cu2) veins. Hind wing (Fig. 3B) with crossveins connecting subcostal (Sc) and first radial (R_1) veins, fifth radial (R_5) and first medial (M) veins (r-m), and M_{3+4} and first cubital (Cu1) present.

Male genitalia. Segment IX longitudinally short in lateral view (Fig. 4A), anterior and posterior margins slightly concave, dorsal half slightly longer than ventral. Dorsal surface of segment X membranous, slightly inflated, shallowly notched mesally in dorsal view (Fig. 4C). Dorsal branch of segment X short and rounded in lateral view. Anal sclerites partially fused to each other basally and to segment X, in lateral view, directed ventrad. First article of inferior appendages (Fig. 4A) rect-
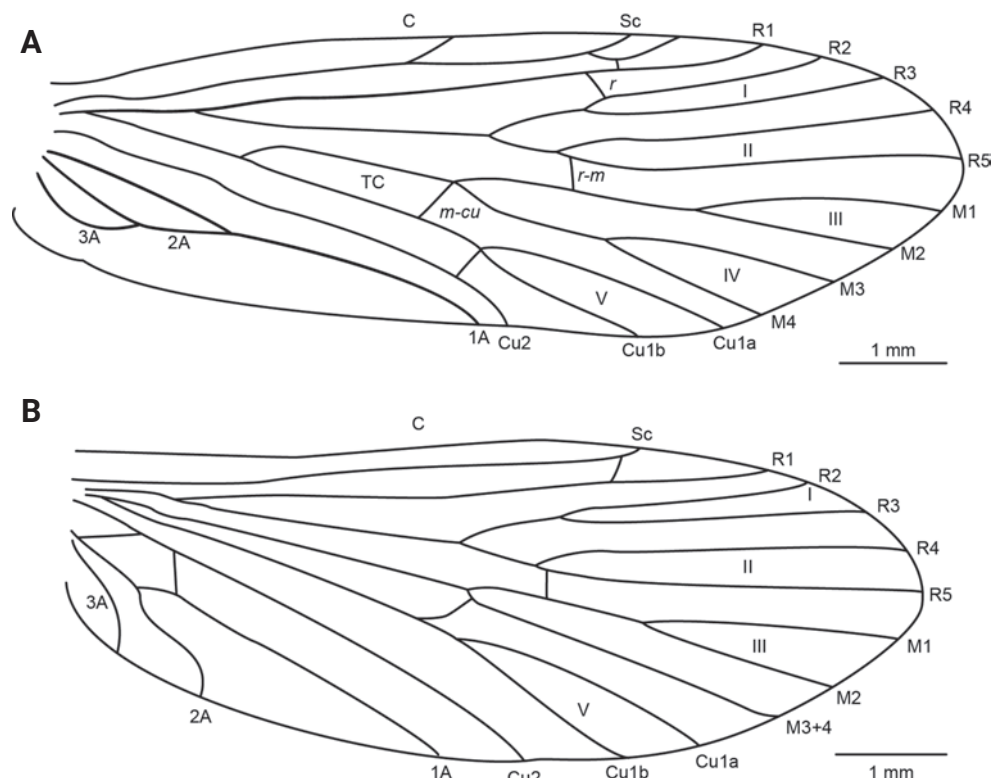
Figure 3. *Rhyacophila lignumvallis* sp. nov., wing venation. **C**, costal vein; **Sc**, subcostal vein; **R1–R5**, first to fifth branches of the radial vein; **M1–M4**, first to fourth branches of the medial vein; **M3+4**, medial vein 3+4 (hindwing); **Cu1a**, anterior branch of first cubital vein; **Cu1b**, posterior branch of first cubital vein; **Cu2**, second cubital vein; **1A–3A**, first to third anal veins; **r**, radial crossvein; **r-m**, radiomedial crossvein; **m-cu**, mediocubital crossvein; **I–V**, first to fifth wing forks; **TC**, thyridial cell. Scale bar: 1 mm. Illustrations were produced by Ernesto Rázuri-Gonzales.

angular in lateral view, slightly broader basally than apically; in ventral view (Fig. 4B), slightly broader apically than basally, with a small setose bump basally on mesal surface. Second article of inferior appendages (Fig. 4A) quadrangular in lateral view, dorsal and ventral margins slightly diverging, posterodorsal margin straight, at a 130° angle to dorsal margin; in ventral view (Fig. 4B), mitton-shaped, mesal margin with very short, peg-like setae basally and longer setae apically. Phallic apparatus (Fig. 4D) with dorsal appendix straight in lateral view, slightly curved dorsad, rounded apically, longer than parameres and aedeagus; in ventral view, straight, lateral margins slightly sinuous, rounded apically. Parameres in lateral view (Fig. 4D) broader than aedeagus, slightly curved posterodorsad, ventral margin straight, dorsal margin slightly sinuous, rounded apically; in ventral view (Fig. 4E), club-shaped, directed mesad. Aedeagus in lateral view (Fig. 4D) slender, slightly sinuous, tapering towards its apex; in ventral view, slender and straight.

Etymology. We dedicate this species to Dr Ralph W. Holzenthal to honor his contributions to caddisfly taxonomy and systematics. *Lignumvallis*, wood valley, is derived from the Latin translation of Ralph's last name.

Habitat. The river Vecchio is a crystal-clear, slow-flowing stream with a heterogeneous bottom substrate that varies from sandy patches to gravel to boulders. Stabile substrates were densely covered by *Agapetus cyrnensis* pupae. As many spring trickles enter the river on its left margin and the specimen was collected by sweeping the vegetation, the habitat of *R. lignumvallis* sp. nov. remains unknown.
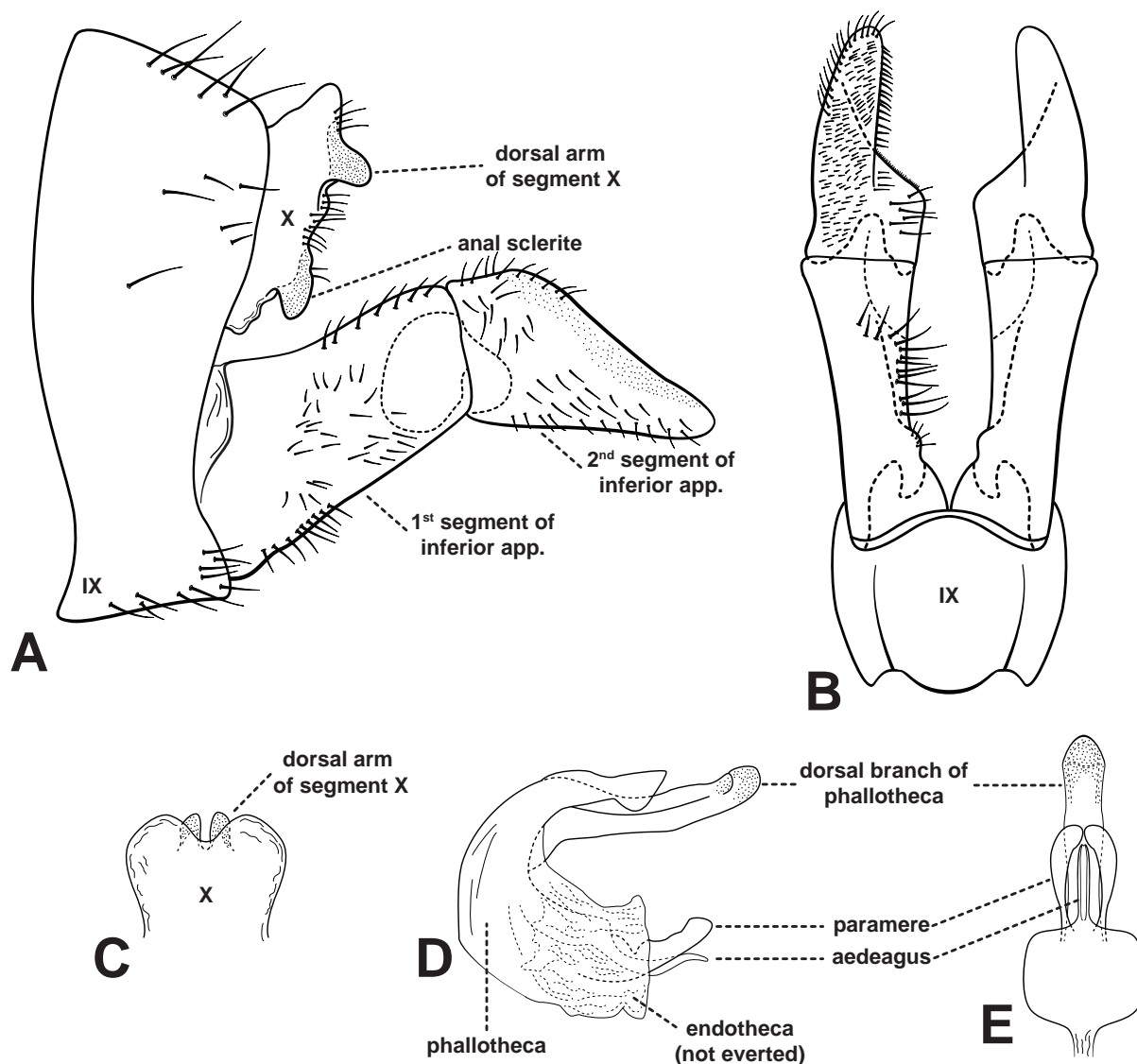
Figure 4. *Rhyacophila lignumvallis* sp. nov., male genitalia, lateral view (**A**), ventral view (**B**), segment X in dorsal view (**C**), phallic apparatus in lateral view (**D**), and phallic apparatus in ventral view (**E**). Illustrations were produced by Ernesto Rázuri-Gonzales.

Discussion

Despite being one of the most well-known faunas in the world, on average more than 770 new animal species are described from Europe each year (Fontaine et al. 2012), with many taxonomic groups not yet reaching a plateau (e.g., Mateos et al. 2017). This trend is particularly pronounced among endemic species, with conservative estimates suggesting that up to one-fifth of endemic taxa from Europe have not yet been described (Essl et al. 2013). Many of these narrowly distributed species are characterized by inhabiting very small, isolated habitats and generally having small populations, making them especially vulnerable to environmental changes (Hering et al. 2009; Essl et al. 2013). This vulnerability is augmented in species occurring at higher elevations that may be subject to "summit trap effects" (Bálint et al. 2011; Domisch et al. 2011; Sauer et al. 2011; Taubmann et al. 2011). Discovering and potentially safeguarding these species prior to their extirpation should be a priority in conservation efforts.
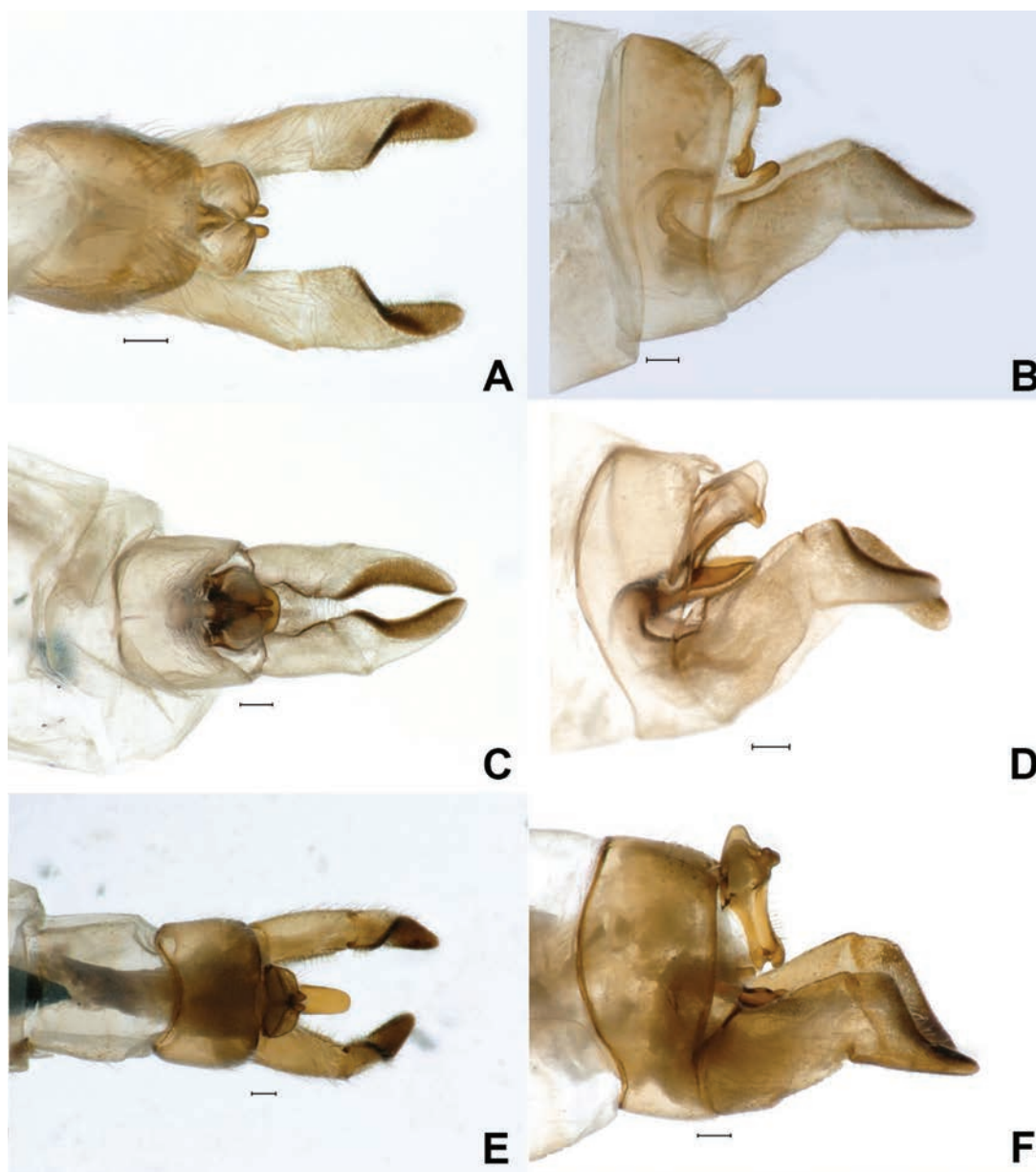
Figure 5. *Rhyacophila lignumvallis* sp. nov., male genitalia, dorsal view (**A**), lateral view (**B**). *R. pubescens*, male genitalia, dorsal view (**C**), lateral view (**D**). *R. tsurakiana*, male genitalia, dorsal view (**E**), lateral view (**F**). Scale bars: 100 µm. Specimens were photographed by W. Graf.

In the case of caddisflies, southern Europe (e.g., Spain, Italy, and the Balkan Peninsula), mountainous regions (e.g., the Alps and the Pyrenees), and the Caucasus have been shown to be particularly species-rich and centers of endemism (Pauls et al. 2006; Previšić et al. 2014; Graf et al. 2015; Schmidt-Kloiber et al. 2017). Although caddisflies are well-studied in most of Europe, further studies in these highly diverse areas are necessary to better understand their richness in this continent and will likely yield many more new species.

The *Rhyacophila tristis* group now includes 29 species distributed throughout central-southern Europe and Western Asia, with many of them occurring in biodiversity centers in these regions (e.g., southern Europe and the Balkans, Suppl. material 1). Additionally, many species in this group are only known from

a single locality, a single or very few specimens, or with unknown females/immature stages. For example, the single adult specimen of *R. lignumvallis* sp. nov. was associated with larval specimens from Corsica, previously identified as *R. pubescens* (Engelhardt 2009). Further sampling will clarify the potential presence of *R. pubescens* on the island. This suggests that the taxonomy of this group is far from complete, particularly for juvenile stages.

Aquatic insects have traditionally been neglected in genomic research (Hotaling et al. 2020). Using 40× coverage of short-read sequencing, we were able to obtain a draft nuclear and complete mitogenome assembly for the holotype of *R. lignumvallis* sp. nov. The assembly of the newly described species was 644,010,216 bp in length, which is close to the estimate obtained by Genomescope2. With an N50 of 5.6 Kbp, the genome assembly is less contiguous than previously published *Rhyacophila* genomes (*R. brunnea* Banks, 1911 and *R. evoluta* McLachlan, 1879 in Heckenhauer et al. (2023)). This lower contiguity is probably due to the sequencing technologies used (Oxford Nanopore long-reads followed by polishing with Illumina short-reads for the *R. brunnea* genome assembly vs. Illumina short-reads only for the *R. lignumvallis* sp. nov. genome) and/or sequencing coverage (97× and 116× Illumina filtered reads for the two *R. evoluta* genome assemblies vs. 40× in the new species) (Heckenhauer et al. 2022).

The percentage of BUSCOs recovered in the draft genome assembly was 82.5%. Of these, 47.9% were complete and 34.6% were fragmented. Meanwhile, the previously generated *Rhyacophila* genomes had a complete BUSCO score of 95.4% for *R. brunnea* (only 2.5% fragmented) and 74.1/75.1% for two *R. evoluta* specimens (17.9/18.7% fragmented) (Heckenhauer et al. 2022). The discrepancy in the amount of complete and fragmented BUSCOs among these congeners is probably due to the reasons outlined for the contiguity.

Genome assembly quality can be assessed using various metrics, such as contiguity and BUSCO completeness (Gurevich et al. 2013; Heckenhauer et al. 2022). Clearly, this genomic characterization is far from a reference genome quality, but nevertheless permanently connects the species name, the underlying morphology as preserved in the type specimen with the genetic make-up of the most representative specimen of the species (e.g., Hebert and Gregory 2005; Padial and de la Riva 2007; Pohl et al. 2012; Egan et al. 2017; Heckenhauer et al. 2023). This information is valuable for studying the systematics and evolution of the species in question as described in Heckenhauer et al. (2023). Additionally, the complete mitogenome includes the DNA barcode, which has already become important to species descriptions and can be used to monitor the occurrence of this species in freshwater bodies.

Acknowledgments

Additional information

Conflict of interest

The authors have declared that no competing interests exist.

Ethical statement

No ethical statement was reported.

Funding

Author contributions

ER: investigation, data curation, formal analysis, writing – original draft, writing – review and editing, visualization. WG: investigation, writing – original draft, writing – review and editing, visualization. JH: data curation, formal analysis, writing – original draft, writing – review and editing. JS: investigation, writing – original draft, writing – review and editing. SUP: study design, data curation, investigation, writing – original draft, writing – review and editing.

Author ORCIDs

Ernesto Rázuri-Gonzales https://orcid.org/0000-0002-7554-0816
Wolfram Graf https://orcid.org/0000-0001-6559-0644
Jacqueline Heckenhauer https://orcid.org/0000-0001-8771-9154
Julio V. Schneider https://orcid.org/0000-0002-9823-6569
Steffen U. Pauls https://orcid.org/0000-0002-6451-3425

Data availability

All of the data that support the findings of this study are available in the main text or Supplementary Information.

References

Andrews S (2019) FastQC: a quality control tool for high throughput sequence data. v. 0.11.9, http://www.bioinformatics.babraham.ac.uk/projects/fastqc/

Bálint M, Domisch S, Engelhardt CHM, Haase P, Lehrian S, Sauer J, Theissinger K, Pauls SU, Nowak C (2011) Cryptic biodiversity loss linked to global climate change. Nature Climate Change 1: 313–318. https://doi.org/10.1038/nclimate1191

Bankevich A, Nurk S, Antipov D, Gurevich AA, Dvorkin M, Kulikov AS, Lesin VM, Nikolenko SI, Pham S, Prjibelski AD, Pyshkin AV, Sirotkin AV, Vyahhi N, Tesler G, Alekseyev MA, Pevzner PA (2012) SPAdes: A New Genome Assembly Algorithm and Its Applications to Single-Cell Sequencing. Journal of Computational Biology 19: 455–477. https://doi.org/10.1089/cmb.2012.0021

Banks N (1911) Description of new species of North American neuropteroid insects. Transactions of the American Entomological Society 37: 335–360, plates 311–313.

Bianchini G, Sánchez-Baracaldo P (2024) TreeViewer: Flexible, modular software to visualise and manipulate phylogenetic trees. Ecology and Evolution 14: e10873. https://doi.org/10.1002/ece3.10873

Blahnik RJ, Holzenthal RW (2004) Collection and curation of Trichoptera, with an emphasis on pinned material. Nectopsyche, Neotropical Trichoptera Newsletter 1: 8–20. http://hdl.handle.net/11299/190744

Blahnik RJ, Holzenthal RW, Prather AL (2007) The lactic acid method for clearing Trichoptera genitalia. In: Bueno-Soria J, Barba-Álvarez R, Armitage BJ (Eds) Proceedings of the 12th International Symposium on Trichoptera. The Caddis Press, Columbus, Ohio, 9–14.

Bolger AM, Lohse M, Usadel B (2014) Trimmomatic: a flexible trimmer for Illumina sequence data. Bioinformatics 30: 2114–2120. https://doi.org/10.1093/bioinformatics/btu170

Botosaneanu L (1952) *Rhyacophila orghidani* n. sp. (Trichoptera Rhyacophilinae) din Muntii Apuseni ai Republicii Populare Române. Comunicările Academiei Republicii Populare Române 2: 721–724.

Botosaneanu L (1960) Trichoptères de Yougoslavie recueillis en 1955 par le Dr. F. Schmid. Deutsche Entomologische Zeitschrift 7: 261–293 https://doi.org/10.1002/mmnd.19600070304

Botosaneanu L (1995) Additional documents to the knowledge of the Trichoptera of Romania, with data on European taxa from outside this country (Insecta: Trichoptera). Faunistische Abhandlungen Staatliches Museum für Tierkunde Dresden 20: 57–88.

Botosaneanu L, Marinkovic-Gospodnetic M (1967) Sur quelques *Rhyacophila* du groupe de *tristis* (Trichoptera). Annales de la Société Entomologique de France (NS) 3: 1145–1151.

Camacho C, Coulouris G, Avagyan V, Ma N, Papadopoulos J, Bealer K, Madden TL (2009) BLAST+: architecture and applications. BMC Bioinformatics 10: 421. https://doi.org/10.1186/1471-2105-10-421

Coppa G, Graf W, Tachet H (2012) A revised description of the larvae of three species of the *Rhyacophila tristis* group: *Rhyacophila aquitanica*, *Rhyacophila pubescens* and *Rhyacophila tristis* (Trichoptera: Rhyacophilidae). Annales de Limnologie 48: 215–223. https://doi.org/10.1051/limn/2012014

Dierckxsens N, Mardulyn P, Smits G (2016) NOVOPlasty: de novo assembly of organelle genomes from whole genome data. Nucleic Acids Research 45: e18. https://doi.org/10.1093/nar/gkw955

Döhler W (1950) Zur Kenntnis der Gattung *Rhyacophila* im mitteleuropaischen Raum (Trichoptera). Archiv für Hydrobiologie 44: 271–293.

Domisch S, Jähnig SC, Haase P (2011) Climate-change winners and losers: stream macroinvertebrates of a submontane region in Central Europe. Freshwater Biology 56: 2009–2020. https://doi.org/10.1111/j.1365-2427.2011.02631.x

Egan SP, Weinersmith KL, Liu S, Ridenbaugh RD, Zhang YM, Forbes AA (2017) Description of a new species of Euderus Haliday from the southeastern United States (Hymenoptera, Chalcidoidea, Eulophidae): the crypt-keeper wasp. ZooKeys 645: 37–49. https://doi.org/10.3897/zookeys.645.11117

Engelhardt C (2009) Phylogeny and phylogeography of the caddisfly *Rhyacophila pubescens*, PICTET 1834, (Trichoptera), with special consideration of its habitat specificity. PhD Thesis, Universität Duisburg-Essen, Essen, 120 pp.

Engelhardt CHM, Haase P, Pauls SU (2011) From the Western Alps across Central Europe: postglacial recolonisation of the tufa stream specialist *Rhyacophila pubescens* (Insecta, Trichoptera). Frontiers in Zoology 8: 10 [14 pp]. https://doi.org/10.1186/1742-9994-8-10

Essl F, Rabitsch W, Dullinger S, Moser D, Milasowszky N (2013) How well do we know species richness in a well-known continent? Temporal patterns of endemic and widespread species descriptions in the European fauna. Global Ecology and Biogeography 22: 29–39. https://doi.org/10.1111/j.1466-8238.2012.00787.x

Fontaine B, van Achterberg K, Alonso-Zarazaga MA, Araujo R, Asche M, Aspöck H, Aspöck U, Audisio P, Aukema B, Bailly N, Balsamo M, Bank RA, Belfiore C, Bogdanowicz W, Boxshall G, Burckhardt D, Chylarecki P, Deharveng L, Dubois A, Enghoff H, Fochetti R, Fontaine C, Gargominy O, Lopez MSG, Goujet D, Harvey MS, Heller K-G, van Helsdingen P, Hoch H, De Jong Y, Karsholt O, Los W, Magowski W, Massard JA, McInnes SJ, Mendes LF, Mey E, Michelsen V, Minelli A, Nafrıa JMN, van Nieukerken EJ, Pape T, De Prins W, Ramos M, Ricci C, Roselaar C, Rota E, Segers H, Timm T, van Tol J, Bouchet P (2012) New species in the old world: Europe as a frontier in biodiversity exploration, a test bed for 21st century taxonomy. PLOS ONE 7: e36881. https://doi.org/10.1371/journal.pone.0036881

Graf W, Vitecek S, Previsic A, Malicky H (2015) New species of Limnephilidae (Insecta: Trichoptera) from Europe: Alps and Pyrenees as harbours of unknown biodiversity. Zootaxa 3911: 381–395. https://doi.org/10.11646/zootaxa.3911.3.5

Gurevich A, Saveliev V, Vyahhi N, Tesler G (2013) QUAST: quality assessment tool for genome assemblies. Bioinformatics 29: 1072–1075. https://doi.org/10.1093/bioinformatics/btt086

Hagen HA (1859) Die Phryganiden Pictet's nach typen bearbeitet (continued in 1860 and 1861). Stettiner Entomologische Zeitung 20: 131–170.

Hebert PDN, Gregory TR (2005) The Promise of DNA Barcoding for Taxonomy. Systematic Biology 54: 852–859. https://doi.org/10.1080/10635150500354886

Heckenhauer J, Frandsen PB, Sproul JS, Li Z, Paule J, Larracuente AM, Maughan PJ, Barker MS, Schneider JV, Stewart RJ, Pauls SU (2022) Genome size evolution in the diverse insect order Trichoptera. GigaScience 11. https://doi.org/10.1093/gigascience/giac011

Heckenhauer J, Rázuri-Gonzales E, Mwangi FN, Schneider J, Pauls SU (2023) Holotype sequencing of *Silvatares holzenthali* Rázuri-Gonzales, Ngera & Pauls, 2022 (Trichoptera, Pisuliidae). ZooKeys 1159. https://doi.org/10.3897/zookeys.1159.98439

Hering D, Schmidt-Kloiber A, Murphy J, Lücke S, Zamora-Muñoz C, López-Rodríguez MJ, Huber T, Graf W (2009) Potential impact of climate change on aquatic insects: a sensitivity analysis for European caddisflies (Trichoptera) based on distribution patterns and ecological preferences. Aquatic Sciences 71: 3–14. https://doi.org/10.1007/s00027-009-9159-5

Hoang DT, Chernomor O, von Haeseler A, Minh BQ, Vinh LS (2017) UFBoot2: Improving the Ultrafast Bootstrap Approximation. Molecular Biology and Evolution 35: 518–522. https://doi.org/10.1093/molbev/msx281

Holzenthal RW, Blahnik RJ, Prather AL, Kjer KM (2007) Order Trichoptera Kirby, 1813 (Insecta), caddisflies. Zootaxa 1668: 639–698. https://doi.org/10.11646/zootaxa.1668.1.29

Hotaling S, Kelley JL, Frandsen PB (2020) Aquatic Insects Are Dramatically Underrepresented in Genomic Research. Insects 11: 601. https://doi.org/10.3390/insects11090601

Hwang C-L (1958) Descriptions of Chinese caddis flies (Trichoptera). Acta Entomologica Sinica 10: 279–285.

Ivanov VD (1990) Structure and function of setose warts of caddisflies [in Russian]. Latvijas Entomologs 33: 96–110.

Kalyaanamoorthy S, Minh BQ, Wong TKF, von Haeseler A, Jermiin LS (2017) ModelFinder: fast model selection for accurate phylogenetic estimates. Nature Methods 14: 587–589. https://doi.org/10.1038/nmeth.4285

Klapálek F (1894) Descriptions of new species of *Raphidia*, L., and of three new species of Trichoptera from the Balkan Peninsula, with critical remarks on *Panorpa gibberosa*, McLachlan. Transactions of the Entomological Society of London 1894: 489, 495. https://doi.org/10.1111/j.1365-2311.1894.tb02097.x

Kumanski KP (1980) Description of three new caddis-flies (Trichoptera) from Bulgaria. Rivista di Idrobiologia 19: 197–206.

Kumanski KP (1998) *Rhyacophila margaritae* – a new insect species (Trichoptera: Rhyacophilidae) from Bulgaria. Dokladi na Bulgarskata Akademiya na Naukite 51: 59–62.

Laetsch DR, Blaxter ML (2017) BlobTools: Interrogation of genome assemblies. F1000Research 6. https://doi.org/10.12688/f1000research.12232.1

Li H (2013) Aligning sequence reads, clone sequences and assembly contigs with BWA-MEM. arXiv [q-Bio.GN]. https://doi.org/10.48550/arXiv.1303.3997

Malicky H (1984) Fünf neue griechische Köcherfliegen (Trichoptera). Mitteilungen der Entomologischen Gesellschaft Basel 34: 96–102.

Manni M, Berkeley MR, Seppey M, Zdobnov EM (2021) BUSCO: Assessing Genomic Data Quality and Beyond. Current Protocols 1: e323. https://doi.org/10.1002/cpz1.323

Marçais G, Kingsford C (2011) A fast, lock-free approach for efficient parallel counting of occurrences of k-mers. Bioinformatics 27: 764–770. https://doi.org/10.1093/bioinformatics/btr011

Mateos E, Sluys R, Riutort M, Álvarez-Presas M (2017) Species richness in the genus *Microplana* (Platyhelminthes, Tricladida, Microplaninae) in Europe: as yet no asymptote in sight. Invertebrate Systematics 31: 269–301. https://doi.org/10.1071/IS16038

McLachlan R (1879) A monographic revision and synopsis of the Trichoptera of the European fauna. Part 8. John van Voorst, London, 429–500, plates 445–451 pp.

Meng G, Li Y, Yang C, Liu S (2019) MitoZ: a toolkit for animal mitochondrial genome assembly, annotation and visualization. Nucleic Acids Research 47: e63. https://doi.org/10.1093/nar/gkz173

Minh BQ, Schmidt HA, Chernomor O, Schrempf D, Woodhams MD, von Haeseler A, Lanfear R (2020) IQ-TREE 2: New Models and Efficient Methods for Phylogenetic Inference in the Genomic Era. Molecular Biology and Evolution 37: 1530–1534. https://doi.org/10.1093/molbev/msaa015

Moretti GP (1981) New Trichoptera species and subspecies found in Italy. In: Moretti GP (Ed.) Proceedings of the 3rd International Symposium on Trichoptera. Dr. W. Junk, The Hague, 165–192. https://doi.org/10.1007/978-94-009-8641-1_22

Mosely ME (1930) Corsican Trichoptera. Eos – Revista Española Entomología 6: 147–184.

Mosely ME (1932) Corsican Trichoptera and Neuroptera (s. l.). Eos – Revista Española de Entomología 8: 165–184.

Nelson LA, Wallman JF, Dowton M (2007) Using COI barcodes to identify forensically and medically important blowflies. Medical and Veterinary Entomology 21: 44–52. https://doi.org/10.1111/j.1365-2915.2007.00664.x

Okonechnikov K, Conesa A, García-Alcalde F (2016) Qualimap 2: advanced multi-sample quality control for high-throughput sequencing data. Bioinformatics 32: 292–294. https://doi.org/10.1093/bioinformatics/btv566

Oláh J, Vinçon G, Coppa G (2021) On the Trichoptera of Italy with delineation of incipient sibling species. Opuscula Zoologica (Budapest) 52: 03–67. https://doi.org/10.18348/opzool.2021.1.3

Oláh J, Beshkov S, Ibrahimi H, Kovács T, Oláh Jr J, Vinçon G (2022) On the Trichoptera of the Balkan: survey of species complexes of *Polycentropus ierapetra*, *Rhyacophila balcanica*, *R. bosnica* and *Notidobia nekibe*. Opuscula Zoologica (Budapest) 53: 67–111. https://doi.org/10.18348/opzool.2022.1.67

Padial JM, de la Riva I (2007) Integrative taxonomists should use and produce DNA barcodes. Zootaxa 1586: 67–68. https://doi.org/10.11646/zootaxa.1586.1.7

Pauls SU, Lumbsch HT, Haase P (2006) Phylogeography of the montane caddisfly *Drusus discolor*: evidence for multiple refugia and periglacial survival. Molecular Ecology 15: 2153–2169. https://doi.org/10.1111/j.1365-294X.2006.02916.x

Pictet FJ (1834) Recherches pour servir à l'histoire et l'anatomie des Phryganides. A. Cherbuliez, Geneva, plates 1–20 + 235 [220 plates]. https://doi.org/10.5962/bhl.title.8547

Pohl H, Niehuis O, Gloyna K, Misof B, Beutel R (2012) A new species of *Mengenilla* (Insecta, Strepsiptera) from Tunisia. ZooKeys 198: 79–102. https://doi.org/10.3897/zookeys.198.2334

Previšić A, Graf W, Vitecek S, Kučinić M, Bálint M, Keresztes L, Pauls SU, Waringer J (2014) Cryptic diversity of caddisflies in the Balkans: the curious case of *Ecclisopteryx* species (Trichoptera: Limnephilidae). Arthropod Systematics and Phylogeny 72: 309–329. https://doi.org/10.3897/asp.72.e31792

Ranallo-Benavidez TR, Jaron KS, Schatz MC (2020) GenomeScope 2.0 and Smudgeplot for reference-free profiling of polyploid genomes. Nature Communications 11: 1432. https://doi.org/10.1038/s41467-020-14998-3

Rohland N, Reich D (2012) Cost-effective, high-throughput DNA sequencing libraries for multiplexed target capture. Genome Research 22: 939–946. https://doi.org/10.1101/gr.128124.111

Ross HH (1956) Evolution and Classification of the Mountain Caddisflies. University of Illinois Press, Urbana, 213 pp.

Sauer J, Domisch S, Nowak C, Haase P (2011) Low mountain ranges: summit traps for montane freshwater species under climate change. Biodiversity and Conservation 20: 3133–3146. https://doi.org/10.1007/s10531-011-0140-y

Schmid F (1970) Le genre *Rhyacophila* et la famille des Rhyacophilidae (Trichoptera). Memoires de la Société Entomologique du Canada 66: 1–230. https://doi.org/10.4039/entm10266fv

Schmidt-Kloiber A, Neu PJ, Malicky M, Pletterbauer F, Malicky H, Graf W (2017) Aquatic biodiversity in Europe: a unique dataset on the distribution of Trichoptera species with important implications for conservation. Hydrobiologia 797: 11–27. https://doi.org/10.1007/s10750-017-3116-4

Sun C-H, Yang L-F (1995) Studies on the genus *Rhyacophila* (Trichoptera) in China (1). Braueria 22: 27–32.

Taubmann J, Theissinger K, Feldheim KA, Laube I, Graf W, Haase P, Johannesen J, Pauls SU (2011) Modelling range shifts and assessing genetic diversity distribution of the montane aquatic mayfly Ameletus inopinatus in Europe under climate change scenarios. Conservation Genetics 12: 503–515. https://doi.org/10.1007/s10592-010-0157-x

Ulmer G (1927) Einige neue Trichopteren aus Asien. Entomologische Mitteilungen, Deutsche Entomologische Museum 16: 172–182.

Valladolid M, Waringer J, Arauzo M, Chvojka P, Dorda BA, Komzák P, Lodovici O, Rey I (2023) The *Rhyacophila fasciata* Species Complex (Trichoptera: Rhyacophilidae) in Central Europe with description of a new species, *Rhyacophila loeffleri* Valladolid & Waringer, n. sp., based on morphological, genetic and ecological evidence. Zootaxa 5325: 451–482. https://doi.org/10.11646/zootaxa.5325.4.1

Waldvogel A-M, Wieser A, Schell T, Patel S, Schmidt H, Hankeln T, Feldmeyer B, Pfenninger M (2018) The genomic footprint of climate adaptation in *Chironomus riparius*. Molecular Ecology 27: 1439–1456. https://doi.org/10.1111/mec.14543

Wood DE, Salzberg SL (2014) Kraken: ultrafast metagenomic sequence classification using exact alignments. Genome Biology 15: R46. https://doi.org/10.1186/gb-2014-15-3-r46

Supplementary material 1

Blobtools graphs for the *Rhyacophila lignumvalle* sp. nov. assembly

Authors: Ernesto Rázuri-Gonzales, Wolfram Graf, Jacqueline Heckenhauer, Julio V. Schneider, Steffen U. Pauls

Data type: docx

Link: https://doi.org/10.3897/zookeys.1218.132275.suppl1

Supplementary material 2

Genomic methods and characterization for the *Rhyacophila tsurakiana* genome assembly

Authors: Ernesto Rázuri-Gonzales, Wolfram Graf, Jacqueline Heckenhauer, Julio V. Schneider, Steffen U. Pauls

Data type: docx

Link: https://doi.org/10.3897/zookeys.1218.132275.suppl2

Supplementary material 3

Geographic distribution of species in the *Rhyacophila tristis* species group

Authors: Ernesto Rázuri-Gonzales, Wolfram Graf, Jacqueline Heckenhauer, Julio V. Schneider, Steffen U. Pauls

Data type: docx

Explanation note: This list includes the geographic distribution of the 25 currently known species in the *Rhyacophila tristis* species group based on literature records. We only include papers with geographic data.

Link: https://doi.org/10.3897/zookeys.1218.132275.suppl3

ZooKeys

Research Article

A Taxonomic Odyssey: An annotated checklist of *Peromyscus* (Cricetidae, Rodentia) in Honduras

Celeste M. López[1,2], Manfredo A. Turcios-Casco[1,2], Eric van den Berghe[3], Nicté Ordóñez-Garza[4,5], Martin R. Alvarez[1]

1 Programa de Pós-Graduação em Zoologia, Departamento de Ciências Biológicas, Universidade Estadual de Santa Cruz, Ilhéus, BA, Brazil
2 Asociación para la Sostenibilidad e Investigación Científica en Honduras (ASICH), Francisco Morazán, Honduras
3 Centro Zamorano de Biodiversidad, apartado 93, Ambiente y Desarrollo, Escuela Agrícola Panamericana, Francisco Morazán, Honduras
4 Department of Ecology and Evolutionary Biology, University of Michigan, Ann Arbor, USA
5 Michigan Pathogen Biorepository, University of Michigan, Ann Arbor, USA
Corresponding author: Celeste M. López (cmlopez.ppgzoo@uesc.br)

OPEN ACCESS

Abstract

Deer mice, *Peromyscus*, thrive in diverse environments and altitudes across North and Central America. The number of extant species continues to be debated with species counts ranging from 53 to 83. This study represents the first comprehensive historical and taxonomic account of the genus *Peromyscus* for Honduras. We systematically compiled records from all available sources, incorporating verified genetic and morphological evidence. We confirm the presence of *P. beatae*, *P. cordillerae*, *P. nicaraguae*, *P. salvadorensis* and *P. stirtoni* for Honduras. The distribution maps provided here include confirmed records and approximate localities in a few cases and offer insights into the geographical distribution of these species in Honduras. Conducting a comprehensive assessment of the taxonomic status of *Peromyscus* in Honduras is imperative to achieve accurate conservation assessments within the larger Mesoamerican landscape. The present review establishes the baseline for future research on deer mice in Honduras, aiding in the validation of distributions and ecological data for the poorly understood genus *Peromyscus* in the country.

Key words: Central America, Deer mice, geographical distribution, historical review, systematics, taxonomy

Introduction

Deer mice, family Cricetidae Fischer, 1817, subfamily Neotominae Merriam, 1894 (Pardiñas et al. 2017), genus *Peromyscus* Gloger, 1841 defined by Platt et al. (2015), are a diverse group. According to Dawson (2005), deer mice underwent significant diversification during the Pleistocene, and they are currently distributed from Alaska to Panamá (Hall 1981; Bradley et al. 2016; Pérez-Consuegra and Vázquez-Domínguez 2016). *Peromyscus* thrive in diverse habitats, encompassing deserts and rain forests in both temperate and tropical climates (Tiemann-Boege et al. 2000) from sea level to 4300 meters above sea level (Bedford and Hoekstra 2015).

The high rate of diversification has posed a challenge in clarifying the taxonomic relationships within this genus and has generated ongoing controversy regarding the number of *Peromyscus* species (Osgood 1909; Carleton 1989; Bradley et al. 2007; Miller and Engstrom 2008; Pérez-Consuegra and Vázquez-Domínguez 2015). Hooper and Musser (1964) initially proposed 59 species within the genus *Peromyscus*. Subsequently, Hooper (1968) reduced the count to 57 species, upheld by Carleton (1989) and Musser and Carleton (1993). However, Musser and Carleton (2005) reduced the count to 56 species. Later, Platt et al. (2015), confirmed 53 species based on genetic analysis. Pardiñas et al. (2017) and Hernández-Canchola et al. (2022) then suggested 66 species. Presently, the Integrated Taxonomic Information System−ITIS (2024) recognizes 58 *Peromyscus* species, in contrast with the 83 species cataloged by the American Society of Mammalogists in their Mammal Diversity Database (ASM 2024).

In the last ten years, we have witnessed a significant shift in our understanding of deer mice taxonomy and systematics based on a series of prominent research studies (e.g., Pérez-Consuegra and Vázquez-Domínguez 2015, 2016; Platt et al. 2015; Bradley et al. 2016, 2017; Álvarez-Castañeda et al. 2019; Kilpatrick et al. 2021; Bradley et al. 2022). These studies have been pivotal in understanding the systematic, taxonomic, and biogeographical diversity within *Peromyscus* in the Mesoamerican region.

In Central America, approximately 15 species of deer mice have been documented (Musser 1969; Bradley et al. 2000; Ordóñez-Garza et al. 2010; Trujano-Álvarez and Álvarez-Castañeda, 2010; Lorenzo et al. 2016; Matson et al. 2016; Pérez-Consuegra and Vázquez-Domínguez 2016; Álvarez-Castañeda et al. 2019; Ramírez-Fernández et al. 2023; ASM 2024). However, in most Central American countries, the total number of species has not yet been conclusively determined. This is due to the synonymy of some species (e.g., Kilpatrick et al. 2021). while some subspecies have been elevated to species level (e.g., Pérez-Consuegra and Vázquez-Domínguez 2015). This shifting landscape highlights the taxonomic complexity within this genus and underscores the need for ongoing research to achieve a more precise understanding of the number of species in northern Central America, including Honduras. For example, 13 species are recognized in Guatemala (five endemic), four in El Salvador, and three in Nicaragua (ASM 2024). We explored the latest scientific literature and historical revisions of *Peromyscus*, specifically focusing on specimens from Honduras to construct a comprehensive annotated checklist of this genus in Honduras. We relied on specimens housed in museums or that were confirmed by genetic and morphological studies to generate distribution maps.

Materials and methods

Study area

Honduras covers 112,492 km^2 making it the second-largest country in the Central American Isthmus (Hernández Oré et al. 2016). Positioned at the core of Central America, this region is one of the Earth's biodiversity hotspots (Mittermeier et al. 1999), owing to its elevation and climatic diversity.

Geologically, the Honduran territory is part of the Chortís Block (Fig. 1), which includes the western highlands and the central plateau of Chortís (Marshall 2007)
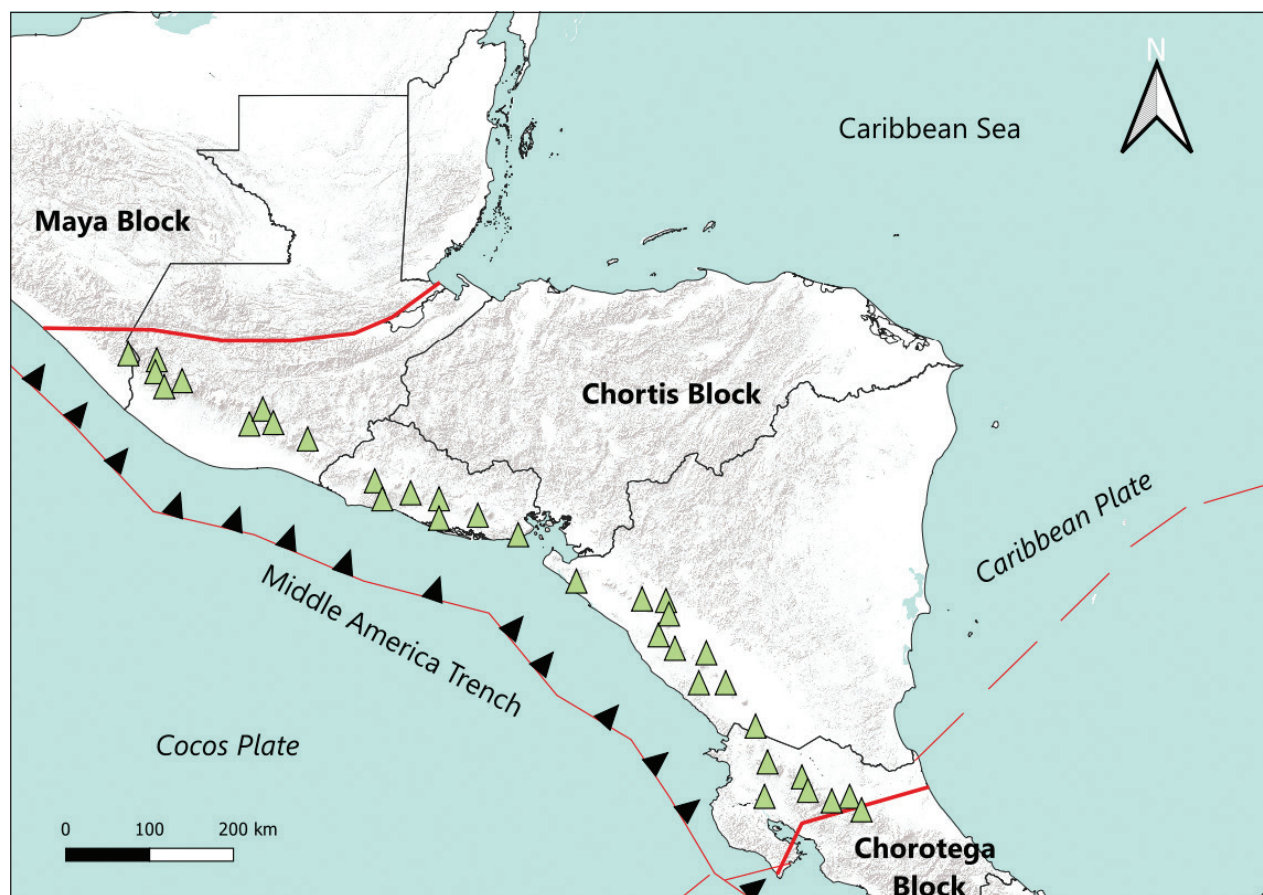
Figure 1. Representation of the Chortís Block within Central America. Adapted from Marshall (2007).

in the Isthmus of Tehuantepec (Dengo 1968). This area is characterized by mountain ranges separated by a discontinuous series of north-trending small rift valleys, featuring late Miocene to Quaternary soils (Burkart and Self 1985; Marshall 2007). The mountainous geography results in notable elevations in various parts of the country with notable peaks that include 2870 m a.s.l. in Celaque National Park to the west, 2454 m a.s.l. in the Nombre de Dios mountain range, and 2435 m a.s.l. in Pico Bonito National Park to the north. In the northwest, in the Santa Barbara Mountain National Park elevations reach 2777 m a.s.l., whereas in the central region they reach 2420 m a.s.l., and in the eastern region, they attain 2351 m a.s.l. (Townsend 2014; Matson et al. 2016). This mountainous topography gradually gives way to the Lowland Province of the Mosquitia Coast (<450 m a.s.l.), characterized by an extensive alluvial plain in the eastern strip of the Caribbean coast (Marshall 2007). The Honduran Pacific coast, featuring the Gulf of Fonseca, is characterized by extensive estuaries, lagoon systems, and mangrove forest in coastal plains, punctuated by volcanoes (Bengtson 1926; Dunbar et al. 2020).

Preserved specimens

We compiled historical records of *Peromyscus* in Honduras using Goodwin (1941, 1942) as a basis, as well as information available on Global Biodiversity Information Facility–GBIF.org (2023) concerning the specimens housed in the museums. This allowed us to gather a broad range of taxonomic and distributional information on *Peromyscus* in Honduras. We also reviewed the

modifications over time in the taxonomic classification of the species of *Peromyscus* living in Honduras (e.g., Hall and Kelson 1959; Musser 1969; Carleton 1989; Bradley et al. 2000, 2007; Ordóñez-Garza et al. 2010; Trujano-Álvarez and Álvarez-Castañeda 2010; Pérez-Consuegra and Vázquez-Domínguez 2015, 2016; Bradley et al. 2016; Matson et al. 2016; Kilpatrick et al. 2021; Bradley et al. 2022; León-Tapia at al. 2022).

Taxonomic accounts

We considered only those species, whose identification has been confirmed by external and cranial morphology and morphometry (Goodwin 1942; Musser 1969; Carleton 1979; Matson et al. 2016). We also reviewed the literature (Hall 1981; Musser and Carleton 2005; Trujano-Álvarez and Álvarez-Castañeda 2010), karyotypic analyses (Bradley and Ensink 1987; Peppers et al. 1999), cytological-taxonomic studies (von Lehmann and Schaefer 1979), as well as biogeography and phylogenetic studies (Sullivan et al. 1997; Bradley et al. 2000; Bradley et al. 2007; Pérez-Consuegra and Vásquez-Domínguez 2015, 2016; Bradley et al. 2016; Kilpatrick et al. 2021). This information is summarized in Tables 1−3.

The GBIF.org dataset (2023) of museum specimens was downloaded for the distributions of *P. beatae* Thomas, 1903 and *P. stirtoni* Dickey, 1928 because these are the only species that had not experienced substantial taxonomic changes; and for *P. stirtoni* we did not present any table because its epithet has not changed since its description (Jones 1990). Citizen science observations (e.g., iNaturalist) were not considered for any species; additionally, we present the elevation ranges as well as the departments and the ecoregions, where their occurrence has been confirmed (see Figs 2−6; Suppl. material 1).

Distribution map

For the creation of the distribution maps, we used QGIS Desktop software version 3.28.11 and included only the records that were confirmed following the previously mentioned criteria. Specimens without locality coordinates were approximated based on the verbatim descriptions (see Figs 2−6; Suppl. material 1). Elevations were also corroborated (see observations in Suppl. material 1). The ecoregions defined by Olson et al. (2001), were presented for each species (see Figs 2−6; Suppl. material 1).

Table 1. Summary of the systematic history and taxonomical arrangements of *P. beatae* in Honduras.

Reference	Taxonomical history of *P. beatae*	Scope of their methodology
Goodwin (1942)	*P. boylii sacarensis* was the only one of *P. boylii* group	External and cranial morphology and morphometry of collected specimens
Hall (1981)	*P. b. sacarensis* was maintained as a subspecies	Based on external and cranial descriptions of museum specimens and marginal records of the distribution
Bradley and Ensink (1987)	Continued to recognize the subspecies *P. b. sacarensis*	Karyotypic analyses
Bradley et al. (2000)	Reassigned *P. b. sacarensis* with *P. beatae*	Analysis of the mitochondrial cytochrome *b* gene in *P. b. sacarensis*
This study	Recognized *P. beatae* as the only species of the *P. boylii* group in Honduras	Bibliographic taxonomic review

Table 2. Summary of the systematic history and taxonomical arrangements of *P. cordillerae* in Honduras.

Reference	Taxonomical history of *P. cordillerae*	Scope of their methodology
Goodwin (1942)	Considered *P. mexicanus saxatilis* and *P. hondurensis* as separate species	External and cranial morphology and morphometry of collected specimens
Musser (1969)	Referred to the specimens previously cited as *P. mexicanus saxatilis* and *P. hondurensis* to be *P. oaxacensis*	External and cranial morphology and morphometry of preserved specimens
von Lehmann and Schaefer (1979)	*P. hondurensis* was still considered a valid species even though it had already been synonymized by previous studies	Cytological-taxonomic studies, including sperm analysis, morphology, and comparative cytochemistry
Carleton (1979)	*P. aztecus oaxacensis* was synonymized with *P. oaxacensis* and *P. hondurensis*	External and cranial morphology and morphometry of preserved specimens.
Hall (1981)	Referred to specimens previously cited as *P. oaxacensis* and *P. hondurensis* to be *P. oaxacensis*	Based on external and cranial descriptions of museum specimens and marginal records of the distribution
Sullivan et al. (1997)	Presented evidence indicating that subspecies *P. a. oaxacensis* in the south and east of the Isthmus of Tehuantepec represents a distinct species	Phylogeography based on phylogenetic analyses of 668 bp of the mitochondrial cytochrome *b* gene
Musser and Carleton (2005)	Continued to recognize the subspecies *P. a. oaxacensis*, emphasizing the need for further scrutiny in the populations mentioned by Sullivan et al. (1997)	Bibliographical review
Matson et al. (2016)	Considered *P. oaxacensis* as the species for Honduras within the *P. aztecus* group*	External and cranial morphology and morphometry of collected specimens
Kilpatrick et al. (2021)	Recognized the subspecies *P. cordillerae hondurensis* for the population in Honduras considered as *P. a. oaxacensis*	Molecular data from the mitochondrial cytochrome *b* gene
This study	Consider *P. cordillerae hondurensis* for all representatives of the *Peromyscus aztecus* group for Honduras including the following synonyms: *P. oaxacensis*, *P. hondurensis*, *P. aztecus*, and *P. a. oaxacensis*	Bibliographic taxonomic review

*Matson et al. (2016) relied on the description by Bradley et al. (2014) for their records in eastern Honduras. However, Bradley et al. (2014) did not utilize specimens from the *P. aztecus* group from Honduras in their comparisons.

Table 3. Summary of the systematic history and taxonomical arrangements of *P. nicaraguae* and *P. salvadorensis* in Honduras.

Reference	Summarized taxonomical history of *P. nicaraguae* and *P. salvadorensis*	Scope of their methodology
Goodwin (1942)	Considered *P. mexicanus saxatilis* and *P. guatemalensis tropicalis* as separate species	External and cranial morphology and morphometry of collected specimens
Musser (1969)	Referred to specimens cited as of *P. guatemalensis tropicalis* to be *P. m. saxatilis*	External and cranial morphology and morphometry of preserved specimens
Hall (1981)	Maintained *P. m. saxatilis* as the species to occur in Honduras	Based on external and cranial descriptions of museum specimens and marginal records of the distribution
Bradley and Ensink (1987)	Supported the recognition of *P. m. saxatilis* for Honduras	Karyotypic analyses
Trujano-Álvarez and Álvarez-Castañeda (2010)	Considered *P. m. saxatilis* to occur in Honduras	Mammalian Species review for *P. mexicanus*
Pérez-Consuegra and Vázquez-Domínguez (2015, 2016)	Resurrected *P. nicaraguae* and *P. salvadorensis* from synonymy with *P. m. saxatilis*	Molecular analyses of the mitochondrial cytochrome *b* gene, phylogenetic studies, and assessments of genetic diversity and lineage differentiation
Bradley et al. (2016)	Reaffirmed *P. nicaraguae* as a valid species in Honduras.	Mitochondrial DNA analysis of the cytochrome *b* gene
Matson et al. (2016)	Supported the designation of *P. nicaraguae* and *P. salvadorensis* as proper species that occurs in Honduras	External and cranial morphology and morphometry of collected specimens
This study	Recognized *P. nicaraguae* as well as two morphotypes of *P. salvadorensis* supporting the hypothesis of Pérez-Consuegra et al. (2015, 2016)	Bibliographic taxonomic review

Museum abbreviations

The museum abbreviations are as follows: **AMNH** = American Museum of Natural History; **CMNH** = Carnegie Museum of Natural History; **TCWC** = Biodiversity Research and Teaching Collections, Texas A&M University; **TTU** = Texas Tech University Museum; **UF** = Florida Museum of Natural History; **USNM** = Smithsonian Institution, National Museum of Natural History; and **UNAH** = Universidad Nacional Autónoma de Honduras.

Results

Based on our examination it seems that five species are present in the territory of Honduras, and 825 specimens of *Peromyscus* are housed in the zoological collections in natural history museums; from the latter, we only considered 254 specimens that were confirmed by recent studies and in accordance with the current taxonomy (see Suppl. material 1). About a third of these museum specimens have been employed in studies to report on this group within the country (see Bradley et al. 2000, 2007, 2016, 2022; Pérez-Consuegra and Vázquez-Domínguez 2015, 2016; Matson et al. 2016).

Species accounts

Based on our review, the species of *Peromyscus* that occur in Honduras are described below.

Rodentia Bowdich, 1821
Myomorpha Brandt, 1855
Muroidea Illiger, 1811
Cricetidae Fischer, 1817
Neotominae Merriam, 1894
***Peromyscus* Gloger, 1841**
***Peromyscus boylii* group**

***Peromyscus beatae* Thomas, 1903**

Distribution. Comayagua, Francisco Morazán, and Lempira departments (Fig. 2).
   Ecoregions and elevation. Central American montane, dry, and pine-oak forests (300–2850 m a.s.l.).
   Comments. The taxonomic classification of the *P. boylii* group has not undergone significant changes. However, Bradley et al. (2000) analyzed the taxonomy of the subspecies *P. boylii sacarensis* Dickey, 1928 using DNA sequences from the mitochondrial cytochrome *b* gene. As a result of this study, it is now considered as *P. beatae* (Bradley et al. 2000, 2017) (Table 1). Thus, specimens previously identified as *P. b. sacarensis* in Honduras should now be recognized as individuals of *P. beatae*. We verified the coordinates provided by Bradley et al. (2000), and the approximate coordinates corresponding to "2 mi NE El Hatillo" and "10 mi SE Tegucigalpa" and found them to be incorrectly attributed to the Olancho Department; these specimens belong to the department of Francisco Morazán. Cassola (2016) suggested the occurrence of *P. beatae* in other regions in western Honduras, but no tangible evidence corroborates this speculation.

***Peromyscus aztecus* group**

***Peromyscus cordillerae* Dickey, 1928**

Distribution. Lempira and La Paz departments (Fig. 3).
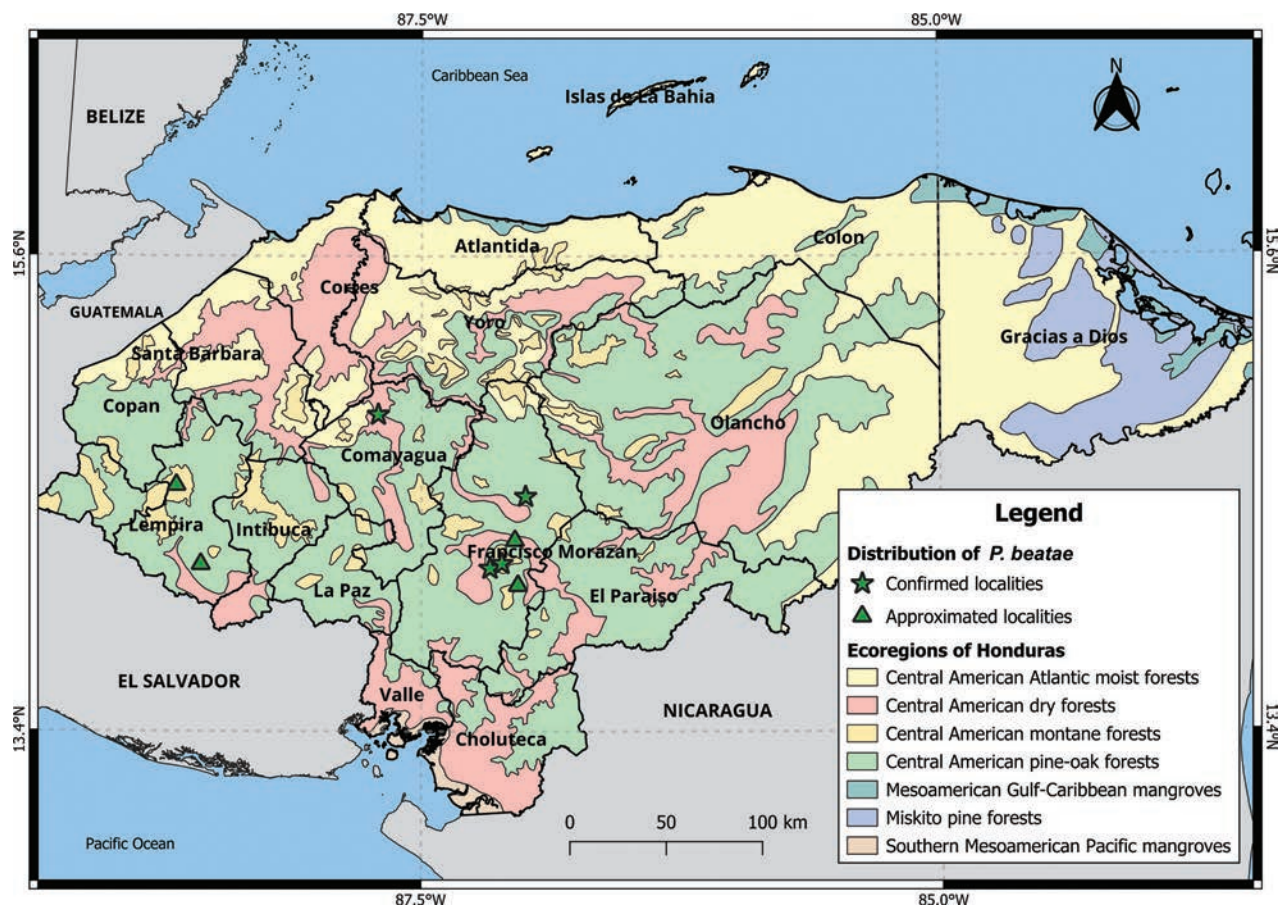   **Ecoregions and elevation.** Central American dry and pine-oak forests (1129–1984 m a.s.l.).

Figure 2. Distribution of *P. beatae* in Honduras.

Comments. The individuals from Honduras that Goodwin (1942) had identified as *P. mexicanus saxatilis* Merriam, 1898 were considered to belong to *P. oaxacensis* Merriam, 1898, (*P. aztecus* group) by Musser (1969). Similarly, Musser (1969) indicated that the species cataloged as *P. hondurensis* Goodwin, 1941 by Goodwin (1942) also belonged to *P. oaxacensis*. Recently, Kilpatrick et al. (2021) treated *P. oaxacensis* as a subspecies of *P. aztecus* (Saussure, 1860) restricted to Mexico. Additionally, *P. cordillerae* refers to all members of the *P. aztecus* species group within the southeast of the Isthmus of Tehuantepec, and two subspecies have been provisionally proposed: one from the Cahuatique locality, as *P. cordillerae cordillerae*, and the other, *P. cordillerae hondurensis* for western Honduras (Table 2). Therefore, we should treat Honduran specimens referenced as *P. oaxacensis*, *P. aztecus*, *P. aztecus oaxacensis*, and *P. hondurensis* as pertaining to *P. c. hondurensis* (Musser 1969; Carleton 1979; Hall 1981; Kilpatrick et al. 2021). This group requires additional study in eastern Honduras and confirmation of its presence in other regions of the country. For example, Matson et al. (2016) identified *P. oaxacensis* (Table 2) based on its external morphology in the Sierra de Agalta National Park, situated in eastern Honduras, in the department of Olancho. This area is not part of the potential distribution proposed by Kilpatrick et al. (2021) which included the departments Choluteca, Comayagua, Copán, El Paraíso, Intibucá, Francisco Morazán, Ocotepeque, Santa Barbara, and Valle. Hence, it is crucial to verify these specimens and historical records before making any taxonomic reassignment.

Figure 3. Distribution of *P. cordillerae* in Honduras.

Peromyscus mexicanus group

Peromyscus nicaraguae J. A. Allen (1908)

Distribution. Colón, Comayagua, Francisco Morazán, and Olancho departments (Fig. 4).

Ecoregions and elevation. Central American montane, Atlantic moist forests, and pine-oak forests (1261–2030 m a.s.l.).

Comments. *Peromyscus nicaraguae*, originally considered a distinct species, was later placed under *P. mexicanus saxatilis*. In a subsequent review, Musser (1969) reexamined the collections presented by Goodwin in 1942 in Honduras and determined that individuals previously identified as *P. guatemalensis tropicalis* Goodwin, 1932 should be reclassified as *P. m. saxatilis*, both taxa being part of the *P. mexicanus* group. A recent taxonomic assessment conducted by Pérez-Consuegra and Vázquez-Domínguez (2015) significantly revised the *P. mexicanus* species group. Three junior synonyms were elevated to independent species status: *P. tropicalis* (formerly *P. g. tropicalis*), *P. nicaraguae* (previously *P. mexicanus nicaraguae*), and *P. salvadorensis* (Dickey 1928) (formerly *P. mexicanus salvadorensis*) (Table 3), these changes were based on the synonymy of *P. m. saxatilis* provided by Trujano-Álvarez and Álvarez-Castañeda (2010). Bradley et al. (2016) reported the northernmost locality in Honduras for this species in Capiro and Calentura National Park, without providing coordinates; therefore, it was approximated. However, the elevations in this area range from 600–1200 m a.s.l., suggesting that the species may occur at lower elevations in Honduras.

Figure 4. Distribution of *P. nicaraguae* in Honduras.

Peromyscus salvadorensis (Dickey 1928)

Distribution. Lempira Department (Fig. 5).

Ecoregions and elevation. Central American montane forests (1430–2870 m a.s.l.). **Comments.** Another species within the *P. mexicanus* group in Honduras is *P. salvadorensis* (Pérez-Consuegra and Vásquez-Domínguez 2015, 2016). Recent research indicates the presence of two lineages in the country: "lineage M" and "lineage L", both displaying cryptic morphometric characteristics indicating a possible undescribed species (Table 3; Pérez-Consuegra and Vásquez-Domínguez 2015). According to Pérez-Consuegra and Vásquez-Domínguez (2016), however, both lineages inhabit mid to high elevations. Nevertheless, the specimens from lineages M and L reported in Pérez-Consuegra and Vásquez-Domínguez (2016), originate exclusively from the Celaque National Park in western Honduras.

P. nicaraguae and *P. salvadorensis* may be cryptic within their distribution ranges (Pérez-Consuegra and Vásquez-Domínguez 2016); however, these species are currently considered allopatric because *P. salvadorensis* has only been confirmed in western Honduras, and *P. nicaraguae* is documented in the central-eastern region of the country.

Peromyscus stirtoni Dickey, 1928

Distribution. Choluteca, Francisco Morazán, El Paraíso, and Valle departments (Fig. 6).
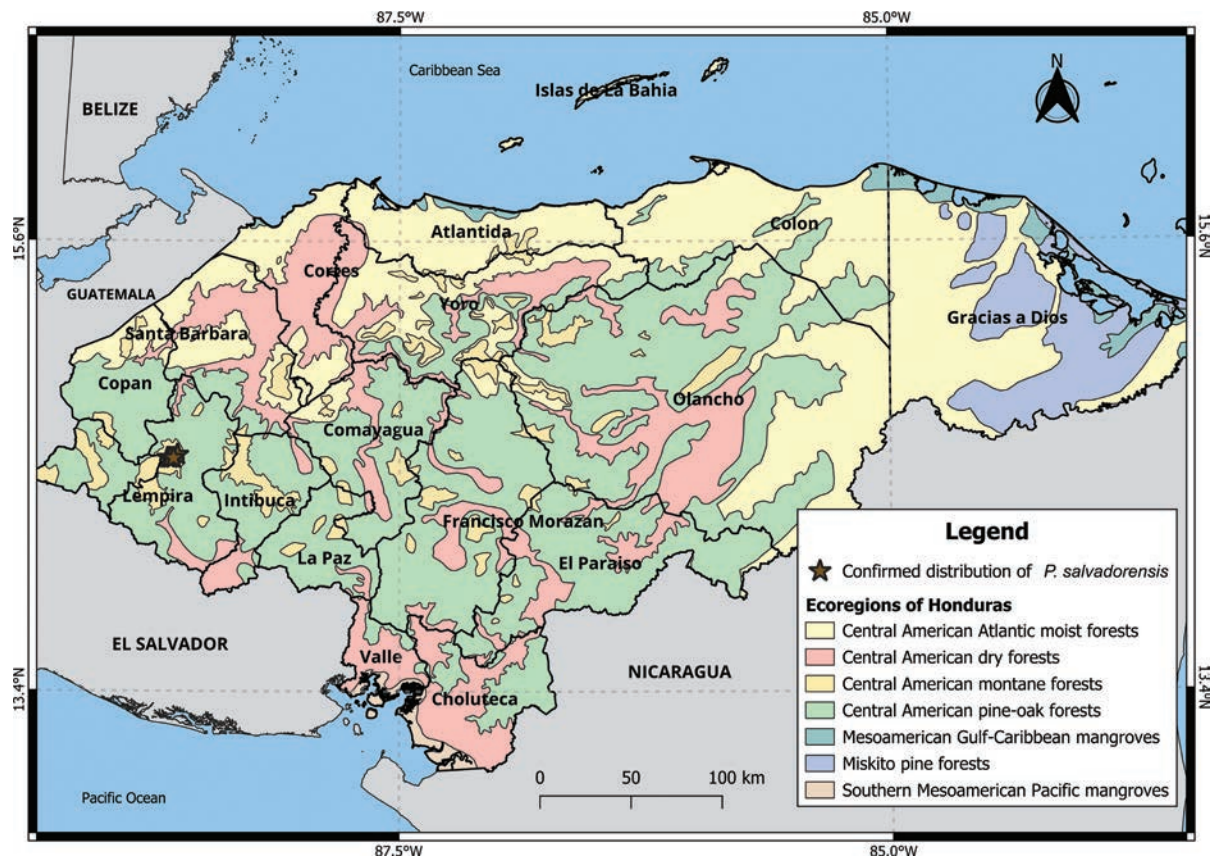
Figure 5. Distribution of *P. salvadorensis* in Honduras.

Figure 6. Distribution of *P. stirtoni* in Honduras.

Ecoregions and elevation. Central American dry and pine-oak forests (200–900 m a.s.l.).

Comments. *P. stirtoni* was initially assigned to the *P. mexicanus* group (Hall and Kelson 1959). However, this placement was questioned and considered provisional by Carleton (1989). Subsequent mtDNA studies conducted by Bradley et al. (2007) and Ordóñez-Garza et al. (2010) suggested that *P. stirtoni* should be placed within the *P. megalops* species group. León-Tapia et al. (2022) reported that *P. stirtoni* forms a well-supported monophyletic lineage, but it is important to note its close relationship with lowland species, including the *P. megalops* group. In contrast, Bradley et al. (2016) considered *P. stirtoni* to be in the *P. mexicanus* group. Timm (2016) suggested that *P. stirtoni* might occur in La Paz, southern Comayagua, Lempira, Ocotepeque, and Intibucá departments, but this remains to be confirmed.

Discussion

The *Peromyscus* genus in Honduras includes five recognized species: *P. beatae*, *P. cordillerae*, *P. nicaraguae*, *P. salvadorensis*, and *P. stirtoni*. However, this count might underestimate the actual diversity, and there could be additional *Peromyscus* species in Honduras. For example, there are potentially isolated populations of *P. nicaraguae* in northern and eastern Honduras (Pérez-Consuegra and Vásquez-Domínguez 2015, 2016; Matson et al. 2016). Similarly, the individuals identified by Matson et al. (2016) as *"P. oaxacensis"*, (currently *P. cordillerae*) in eastern Honduras deposited at the CMNH (Suppl. material 1) could yield additional species. Although the specimens from this museum are undergoing genetic studies (e.g., Pérez-Consuegra and Vásquez-Domínguez 2015, 2016), the review of the individuals identified as *P. oaxacensis* is of utmost importance as morphological and ecological evidence is required to confirm the distribution of *P. cordillerae* in Honduras (Kilpatrick et al. 2021).

The confirmed species count for the country might reflect the limited studies conducted on the genus in Honduras, primarily relying on specimens from museum collectors' or curators' identifications within historical collections. The uncertainty regarding the identity of Honduran *Peromyscus* individuals underscores the importance of validating historical specimens in the respective collections (Turcios-Casco et al. 2024), such as the ones of *Peromyscus* at the AMNH. This museum houses the largest collection of *Peromyscus* specimens (270) from Honduras and is comprised of specimens collected by one prominent mammalian collector for Honduras, C. F. Underwood, dating back to 1937. In contrast, the second-largest collection is deposited at the CMNH, has been used to demonstrate the presence of the genus in the country (Matson et al. 2016) and for taxonomic studies, such as those within the *P. mexicanus* and *P. boylii* groups (see Bradley et al. 2000; Pérez-Consuegra and Vázquez-Domínguez 2015, 2016; Bradley et al. 2016, 2017). Remarkably, there are regions in Honduras where the only known specimens are historical ones. For instance, the sole known specimens of *Peromyscus* from the La Paz Department were collected by C. F. Underwood in the 1930s (Goodwin 1942). Certain isolated specimens are regarded as genetic taxonomic units by some researchers, while others classify them as distinct forms. For instance, Kilpatrick et al. (2021) mentioned that the specimen TTU 83698 (TK 101037) labeled as *P. mexicanus* from La Tigra National Park (Francisco Morazán) was identified as *P. a. oaxacensis* in GenBank. However, the molec-

ular analyses in Kilpatrick et al. (2021) suggest that the sequence of TK 101037 from Honduras aligns more closely with *P. nudipes* J.A. Allen, 1891 (sequence accession number FJ214675); and they proposed the possibility of contamination of this sequence with another taxon. We found no evidence confirming the presence of *P. nudipes* in Honduras. It is possible that similar cases may involve incorrect identification, however, we cannot confirm this possibility because we have not conducted reviews of specimens in scientific collections. On the other hand, *P. gymnotis* Thomas, 1894 is considered as potentially distributed in Honduras according to The International Union for the Conservation of Nature−IUCN (Vázquez and Reid 2016). In addition, Pérez-Consuegra and Vázquez Domínguez (2015) mentioned that *P. salvadorensis* (resurrected and elevated from synonymy with *P. m. saxatilis*) has been confused in the past with *P. gymnotis*. Hence, we propose a comprehensive examination of specimens from western and southwestern Honduras, where the species is anticipated to occur. Additionally, further collections from this region are essential to validate the presence of *P. gymnotis*.

From a conservation perspective, it is crucial to consider taxonomic checklists or reviews, as the work presented herein, because ignoring them can result in inaccurate conservation assessments. For instance, *P. gymnotis* is categorized as Data Deficient (DD) in the Red List of Honduras (WCS 2021). Unfortunately, *P. gymnotis* in Honduras has not been confirmed yet. Regrettably, in some cases, national classifications depend on extrapolating data, such as species expected to inhabit a particular area based on geographic proximity or limited available information, which can be misleading (e.g., Reid 2009). Similarly, *P. beatae* and *P. stirtoni* are categorized as DD in the Honduran Red List (WCS 2021); even though their presence has been confirmed additional information regarding their distribution, ecology, and natural history remains unknown. This classification in the Honduran Red List (WCS 2021) emphasizes the importance of conducting updated studies to accurately determine their true threat level and to propose and implement effective management measures for protecting their populations at the national level. For example, *P. mexicanus* sensu lato could be used to evaluate the effectiveness of protected area management (Cobo-Simón et al. 2018). However, it is essential to consider that in this region, three species of the *P. mexicanus* group (Pérez-Consuegra and Vázquez-Domínguez 2016; Bradley et al. 2016) and four species of the genus (*P. beatae*, *P. cordillerae*, *P. nicaraguae*, and *P. stirtoni*) could potentially coexist (see Figs 2−4, 6); all *Peromyscus* species for Honduras share significant similarities in their external morphology (Musser 1969; Hall 1981; Carleton 1989; Pérez-Consuegra and Vázquez-Domínguez 2015, 2016; León-Tapia et al. 2022).

The *P. mexicanus* group is known for exhibiting allopatric distributions with respect to its congeners, leading to cryptic speciation with conservative morphology (Ornelas et al. 2013; Pérez-Consuegra and Vásquez-Domínguez 2016). This makes precise identification a challenge for research in the country (e.g., Cobo-Simón et al. 2018; Hoskins et al. 2018). Conservative morphology has also been mentioned for other groups of *Peromyscus* occurring in Honduras, such as *P. boylii* (Baird, 1855) and *P. aztecus* (Schmidly et al. 1988; Bradley et al. 2004, 2017), so elucidating both external and cranial morphological differences of *Peromyscus* should be a top priority. This is especially important because geographic variation complicates identification (Hall 1981). Previous studies must be complemented with geographic distribution, ecology, and the use of

modern molecular techniques, such as mitochondrial DNA sequencing and phylogenetic analysis. Bradley et al. (2016) have employed these techniques to clarify the systematics of *P. nudipes* and *P. nicaraguae*, including specimens previously assigned to *P. nudipes hesperus* Harris, 1940 and *P. nudipes orientalis* Goodwin, 1938 from Costa Rica, Honduras, Nicaragua, and Panamá. This integration of molecular data with information from genetic databases like GenBank facilitates the assessment of genetic variability within *Peromyscus*, paving the way for future research in this field (Bradley et al. 2016).

This review serves as a crucial foundation for future investigations, highlighting the need for a comprehensive understanding of species diversity and the taxonomy of *Peromyscus* in the region. By addressing taxonomic uncertainties and consolidating available data, this study paves the way for more accurate conservation assessments and informed management strategies. It also sets a precedent for ongoing research efforts aimed at elucidating the biodiversity and evolutionary history of *Peromyscus* species within the Honduran context.

Acknowledgements

Additional information

Conflict of interest

The authors have declared that no competing interests exist.

Ethical statement

No ethical statement was reported.

Funding

Author contributions

Conceptualization: CML, MATC, NOG, MRA. Funding acquisition: MRA. Investigation: CML, MATC, NOG, EVB, MRA. Supervision: EVB, MRA. Writing – original draft: CML, MATC, NOG, EVB, MRA. Review and editing: CML, MATC, NOG, EVB, MRA.

Author ORCIDs

Celeste M. López https://orcid.org/0000-0002-7002-7511
Manfredo A. Turcios-Casco https://orcid.org/0000-0002-3198-3834

Eric van den Berghe https://orcid.org/0000-0001-7566-0415
Nicté Ordóñez-Garza https://orcid.org/0000-0002-7732-7824
Martin R. Alvarez https://orcid.org/0000-0001-6908-8547

Data availability

All of the data that support the findings of this study are available in the main text or Supplementary Information.

References

Allen JA (1908) Mammals from Nicaragua. Bulletin of the American Museum of Natural History 24: 647–670.

Álvarez-Castañeda ST, Lorenzo C, Segura-Trujillo CA, Pérez-Consuegra SG (2019) Two new species of *Peromyscus* from Chiapas, Mexico, and Guatemala. From field to laboratory: a memorial volume in honor of Robert J. Baker. Special Publications, Museum of Texas Tech University 543–558.

ASM (2024) Mammal Diversity Database. https://www.mammaldiversity.org/explore.html [Accessed on 28 April 2024]

Bedford NL, Hoekstra HE (2015) *Peromyscus mice* as a model for studying natural variation. eLife e06813(4): e06813. https://doi.org/10.7554/eLife.06813

Bengtson NA (1926) Notes on the Physiography of Honduras. Geographical Review 16(3): 403–413. https://doi.org/10.2307/208710

Bradley RD, Ensink J (1987) Karyotypes of five cricetid rodents from Honduras. The Texas Journal of Science 39: 171–175.

Bradley RD, Tiemann-Boege I, Kilpatrick CW, Schmidly DJ (2000) Taxonomic status of *Peromyscus boylii sacarensis*: Inferences from DNA sequences of the mitochondrial cytochrome-b gene. Journal of Mammalogy 81(3): 875–884. https://doi.org/10.1644/1545-1542(2000)081<0875:TSOPBS>2.3.CO;2

Bradley RD, Carroll DS, Haynie ML, Martínez RM, Hamilton MJ, Kilpatrick CW (2004) A new species of *Peromyscus* from western Mexico. Journal of Mammalogy 85(6): 1184–1193. https://doi.org/10.1644/BEL-113.1

Bradley RD, Durish ND, Rogers DS, Miller JR, Engstrom MD, Kilpatrick CW (2007) Toward a molecular phylogeny for *Peromyscus*: Evidence from mitochondrial cytochrome-b sequences. Journal of Mammalogy 88(5): 1146–1159. https://doi.org/10.1644/06-MAMM-A-342R.1

Bradley RD, Ordóñez-Garza N, Sotero-Caio CG, Huynh HM, Kilpatrick CW, Iñíguez-Dávalos LI, Schmidly DJ (2014) Morphometric, karyotypic, and molecular evidence for a new species of *Peromyscus* (Cricetidae: Neotominae) from Nayarit, Mexico. Journal of Mammalogy 95: 176–186. https://doi.org/10.1644/13-MAMM-A-217

Bradley RD, Nuñez-Tabares M, Soniat TJ, Kerr S, Raymond RW, Ordóñez-Garza N (2016) Molecular systematics and phylogeography of *Peromyscus nudipes* (Cricetidae: Neotominae). In: Manning RW, Goetze JR, Yancey FD II (Eds) Contributions in Natural History: A Memorial Volume in Honor of Clyde Jones. Special Publications Museum of Texas Tech University 65: 201–214.

Bradley RD, Ordóñez-Garza N, Ceballos G, Rogers DS, Schmidly DJ (2017) A new species in the *Peromyscus boylii* species group (Cricetidae: Neotominae) from Michoacán, México. Journal of Mammalogy 98(1): 154–165. https://doi.org/10.1093/jmammal/gyw160

Bradley RD, Ordóñez-Garza N, Thompson CW, Wright EA, Ceballos G, Kilpatrick CW, Schmidly DJ (2022) Two new species of *Peromyscus* (Cricetidae: Neotominae) from

the Transverse Volcanic Belt of Mexico. Journal of Mammalogy 103(2): 255–274. https://doi.org/10.1093/jmammal/gyab128

Burkart B, Self S (1985) Extension and rotation of crustal blocks in northern Central America and effect on the volcanic arc. Geology 13(1): 22–26. https://doi.org/10.1130/0091-7613(1985)13<22:EAROCB>2.0.CO;2

Carleton MD (1979) Taxonomic status and relationships of *Peromyscus boylii* from El Salvador. Journal of Mammalogy 60(2): 280–296. https://doi.org/10.2307/1379799

Carleton MD (1989) Systematics and Evolution. In: Kirkland GL, Layne JN (Eds) Advances in the Study of *Peromyscus* (Rodentia). Texas Tech University Press, Lubbock, Texas, 7–141.

Cassola F (2016) *Peromyscus beatae*. The IUCN Red List of Threatened Species 2016: e.T136323A22364310. https://doi.org/10.2305/IUCN.UK.2016-2.RLTS.T136323A22364310.en. [Accessed on October 02, 2024]

Cobo-Simón I, Méndez-Cea B, Portillo H, Elvir F, Vega H, Gallego FJ, Fontecha G (2018) Testing the effectiveness of conservation management within biosphere reserves: The case of the Mexican deer mouse (*Peromyscus mexicanus*) as a bioindicator. Integrative Zoology 14(5): 422–434. https://doi.org/10.1111/1749-4877.12371

Dawson WD (2005) Peromyscine biogeography, Mexican topography and Pleistocene climatology. In: Sánchez-Cordero V, Medellín RA (Eds) Contribuciones mastozoológicas en homenaje a Bernardo Villa. Instituto de Biología, UNAM; Instituto de Ecología, UNAM, CONABIO, 145–156.

Dengo G (1968) Estructura geológica, historia tectónica y morfología de América Central. Ciudad de Mexico, Mexico: Centro Regional de Ayuda Técnica Agencia para el Desarrollo Internacional.

Dickey DR (1928) Five new mammals of the genus *Peromyscus* from El Salvador. Proceedings of the Biological Society of Washington 41: 1–6.

Dunbar SG, Salinas L, Baumbach D (2020) Marine Turtle Species of Pacific Honduras. Marine Turtle Newsletter 160: 1–6.

GBIF.org (2023) GBIF Occurrence Download. https://doi.org/https://doi.org/10.15468/dl.8phy97 [Accessed on September 15, 2023]

Goodwin GG (1941) A new *Peromyscus* from western Honduras. American Museum Novitates, 1121.

Goodwin GG (1942) Mammals of Honduras. Bulletin of the American Museum of Natural History 79: 107–195. https://archive.org/details/bulletin-american-museum-natural-history-79-107-195

Hall E (1981) The Mammals of North America. Vols 1 and 2, Ronald Press, New York, 720 pp.

Hall E, Kelson KR (1959) The mammals of North America. 2 Vols Ronald Press, 674 pp.

Hernández-Canchola G, León-Paniagua L, Esselstyn JA (2022) Mitochondrial DNA and other lines of evidence clarify species diversity in the *Peromyscus truei* species group (Cricetidae: Neotominae). Mammalia 86(4): 380–392. https://doi.org/10.1515/mammalia-2021-0146

Hernández Oré M, De Sousa L, López JH (2016) Honduras: Desatando el potencial económico para mayores oportunidades. Diagnóstico sistemático de país, Banco Mundial, 27 pp.

Hooper ET (1968) Classification. In: King JA (Ed.) Biology of *Peromyscus* (Rodentia). American Society of Mammalogists, Special Publication 2: 27–74.

Hooper ET, Musser GG (1964) Notes on classification of the rodent genus *Peromyscus*. Occasional Papers of the Museum of Zoology, University of Michigan 635: 1–13.

Hoskins HMJ, Burdekin OJ, Dicks K, Slater KY, McCann NP, Jocque M, Castañeda F, Reid N (2018) Non-volant mammal inventory of Cusuco National Park, north-west Honduras: Reporting the presence of Jaguar, *Panthera onca* (Linnaeus, 1758), and demonstrating the effects of zonal protection on mammalian abundance. Check List 14(5): 877–891. https://doi.org/10.15560/14.5.877

ITIS (2024) Integrated Taxonomic Information System. https://www.itis.gov/servlet/SingleRpt/SingleRpt [Accessed on April 18, 2024]

Jones JK (1990) *Peromyscus stirtoni*. Mammalian Species 361: 1–2. https://doi.org/10.2307/3504308

Kilpatrick CW, Pradhan N, Norris RW (2021) A re-examination of the molecular systematics and phylogeography of taxa of the *Peromyscus aztecus* species group, with comments on the distribution of *P. winkelmanni*. Therya 12(2): 331–346. https://doi.org/10.12933/therya-21-1115

León-Tapia MÁ, Rico Y, Fernández JA, Espinosa de los Monteros A (2022) Molecular, morphometric, and spatial data analyses provide new insights into the evolutionary history of the *Peromyscus boylii* species complex (Rodentia: Cricetidae) in the mountains of Mexico. Systematics and Biodiversity 20(1): 1–19. https://doi.org/10.1080/14772000.2022.2127966

Lorenzo C, Álvarez-Castañeda ST, Pérez-Consuegra SG, Patton JL (2016) Revision of the Chiapan deer mouse, *Peromyscus zarhynchus*, with the description of a new species. Journal of Mammalogy 97(3): 910–918. https://doi.org/10.1093/jmammal/gyw018

Marshall JS (2007) The geomorphology and physiographic provinces of Central America. In: Bundschuc J, Alvarado GE (Eds) Central America: Geology, Resources and Hazards.T&F: Tokyo, Japan, 1436 pp. https://doi.org/10.1201/9780203947043.pt2

Matson JO, Eckerlin RP, Consuegra SGP, Ordóñez-Garza N (2016) Small mammals from three mountain ranges in nuclear central America. Annals of the Carnegie Museum 83(4): 269–285. https://doi.org/10.2992/007.083.0403

Miller JR, Engstrom MD (2008) The relationships of major lineages within peromyscine rodents: A molecular phylogenetic hypothesis and systematic reappraisal. Journal of Mammalogy 89(5): 1279–1295. https://doi.org/10.1644/07-MAMM-A-195.1

Mittermeier RA, Myers N, Mittermeier CG (1999) Hotspots: earth's biologically richest and most endangered terrestrial ecoregions. CEMAX, S.A., Mexico City, 430 pp.

Musser GG (1969) Notes on *Peromyscus* (Muridae) of Mexico and Central America. American Museum Novitates 2357: 1–23.

Musser GG, Carleton MD (1993) Family Muridae. In: Wilson DE, Reeder DM (Eds) Mammal Species of the World, a Taxonomic and Geographic Reference. Smithsonian Institution Press Washington, U.S.A., 501–755.

Musser GG, Carleton MD (2005) Superfamily Muroidea. In: Wilson DE, Reeder DM (Eds) Mammal Species of the World, a Taxonomic and Geographic Reference. Baltimore: Johns Hopkins University Press, 894–1531.

Olson DM, Dinerstein E, Wikramanayake ED, Burgess ND, Powell GVN, Underwood EC, D'Amico JA, Itoua I, Strand HE, Morrison JC, Loucks CJ, Allnutt TF, Ricketts TH, Kura Y, Lamoreux JF, Wettengel WW, Hedao P, Kassem KR (2001) Terrestrial ecoregions of the world: A new map of life on Earth. Bioscience 51(11): 933–938. https://doi.org/10.1641/0006-3568(2001)051[0933:TEOTWA]2.0.CO;2

Ordóñez-Garza N, Matson JO, Strauss RE, Bradley RD, Salazar-Bravo J (2010) Patterns of phenotypic and genetic variation in three species of endemic Mesoamerican *Per-*

omyscus (Rodentia: Cricetidae). Journal of Mammalogy 91(4): 848–859. https://doi.org/10.1644/09-MAMM-A-167.1

Ornelas JF, Sosa V, Soltis DE, Daza JM, González C, Soltis PS, Gutiérrez-Rodríguez C, de los Monteros AE, Castoe TA, Bell C, Ruíz-Sanchez E (2013) Comparative Phylogeographic Analyses Illustrate the Complex Evolutionary History of Threatened Cloud Forests of Northern Mesoamerica. PLoS ONE 8(2): e56283. https://doi.org/10.1371/journal.pone.0056283

Osgood WH (1909) Revision of the mice of the American genus *Peromyscus*. North American Fauna 28: 1–285. https://doi.org/10.3996/nafa.28.0001

Pardiñas UFJ, Ruelas D, Brito J, Bradley LC, Bradley RD, Ordóñez Garza N, Kryštufek B, Cook JA, Cuéllar Soto E, Salazar-Bravo J, Shenbrot GI, Chiquito EA, Percequillo AR, Prado JR, Haslauer R, Patton JL, León-Paniagua L (2017) Cricetidae (true hamsters, voles, lemmings and new world rats and mice) -species accounts of Cricetidae. In: Wilson DE, Lacher Jr TE, Mittermeier RA (Eds) Handbook of the Mammals of the World. Barcelona: Lynx Edicions, 280–535.

Peppers JA, Owen JG, Bradley RD (1999) The Karyotype of *Peromyscus Stirtoni* (Rodentia: Muridae). The Southwestern Naturalist 44(1): 109–112.

Pérez-Consuegra SG, Vázquez-Domínguez E (2015) Mitochondrial diversification of the *Peromyscus mexicanus* species group in Nuclear Central America: Biogeographic and taxonomic implications. Journal of Zoological Systematics and Evolutionary Research 53(4): 300–311. https://doi.org/10.1111/jzs.12099

Pérez-Consuegra SG, Vázquez-Domínguez E (2016) Intricate evolutionary histories in montane species: a phylogenetic window into craniodental discrimination in the *Peromyscus mexicanus* species group (Mammalia: Rodentia: Cricetidae). Journal of Zoological Systematics and Evolutionary Research 55(1): 57–72. https://doi.org/10.1111/jzs.12155

Platt RN II, Amman BR, Keith MS, Thompson CW, Bradley RD (2015) What is *Peromyscus*? Evidence from nuclear and mitochondrial DNA sequences suggests the need for a new classification. Journal of Mammalogy 96(4): 708–719. https://doi.org/10.1093/jmammal/gyv067

Ramírez-Fernández JD, Barrantes G, Sánchez-Quirós C, Rodríguez-Herrera B (2023) Habitat use, richness, and abundance of native mice in the highlands of the Talamanca Mountain range, Costa Rica. Therya 14(1): 49–54. https://doi.org/10.12933/therya-23-2227

Reid FA (2009) A field guide to the Mammals of Southeast Mexico and Central America. 2nd edn. New York: Oxford University Press, 346 pp.

Schmidly DJ, Bradley RD, Cato PS (1988) Morphometric differentiation and taxonomy of three chromosomally characterized groups of *Peromyscus boylii* from east-central Mexico. Journal of Mammalogy 69(3): 462–480. https://doi.org/10.2307/1381338

Sullivan J, Markert JA, Kilpatrick CW (1997) Phylogeography and molecular systematics of the *Peromyscus aztecus* species group (Rodentia: Muridae) inferred using parsimony and likelihood. Systematic Biology 46(3): 426–440. https://doi.org/10.1093/sysbio/46.3.426

Tiemann-Boege I, Kilpatrick CW, Schmidly DJ, Bradley RD (2000) Molecular phylogenetics of the *Peromyscus boylii* species group (Rodentia: Muridae) based on mitochondrial cytochrome b sequences. Molecular Phylogenetics and Evolution 16(3): 366–378. https://doi.org/10.1006/mpev.2000.0806

Timm R (2016) *Peromyscus stirtoni*. The IUCN Red List of Threatened Species 2016: e.T16693A22362723. https://dx.doi.org/10.2305/IUCN.UK.20162.RLTS.T16693A22362723.en [Accessed on 02 October 2024]

Townsend JH (2014) Characterizing the Chortís block biogeographic province: Geological, physiographic, and ecological associations and herpetofaunal diversity. Mesoamerican Herpetology 1(2): 204–252.

Trujano-Álvarez AL, Álvarez-Castañeda ST (2010) *Peromyscus mexicanus* (Rodentia: Cricetidae). Mammalian Species 42(858): 111–118. https://doi.org/10.1644/858.1

Turcios-Casco MA, Cardoso Cláudio V, Lee Jr TE (2024) Back to the future: A preserved specimen validates the presence of *Molossus pretiosus* (Molossidae, Chiroptera) in Honduras. ZooKeys 1196: 139–148. https://doi.org/10.3897/zookeys.1196.116144

Vázquez E, Reid F (2016) *Peromyscus gymnotis*. The IUCN Red List of Threatened Species 2016: e.T16666A22361063. https://doi.org/10.2305/IUCN.UK.2016-2.RLTS.T16666A22361063.en [Accessed on 04 October 2024]

von Lehmann VE, Schaefer HE (1979) Cytologisch-taxonomische Studien an einer Kleinsäugeraufsammlung aus Honduras (Spermienmorphologie und vergleichende Cytochemie). Journal of Zoological Systematics and Evolutionary Research 17(3): 226–236. https://doi.org/10.1111/j.1439-0469.1979.tb00703.x

WCS (2021) Lista Roja de especies amenazadas de Honduras. WCS, MiAmbiente, UNAH–VS, ICF, IUCN, Tegucigalpa, M.D.C., Honduras, 139 pp.

Supplementary material 1

Verified records of *Peromyscus* in Honduras

Authors: Celeste M. López, Manfredo A. Turcios-Casco, Eric van den Berghe, Nicté Ordóñez-Garza, Martin R. Alvarez

Data type: xlsx

Explanation note: Verified occurrence list of *Peromyscus* species in Honduras, including the museums where they are deposited, catalog numbers, as well as a description for each record including the department, municipality, and locality with geographical coordinates in decimal format and WGS-84 Datum. Please refer to observations for detailed remarks on each specimen.

Link: https://doi.org/10.3897/zookeys.1218.126535.suppl1

ZooKeys

Cremastobombycia socoromaensis sp. nov., the first South American representative of the micromoth genus *Cremastobombycia* Braun (Lepidoptera, Gracillariidae, Lithocolletinae)

Héctor A. Vargas[1]

1 Departamento de Recursos Ambientales, Facultad de Ciencias Agronómicas, Universidad de Tarapacá, Arica, Chile
Corresponding author: Héctor A. Vargas (havargas@academicos.uta.cl, lepvargas@gmail.com)

Abstract

The micromoth *Cremastobombycia socoromaensis* **sp. nov.** (Lepidoptera, Gracillariidae, Lithocolletinae) from the arid highlands of the western slope of the Andes of northern Chile is described and illustrated. Larvae construct bulged leaf mines on the shrub *Baccharis tola* Phil. (Asteraceae). Pupation occurs in a silk cocoon constructed by the last instar larva inside the mine. The cocoon and the mine surface are pierced by the frontal process of the pupa to allow adult emergence. This discovery represents the first record of *Cremastobombycia* Braun, 1908 in South America.

Key words: Andes, Chile, leaf miner, new record, new species, taxonomy

Introduction

Cremastobombycia Braun, 1908 (Lepidoptera, Gracillariidae, Lithocolletinae) was originally described as a subgenus of *Lithocolletis* Hübner, 1825, currently a synonym of *Phyllonorycter* Hübner, 1823 (De Prins and De Prins 2024), to include five North American micromoth species bearing forewing and hindwing with veins M1 and M2 stalked and labial palpus with the third palpomere slightly longer than the second one (Braun 1908). Furthermore, Braun (1908) indicated some elements of the wing pattern, larval morphology, and mine and cocoon shape shared by these five species. Busck (1910) treated *Cremastobombycia* as a genus, and Meyrick (1912) subsequently designated *Lithocolletis solidaginis* Frey & Boll, 1876 as its type species. Vári (1961) provided a more detailed description based on the study of the adult stage of the type species, including genitalia morphology. De Prins and Kawahara (2012) expanded this definition to include variations in forewing venation and genitalia. Finally, Davis et al. (2013) highlighted a morphological specialization of the hypopharynx of the larva as a distinctive character. Consistent with the evolutionary closeness between *Cremastobombycia* and *Phyllonorycter* suggested early based on morphology (Braun 1908, 1909; Busck 1910), results of molecular analyses have provided support for a sister relationship between these two genera (Kawahara et al. 2011, 2017; De Prins and Kawahara 2012).

Shortly after the original description of *Cremastobombycia*, an additional species was described based on the type material collected in Honolulu, Oahu (Busck 1910). However, this species had previously been purposely introduced to the Hawaiian Islands from Mexico, which represents its native range, as a biocontrol for *Lantana camara* L. (Verbenaceae) (Busck 1910). Thus, after this addition, the genus continued to include species exclusively native to North America, a picture that remained unchanged for almost 100 years, until the recent discovery of two African representatives from Kenya and Tanzania (De Prins and Kawahara 2012). The subsequent discovery of another North American member from Florida (Davis et al. 2013) brought the currently described species of *Cremastobombycia* to nine (De Prins and De Prins 2024). However, this number should continue to grow in the near future, as Davis et al. (2013) reported at least seven other undescribed species from North America.

Cremastobombycia larvae are leaf miners whose feeding activity produces longitudinally very wrinkled mines mainly found on the underside of the leaf (Braun 1908), known as tentiform mines (Davis et al 2013). As in many Gracillariidae lineages, the hypermetamorphic development of *Cremastobombycia* larvae includes two distinct forms: an early sap-feeding form with prognathous mouthparts and flattened thorax and abdomen, and a later tissue-feeding form with hypognathous mouthparts and cylindrical thorax and abdomen (Davis et al. 2013). Host plants have been recorded for the seven North American species (Braun 1908; Busck 1910; Davis et al. 2013; De Prins and De Prins 2024), while those of the two African species remain unknown (De Prins and Kawahara 2012). The available records suggest a main association with Asteraceae, as six species are hosted by plants of this family and only one by members of Verbenaceae (Braun 1908; Busck 1910; Davis et al. 2013; De Prins and De Prins 2024). In contrast, only two species of the highly diverse *Phyllonorycter* are associated with members of Asteraceae (Vári 1961, De Prins and Kawahara 2012).

No *Cremastobombycia* species have been reported from South America (De Prins et al. 2019). However, morphological examination revealed that micromoths obtained from leaf mines collected in the arid highlands of the Andes of northern Chile belong to an undescribed species of this genus. The aim of this contribution is to provide a formal taxonomic description for the first South American member of *Cremastobombycia*.

Materials and methods

Mined leaves of the shrub *Baccharis tola* Phil. (Asteraceae) were collected in May 2023 in the surroundings of Socoroma Village (18°17'22"S, 69°35'12"W) at about 3400 m elevation on the western slope of the Andes in the Parinacota Province of northern Chile. Adults emerged in June 2023. The abdomen of each adult was removed and placed in hot KOH 10% for a few minutes for dissection of the genitalia, which were stained with Eosin Y and Chlorazol Black and mounted on slides with Euparal. Photos of the adults were taken with an iPhone 11 camera attached to a Leica M125 stereomicroscope. Photos of the genitalia were taken with a Leica MC170 HD digital camera attached to a Leica DM1000 LED light microscope. The holotype, paratypes and their genitalia slides are deposited in the "Colección Entomológica de la Universidad de Tarapacá" (IDEA), Arica, Chile.

Results

Cremastobombycia socoromaensis sp. nov.

https://zoobank.org/6E904F72-B578-4B30-8CD2-B6F7A8516AAE
Figs 1−4

Type locality. Chile, Parinacota Province, Socoroma (18°17'22"S, 69°35'12"W), 3400 m elevation on the western slope of the Andes.

Type material. *Holotype*. CHILE • ♂; Parinacota, Socoroma; June, 2023; H.A. Vargas leg.; ex-larva; *Baccharis tola*; May, 2023; "HOLOTYPE *Cremastobombycia socoromaensis* Vargas" [red handwritten label]; IDEA-LEPI-2024-09; HAV-1811 [genitalia slide] (IDEA). *Paratypes*. CHILE • 2♂ 2♀; same data as for the holotype; IDEA-LEPI-2024-10 to IDEA-LEPI-2024-13; HAV-1639, 1719, 1806, 1807 [genitalia slides] (IDEA).

Diagnosis. Among the currently described *Cremastobombycia* species, *C. socoromaensis* sp. nov. is recognized based on wing pattern and genitalia morphology. Male forewing (length 3.6−3.7 mm) is brownish-orange and bears poorly defined creamy-white markings: a short longitudinal sub-basal streak and three costal and two dorsal oblique strigulae. Although female forewing (length 3.0−3.1 mm) is also brownish-orange with a sub-basal streak similar to that of the male, the four well-defined creamy-white transverse fasciae and three well-defined dark brown spots differ from the forewing pattern of the male. Male genitalia of *C. socoromaensis* sp. nov. resemble those of *C. chromolaenae* Davis, 2013 from Florida, United States. However, the poorly defined longitudinal sub-basal streak on the forewing of the former clearly contrasts with the conspicuous white longitudinal streak along the basal third on the forewing of the latter (Davis et al. 2013, figs 2, 3). Furthermore, the posterior projection of the tegumen, the straight margin between the lobes of the transtilla, the vesica with a cornutus in the male genitalia, and the diamond-shaped signum with a transverse fold in the female genitalia allow the recognition of *C. socoromaensis* sp. nov.; as in the male genitalia of *C. chromolaenae* the tegumen lacks a posterior projection, the margin between the lobes of the transtilla is concave, and the vesica lacks a cornutus (Davis et al. 2013, figs 6, 8), and the female genitalia have a strongly bilobed signum (Davis et al. 2013, figs 9−12). The transverse fold of the signum in the female genitalia of *C. socoromaensis* sp. nov. resembles that of *C. lantanella* (De Prins et al. 2019, fig. 436). However, in clear contrast with the male genitalia of the former, those of *C. lantanella* lack a posterior projection of the tegumen, have the saccus shorter than the vinculum width, and lack a cornutus on the vesica (De Prins et al. 2019, fig. 374).

Description. Male (Fig. 1A). *Head*. Vertex with narrow, elongate, raised scales, mostly brownish-orange and a few dark brown; frons with narrow, elongate, smooth brownish-orange scales. Antenna filiform, slightly shorter than forewing, silvery-gray, scape with pecten. Labial palpus straight, drooping, silvery-gray. *Thorax* (forewing length 3.6−3.7 mm). Mostly brownish-orange with scattered creamy-white dorsally; silvery-gray ventrally; legs silvery-gray. Forewing brownish-orange with poorly defined creamy-white markings, including a short longitudinal sub-basal streak and three costal and two dorsal oblique strigulae; first two costal strigulae arising before the middle, third one arising near the apex; dorsal strigulae arising near the middle; scattered dark brown scales between the
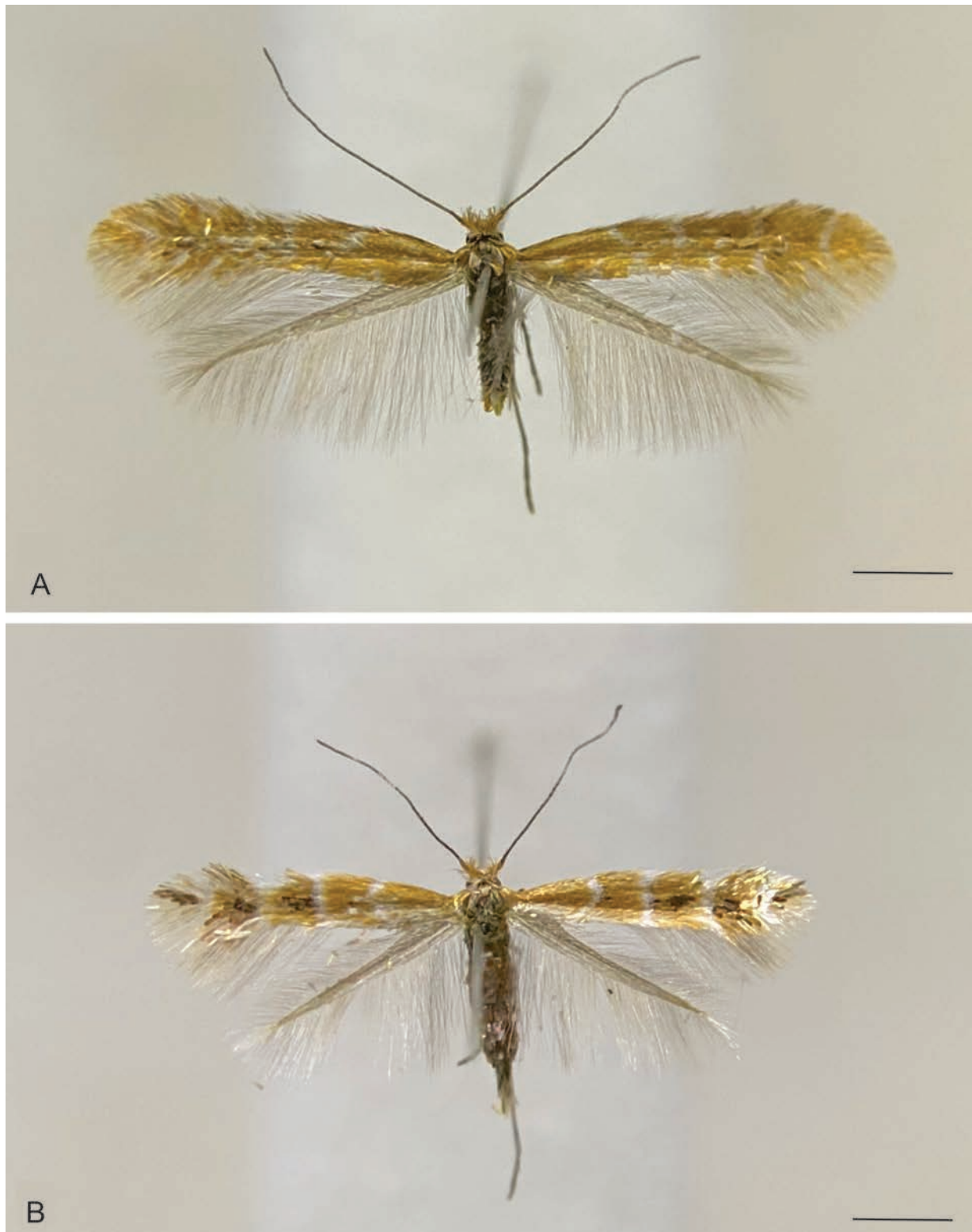
Figure 1. Habitus of *Cremastobombycia socoromaensis* sp. nov. (Lepidoptera, Gracillariidae) **A** holotype, male **B** paratype, female. Scale bars: 1 mm.

two dorsal strigulae and between the second dorsal and the third costal strigulae; fringe brownish-orange. Hindwing uniformly gray with gray fringe. ***Abdomen.*** Mostly gray with scattered creamy-white scales; sternum VIII flap-like, elongate. ***Male genitalia*** (Fig. 2). Tegumen with narrow arms slightly widened on dorsal half,
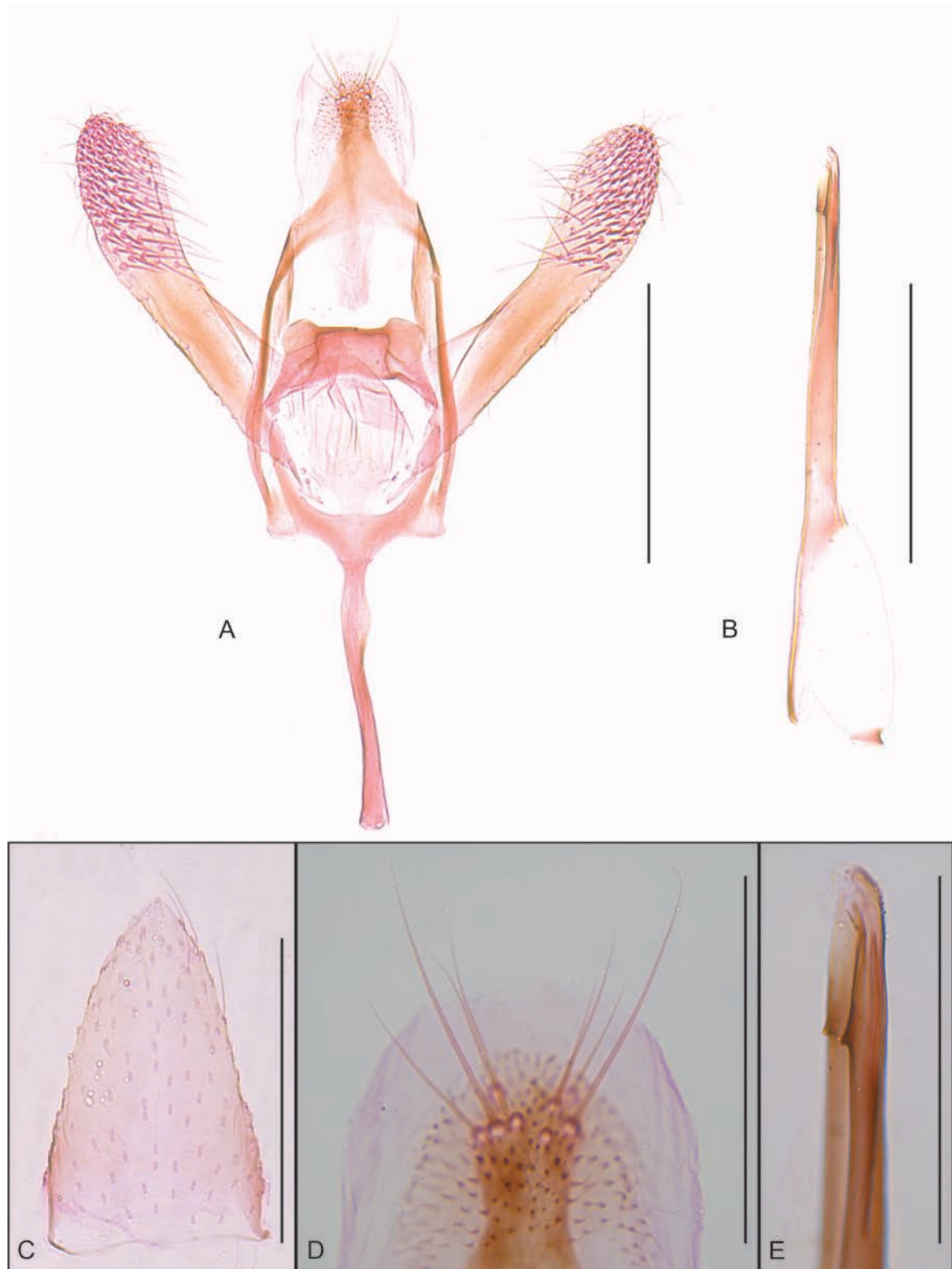
Figure 2. Male genitalia and sternum VIII of *Cremastobombycia socoromaensis* sp. nov. (Lepidoptera, Gracillariidae) **A** male genitalia, phallus removed **B** phallus **C** sternum VIII **D** tegumen apex **E** phallus apex. Scale bars: 0.2 mm (**A, B**); 0.1 mm (**C–E**).

with flat, somewhat triangular posterior projection bearing eight elongate setae near apex. Vinculum U-shaped. Saccus a narrow, elongate, slightly sinuous rod. Subscaphium a narrow, poorly sclerotized longitudinal stripe ending in a broad patch of microtrichiae. Juxta a broad, poorly sclerotized plate joined to posterior
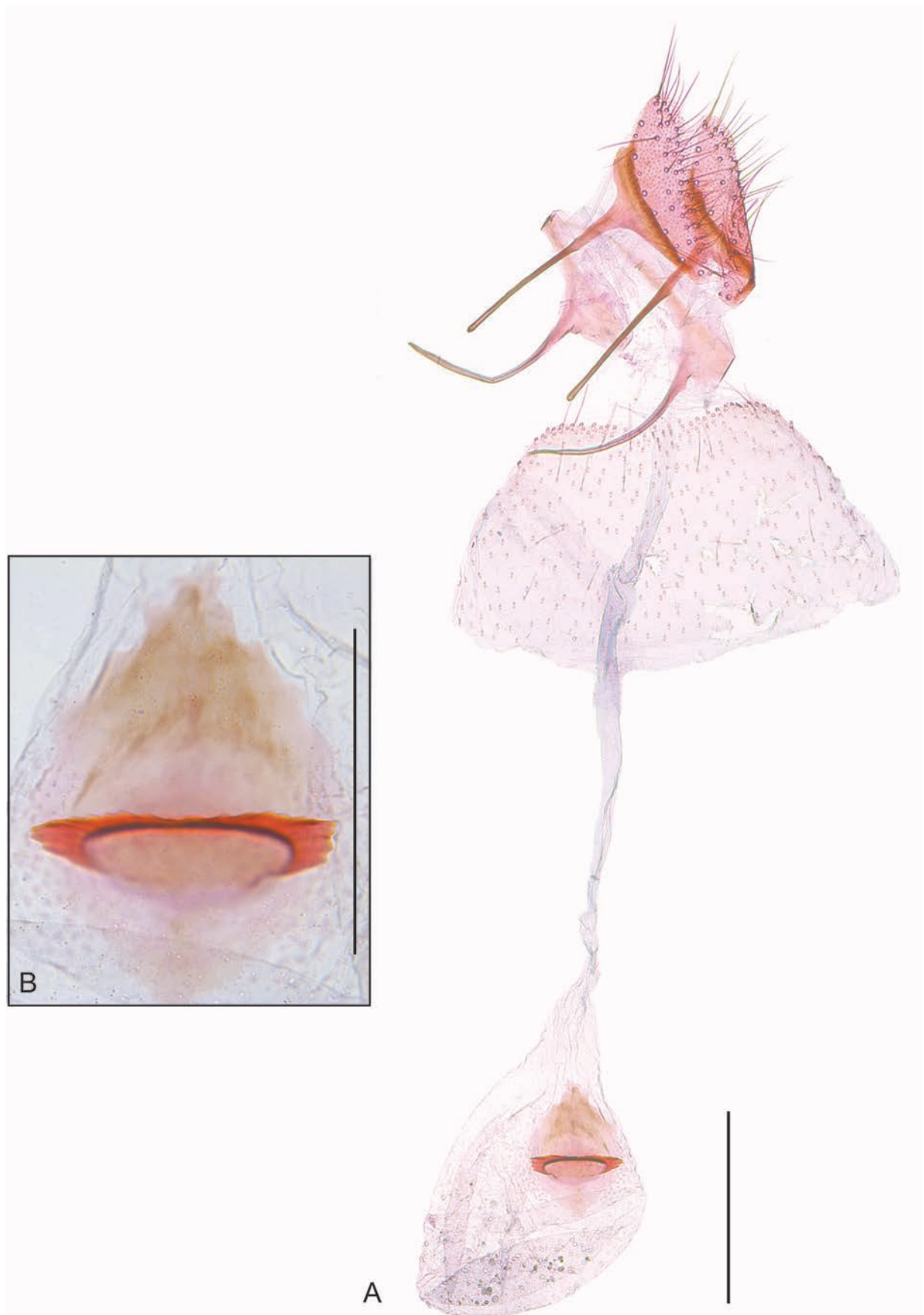
Figure 3. Female genitalia of *Cremastobombycia socoromaensis* sp. nov. (Lepidoptera, Gracillariidae) **A** female genitalia **B** signum. Scale bars: 0.2 mm (**A**); 0.1 mm (**B**).
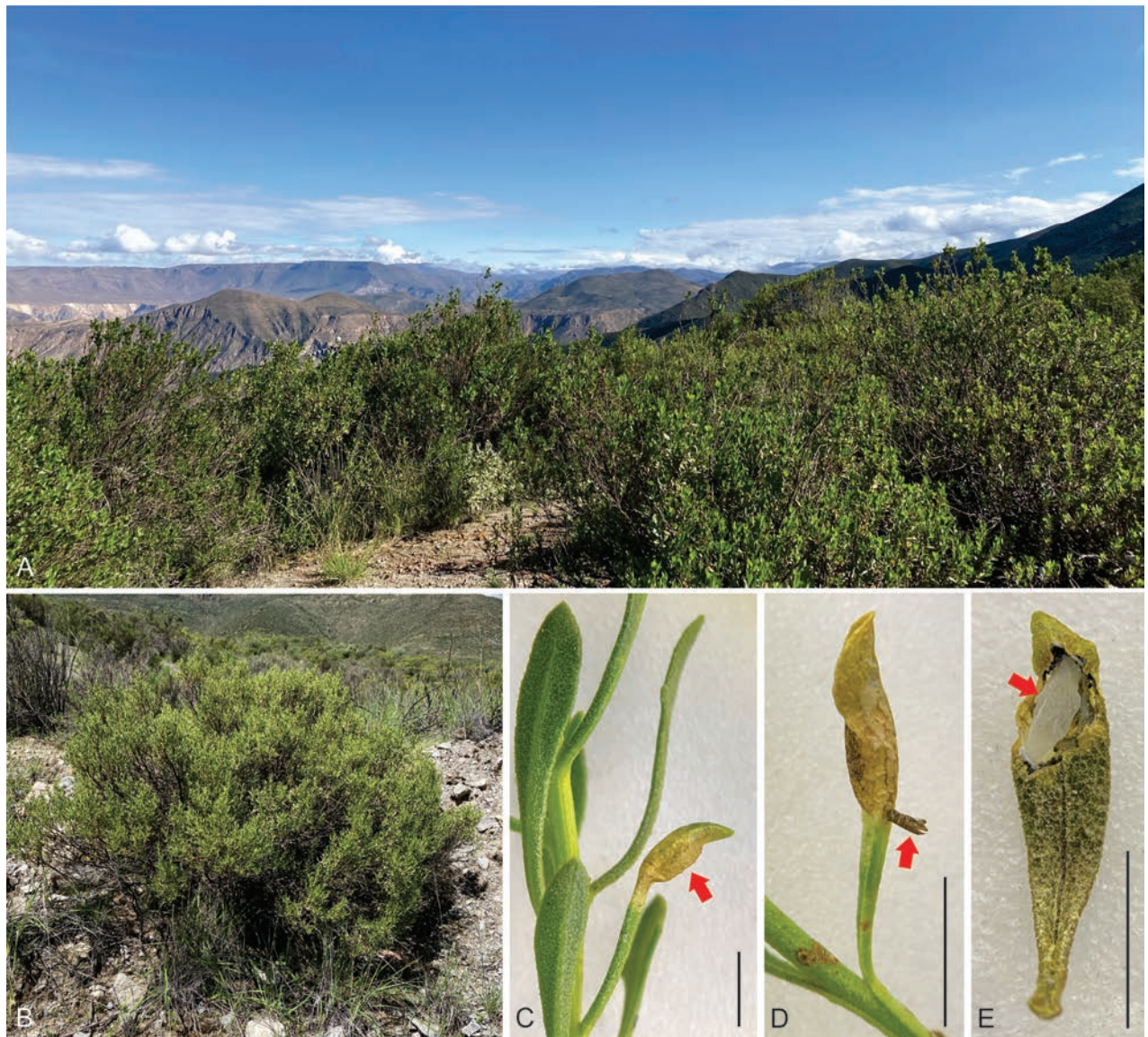
Figure 4. Natural history of *Cremastobombycia socoromaensis* sp. nov. (Lepidoptera, Gracillariidae) **A** habitat at the type locality **B** host plant *Baccharis tola* (Asteraceae) **C** leaf mine (red arrow) on *B. tola* **D** pupal exuvium (red arrow) attached to the mine after adult emergence **E** artificially opened leaf mine showing a pupal cocoon (red arrow). Scale bars: 5 mm.

margin of vinculum by a narrow stripe. Transtilla well-differentiated with two widely separated lobes on anterior margin. Valva elongate, slender, length about 1.5 times the saccus; dorsal margin slightly convex near tip; ventral margin mostly straight; apex widely rounded; median surface with dense patch of stout setae on distal third. Phallus cylindrical, straight, about twice the saccus length; coecum about a third the phallus length; a narrow cleft on distal third with two small spine-like projections on opposed margins; vesica with a narrow, elongate cornutus; ductus ejaculatorius with a ring-shaped sclerite near the tip of the coecum.

Female (Fig. 1B). Mostly similar to male, except for forewing length (3.0–3.1 mm) and maculation pattern; mostly brownish-orange with a poorly defined, short creamy-white longitudinal sub-basal streak and four well-defined creamy-white transverse fasciae, the first one convex, the three other straight; a small dark brown spot on the middle of the outer margin of the first fascia; a great dark brown spot between the outer margin of the second and the inner margin of the

third fasciae and between the outer margin of the third and the inner margin of the fourth fasciae; a small dark brown spot on the outer margin of the fourth fascia. ***Female genitalia*** (Fig. 3). Papillae anales flattened, bearing long setae mostly near posterior margin. Posterior apophyses straight, slightly longer than posterior margin of papillae anales. Anterior apophyses dorsally curved, length similar to posterior apophyses. Ostium near the posterior margin of sternum VII. Ductus bursae membranous, narrow, about three times the posterior apophyses length; ductus seminalis arising near the posterior third of ductus bursae. Corpus bursae membranous, oval, about half the length of ductus bursae; signum a slightly sclerotized diamond-shaped plate on posterior half of corpus bursae with a well-sclerotized semicircular serrated transverse fold near the middle.

Etymology. The specific epithet is derived from the type locality.

Distribution (Fig. 4A). The currently documented range of *C. socoromaensis* sp. nov. is restricted to the type locality in the surroundings of Socoroma Village, at about 3400 m elevation on the western slope of the Andes in the Parinacota Province of northern Chile.

Host plant (Fig. 4B). *Baccharis tola* is the only host plant currently recorded for *C. socoromaensis* sp. nov. This shrub, native to Argentina, Bolivia, Chile and Peru (POWO 2024), is used for medicinal purposes (Villagrán et al. 2003). In northern Chile, *B. tola* inhabits the highlands of the Andes between about 2000–4800 m elevation (Rodriguez et al. 2018).

Natural history (Fig. 4C–E). Eggs of *C. socoromaensis* sp. nov. are laid individually mainly on the adaxial surface of the leaf. Larva and pupa are endophytic. The hypermetamorphic larval development includes early sap-feeding and later tissue-feeding forms. The bulged, elongate mature mine occupies a large proportion of the leaf. The last instar tissue-feeding larva constructs a loose, smooth, cylindrical silk cocoon for pupation attached to the mine by anterior and posterior ends. The cocoon and the mine surface are pierced by the frontal process of the pupa to allow the adult emergence.

Discussion

Besides the morphological attributes of the labial palpus and wing venation of the adult stage highlighted in the original description of *Cremastobombycia*, Braun (1908) indicated that members of this genus use host plants of the family Asteraceae, construct longitudinally very wrinkled (=tentiform) mines on the lower side of the leaf, and pupate in a dense, elongate cocoon suspended inside the mine by silken threads at the anterior and posterior ends. Although these features are found in many of the North American species of *Cremastobombycia*, mines of *C. grindeliella* (Walsingham, 1891) sometimes occur on the upper side of the leaf (Braun 1908), and the hosts of *C. lantanella* belong to the family Verbenaceae (Busck 1910). Meanwhile, host plants, leaf mines and immature stages of the African species remain unknown (De Prins and Kawahara 2012).

The inclusion of *C. socoromaensis* sp. nov. in *Cremastobombycia* is based on its wing venation, which is identical to that of the type species (Meyrick 1912; Vári 1961; Davis et al. 2013), and its genitalia morphology, which fits the pattern previously described for this genus (Vári 1961; De Prins and Kawahara 2012; Davis et al. 2013). Furthermore, *B. tola* belongs to the family most frequently reported as host to members of *Cremastobombycia* (De Prins and De Prins

2024). Although preliminary observations using light microscopy suggest that the last instar tissue-feeding larva of *C. socoromaensis* sp. nov. bears six lobes like those indicated by Davis et al. (2013) as a distinctive feature of the genus, further studies using scanning electron microscopy will be needed to perform detailed observations of these small structures.

Cremastobombycia socoromaensis sp. nov. is the first species of the genus described from South America. Like other recent studies (Cerdeña et al. 2020, 2022; Vargas-Ortiz et al. 2020), this discovery highlights the need to continue the search for leaf miners associated with plants native to the western slope of the central Andes to improve the understanding of the diversity of Gracillariidae which remains overlooked in these arid environments.

Acknowledgements

Additional information

Conflict of interest

The author has declared that no competing interests exist.

Ethical statement

No ethical statement was reported.

Funding

Author contributions

The author solely contributed to this work.

Author ORCIDs

Héctor A. Vargas https://orcid.org/0000-0002-5355-3157

Data availability

All of the data that support the findings of this study are available in the main text.

References

Braun A (1908) Revision of the North American species of the genus *Lithocolethis* Hübner. Transactions of the American Entomological Society 34: 269−357. https://doi.org/10.5962/bhl.title.17825

Braun AF (1909) Phylogeny of the Lithocolletid group. (Preliminary Survey.). Canadian Entomologist 41: 419−423. https://doi.org/10.4039/Ent41419-12

Busck A (1910) New Central-American Microlepidoptera introduced into the Hawaiian Islands. Proceedings of the Entomological Society of Washington 12: 132−135.

Cerdeña J, Farfán J, Vargas HA, Brito R, Gonçalves GL, Lazo A, Moreira GRP (2020) *Phyllocnistis furcata* sp. nov.: A new species of leaf-miner associated with *Baccharis* (As-

teraceae) from Southern Peru (Lepidoptera, Gracillariidae). ZooKeys 996: 121–145. https://doi.org/10.3897/zookeys.996.53958

Cerdeña J, Farfán J, Vargas HA, Huanca-Mamani W, Gonçalves GL, Moreira GRP (2022) A contribution to the knowledge of leaf-mining *Phyllocnistis* Zeller, 1848 associated with *Baccharis* (Asteraceae), with description of two new species from Peru (Lepidoptera: Gracillariidae). Zootaxa 5104: 196–208. https://doi.org/10.11646/zootaxa.5104.2.2

Davis DR, Diaz R, Overholt WA (2013) Systematics and biology of *Cremastobombycia chromolaenae*, new species (Gracillariidae), a natural enemy of *Chromolaena odorata* (L.) King and H. Robinson (Asteraceae). Journal of the Lepidopterists Society 67: 35–41. https://doi.org/10.18473/lepi.v67i1.a4

De Prins J, De Prins W (2024) Global Taxonomic Database of Gracillariidae (Lepidoptera). http://www.gracillariidae.net [accessed 05 August 2024]

De Prins J, Kawahara AY (2012) Systematics, revisionary taxonomy, and biodiversity of Afrotropical Lithocolletinae (Lepidoptera: Gracillariidae). Zootaxa 3594: 1–283. https://doi.org/10.11646/zootaxa.3594.1.1

De Prins J, Arévalo-Maldonado H, Davis DR, Landry B, Vargas HA, Davis MM, Brito R, Fochezato J, Oshima I, Moreira GRP (2019) An illustrated catalogue of the Neotropical Gracillariidae (Lepidoptera) with new data on primary types. Zootaxa 4575: 1–110. https://doi.org/10.11646/zootaxa.4575.1.1

Kawahara AY, Ohshima I, Kawakita A, Regier JC, Mitter C, Cummings MP, Davis DR, Wagner DL, De Prins J, Lopez-Vaamonde C (2011) Increased gene sampling strengthens support for higher-level groups within leaf-mining moths and relatives (Lepidoptera: Gracillariidae). BMC Evolutionary Biology 11: 182. https://doi.org/10.1186/1471-2148-11-182

Kawahara AY, Plotkin D, Ohshima I, Lopez-Vaamonde C, Houlihan PR, Breinholt JW, Kawakita A, Xiao L, Regier JC, Davis DR, Kumata T, Sohn J-C, De Prins J, Mitter C (2017) A molecular phylogeny and revised higher-level classification for the leaf-mining moth family Gracillariidae and its implications for larval host-use evolution. Systematic Entomology 42: 60–81. https://doi.org/10.1111/syen.12210

Meyrick E (1912) Lepidoptera Heterocera (Tineae). Fam. Gracilariadae. In: Wytsman P (Ed.) Genera Insectorum. Fascicule 128. V. Verteneuil & L. Desmet, Imprimeurs-Éditeurs, Bruxelles, 1–36.

POWO (2024) Plants of the World Online. Royal Botanic Gardens, Kew. https://powo.science.kew.org/ [Retrieved 21 August 2024]

Rodriguez R, Marticorena C, Alarcón D, Baeza C, Cavieres L, Finot VL, Fuentes N, Kiessling A, Mihoc M, Pauchard A, Ruiz E, Sanchez P, Marticorena A (2018) Catálogo de las plantas vasculares de Chile. Gayana. Botánica 75: 1–430. https://doi.org/10.4067/S0717-66432018000100001

Vargas-Ortiz M, Aliaga-Pichihua G, Lazo-Rivera A, Cerdeña J, Farfán J, Huanca-Mamani W, Vargas HA (2020) Cryptic Diversity in the Monotypic Neotropical Micromoth Genus *Angelabella* (Lepidoptera: Gracillariidae) in the Peru-Chile Desert. Insects 11: 677. https://doi.org/10.3390/insects11100677

Vári L (1961) South African Lepidoptera. Vol. I. Lithocolletidae. Transvaal Museum Memoir 12: 1–238.

Villagrán C, Romo M, Castro V (2003) Etnobotánica del sur de los Andes de la Primera Región de Chile: Un enlace entre las culturas altiplánicas y las de quebradas altas del Loa superior. Chungara (Arica) 35: 73–124. https://doi.org/10.4067/S0717-73562003000100005

Research Article

Notes on the genus *Thibetana* (Lepidoptera, Zygaenidae) with description of a new species from China

Xinxin He[1], Chao Jiang[2], Weichun Li[1,3]

1 *College of Agronomy, Jiangxi Agricultural University, Nanchang 330045, China*
2 *State Key Laboratory for Quality Ensurance and Sustainable Use of Dao-di Herbs, National Resource Center for Chinese Materia Medica, China Academy of Chinese Medical Sciences, Beijing 100700, China*
3 *Jiangxi Provincial Key Laboratory of Conservation Biology, Jiangxi Agricultural University, Nanchang 330045, China*
Corresponding author: Weichun Li (weichunlee@126.com)

Abstract

The genus *Thibetana* Efetov & Tarmann, 1995 includes six species occurring in southwest China and Indian Sikkim. In the present paper, *Thibetana weii* Li & He, **sp. nov.**, the seventh species of the genus encountered at the foot of Galongla Snow Mountain, southeast Xizang of China is described. Habitus of the adult and genitalia of the new species are illustrated, and a checklist and a key of all *Thibetana* species are provided.

Key words: New species, Procridinae, taxonomy, Xizang, Zygaenidae

Introduction

The genus *Thibetana* Efetov & Tarmann, 1995 (Zygaenidae, Procridinae) was established to place *Artona sieversi* Alphéraky, 1892 (Efetov and Tarmann 1995). The genus includes six species with an Oriental distribution, occurring in southwest China and Indian Sikkim (Efetov 1997; Efetov and Tarmann 2017; Efetov and Tarmann 2024). Prior to this study, three *Thibetana* species were known from China (Alberti 1954; Efetov 1997; Efetov and Tarmann 2017). The present study aims to add a seventh species to the genus based on specimens collected from Xizang, China.

Material and methods

Specimens were hand-collected at night with a 250W mercury-vapour lamp and killed with ammonium hydroxide. The holotype is deposited in the Insect Museum, Jiangxi Agricultural University, Nanchang, China (JXAUM), and the paratype is deposited in the National Zoological Museum of China, Institute of Zoology, Chinese Academy of Sciences, Beijing, China (NZMCAS).

Terminology for morphological structures follows Efetov (1997). Photographs of adults were taken with a Zeiss AxioCam Icc 5 camera attached to a Zeiss Stereo Discovery V12 microscope. Illustrations of the genitalia were prepared using an Optec DV E3 630 digital camera attached to an Optec BK6000 microscope.

Taxonomy

Genus *Thibetana* Efetov & Tarmann, 1995

Thibetana Efetov & Tarmann, 1995: 74. Type-species: *Artona sieversi* Alphéraky, 1892, by original designation.

Diagnosis. Fore- and hindwings with black ground colour and yellow markings, r2+r3 stalked. Uncus long and thin, valva fan-shaped, and saccus well-developed in male genitalia. Praebursa spherical, translucent, with ring-like sclerotization in female genitalia (Efetov and Tarmann 1995).
   Distribution. China, India.

Checklist of the genus of *Thibetana* Efetov & Tarmann, 1995

Thibetana delavayi (Oberthür, 1894)

Artona delavayi Oberthür, 1894: 29; Alberti 1954: 280, pl. 29, fig. 9.
Thibetana delavayi: Efetov and Tarmann 2017: 583; Efetov and Tarmann 2024: 431.

Distribution. China (Sichuan, Yunnan).

Thibetana keili Efetov & Tarmann, 2017

Thibetana keili Efetov & Tarmann, 2017: 582, figs 1, 2, 7; Efetov and Tarmann 2024: 431.

Distribution. China (Xizang).

Thibetana postalba (Elwes, 1890)

Artona postalba Elwes, 1890: 379, pl. 32, fig. 16.
Thibetana postalba: Efetov and Tarmann 2017: 582, figs 3, 4, 8; Efetov and Tarmann 2024: 431.

Distribution. India (Sikkim).

Thibetana sieversi (Alphéraky, 1892)

Artona sieversi Alphéraky, 1892: 5.
Artona dejeani Oberthür, 1894: 29.
Artona gephyra Hering, 1936: 1.
Thibetana sieversi: Efetov and Tarmann 1995: 74, figs 21, 22; Efetov 1997: 511, figs 4, 7, 10; Efetov and Tarmann 2024: 431.

Distribution. China (Qinghai, Sichuan).

***Thibetana weii* Li & He, sp. nov.**

Distribution. China (Xizang).

***Thibetana witti* Efetov, 1997**

Thibetana witti Efetov, 1997: 509, figs 1, 2, 5, 6, 8, 9; Efetov and Tarmann 2024: 431.

Distribution. China (Xizang).

***Thibetana zebra* (Elwes, 1890)**

Artona zebra Elwes, 1890: 379, pl. 32, fig. 11.
Thibetana zebra: Efetov and Tarmann 2017: 583, figs 5, 6; Efetov and Tarmann 2024: 431.

Distribution. India (Sikkim).

Key to the genus of *Thibetana* Efetov & Tarmann, 1995

1	Hindwing upperside with two yellow spots	**2**
–	Hindwing upperside with one yellow spot	**3**
2	Forewing upperside with one yellow spot at base	***T. weii* sp. nov.**
–	Forewing upperside with two yellow spots at base	***T. zebra***
3	Forewing upperside with a single or two yellow spots	**4**
–	Forewing upperside with four yellow spots	**5**
4	Forewing upperside with a single yellow spot	***T. delavayi***
–	Forewing upperside with two yellow spots	***T. sieversi***
5	Sacculus without process, juxta longer than uncus in male genitalia	***T. witti***
–	Sacculus with a round lobe, juxta shorter than uncus in male genitalia	**6**
6	Saccus as long as uncus in male genitalia	***T. keili***
–	Saccus twice as long as uncus in male genitalia	***T. postalba***

***Thibetana weii* Li & He, sp. nov.**
https://zoobank.org/B0F6360A-BF60-4222-93BD-D679E9DDB208

Type materials. *Holotype* • ♂, Сʜɪɴᴀ, Xizang Autonomous Region, Mêdog County, the foot of Galongla Snow Mountain (29°44.2947'N, 95°40.6068'E), 3415 m, 31 July 2024, Weichun Li et al. leg. ***Paratype*** • 1 ♀, same data as holotype.

Diagnosis. Forewing upperside with ovate yellow spot at base, two ovate spots near middle, and an 8-shaped yellow spot at distal part; hindwing upperside with subtriangular yellow spot and oblong yellow spot. In male genitalia, sacculus nearly rectangular, dentated on outer margin, ending with spine-like process on ventral margin.

Description. *External morphology of imago* (Fig. 1). Forewing length 8.5–9.0 mm. Frons yellow mixed black. Vertex black. Labial palpus approximately

one and half as long as compound eye's diameter, pale brown mixed with yellow. Male antenna pinnate except distal one-sixth serrate; female antenna serrate. Compound eye ovate, black, edged with yellow scales; ocellus round, black. Chaetosema well-developed, gray. Tegula yellow. Thorax black. Upperside of forewing black, bearing ovate yellow spot at base, two ovate yellow spots near middle, and an 8-shaped yellow spot at outer side of discoidal cell, cilia yellow; underside of forewing pattern same as upperside except for long and thin yellow stripe at basal one-fourth of costa, and longitudinal yellow stripe extending from
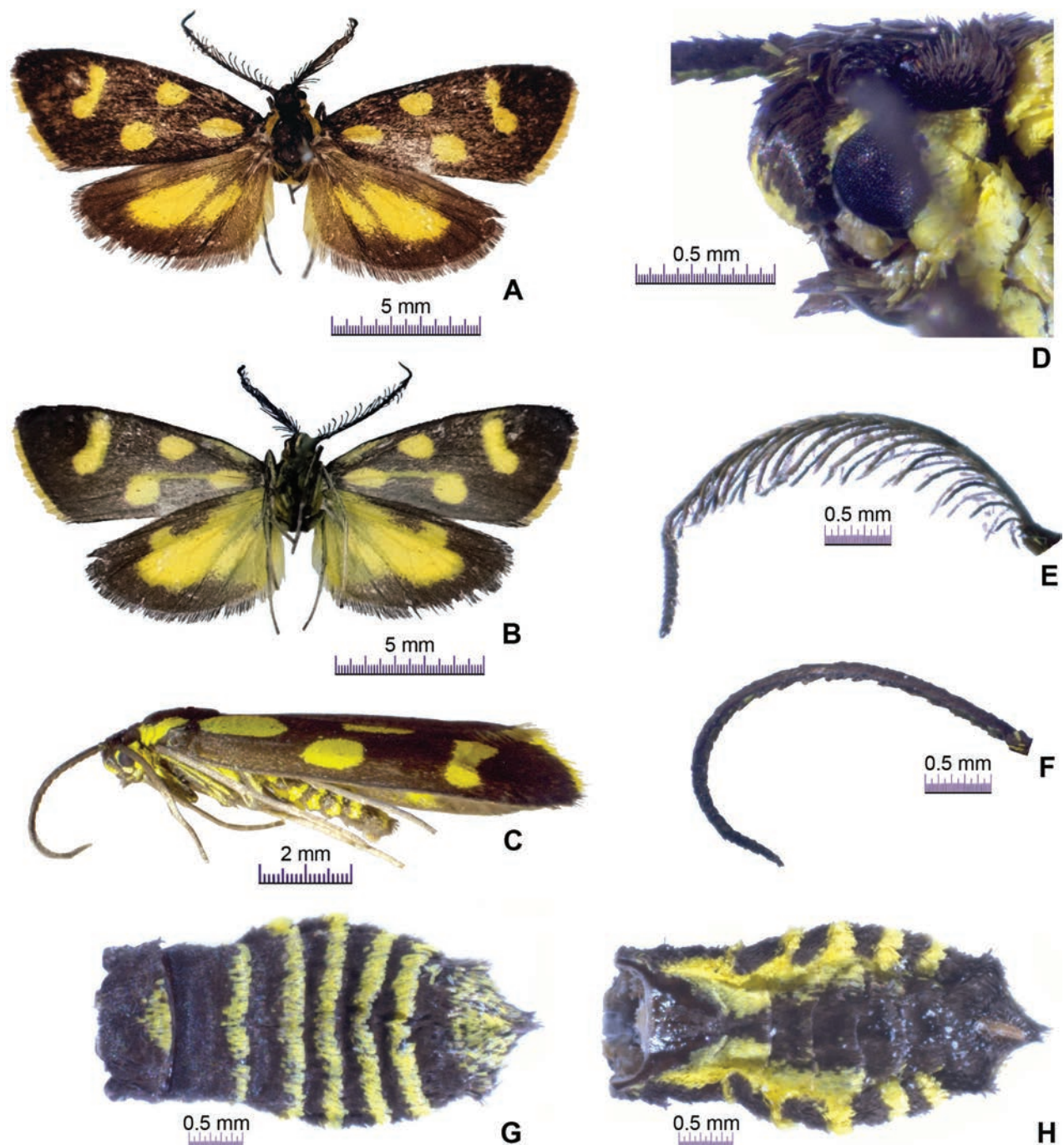
Figure 1. *Thibetana weii* Li & He, sp. nov. **A** male habitus (holotype), dorsal view **B** ditto, ventral view **C** female habitus (paratype), lateral view **D** ditto, head, lateral view **E** male antenna (holotype), lateral view **F** female antenna (paratype), lateral view **G** female abdomen (paratype), dorsal view **H** ditto, ventral view.

basal one fourth to half part of forewing. Upperside of hindwing blackish-brown, with subtriangular yellow spot and oblong yellow spot, cilia blackish-brown; underside of hindwing yellow, costa, outer region, and apex blackish-brown. Legs greyish brown, femur yellow in lateral view. Dorsal side of abdomen blackish-brown, first segment covered with yellow scales in middle, second to sixth segments densely covered with yellow scales on distal margin, distal segment scattered with yellow scales; ventral side of abdomen blackish-brown, second to sixth segments densely covered with yellow scales near lateral margin.

Male genitalia (Fig. 2A). Uncus thin and long, distal apex pointed. Tegumen arm slightly longer than uncus. Valva slightly broader near middle, distal one-third nearly triangular, and gently concave at approximately distal one-fourth on ventral margin; costa strongly sclerotized, reaching apex of valva; sacculus nearly rectangular, about one-fourth as long as valva, dentated on outer margin, ending with spine-like process on ventral margin. Saccus well-developed, as long as uncus, distal tip round. Juxta ovate. Phallus cylindrical as long as valva, without cornuti.

Female genitalia (Fig. 2B). Papillae analis about two thirds as long as apophysis posterioris. Apophysis anterioris thin and long, nearly as long as apophysis posterioris. Praebursa spherical, translucent, with ring-like sclerotization. Ductus bursae inconspicuous. Corpus bursae ovate; signum small, bearing two spine-like projections; appendix bursae irregular shaped.

Etymology. In honour of Dr. Fuwen Wei, a renowned conservation biologist, who contributes profoundly to biodiversity, zoological evolution and conservation biology. We suggest the Chinese common name as "魏氏藏斑蛾".
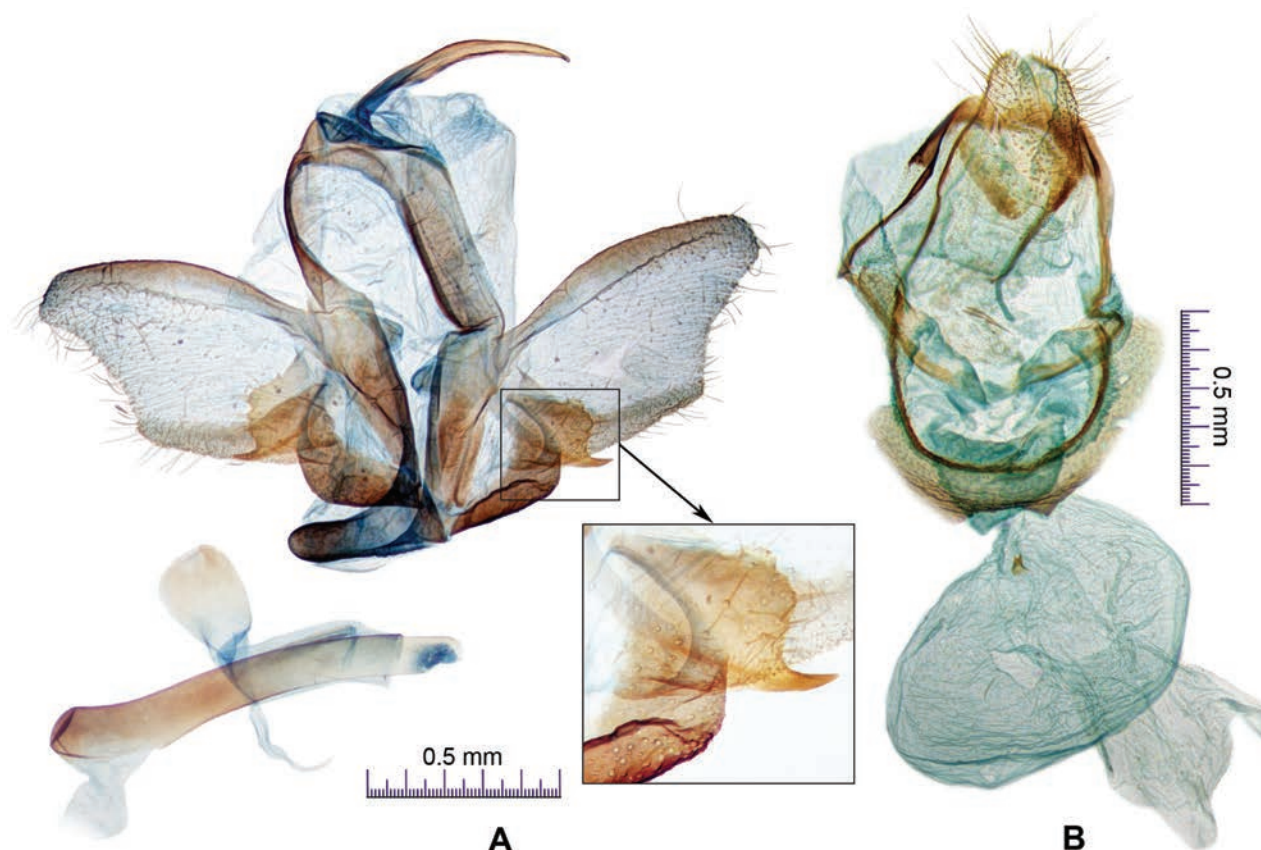

Figure 2. *Thibetana weii* Li & He, sp. nov. **A** male genitalia (holotype), ventral view **B** female genitalia (paratype), ventral view.

Distribution. China (Xizang).

Remarks. The new species is similar to *Thibetana zebra* (Elwes, 1890) in the forewing pattern, but can be distinguished from the latter species by the upper-side of the hindwing with a subtriangular yellow spot and an oblong yellow spot (Fig. 1A). In *T. zebra*, the second spot on the upperside of the hindwing is thin and long (Efetov and Tarmann 2017: fig. 5).

Acknowledgements

Additional information

Conflict of interest

The authors have declared that no competing interests exist.

Ethical statement

No ethical statement was reported.

Funding

Author contributions

Investigation: CJ. Writing - original draft: XH. Writing - review and editing: WL.

Author ORCIDs

Chao Jiang https://orcid.org/0000-0003-1841-1169
Weichun Li https://orcid.org/0000-0003-0154-861

Data availability

All of the data that support the findings of this study are available in the main text.

References

Alberti B (1954) Uber die stammesgeschichtliche Gliederung der Zygaenidae nebst Revision einiger Gruppen (Insecta, Lepidoptera). Mitteilungen aus dem Zoologischen Museum in Berlin 30: 115–480. https://doi.org/10.1002/mmnz.19540300202

Alphéraky S (1892) Lépidoptères rapportés de la Chine et de la Mongolie par G. N. Potanine. In: Romanoff NM (Ed.) Mémoires sur les Lépidoptères 6. St. Pétersbourg, 1–81.

Efetov KA (1997) *Thibetana witti* sp. nov. from Tibet (Lepidoptera, Zygaenidae, Procridinae). Entomofauna 18: 509–512.

Efetov KA, Tarmann GM (1995) An annotated check-list of the Palaearctic Procridinae (Lepidoptera: Zygaenidae), with descriptions of new taxa. Entomologist's Gazette 46: 63–103.

Efetov KA, Tarmann GM (2017) *Thibetana keili* Efetov & Tarmann, a new species of the genus *Thibetana* Efetov & Tarmann, 1995, from Tibet (Lepidoptera: Zygaenidae, Procridinae, Artonini). SHILAP Revista De lepidopterología 45(180): 581–587. https://doi.org/10.57065/shilap.879

Efetov KA, Tarmann GM (2024) An annotated catalogue of the Procridinae of the World (Lepidoptera: Zygaenidae). SHILAP Revista De lepidopterología 52 (207): 409–547. https://doi.org/10.57065/shilap.956

Elwes HJ (1890). On some new moths from India. Proceedings of the Zoological Society of London 1890: 378–401.

Hering M (1936) Schwedisch-chinesische wissenschaftliche Expedition nach den nordwestlichen Provinzen Chinas, unter Leitung von Dr. Sven Hedin und Prof. Sü Pingchang. Insekten gesammelt vom schwedischen Arzt der Expedition Dr. David Hummel 1927–1930. Teil 40. Lepidoptera, Bombyces. Arkiv för Zoologie 27(A) 32: 1–7.

Oberthür PC (1894) Faunes entomologiques Descriptions d'Insectes nouveaux ou peu connus. Chalcosiidae, Zygaenidae. Études d'Entomologie 19: 25–32.